RTD-TDR-63-4239

PRESSURE MEASUREMENTS FOR MACH FIVE FLOWS OVER A BLUNT PYRAMIDAL CONFIGURATION WITH AERODYNAMIC CONTROLS

PART OF AN INVESTIGATION OF HYPERSONIC FLOW SEPARATION AND CONTROL CHARACTERISTICS

DEPARTMENT OF AERONAUTICS
U. S. Naval Postgraduate School
Monterey, California

TECHNICAL DOCUMENTARY REPORT No. RTD-TDR-63-4239

JANUARY 1964

AIR FORCE FLIGHT DYNAMICS LABORATORY
RESEARCH AND TECHNOLOGY DIVISION
AIR FORCE SYSTEMS COMMAND
WRIGHT-PATTERSON AIR FORCE BASE, OHIO

Project 8219, Task No. 821902

(Prepared under Contract No. AF 33(616)-8130 by the
Research Department, Grumman Aircraft Engineering Corporation
Bethpage, New York
Author: Louis G. Kaufman II)

NOTICES

When Government drawings, specifications, or other data are used for any purpose other than in connection with a definitely related Government procurement operation, the United States Government thereby incurs no responsibility nor any obligation whatsoever; and the fact that the Government may have formulated furnished, or in any way supplied the said drawings, specifications, or other data, is not to be regarded by implication or otherwise as in any manner licensing the holder or any other person or corporation, or conveying any rights or permission to manufacture, use, or sell any patented invention that may in any way be related thereto.

Qualified requsters may obtain copies of this report from the Defense Documentation Center (DDC), (formerly ASTIA), Cameron Station, Bldg. 5, 5010 Duke Street, Alexandria, Virginia, 22314.

This report has been released to the Office of Technical Services, U.S. Department of Commerce, Washington 25, D. C., in stock quantities for sale to the general public.

Copies of this report should not be returned to the Research and Technology Division, Wright-Patterson Air Force Base, Ohio, unless return is required by security considerations, contractual obligations, or notice on a specific document.

500 - March 1964 - 162-28-532

FOREWORD

This report presents the results of a portion of the experimental program for the investigation of hypersonic flow separation and control characteristics being conducted by the Research Department of Grumman Aircraft Engineering Corporation, Bethpage, New York. Mr. Donald E. Hoak of the Flight Control Laboratory, Aeronautical Systems Division, located at Wright-Patterson Air Force Base, Ohio, is the Air Force Project Engineer for the program, which is being supported primarily under Contract AF33(616)-8130, Air Force Task 821902.

The author wishes to express his appreciation to the staff of the von Karman Facility for their helpfulness in conducting the tests and particularly to Messrs. Schueler, Donaldson, Baer, and Burchfield for providing the machine plotted graphs of the experimental data included in this report. Ozalid reproducible copies of the tabulated data are available on loan from the Flight Control Laboratory.

ABSTRACT

Pressure data were obtained for Mach 5 flows over a blunt pyramidal configuration composed of a 70-degree sweepback delta wing surface and two dihedral surfaces. Trailing edge flap deflections were varied up to 40 degrees on all surfaces and the model was tested with and without canards and ventral fins. The model was pitched at angles of attack from -30 degrees to +45 degrees and at sideslip angles up to 15 degrees for a Reynolds number, based on model length, of 4.6 million.

PUBLICATION REVIEW

This report has been reviewed and is approved.

FOR THE COMMANDER:

Charles B. Westbrook

Charles B. Westbrook
Chief, Aerospace Mechanics Branch
Flight Control Laboratory

TABLE OF CONTENTS

Item	Page
Introduction	1
Model	1
Test Conditions	2
Data Reduction and Accuracy	3
Results	3
References	5

LIST OF ILLUSTRATIONS

Figure		Page
1	General Outline of Models and Remarks for Over-all Program	10
2	Photographs of Model Installed in the AEDC 40-inch Supersonic Tunnel	11
3	Instrumentation on Model	13
4-15	Oil Film Photographs*	16
16-27	Schlieren Flow Photographs*	28
28-78	Pressure Coefficient Data Plots*	40

*See Table II, p.7 , for figure numbers corresponding to particular test conditions.

LIST OF SYMBOLS

C_p	pressure coefficient, $C_p \equiv (p - p_\infty)/q_\infty$
M_∞	free stream Mach number
p	pressure (psia)
p_o	stagnation pressure (psia)
p_∞	free stream static pressure (psia)
q_∞	free stream dynamic pressure (psia)
Re_∞/ft	Reynolds number per foot, $Re_\infty/ft \equiv \rho_\infty U_\infty/\mu_\infty$
T_o	stagnation temperature (°R)
T_∞	free stream static temperature (°R)
U_∞	free stream velocity (ft/sec)
X'	nondimensional streamwise distance from virtual apex to planform projection (see Fig. 3)
Y'	nondimensional spanwise distance measured outboard from the model centerline
α	angle of attack (degrees), positive for nose up
β	sideslip angle (degrees), positive for nose left
μ_∞	viscosity of air in the free stream (slugs/ft sec)
ρ_∞	density of air in the free stream (slugs/ft^3)

INTRODUCTION

The experimental data generated for an investigation of hypersonic flow separation and aerodynamic control characteristics are to be presented in a series of reports, of which this is one. Pressure, heat transfer, and force data are to be obtained for hypersonic flows over "basic geometries," such as a wedge mounted on a flat plate, and for "typical" hypersonic flight configurations with aerodynamic control surfaces. The experimental portion of the program requires a total of 11 models (see Fig. 1, page 10); 8 for tests in the von Karman Facility of the Arnold Engineering Development Center and 3 for tests in the Grumman Hypersonic Shock Tunnel (Refs. 1 and 2). The data obtained from AEDC tests of one of the models are given in this report (see Foreword).

This report presents pressure data obtained at $M_\infty = 5$ in the AEDC 40-inch Supersonic Tunnel on a blunt pyramidal configuration having four, remotely controlled, trailing edge flaps. The same model was tested in the AEDC 50-inch Mach 8 Tunnel to obtain pressure and aerodynamic heating rate distributions (Ref. 3). Flap hinge and twist moments and normal force were obtained along with six component force data on a geometrically similar model tested at the same model length Reynolds number in the 40-inch Supersonic Tunnel and also in the 50-inch Mach 8 Tunnel. A third geometrically similar model, with limited pressure and heat transfer instrumentation, is to be tested in the Grumman Hypersonic Shock Tunnel (see Fig. 1).

MODEL

Photographs of the model installed in the 40-inch Supersonic Tunnel are shown in Fig. 2. The lower surface of the model is a blunt delta wing with 70 degree sweepback. The plane parts of the dihedral surfaces are right triangles connected by a cylindrical segment which forms the ridge line of the model. The three cylindrical leading edges and the spherical nose have the same radius (also the same as for Configurations "C" shown in Fig. 1). The cross-sectional shape of the model was chosen to be the same as one of the ASD - General Applied Sciences Laboratory pyramidal models tested in the AEDC Hotshot 2 hypervelocity facility (Ref. 4).

Manuscript released by the author September 1963 for publication as an RTD Technical Documentary Report.

The model has four, remotely controlled, trailing edge flaps, two on the lower surface and one on each dihedral surface. As shown in Fig. 3, the flaps have rectangular planforms and their hinge lines are parallel to the base of the model (perpendicular to the ridge line). The chords of the remotely controlled flaps are 15 per cent of the virtual planform length of the model. In addition to these flaps, which were deflected at various angles up to 40 degrees, the model was tested with one pair of instrumented flaps, mounted on the lower surface, having a deflection angle of 20 degrees and a chord equal to 25 per cent of the model reference length (Fig. 3).

Tests were also conducted with a ventral fin mounted between the flaps on the lower surface. The wedge shaped fin has a total included angle of 30 degrees, was set at fin (or rudder) deflection angles of 0 and 15 degrees, and is geometrically similar to the instrumented fin of Configuration "B" shown in Fig. 1.

Pressure tap locations are shown in Fig. 3. Also shown in this figure are the thermocouple locations and the removable canard used for the Mach 8 tests. There are 5 streamwise lines of pressure taps on the lower surface; 10 taps are positioned along the streamwise centerline of the flap and 8 taps are on the model centerline. The dihedral surface has a similar array of taps in lines parallel to the ridge line; 10 taps along the streamwise centerline of the flap and 8 taps on the ridge line.

TEST CONDITIONS

The data presented herein were obtained from Mach 5 tests in the AEDC 40-inch Supersonic Tunnel (Ref. 3). The model was pitched from 30 degrees nose down to 45 degrees nose up for various flap settings for a free stream Reynolds number per foot of 3.3 million (corresponding to a Reynolds number of 4.6 million, based on free stream conditions and the model reference length). As indicated in Table I, pressure data were also obtained for a limited number of conditions at a 14 degree sideslip angle.

The configuration, flap settings, and angles of attack and sideslip are shown in Table I, along with the tunnel test conditions. In keeping with standard aeronautical terminology, the flap deflection angles are considered positive downward. Thus, the flaps on the lower surface were deflected at positive angles and the flaps on the dihedral, upper surfaces were deflected at negative angles.

The angles are measured in a plane normal to the flap hinge lines. The 15 degree ventral fin (rudder) setting is indicated in Fig. 3 and is set to trim at positive sideslip angle (nose left).

At $\alpha = 14.3$ degrees, the dihedral surfaces are parallel to the free stream and all flap hinge lines are normal to the free stream flow.

DATA REDUCTION AND ACCURACY

The data were reduced to standard pressure coefficient form:

$$C_p = \frac{p - p_\infty}{q_\infty}$$

where p is the measured pressure; p_∞ is the free stream static pressure; and q_∞ is the free stream dynamic pressure. The inaccuracy in the measured pressure varies from ± 0.005 psia for pressures below 1.00 psia, to ± 0.075 psia for pressures greater than 15 psia. Whence, depending upon the values of C_p and Re_∞/ft, the pressure coefficient accuracy varies from about ± 0.009 to ± 0.020. Variations in the tunnel conditions affect the accuracy of the tabulated pressure coefficient data to a negligible extent; the tunnel conditions shown in Table I were kept constant to well within one per cent of the values shown.

The automatic plotting machines, used in presenting the data herein, introduce another source of possible error. The discrepancy in the plotted pressure coefficients due to this machine error should not exceed ± 0.01. Nevertheless, there is always the possibility that a point will be completely misplotted. Each graph has been inspected and questionable points checked with the tabulated pressure coefficients.

Finally, the remotely controlled flap settings were estimated to be accurate to well within half a degree.

RESULTS

Table II summarizes the Mach 5 flow data obtained on the model and indicates the corresponding figure numbers where the sets of data are presented. The AEDC group number is presented in the last

column. This number indicates the order in which the data were obtained and is to be used when referring to the tabulated data.

Although obtained on the geometrically similar force model, at the same Mach number and model length Reynolds number, oil film and schlieren flow photographs are included herein as an aid to interpreting the pressure data. The test conditions for the fluorescent oil film and schlieren flow photographs are indicated in Table II.

Four pages are required for each figure containing pressure coefficient plots. Streamwise plots of the pressure coefficients on the lower surface, at five spanwise stations, are presented on the first page of each figure. On the second page are presented pressure coefficient plots at five spanwise stations on the dihedral surface of the model. These plots are taken along lines of pressure taps parallel to the ridge line of the model; they are parallel to the free stream at $\alpha = 14.3^{o}$. Spanwise plots of the pressure coefficients obtained on the lower surface are presented on the third page of each figure. Plots of the dihedral surface pressure coefficients, taken along the surface in planes parallel to the base of the model (perpendicular to the ridge line) are presented on the fourth page.

As indicated in Fig. 3, X' is the nondimensional streamwise distance from the planform virtual apex to the projection of a pressure tap on the planform. The projections are in planes parallel to the base of the model. Thus, for example, the dihedral flap hinge lines are at X' = 0.85 and the hinge lines of the pair of shorter flaps on the lower surface are also at X' = 0.85.

An outline of the model is shown on each graph. Heavy lines on the model outlines indicate the streamwise and spanwise lines of pressure taps for the data shown on the same page.

Although the accuracy of the plotted data should suffice for engineering purposes, ozalid reproducible copies of the tabulated data are available on load (see Foreward). The plotted data may be read accurately using standard 20/inch grid, tracing graph paper overlays.

REFERENCES

1. Kaufman, L.G. II, Oman, R.A., Hartofilis, S.A., Meckler, L.H., Evans, W.J., and Weiss, D., A Review of Hypersonic Flow Separation and Control Characteristics, ASD-TDR-62-168, March 1962.

2. Evans, W.J., and Kaufman, L.G. II, Pretest Report on Hypersonic Flow Separation and Control Models for AEDC Tunnels A, B, Hotshot 2 and Grumman Hypersonic Shock Tunnel, Grumman Research Department Memorandum RM-209, July 1962.

3. Arnold Center, Test Facilities Handbook, Arnold Air Force Station, January 1961.

4. Wallace, A.R., and Swain, W.N., Pressure Distribution Tests on a 60° and 70° Delta Wing at Mach Numbers 20 to 22, AEDC-TN-61-14, February 1961, CONFIDENTIAL REPORT.

5. Kaufman, L.G. II, Pressure and Heat Transfer Measurements for Hypersonic Flows Over Expansion Corners and Ahead of Ramps, Part I: Mach 5 and 8 Data for Expansion Corner Flows, Part II: Mach 5 Pressure Data for Flows Ahead of Ramps, Part III: Mach 8 Pressure Data for Flows Ahead of Ramps, Part IV: Mach 8 Heat Transfer Data for Flows Ahead of Ramps, to be published as an ASD Technical Documentary Report.

6. Kaufman, L.G. II, and Meckler, L., Pressure and Heat Transfer Measurements at Mach 5 and 8 for a Fin-Flat Plate Model, ASD-TDR-63-235, February 1963.

7. Hartofilis, S.A., Pressure Measurements at Mach 19 for a Winged Re-entry Configuration, ASD-TDR-63-319, March 1963.

8. Meckler, L., Static Aerodynamic Characteristics at Mach 5 and 8 for an Aerodynamically Controllable Winged Re-entry Configuration, to be published as an ASD Technical Documentary Report.

TABLE I

TEST CONDITIONS

Tunnel Conditions	M_∞ = 5.01	p_∞ = 0.134 psia	p_o = 72 psia
	Re_∞/ft = 3,300,000	q_∞ = 2.35 psia	T_o = 620°R

Configuration	Flap Settings			Angles of Attack and Sideslip						
	Bottom Flaps	Left Flap	Right Flap	Values of α at β = 0°						Values of α at β = 14°
Basic pyramidal configuration	0	-40	-40			0	14.3*	33	45	
	0	-30	-30			0	14.3	33	45	
	0	-20	-20				14.3	33	45	
	0	-10	-10				14.3	33	45	
	0	0	0	-30	-15	0	14.3	33	45	0 14.3*
	10	0	0			0				
	20	0	0	-30	-15	0	14.3		45	
	30	0	0			0				
	40	0	0	-30	-15	0	14.3			
	0	-20	0				14.3			
	0	-40	0			0	14.3			0 14.3
+ Fin (δ = 0)	0	0	0				14.3			14.3
+ Fin (δ_{fin} = 15°)	0	0	0			0	14.3			0 14.3
	20	0	0				14.3			
	40	0	0			0	14.3			
+ Longer chord flaps	20	0	0	-30	-15	0	14.3			

*Dihedral surfaces parallel to free stream flow at α = 14.3°.

TABLE II

TEST DATA FIGURE NUMBERS

Part I - Flow Photographs

Configuration	Flap Settings* Bottom	Left	Right	α (deg)	β (deg)	Figure Number*	A E D C Photo No.
Basic Pyramidal	0	-40	-40	-30	0	4	33 311
	↓	↓	↓	-15	↓	5	33 310
	↓	↓	↓	0	↓	6	33 309
	↓	↓	↓	+14.3*	↓	7	33 308
	↓	-20	-20	+14.3	↓	8	33 307
	↓	0	0	+14.3	↓	9	33 306
	-40	0	0	-30	0	10	33 305
	↓	↓	↓	-15	↓	11	33 304
	↓	↓	↓	0	↓	12	33 301
	↓	↓	↓	+14.3	↓	13	33 302
	20	↓	↓	0	↓	14	33 299
	20	↓	↓	+12	↓	15	33 300
	0	0	0	0	0	16	820
	↓	↓	↓	+7	↓	17	821
	↓	↓	↓	+14.3	↓	18	822
	↓	-40	↓	+14.3	↓	19	832
	40	0	0	0	0	20	807
	↓	↓	↓	+5	↓	21	808
	↓	↓	↓	+10	↓	22	809
	↓	↓	↓	+14.3	↓	23	810
	↓	↓	↓	+20	↓	24	811
	↓	↓	↓	+25	↓	25	812
	↓	↓	↓	+30	↓	26	813
+ Fin (δ= 0)	0	0	0	0	0	27a	816
	0	0	0	+14.3	0	27b	817

*Notes: Flap settings, indicated in degrees, are measured in planes normal to the flap hinge lines.

Figs. 4-15 are oil film flow photographs and Figs. 16-26 are schlieren photographs obtained on the geometrically similar force model at the same model length Reynolds number.

The dihedral surface are parallel to the free stream flow at α = 14.3 degrees.

TABLE II

TEST DATA FIGURE NUMBERS

Part II - Pressure Coefficient Plots

CONFIGURATION*	FLAP SETTINGS (deg) BOT'M	LEFT	RIGHT	α (deg)	β (deg)	FIGURE NUMBER	A E D C GROUP NO.
Basic (pyramidal)	0	0	0	-30	0	28	124
	20	↓	↓	↓	↓	29	127
	40					30	128
+ Long flaps	20	0	0			31	142
Basic	0	0	0	-15	0	32	125
	20	↓	↓	↓	↓	33	126
	40					34	129
+ Long flaps	20	0	0			35	143
Basic	0	-40	0	0	+14	36	138
	↓	-40	0	↓	0	37	121
		-40	-40		↓	38	122
		-30	-30			39	123
		0	0			40	135
		0	0		+14	41	139
+ Fin (δ = 15°)	0	0	0		+14	42	150
	0	0	0		0	43	151
Basic	10	0	0		↓	44	140
	20	0	0			45	132
+ Long flaps	20	0	0			46	144
Basic	30	0	0			47	131
	40	0	0			48	130
+ Fin (δ = 15°)	40	0	0	↓	↓	49	152
Basic	0	-40	0	+14.3*	+14	50	137
	↓	-40	0	↓	0	51	120
		-40	-40		↓	52	115
		-30	-30			53	116
		-20	-20			54	117
		-20	0			55	119
		-10	-10			56	118
		0	0			57	134
		0	0	↓	+14	58	136

+ Fin (δ = 0)	0	0	0	+14.3*	+14	59	147
	0	0	0		0	60	146
+ Fin (δ = 15°)	0	0	0		0	61	148
	0	↓	↓		+14	62	149
	20				0	63	153
	40				↓	64	154
Basic	40	0	0			65	141
	20	0	0			66	133
+ Long flaps	20	0	0			67	145
Basic	0	-40	-40	+33	0	68	114
	↓	-30	-30	↓	↓	69	111
		-20	-20			70	110
		-10	-10			71	107
		0	0			72	106
	0	-40	-40	+45	0	73	113
	↓	-30	-30	↓	↓	74	112
		-20	-20			75	109
		-10	-10			76	108
		0	0			77	101
	20	0	0			78	102

*Notes:

Configuration: Basic pyramidal is with short chord (15%) bottom flaps and without ventral fin. + Long flaps indicates the 25% virtual length flaps are on the lower surface. + Fin indicates the ventral fin is on the basic model with the short chord flaps, the fin deflection is either 0 or 15°, as indicated.

Flap Settings: Indicated in degrees and measured in a plane normal to the flap hinge lines; the bottom flaps always operate as a pair and have equal settings.

At α = 14.3° the dihedral surfaces are parallel to the free stream flow.

Positive sideslip angle is nose left.

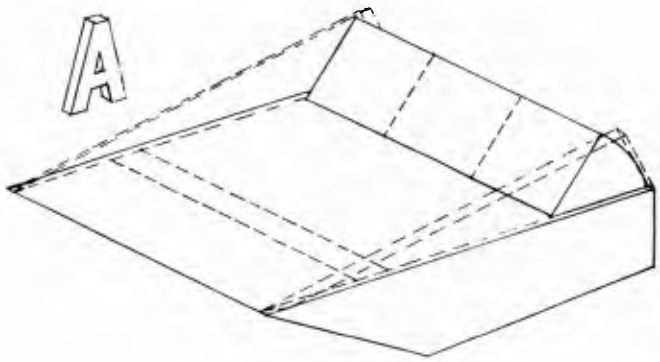

Separated Flows ahead of a Ramp
Fore and aft flaps, end plates
3 separate models:

1) Pressure and heat transfer, AEDC Tunnels A & B, M = 5 & 8, results in Ref. 5.

2) Controlled wall temperature, pressure, AEDC Tunnel B, M = 8, results not available yet.

3) Pressure and heat transfer, Grumman Shock Tunnel, M ≈ 13 & 19, results not available yet.

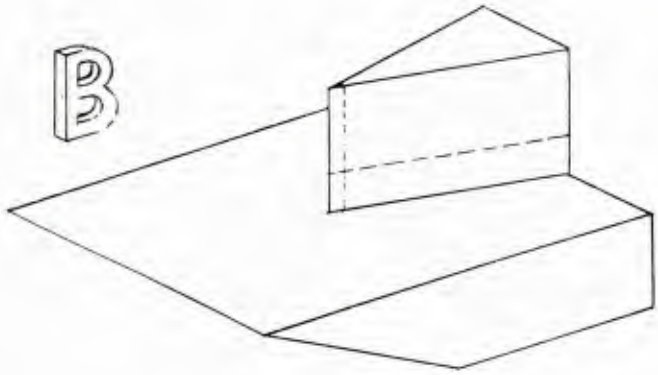

Wedge - Plate Interaction
Small and large fins with sharp and blunt leading edges
2 separate models:

1) Pressure and heat transfer, AEDC Tunnels A & B, M = 5 & 8, results in Ref. 6.

2) Pressure and heat transfer, Grumman Shock Tunnel, M ≈ 13 & 19, results not available yet.

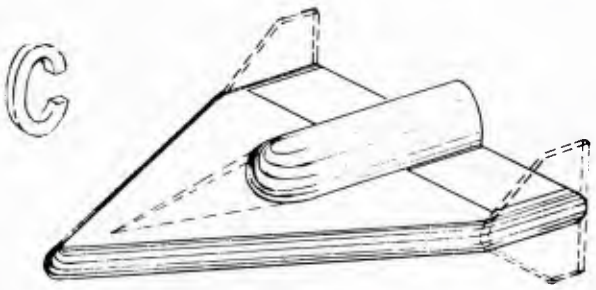

Clipped Delta, Blunt L.E.
Center body, T.E. flaps, drooped nose, spoiler, tip fins
3 separate models:

1) Pressure and heat transfer, AEDC Tunnels A & B, M = 5 & 8, results not available yet.

2) Pressure, AEDC Hotshot 2, M ≈ 19, results in Ref. 7.

3) Six component force, AEDC Tunnels A & B, M = 5 & 8, results in Ref. 8.

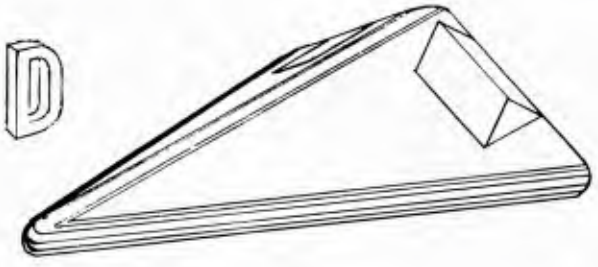

Delta, Blunt L.E., Dihedral
T.E. flaps, canard, ventral fin
3 separate models:

1) Pressure and heat transfer, AEDC Tunnels A & B, M = 5 & 8, results herein.

2) Pressure and heat transfer, Grumman Shock Tunnel, M ≈ 19, results not available yet.

3) Six component force, AEDC Tunnels A & B, M = 5 & 8, results not available yet.

Fig. 1 General Outline of Models and Remarks for Over-all Program

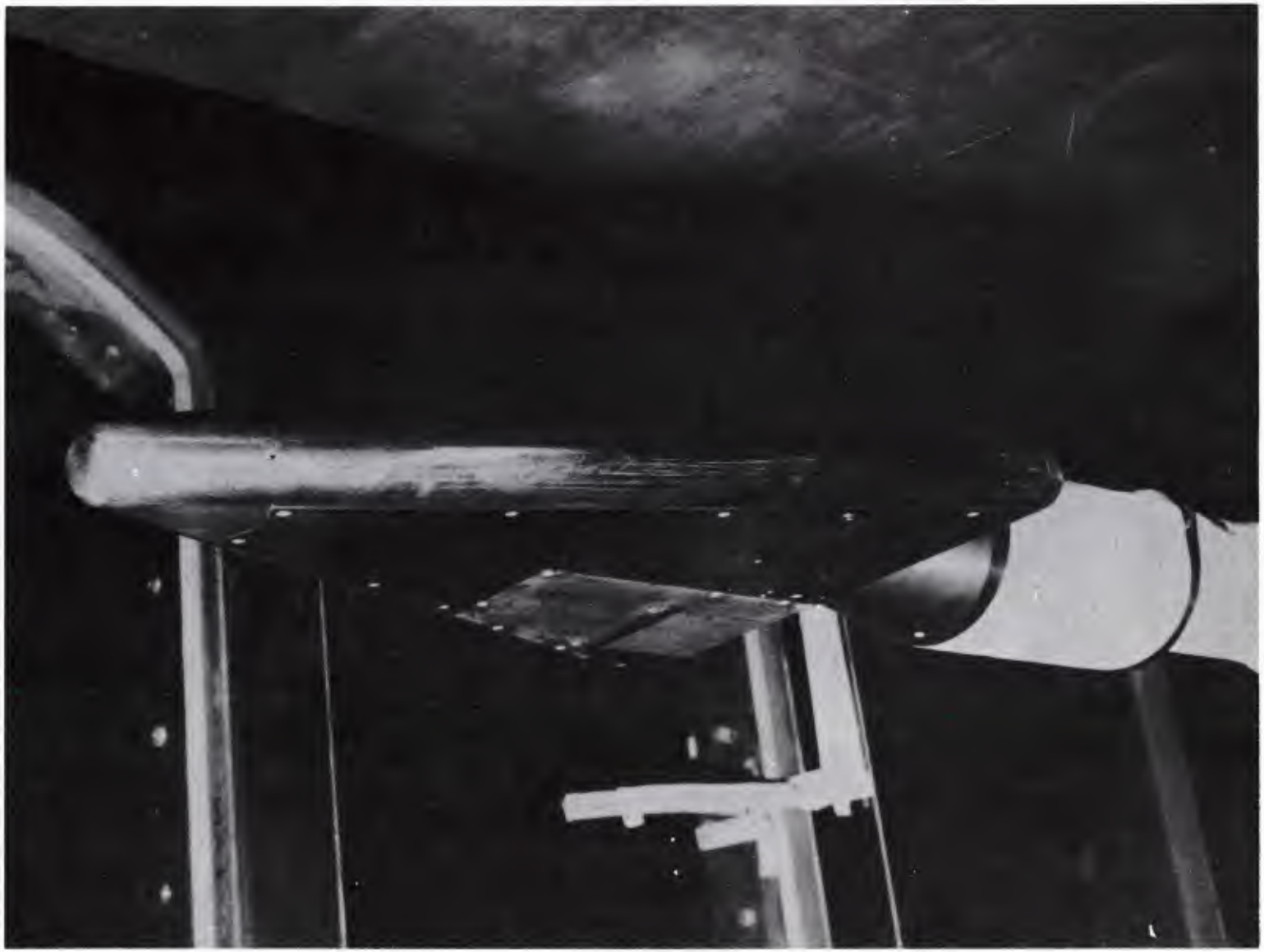

Fig. 2 Photograph of Model Installed in the AEDC 40-inch Supersonic Tunnel
a) Lower Surface

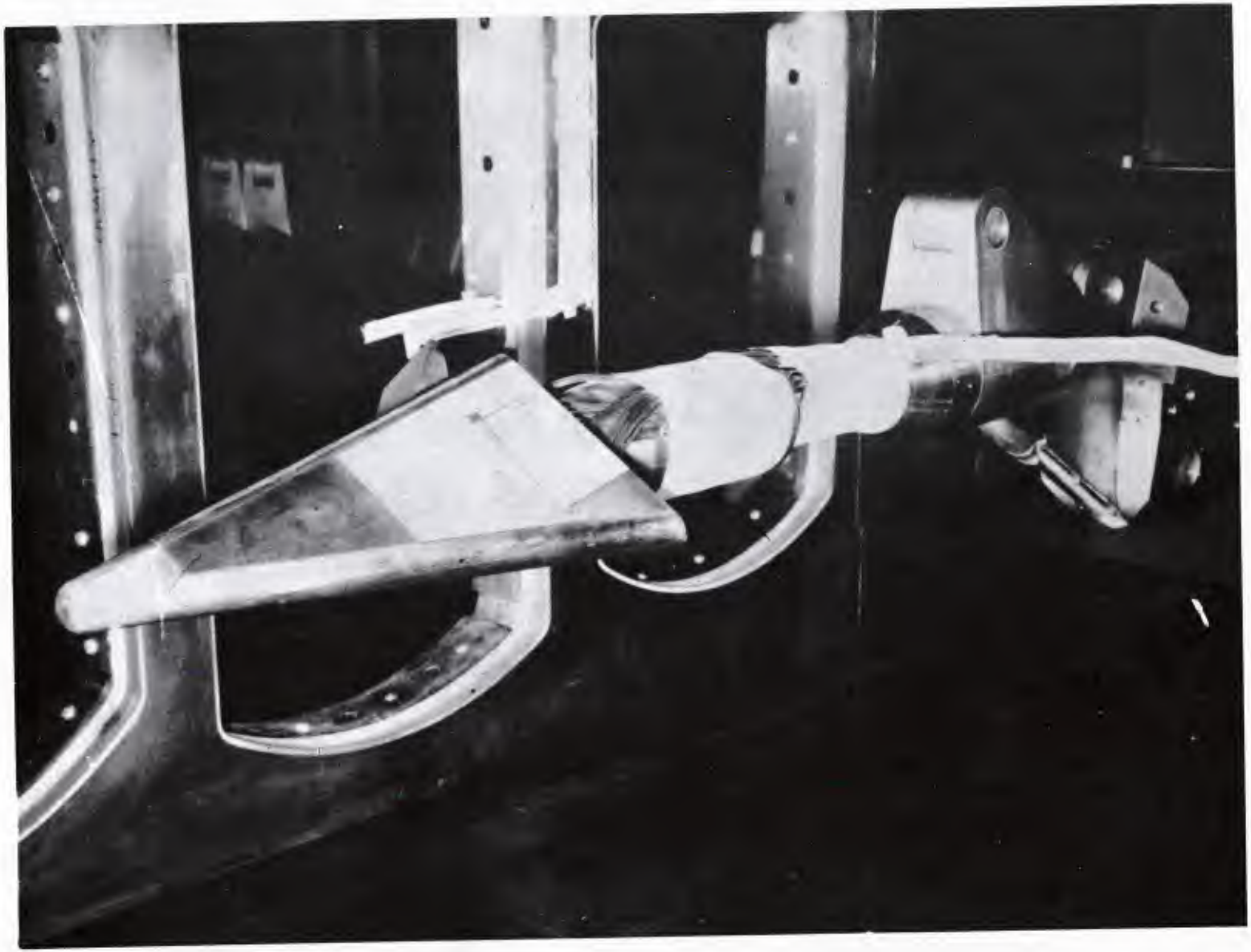

Fig. 2 Photograph of Model Installed in the AEDC 40-inch Supersonic Tunnel
b) Upper Surface

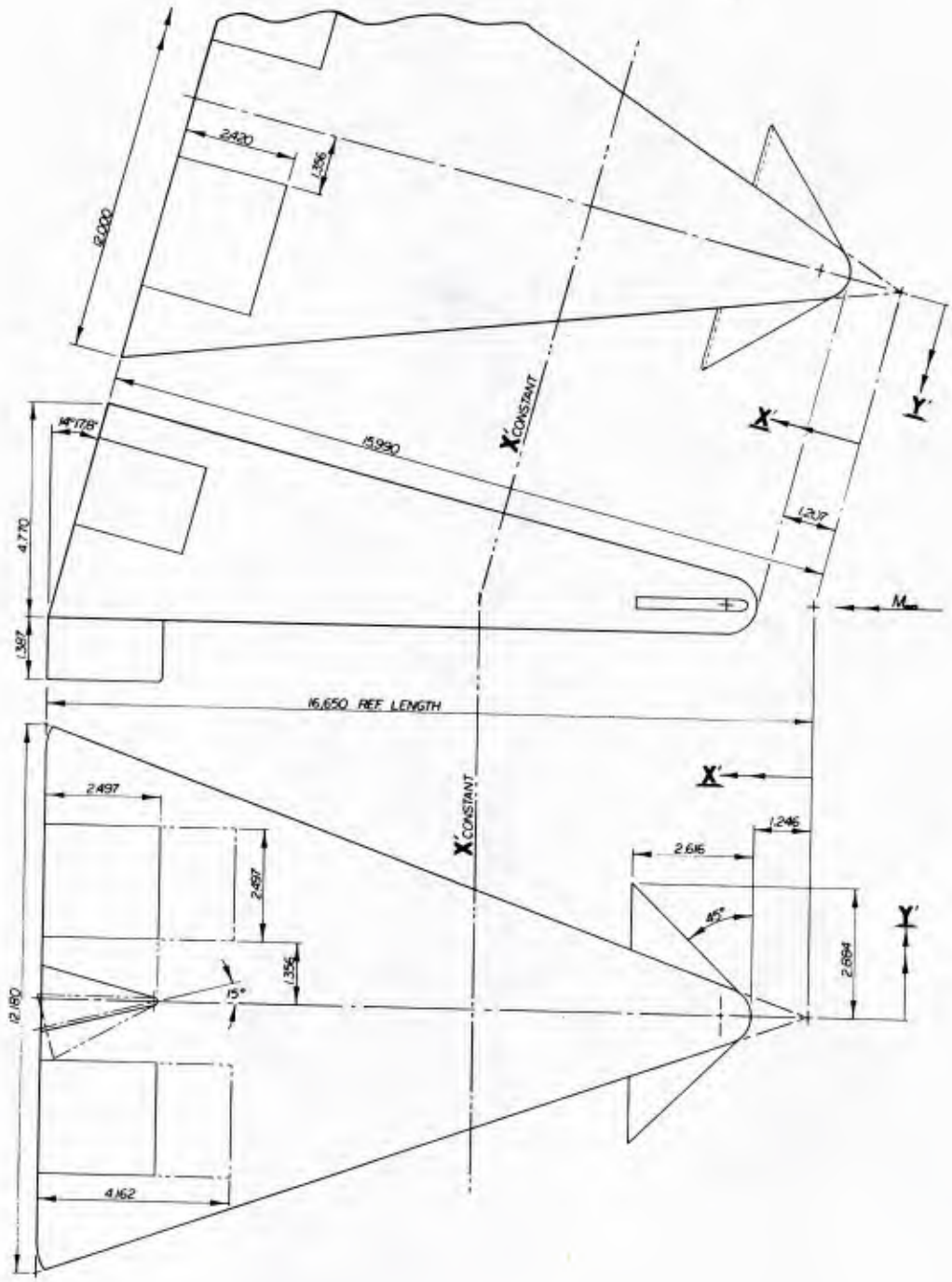

Fig. 3 Instrumentation on Model
(sheet 1 of 3)

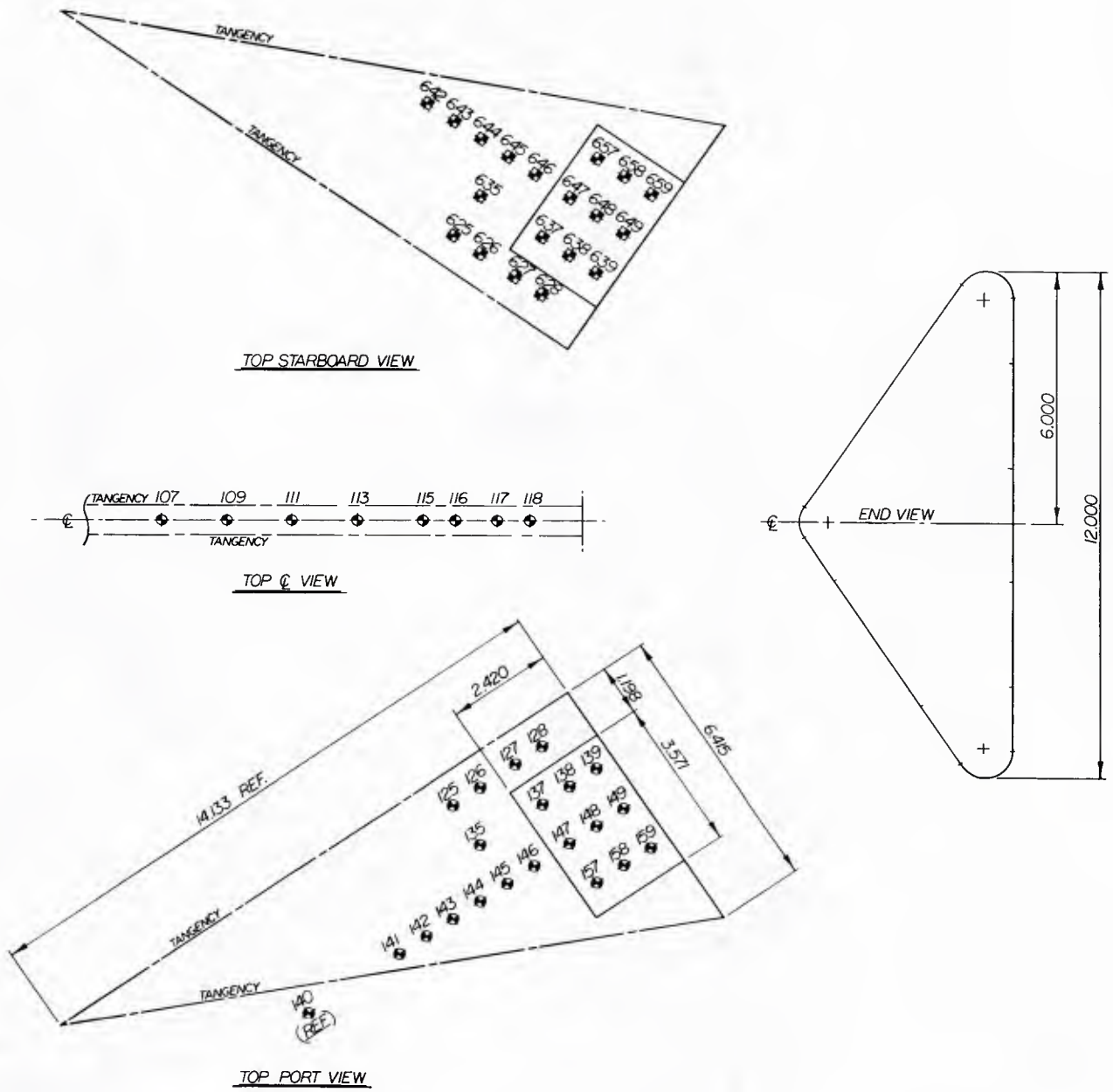

Fig. 3 Instrumentation on Model
(sheet 2 of 3)

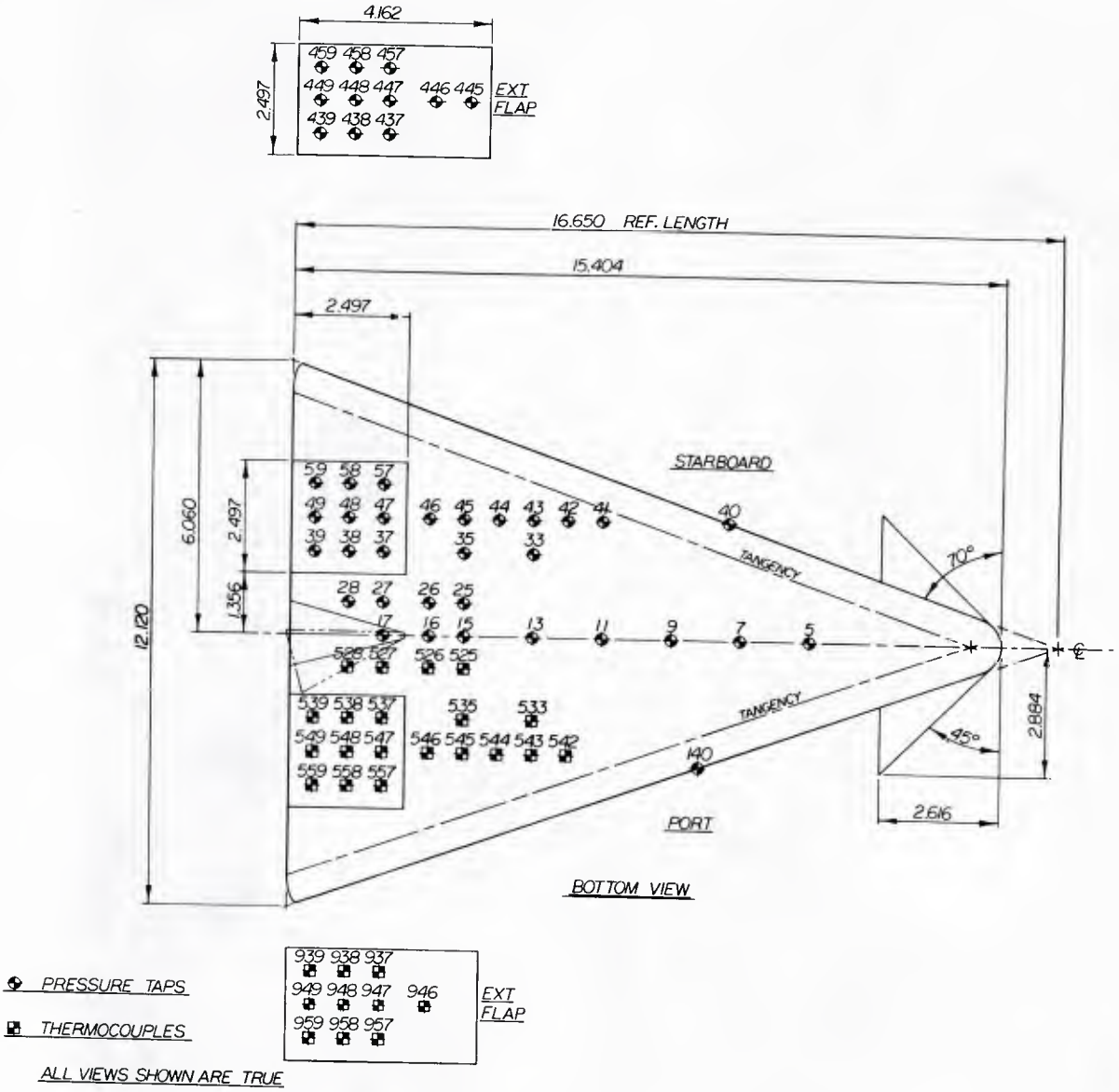

Fig. 3 Instrumentation on Model
(sheet 3 of 3)

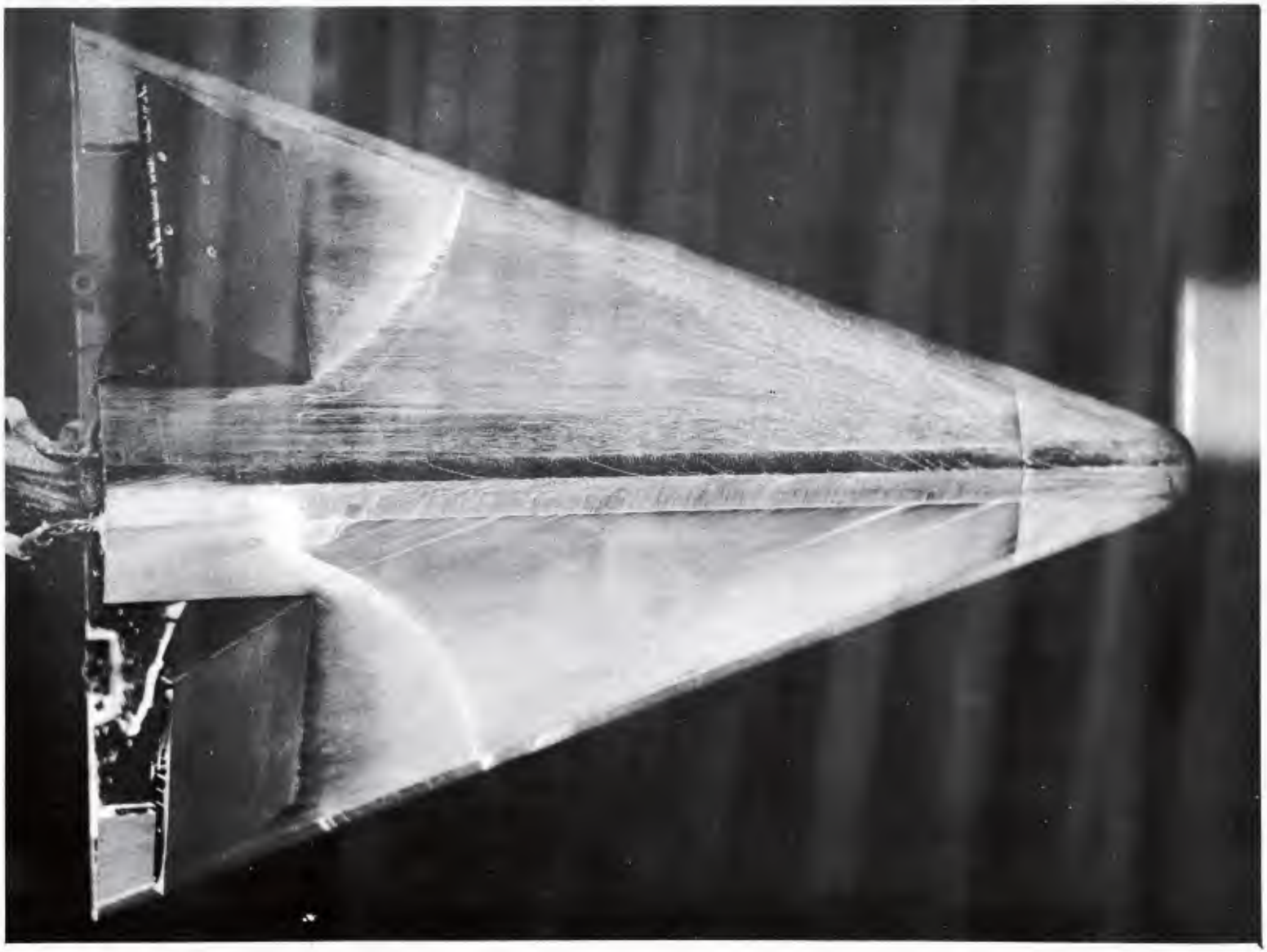

Fig. 4 Oil Film Photograph of Upper Surface; $\alpha = -30^{\circ}$, Upper Flaps Deflected 40°

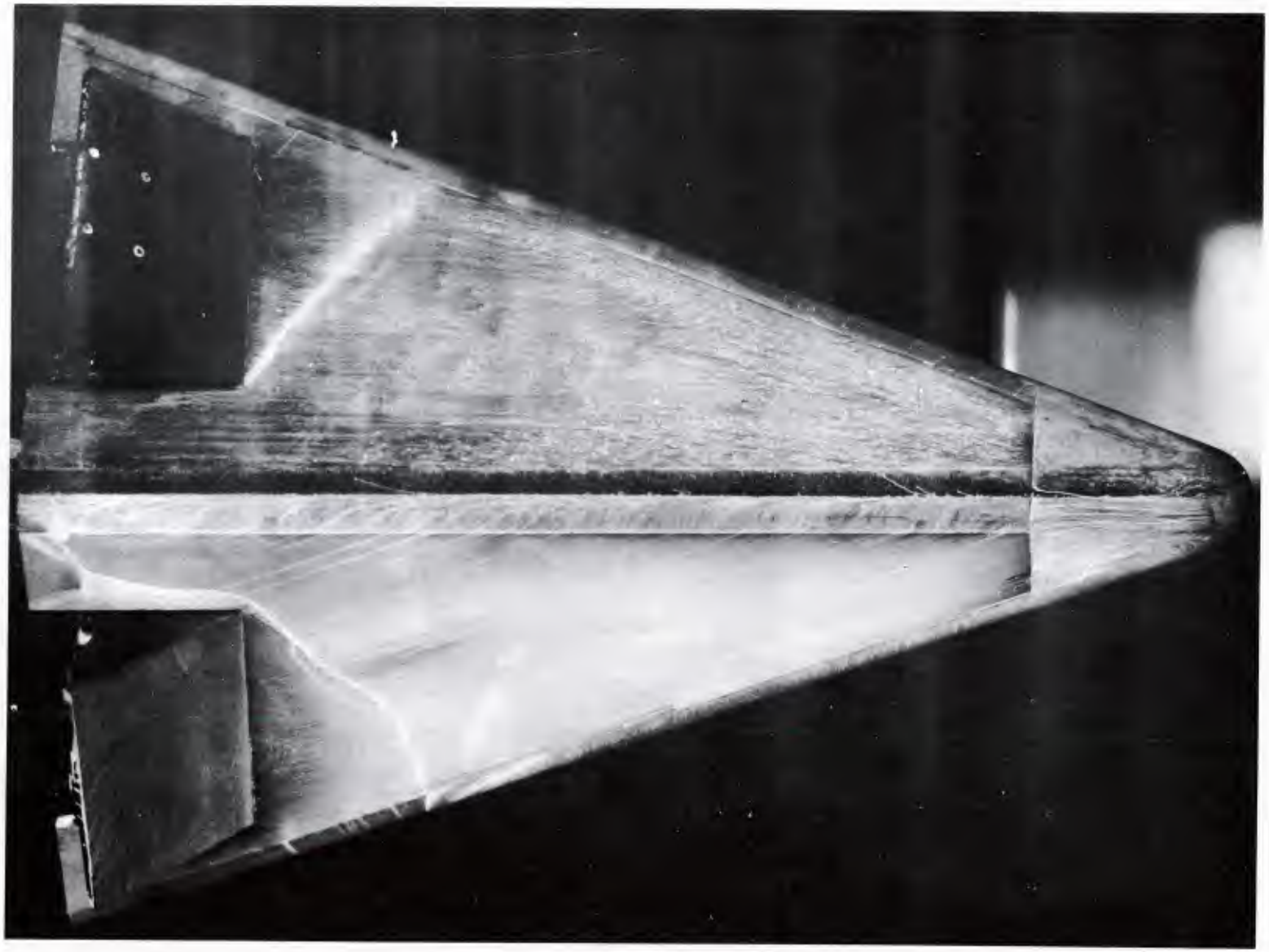

Fig. 5 Oil Film Photograph of Upper Surface; $\alpha = -15^{o}$, Upper Flaps Deflected 40°

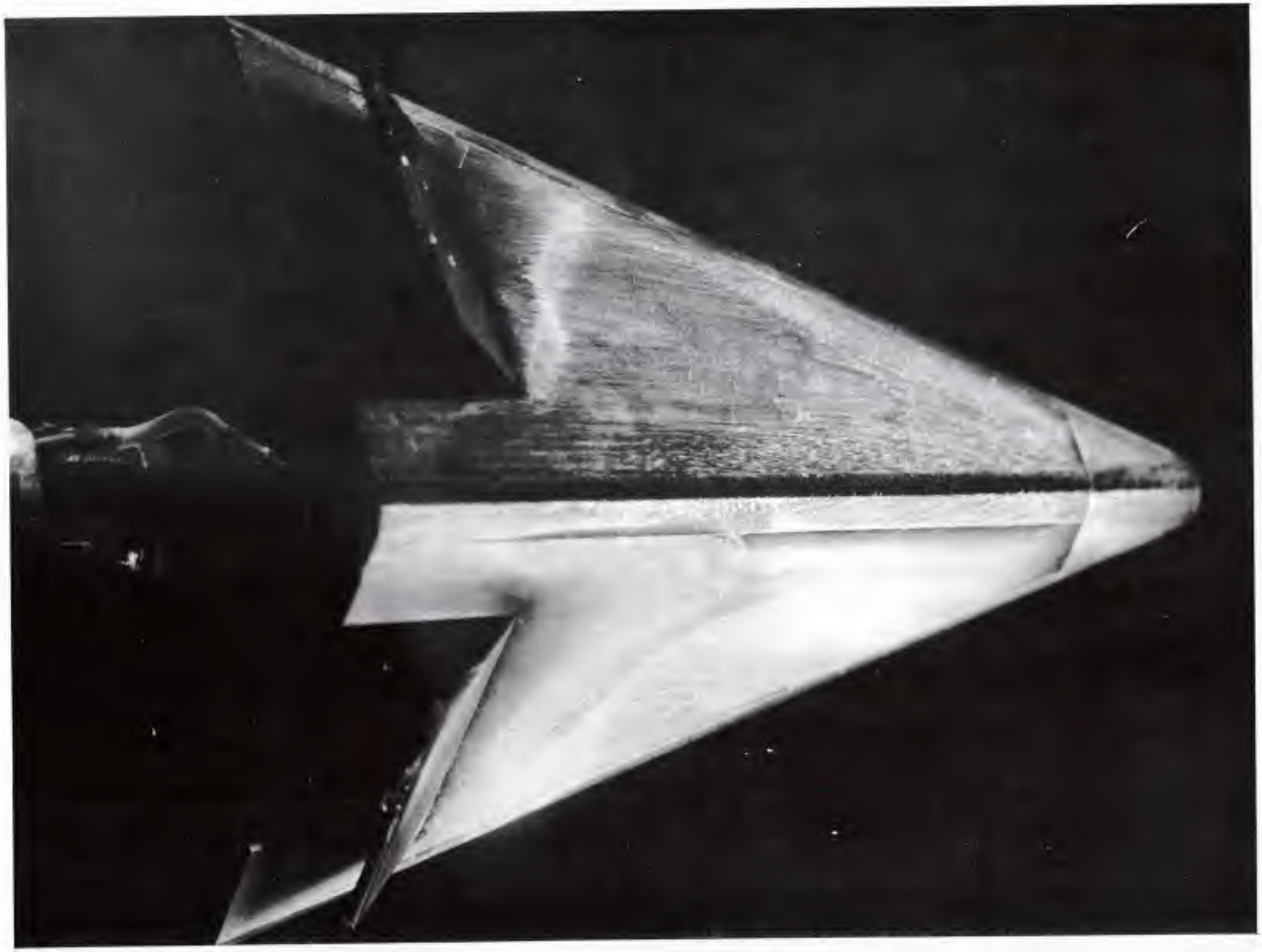

Fig. 6 Oil Film Photograph of Upper Surface; $\alpha = 0$, Upper Flaps Deflected 40°

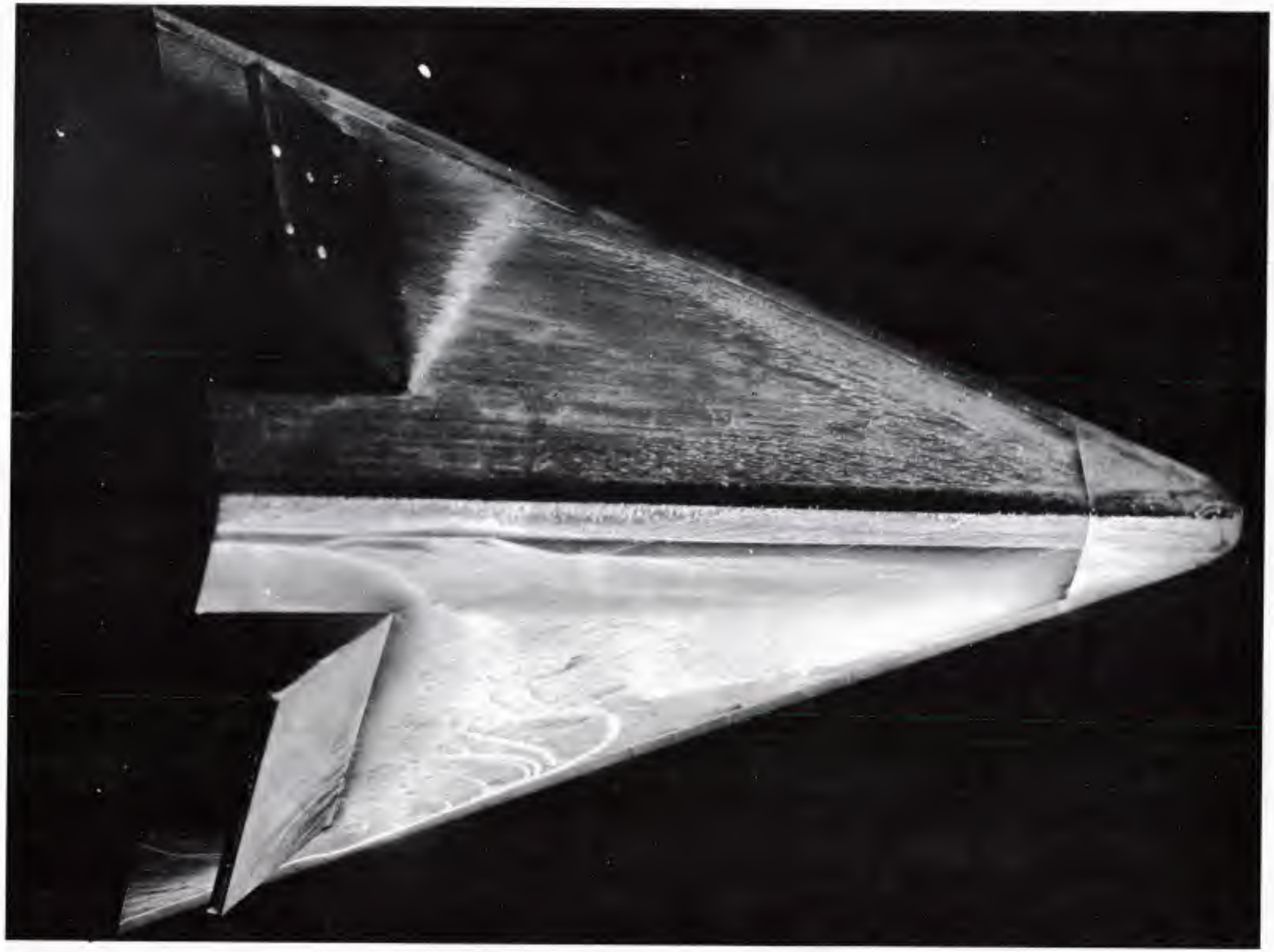

Fig. 7 Oil Film Photograph of Upper Surface; $\alpha = +14.3^{\circ}$, Upper Flaps Deflected 40°

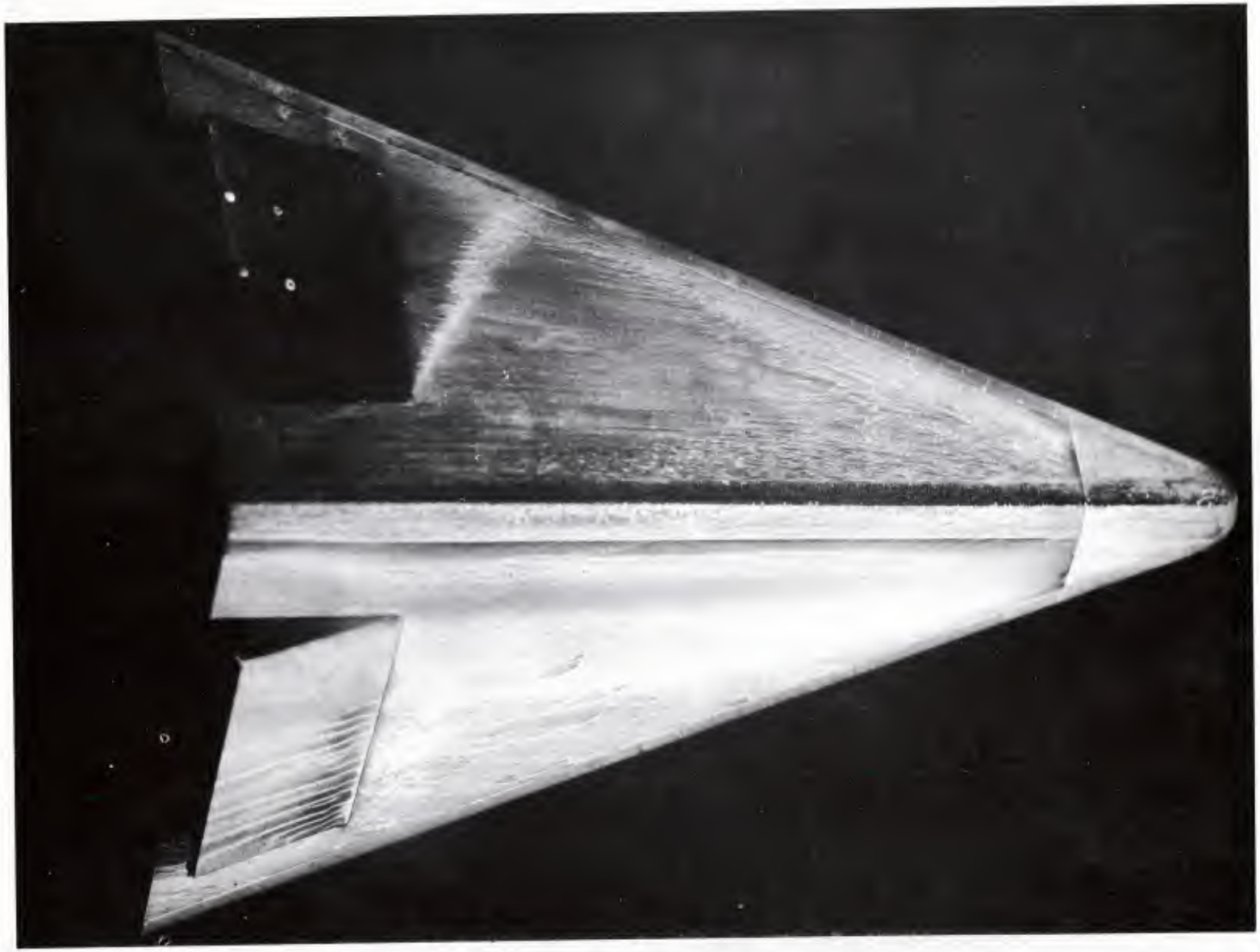

Fig. 8 Oil Film Photograph of Upper Surface; $\alpha = +14.3^{o}$, Upper Flaps Deflected 20°

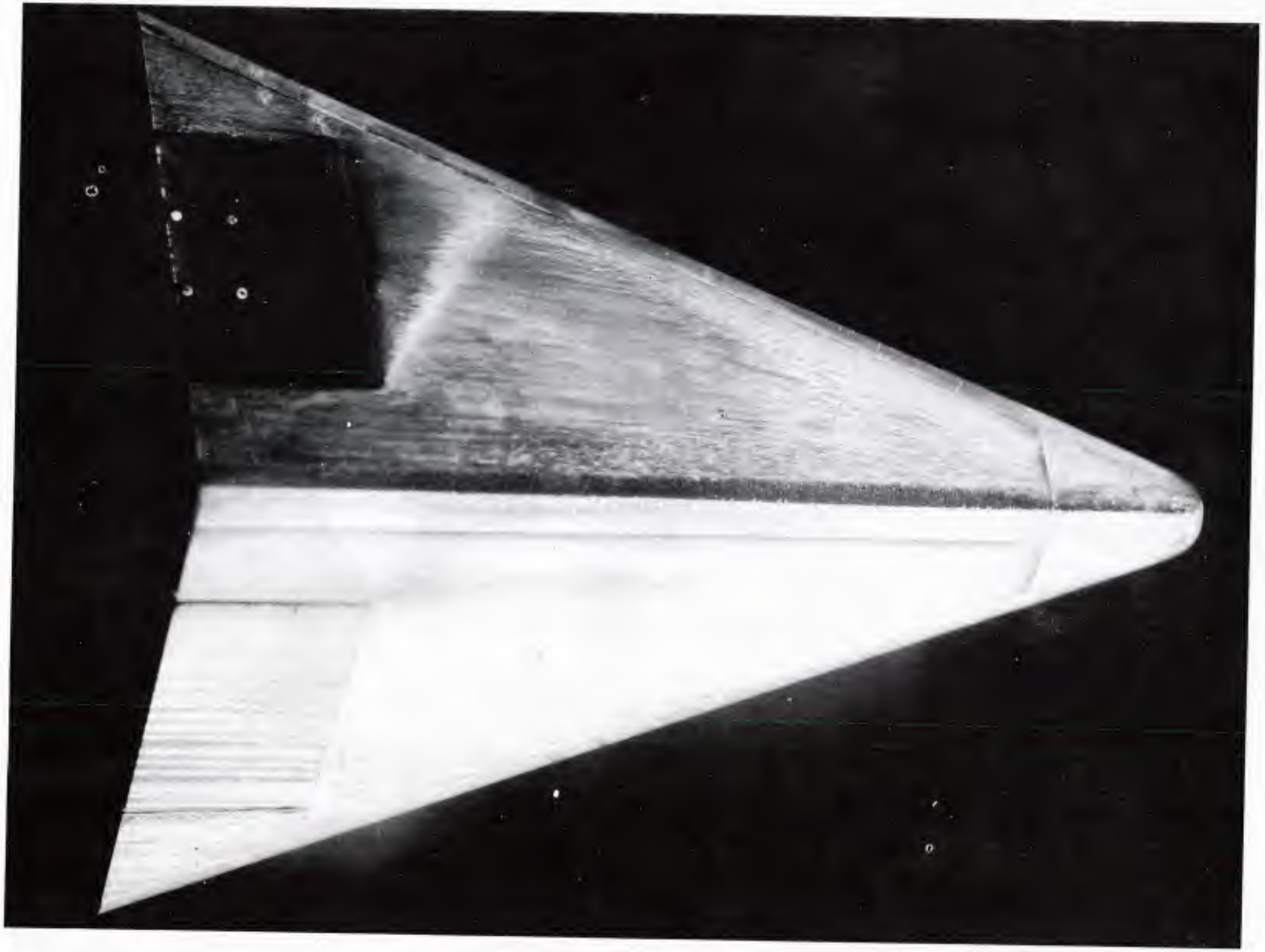

Fig. 9 Oil Film Photograph of Upper Surface; $\alpha = +14.3^{o}$, No Flap Deflections

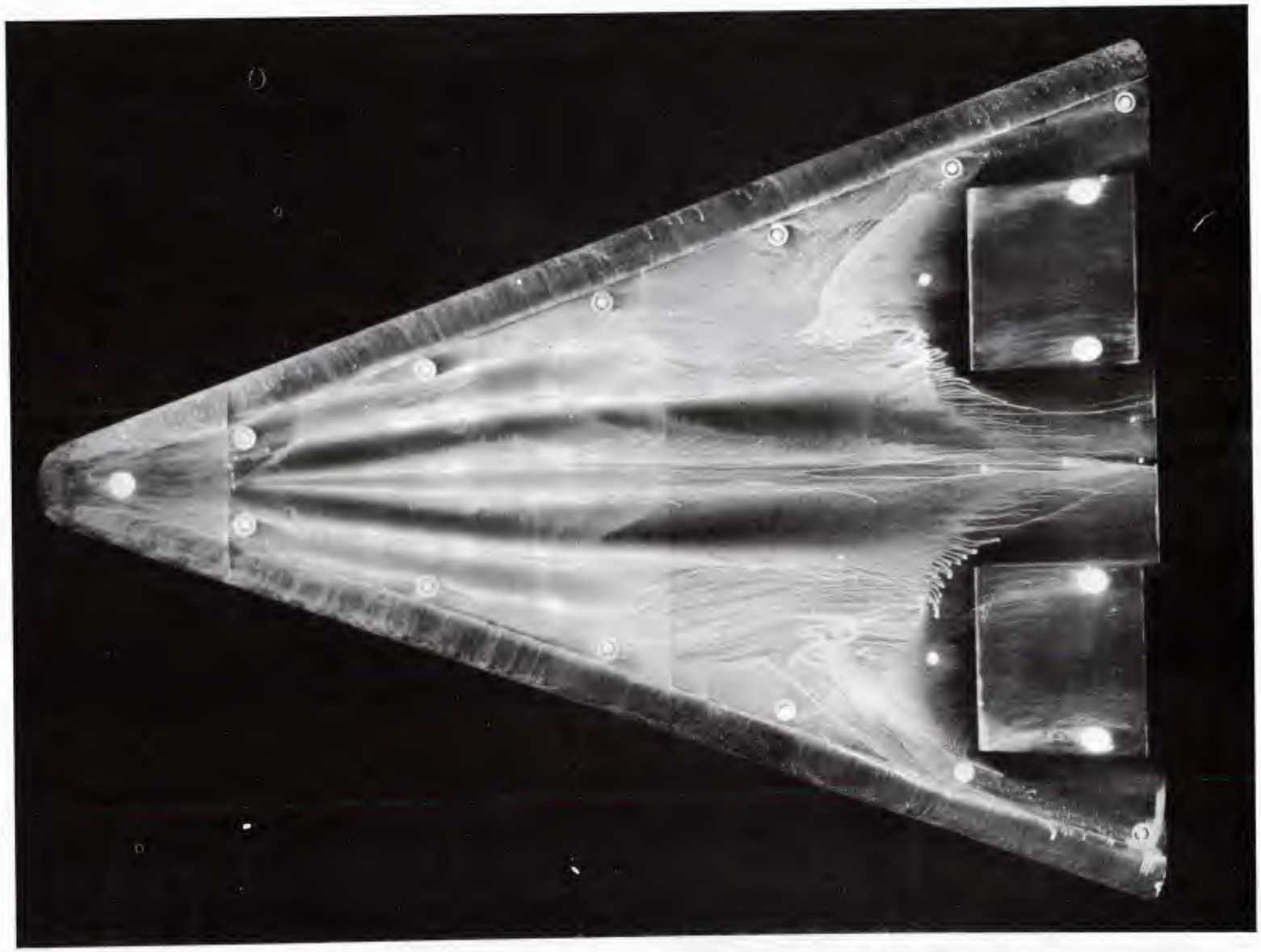

Fig. 10 Oil Film Photograph of Lower Surface; $\alpha = -30^{\circ}$, Bottom Flaps Deflected 40°

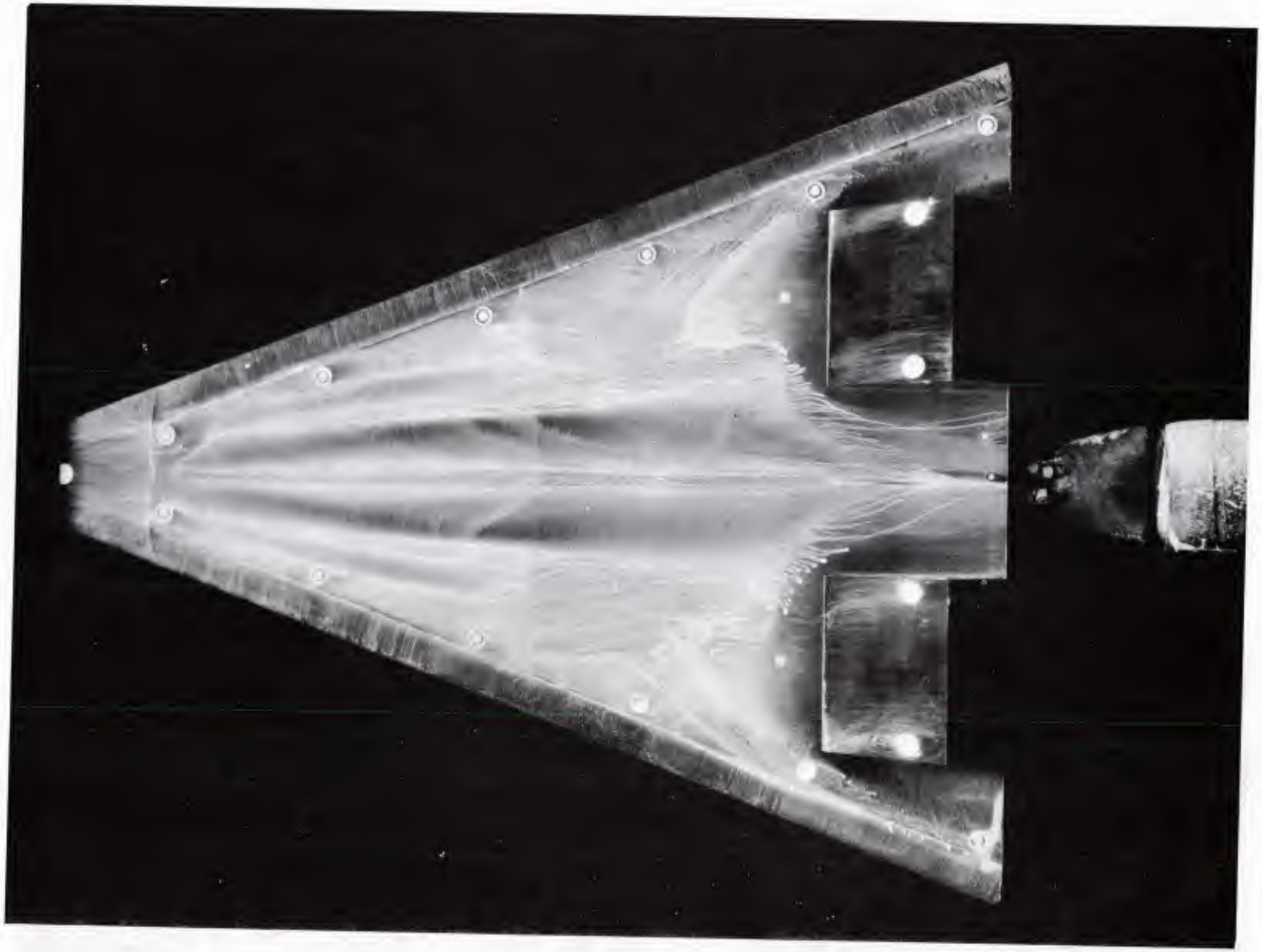

Fig. 11 Oil Film Photograph of Lower Surface; $\alpha = -15^{o}$, Bottom Flaps Deflected 40°

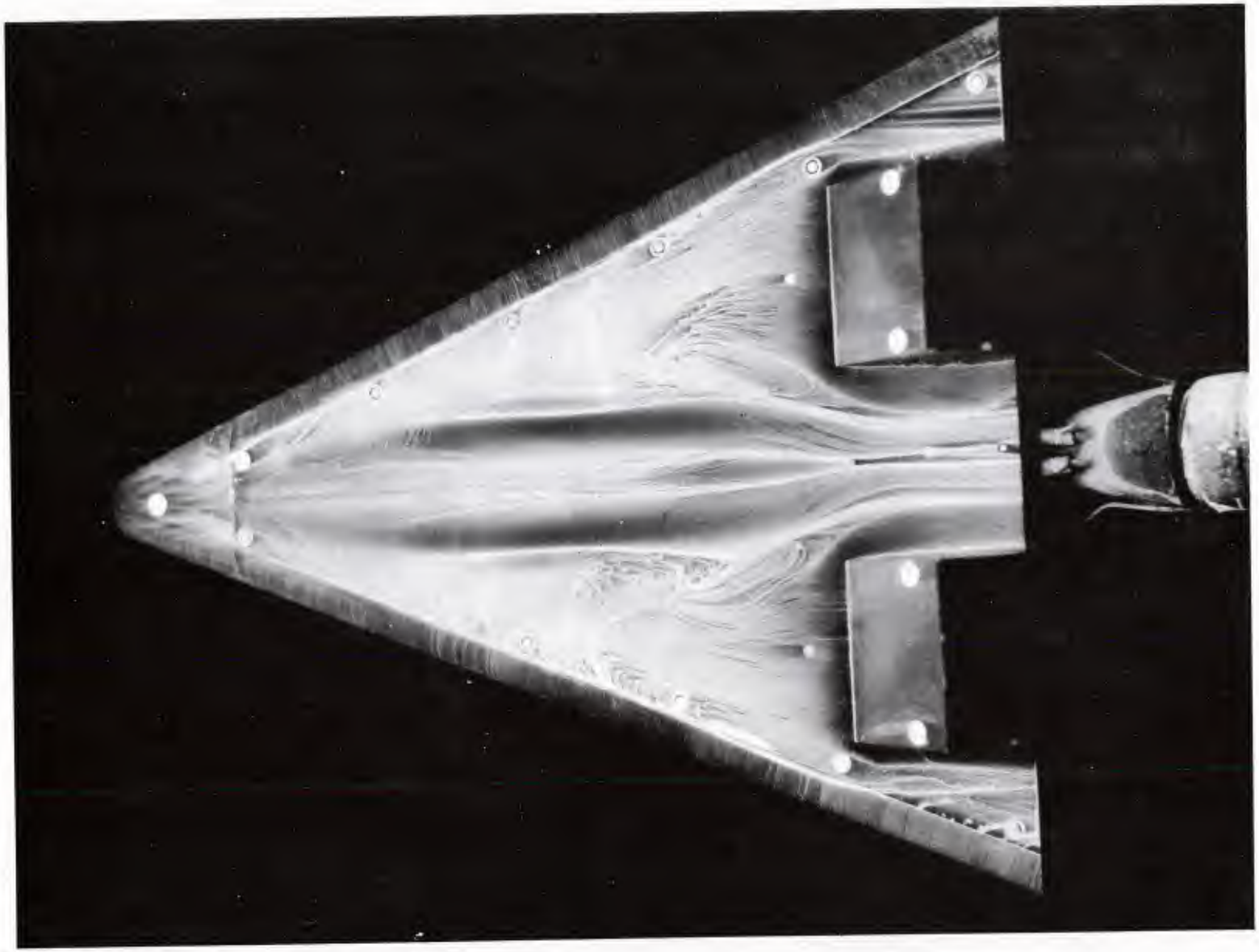

Fig. 12 Oil Film Photograph of Lower Surface; $\alpha = 0$, Bottom Flaps Deflected 40°

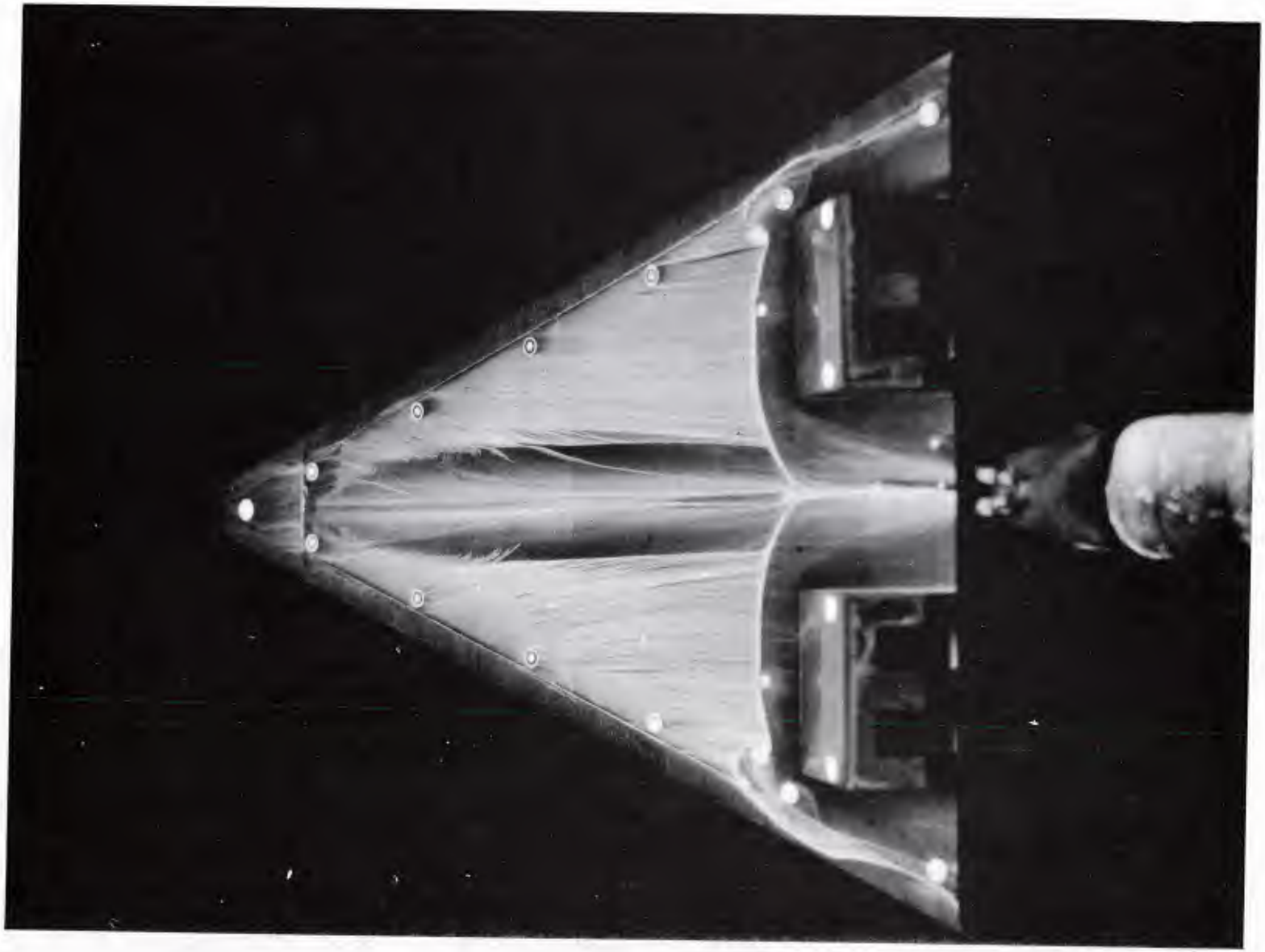

Fig. 13 Oil Film Photograph of Lower Surface; $\alpha = +14.3^{\circ}$, Bottom Flaps Deflected 40°

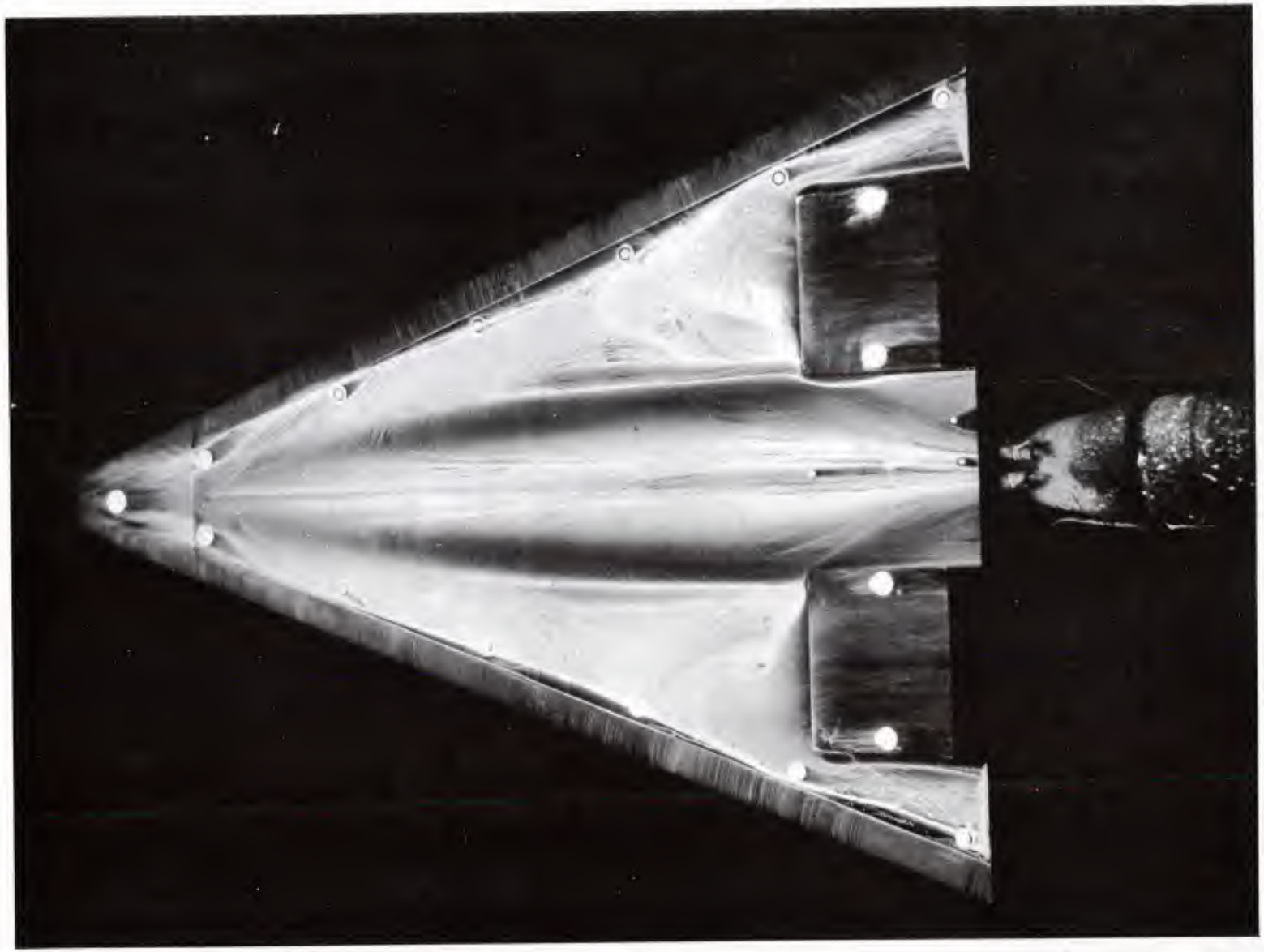

Fig. 14 Oil Film Photograph of Lower Surface; $\alpha = 0$, Bottom Flaps Deflected 20°

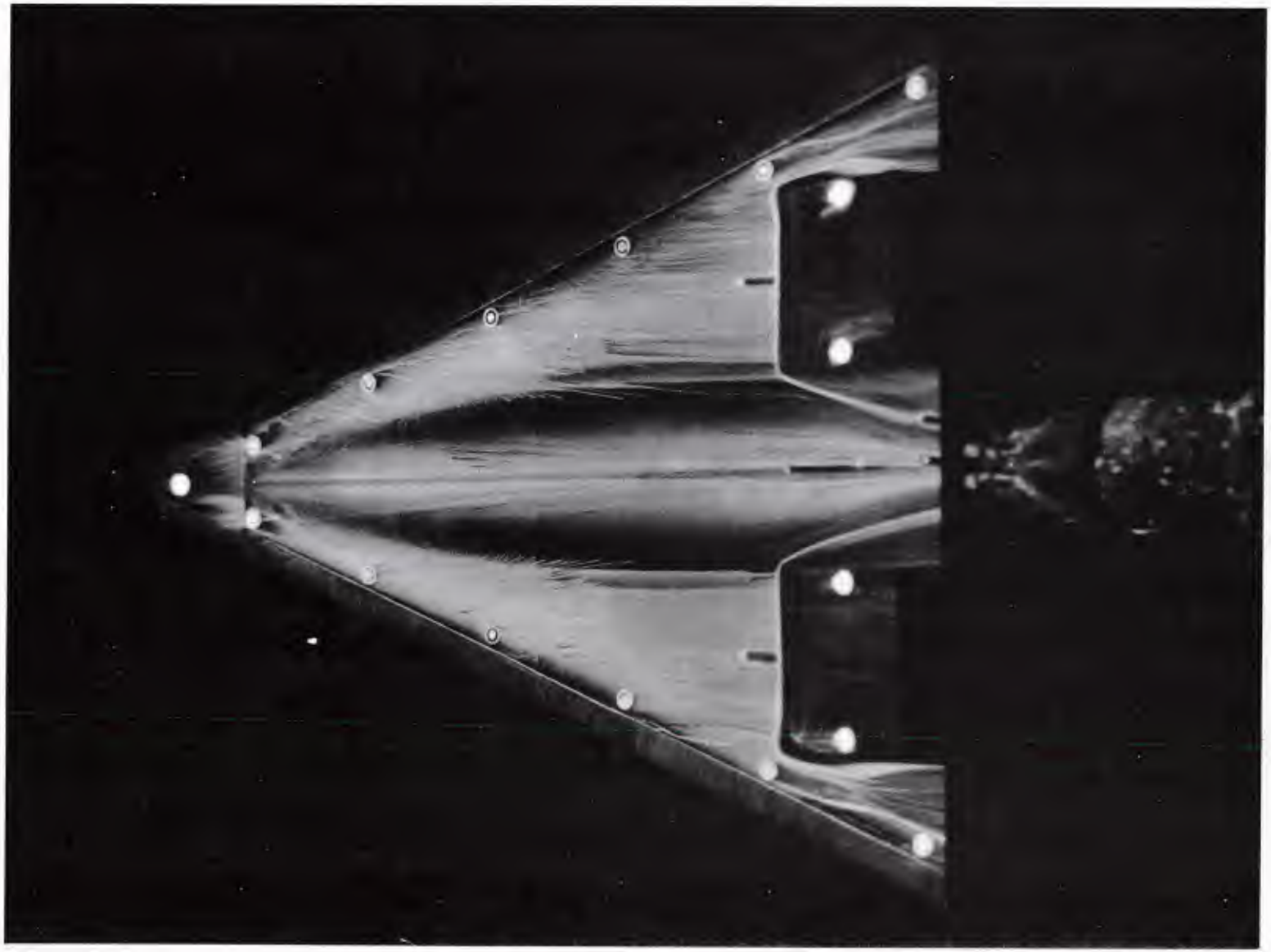

Fig. 15 Oil Film Photograph of Lower Surface; $\alpha = +12^{o}$, Bottom Flaps Deflected 20°

820
A E D C

Fig. 17 Schlieren Flow Photograph; $\alpha = +7^{\circ}$, No Flap Deflections

822
A E D C

Fig. 19 Schlieren Flow Photograph; $\alpha = +14.3^{\circ}$, Upper Left Flap Deflected 40°

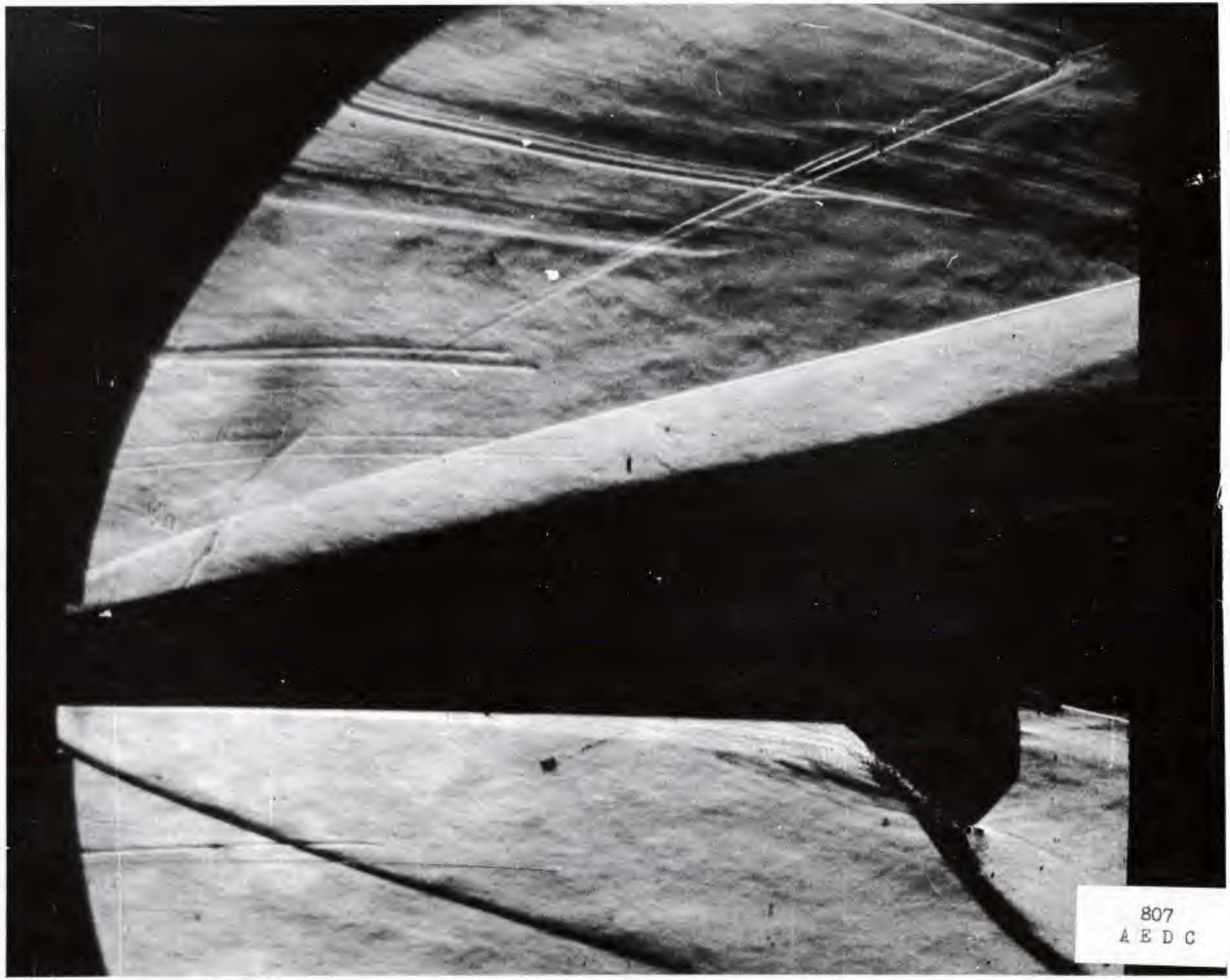

Fig. 20 Schlieren Flow Photograph: $\alpha = 0$, Bottom Flaps Deflected 40°

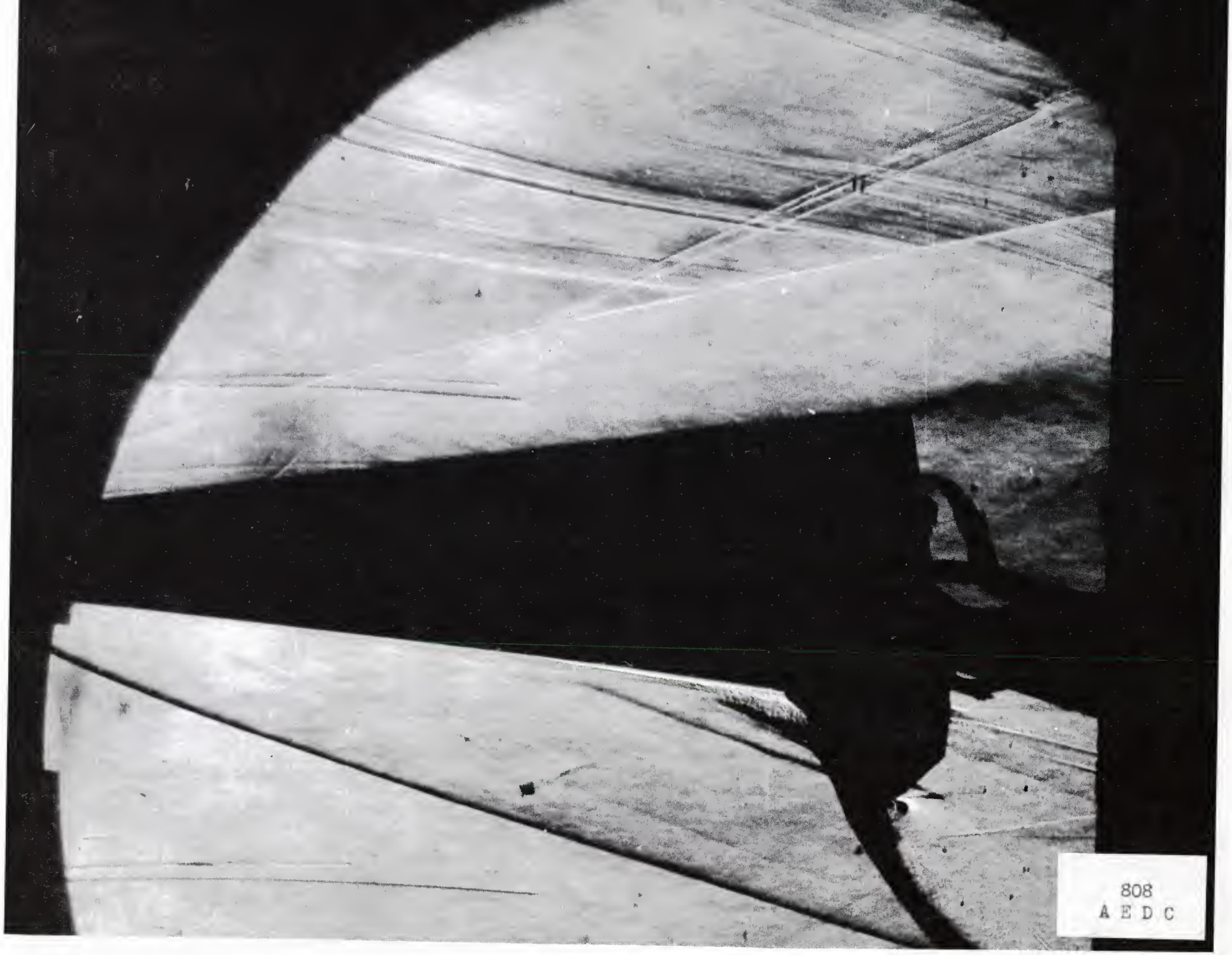

Fig. 21 Schlieren Flow Photograph; $\alpha = +5^{\circ}$, Bottom Flaps Deflected 40°

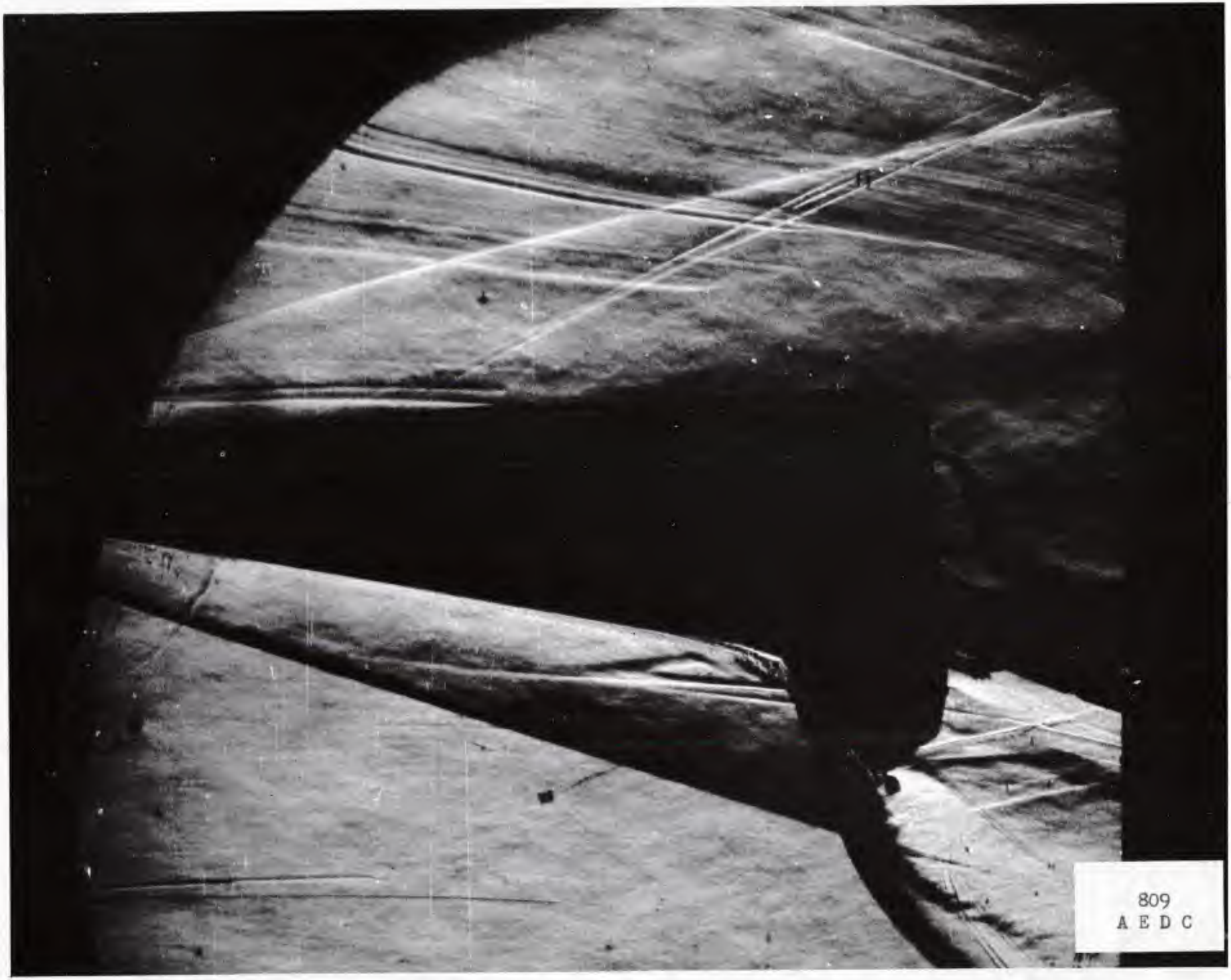

Fig. 22. Sublimer Flow Photograph; $\alpha = +10^{\circ}$, Bottom Flaps Deflected 40°

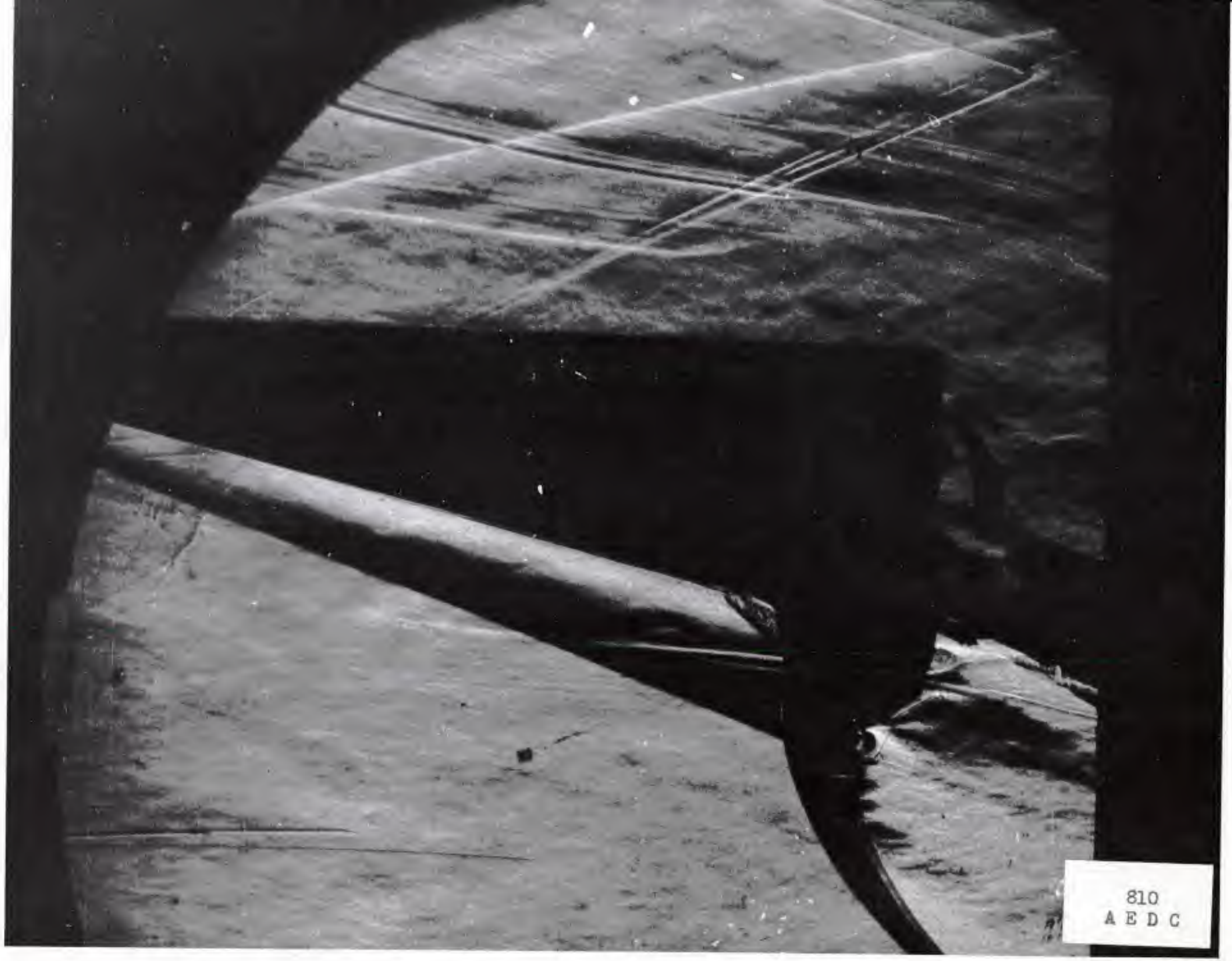

Fig. 23 Schlieren Flow Photograph; $\alpha = +14.3^{\circ}$, Bottom Flaps Deflected 40°

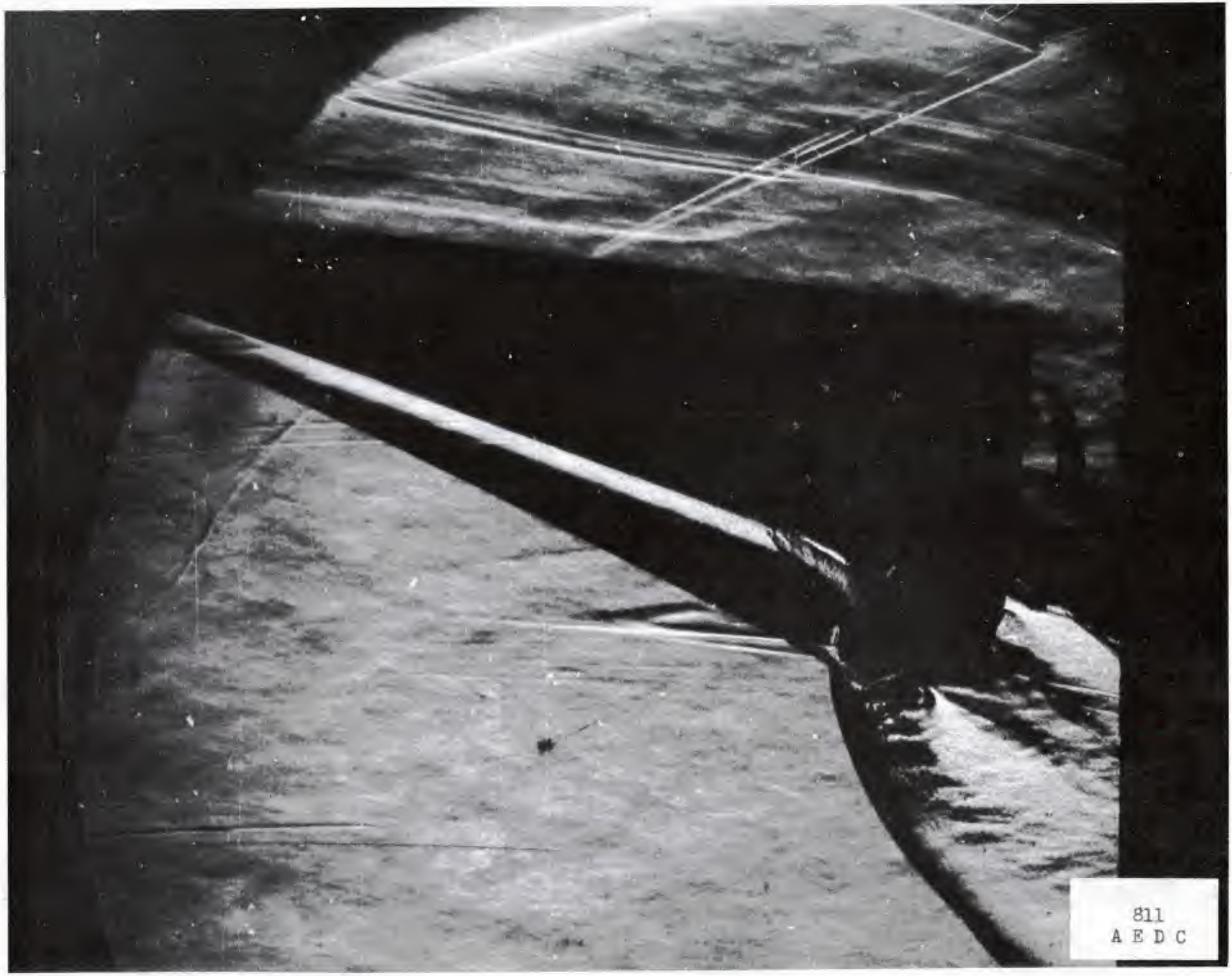

Fig. 24. Schlieren Flow Photograph: $\alpha = +20^{\circ}$, Bottom Flaps Deflected 40°

Fig. 25 Schlieren Flow Photograph; $\alpha = +25^{\circ}$, Bottom Flaps Deflected 40°

Fig. 26 Schlieren Flow Photograph: $\alpha = +30^{\circ}$, Bottom Flaps Deflected 40°

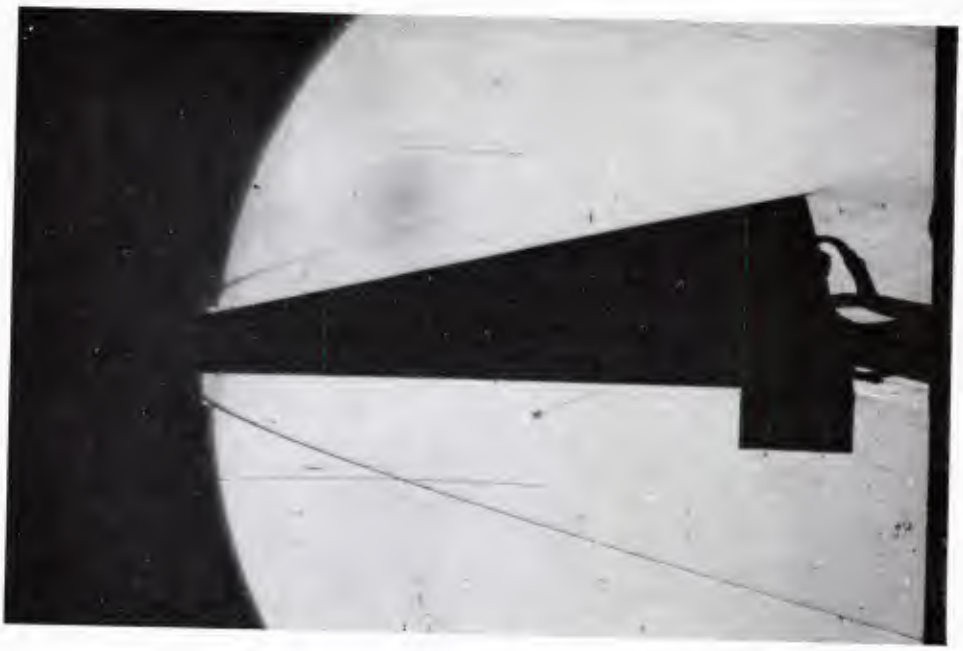

a) $\alpha = 0$

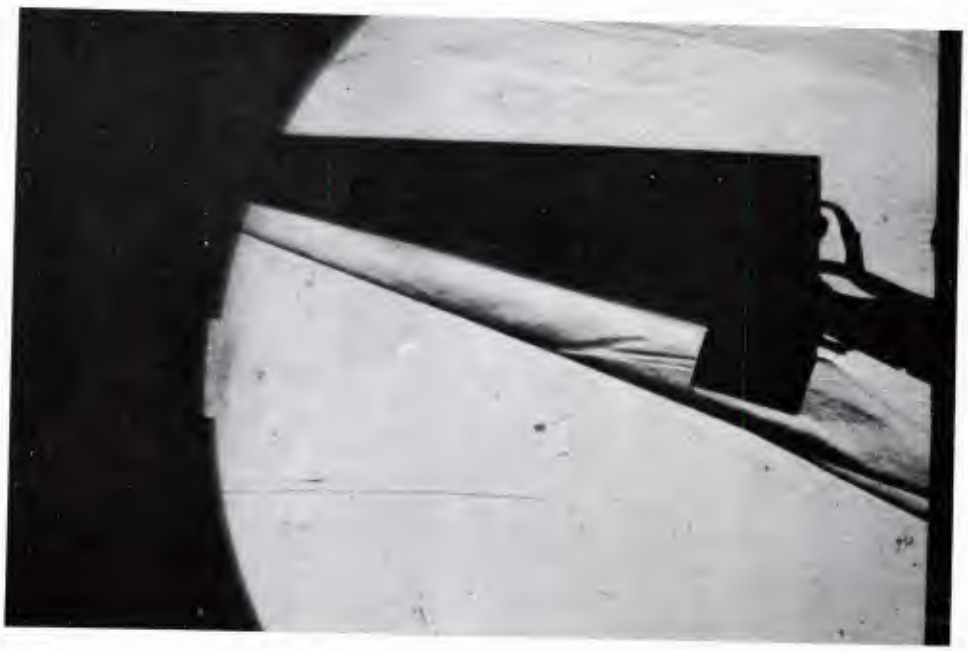

b) $\alpha = 14.3^{o}$

Fig. 27 Schlieren Flow Photographs; Ventral Fin on Lower Surface, No Flap or Fin Deflections

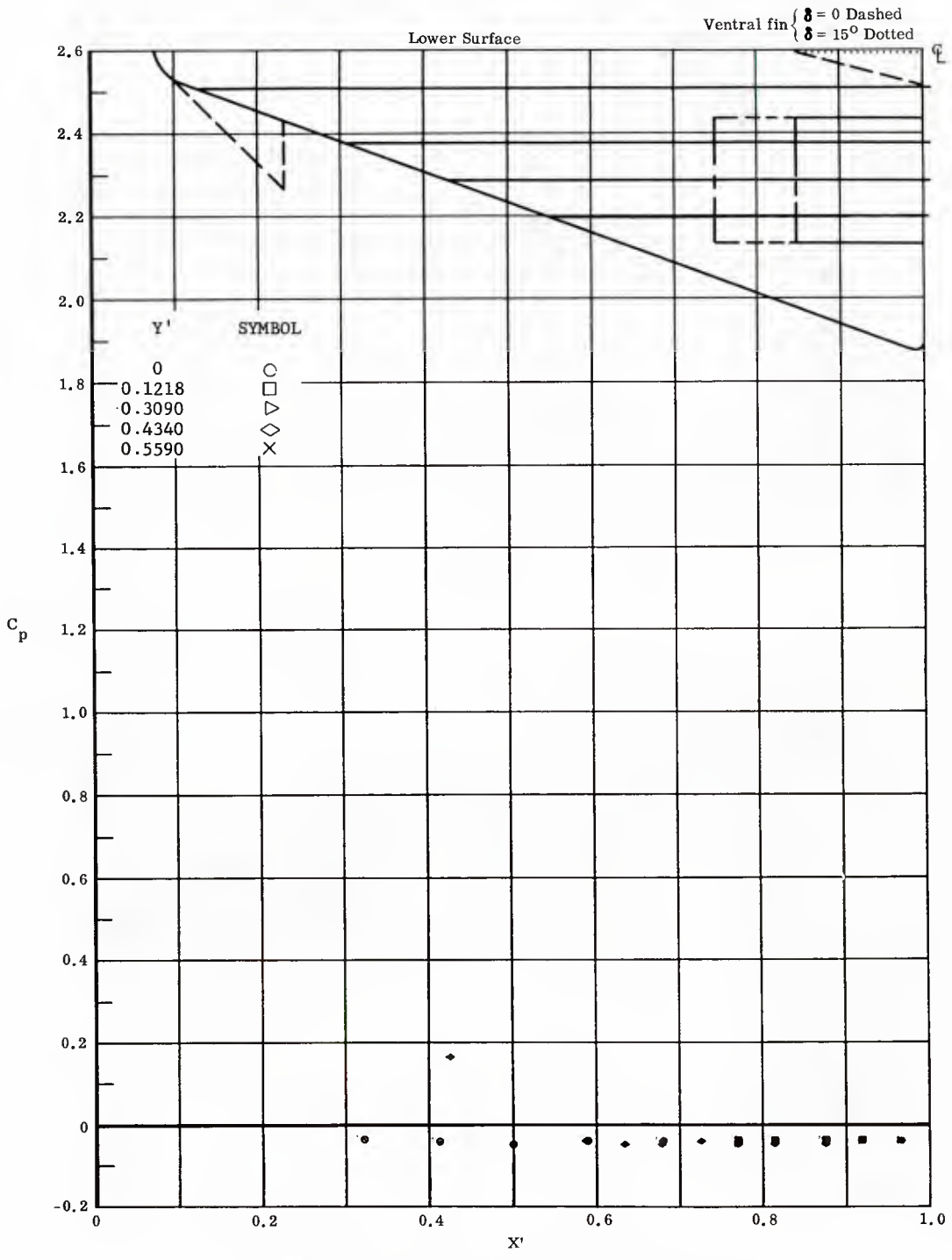

Fig. 28 Streamwise Distributions of Pressure Coefficients on Lower Surface
Basic Configuration, No Flap Deflections, $\alpha = -30°$, $\beta = 0$

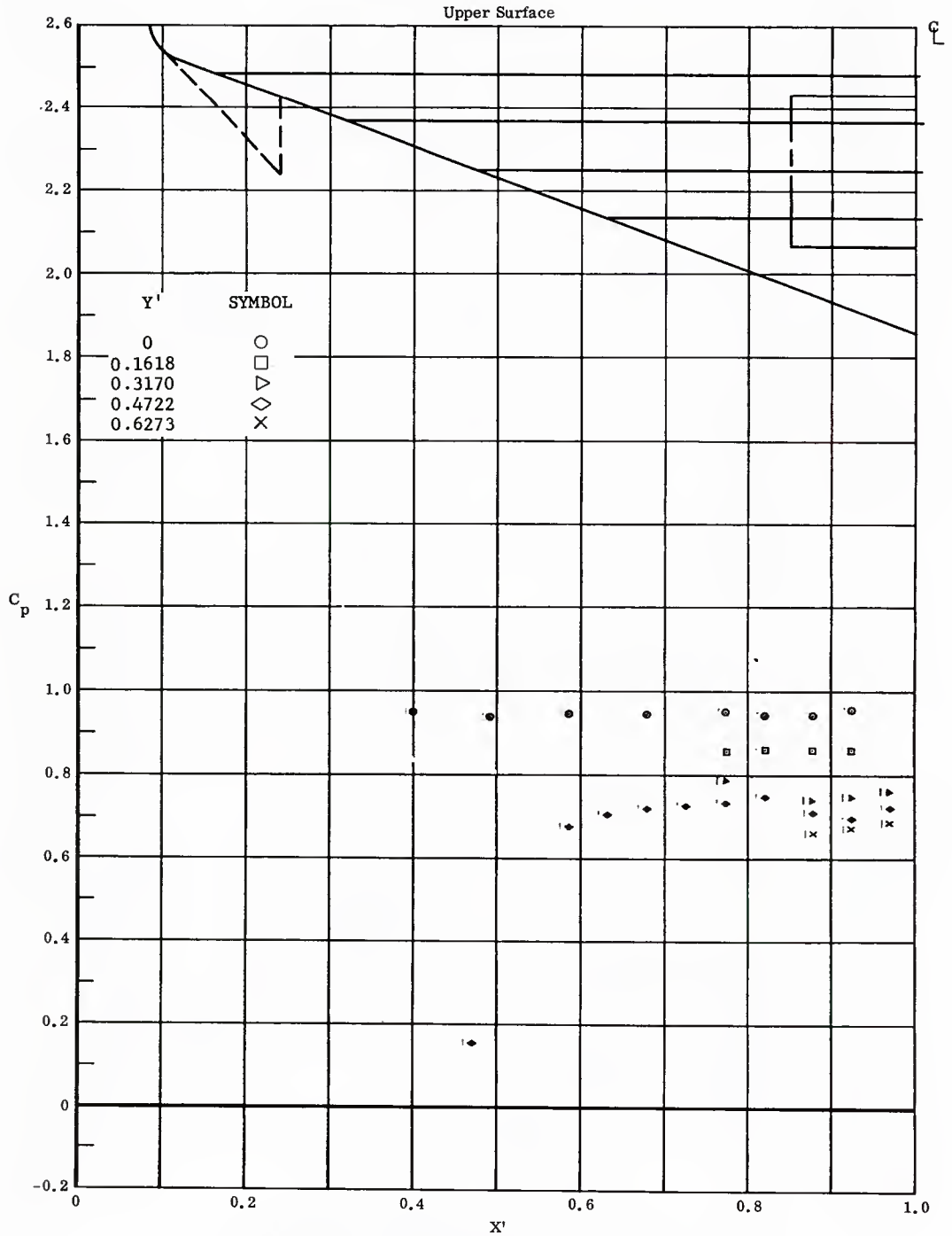

Fig. 28 Streamwise Distributions of Pressure Coefficients on Upper Surface Basic Configuration, No Flap Deflections, $\alpha = -30^\circ$, $\beta = 0$

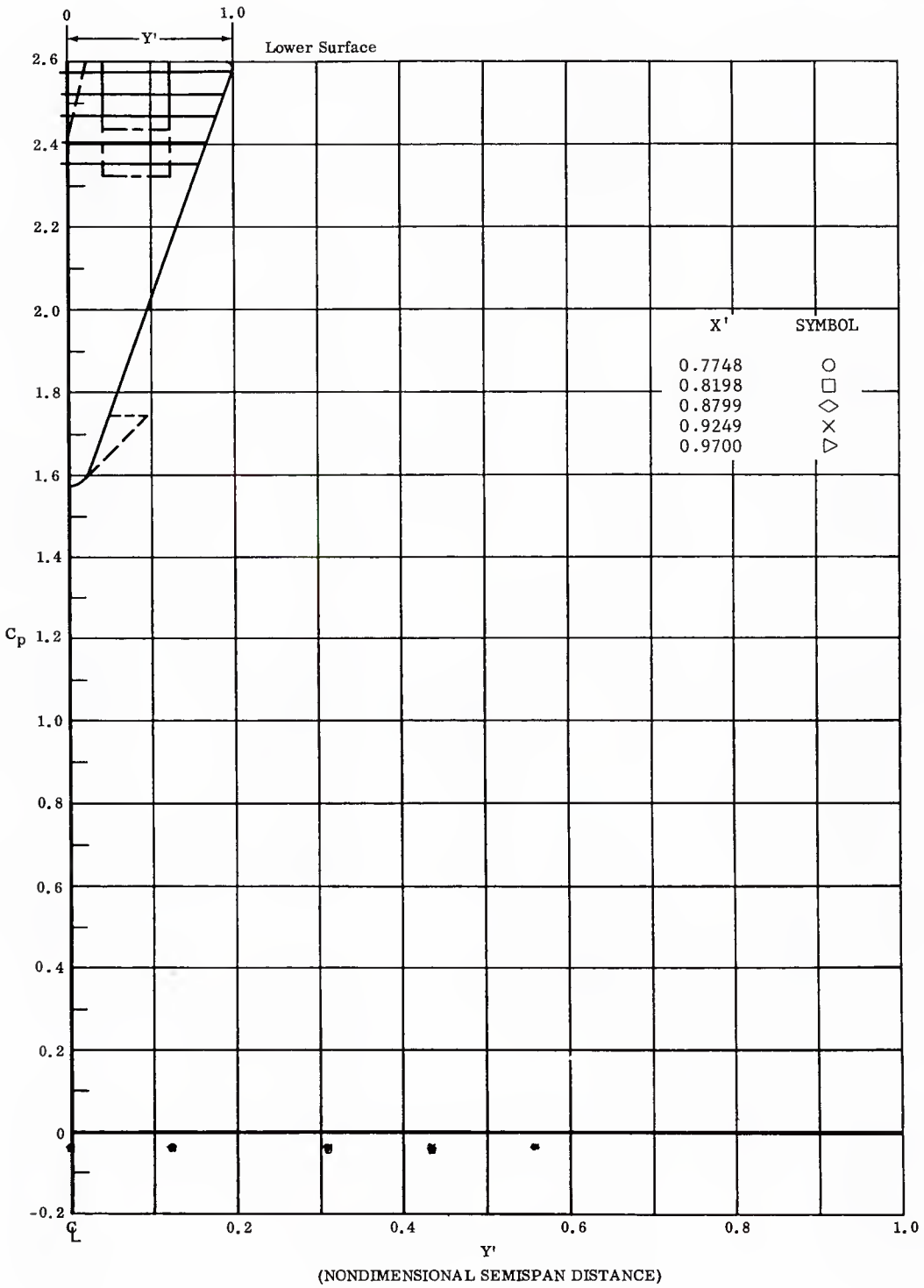

Fig. 28 Spanwise Distributions of Pressure Coefficients on Lower Surface Basic Configuration, No Flap Deflections, $\alpha = -30°$, $\beta = 0$

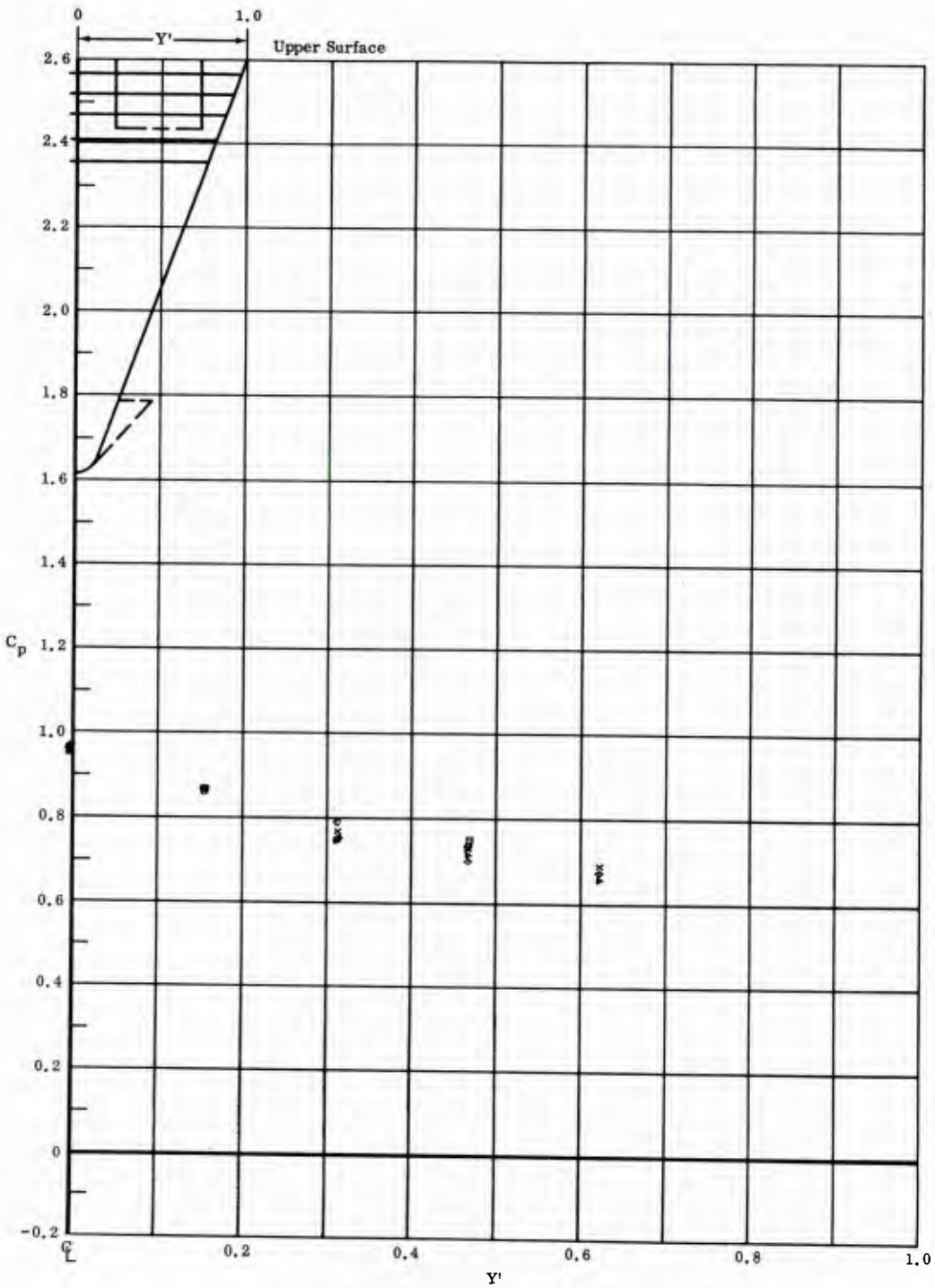

Fig. 28 Spanwise Distributions of Pressure Coefficients on Upper Surface
Basic Configuration, No Flap Deflections, α = -30°, β = 0

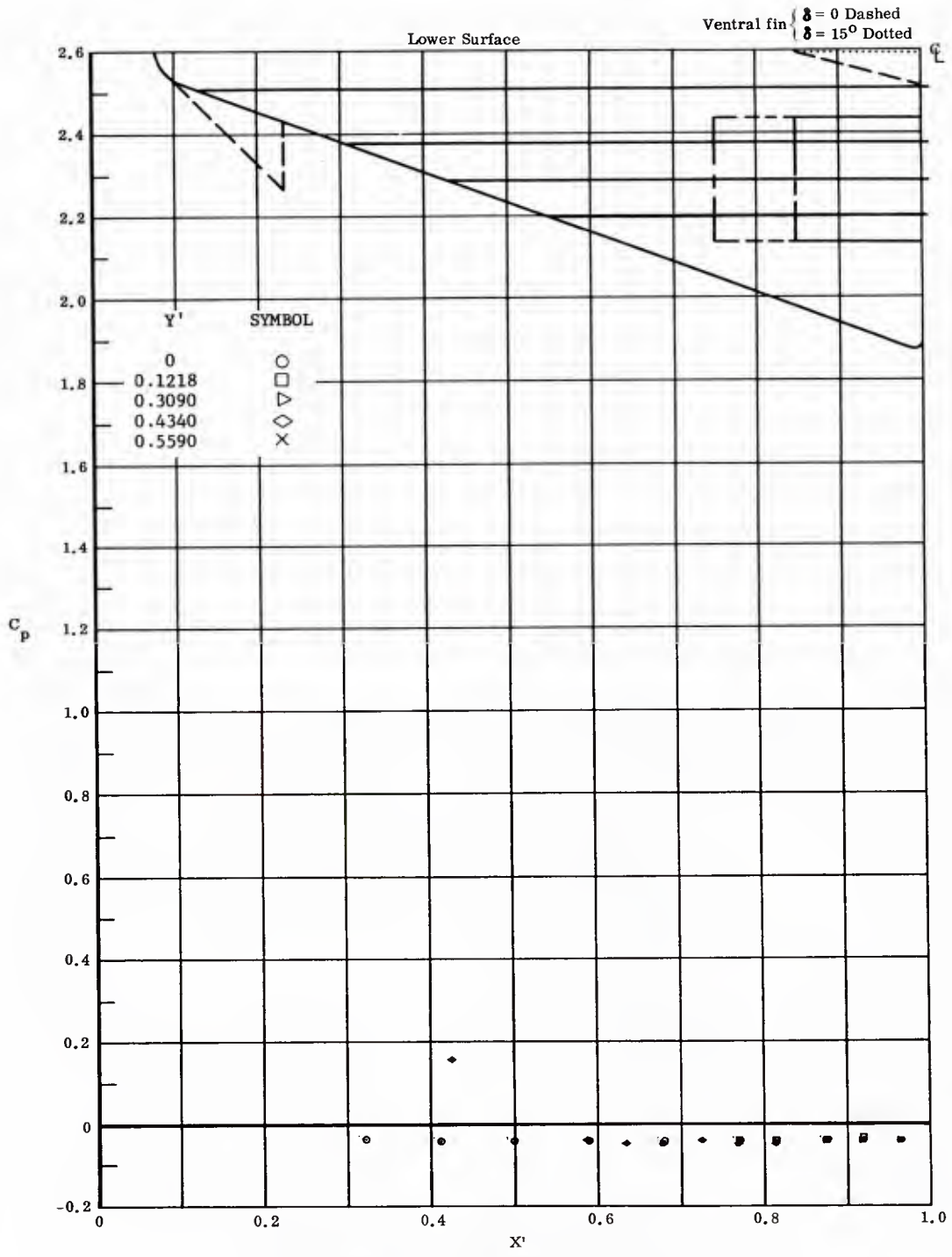

Fig. 29 Streamwise Distributions of Pressure Coefficients on Lower Surface Basic Configuration, Bottom Flaps Deflected 20°, α = -30°, β = 0

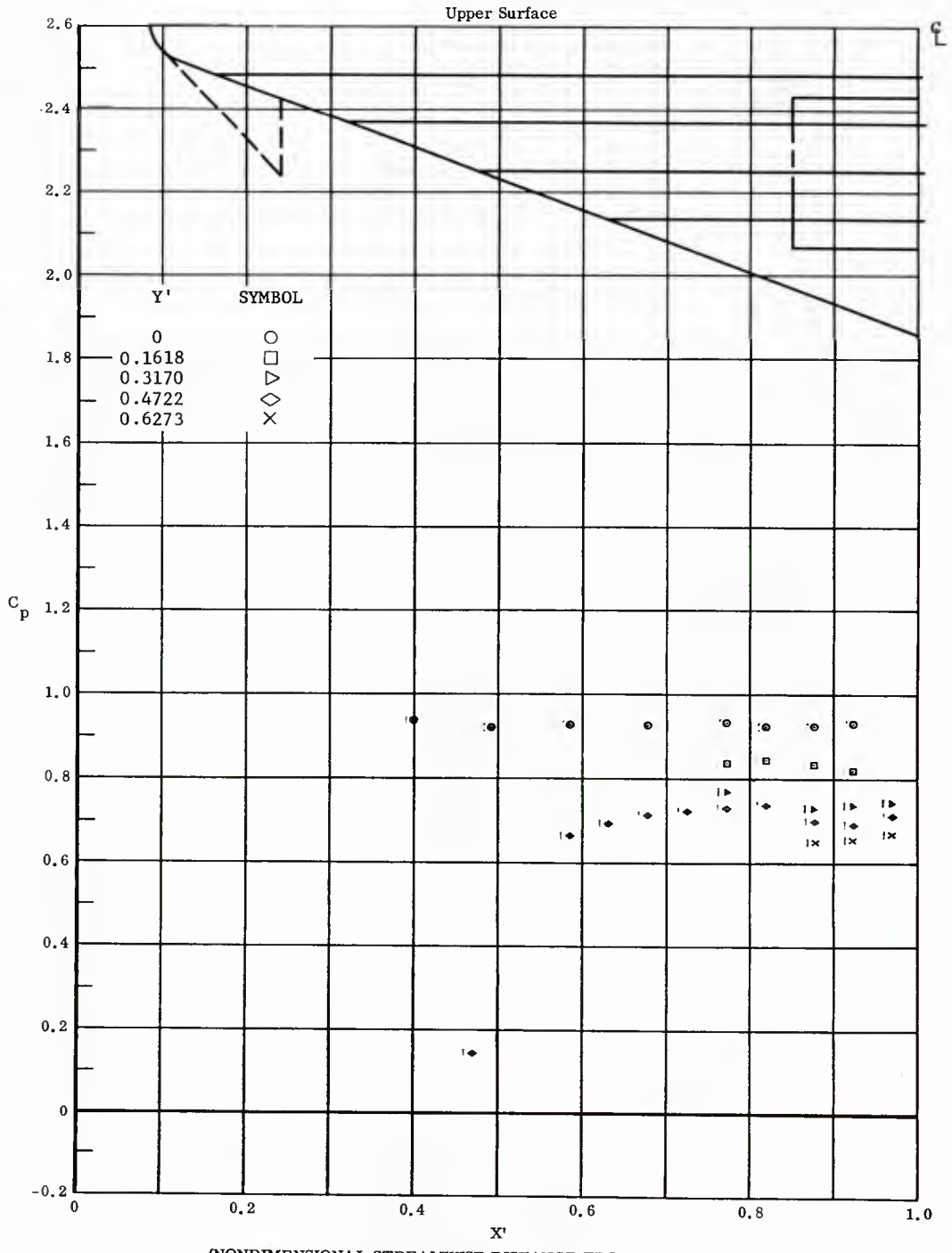

Fig. 29 Streamwise Distributions of Pressure Coefficients on Upper Surface Basic Configuration, Bottom Flaps Deflected 20°, α = -30°, β = 0

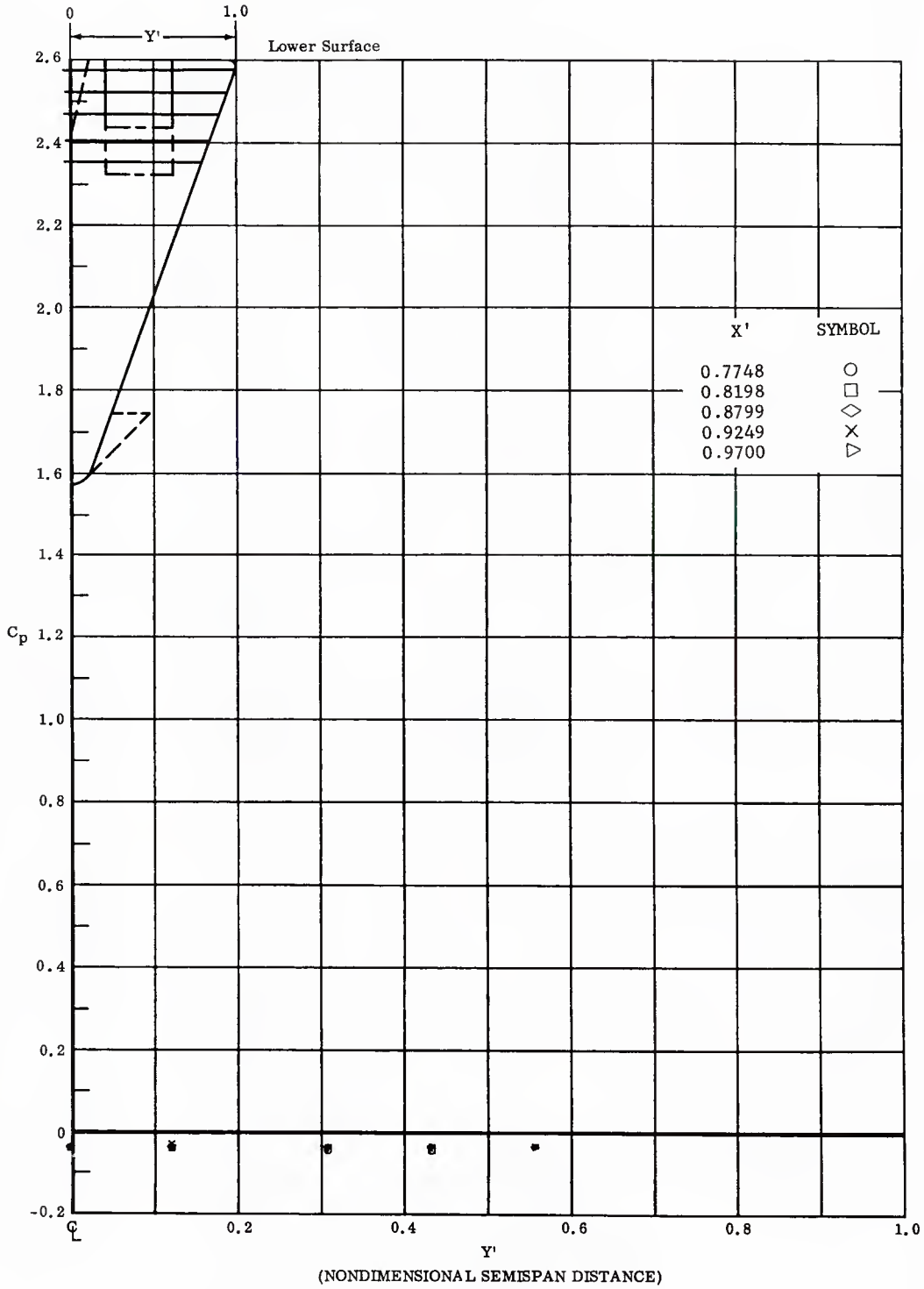

Fig. 29 Spanwise Distributions of Pressure Coefficients on Lower Surface Basic Configuration, Bottom Flaps Deflected 20°, α = -30°, β = 0

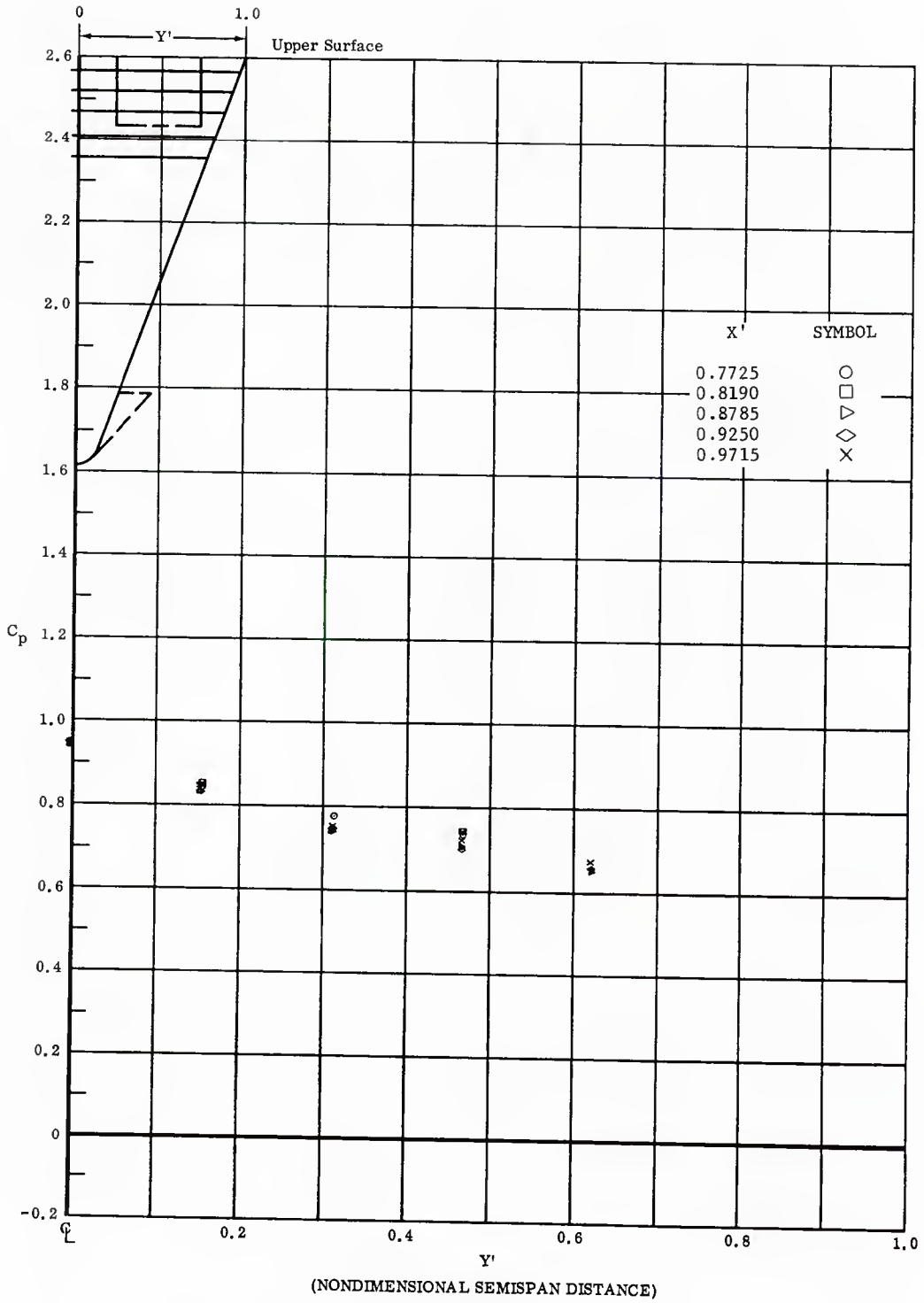

Fig. 29 Spanwise Distributions of Pressure Coefficients on Upper Surface Basic Configuration, Bottom Flaps Deflected 20°, α = -30°, β = 0

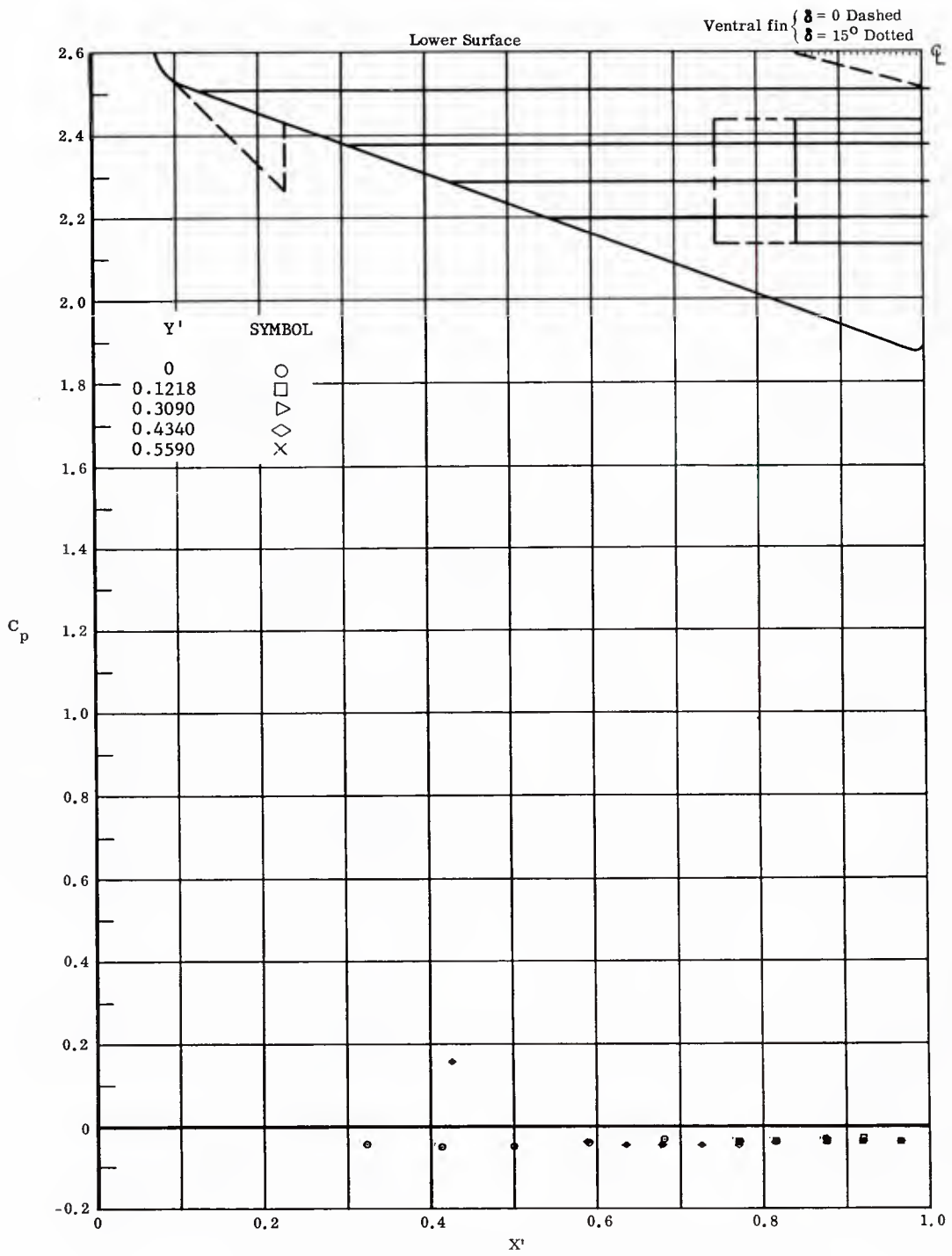

Fig. 30 Streamwise Distributions of Pressure Coefficients on Lower Surface Basic Configuration, Bottom Flaps Deflected 40°, α = -30°, β = 0

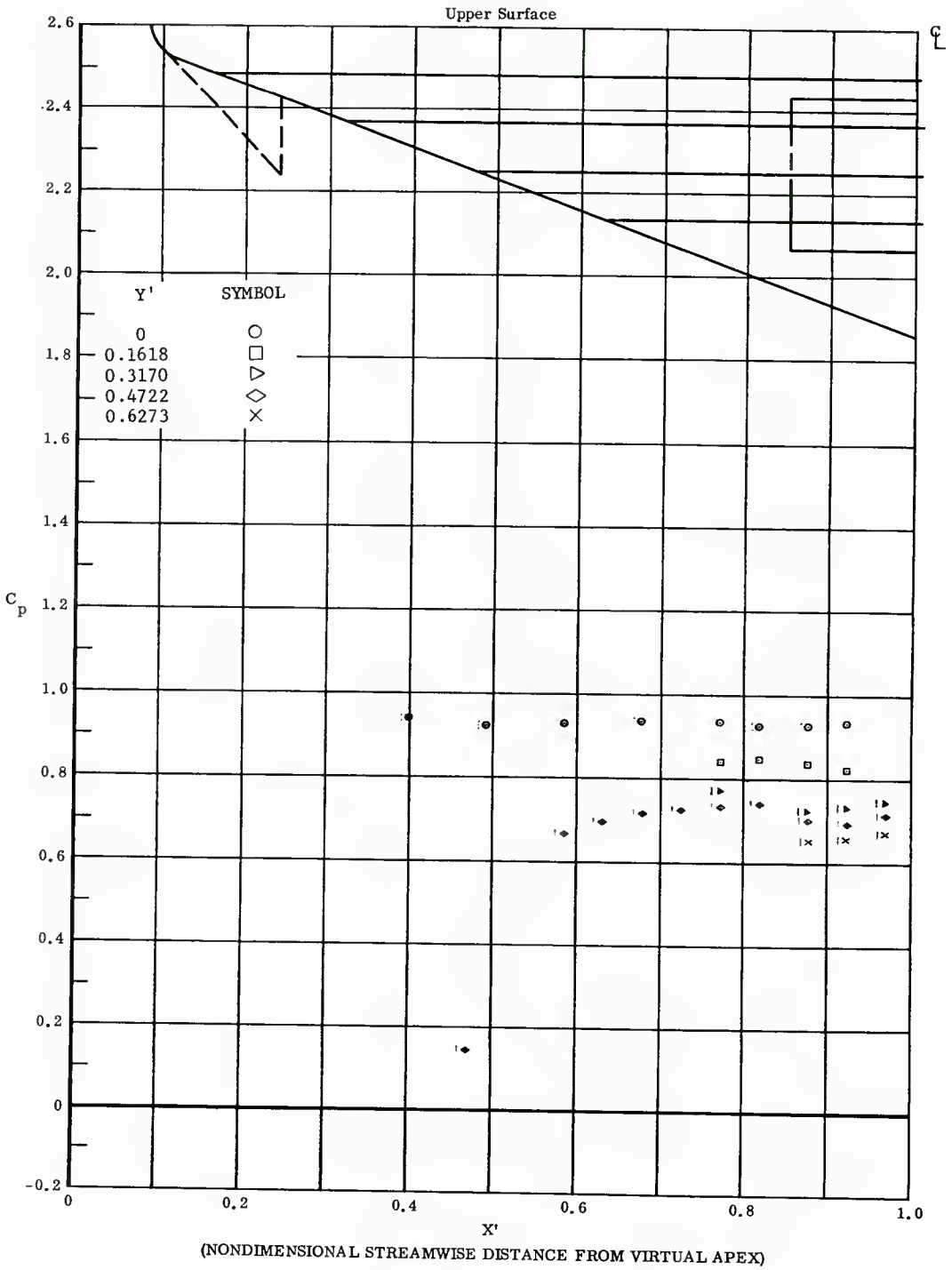

Fig. 30 Streamwise Distributions of Pressure Coefficients on Upper Surface Basic Configuration, Bottom Flaps Deflected 40°, α = -30°, β = 0

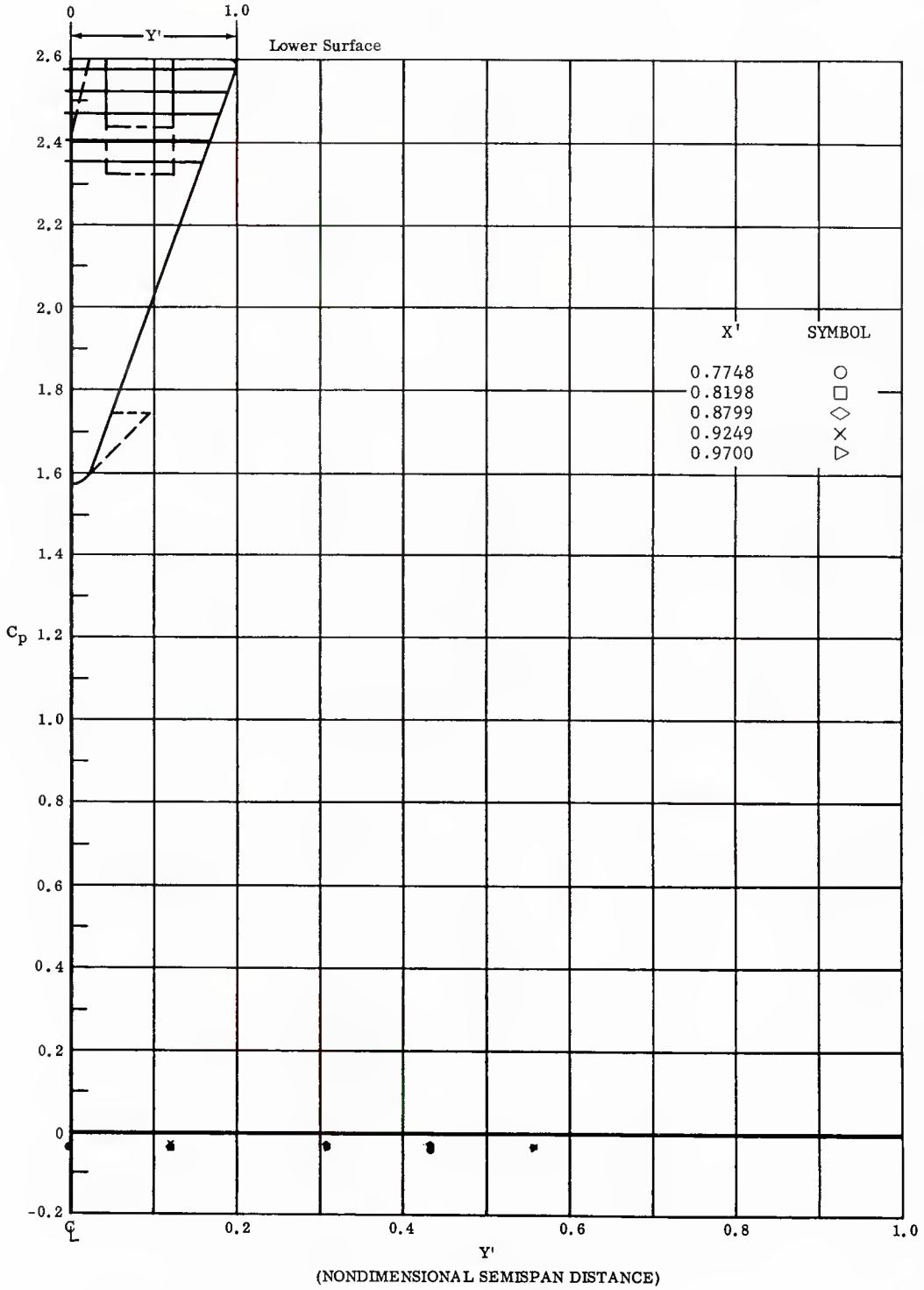

Fig. 30 Spanwise Distributions of Pressure Coefficients on Lower Surface
Basic Configuration, Bottom Flaps Deflected 40°, α = -30°, β = 0

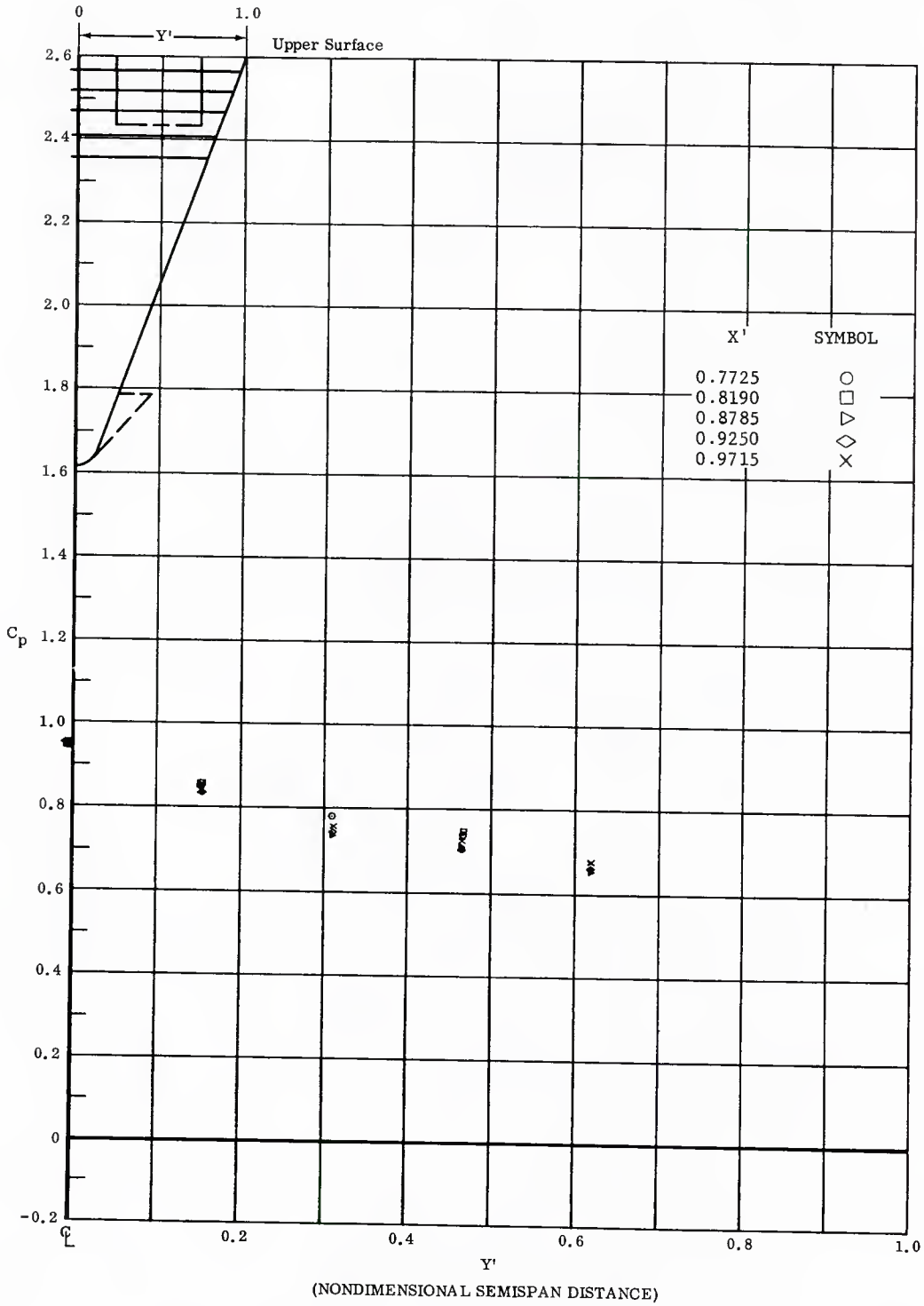

Fig. 30 Spanwise Distributions of Pressure Coefficients on Upper Surface Basic Configuration, Bottom Flaps Delfected 40°, $\alpha = -30°$, $\beta = 0$

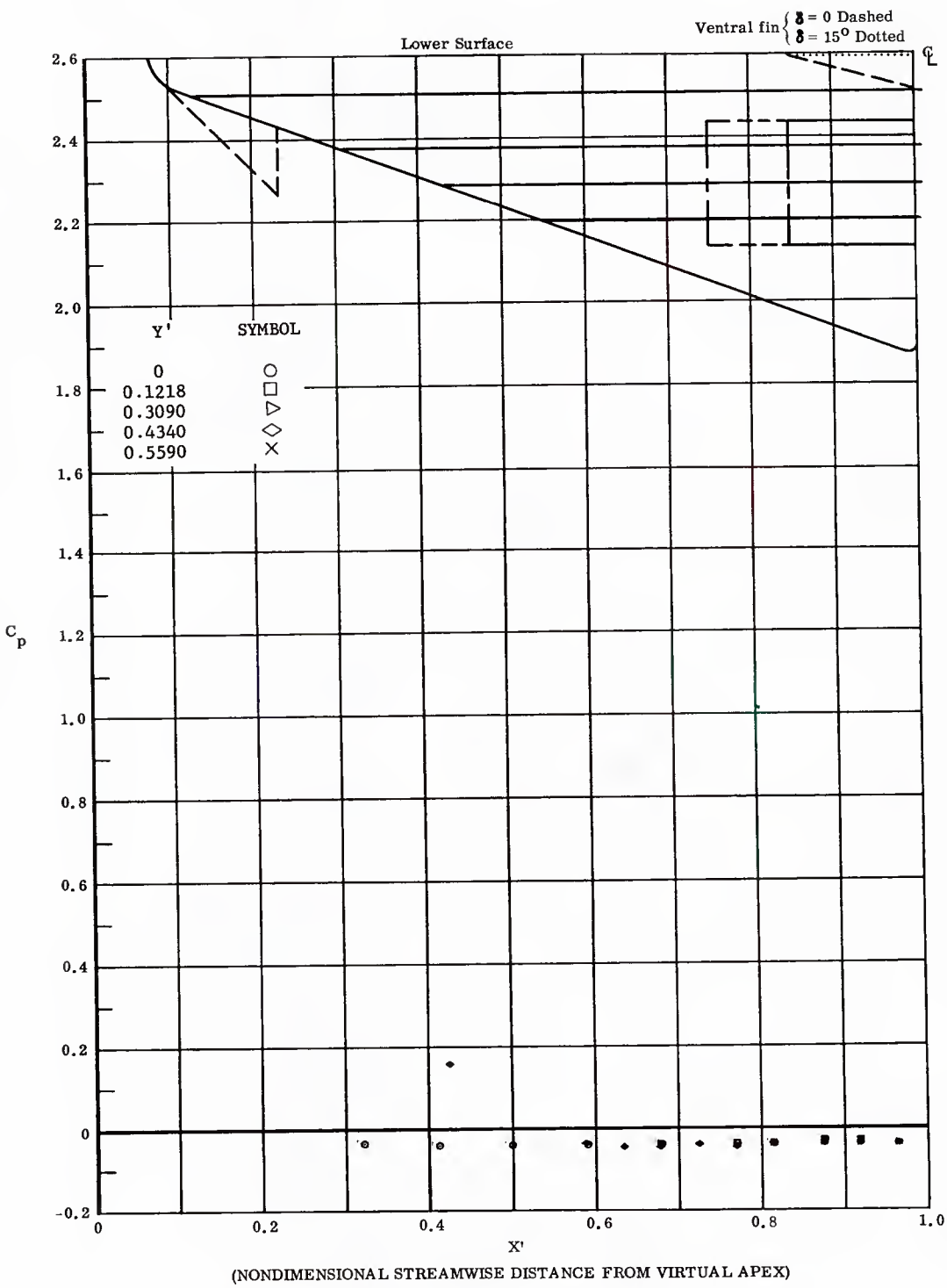

Fig. 31 Streamwise Distributions of Pressure Coefficients on Lower Surface
Extended (Long Chord) Flaps on Lower Surface,
Bottom Flaps Deflected 20°, α = -30°, β = 0

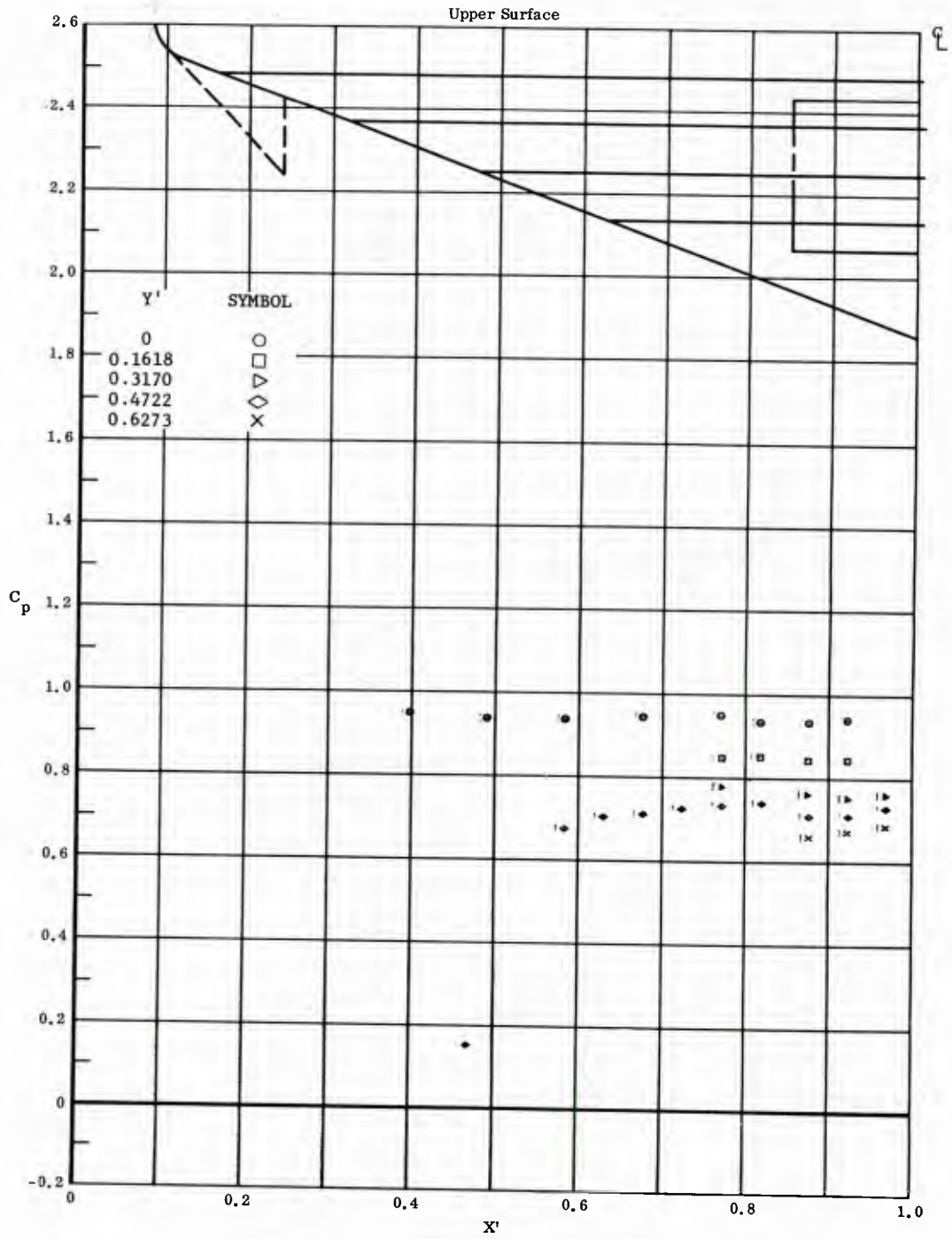

Fig. 31 Streamwise Distributions of Pressure Coefficients on Upper Surface Extended (Long Chord) Flaps on Lower Surface, Bottom Flaps Deflected 20°, $\alpha = -30°$, $\beta = 0$

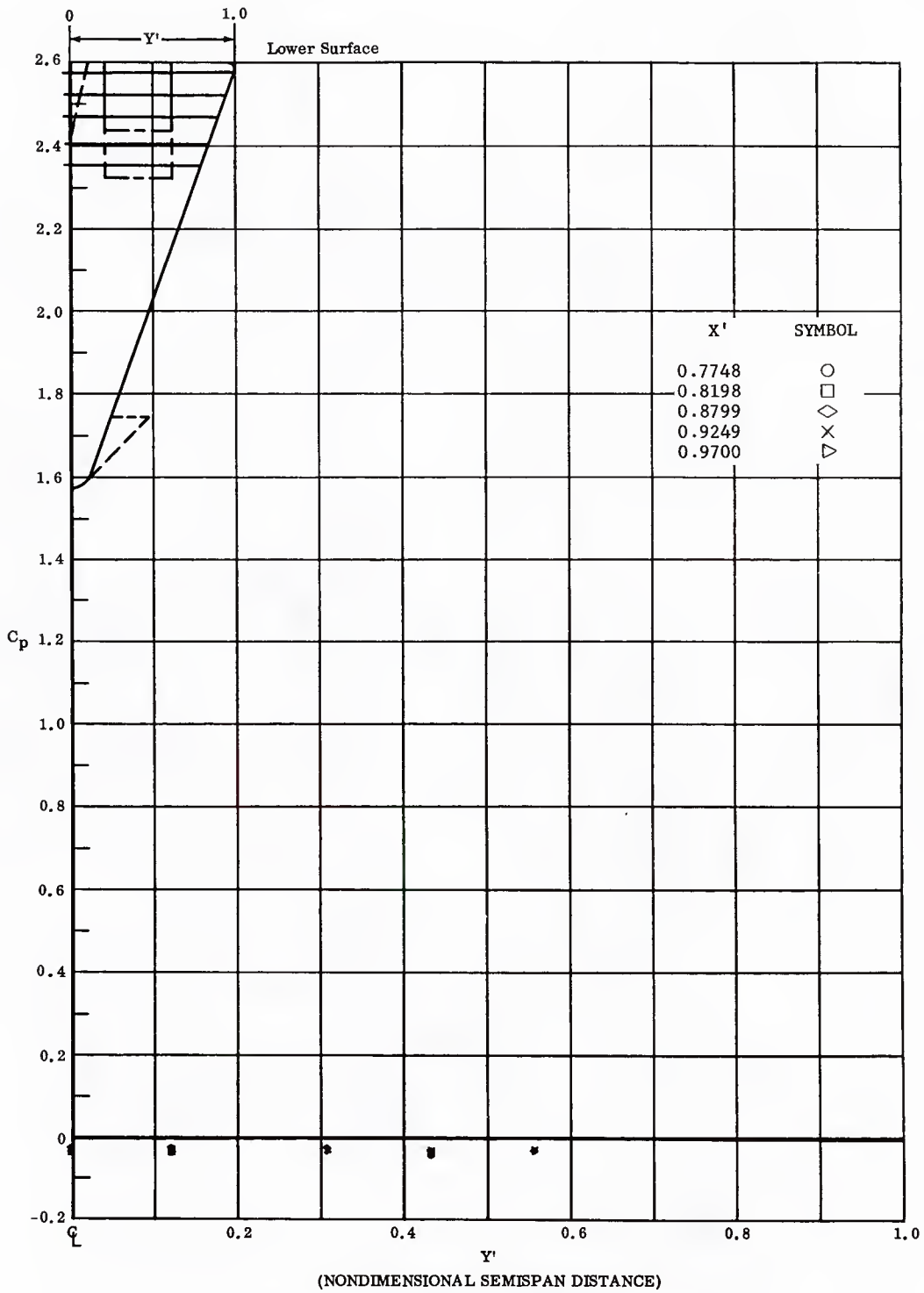

Fig. 31 Spanwise Distributions of Pressure Coefficients on Lower Surface Extended (Long Chord) Flaps on Lower Surface, Bottom Flaps Deflected 20°, α = -30°, β = 0

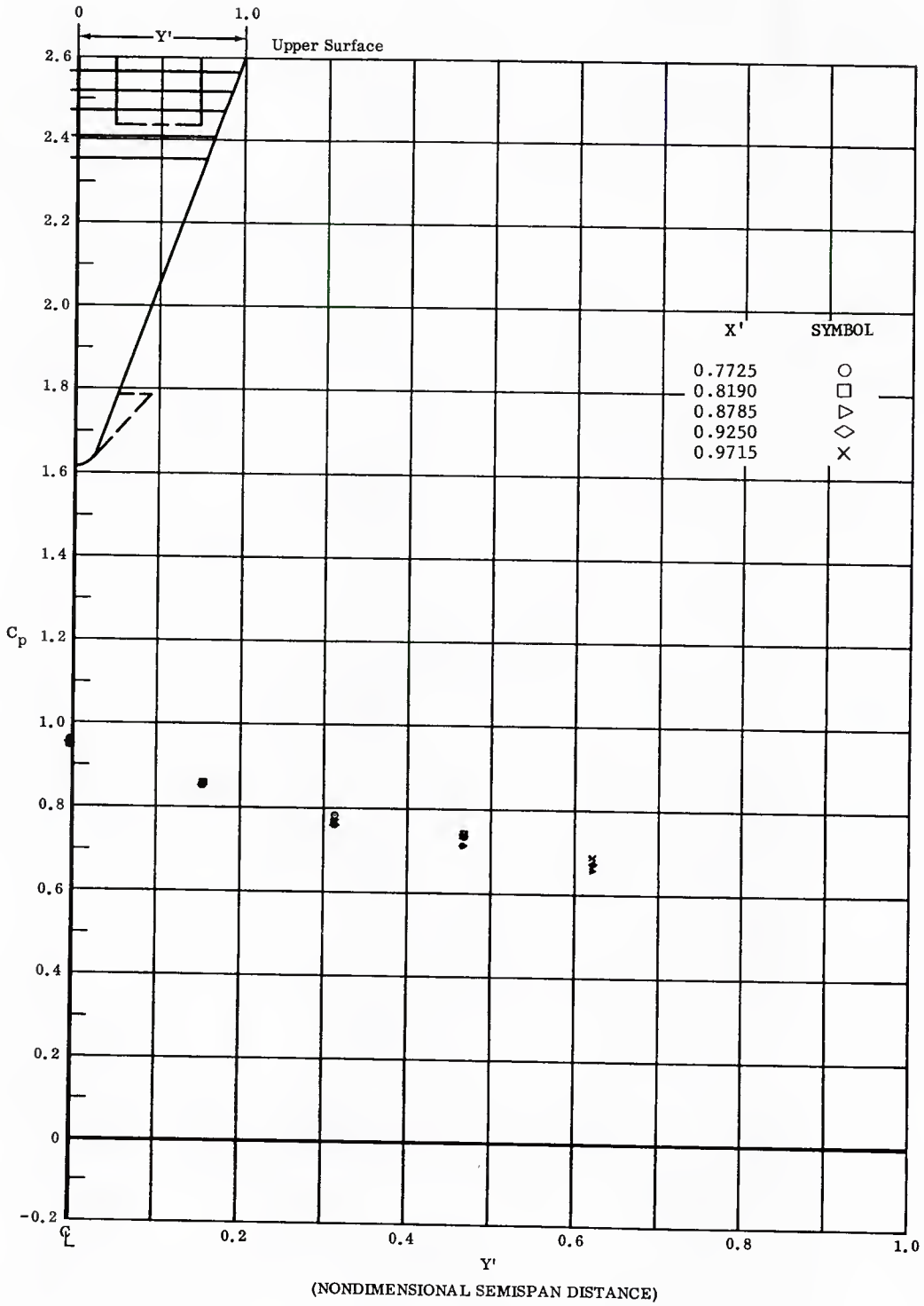

Fig. 31 Spanwise Distributions of Pressure Coefficients on Upper Surface Extended (Long Chord) Flaps on Lower Surface, Bottom Flaps Deflected 20°, α = -30°, β = 0

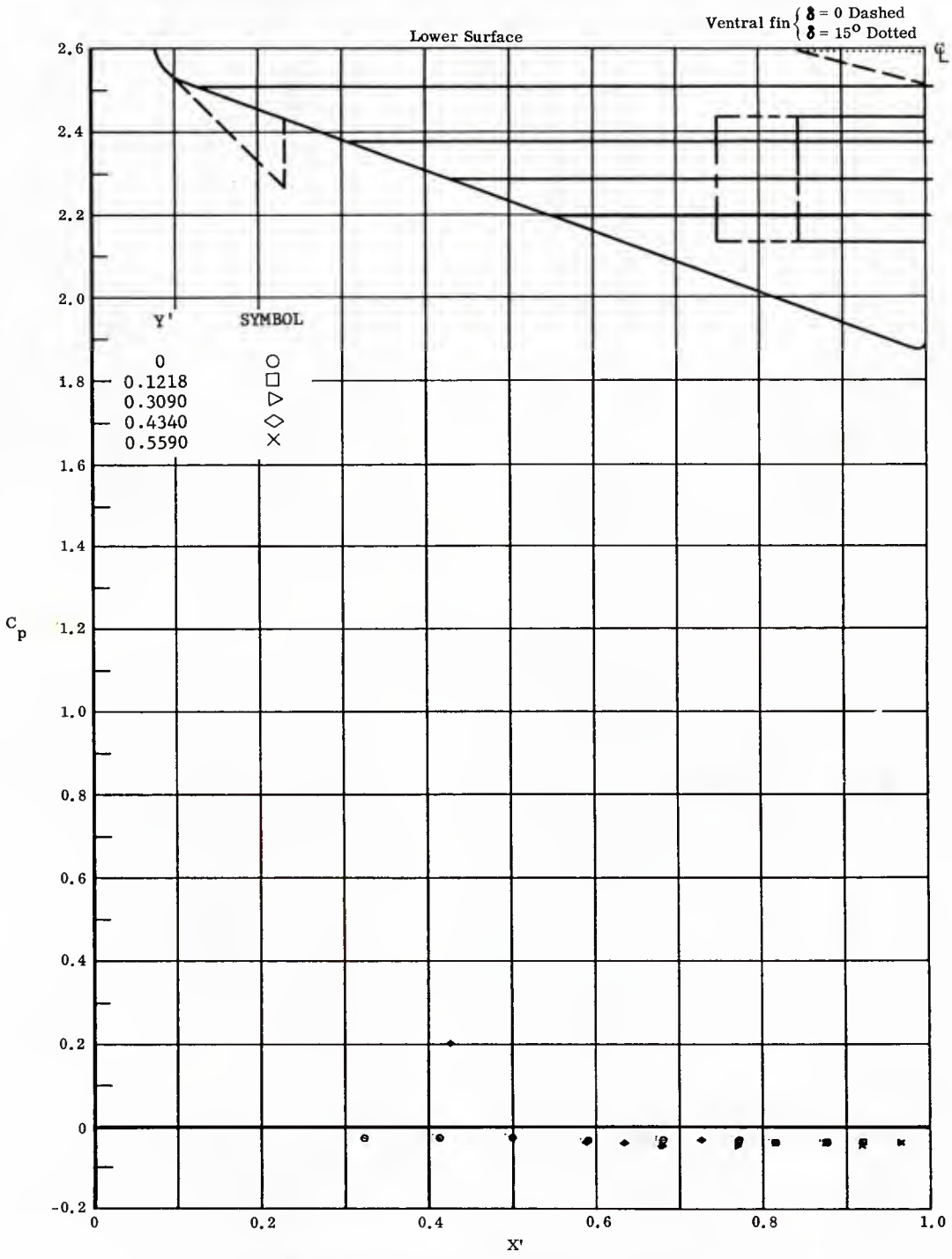

Fig. 32 Streamwise Distributions of Pressure Coefficients on Lower Surface
Basic Configuration, No Flap Deflections, $\alpha = -15°$, $\beta = 0$

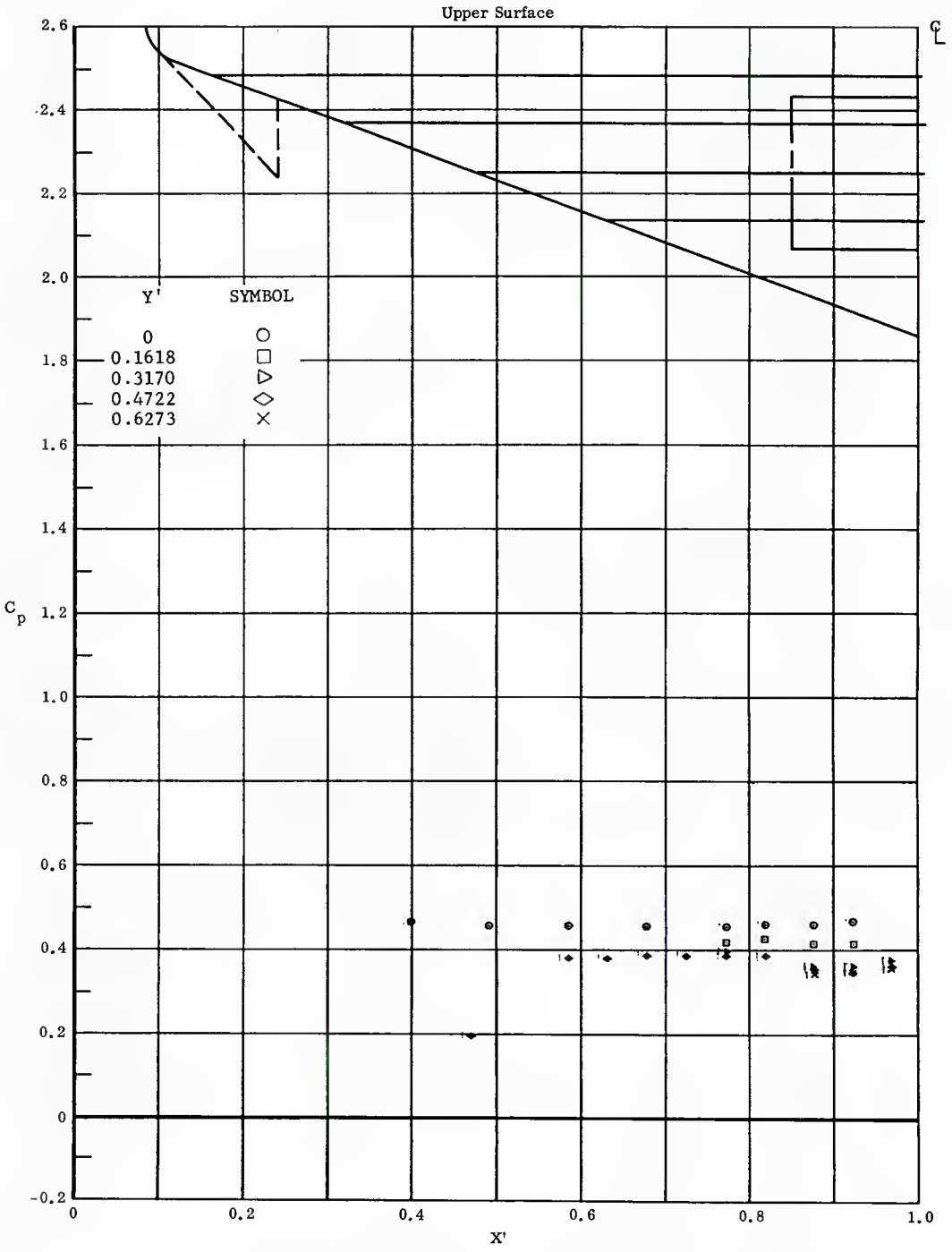

Fig. 32 Streamwise Distributions of Pressure Coefficients on Upper Surface
Basic Configuration, No Flap Deflections, $\alpha = -15°$, $\beta = 0$

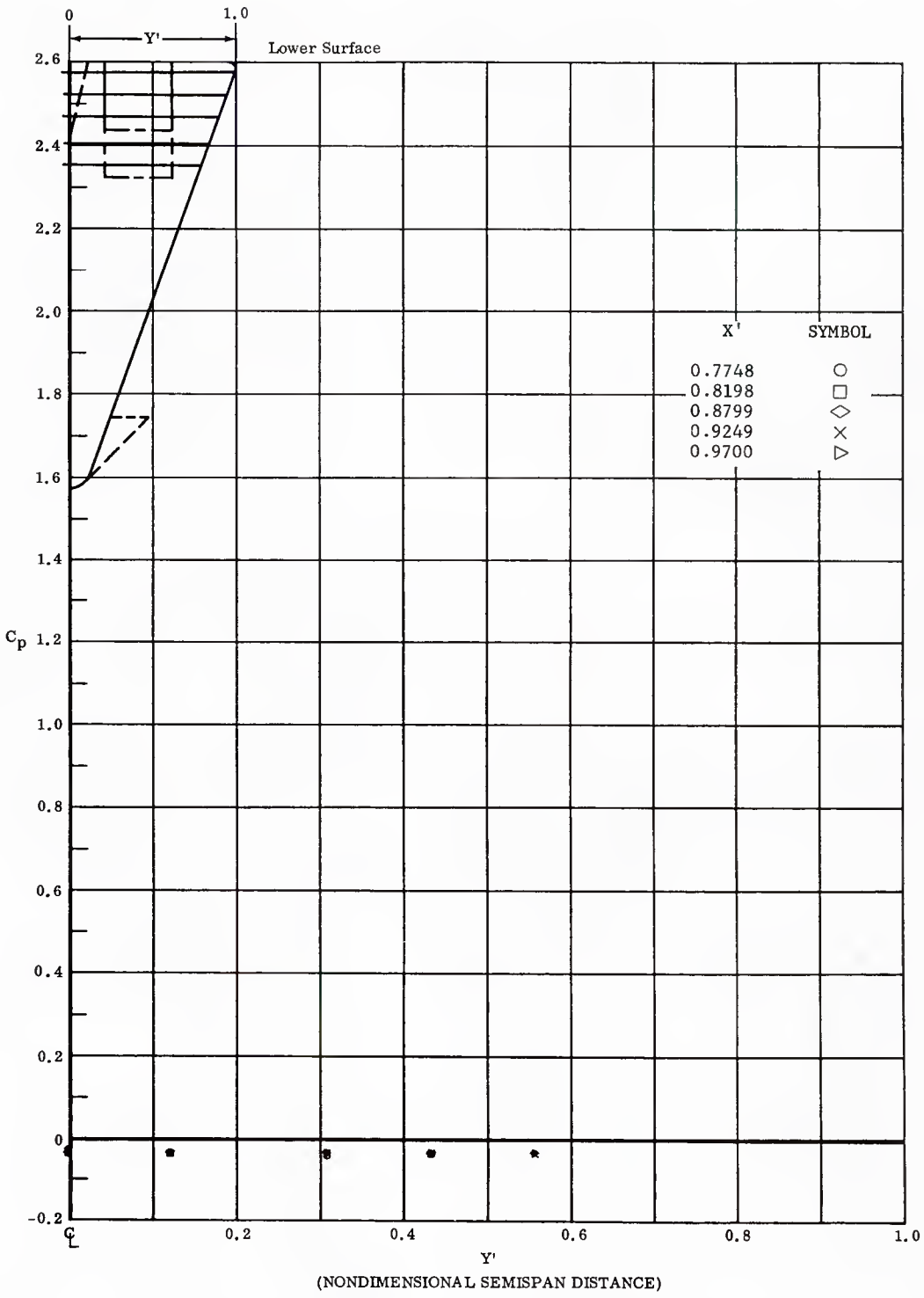

Fig. 32 Spanwise Distributions of Pressure Coefficients on Lower Surface Basic Configuration, No Flap Deflections, $\alpha = -1.5^{\circ}$, $\beta = 0$

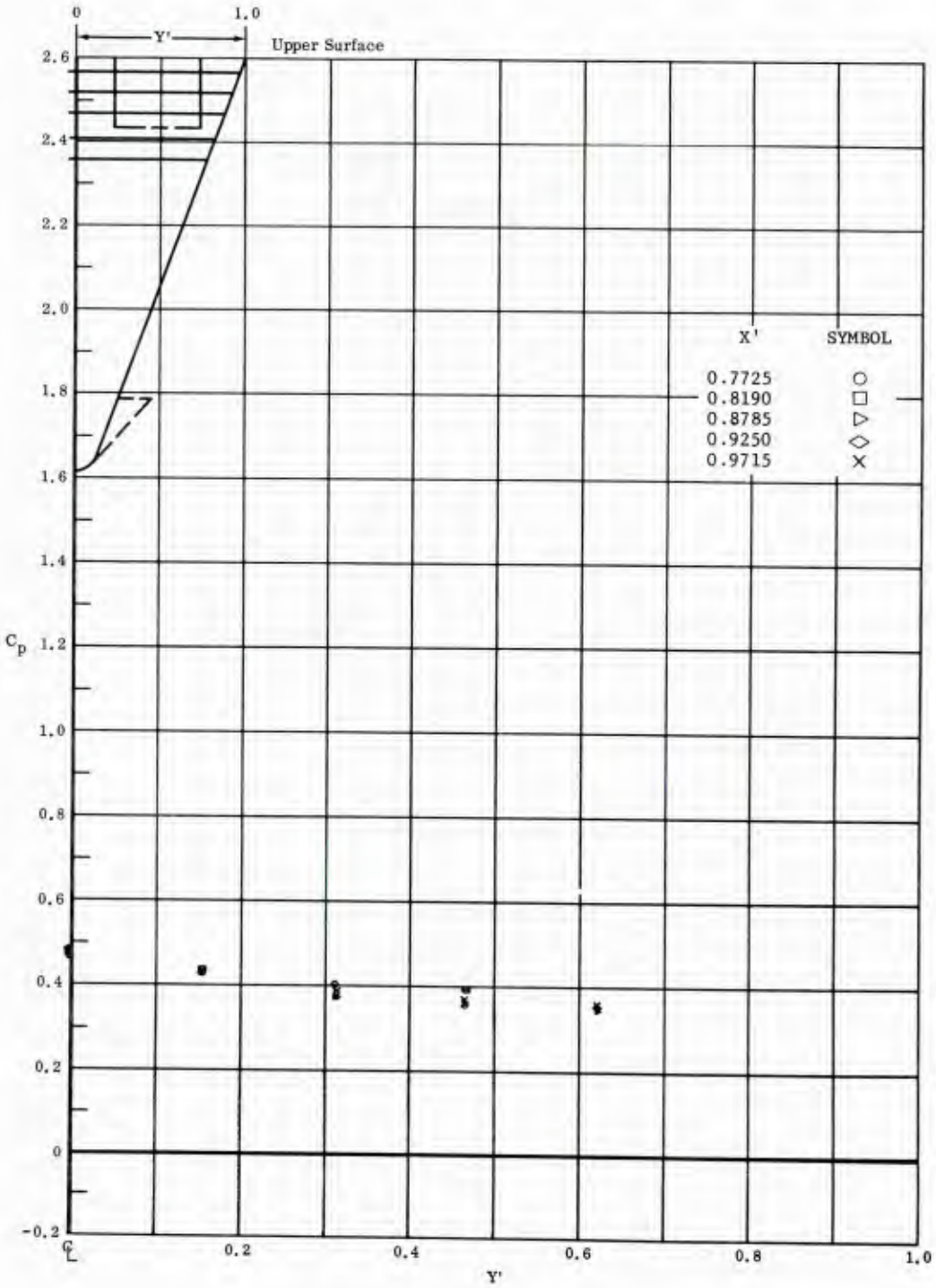

Fig. 32 Spanwise Distributions of Pressure Coefficients on Upper Surface Basic Configuration, No Flap Deflections, $\alpha = -15°$, $\beta = 0$

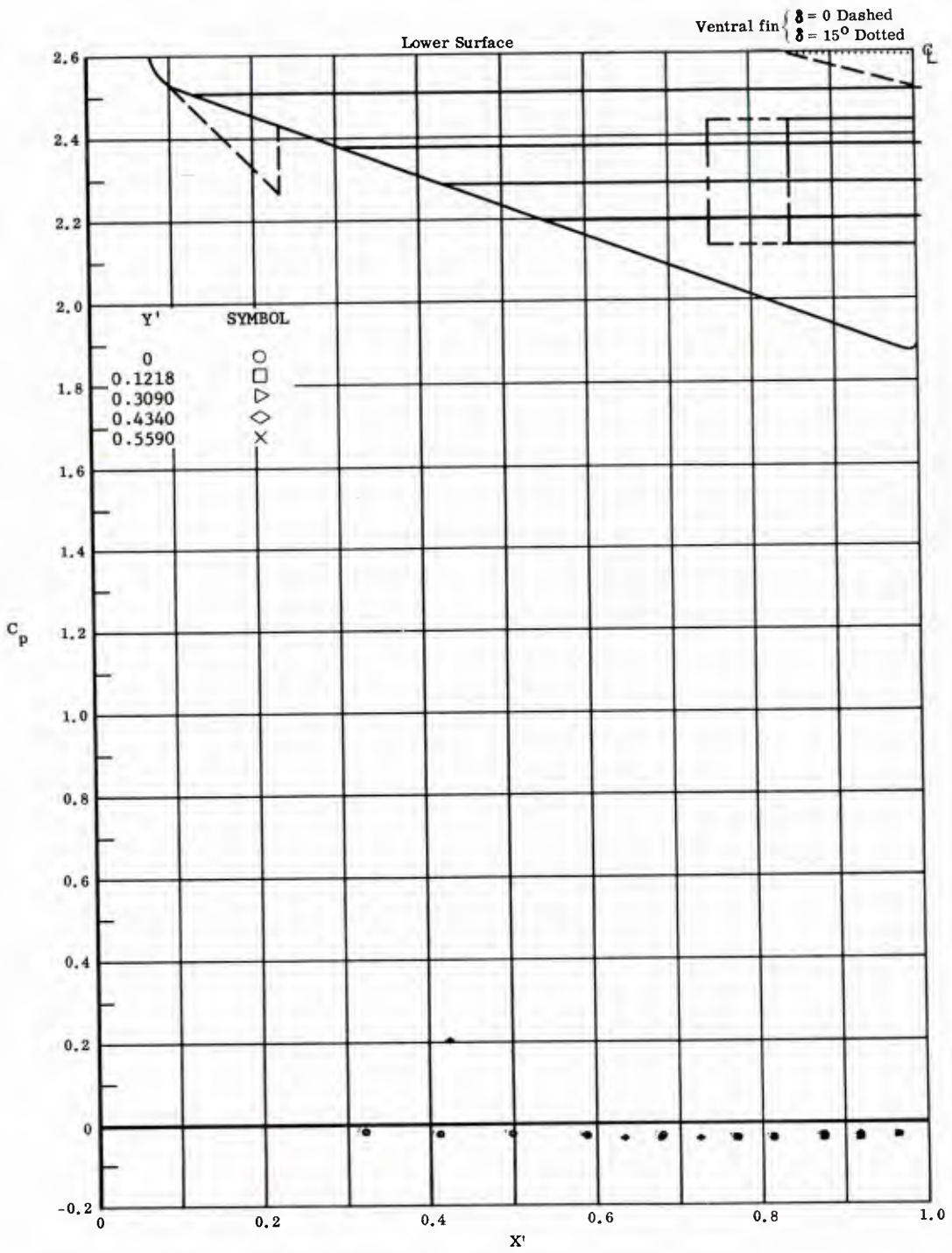

Fig 33 Streamwise Distributions of Pressure Coefficients on Lower Surface Basic Configuration, Bottom Flaps Deflected 20°, $\alpha = -15°$, $\beta = 0$

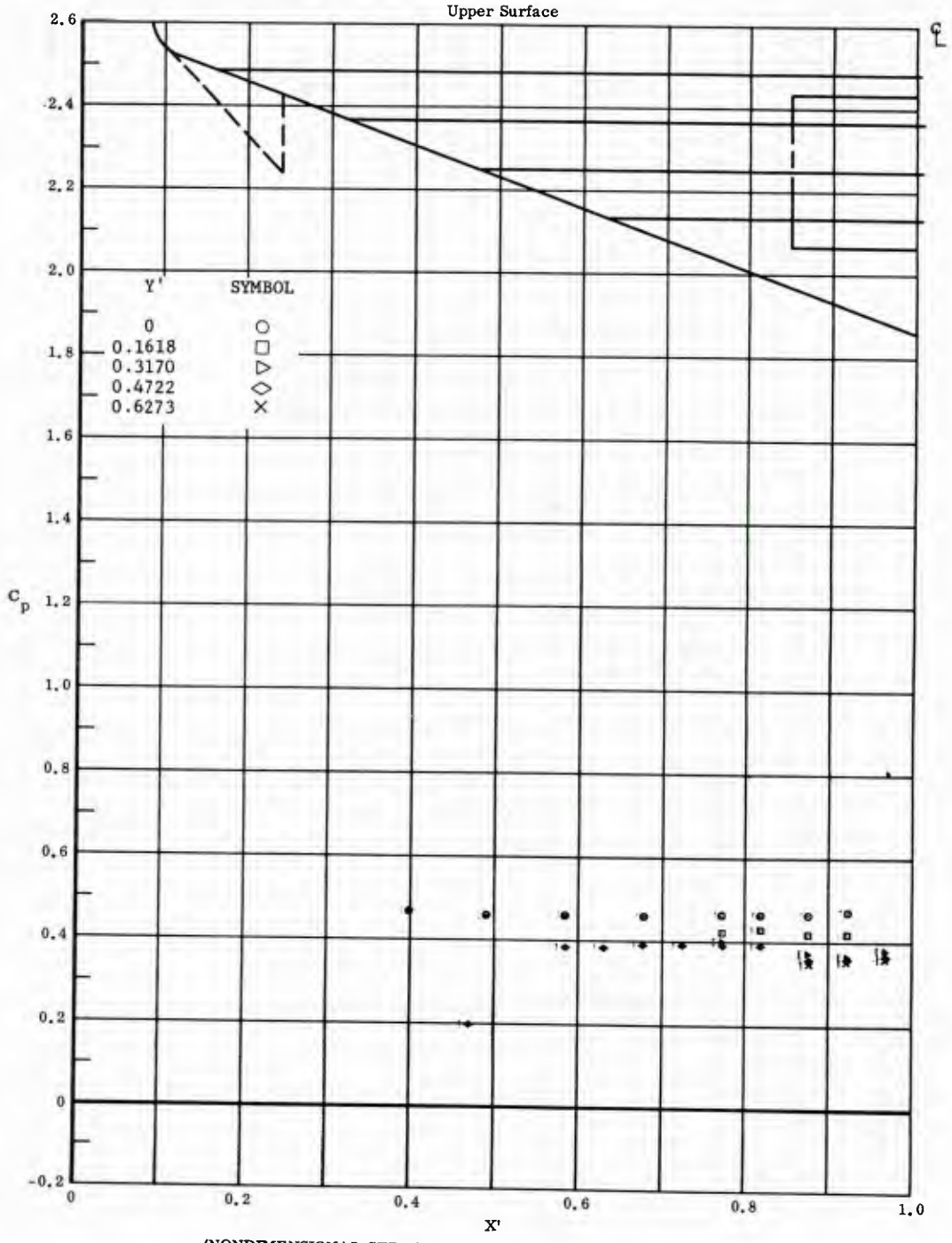

Fig. 33 Streamwise Distributions of Pressure Coefficients on Upper Surface Basic Configuration, Bottom Flaps Deflected 20°, α = -15°, β = 0

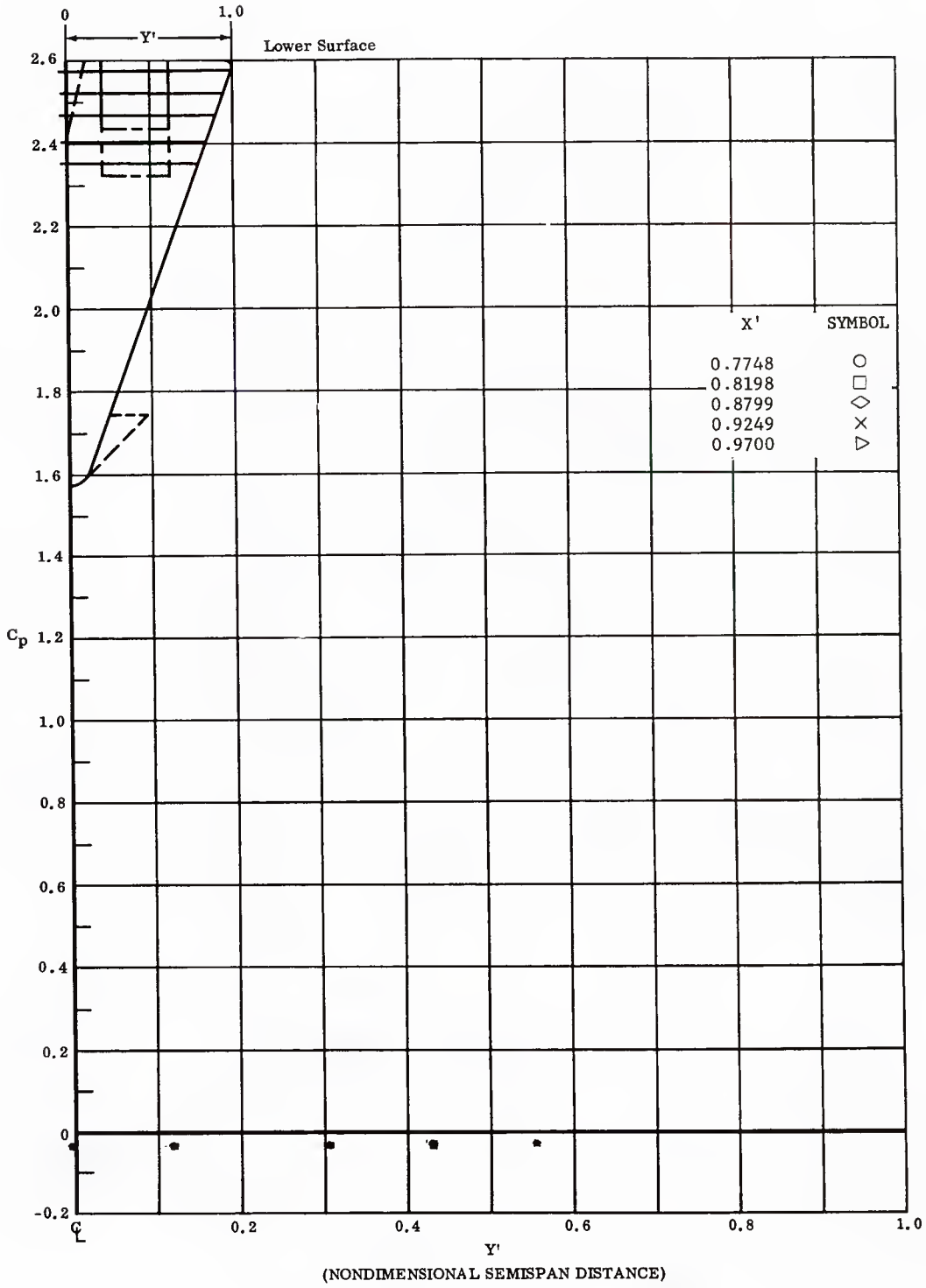

Fig. 33 Spanwise Distributions of Pressure Coefficients on Lower Surface
Basic Configuration, Bottom Flaps Deflected 20°, α = -15°, β = 0

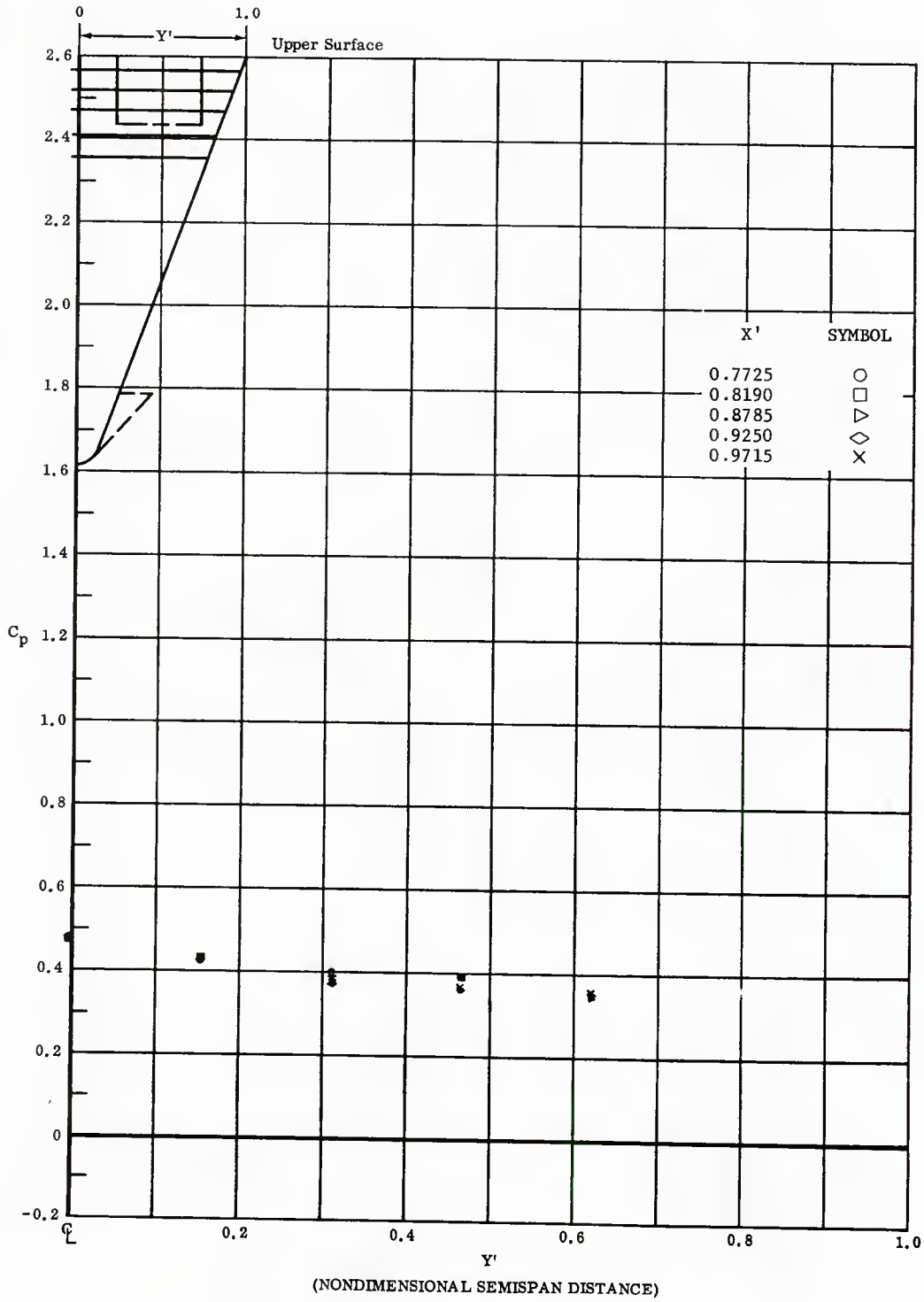

Fig. 33 Spanwise Distributions of Pressure Coefficients on Upper Surface Basic Configuration, Bottom Flaps Deflected 20°, α = -15°, β = 0

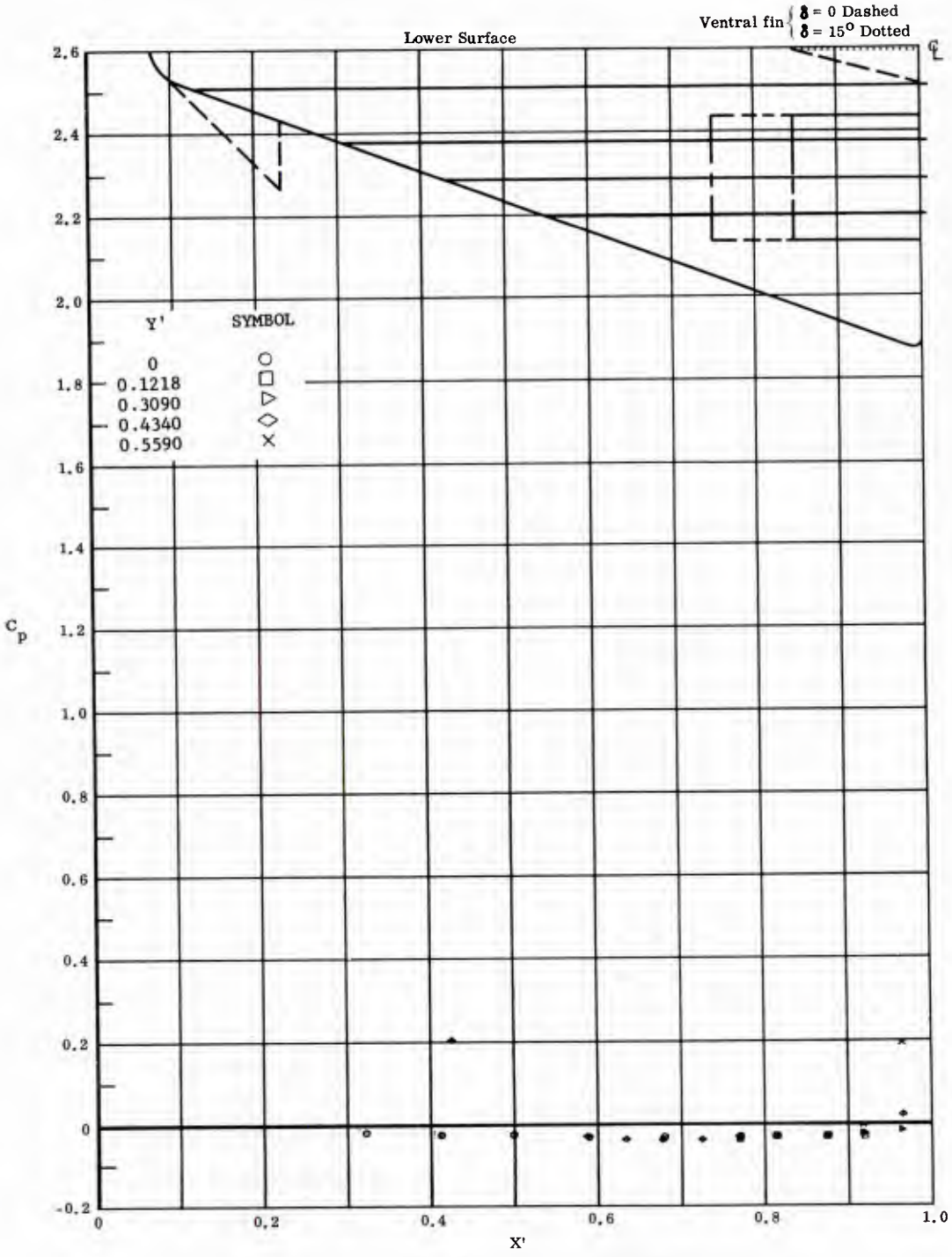

Fig. 34 Streamwise Distributions of Pressure Coefficients on Lower Surface
Basic Configuration, Bottom Flaps Deflected 40°, α = -15°, β = 0

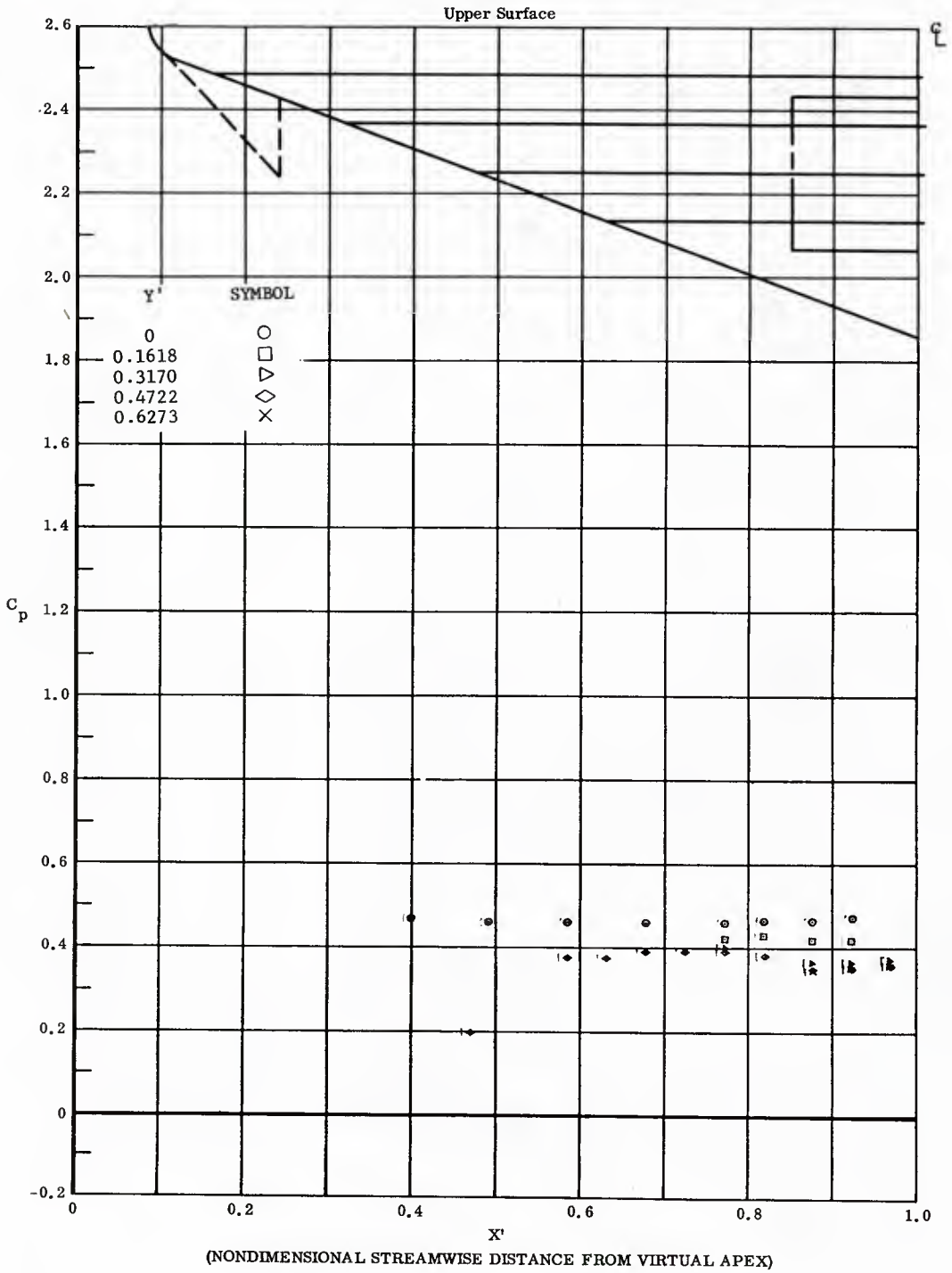

Fig. 34 Streamwise Distributions of Pressure Coefficients on Upper Surface Basic Configuration, Bottom Flaps Deflected 40°, α = -15°, β = 0

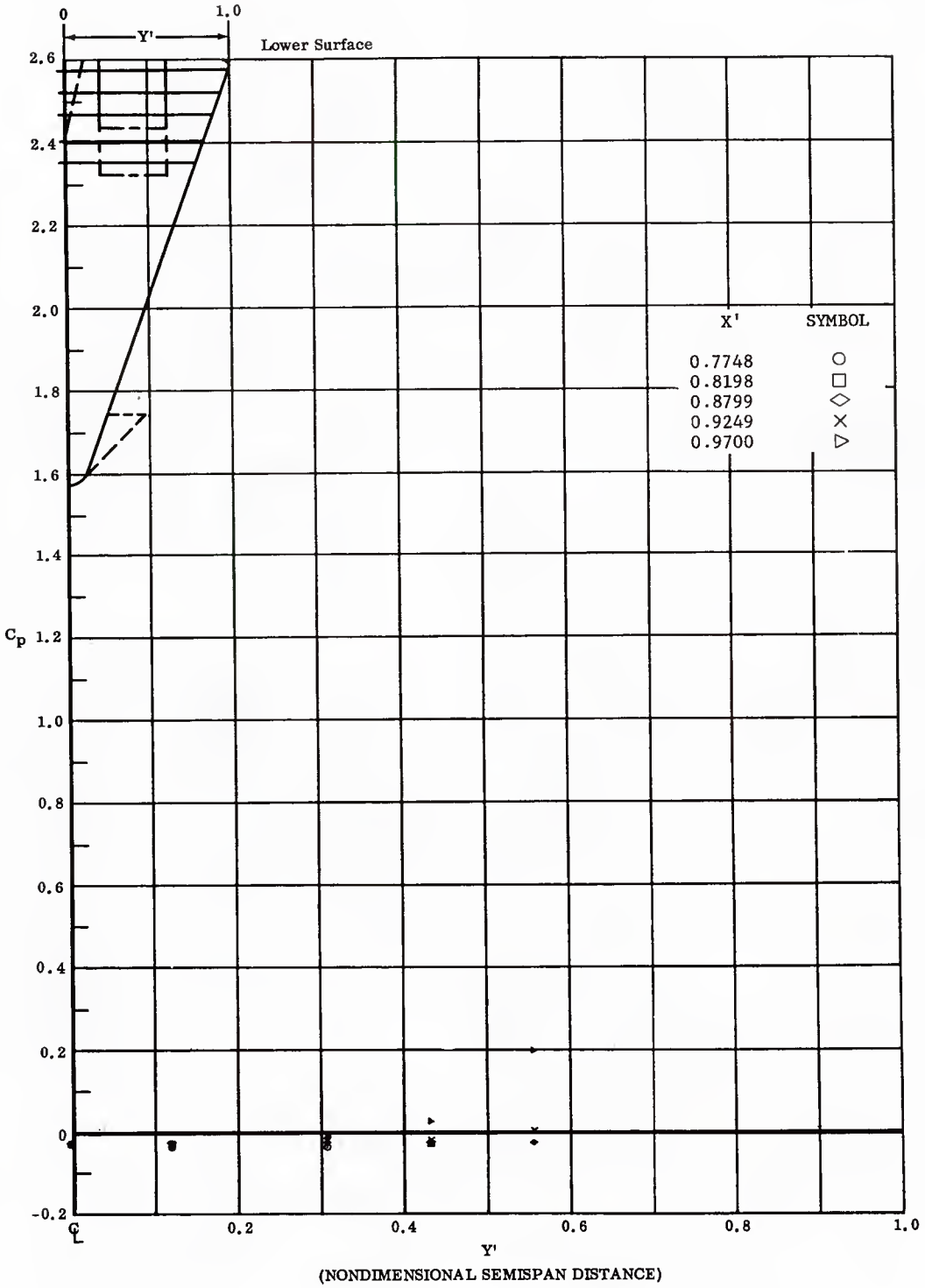

Fig. 34 Spanwise Distributions of Pressure Coefficients on Lower Surface Basic Configuration, Bottom Flaps Deflected 40°, α = -15°, β = 0

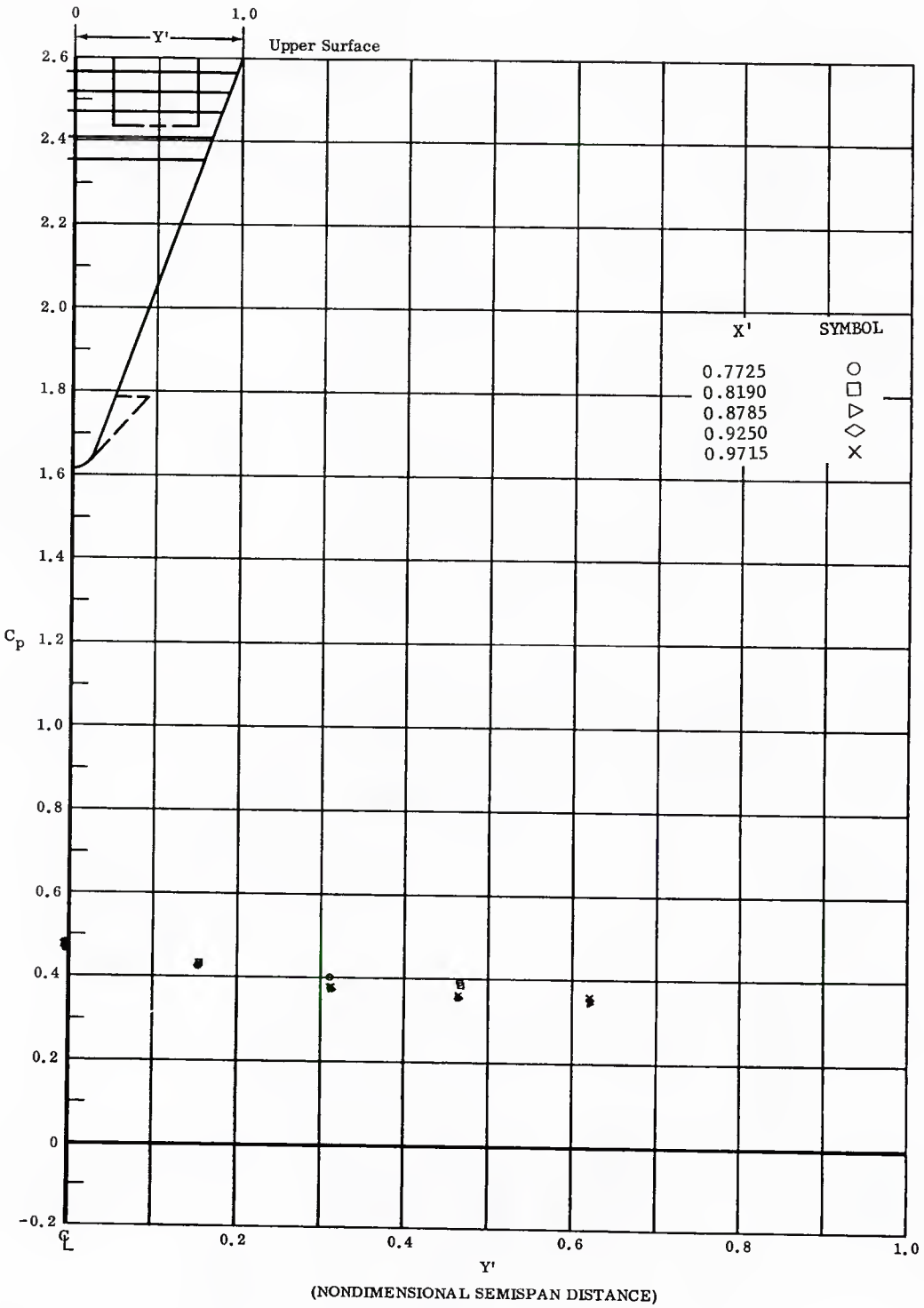

Fig. 34 Spanwise Distributions of Pressure Coefficients on Upper Surface Basic Configuration, Bottom Flaps Deflected 40°, α = -15°, β = 0

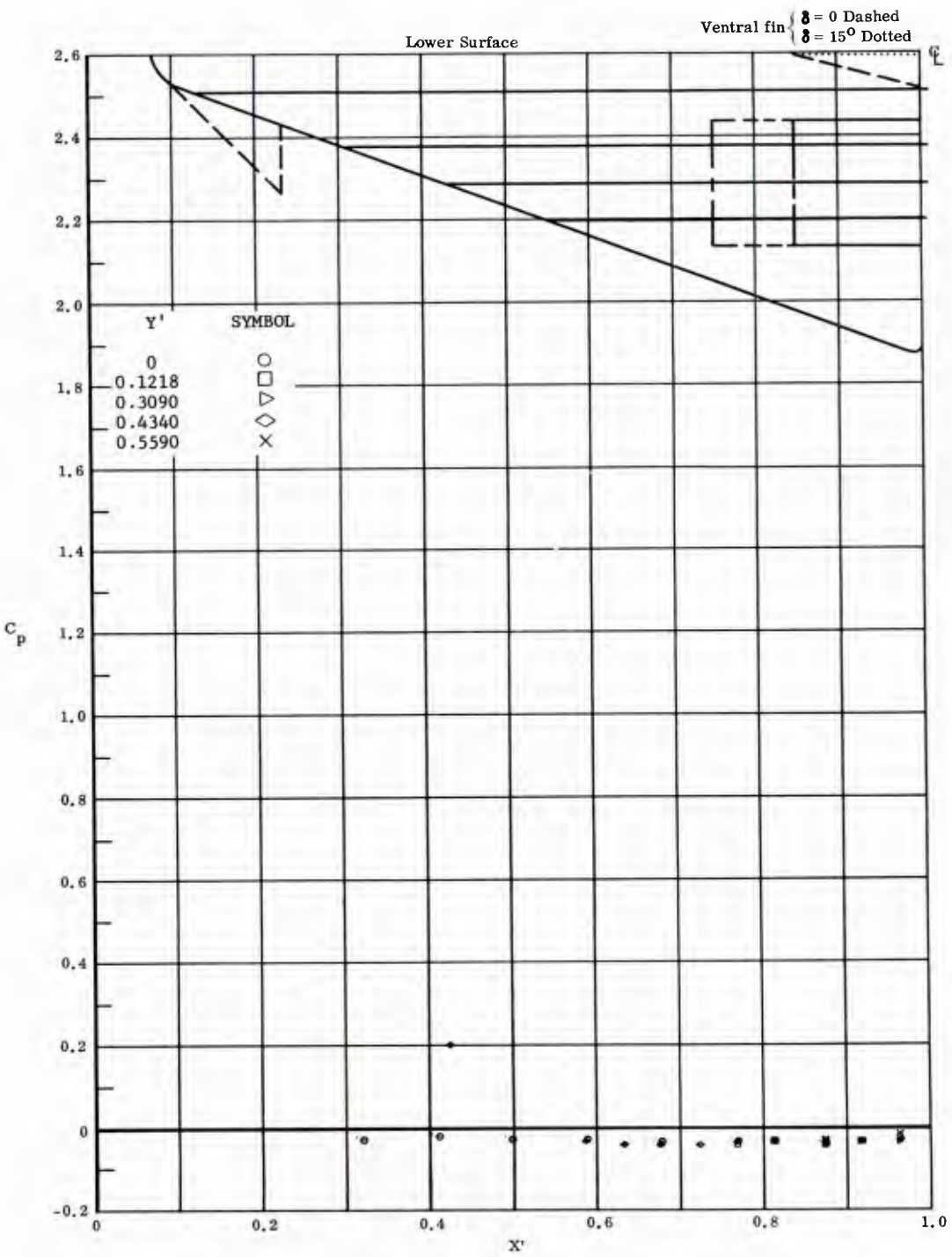

Fig. 35 Streamwise Distributions of Pressure Coefficients on Lower Surface Extended (Long Chord) Flaps on Lower Surface, Bottom Flaps Deflected 20°, α = -15°, β = 0

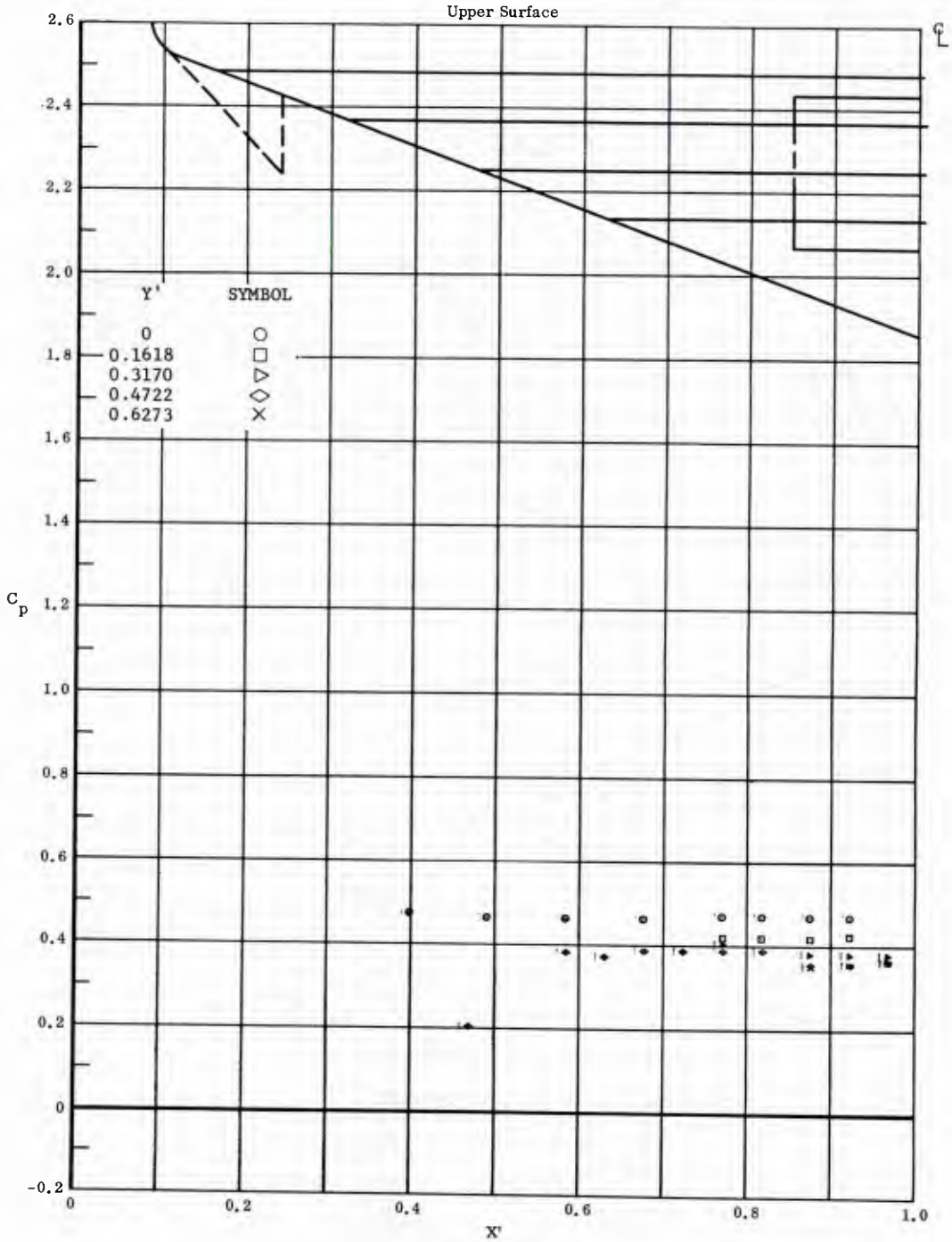

Fig. 35 Streamwise Distributions of Pressure Coefficients on Upper Surface Extended (Long Chord) Flaps on Lower Surface, Bottom Flaps Deflected 20°, α = -15°, β = 0

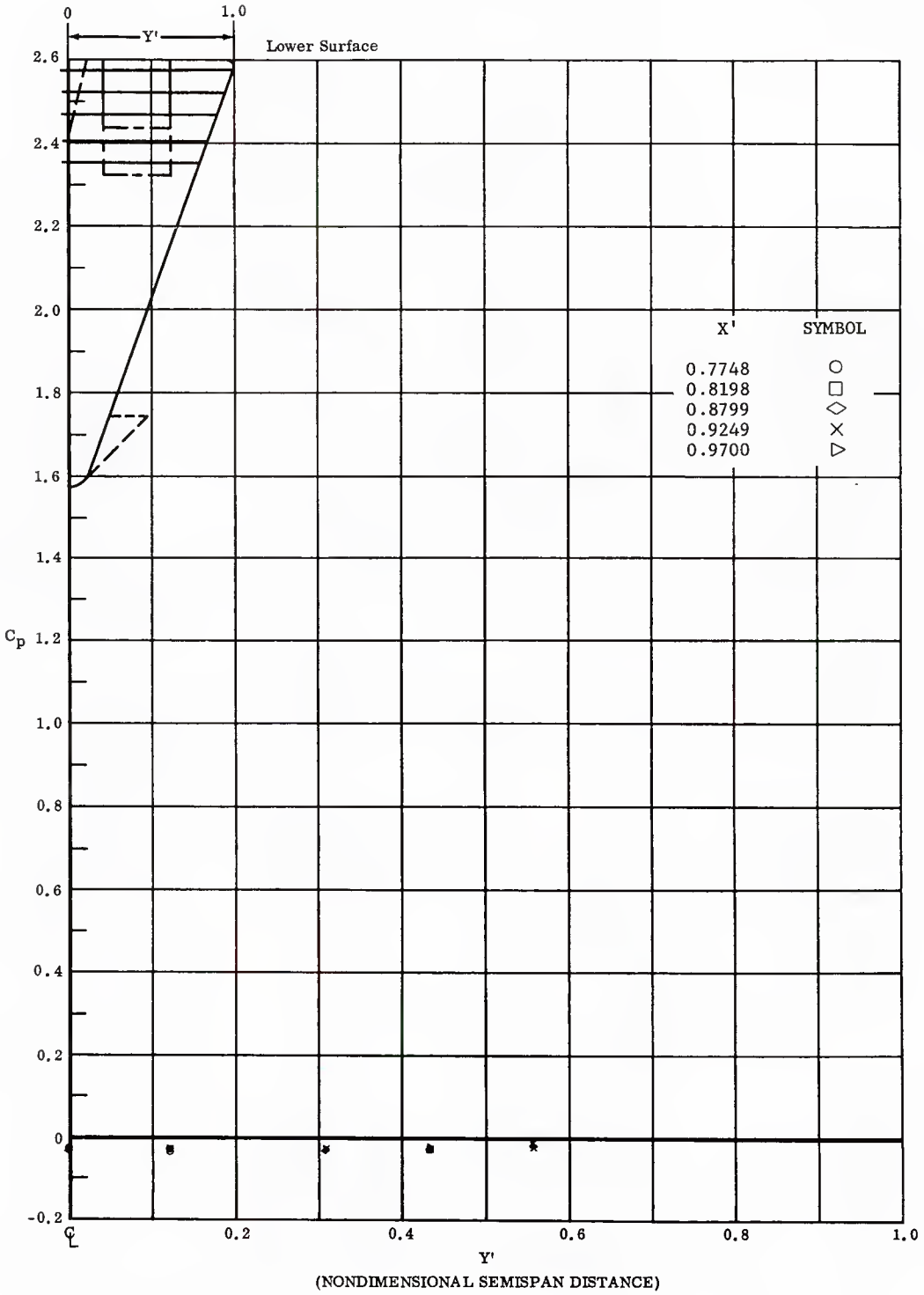

Fig. 35 Spanwise Distributions of Pressure Coefficients on Lower Surface Extended (Long Chord) Flaps on Lower Surface, Bottom Flaps Deflected 20°, α = -15°, β = 0

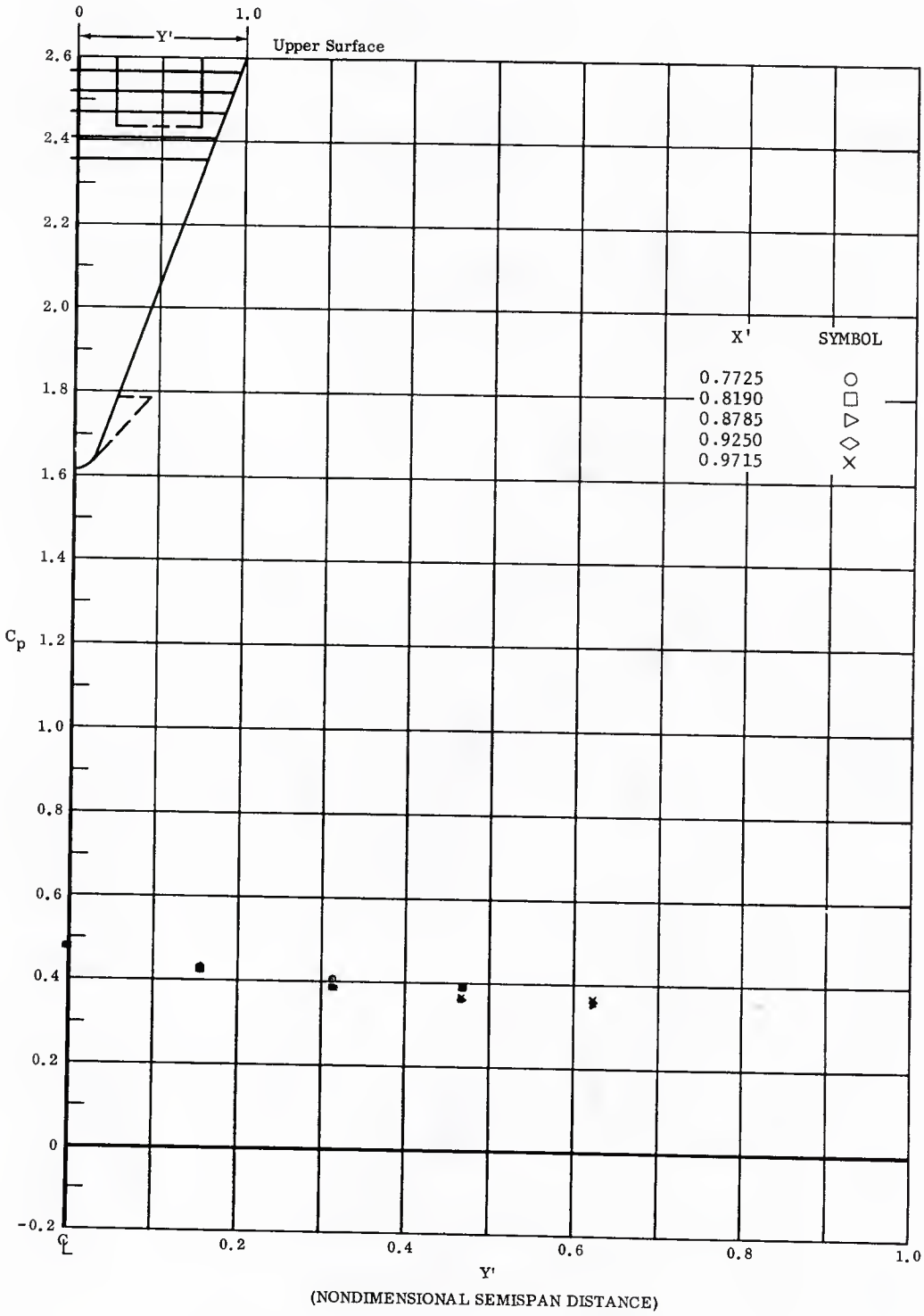

Fig. 35 Spanwise Distributions of Pressure Coefficients on Upper Surface
Extended (Long Chord) Flaps on Lower Surface
Bottom Flaps Deflected 20°, α = -15°, β = 0

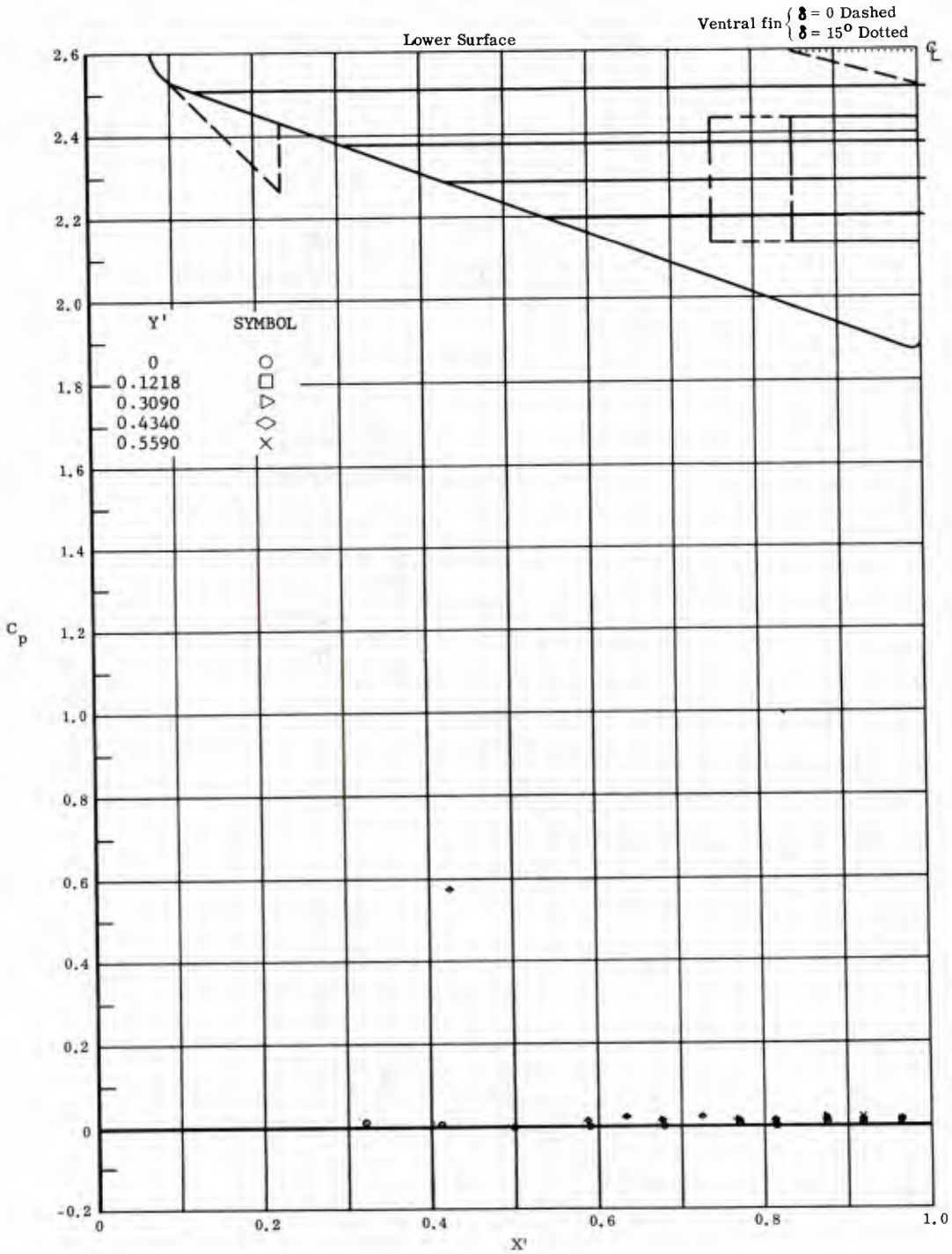

(NONDIMENSIONAL STREAMWISE DISTANCE FROM VIRTUAL APEX)

Fig. 36 Streamwise Distributions of Pressure Coefficients on Lower Surface
Basic Configuration, Left (Upper) Flap Deflected -40°, α = 0, β = +14°

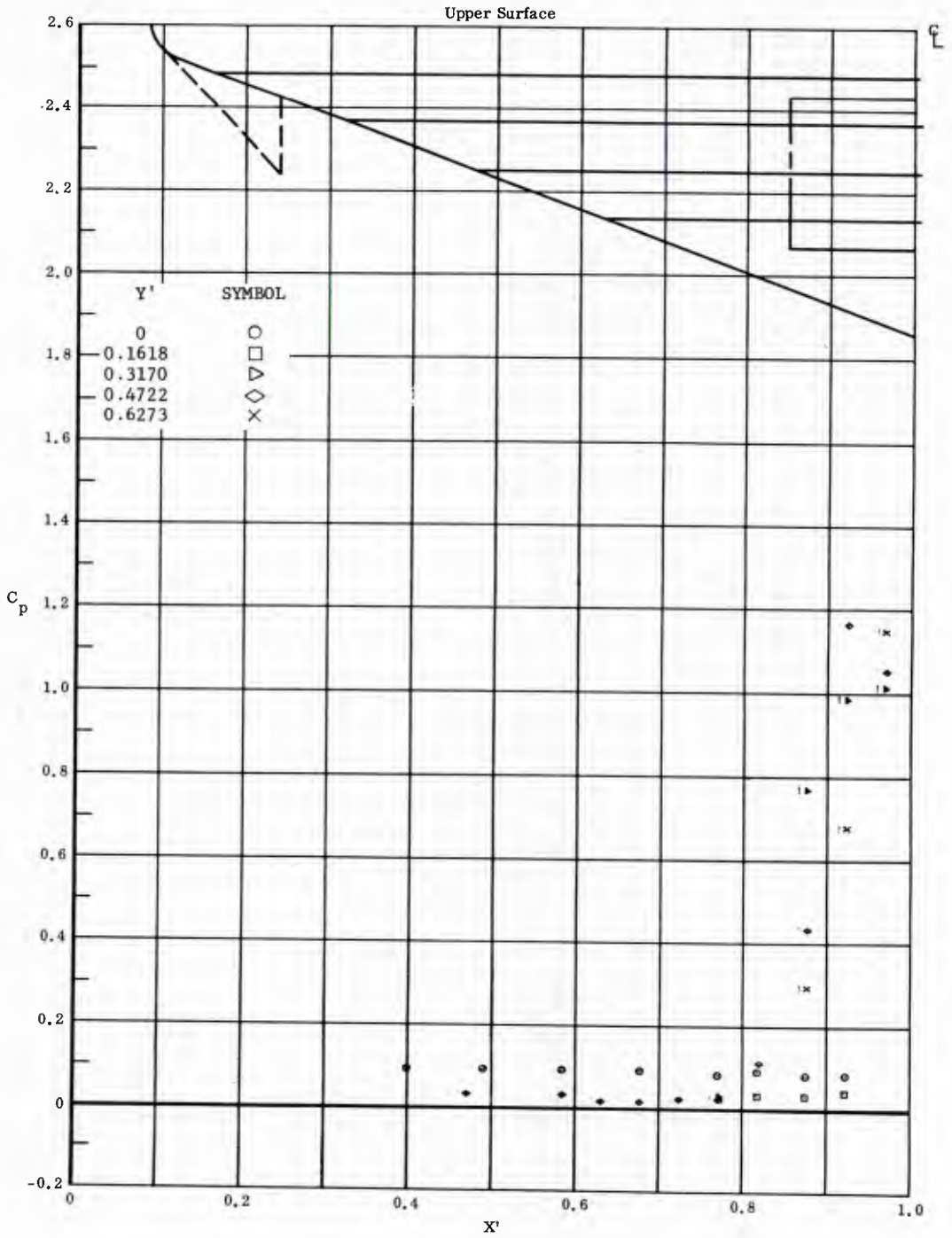

Fig. 36 Streamwise Distributions of Pressure Coefficients on Upper Surface Basic Configuration, Left (Upper) Flap Deflected -40°, α = 0, β = +14°

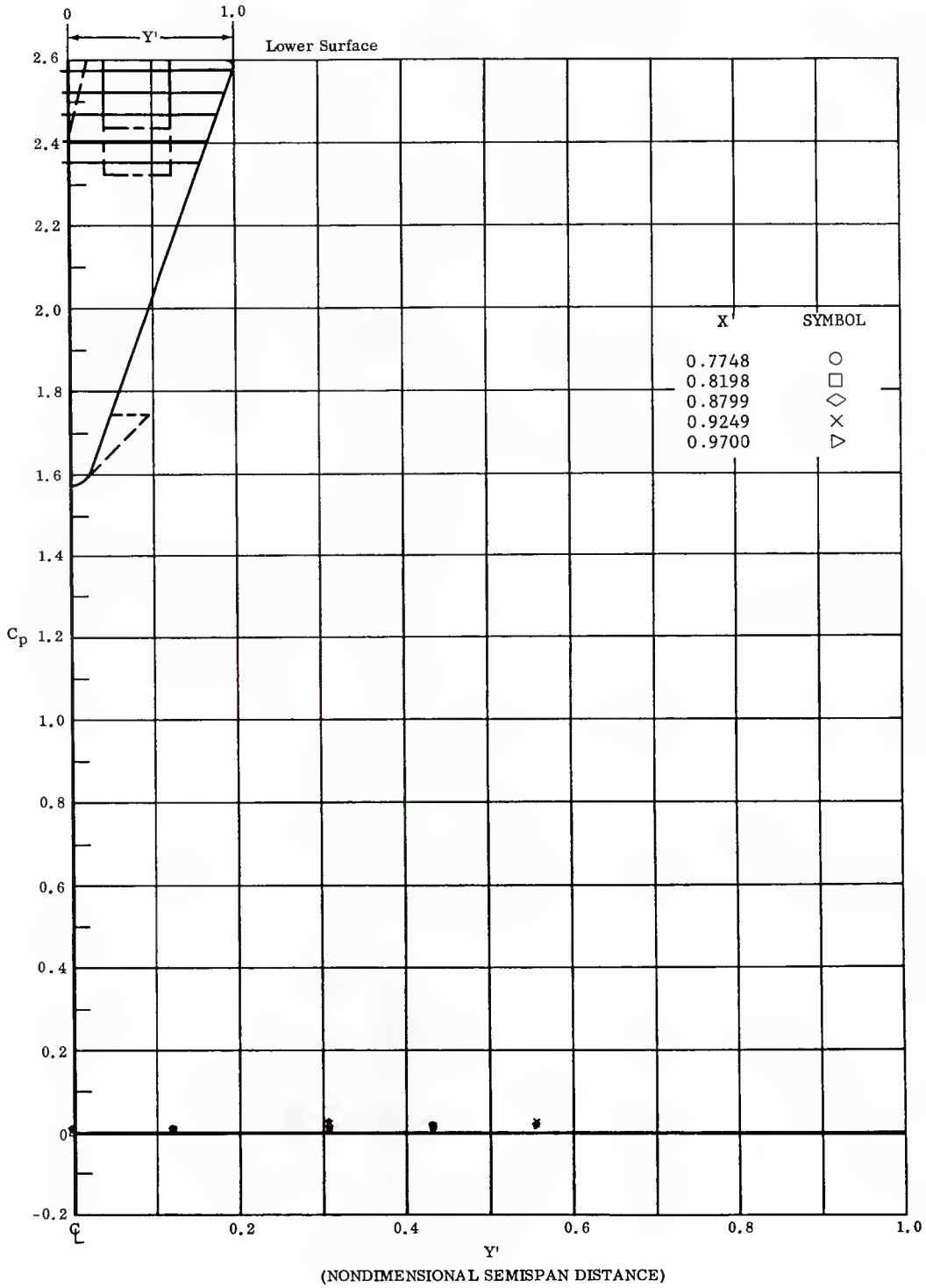

Fig. 36 Spanwise Distributions of Pressure Coefficients on Lower Surface
Basic Configuration, Left (Upper) Flap Deflected -40°, α = 0, β = +14°

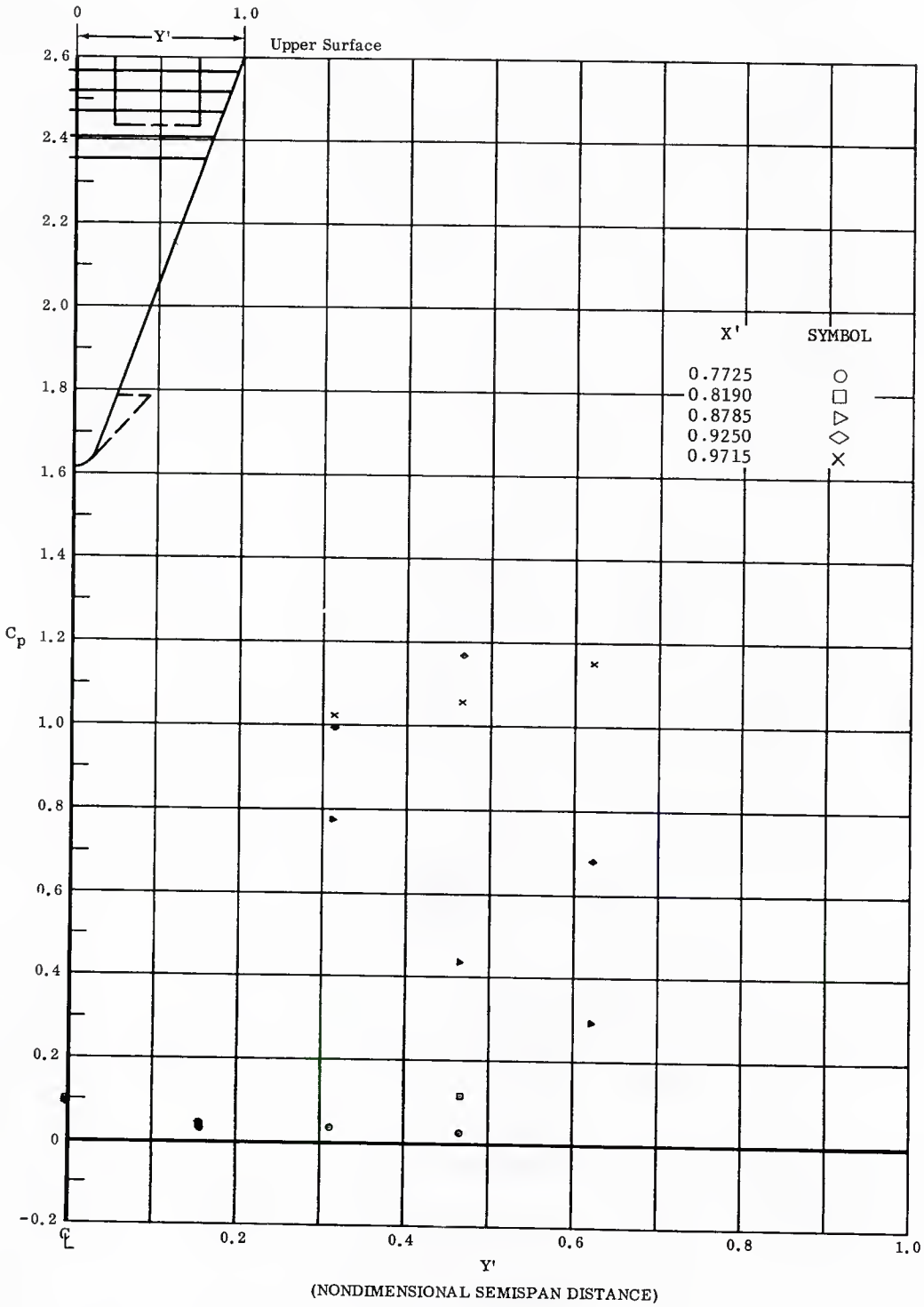

Fig. 36 Spanwise Distributions of Pressure Coefficients on Upper Surface
Basic Configuration, Left (Upper) Flap Deflected -40°, α = 0, β = +14°

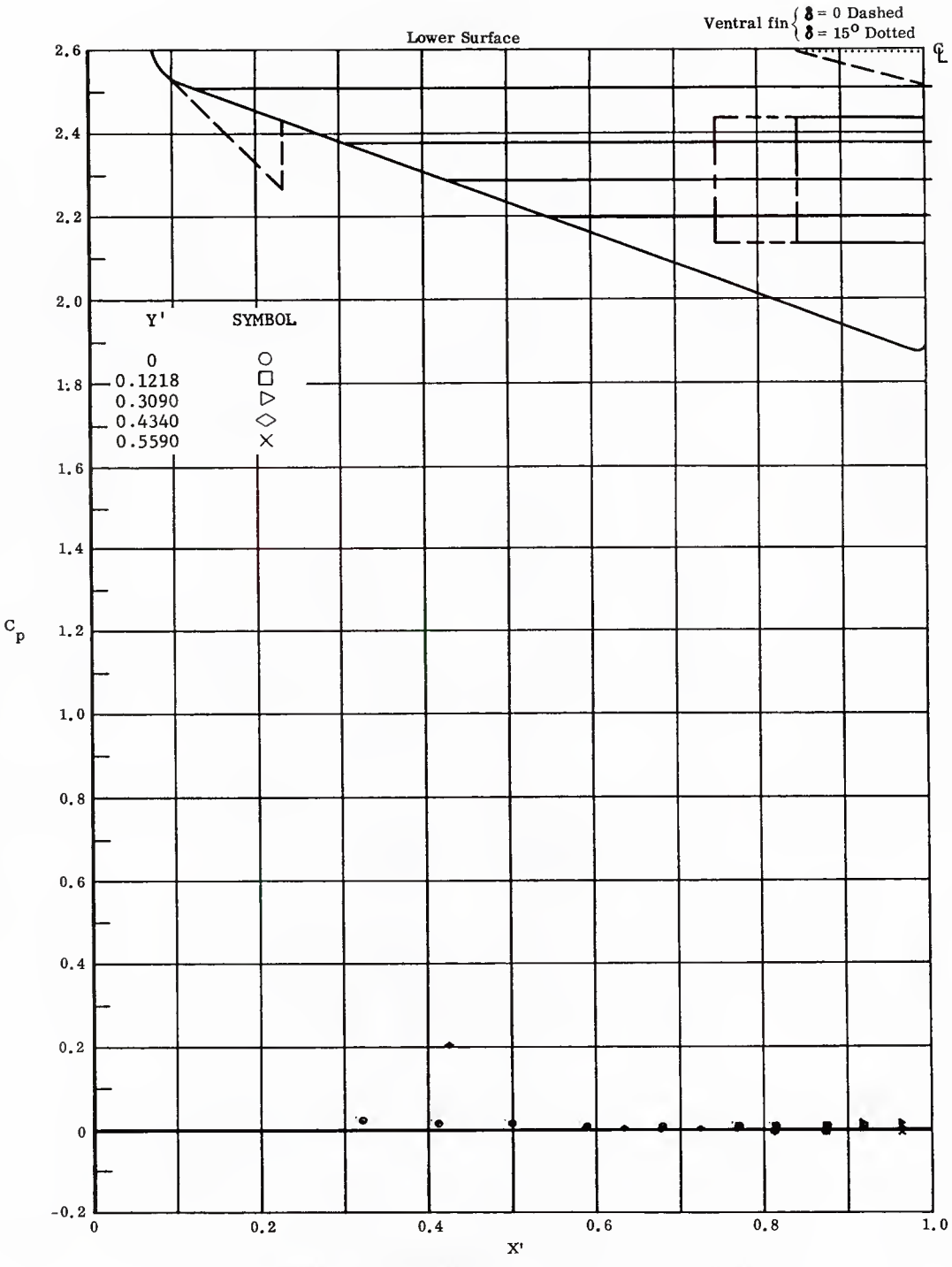

Fig. 37 Streamwise Distributions of Pressure Coefficients on Lower Surface
Basic Configuration, Left (Upper) Flap Deflected -40°, α = 0, β = 0

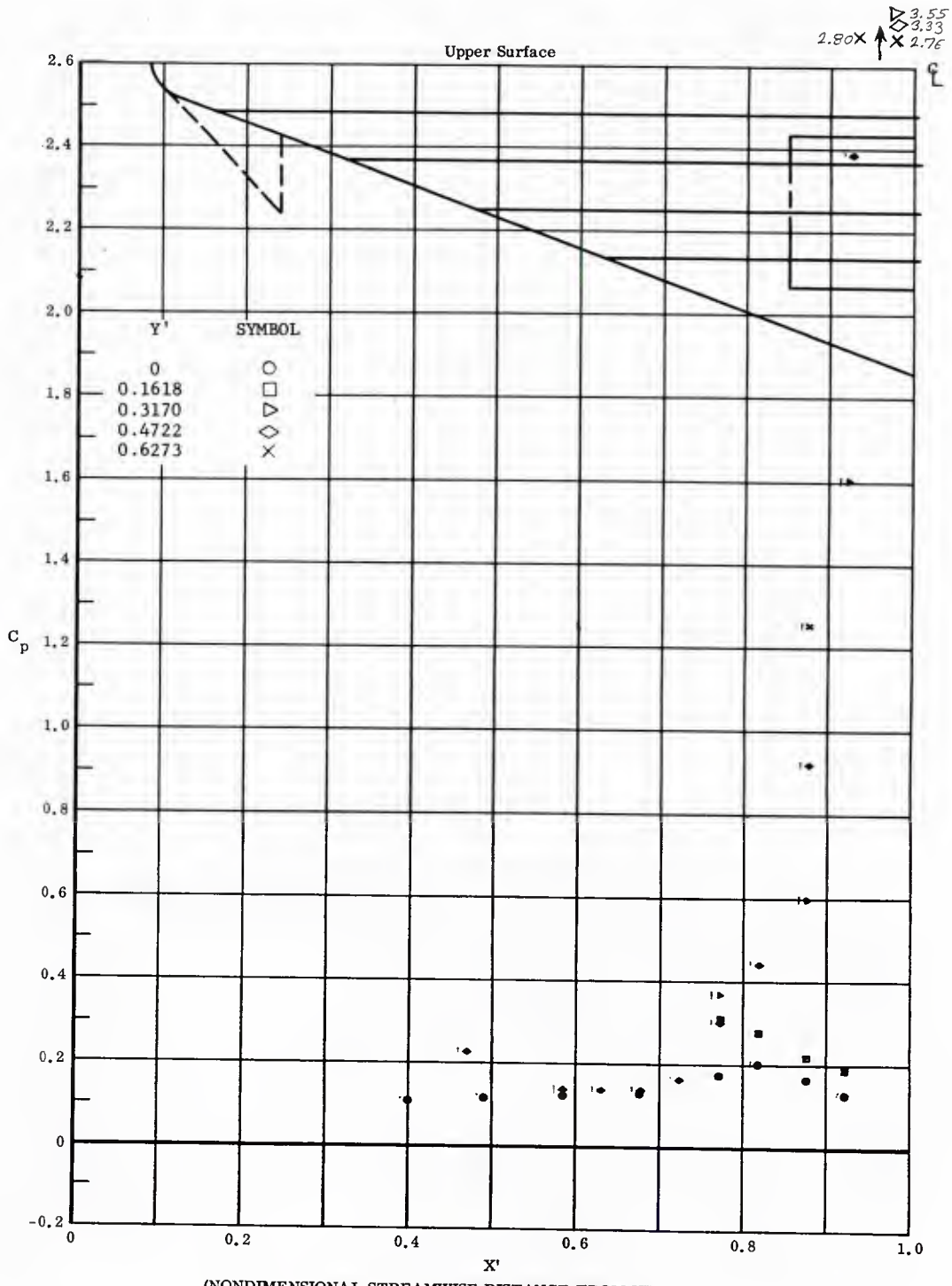

Fig. 37 Streamwise Distributions of Pressure Coefficients on Upper Surface Basic Configuration, Left (Upper) Flap Deflected -40°, α = 0, β = 0

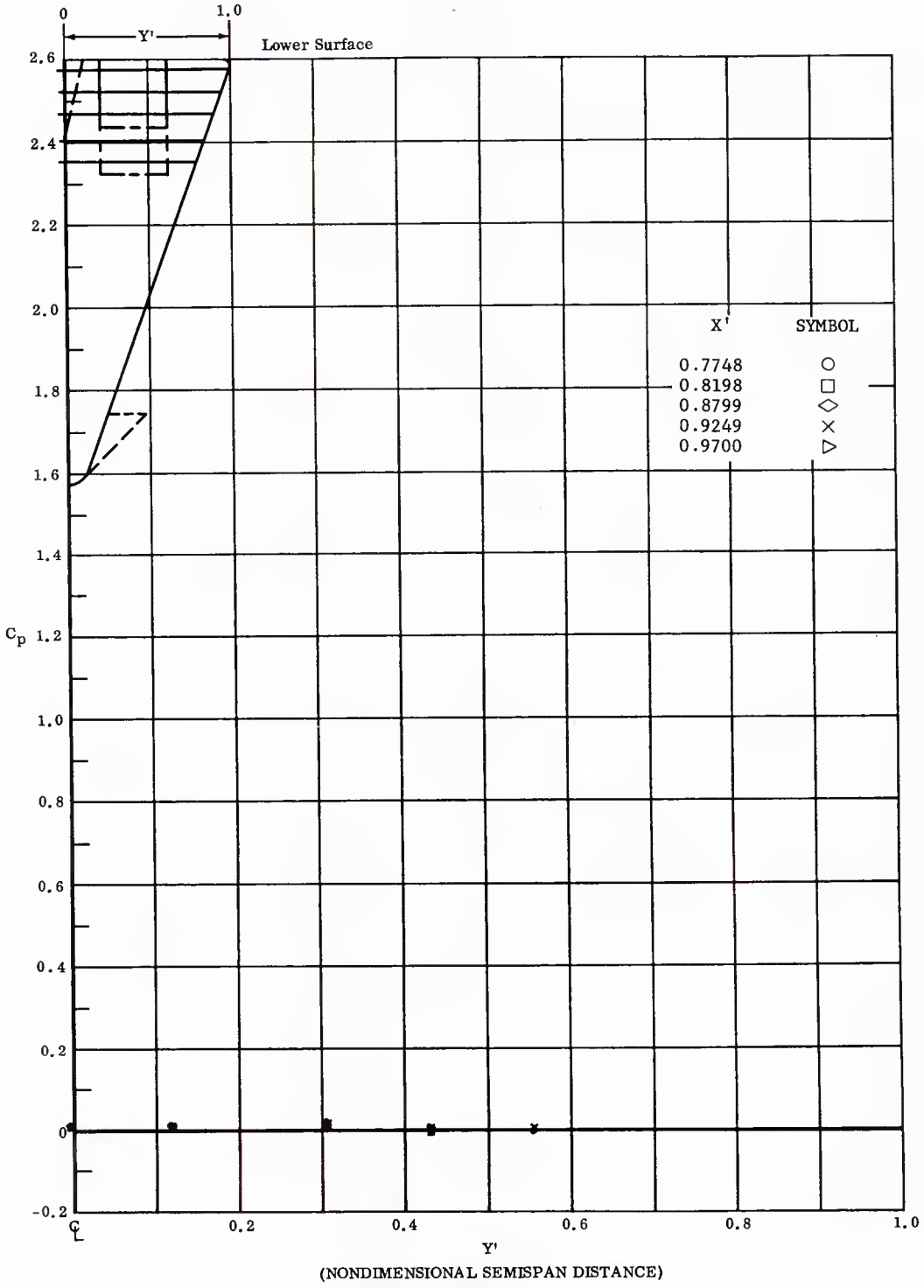

Fig. 37 Spanwise Distributions of Pressure Coefficients on Lower Surface Basic Configuration, Left (Upper) Flap Deflected -40°, $\alpha = 0$, $\beta = 0$

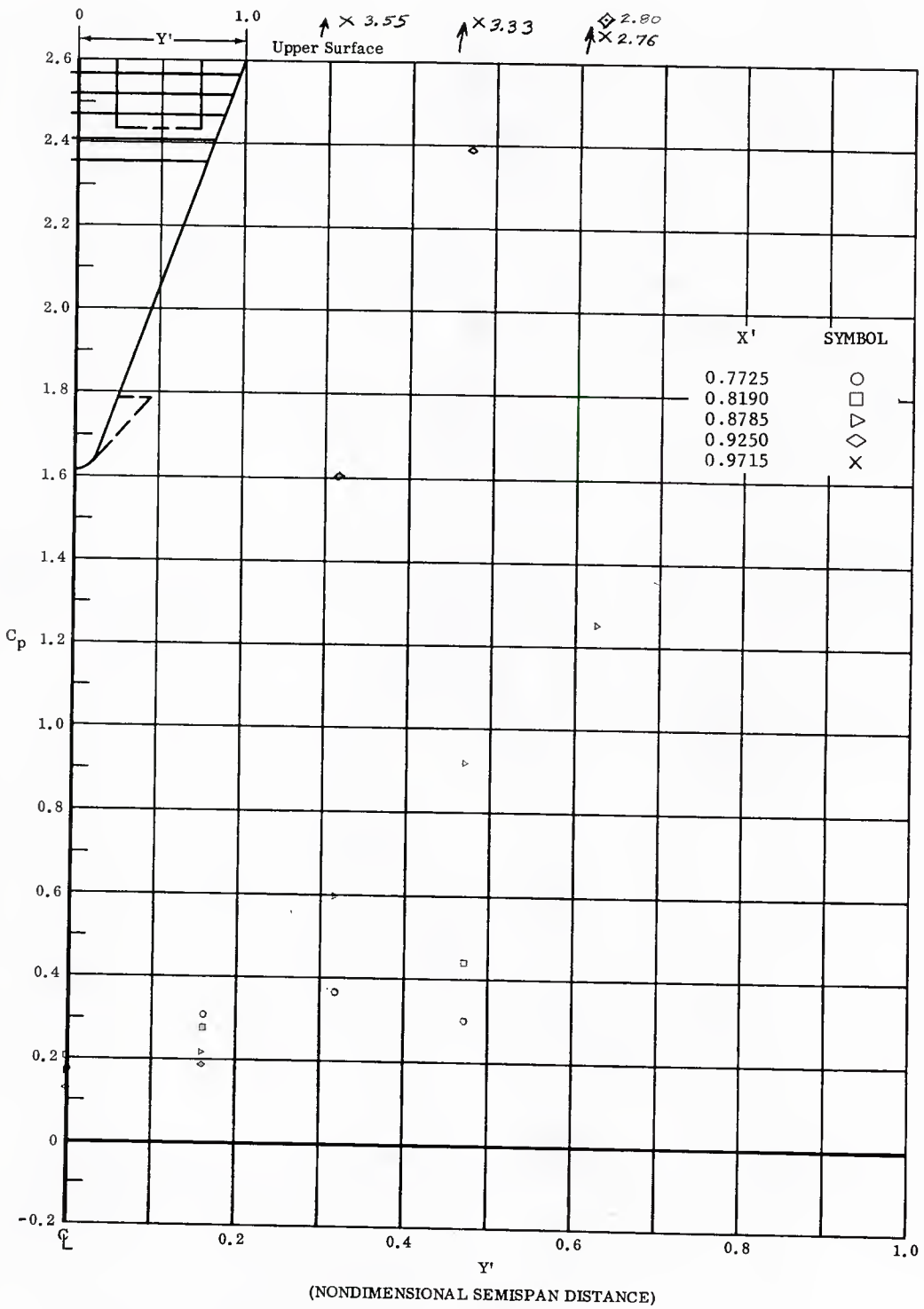

Fig. 37 Spanwise Distributions of Pressure Coefficients on Upper Surface
Basic Configuration, Left (Upper) Flap Deflected -40°, $\alpha = 0$, $\beta = 0$

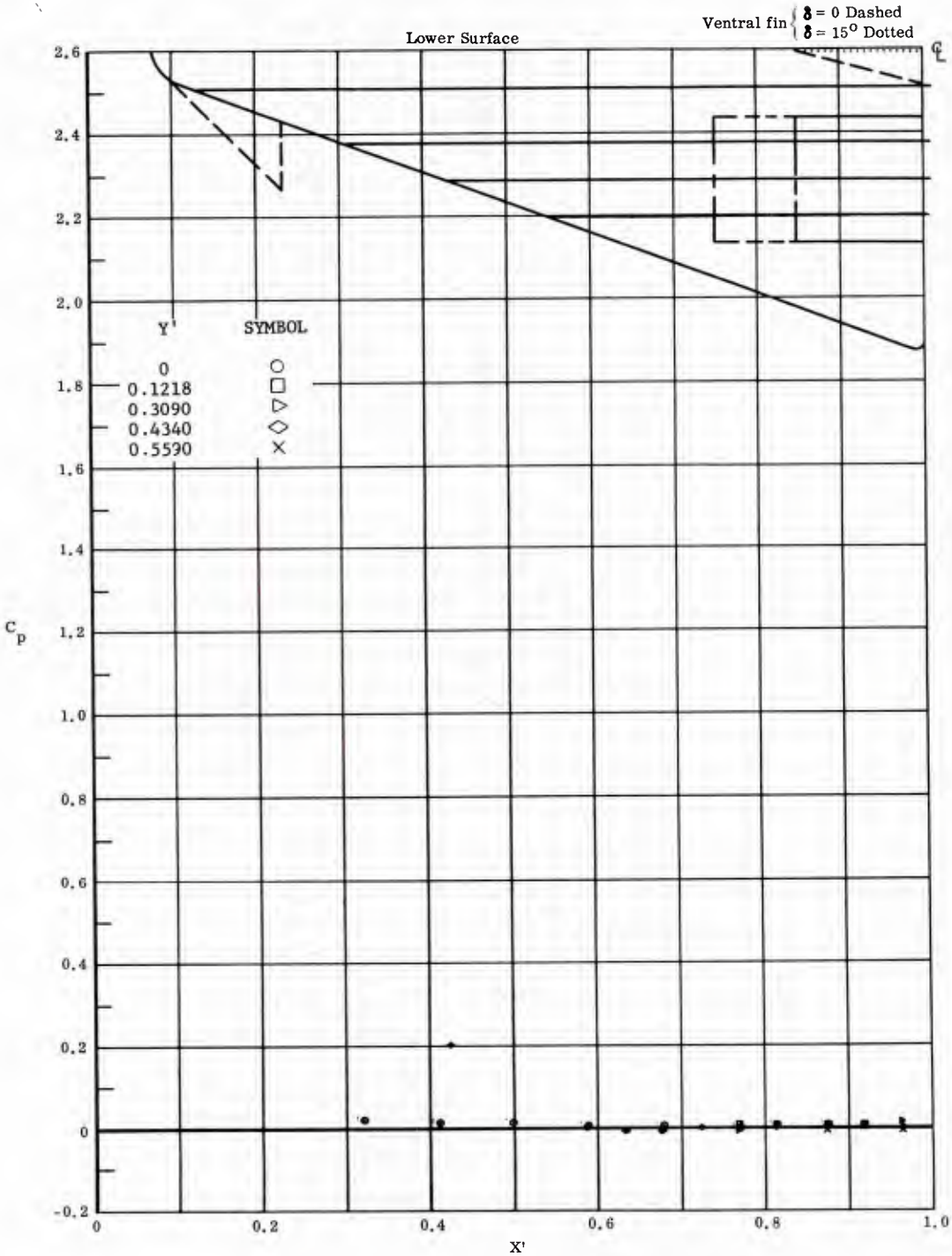

(NONDIMENSIONAL STREAMWISE DISTANCE FROM VIRTUAL APEX)

.Fig. 38 Streamwise Distributions of Pressure Coefficients on Lower Surface Basic Configuration, Left and Right (Upper) Flaps Deflected -40°, $\alpha = 0$, $\beta = 0$

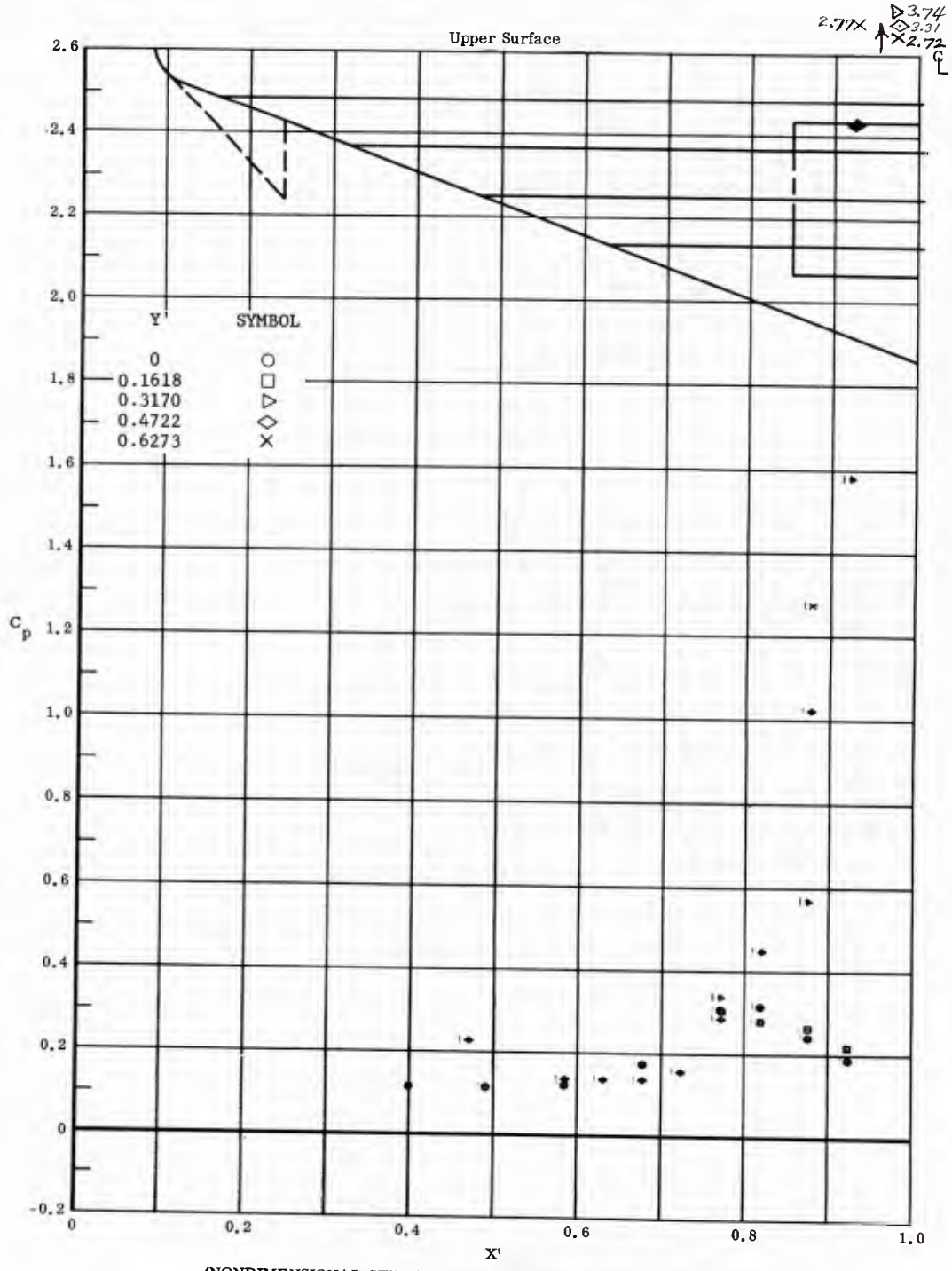

Fig. 38 Streamwise Distributions of Pressure Coefficients on Upper Surface Basic Configuration, Left and Right (Upper) Flaps Deflected -40°, $\alpha = 0$, $\beta = 0$

Ventral Fin	
OFF	
ON δ = 0	
ON δ = 15	

Canard	OFF
	ON
Bottom Flap Chord	Short
	Long

δ_1 = M_∞ = α = β =

δ_2 = $Re_\infty/10^6$ ft =

δ_3 =

122

Graph Dp-3

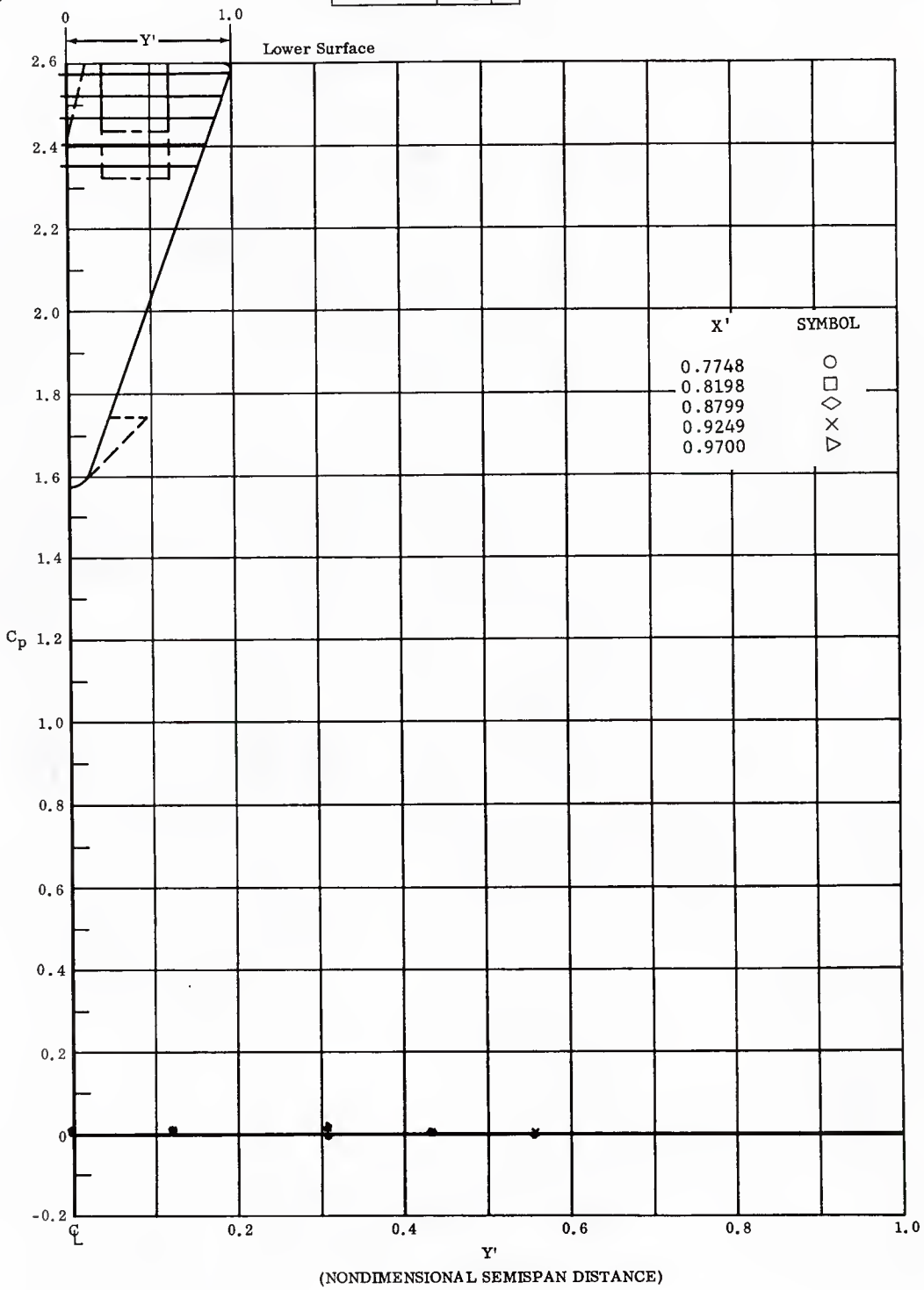

Fig. 38 Spanwise Distributions of Pressure Coefficients on Lower Surface Basic Configuration, Left and Right (Upper) Flaps Deflected -40°, α = 0, β = 0

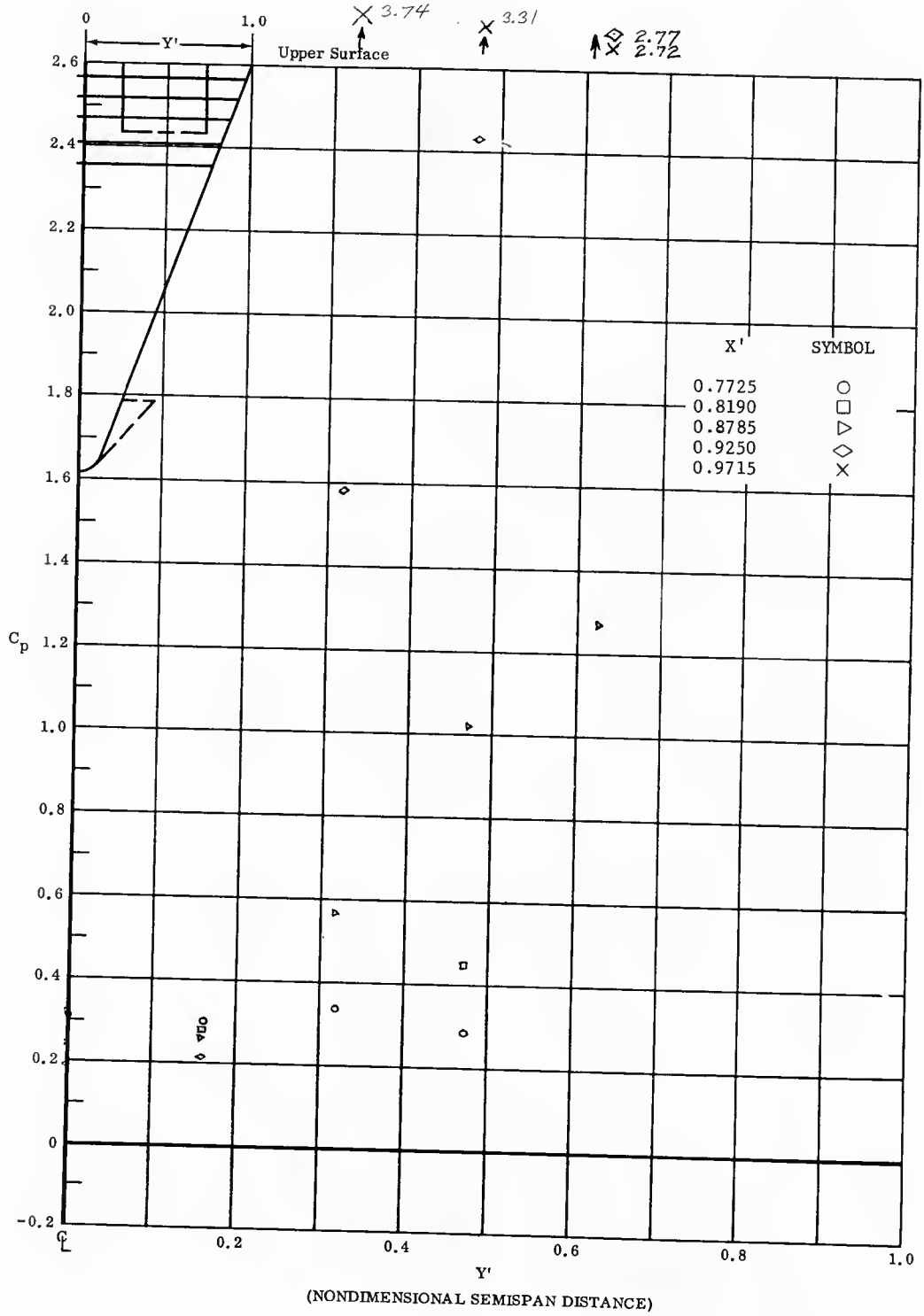

Fig. 38 Spanwise Distributions of Pressure Coefficients on Upper Surface Basic Configuration, Left and Right (Upper) Flaps Deflected -40°, $\alpha = 0$, $\beta = 0$

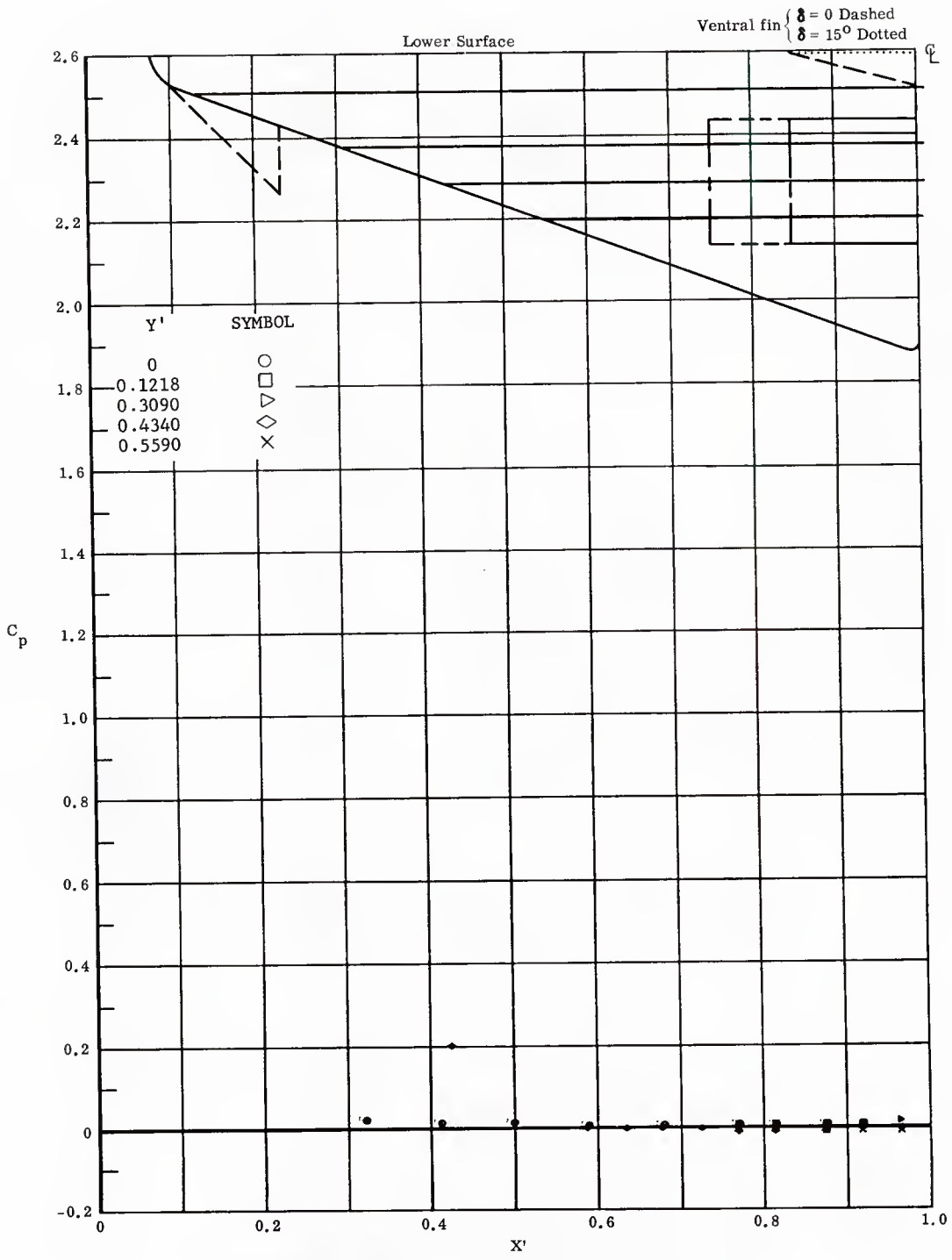

Fig. 39 Streamwise Distributions of Pressure Coefficients on Lower Surface Basic Configuration, Left and Right (Upper) Flaps Deflected -30°, $\alpha = 0$, $\beta = 0$

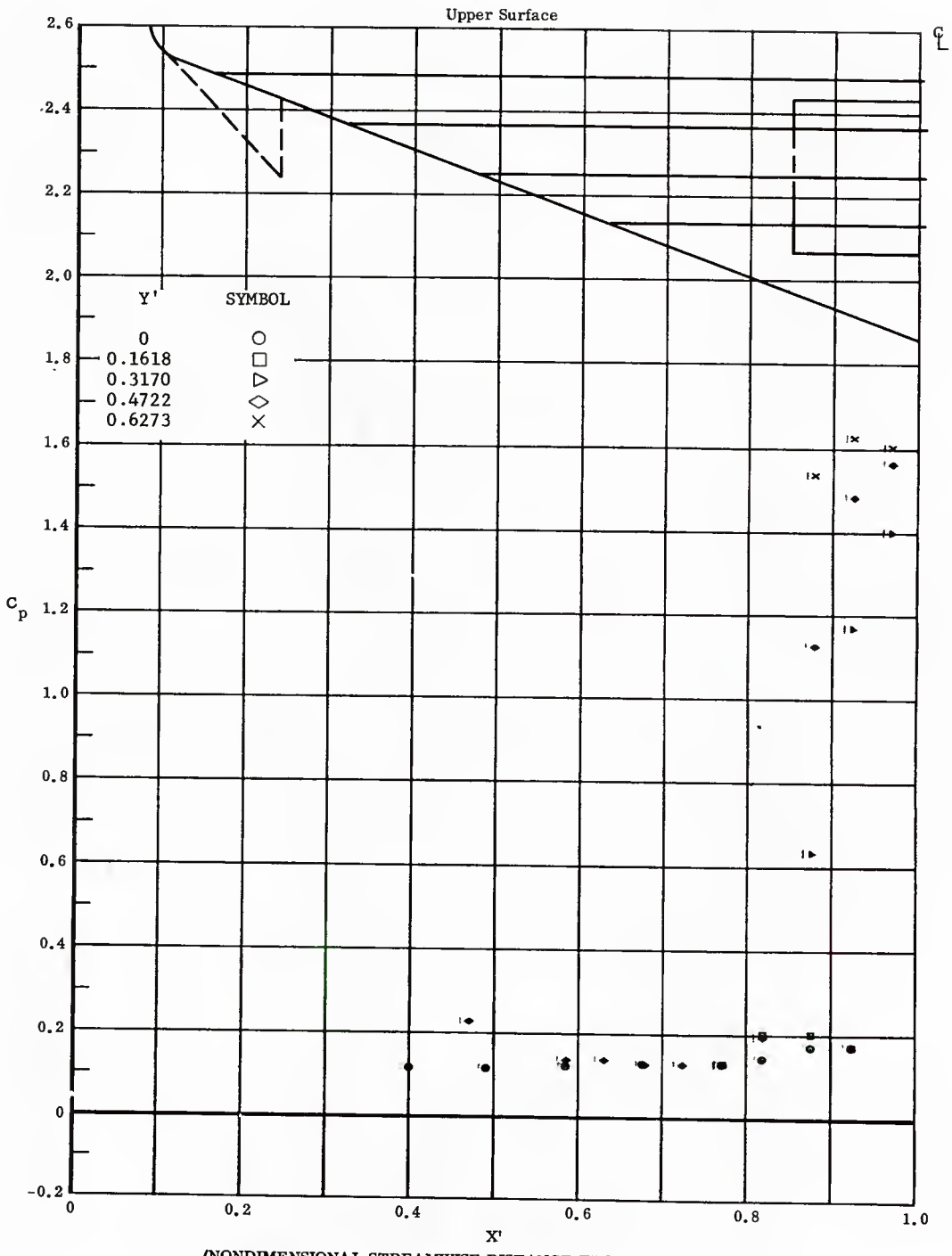

Fig. 39 Streamwise Distributions of Pressure Coefficients on Upper Surface Basic Configuration, Left and Right (Upper) Flaps Deflected -30°, $\alpha = 0$, $\beta = 0$

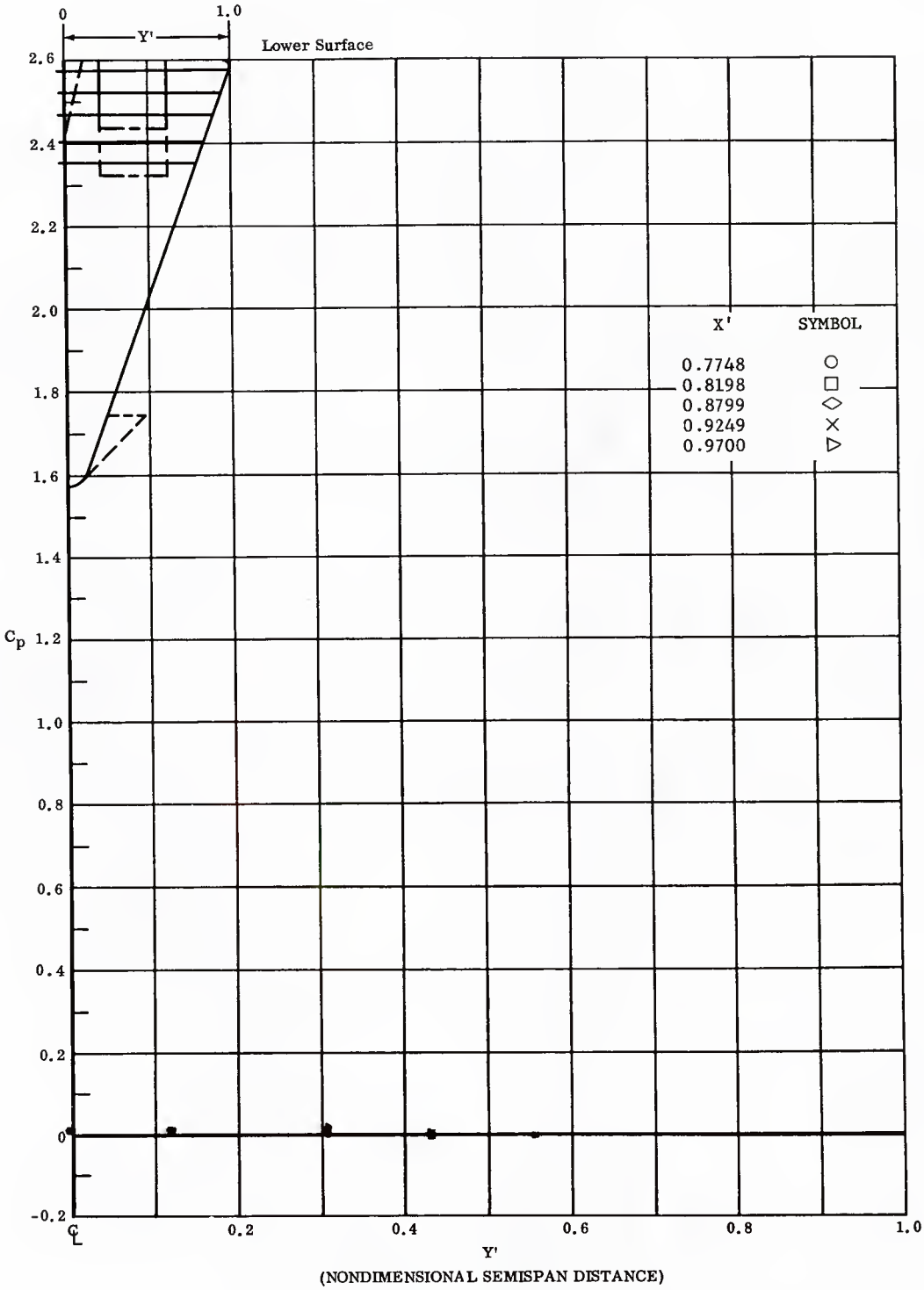

Fig. 39 Spanwise Distributions of Pressure Coefficients on Lower Surface Basic Configuration, Left and Right (Upper) Flaps Deflected -30°, $\alpha = 0$, $\beta = 0$

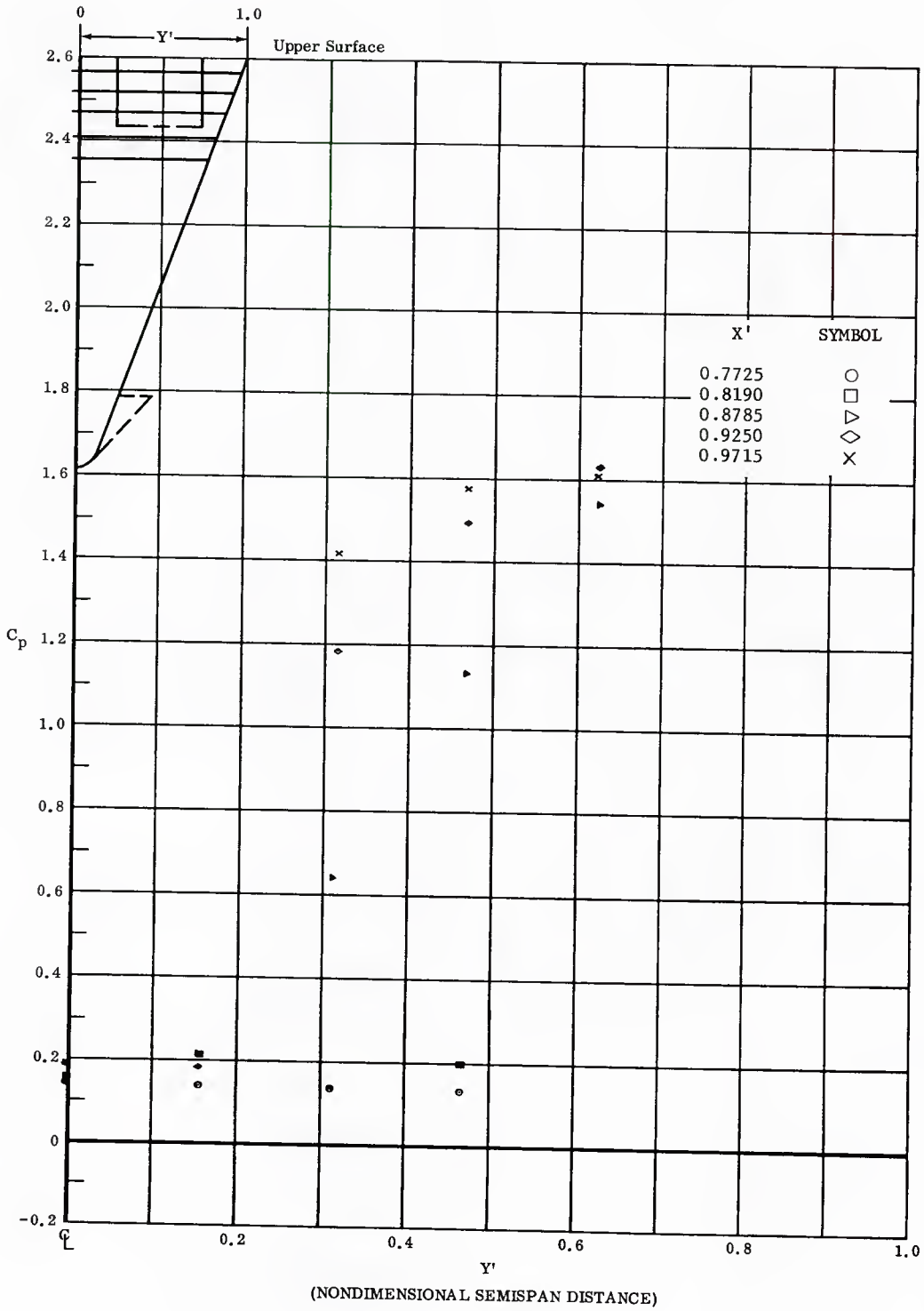

Fig. 39 Spanwise Distributions of Pressure Coefficients on Upper Surface Basic Configuration, Left and Right (Upper) Flaps Deflected -30°, $\alpha = 0$, $\beta = 0$

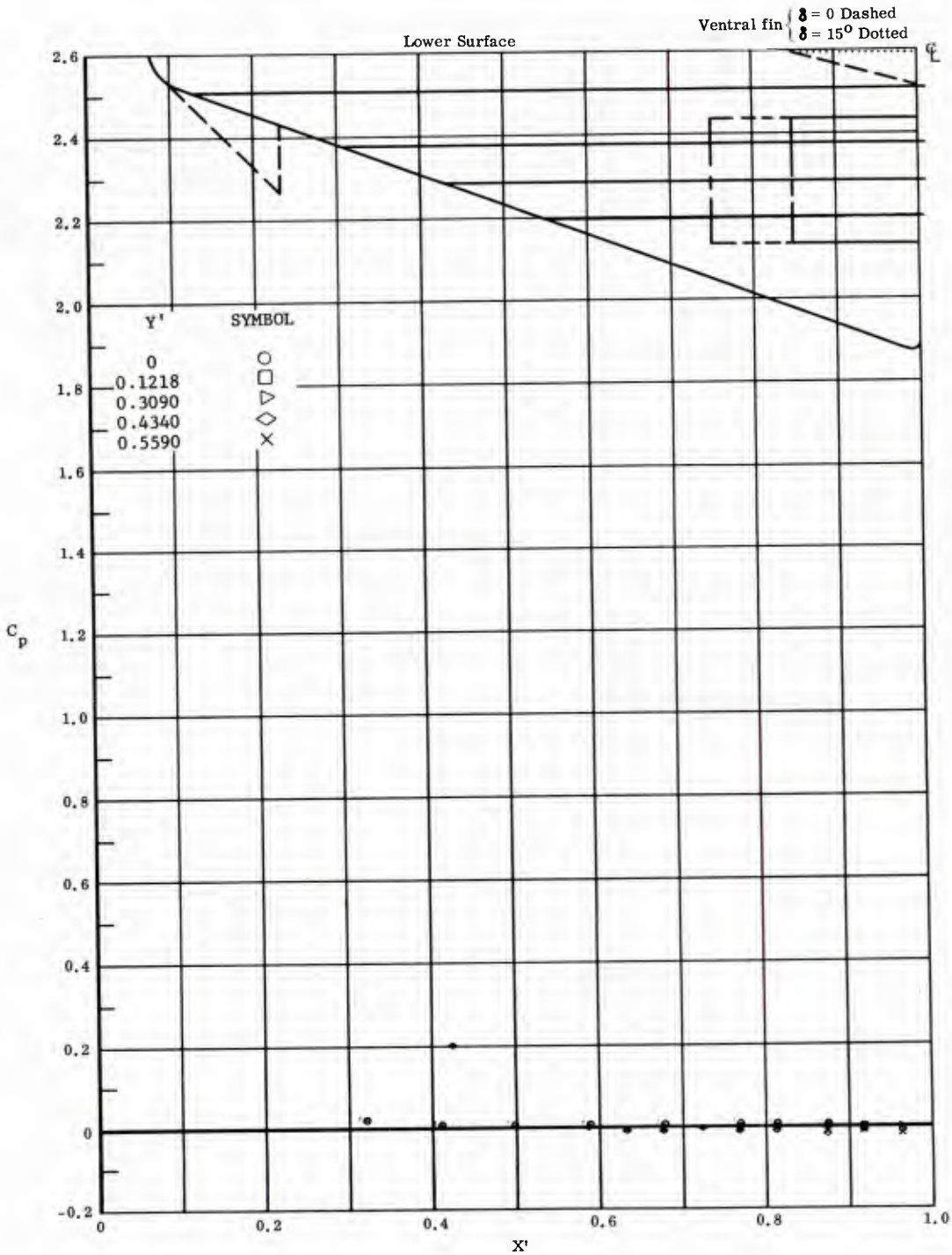

Fig. 40 Streamwise Distributions of Pressure Coefficients on Lower Surface Basic Configuration, No Flap Deflections, $\alpha = 0$, $\beta = 0$

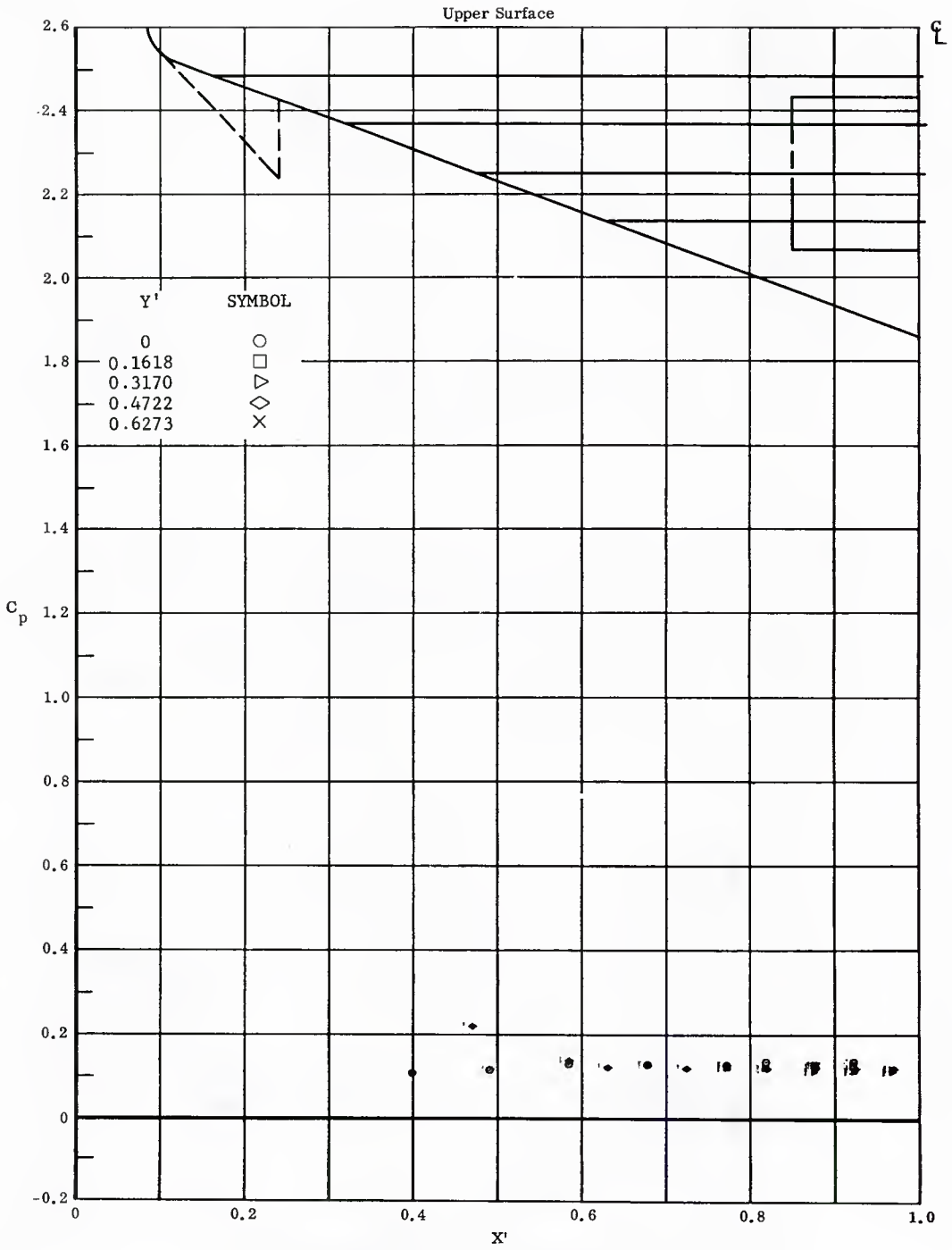

Fig. 40 Streamwise Distributions of Pressure Coefficients on Upper Surface Basic Configuration, No Flap Deflections, $\alpha = 0$, $\beta = 0$

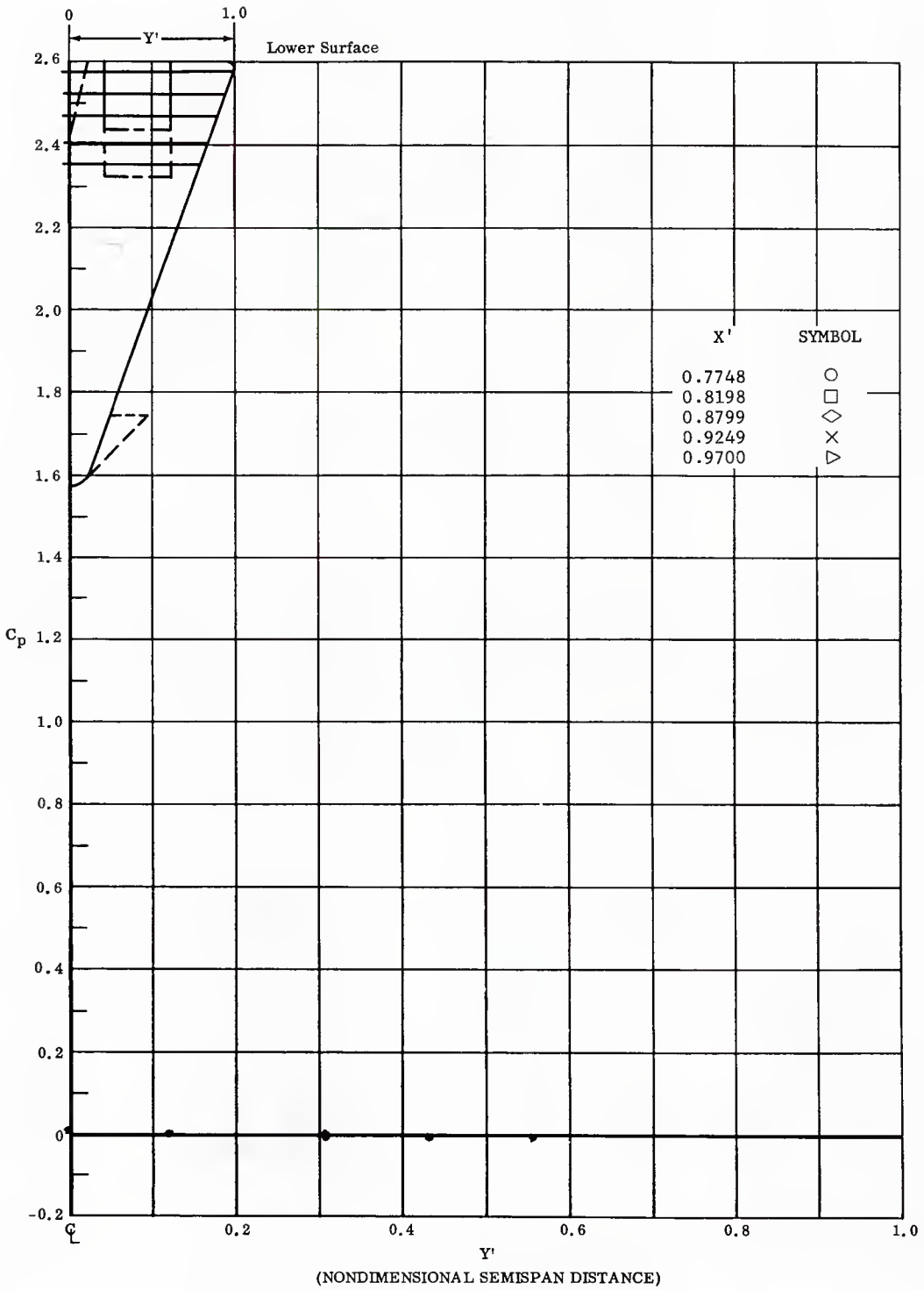

Fig. 40 Spanwise Distributions of Pressure Coefficients on Lower Surface
Basic Configuration, No Flap Deflections, $\alpha = 0$, $\beta = 0$

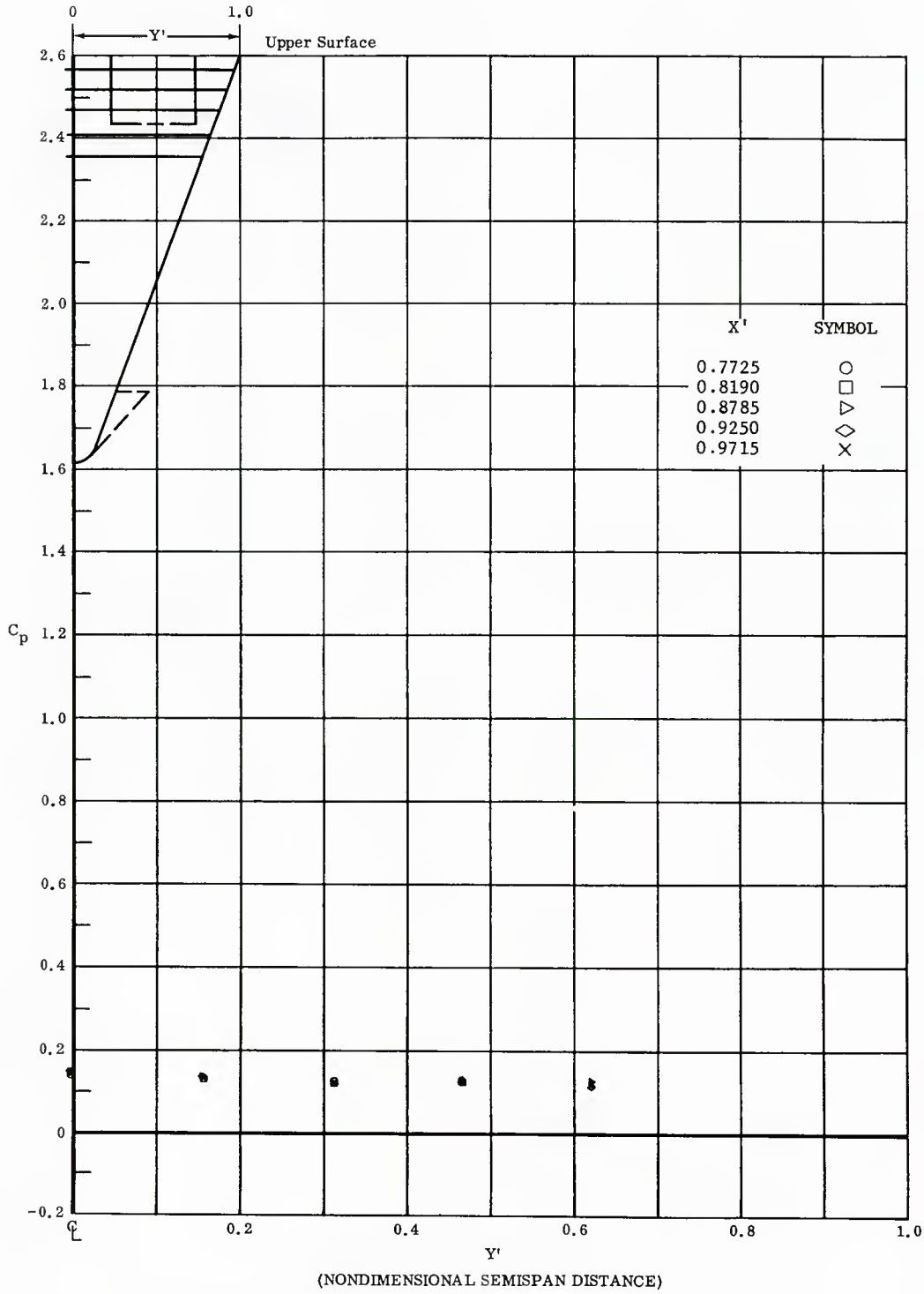

Fig. 40 Spanwise Distributions of Pressure Coefficients on Upper Surface
Basic Configuration, No Flap Deflections, $\alpha = 0$, $\beta = 0$

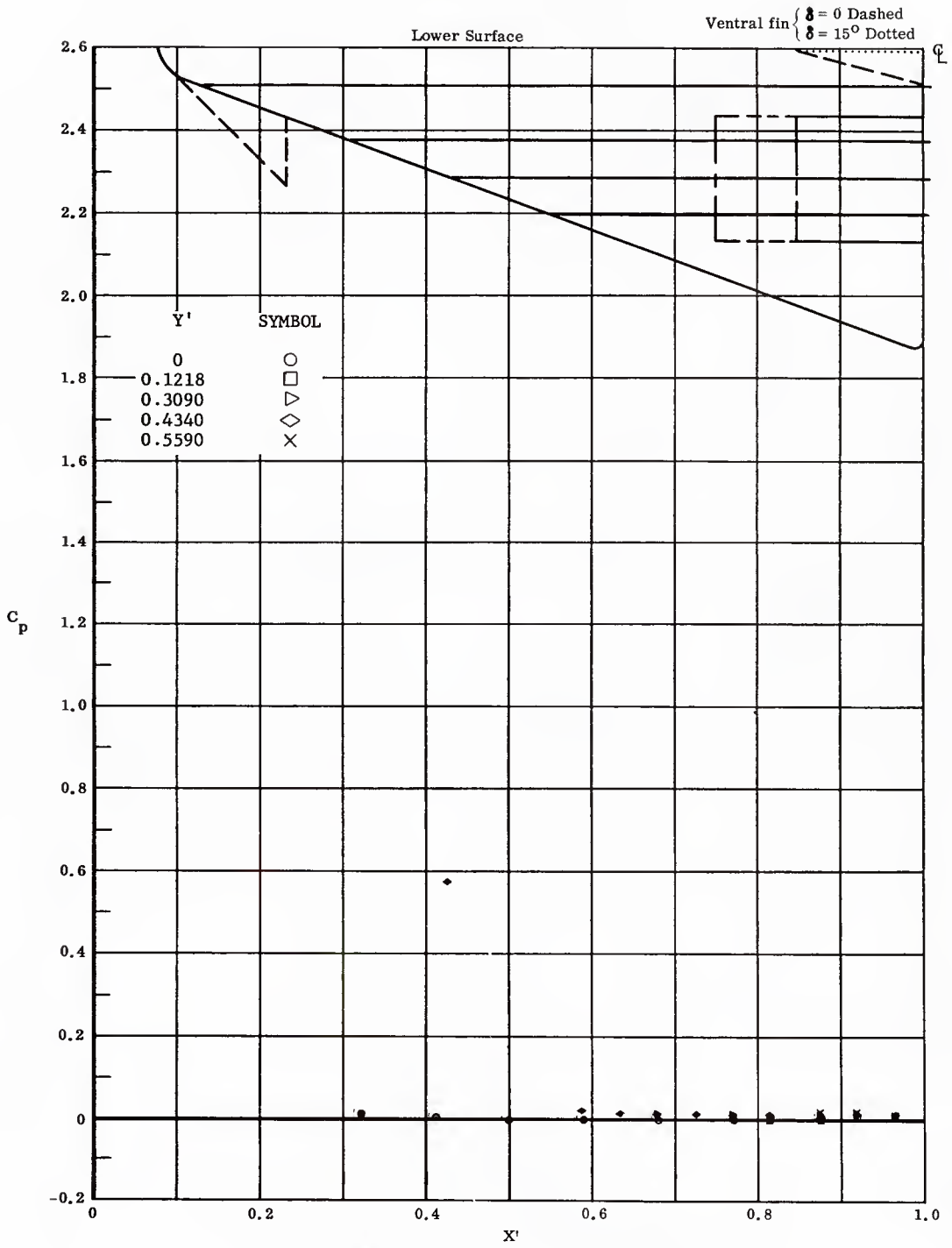

Fig. 41 Streamwise Distributions of Pressure Coefficients on Lower Surface
Basic Configuration, No Flap Deflections, $\alpha = 0$, $\beta = +14^\circ$

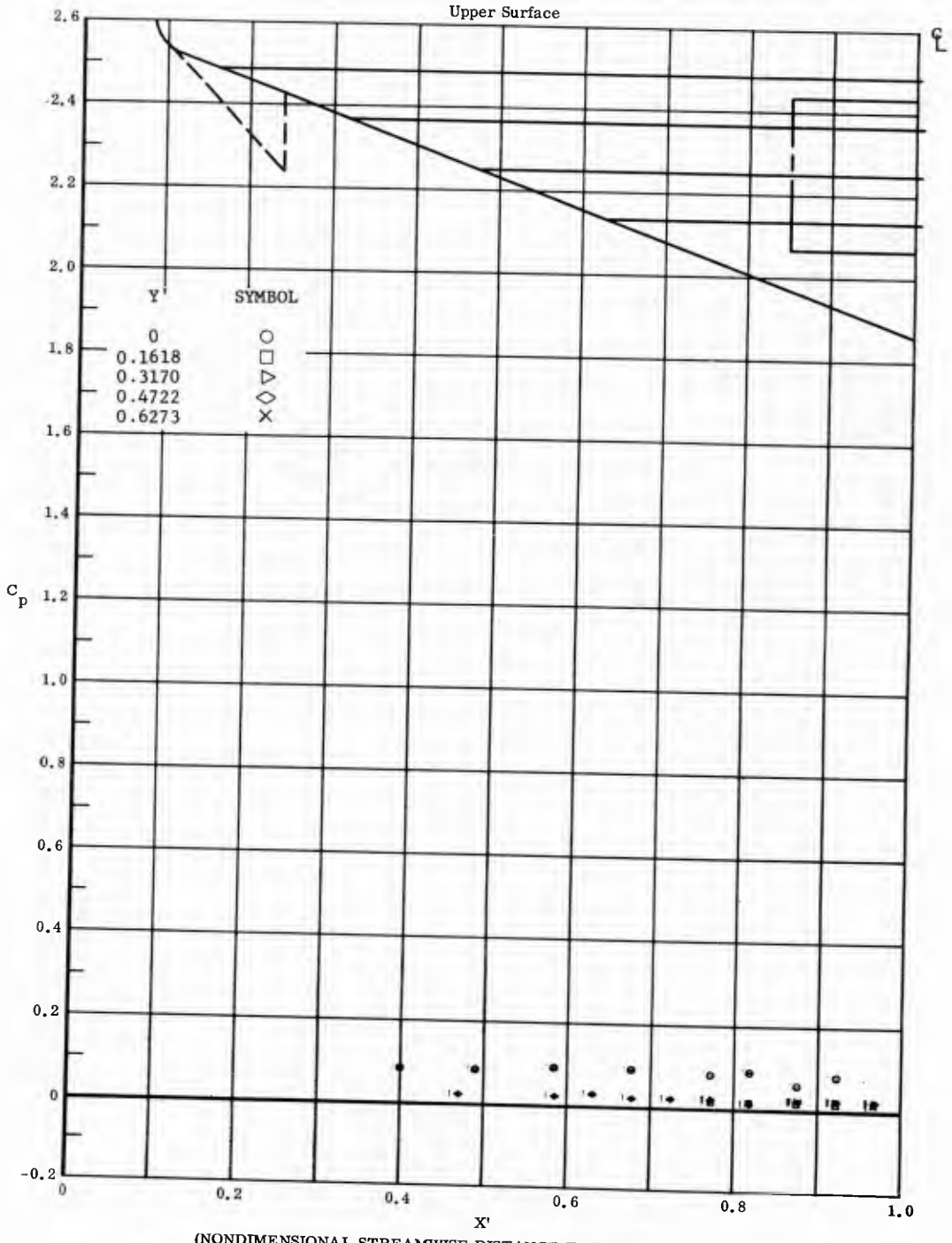

Fig. 41 Streamwise Distributions of Pressure Coefficients on Upper Surface Basic Configuration, No Flap Deflections, $\alpha = 0$, $\beta = +4^\circ$

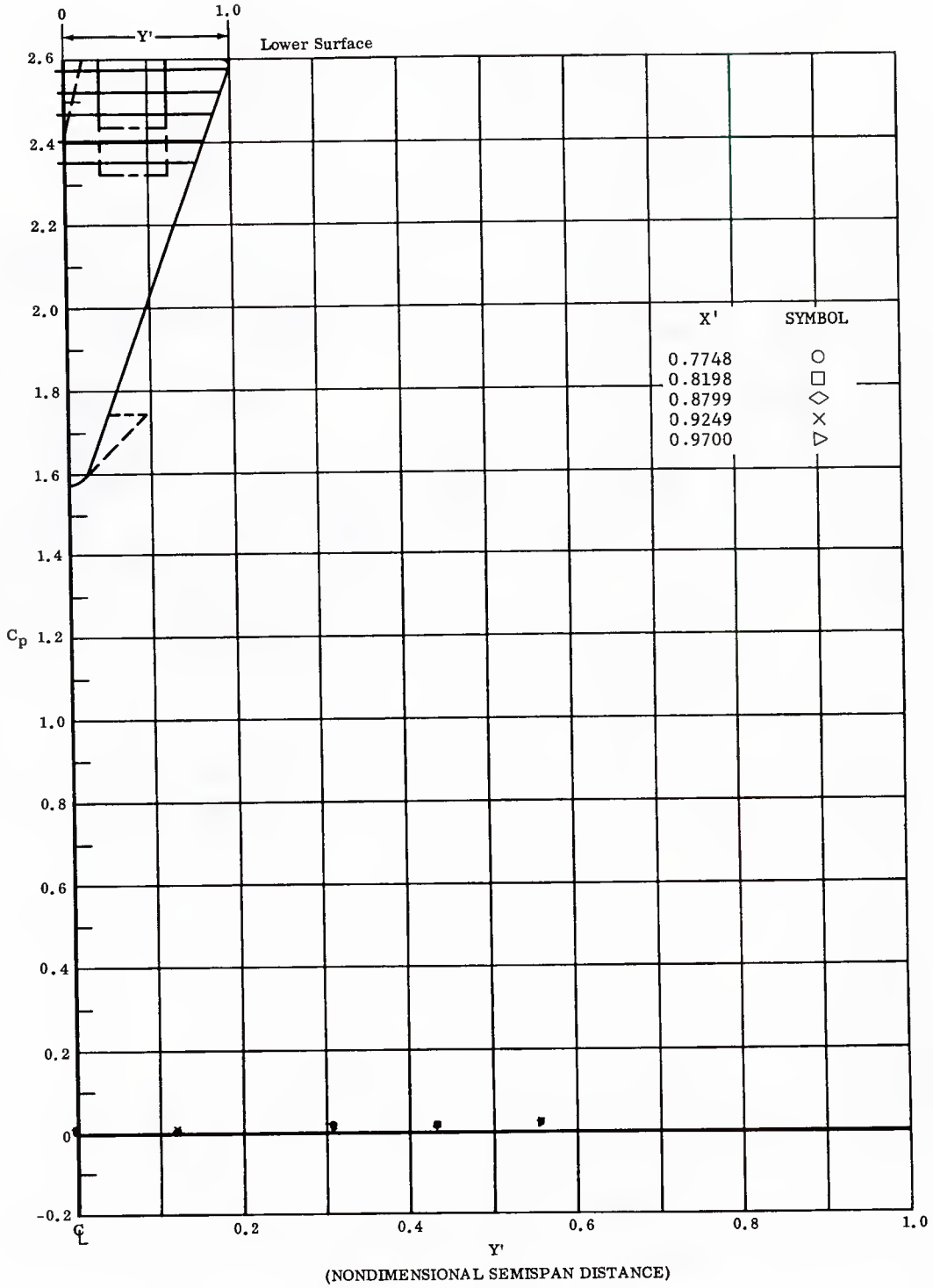

Fig. 41 Spanwise Distributions of Pressure Coefficients on Lower Surface Basic Configuration, No Flap Deflections, $\alpha = 0$, $\beta = +14°$

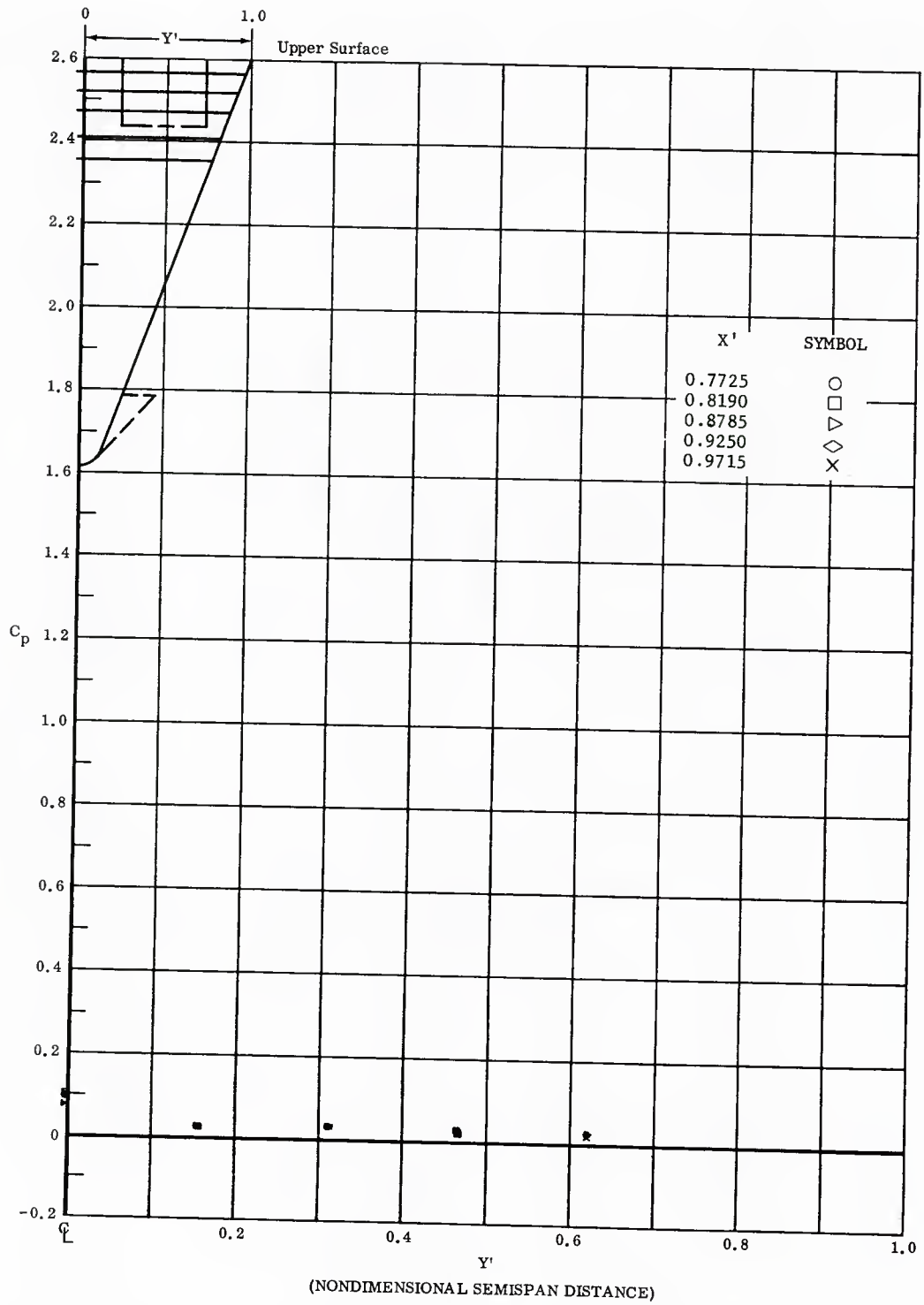

Fig. 41 Spanwise Distributions of Pressure Coefficients on Upper Surface Basic Configuration, No Flap Deflections, $\alpha = 0$, $\beta = +4°$

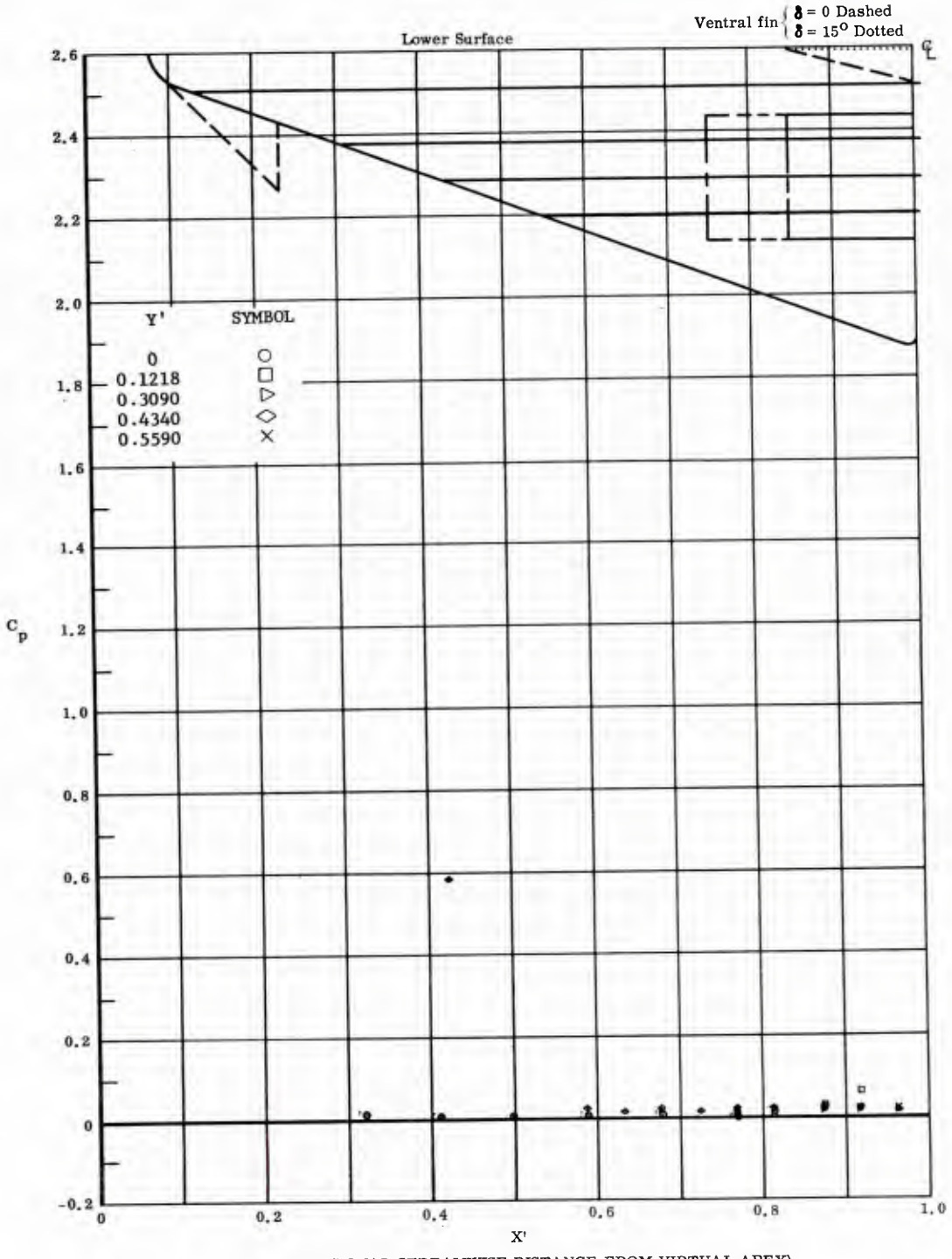

Fig. 42 Streamwise Distributions of Pressure Coefficients on Lower Surface Ventral Fin on Lower Surface Deflected 15°, No Flap Deflections, $\alpha = 0$, $\beta = +11°$

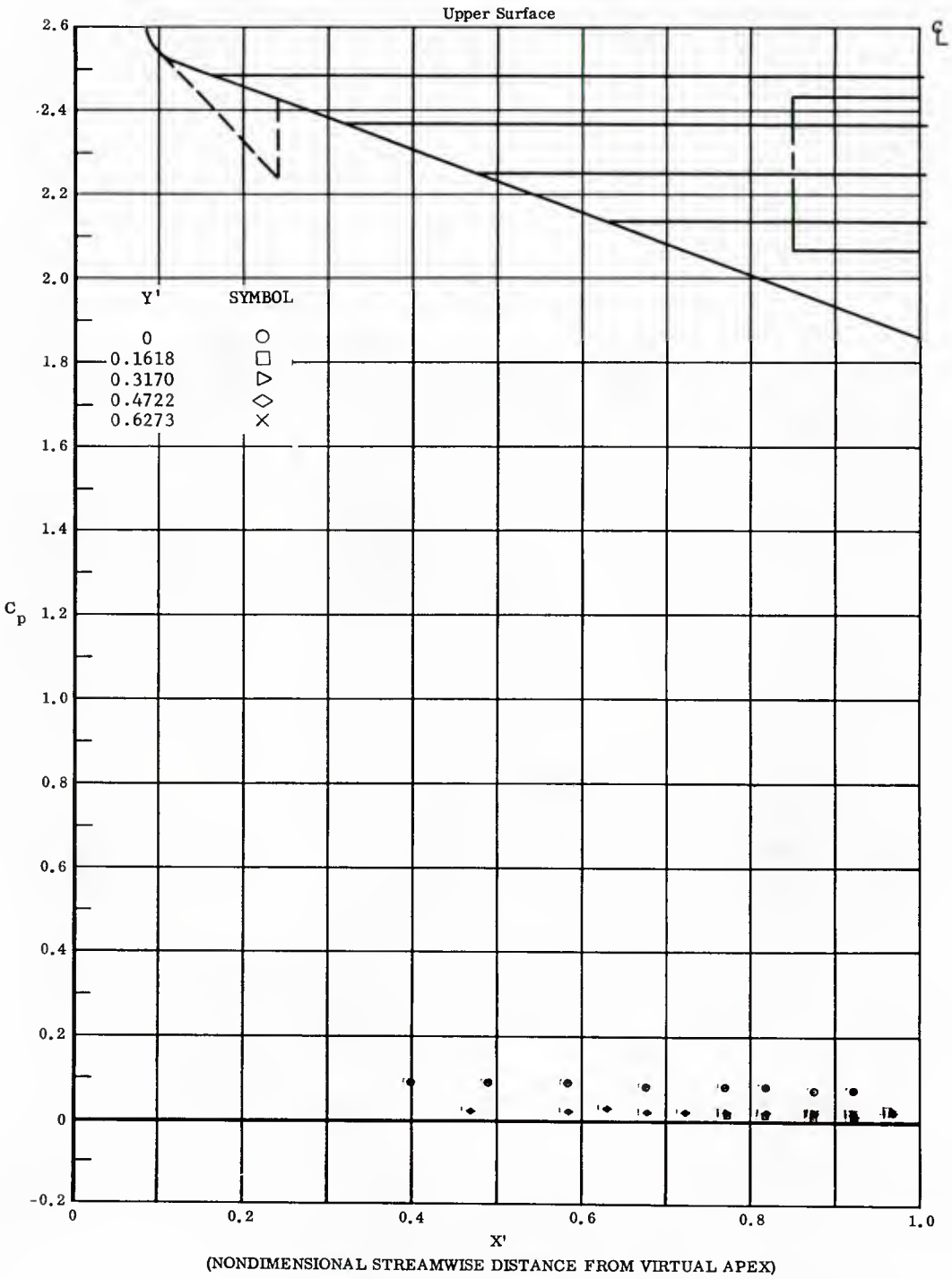

Fig. 42 Streamwise Distributions of Pressure Coefficients on Upper Surface Ventral Fin on Lower Surface Deflected 15°, No Flap Deflections, $\alpha = 0, \beta = +14°$

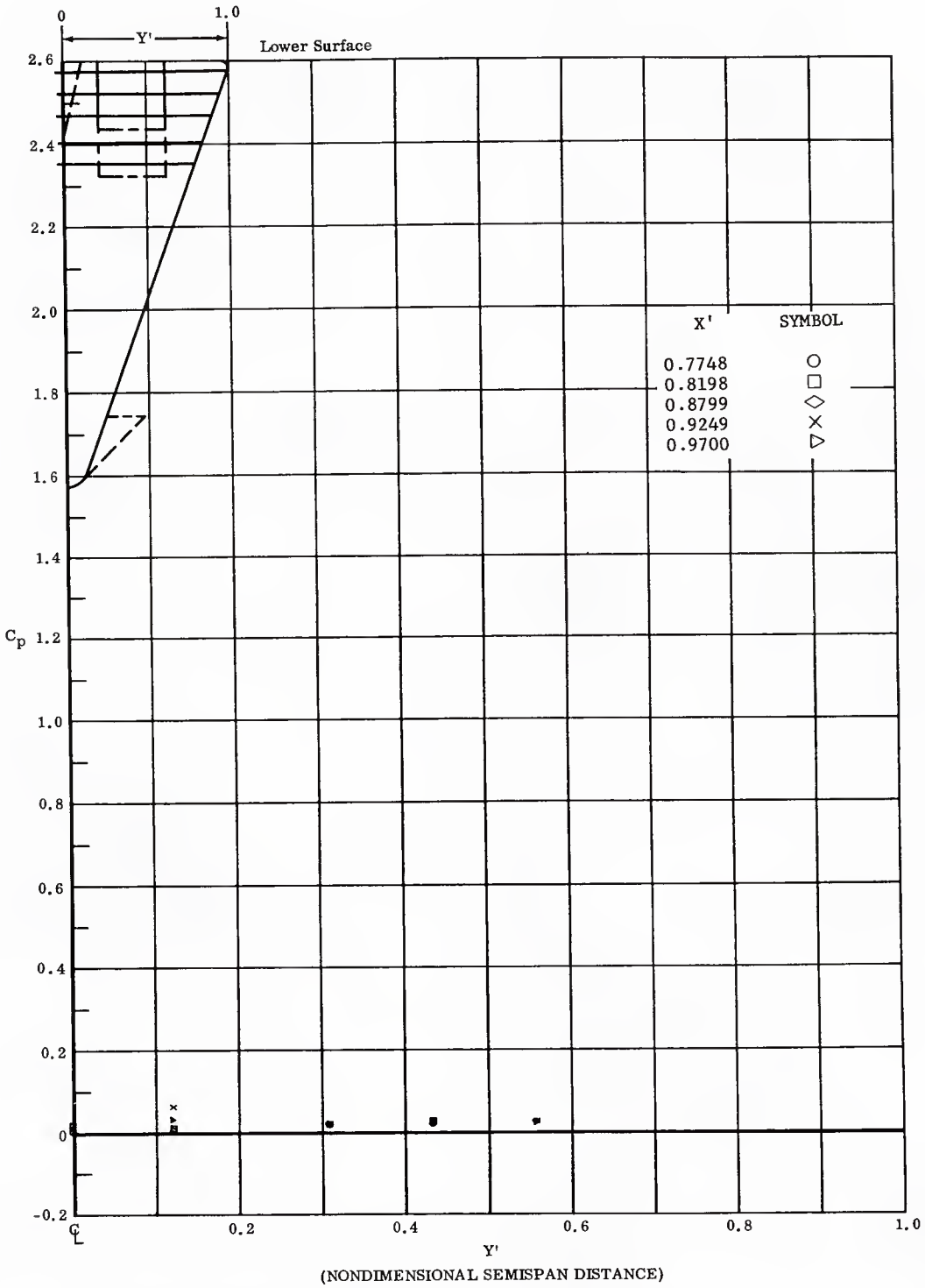

Fig. 42 Spanwise Distributions of Pressure Coefficients on Lower Surface Ventral Fin on Lower Surface Deflected 15°, No Flap Delfections, $\alpha = 0$, $\beta = +14°$

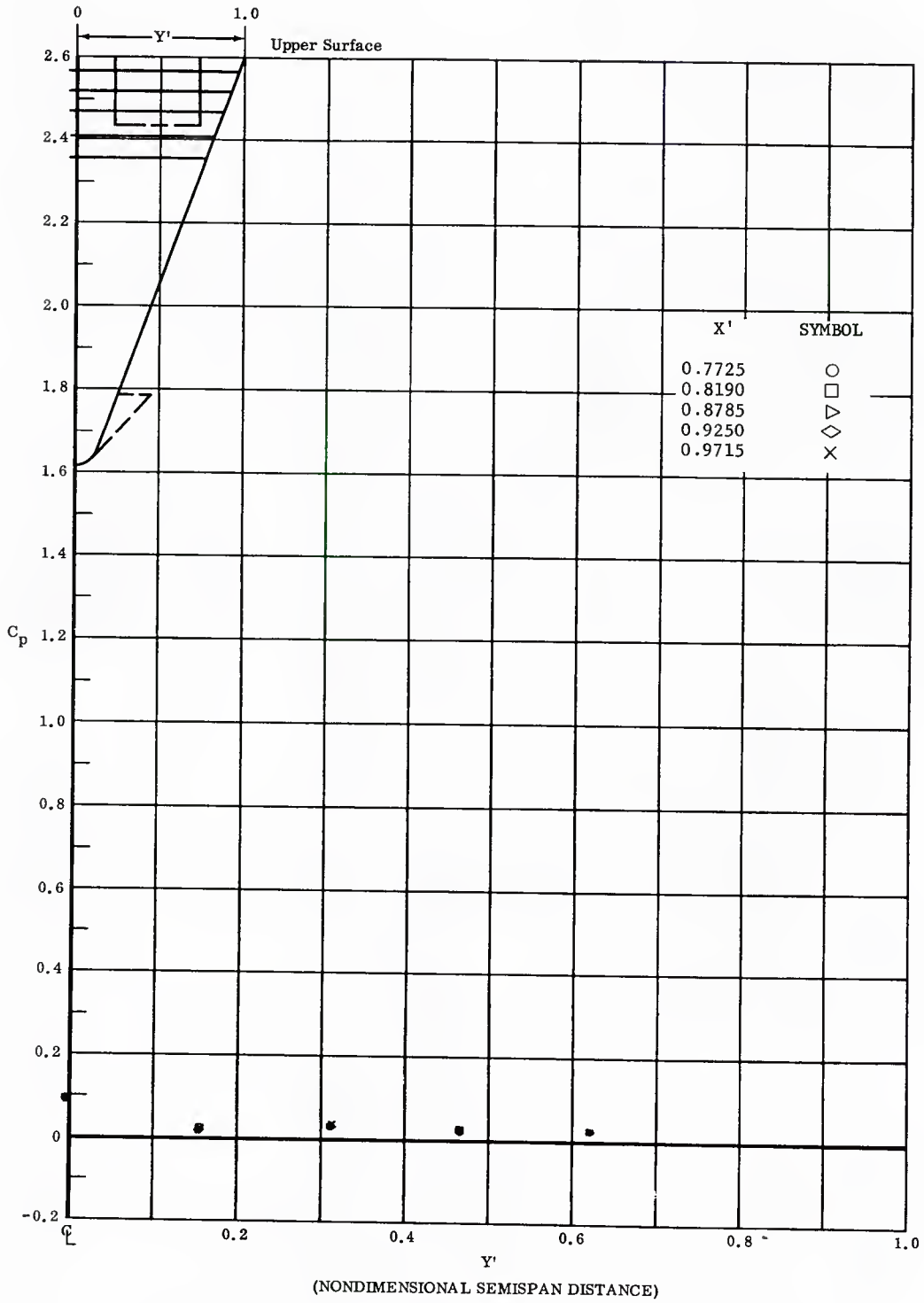

Fig. 42 Spanwise Distributions of Pressure Coefficients on Upper Surface Ventral Fin on Lower Surface Deflected 15°, No Flap Deflections, $\alpha = 0, \beta = +14°$

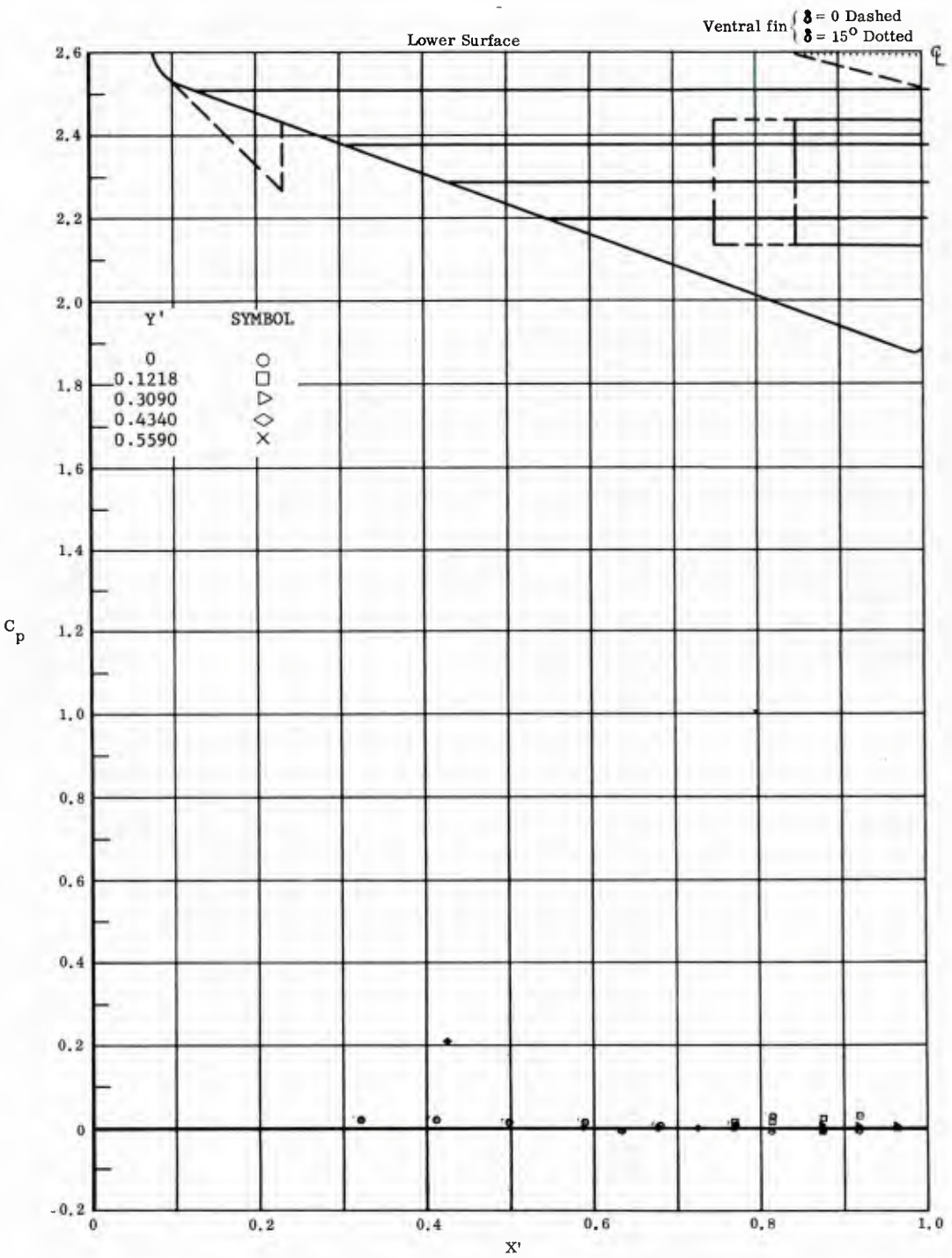

Fig. 43 Streamwise Distributions of Pressure Coefficients on Lower Surface Ventral Fin on Lower Surface Deflected 15°, No Flap Deflections, $\alpha = 0$, $\beta = 0$

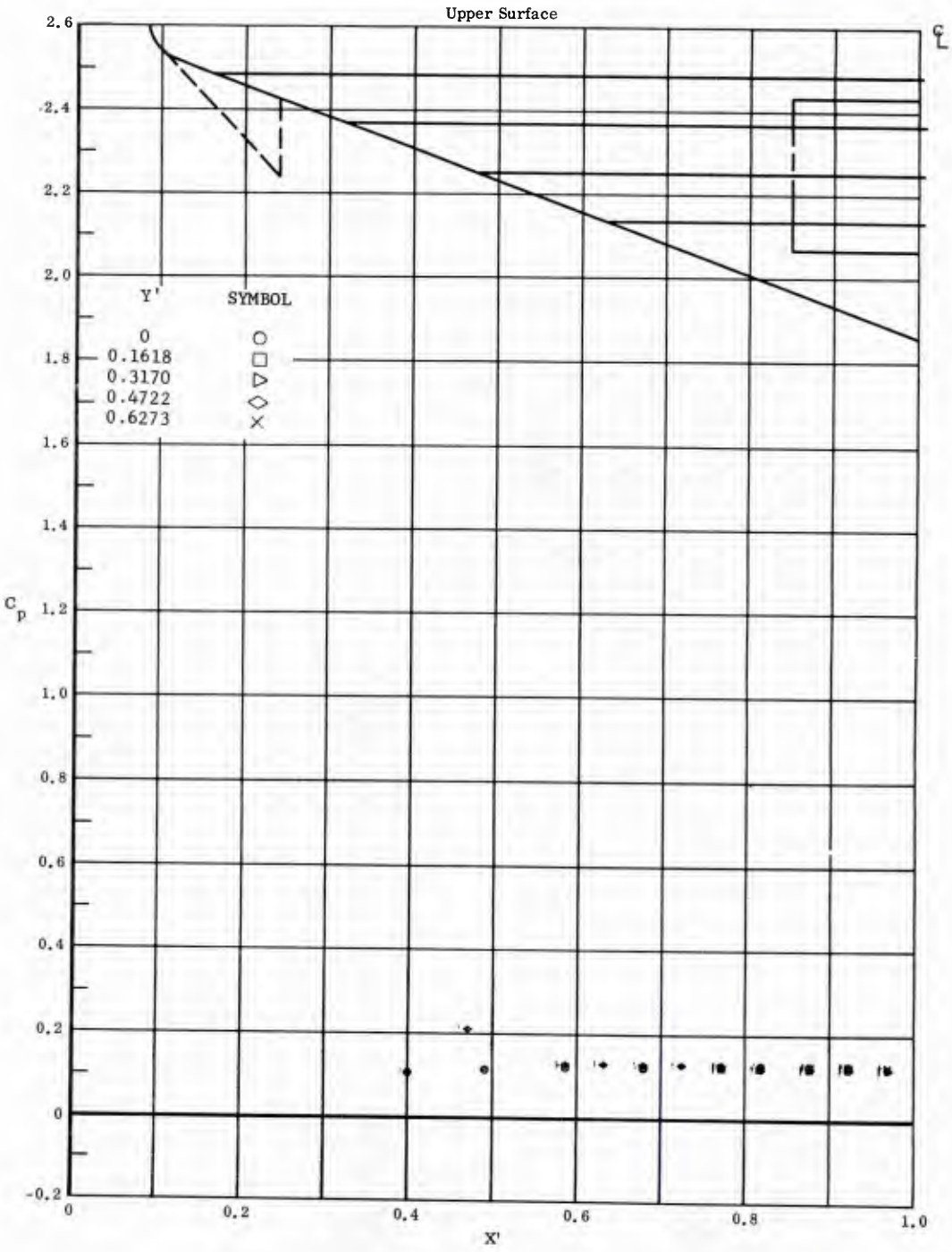

Fig. 43 Streamwise Distributions of Pressure Coefficients on Upper Surface Ventral Fin on Lower Surface Deflected 15°, No Flap Deflections, $\alpha = 0$, $\beta = 0$

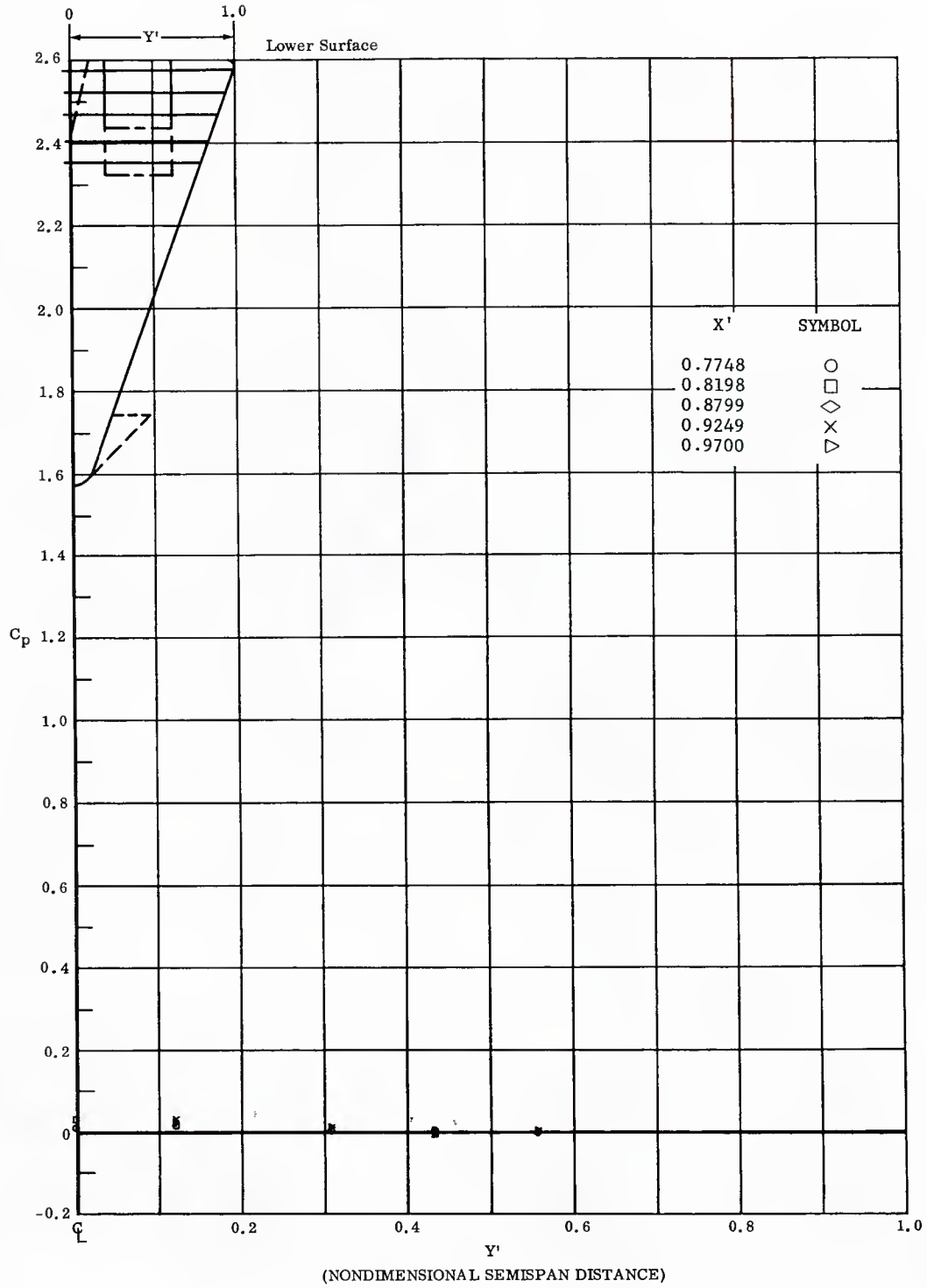

Fig. 43 Spanwise Distributions of Pressure Coefficients on Lower Surface Ventral Fin on Lower Surface Deflected 15°, No Flap Deflections, $\alpha = 0, \beta = 0$

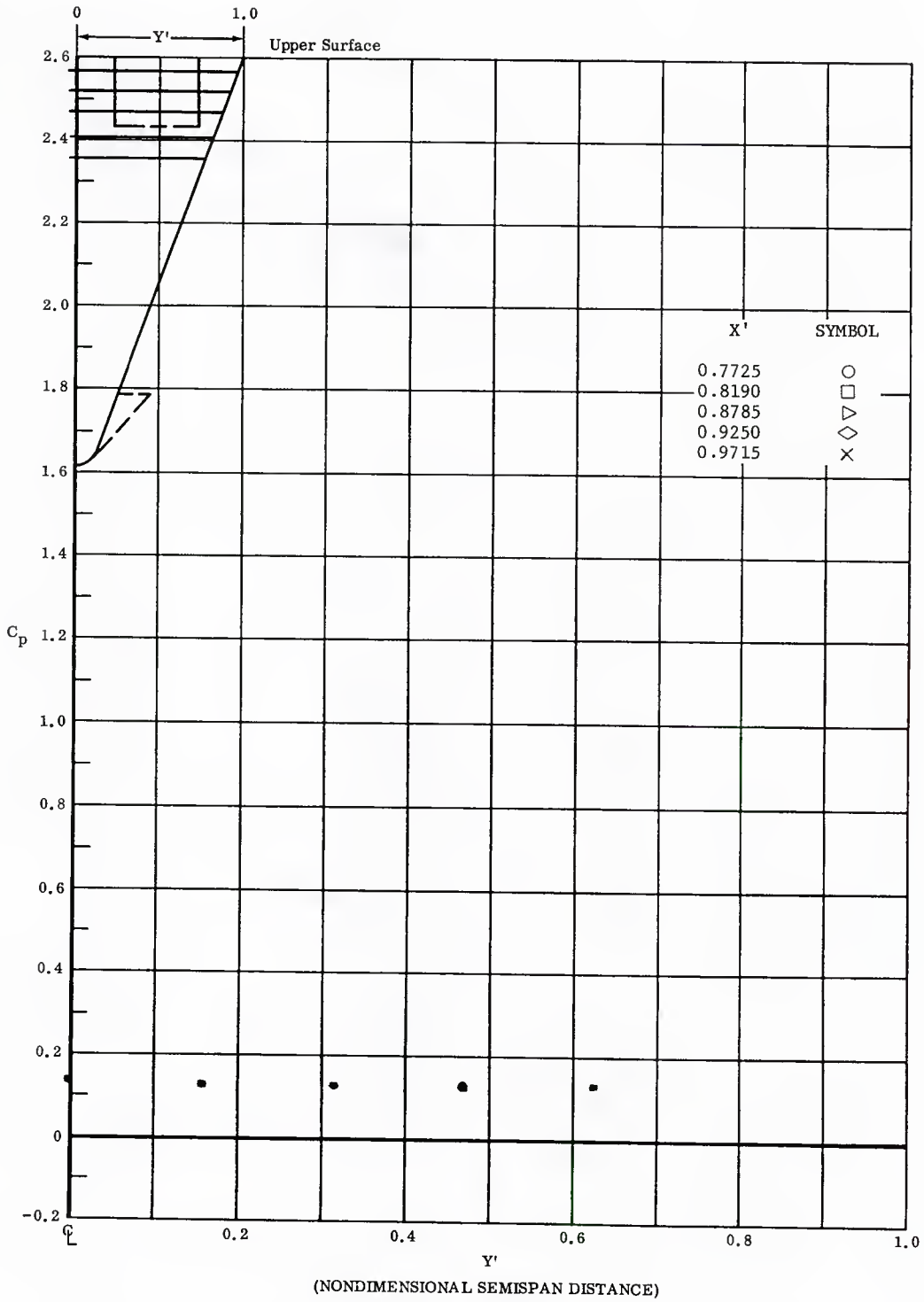

Fig. 43 Spanwise Distributions of Pressure Coefficients on Upper Surface Ventral Fin on Lower Surface Deflected 15°, No Flap Deflections, $\alpha = 0, \beta = 0$

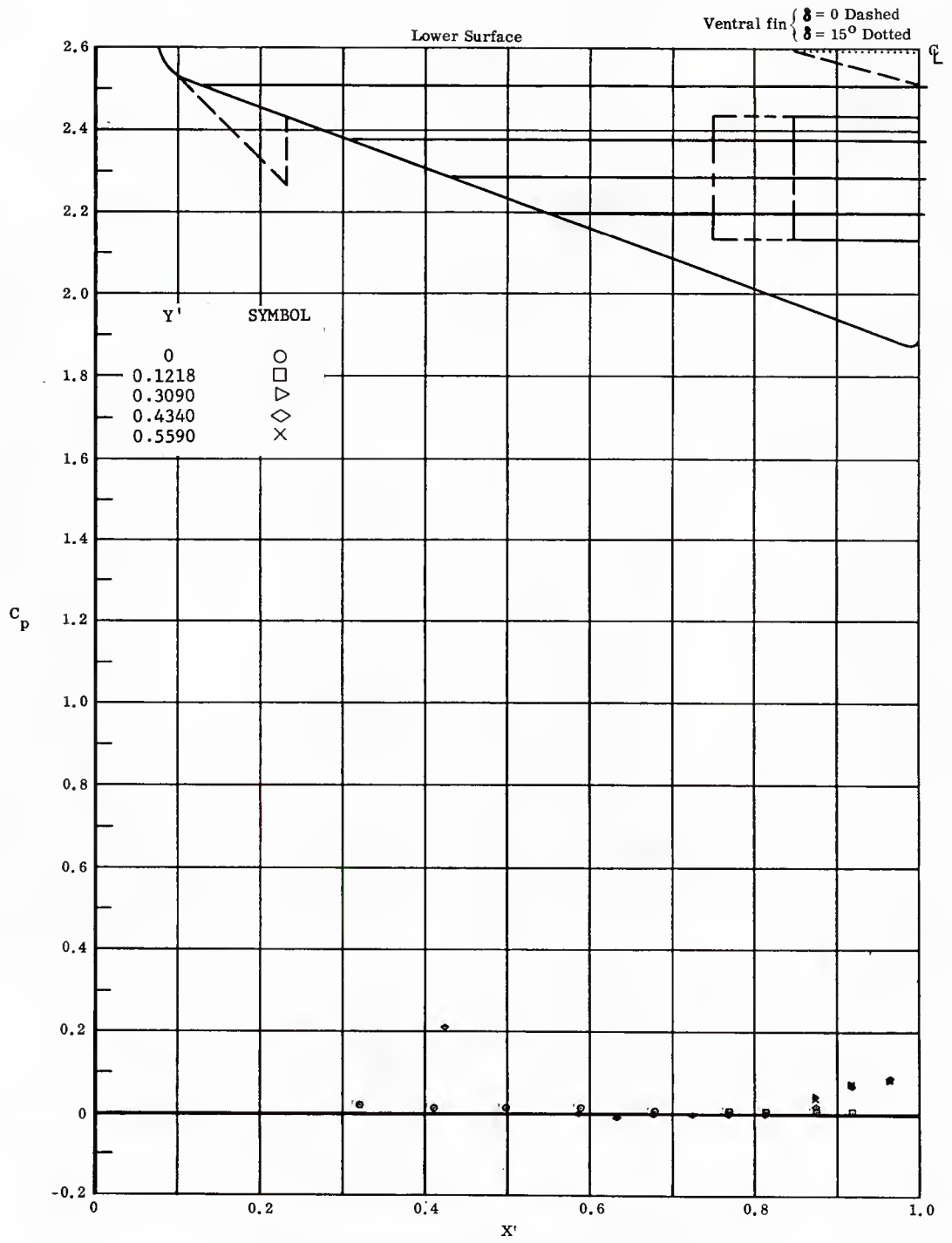

Fig. 44 Streamwise Distributions of Pressure Coefficients on Lower Surface
Basic Configuration, Bottom Flaps Deflected 10°, α = 0, β = 0

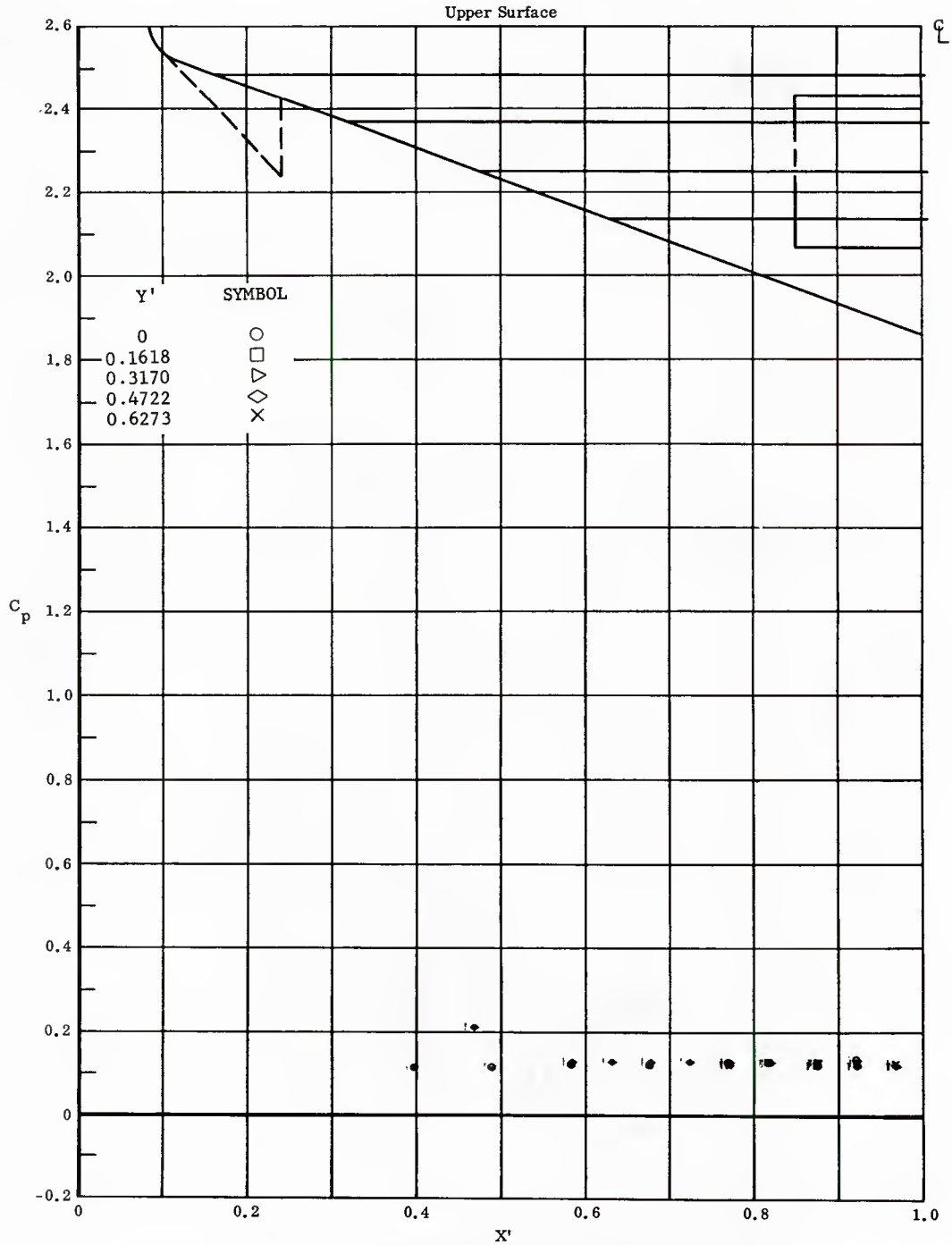

Fig. 44 Streamwise Distributions of Pressure Coefficients on Upper Surface
Basic Configuration, Bottom Flaps Deflected 10°, $\alpha = 0$, $\beta = 0$

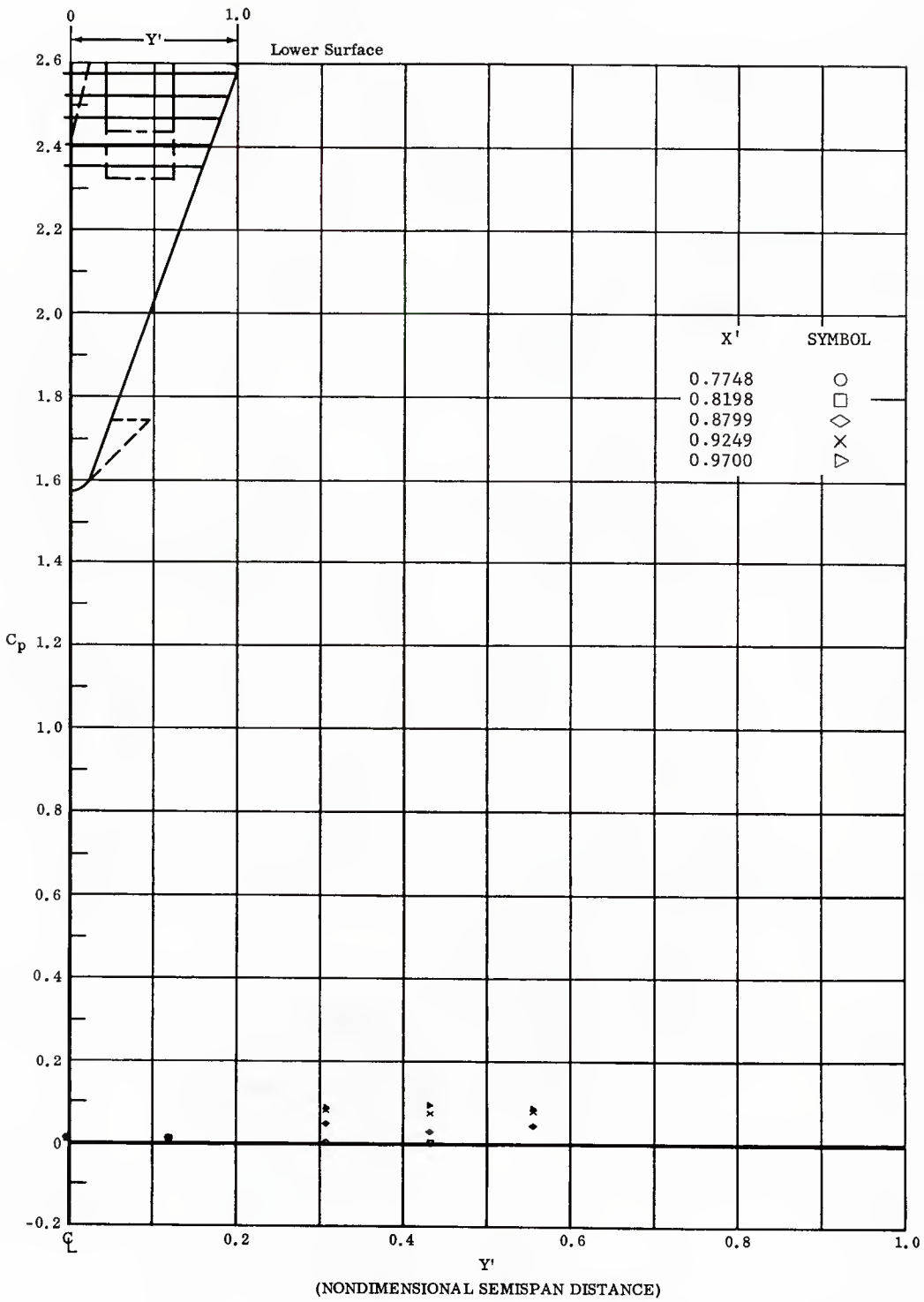

Fig. 44 Spanwise Distributions of Pressure Coefficients on Lower Surface
Basic Configuration, Bottom Flaps Deflected 10°, $\alpha = 0$, $\beta = 0$

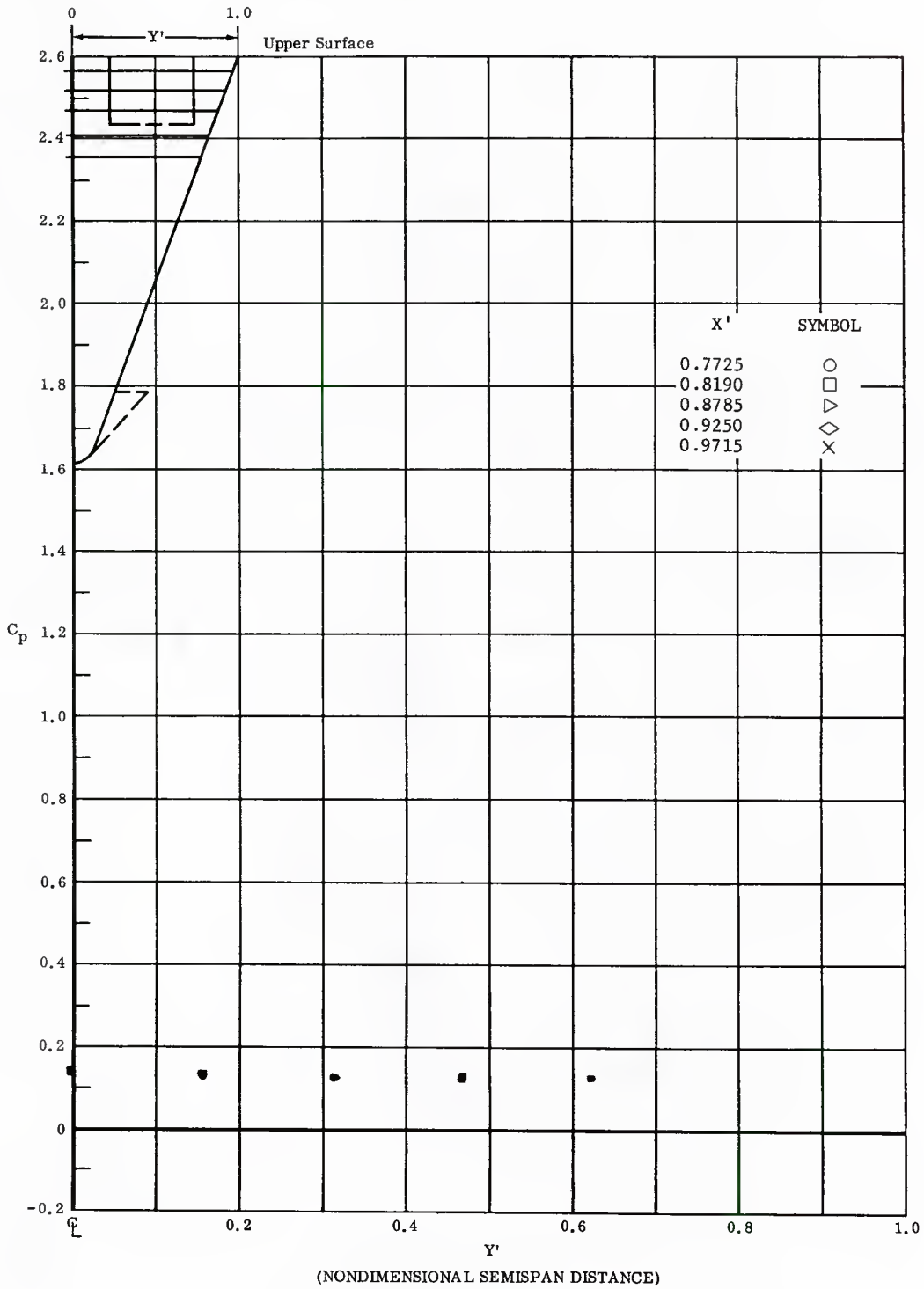

Fig. 44 Spanwise Distributions of Pressure Coefficients on Upper Surface Basic Configuration, Bottom Flaps Deflected 10°, $\alpha = 0$, $\beta = 0$

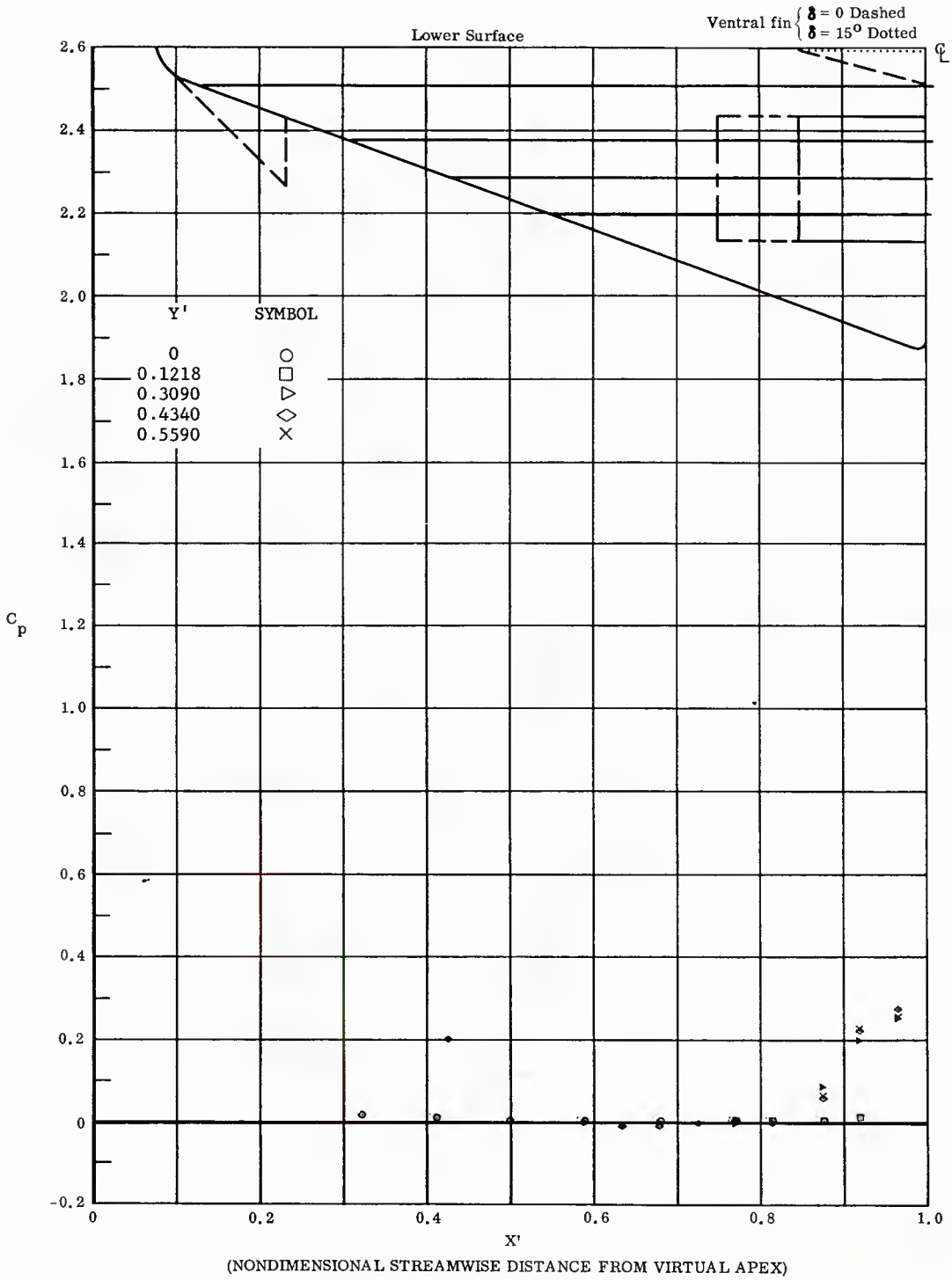

Fig. 45 Streamwise Distributions of Pressure Coefficients on Lower Surface
Basic Configuration, Bottom Flaps Deflected 20°, $\alpha = 0$, $\beta = 0$

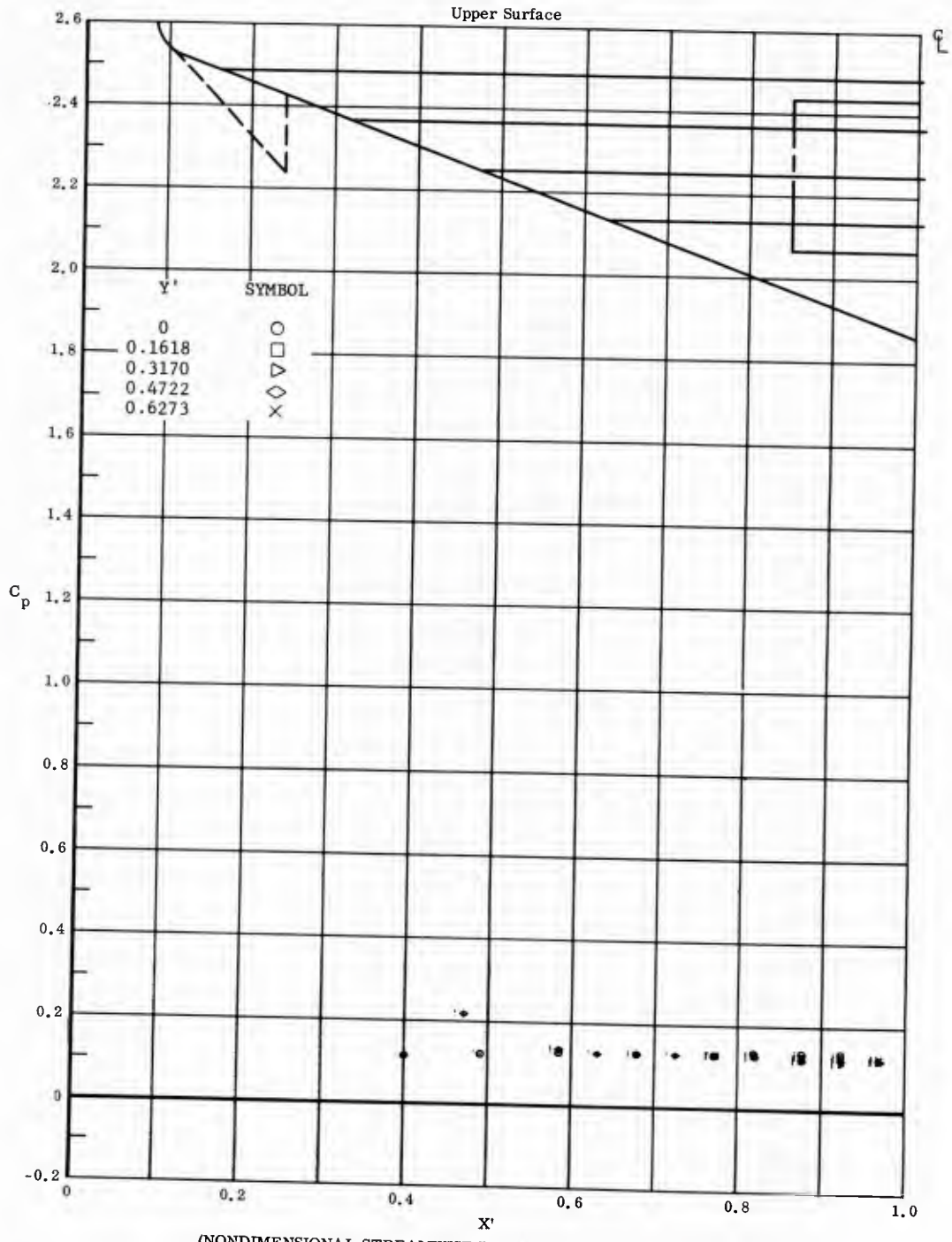

Fig. 45 Streamwise Distributions of Pressure Coefficients on Upper Surface Basic Configuration, Bottom Flaps Deflected 20°, $\alpha = 0$, $\beta = 0$

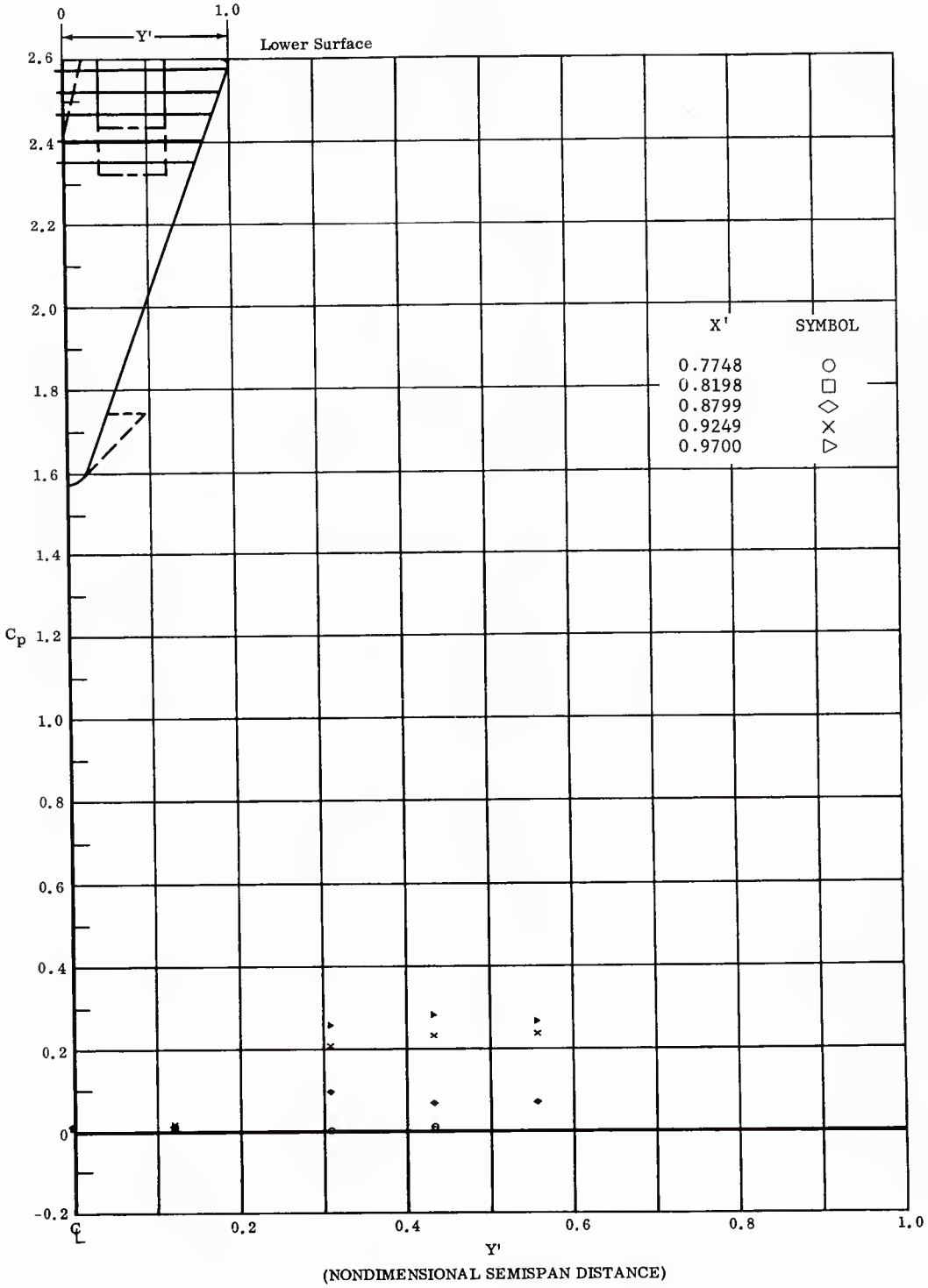

Fig. 45 Spanwise Distributions of Pressure Coefficients on Lower Surface
Basic Configuration, Bottom Flaps Deflected 20°, $\alpha = 0$, $\beta = 0$

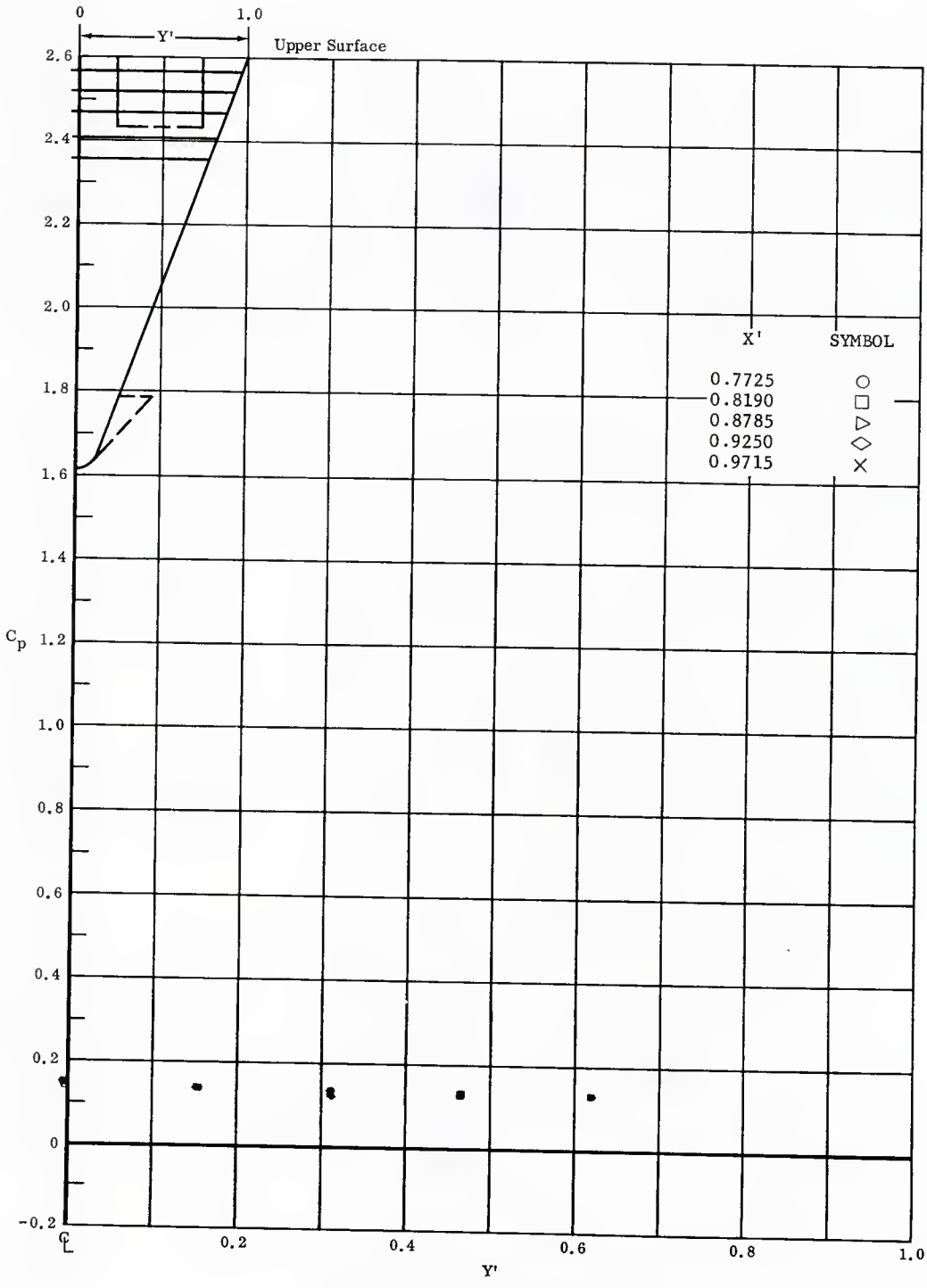

Fig. 45 Spanwise Distributions of Pressure Coefficients on Upper Surface Basic Configuration, Bottom Flaps Deflected 20°, $\alpha = 0$, $\beta = 0$

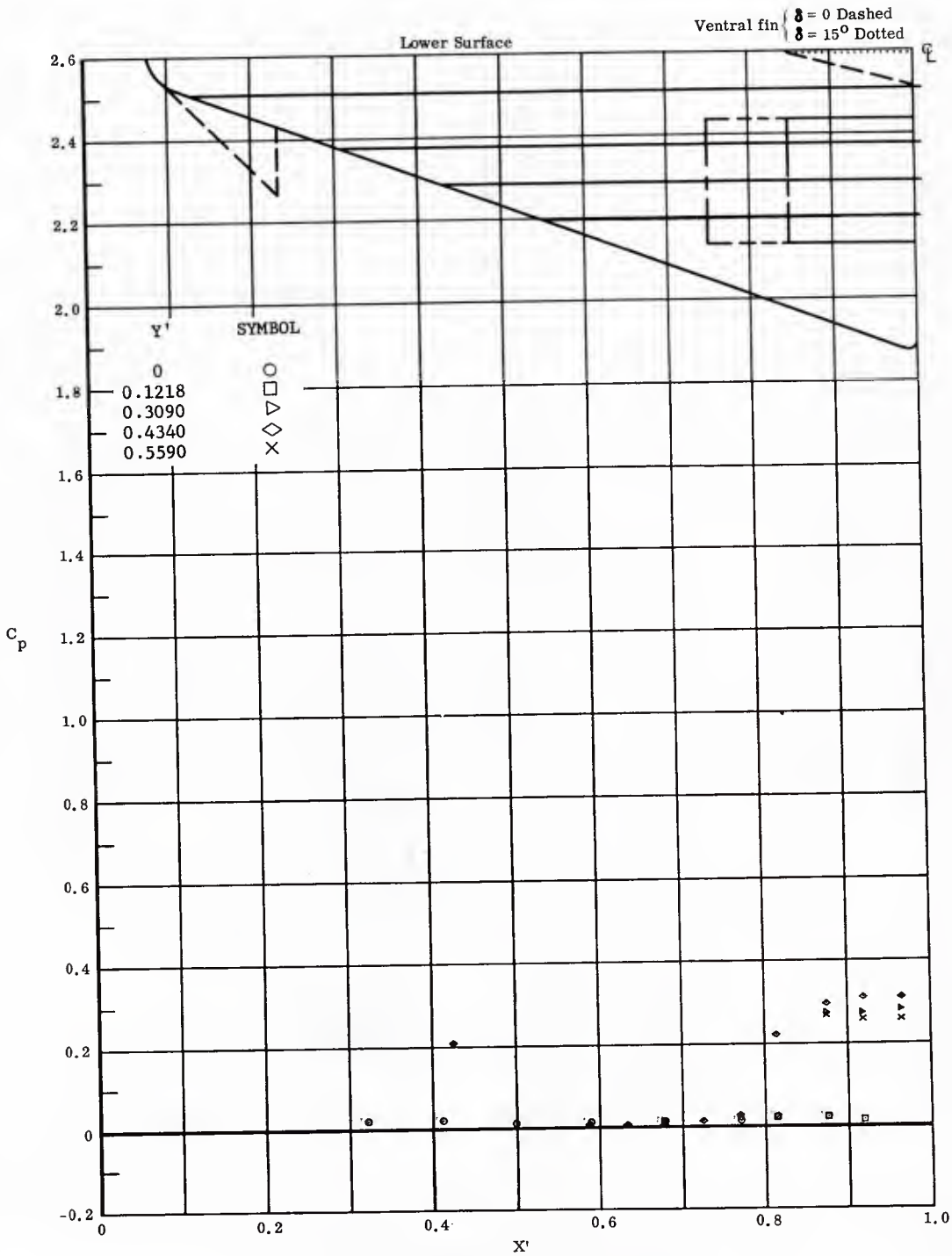

Fig. 46 Streamwise Distributions of Pressure Coefficients on Lower Surface
Extended (Long Chord) Flaps on Lower Surface,
Bottom Flaps Deflected 20°, α = 0, β = 0

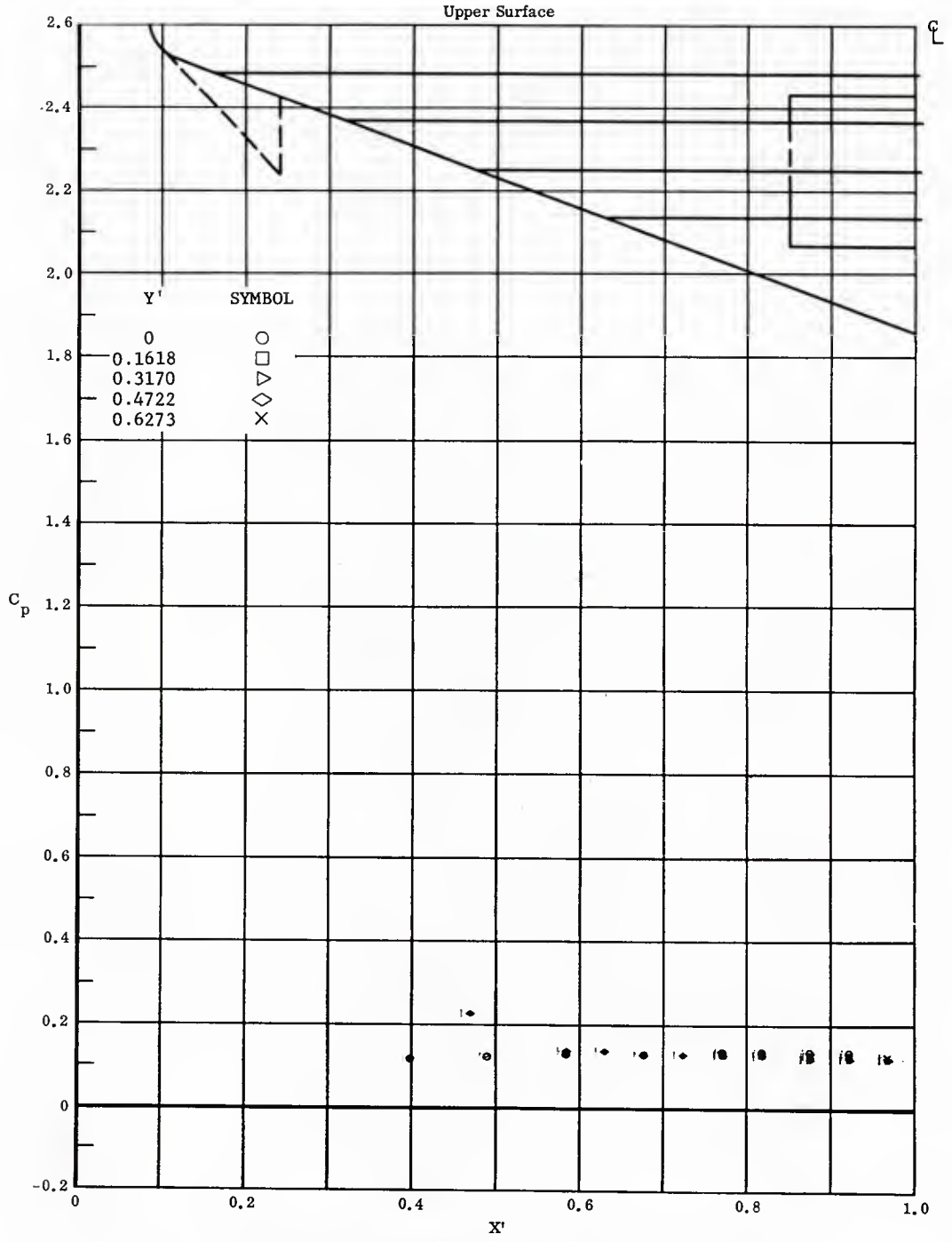

Fig. 46 Streamwise Distributions of Pressure Coefficients on Upper Surface Extended (Long Chord) Flaps on Lower Surface, Bottom Flaps Deflected 20°, $\alpha = 0$, $\beta = 0$

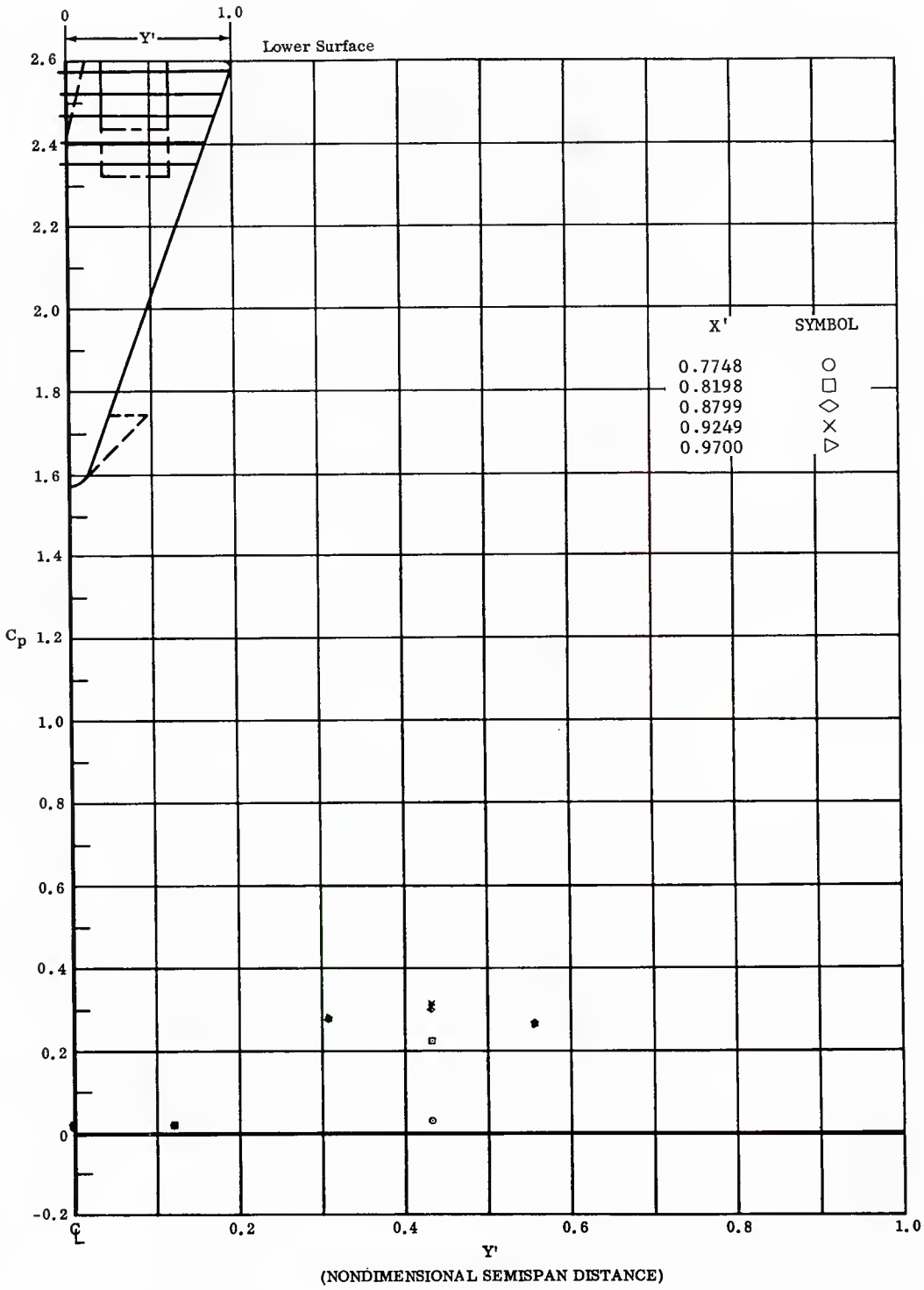

Fig. 46 Spanwise Distributions of Pressure Coefficients on Lower Surface Extended (Long Chord) Flaps on Lower Surface, Bottom Flaps Deflected 20°, $\alpha = 0$, $\beta = 0$

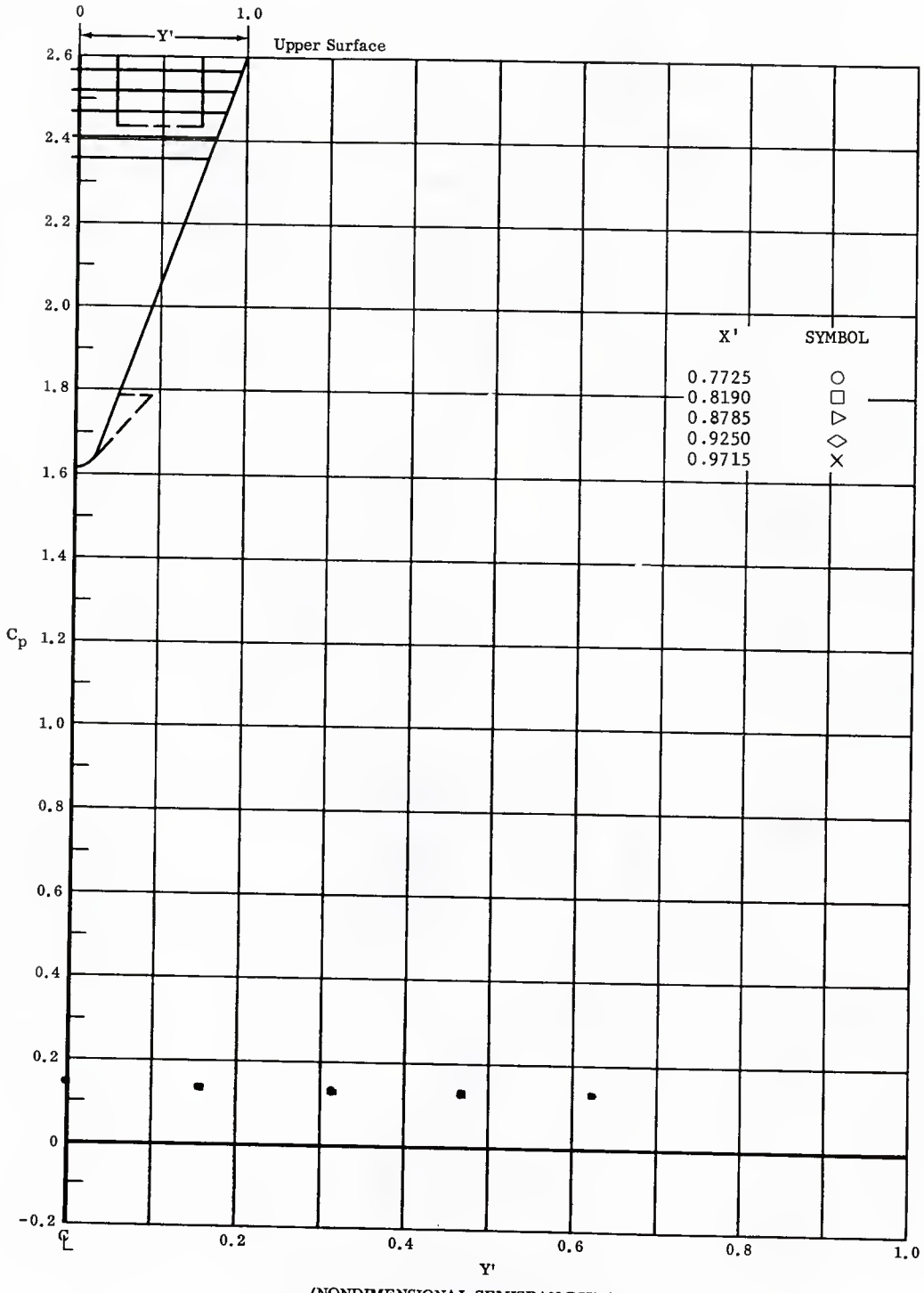

Fig. 46 Spanwise Distributions of Pressure Coefficients on Upper Surface
Extended (Long Chord) Flaps on Lower Surface,
Bottom Flaps Deflected 20°, $\alpha = 0$, $\beta = 0$

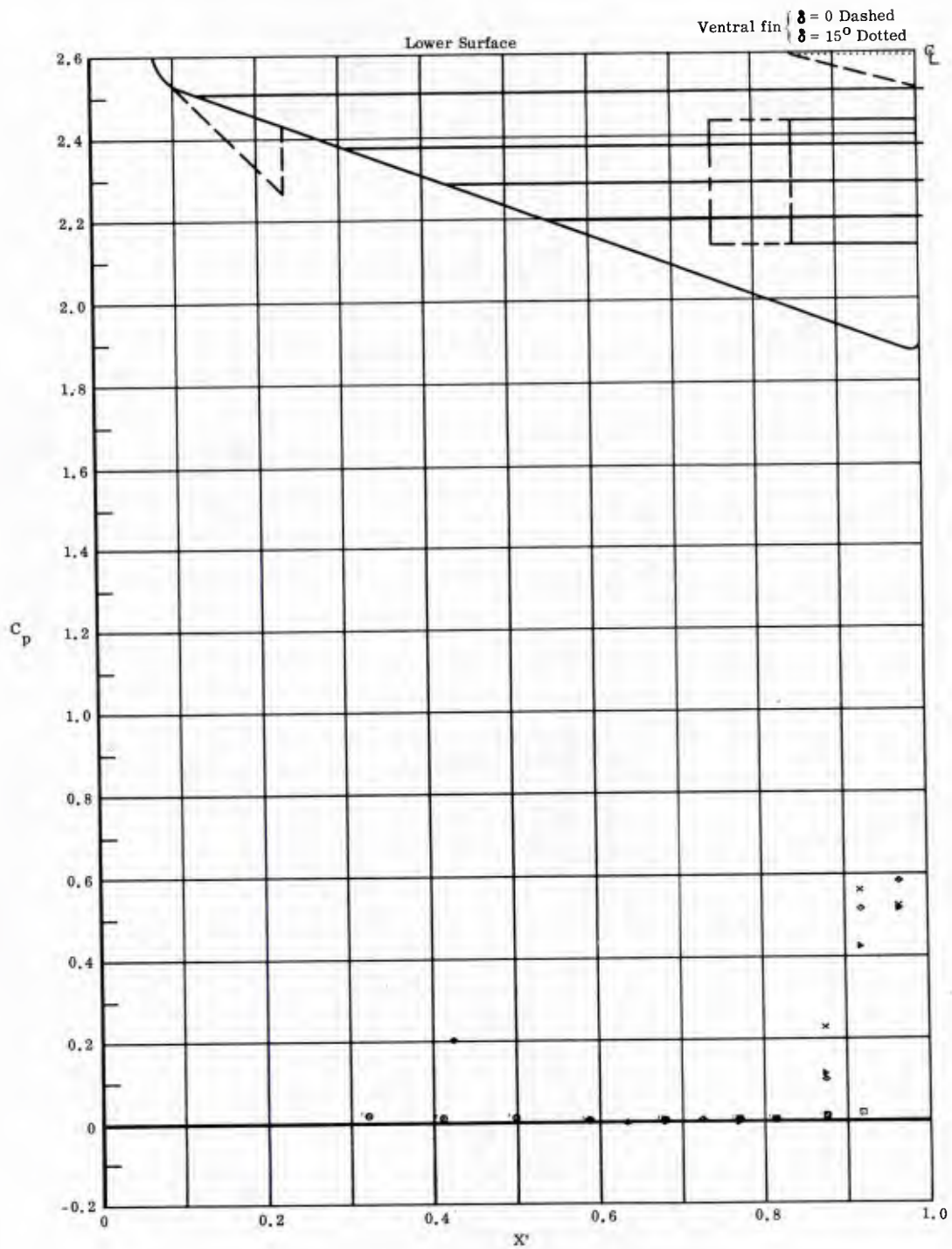

Fig. 47 Streamwise Distributions of Pressure Coefficients on Lower Surface Basic Configuration, Bottom Flaps Deflected 30°, $\alpha = 0$, $\beta = 0$

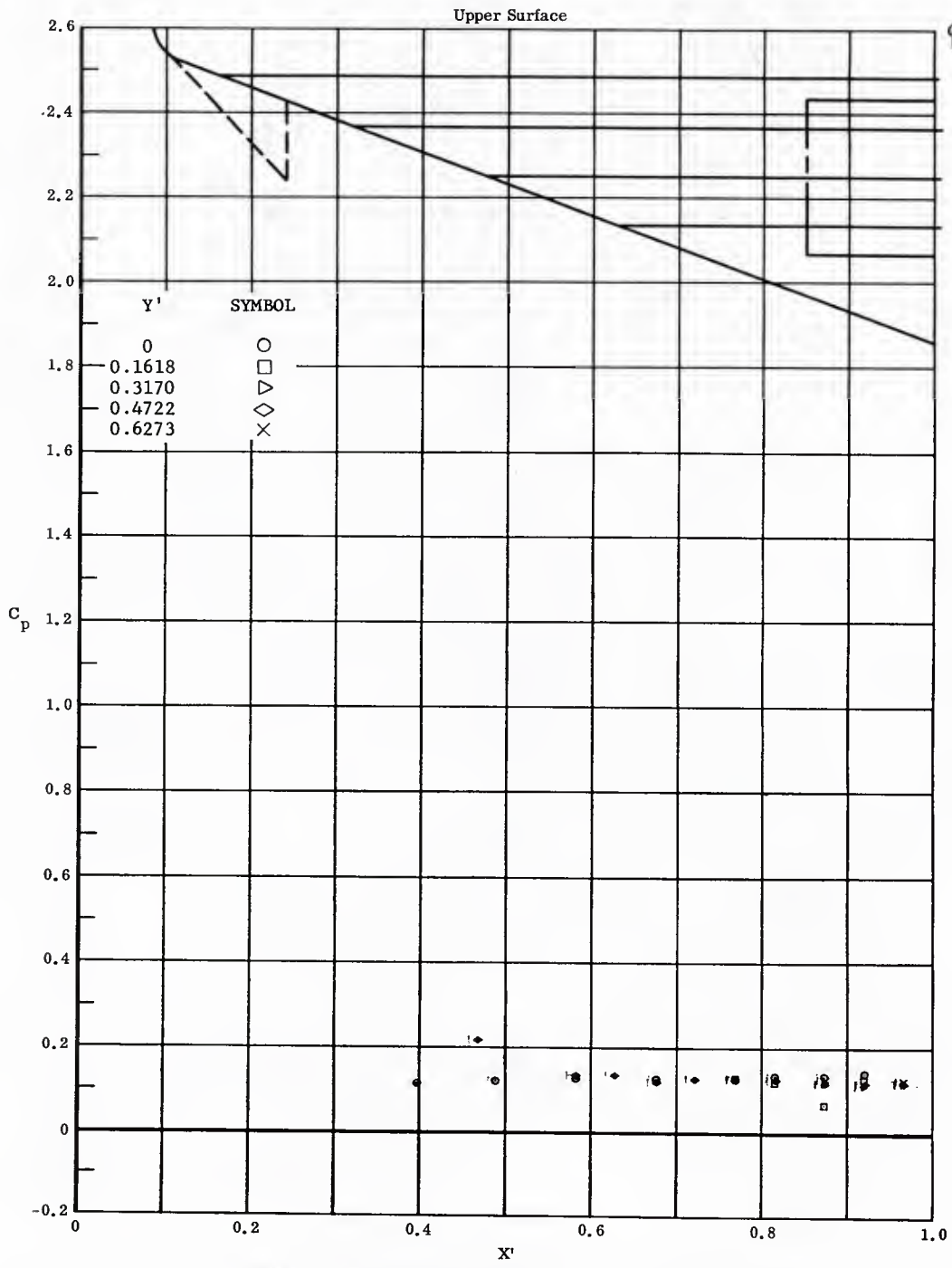

Fig. 47 Streamwise Distributions of Pressure Coefficients on Upper Surface Basic Configuration, Bottom Flaps Deflected 30°, $\alpha = 0$, $\beta = 0$

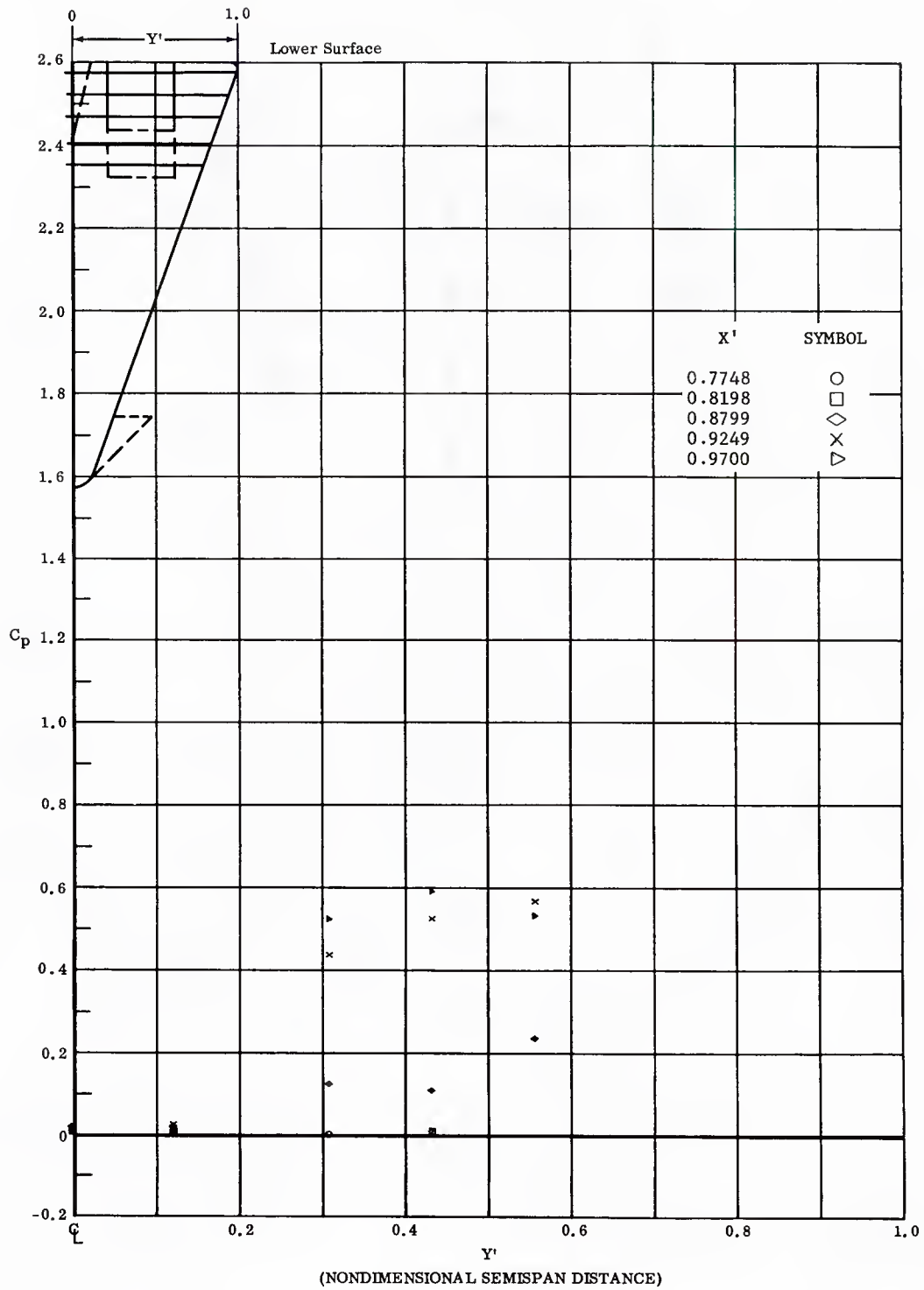

Fig. 47 Spanwise Distributions of Pressure Coefficients on Lower Surface
Basic Configuration, Bottom Flaps Deflected 30°, $\alpha = 0$, $\beta = 0$

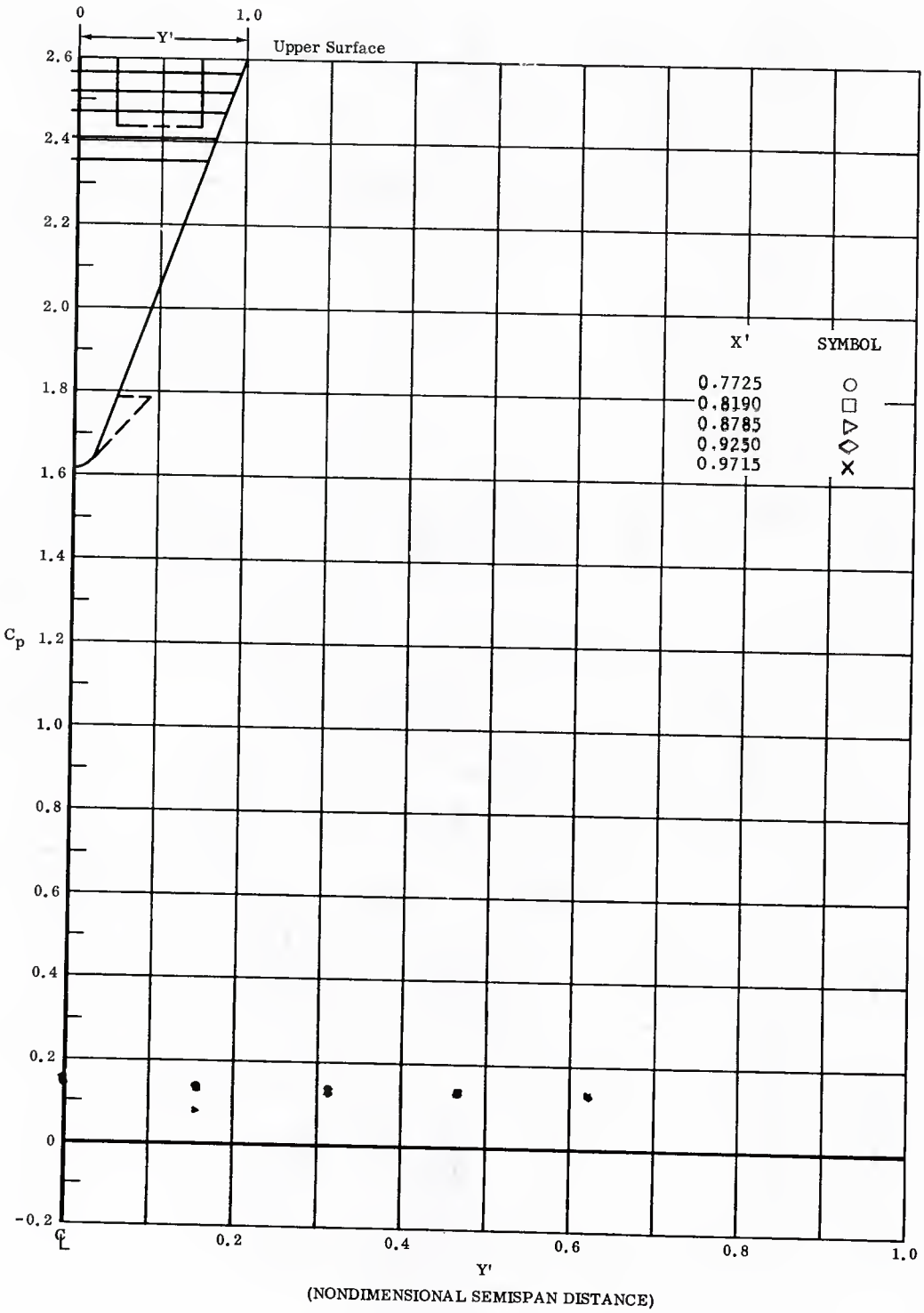

Fig. 47 Spanwise Distributions of Pressure Coefficients on Upper Surface Basic Configuration, Bottom Flaps Deflected 30°, $\alpha = 0$, $\beta = 0$

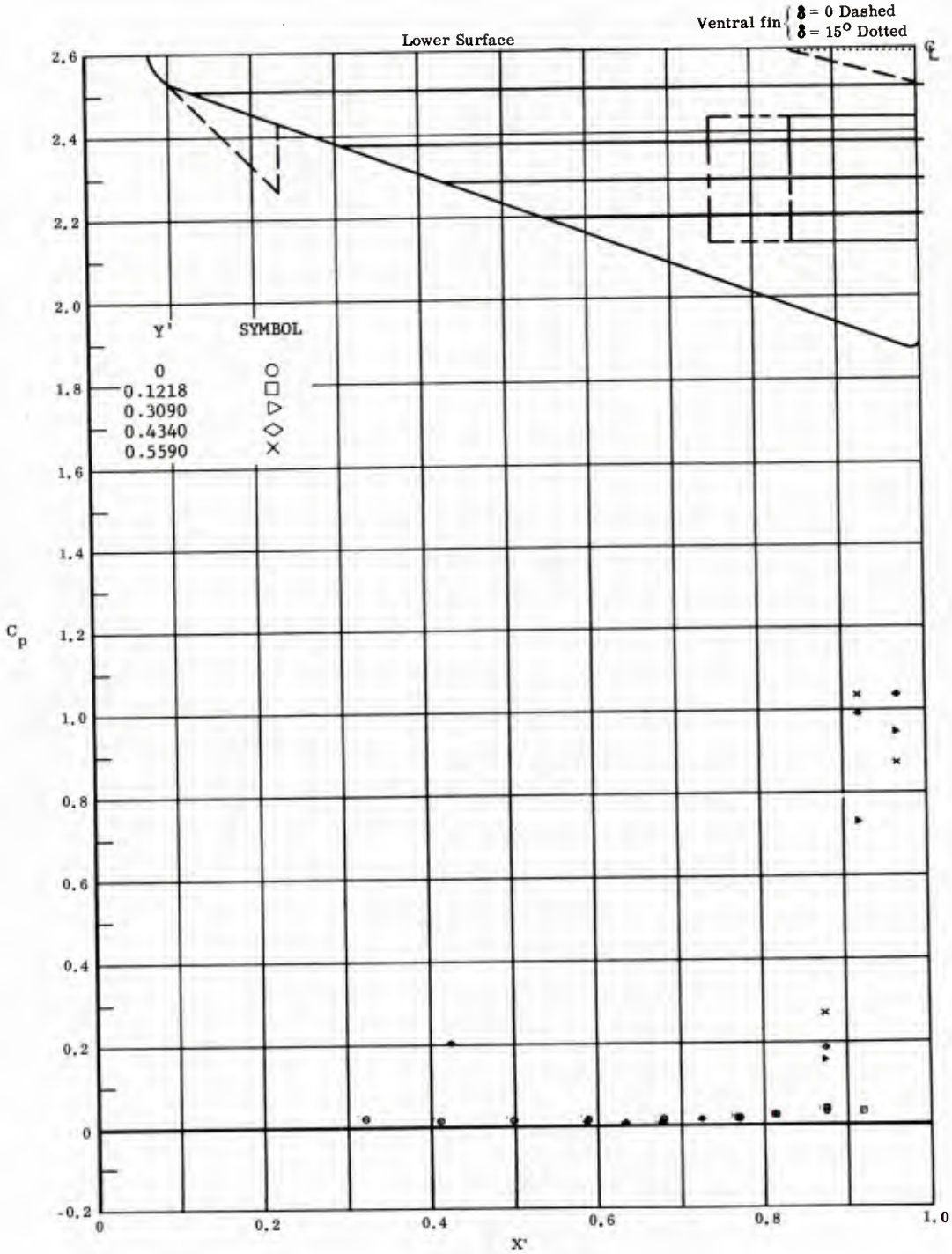

Fig. 48 Streamwise Distributions of Pressure Coefficients on Lower Surface
Basic Configuration, Bottom Flaps Deflected 40°, $\alpha = 0$, $\beta = 0$

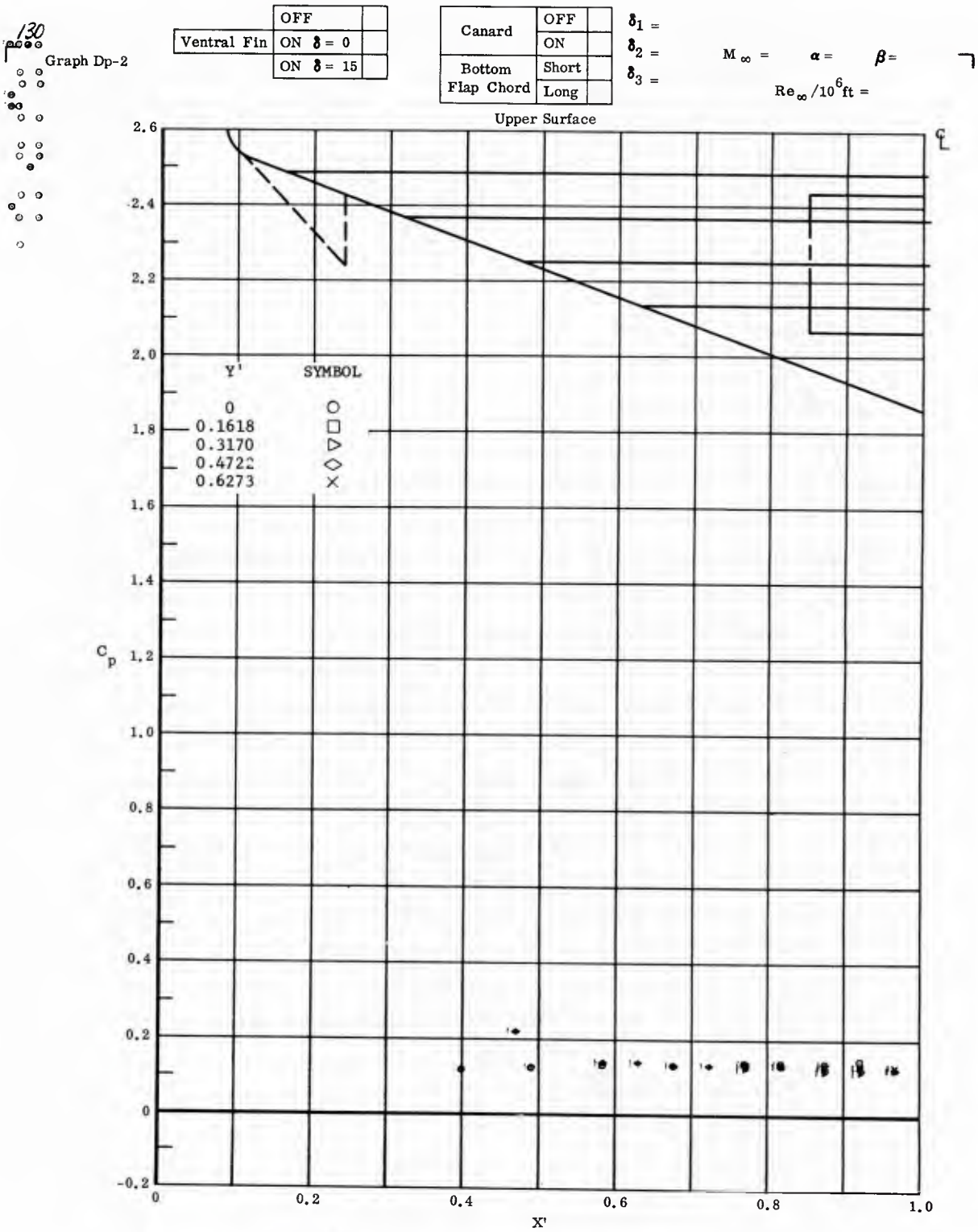

Fig. 48 Streamwise Distributions of Pressure Coefficients on Upper Surface
Basic Configuration, Bottom Flaps Deflected 40°, $\alpha = 0$, $\beta = 0$

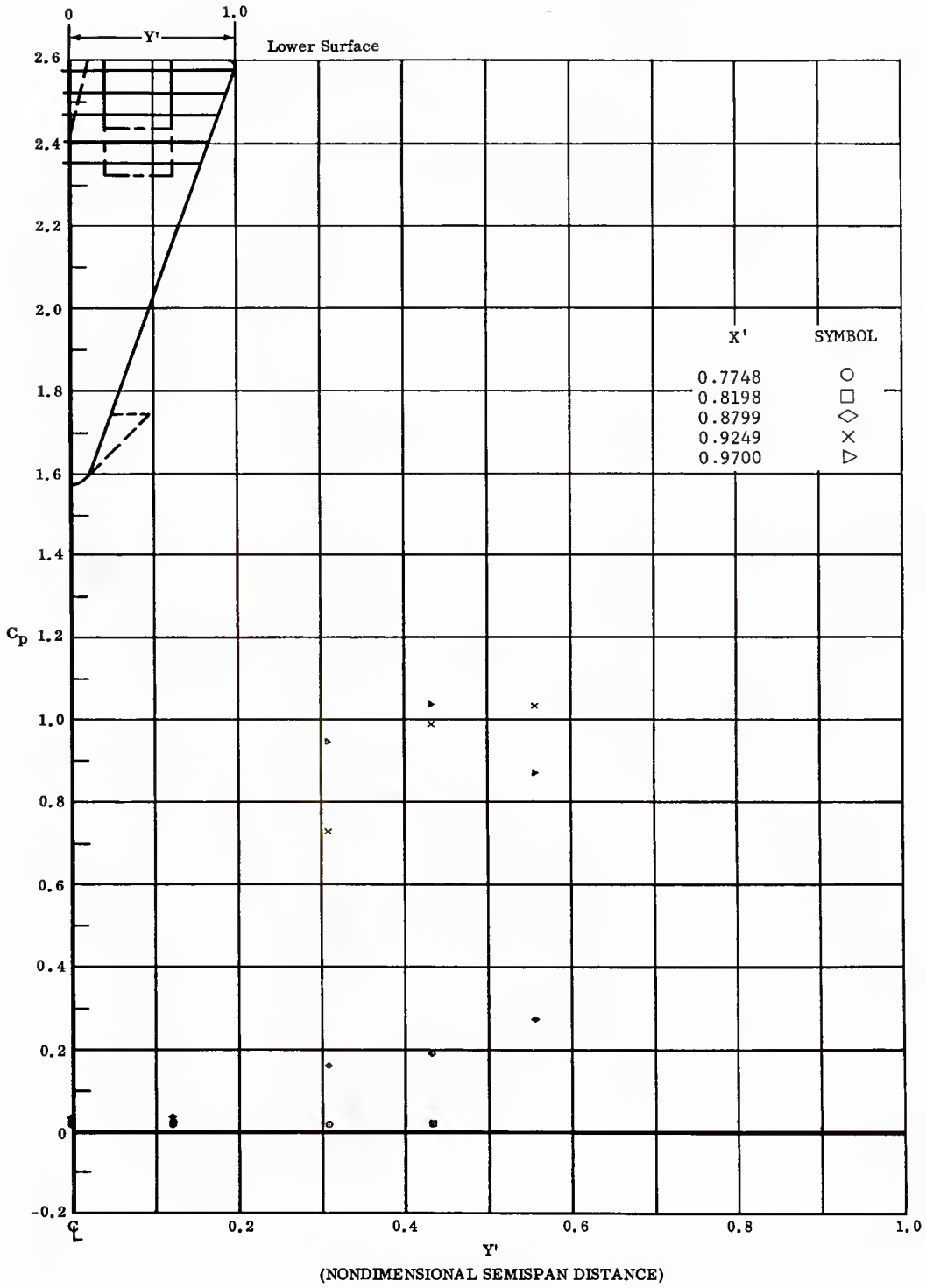

Fig. 48 Spanwise Distributions of Pressure Coefficients on Lower Surface
Basic Configuration, Bottom Flaps Deflected 40°, $\alpha = 0$, $\beta = 0$

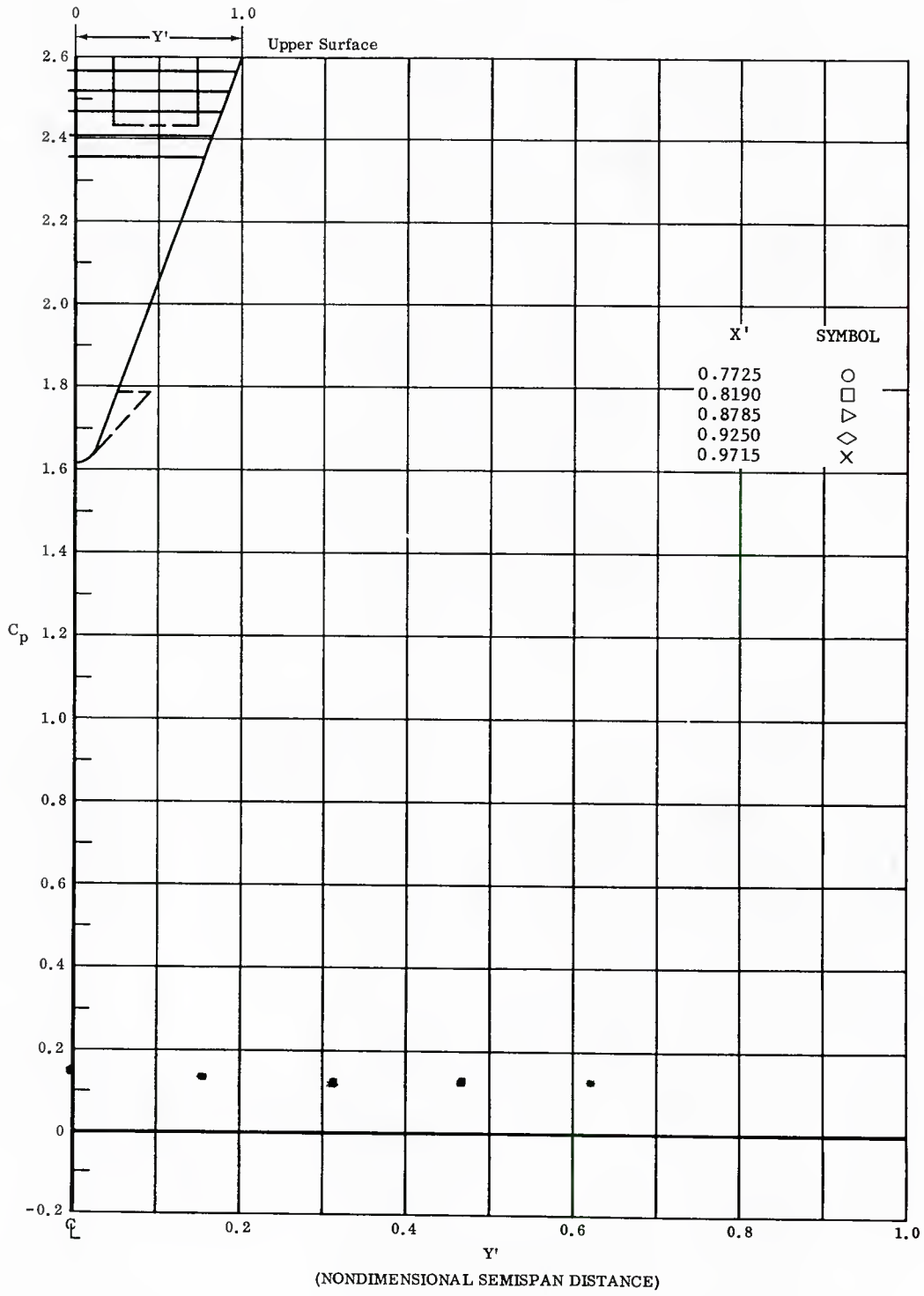

Fig. 48 Spanwise Distributions of Pressure Coefficient on Upper Surface Basic Configuration, Bottom Flaps Deflected 40°, $\alpha = 0$, $\beta = 0$

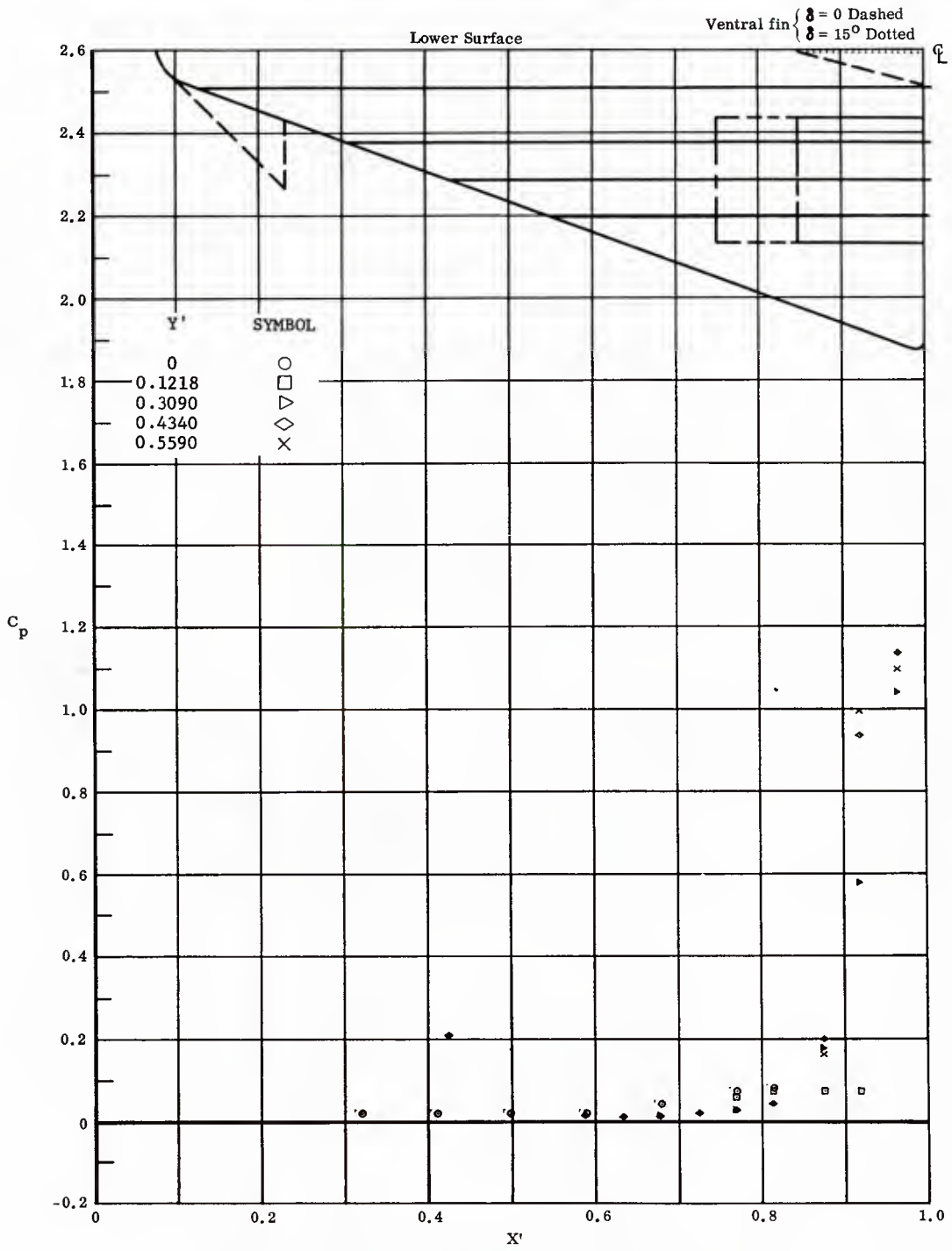

Fig. 49 Streamwise Distributions of Pressure Coefficients on Lower Surface
Ventral Fin on Lower Surface Deflected 15°, Bottom Flaps Deflected 40
$\alpha = 0, \beta = 0$

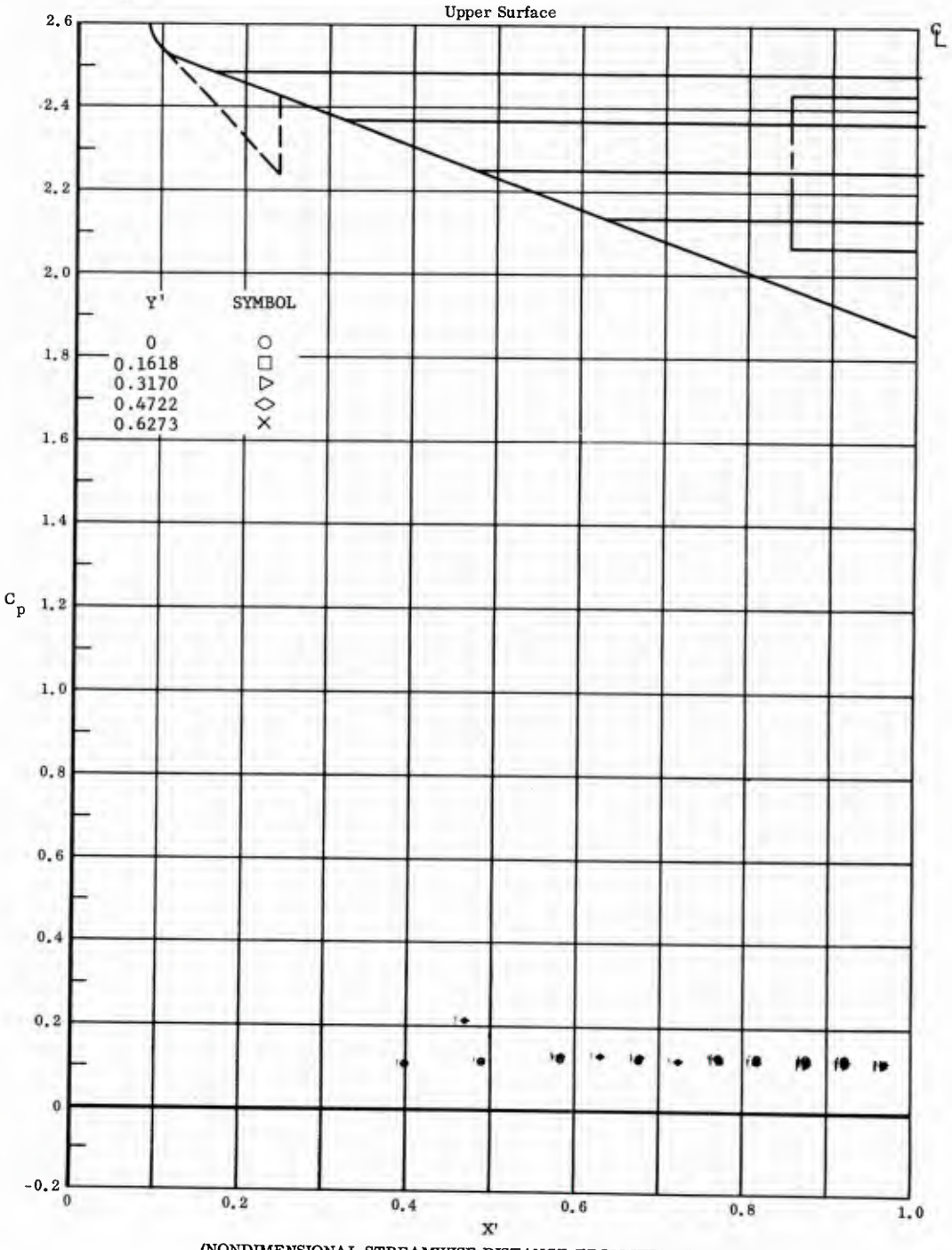

Fig. 49 Streamwise Distributions of Pressure Coefficients on Upper Surface Ventral Fin on Lower Surface Deflected 15°, Bottom Flaps Deflected 40 $\alpha = 0$, $\beta = 0$

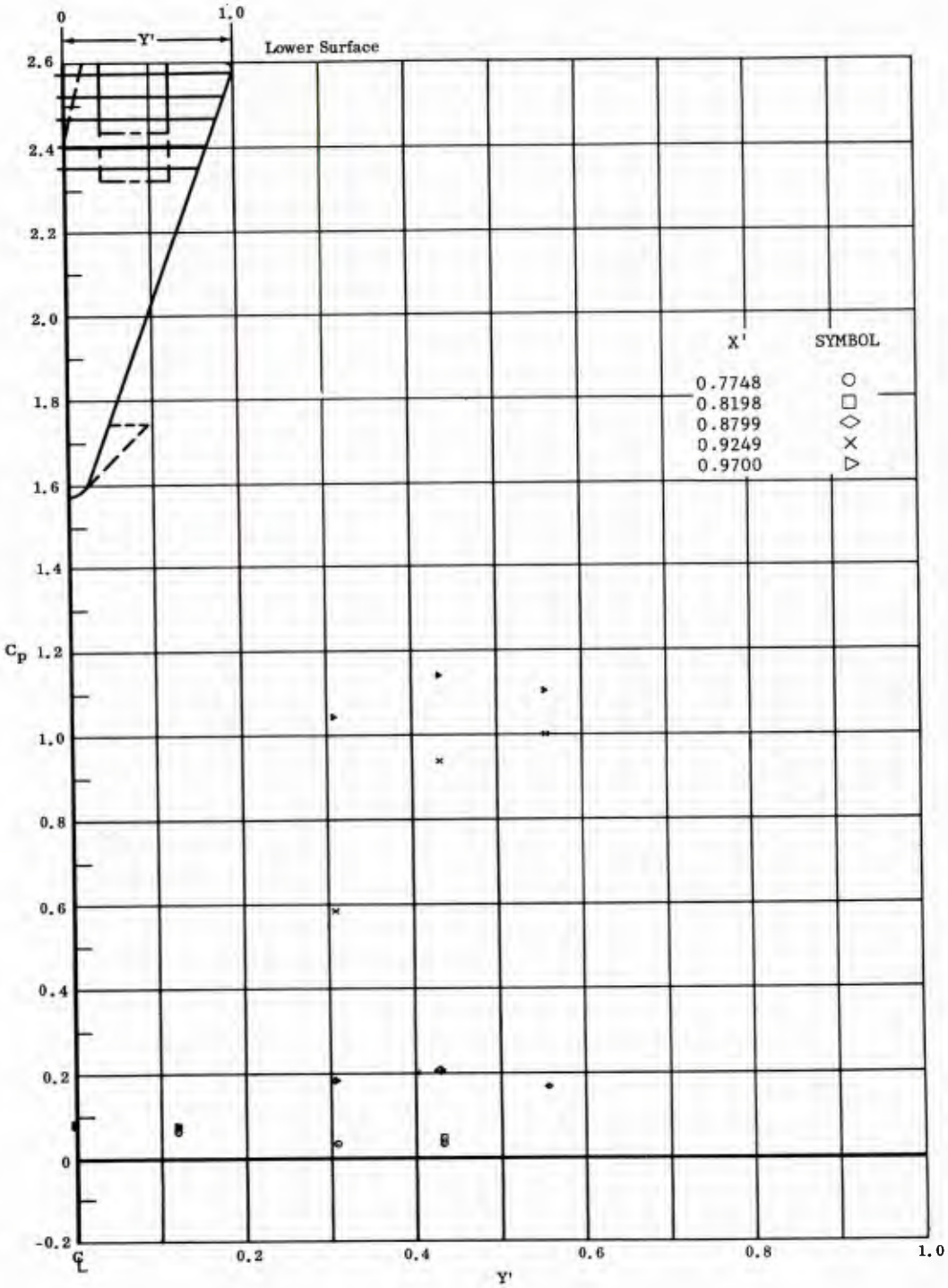

Fig. 49 Spanwise Distributions of Pressure Coefficients on Lower Surface Ventral Fin on Lower Surface Deflected 15°, Bottom Flaps Deflected 40°, $\alpha = 0$, $\beta = 0$

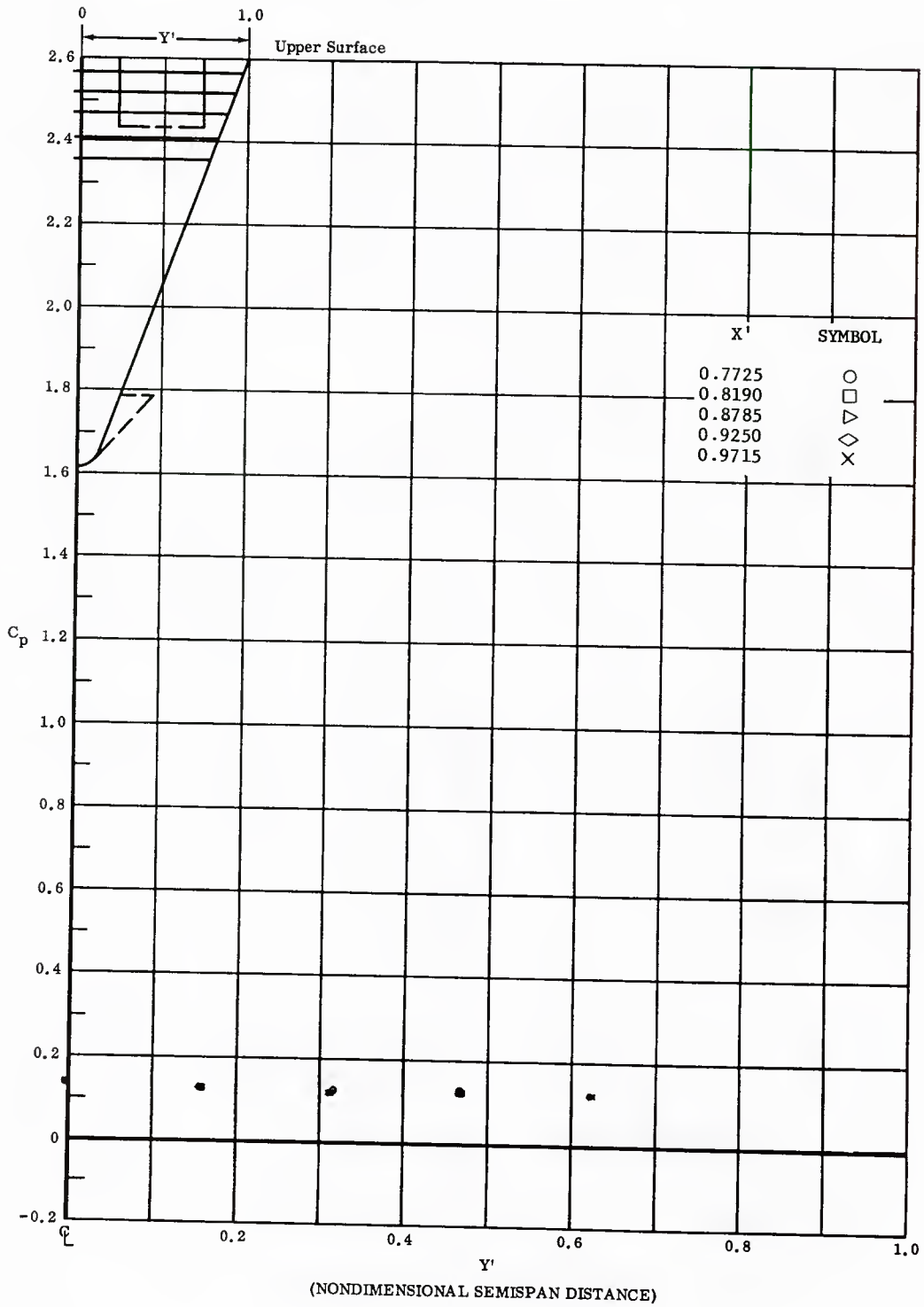

Fig. 49 Spanwise Distributions of Pressure Coefficients on Upper Surface Ventral Fin on Lower Surface Deflected 15°, Bottom Flaps Deflected 40°, $\alpha = 0$, $\beta = 0$

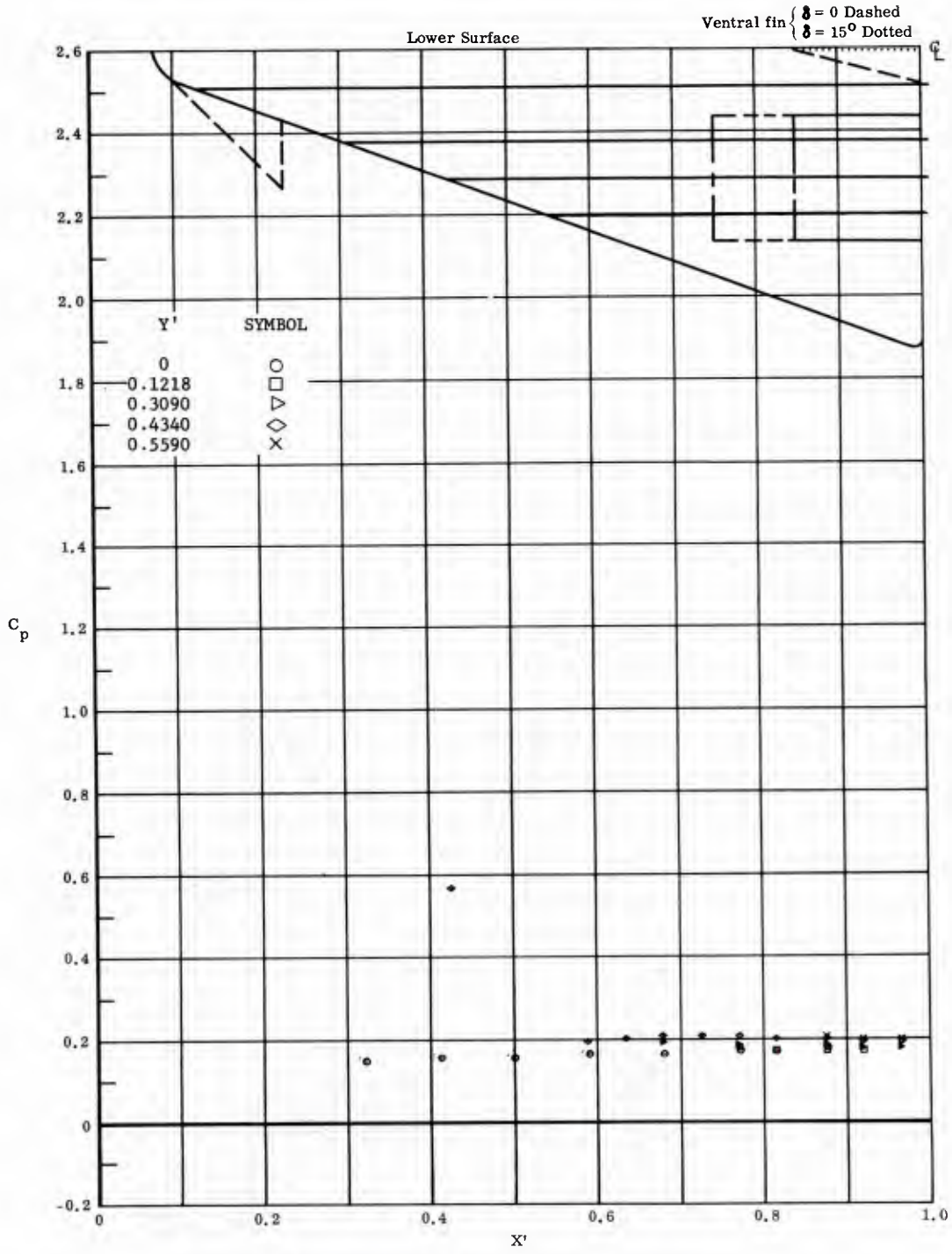

Fig. 50 Streamwise Distributions of Pressure Coefficients on Lower Surface Basic Configuration, Left (Upper) Flap Deflected -40°, α = +14.3°, β = +14°

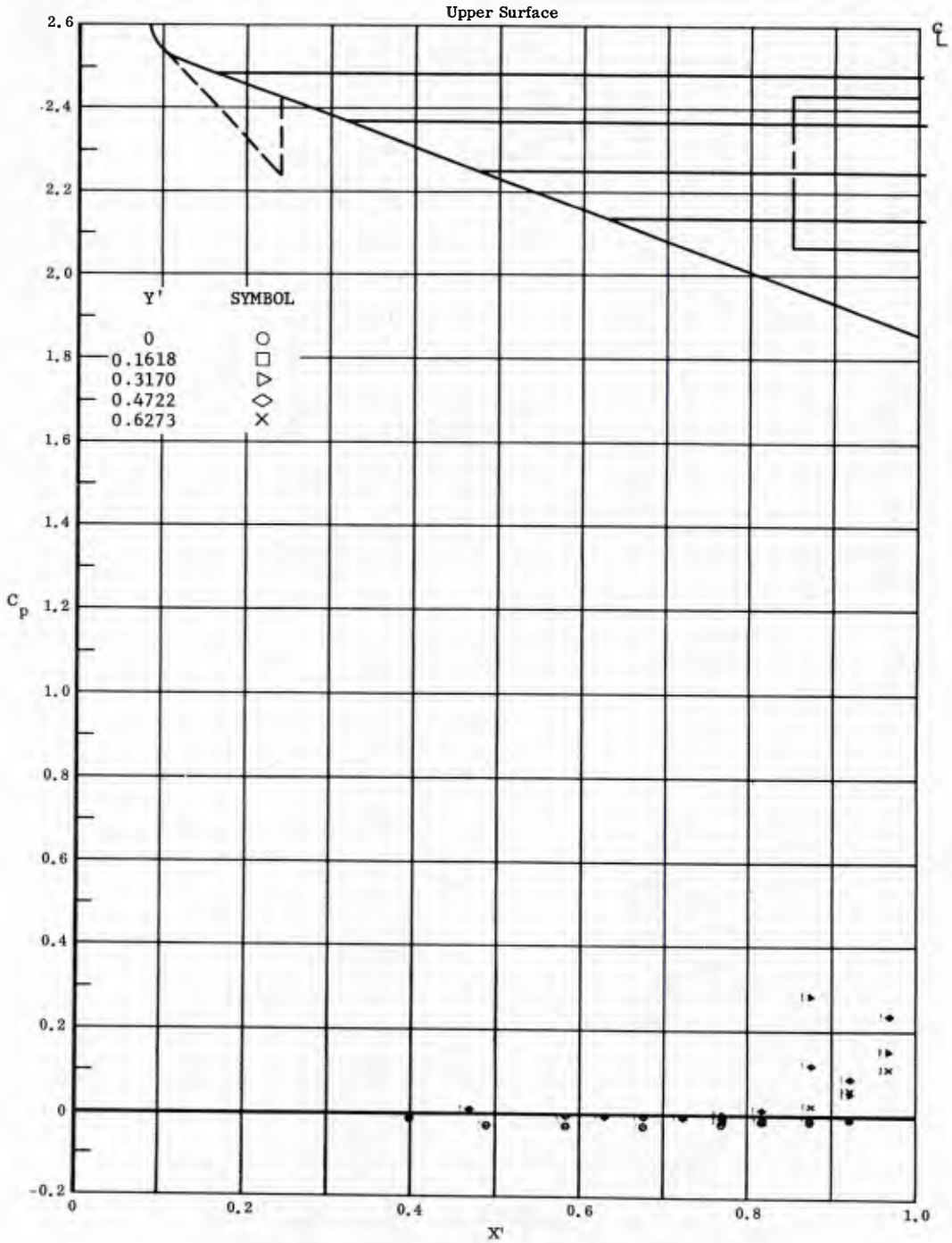

Fig. 50 Streamwise Distributions of Pressure Coefficients on Upper Surface Basic Configuration, Left (Upper) Flap Deflected -40°, α = +14.3° β = +14°

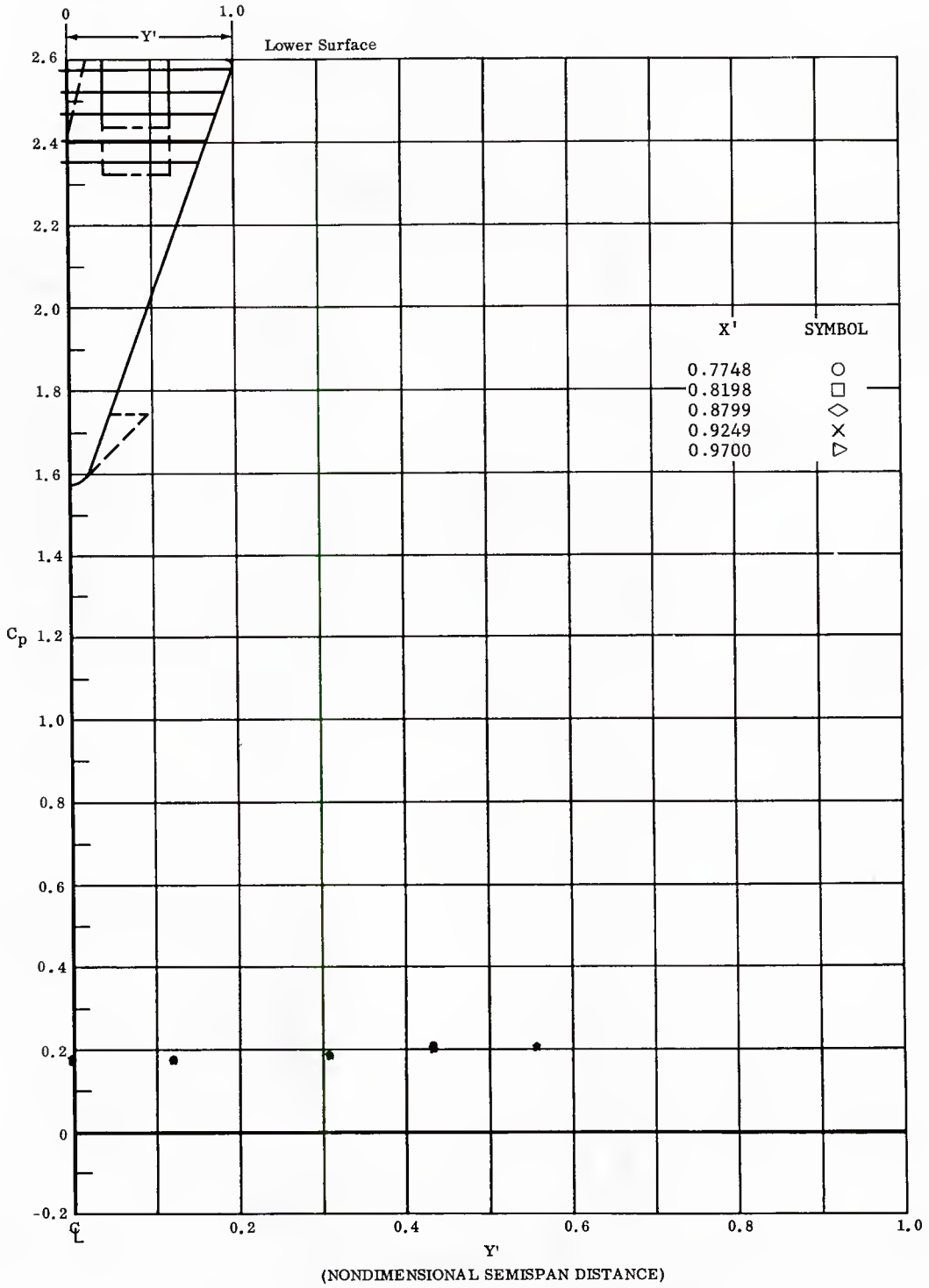

Fig. 50 Spanwise Distributions of Pressure Coefficients on Lower Surface Basic Configuration, Left (Upper) Flap Deflected -40°, α = +14.3°, β = +11°

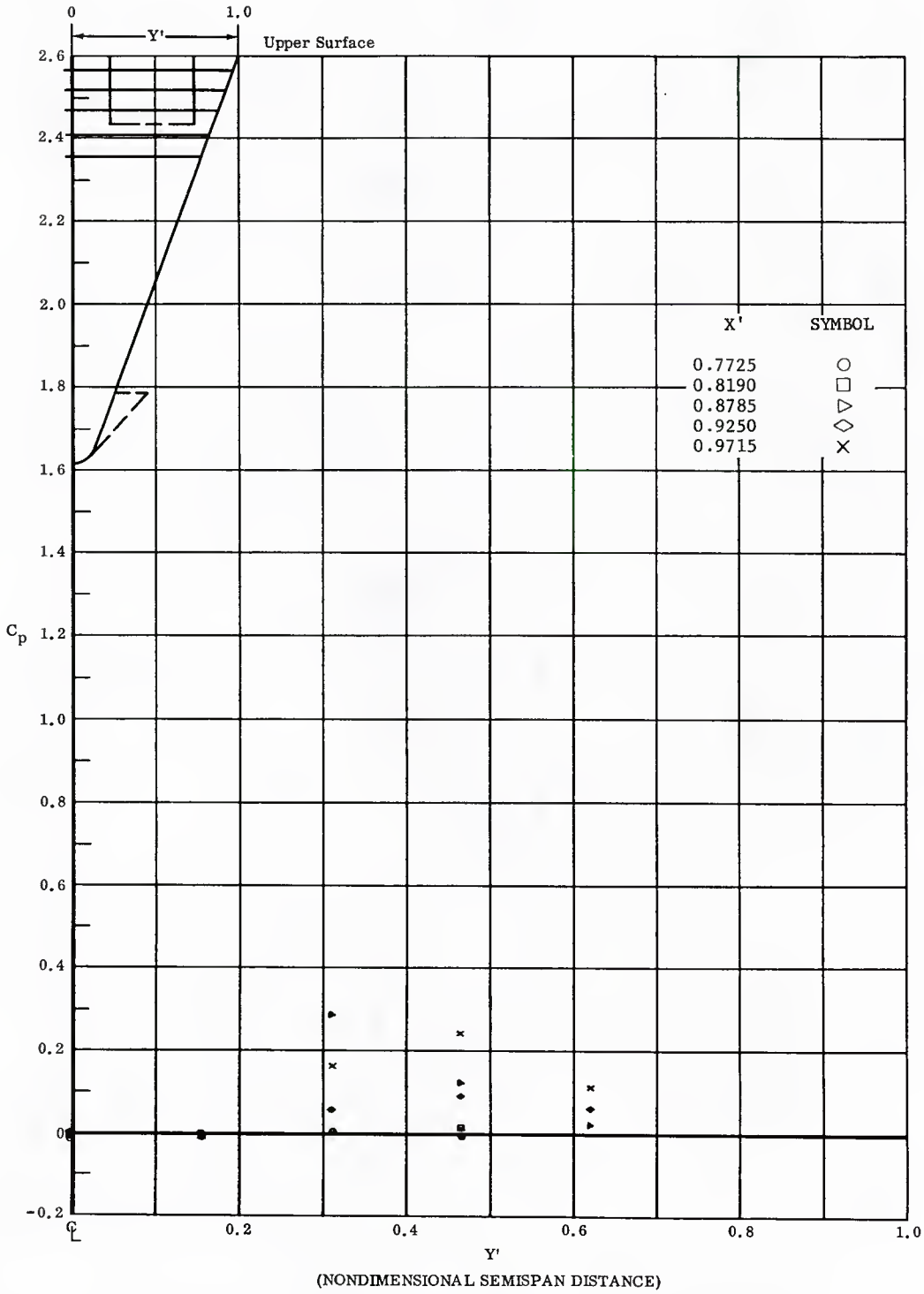

Fig. 50 Spanwise Distributions of Pressure Coefficients on Upper Surface Basic Configuration, Left (Upper) Flap Deflected -40°, α = +14.3° β = +14°

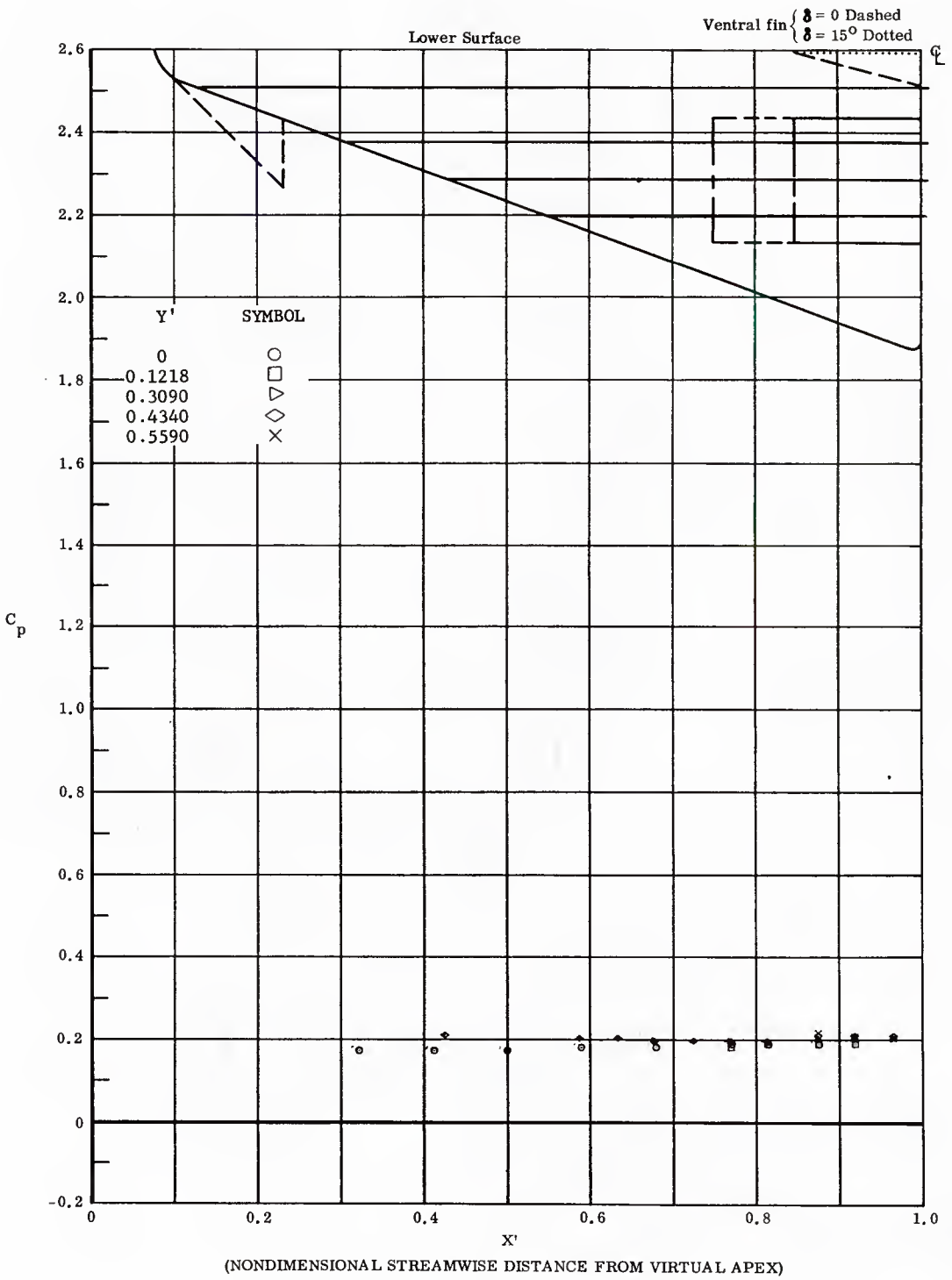

Fig. 51 Streamwise Distributions of Pressure Coefficients on Lower Surface Basic Configuration, Left (Upper) Flap Deflected -40°, α = +14.3°, β = 0

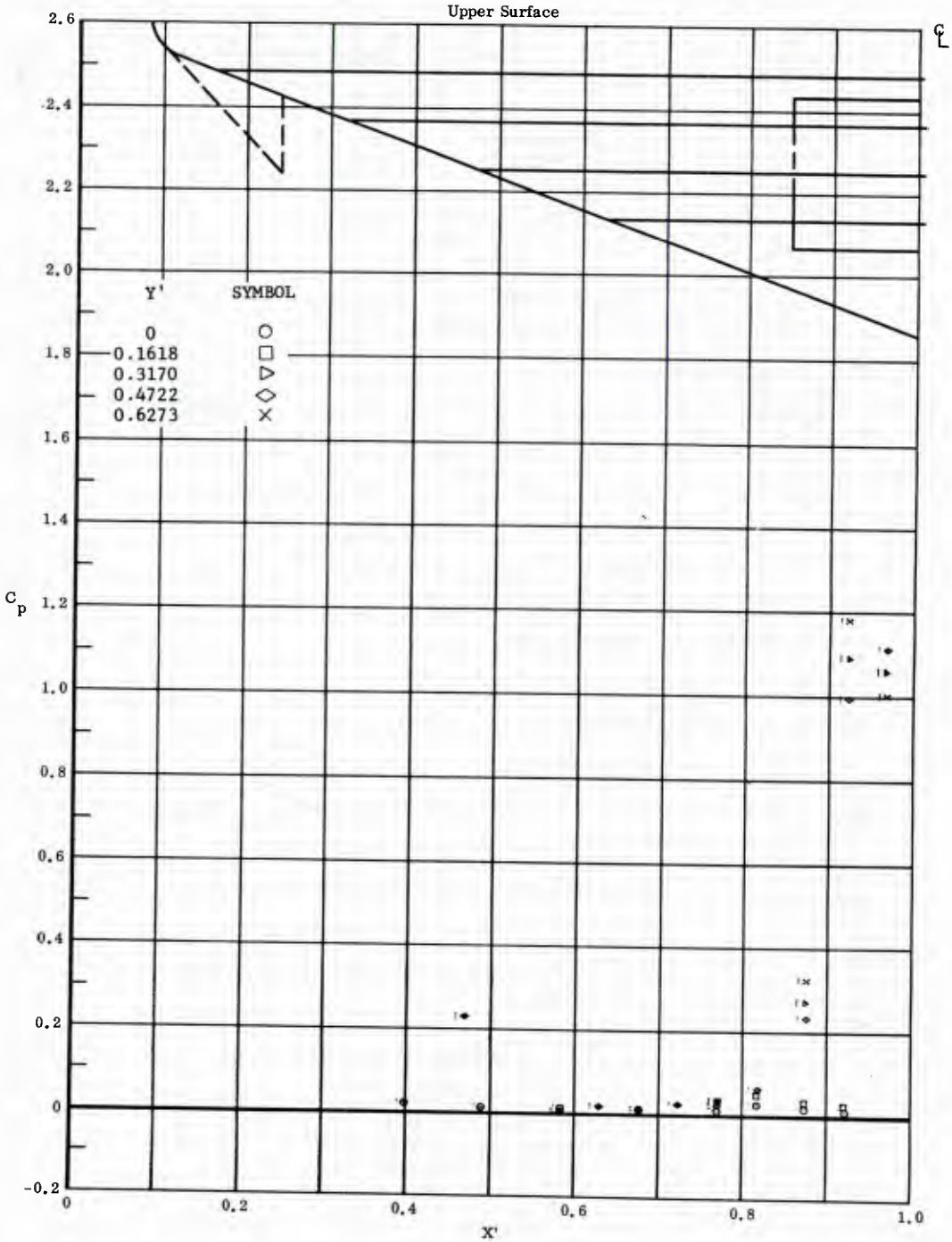

Fig. 51 Streamwise Distributions of Pressure Coefficients on Upper Surface Basic Configuration, Left (Upper) Flap Deflected -40°, α = +14.3°, β = 0

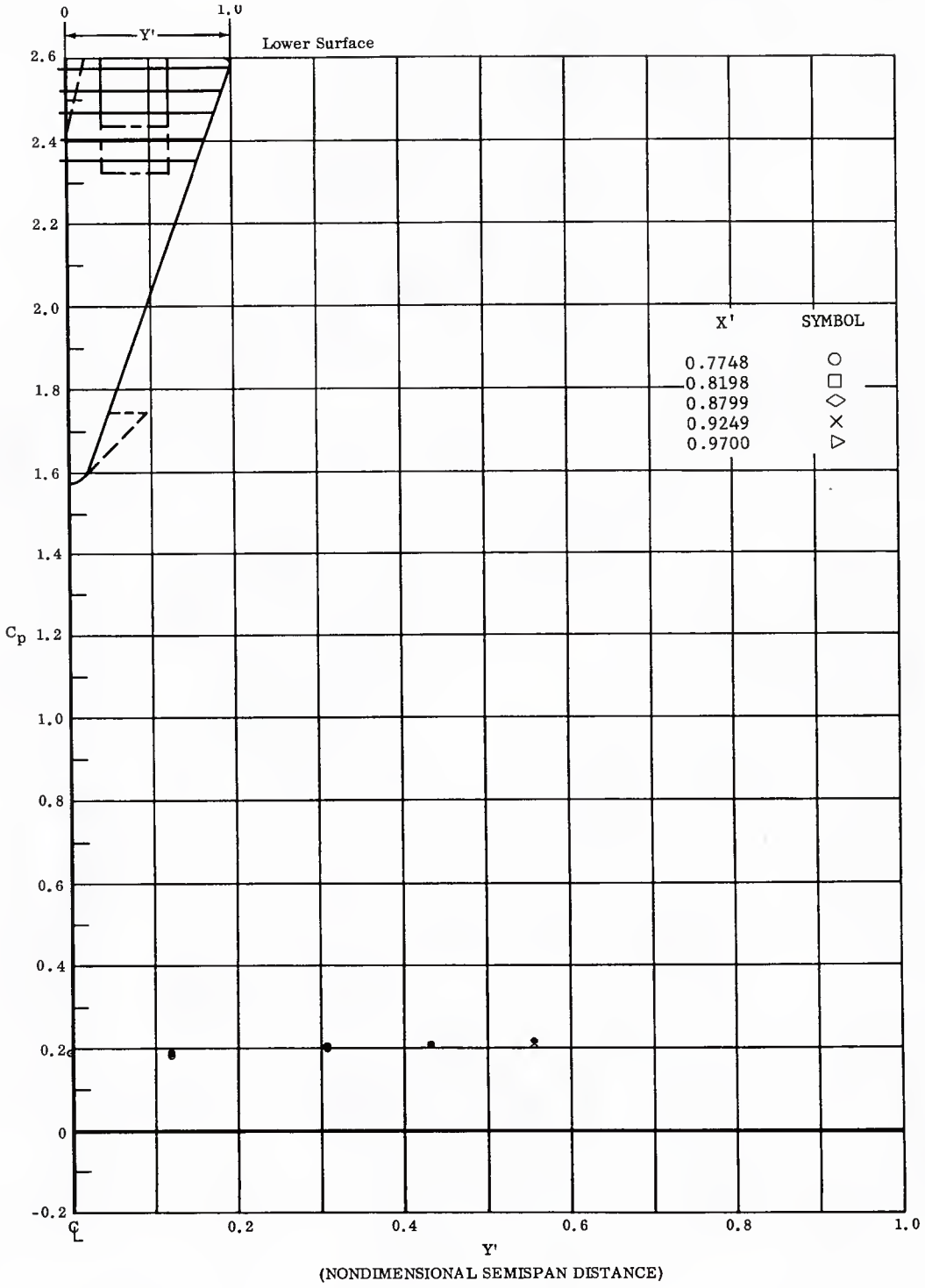

Fig. 51 Spanwise Distributions of Pressure Coefficients on Lower Surface Basic Configuration, Left (Upper) Flap Deflected -40°, α = +14.3°, β = 0

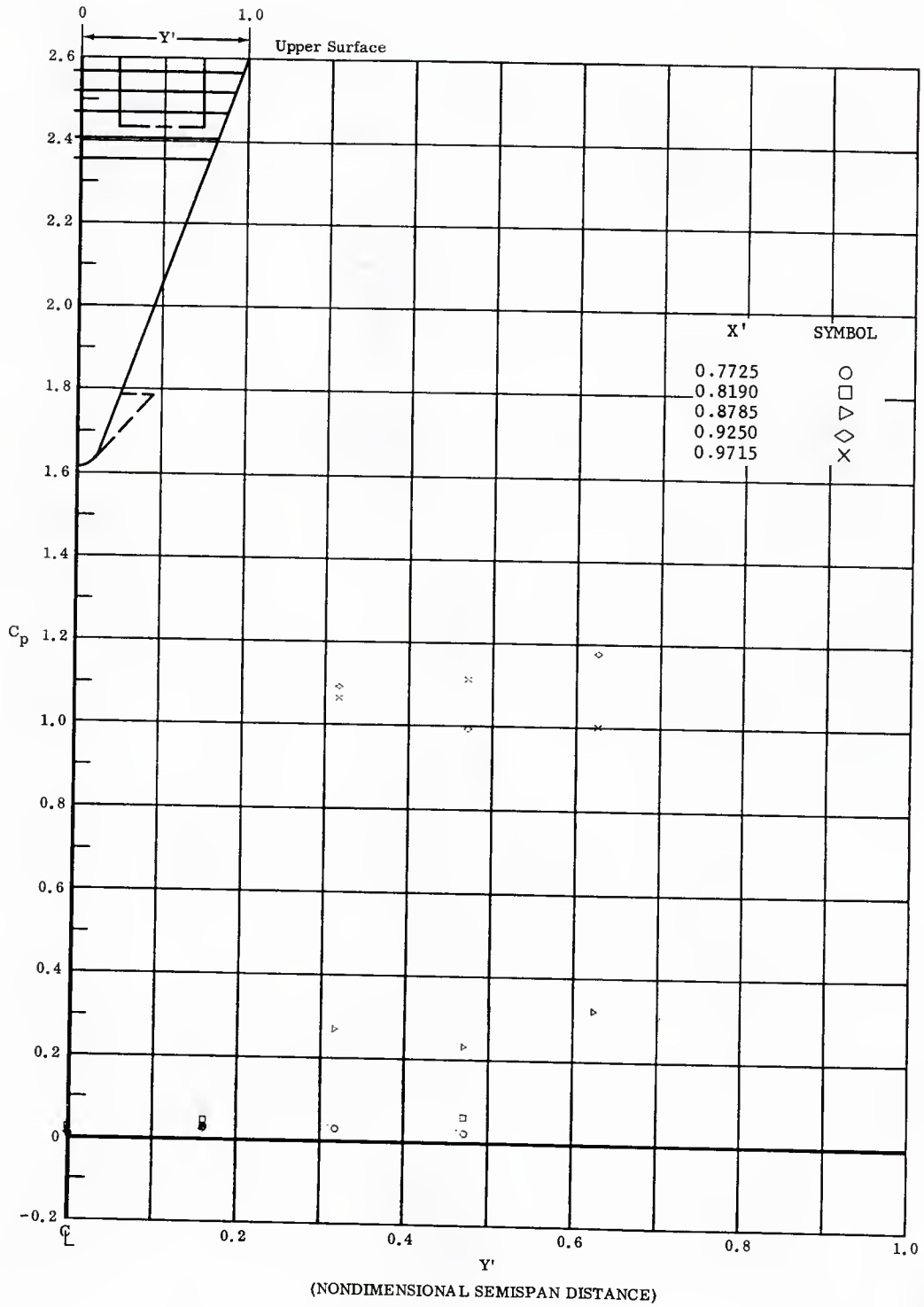

Fig. 51 Spanwise Distributions of Pressure Coefficients on Upper Surface Basic Configuration, Left (Upper) Flap Deflected -40°, α = +14.3°, β = 0

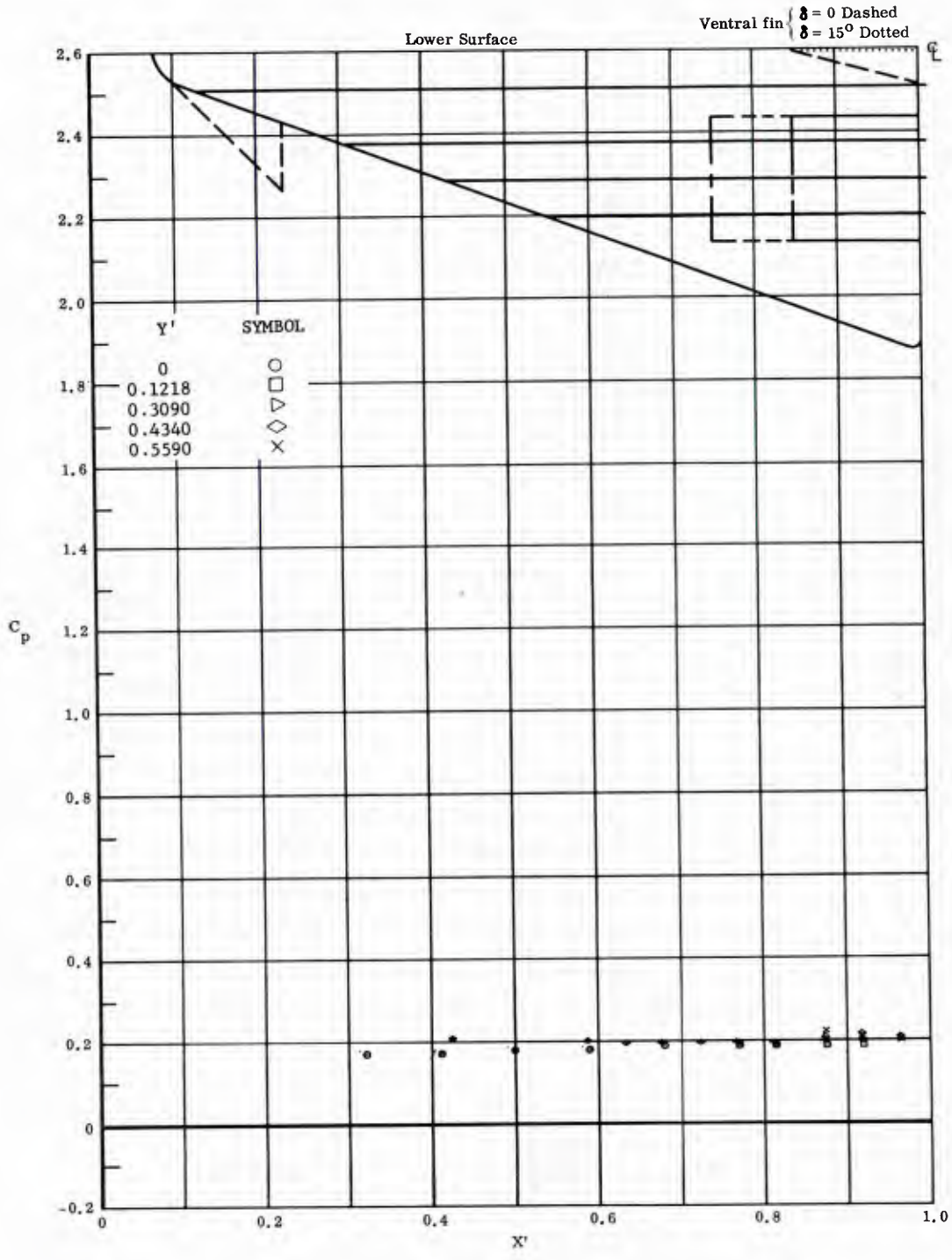

Fig. 52 Streamwise Distributions of Pressure Coefficients on Lower Surface Basic Configuration, Left and Right (Upper) Flaps Deflected -40°, $\alpha = +14.3°, \beta = 0$

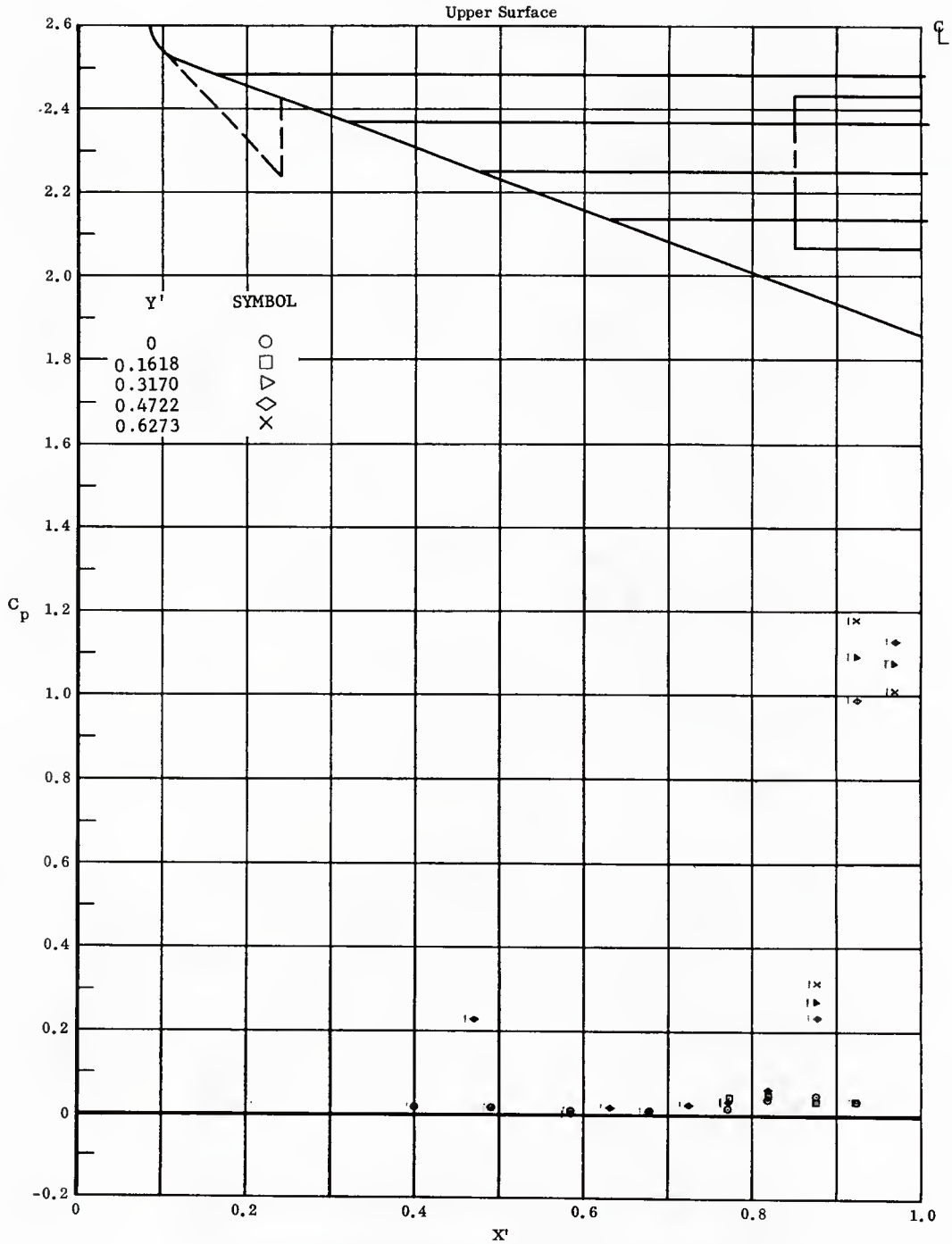

Fig. 52 Streamwise Distributions of Pressure Coefficients on Upper Surface Basic Configuration, Left and Right (Upper) Flaps Deflected -40°, $\alpha = +14.3°$, $\beta = 0$

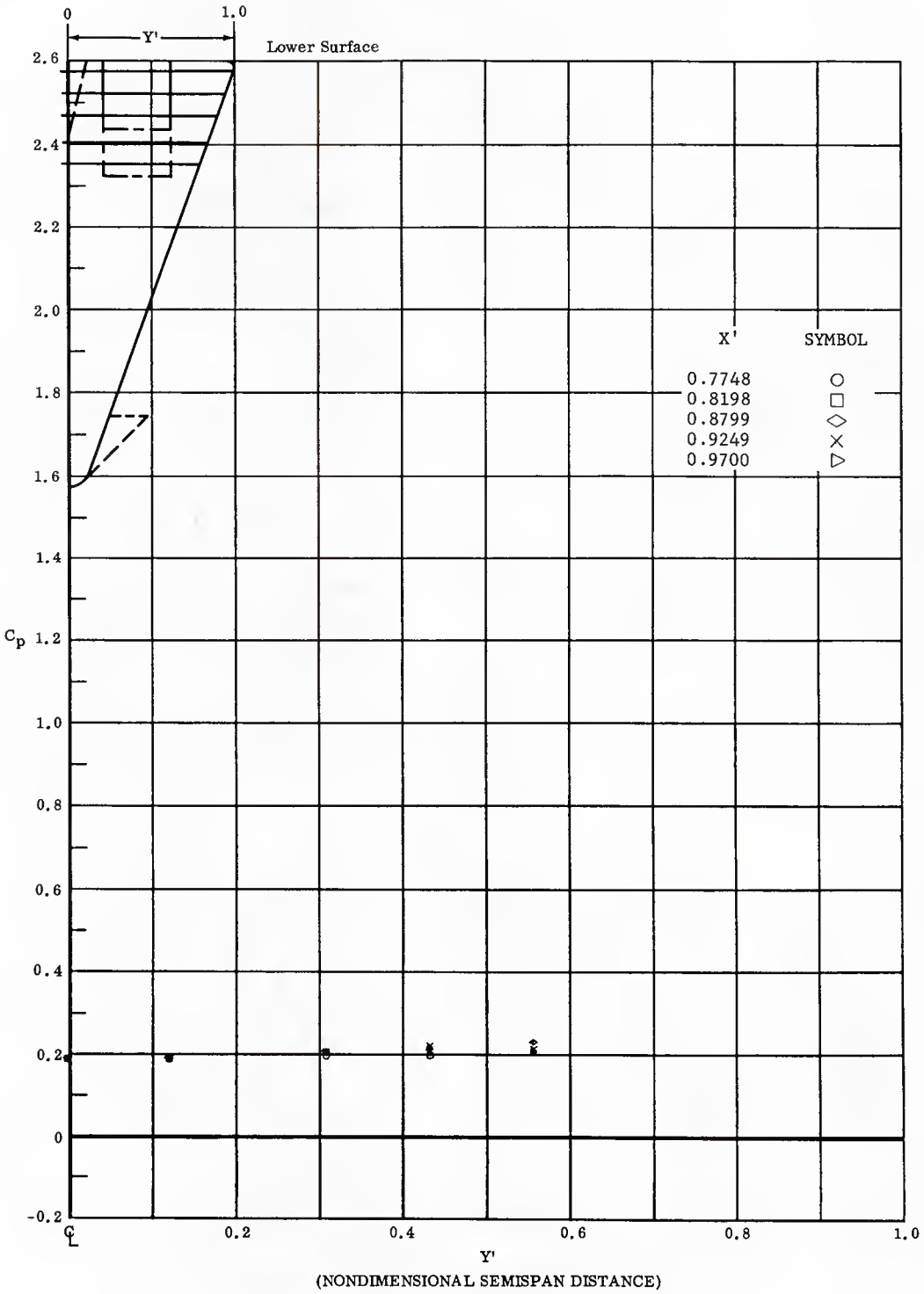

Fig. 52 Spanwise Distributions of Pressure Coefficients on Lower Surface Basic Configuration, Left and Right (Upper) Flaps Deflected -40°, $\alpha = +14.3°$, $\beta = 0$

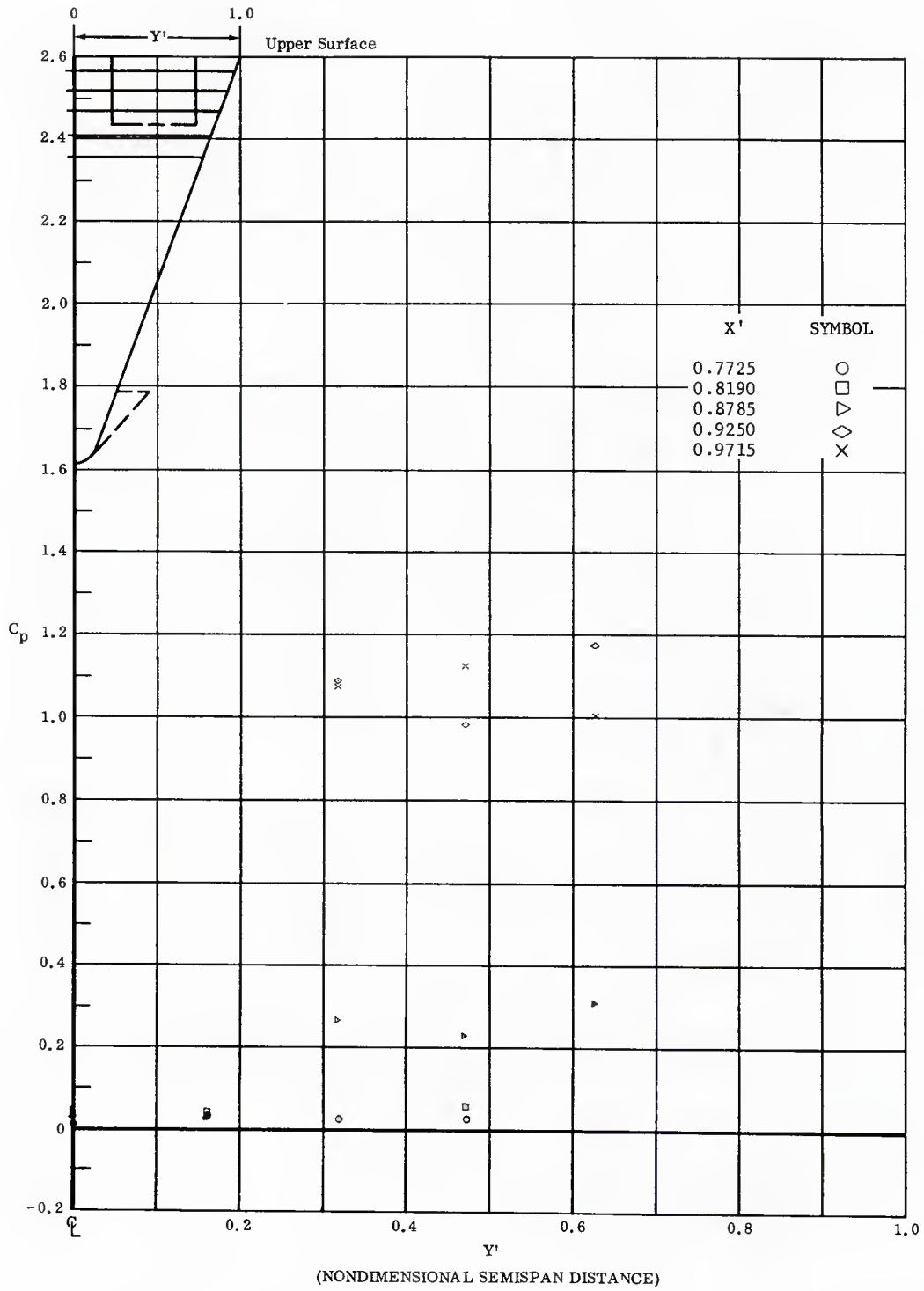

Fig. 52 Spanwise Distributions of Pressure Coefficients on Upper Surface Basic Configuration, Left and Right (Upper) Flaps Deflected -40°, $\alpha = +14.3°$, $\beta = 0$

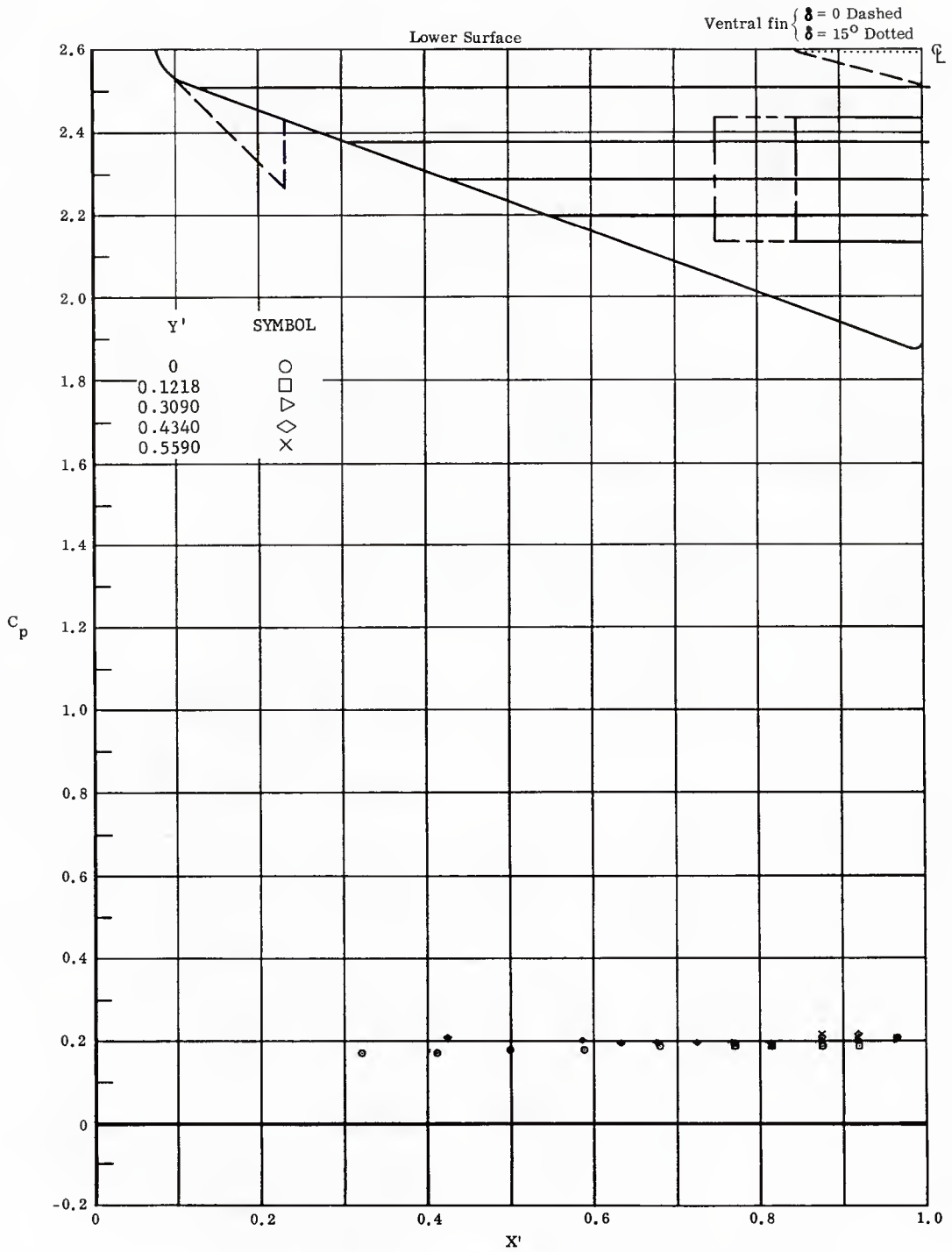

Fig. 53 Streamwise Distributions of Pressure Coefficients on Lower Surface Basic Configuration, Left and Right (Upper) Flaps Deflected -30°, α =+14.3°, β = 0

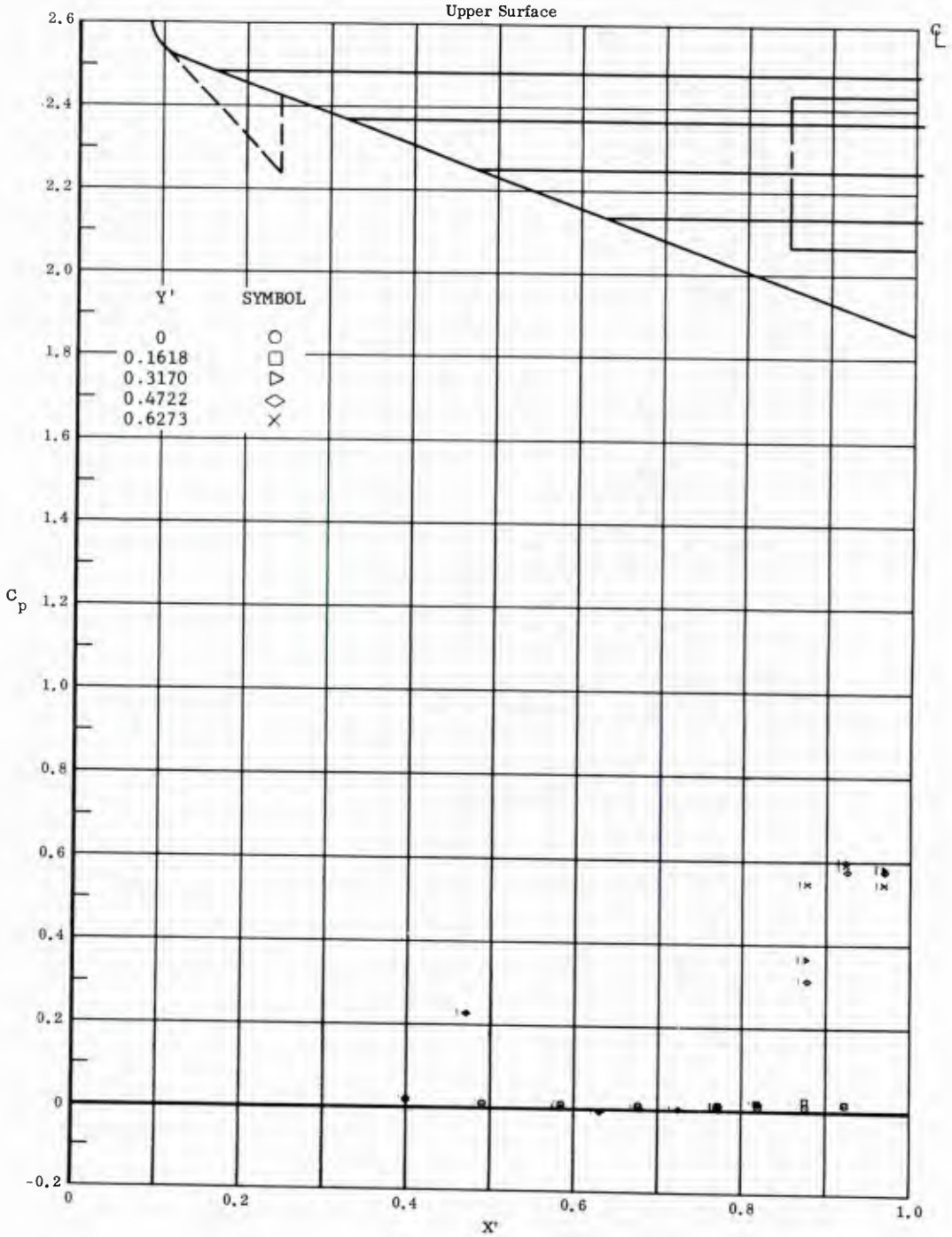

Fig. 53 Streamwise Distributions of Pressure Coefficients on Upper Surface Basic Configuration, Left and Right (Upper) Flaps Deflected -30°, $\alpha = +14.3°$, $\beta = 0$

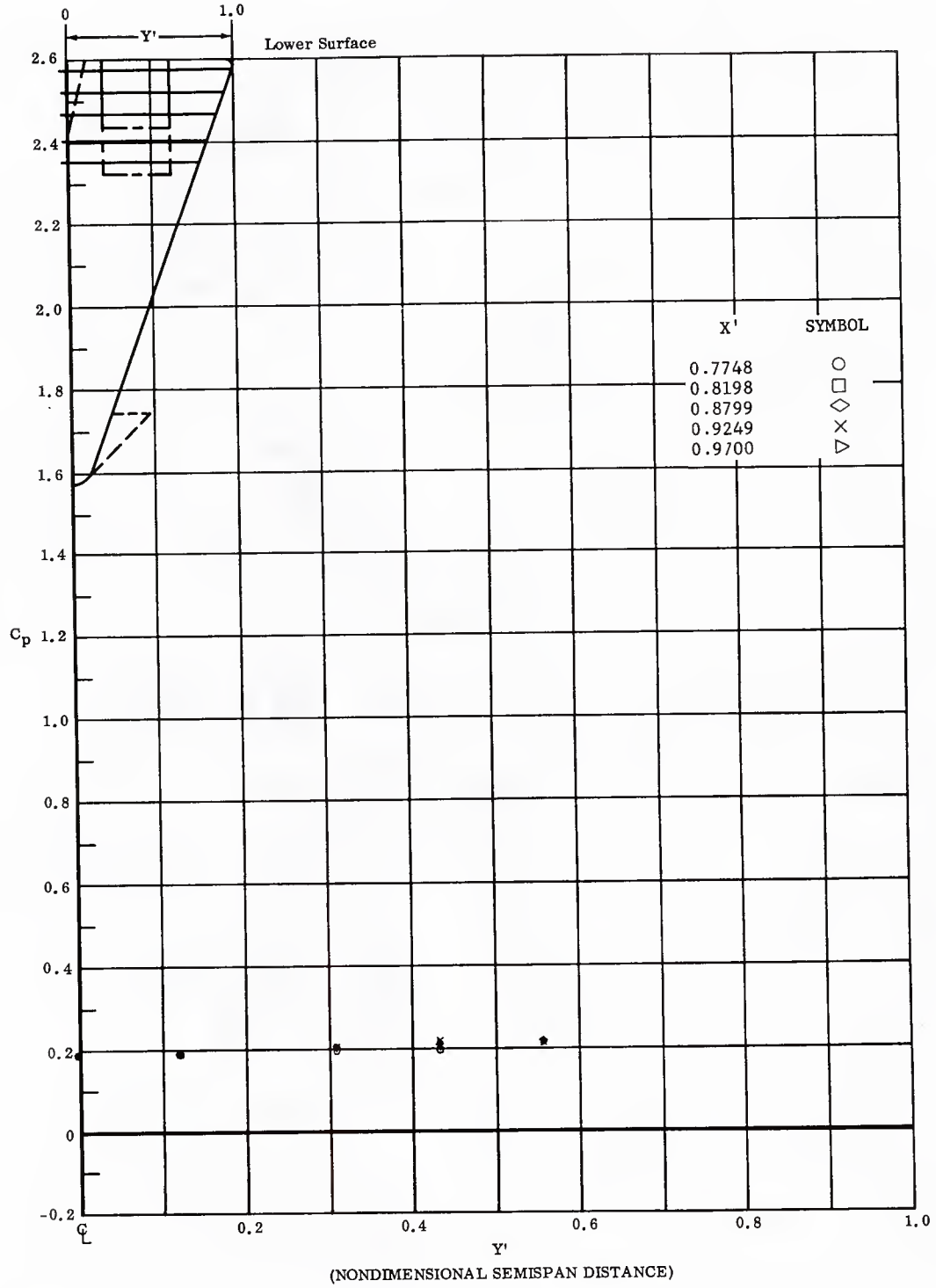

Fig. 53 Spanwise Distributions of Pressure Coefficients on Lower Surface Basic Configuration, Left and Right (Upper) Flaps Deflected -30°, α = +14.3°, β = 0

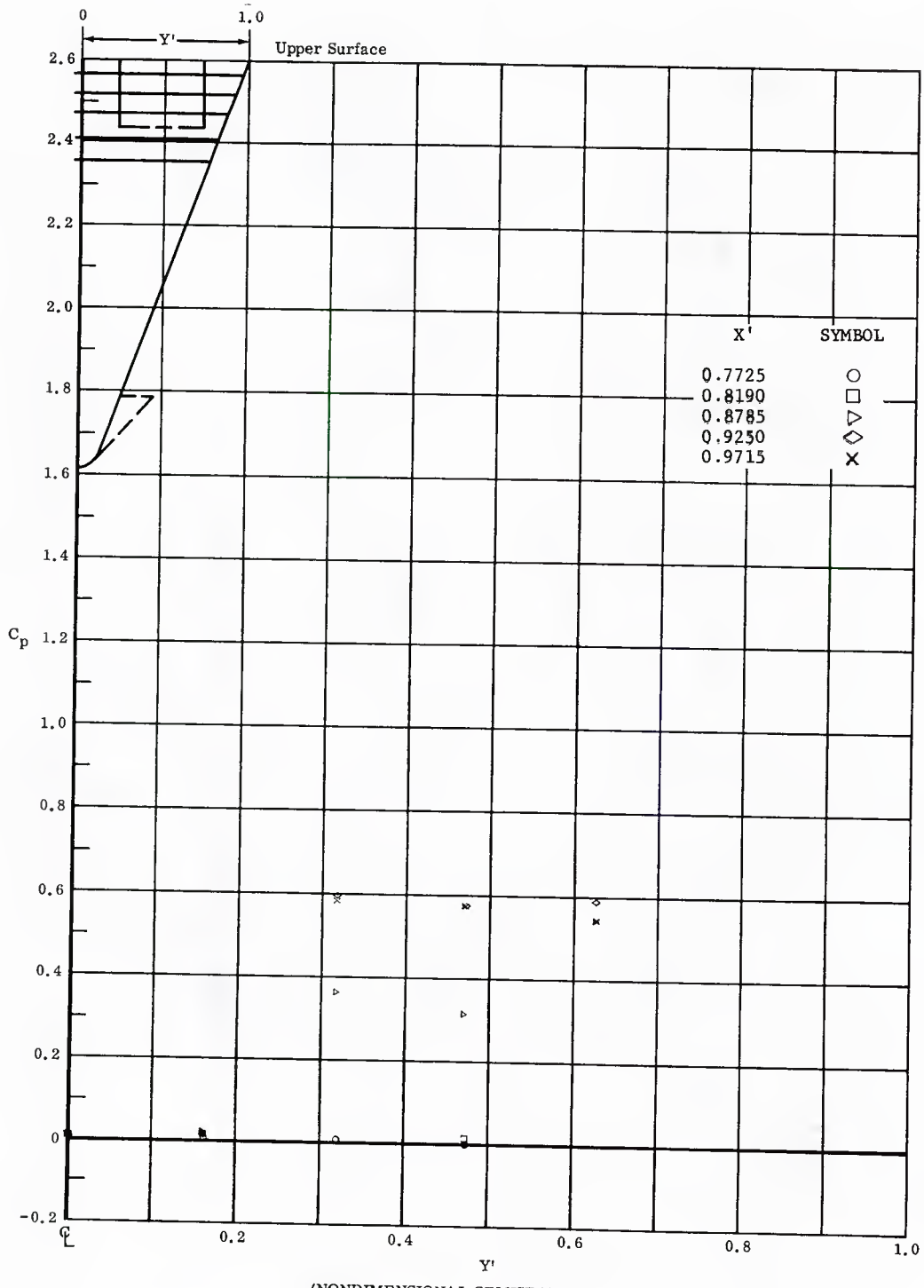

Fig. 53 Spanwise Distributions of Pressure Coefficients on Upper Surface Basic Configuration, Left and Right (Upper) Flaps Deflected -30°, α = +14.3°, β = 0

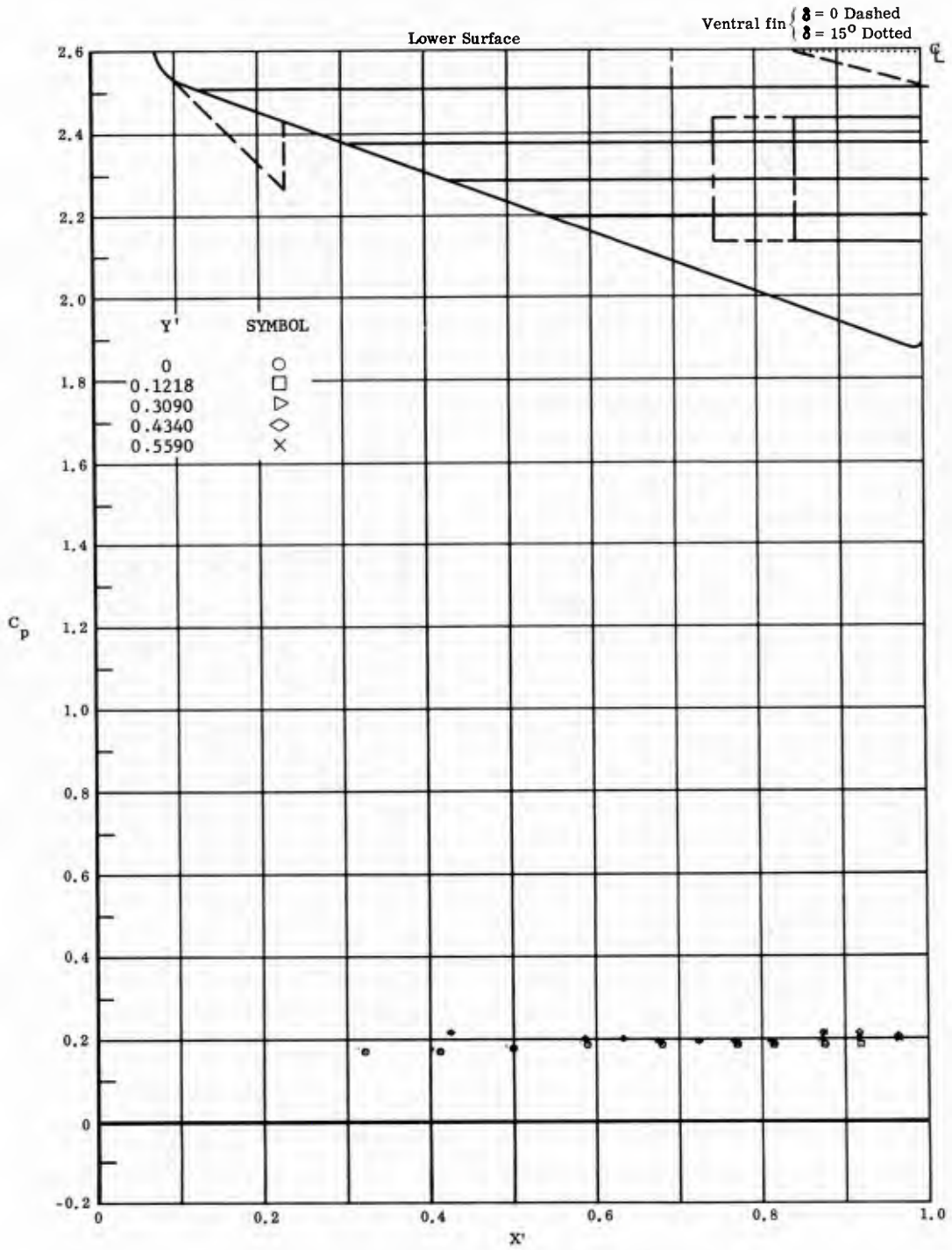

Fig. 54 Streamwise Distributions of Pressure Coefficients on Lower Surface Basic Configuration, Left and Right (Upper) Flaps Deflected -20°, $\alpha = +14.3°$, $\beta = 0$

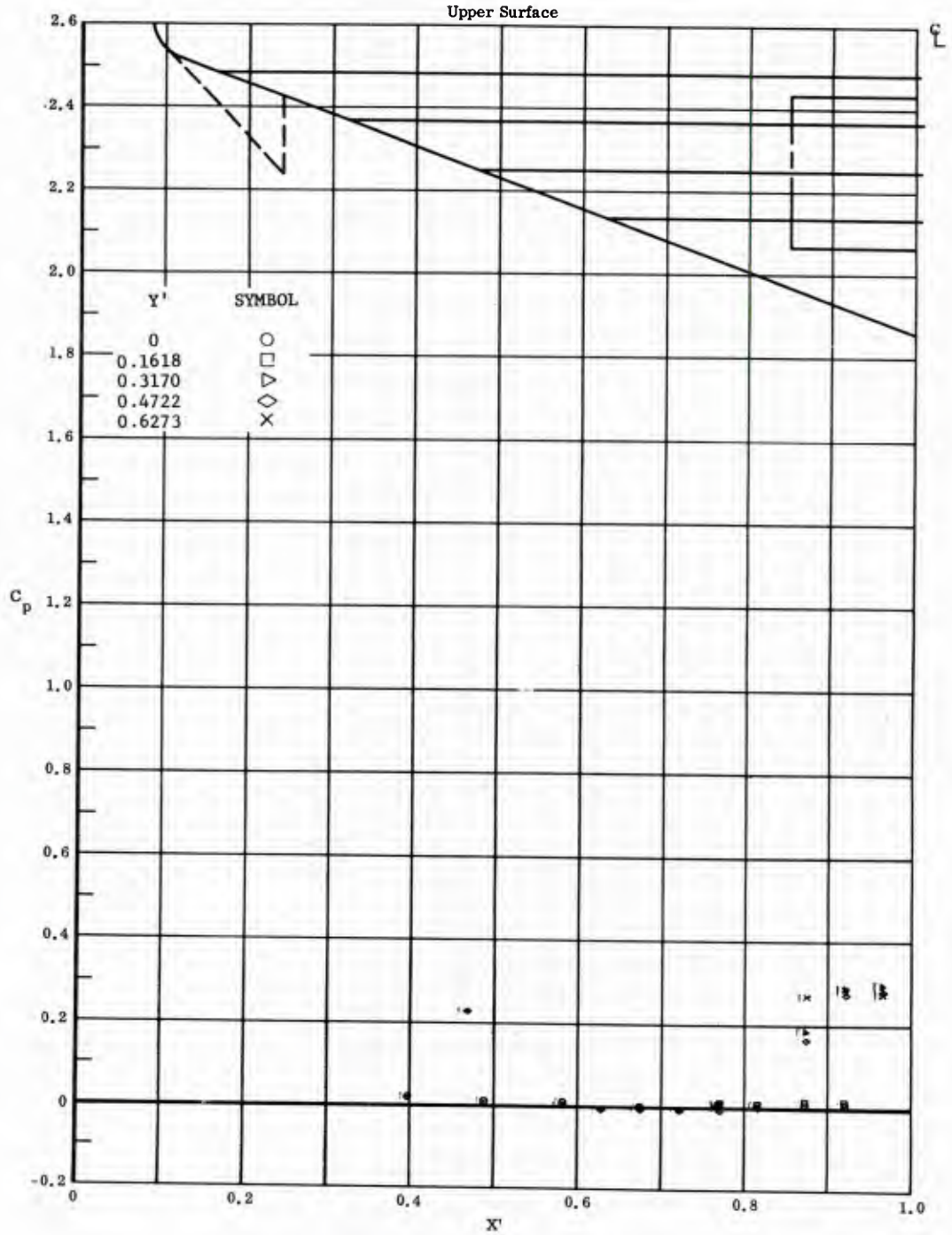

Fig. 54 Streamwise Distributions of Pressure Coefficients on Upper Surface. Basic Configuration, Left and Right (Upper) Flaps Deflected -20°, $\alpha = +14.3°$, $\beta = 0$

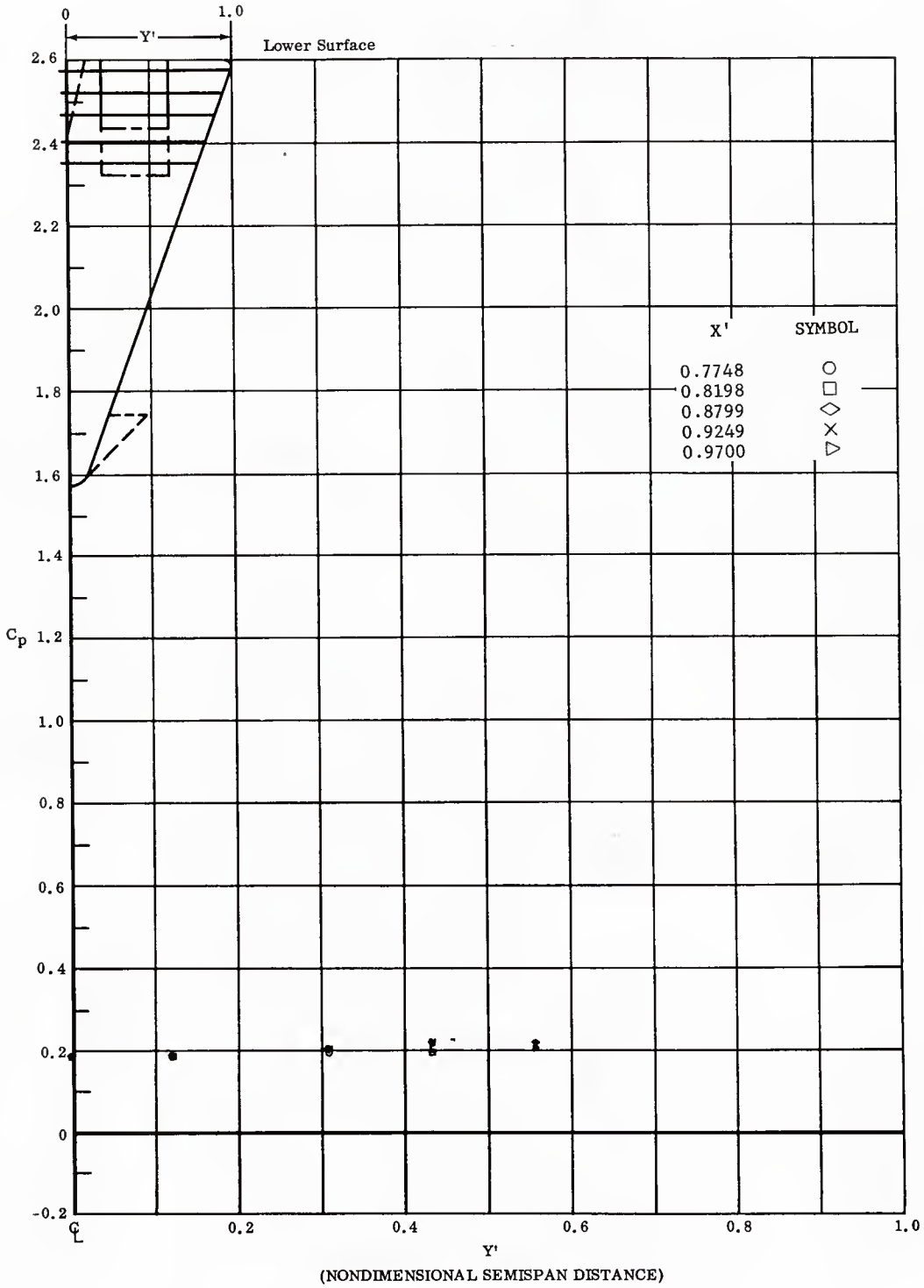

Fig. 54 Spanwise Distributions of Pressure Coefficients on Lower Surface Basic Configuration, Left and Right (Upper) Flaps Deflected -20°, $\alpha = +14.3°$, $\beta = 0$

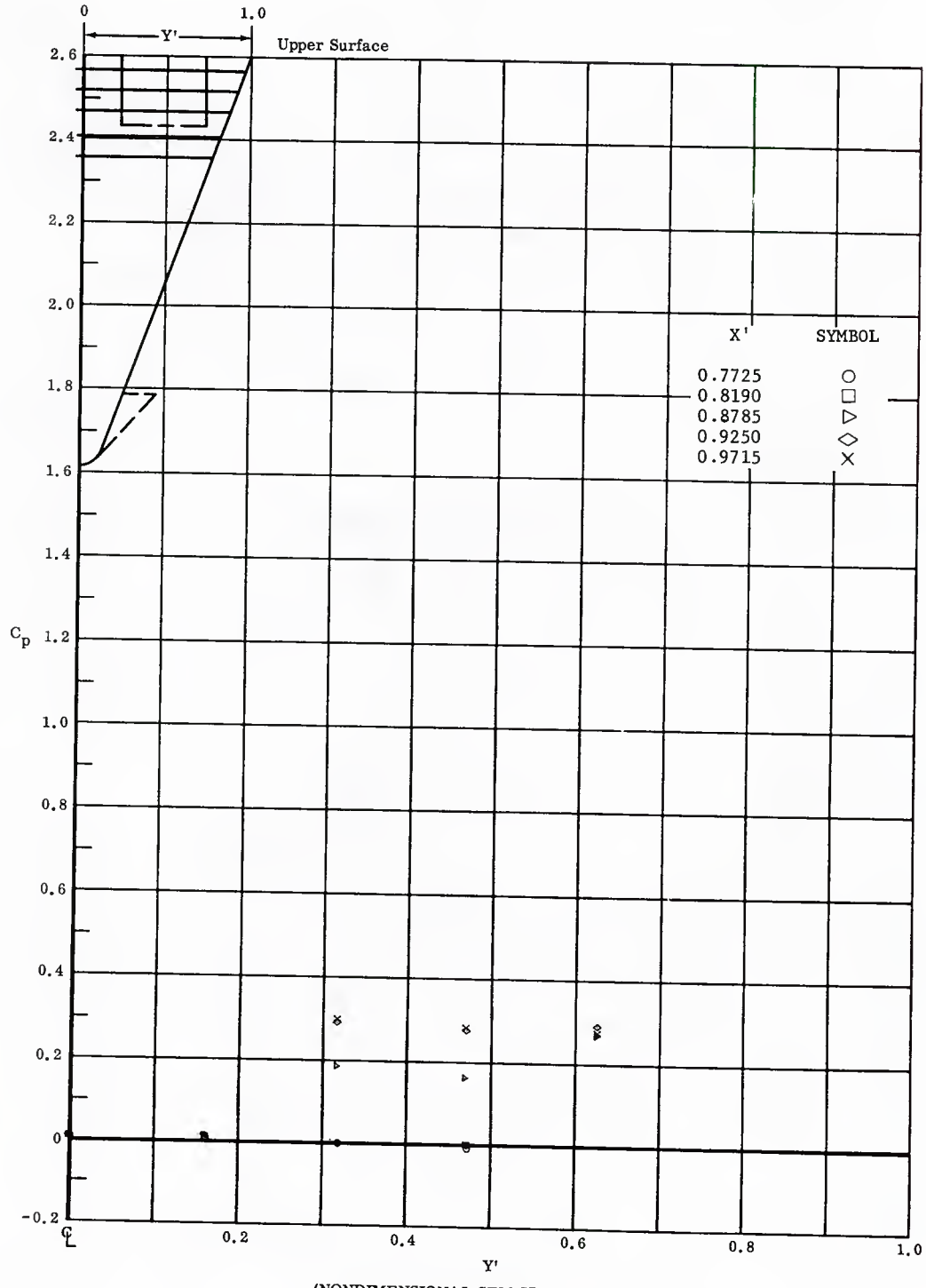

Fig. 54 Spanwise Distributions of Pressure Coefficients on Upper Surface Basic Configuration, Left and Right (Upper) Flaps Deflected -20°, $\alpha = +14.3°$, $\beta = 0$

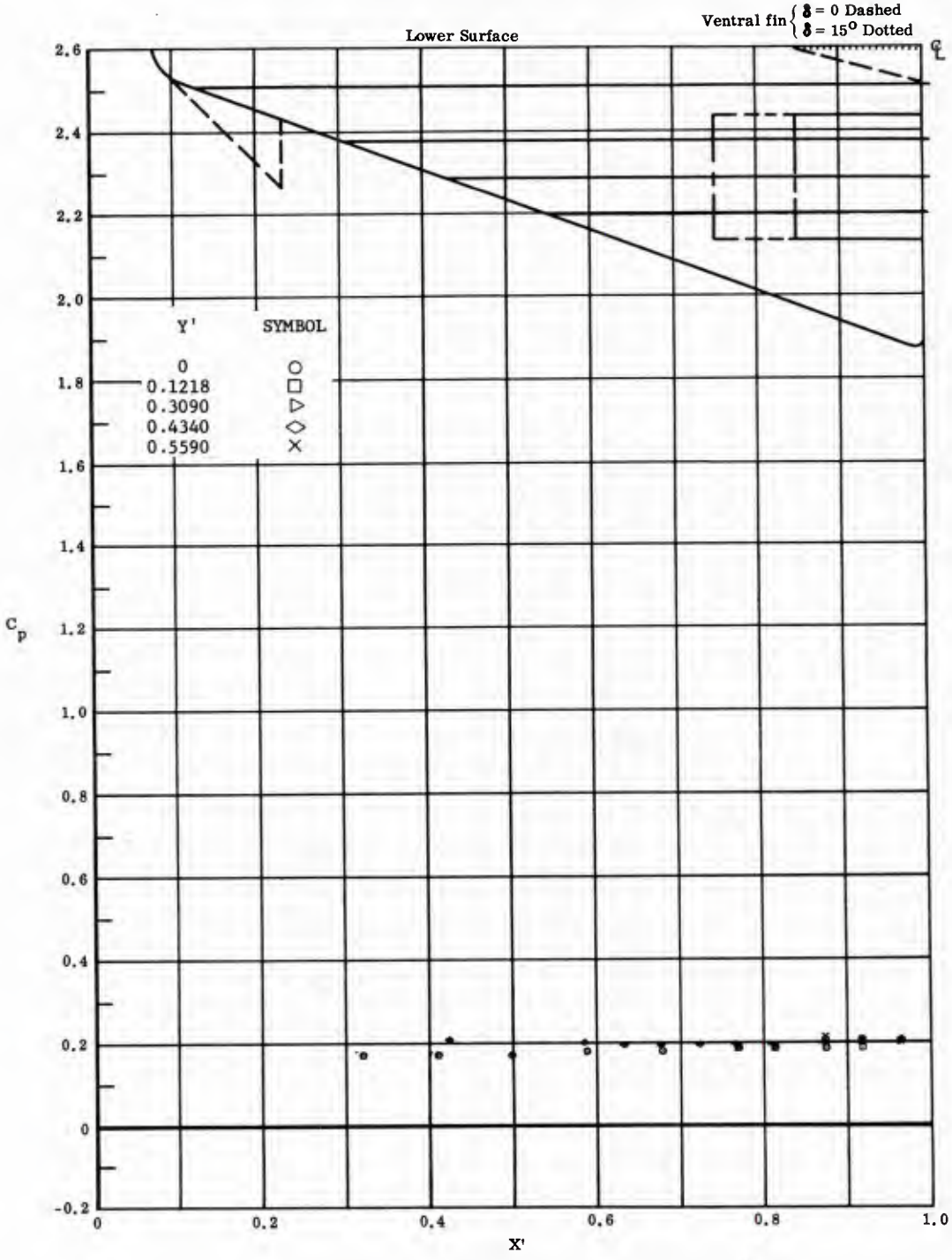

Fig. 55 Streamwise Distributions of Pressure Coefficients on Lower Surface Basic Configuration, Left (Upper) Flap Deflected -20°, α =+14.3°, β =

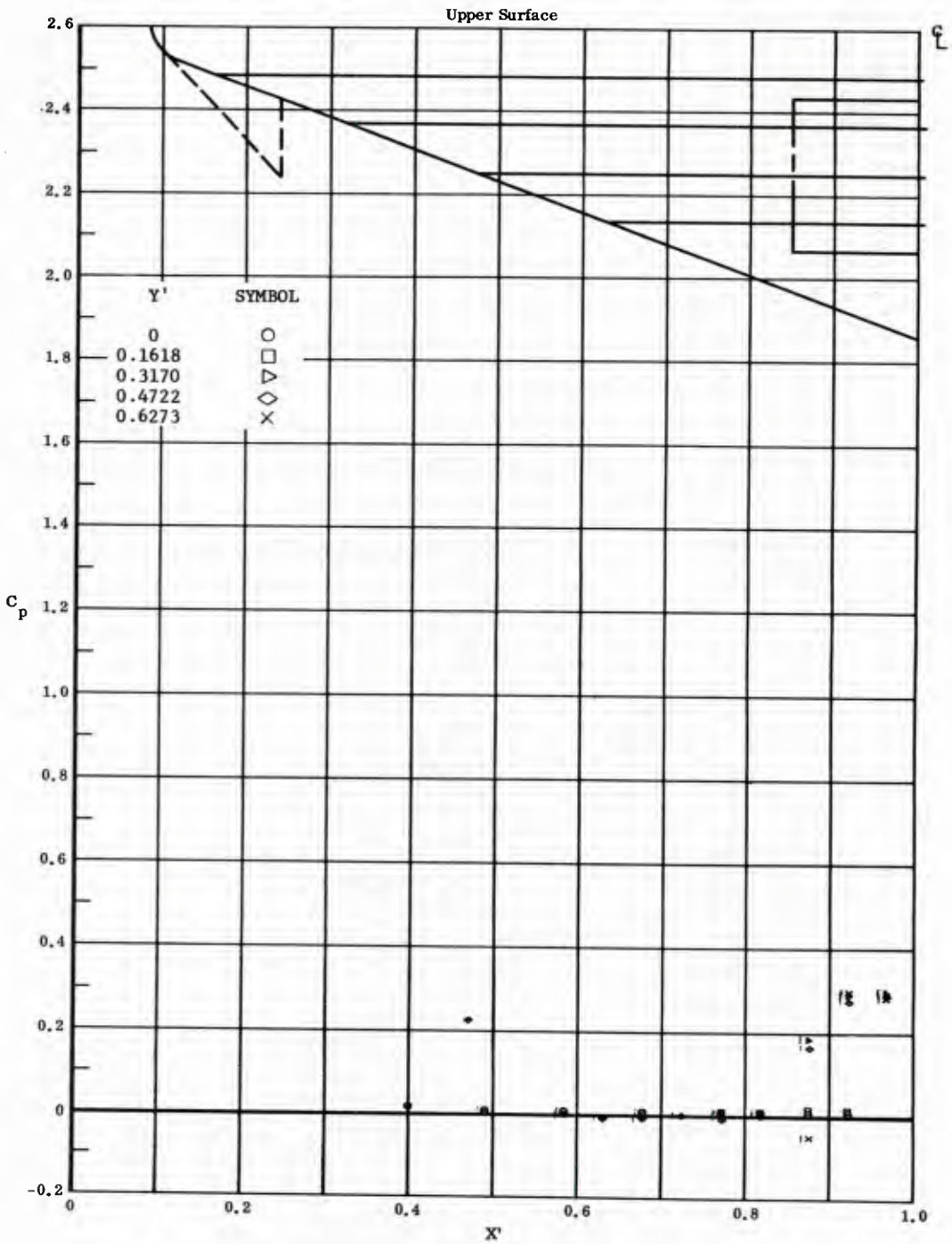

Fig. 55 Streamwise Distributions of Pressure Coefficients on Upper Surface Basic Configuration, Left (Upper) Flap Deflected -20°, α =+14.3°, β = 0

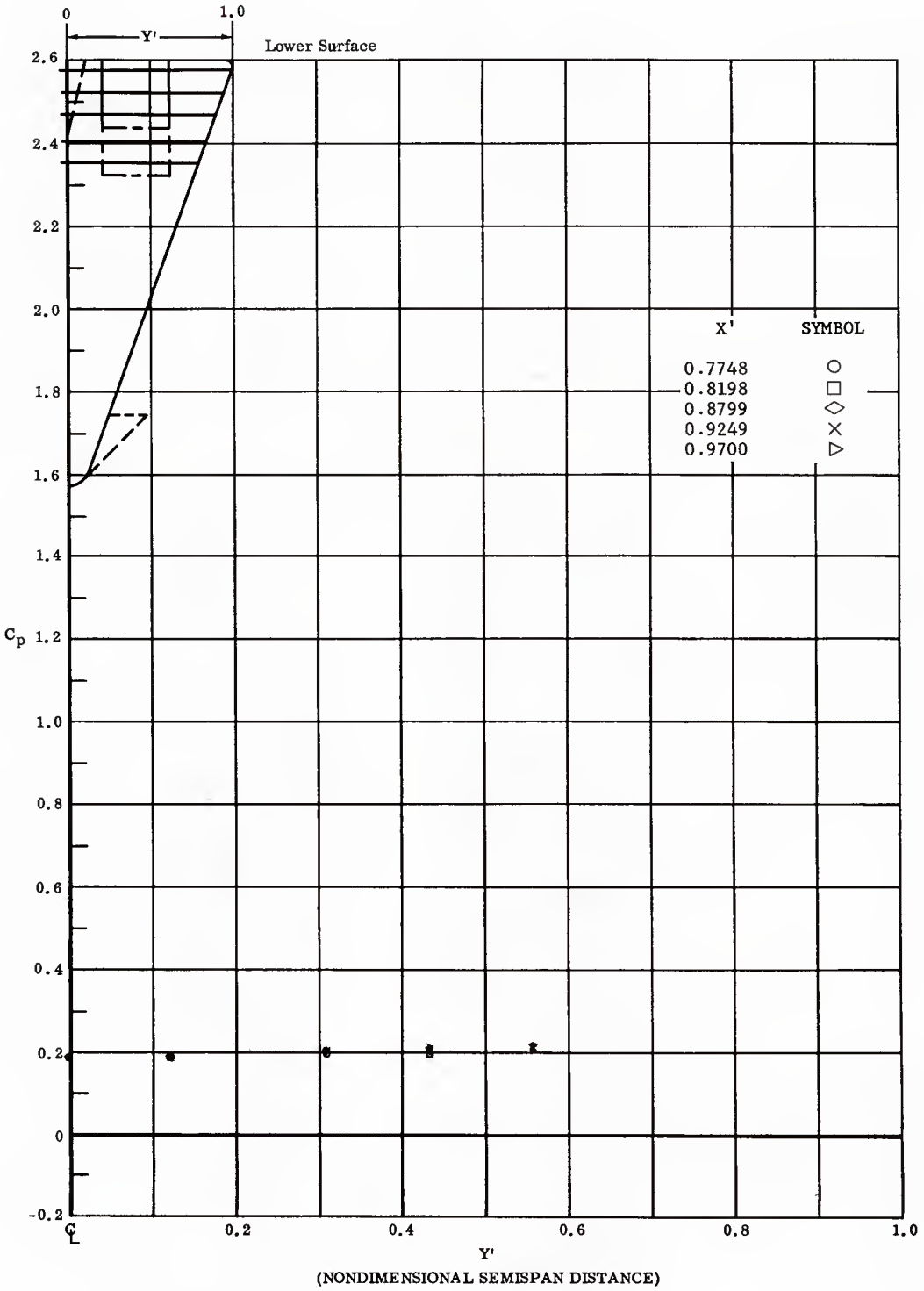

Fig. 55 Spanwise Distributions of Pressure Coefficients on Lower Surface
Basic Configuration, Left (Upper) Flap Deflected -20°, α = +14.3°, β = 0

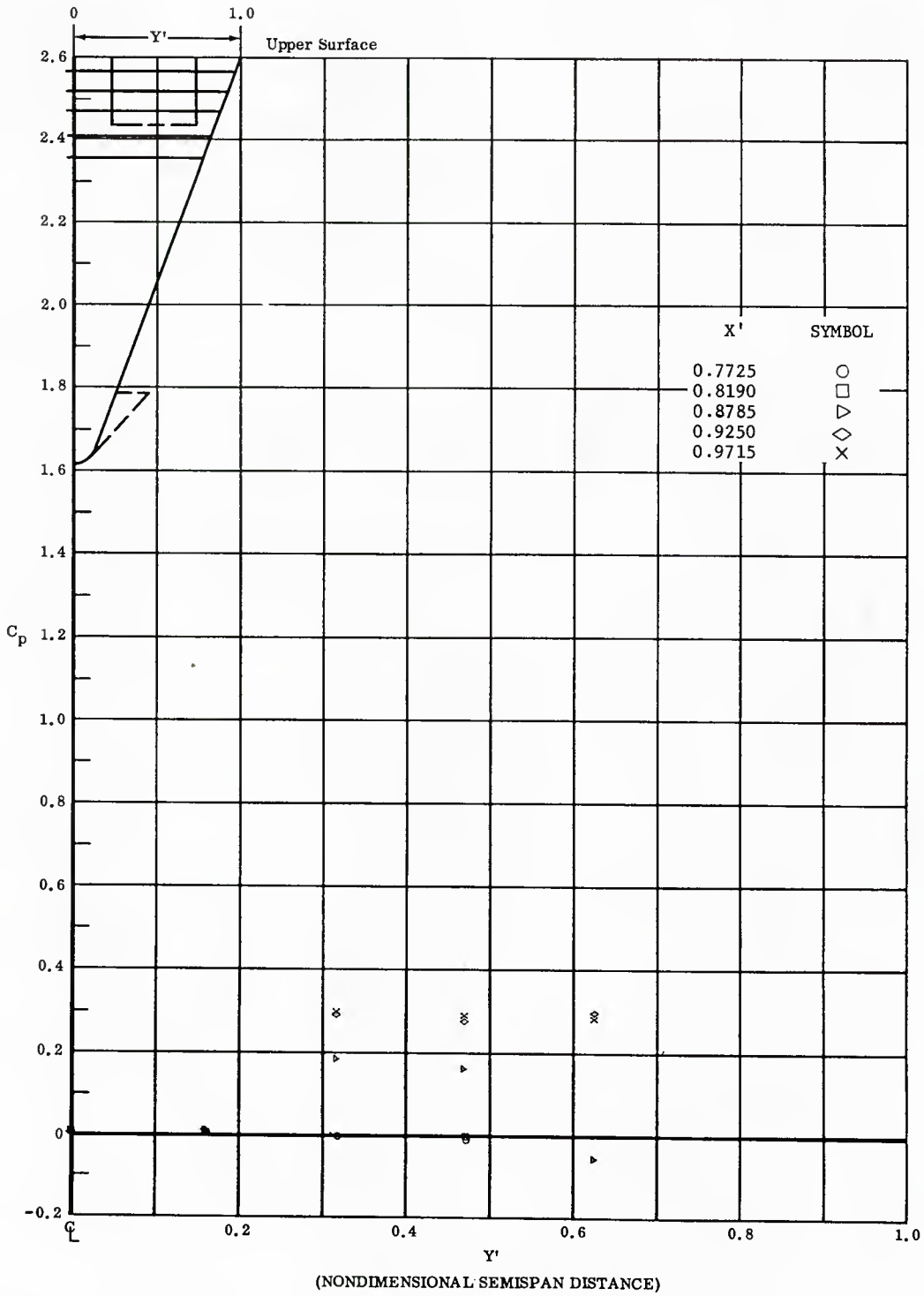

Fig. 55 Spanwise Distributions of Pressure Coefficients on Upper Surface
Basic Configuration, Left (Upper) Flap Deflected -20°, $\alpha = 14.3°$, $\beta = 0$

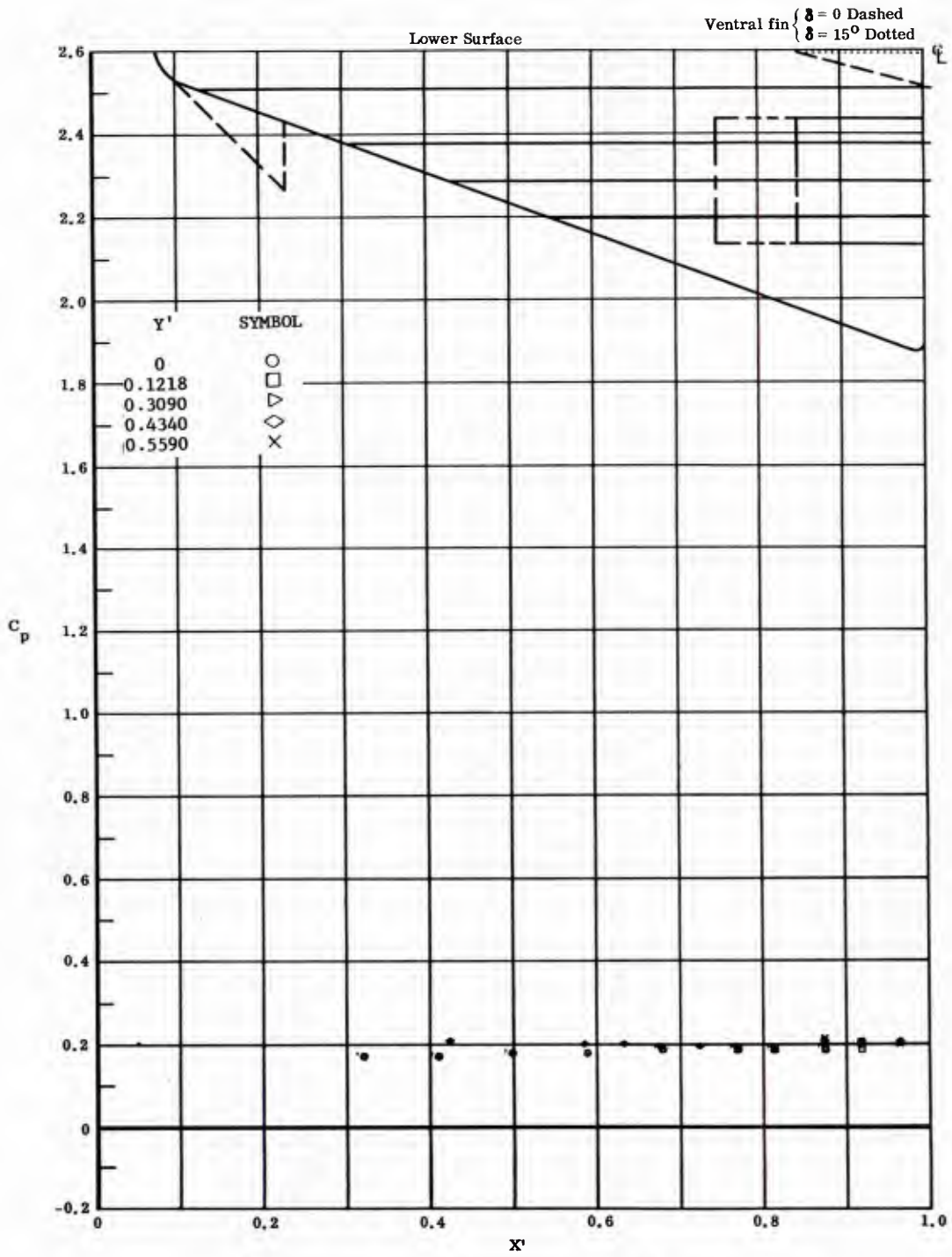

Fig. 56 Streamwise Distributions of Pressure Coefficients on Lower Surface Basic Configuration, Left and Right (Upper) Flaps Deflected -10°, α=+14.3°, β = 0

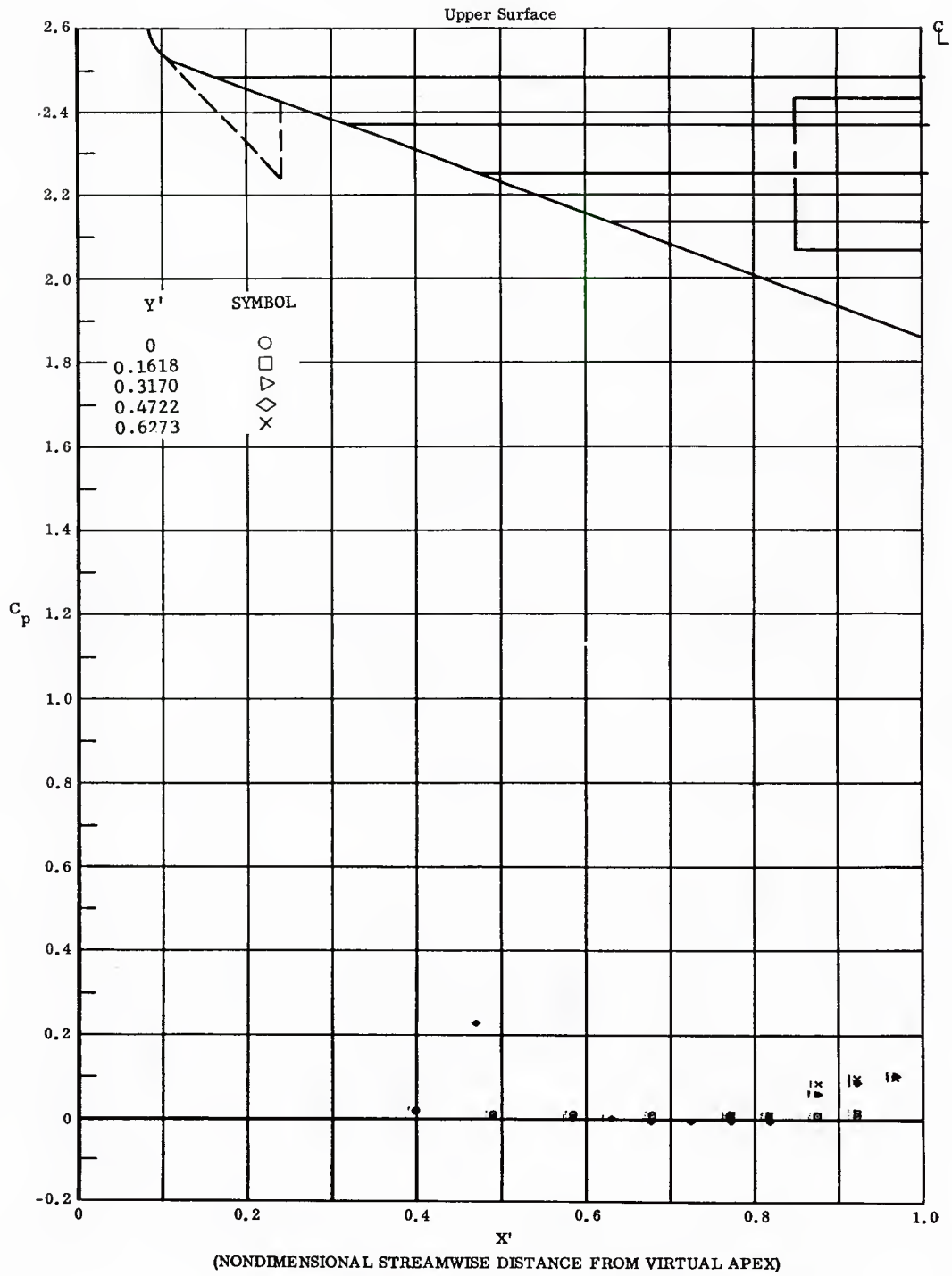

Fig. 56 Streamwise Distributions of Pressure Coefficients on Upper Surface Basic Configuration, Left and Right (Upper) Flaps Deflected -10°, $\alpha = +14.3°$, $\beta = 0$

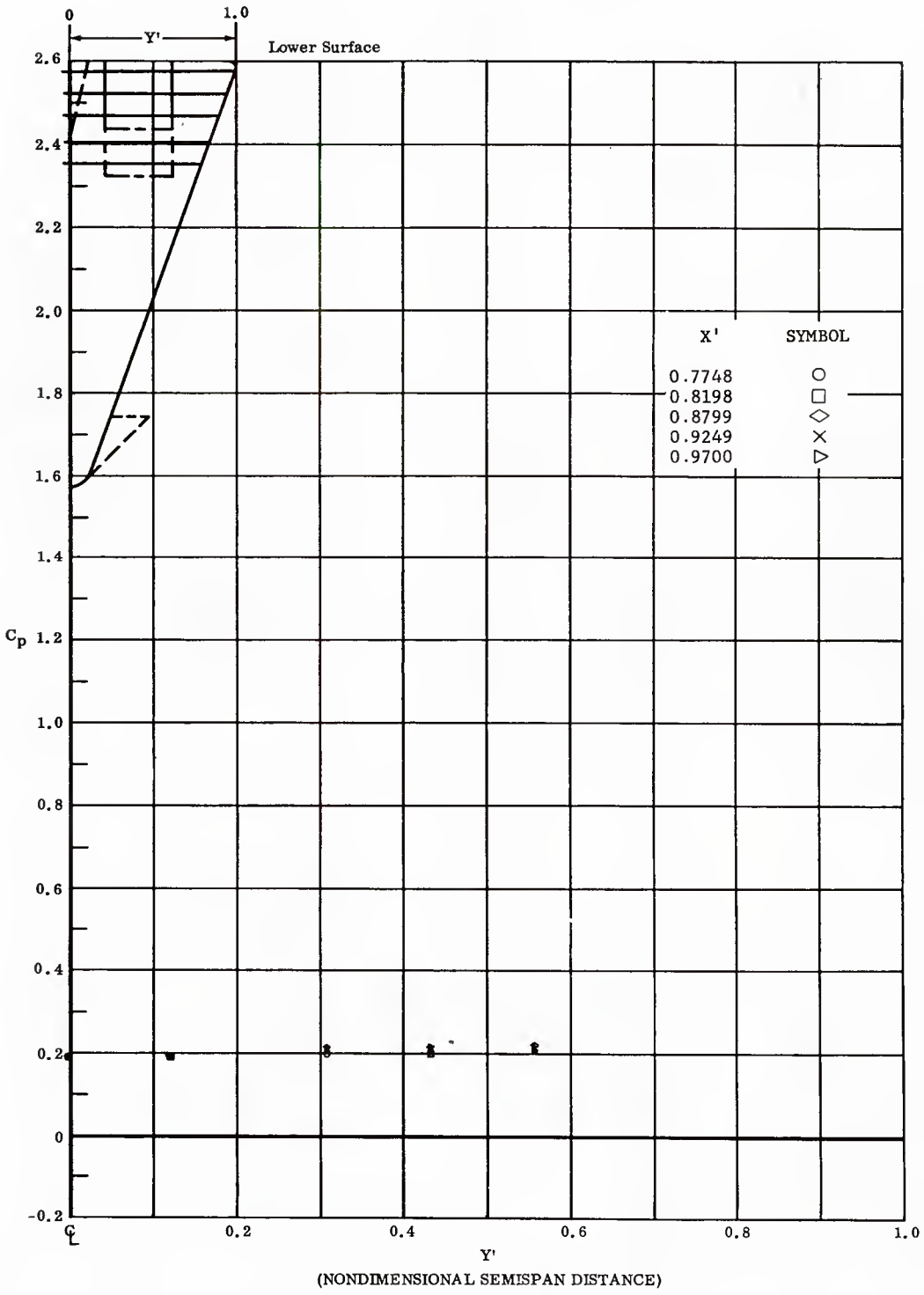

Fig. 56 Spanwise Distributions of Pressure Coefficients on Lower Surface Basic Configuration, Left and Right (Upper) Flaps Deflected -10°, α=+14.3°, β = 0

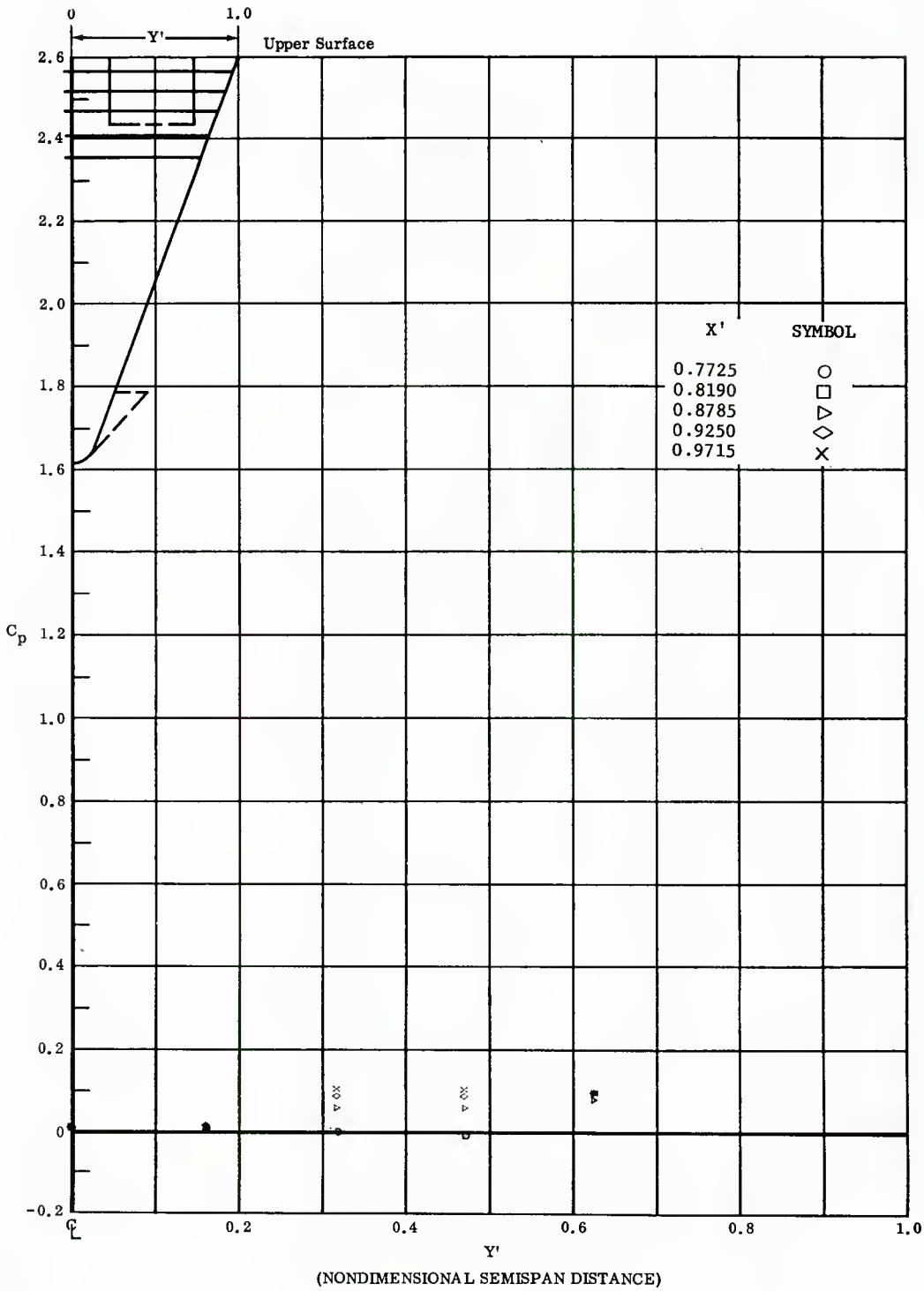

Fig. 56 Spanwise Distributions of Pressure Coefficients on Upper Surface Basic Configuration, Left and Right (Upper) Flaps Deflected -10°, $\alpha = +14.3°$, $\beta = 0$

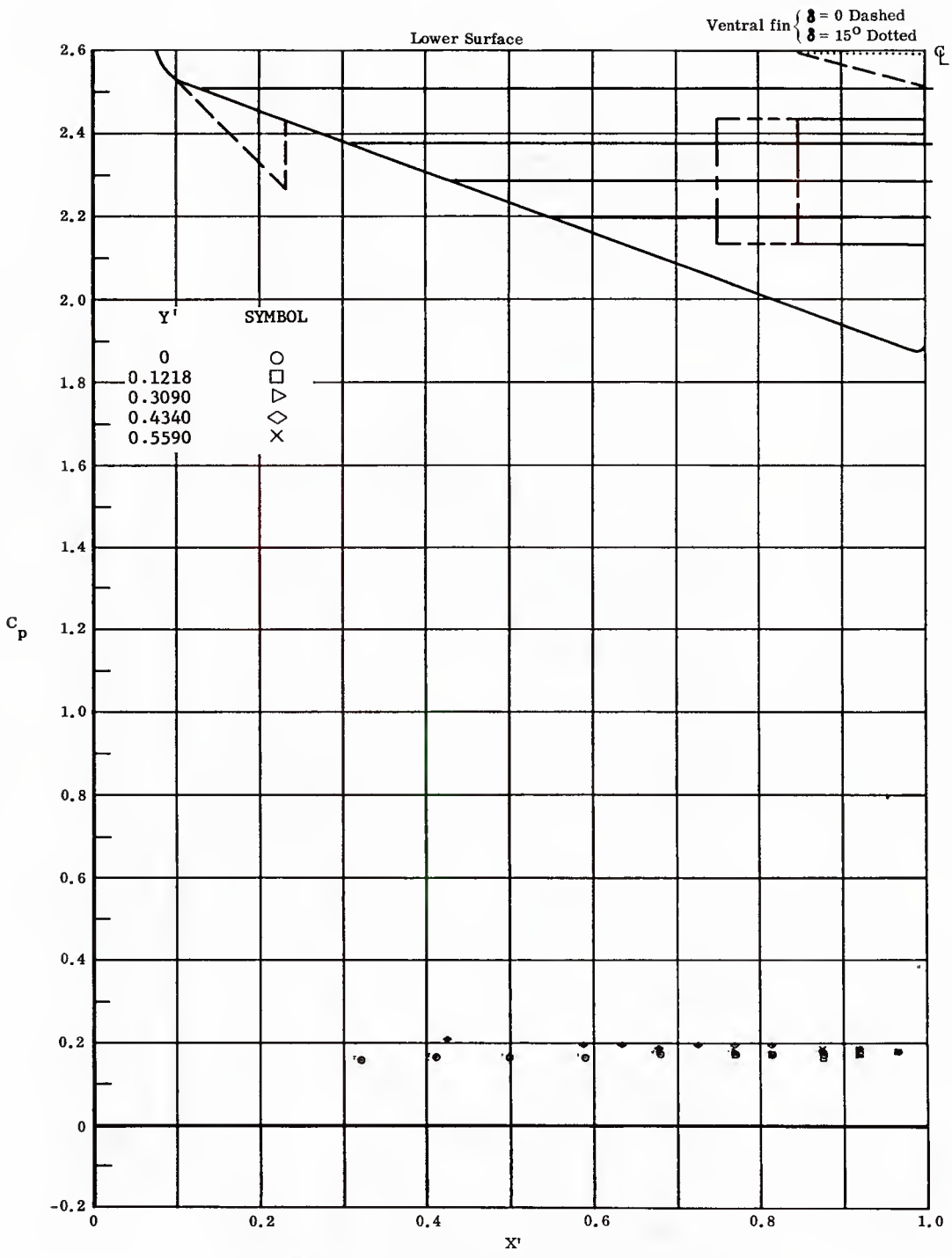

Fig. 57 Streamwise Distributions of Pressure Coefficients on Lower Surface
Basic Configuration, No Flap Deflections, α = +14.3°, β = 0

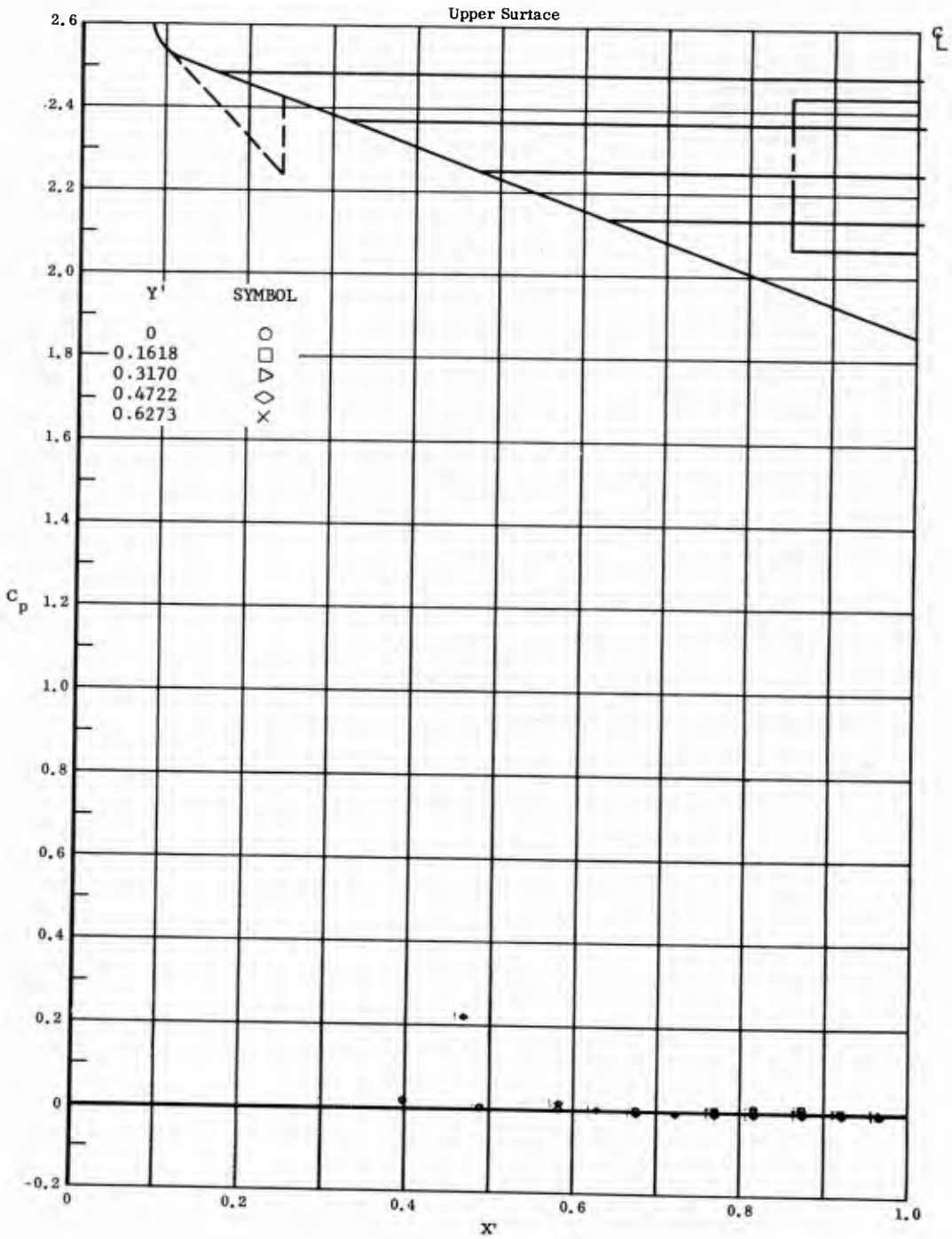

Fig. 57 Streamwise Distributions of Pressure Coefficients on Upper Surface Basic Configuration, No Flap Deflections, $\alpha = +14.3°$, $\beta = 0$

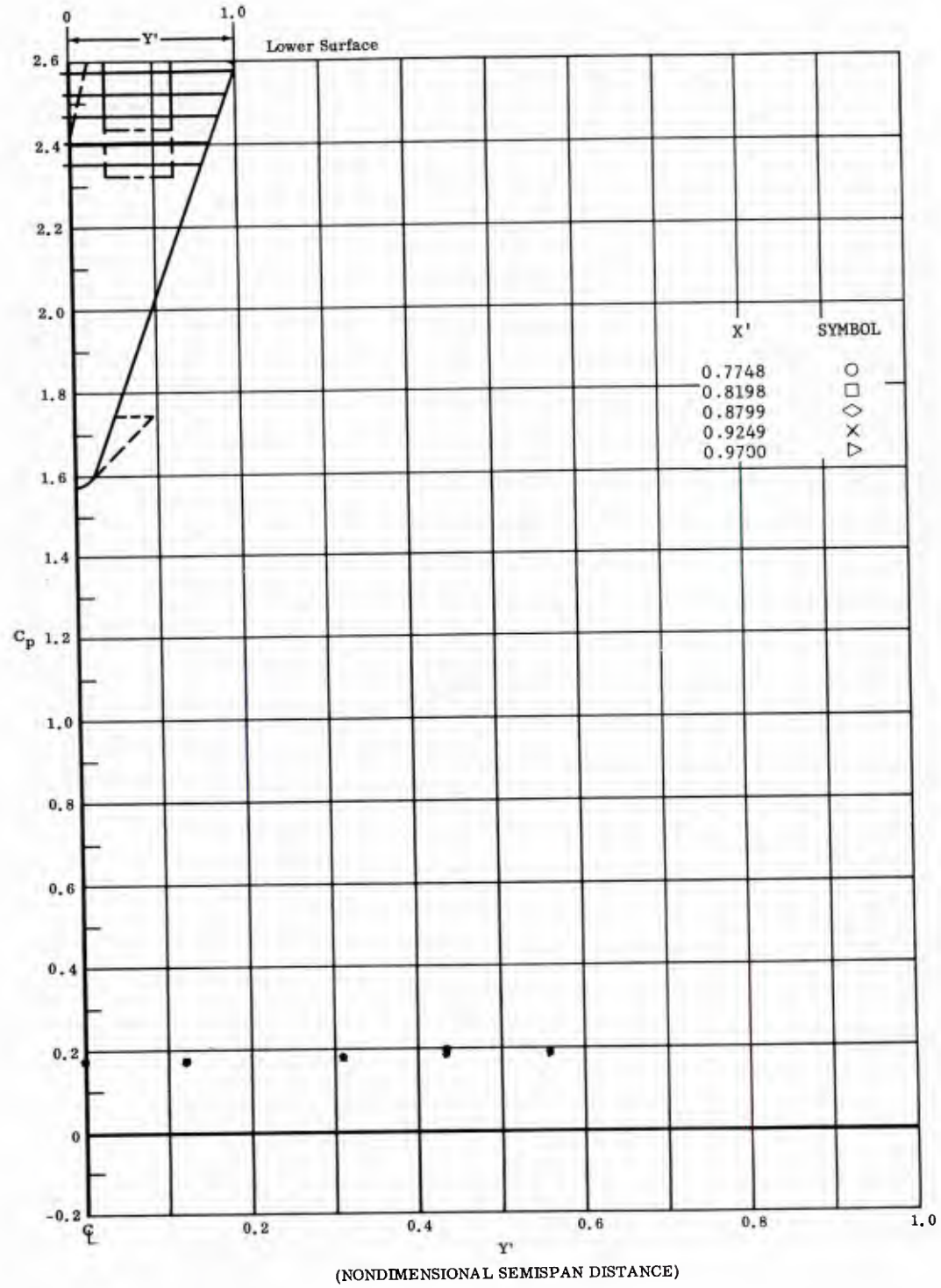

Fig. 57 Spanwise Distributions of Pressure Coefficients on Lower Surface
Basic Configuration, No Flap Deflections, α = +14.3°, β = 0

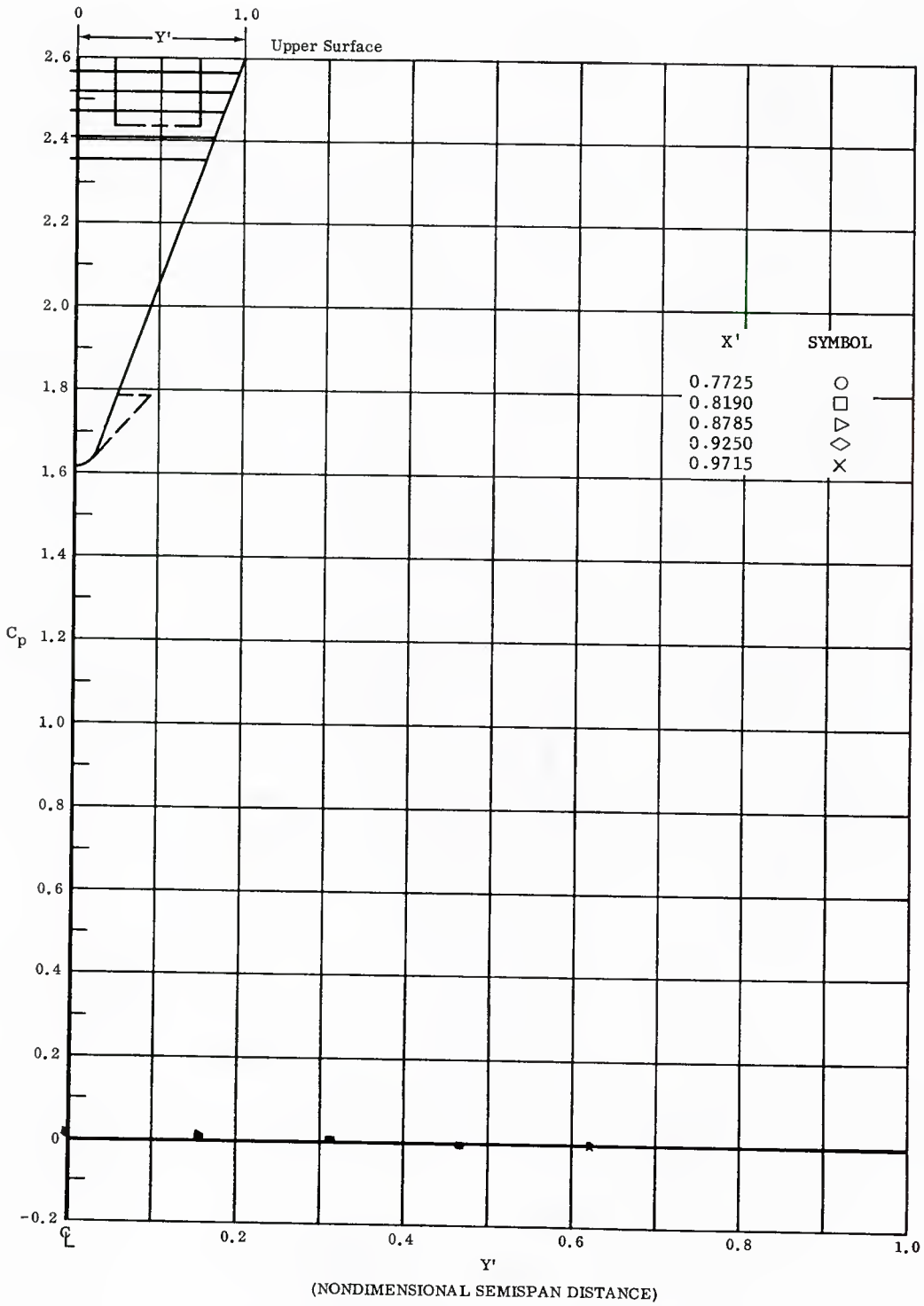

Fig. 57 Spanwise Distributions of Pressure Coefficients on Upper Surface
Basic Configuration, No Flap Deflections, α = +14.3°, β = 0

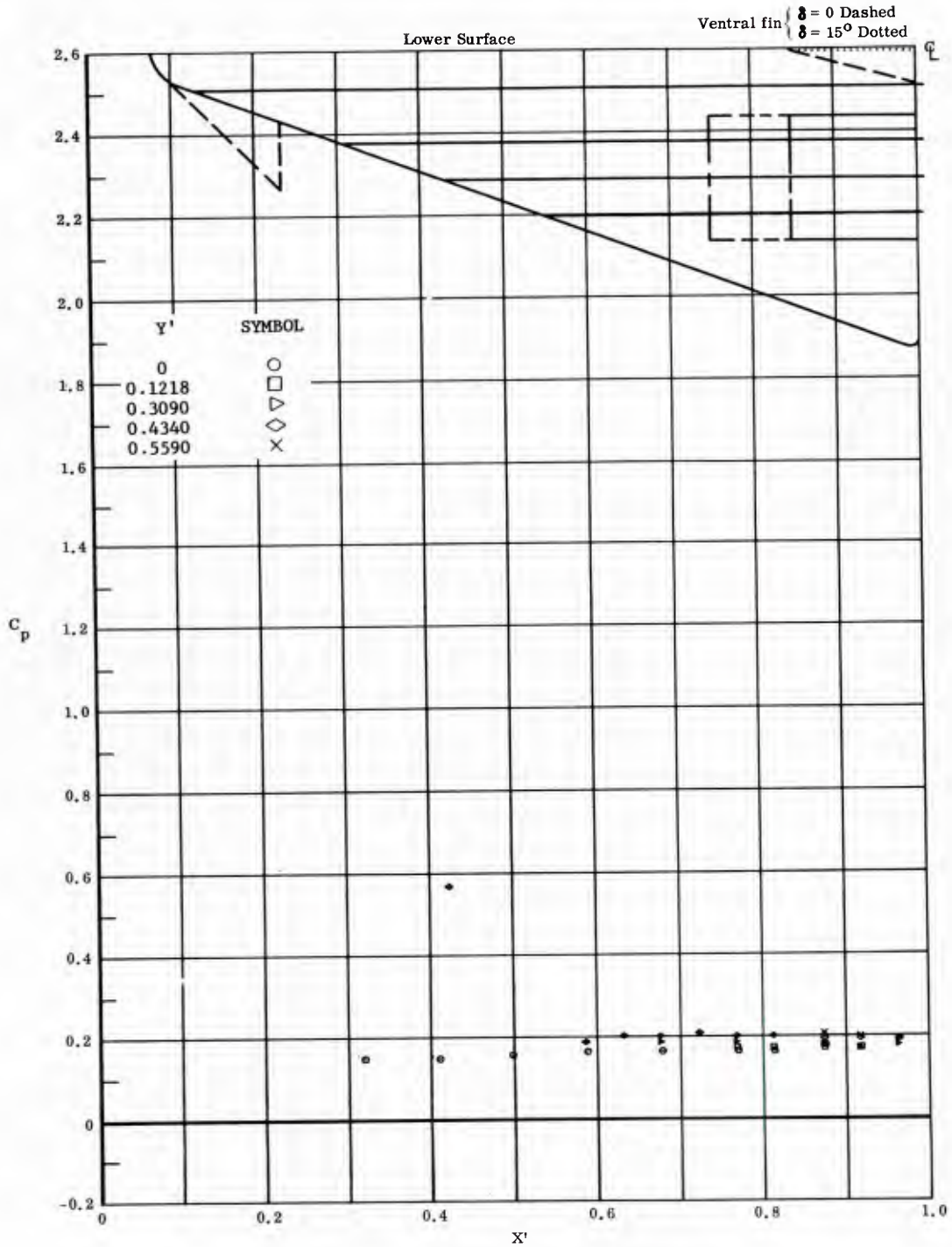

Fig. 58 Streamwise Distributions of Pressure Coefficients on Lower Surface
Basic Configuration, No Flap Deflections, α = +14.3°, β = +14°

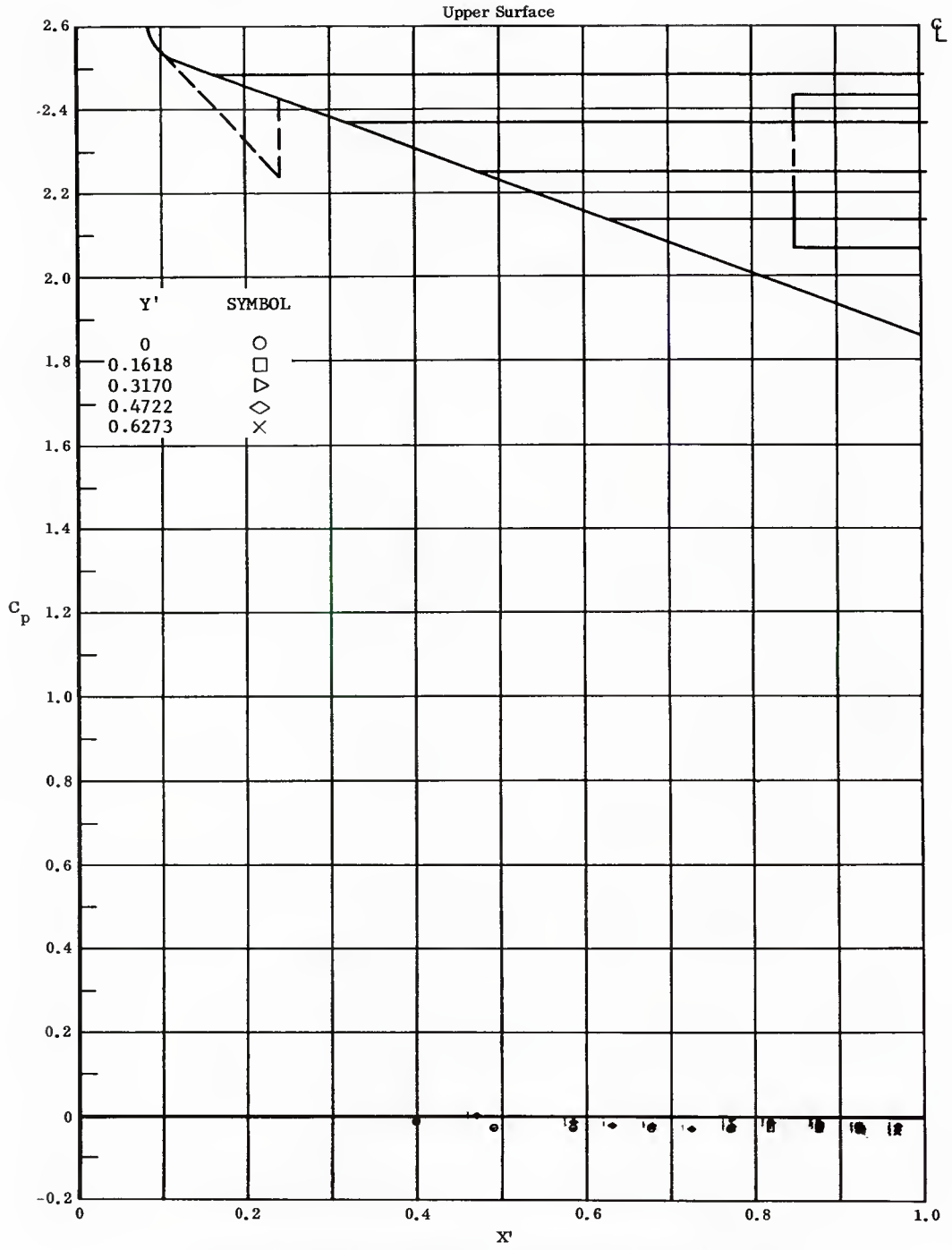

Fig. 58 Streamwise Distributions of Pressure Coefficients on Upper Surface
Basic Configuration, No Flap Deflections, α = +14.3°, β = +14°

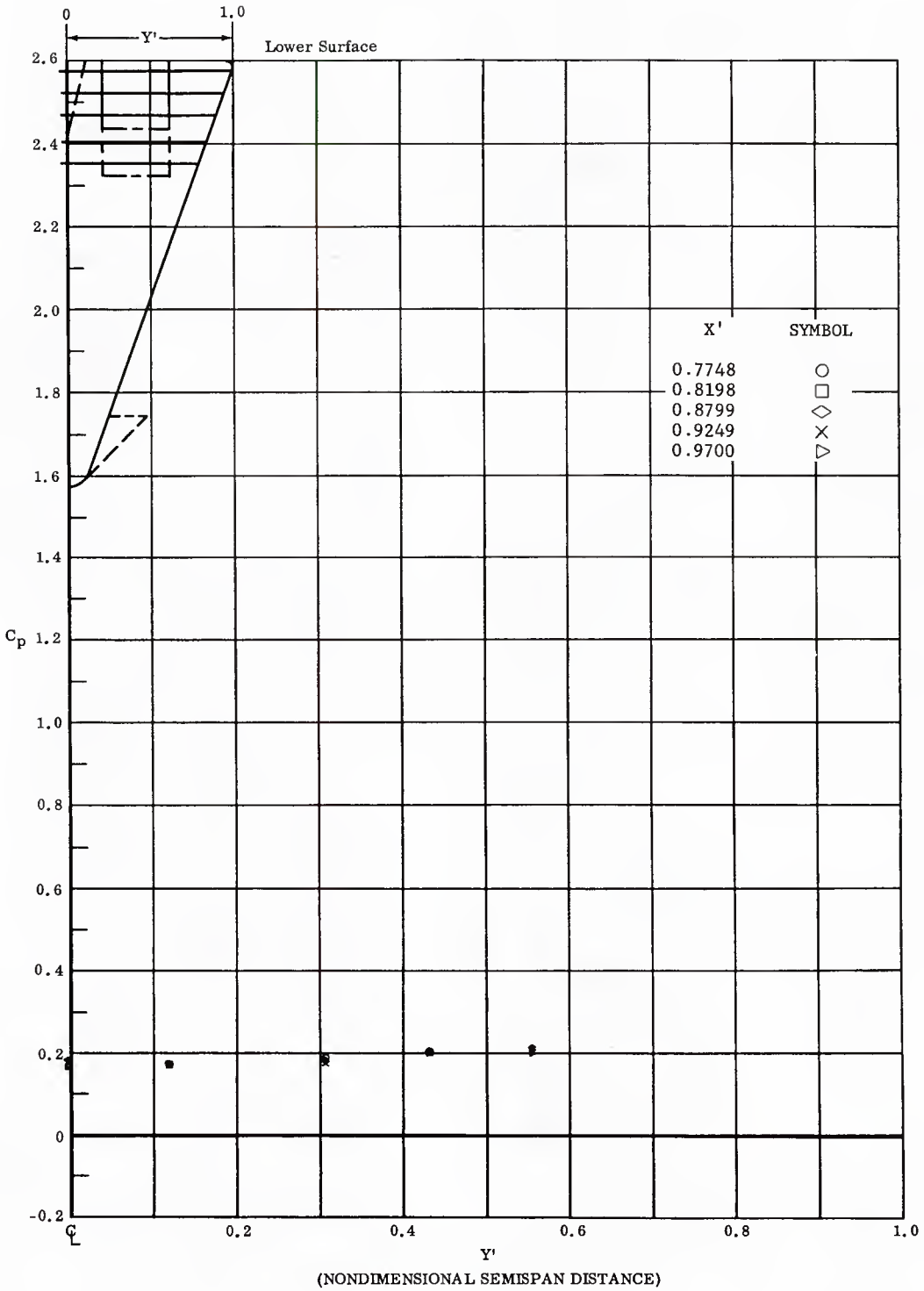

Fig. 58 Spanwise Distributions of Pressure Coefficients on Lower Surface
Basic Configuration, No Flap Deflections, α = +14.3°, β = +14°

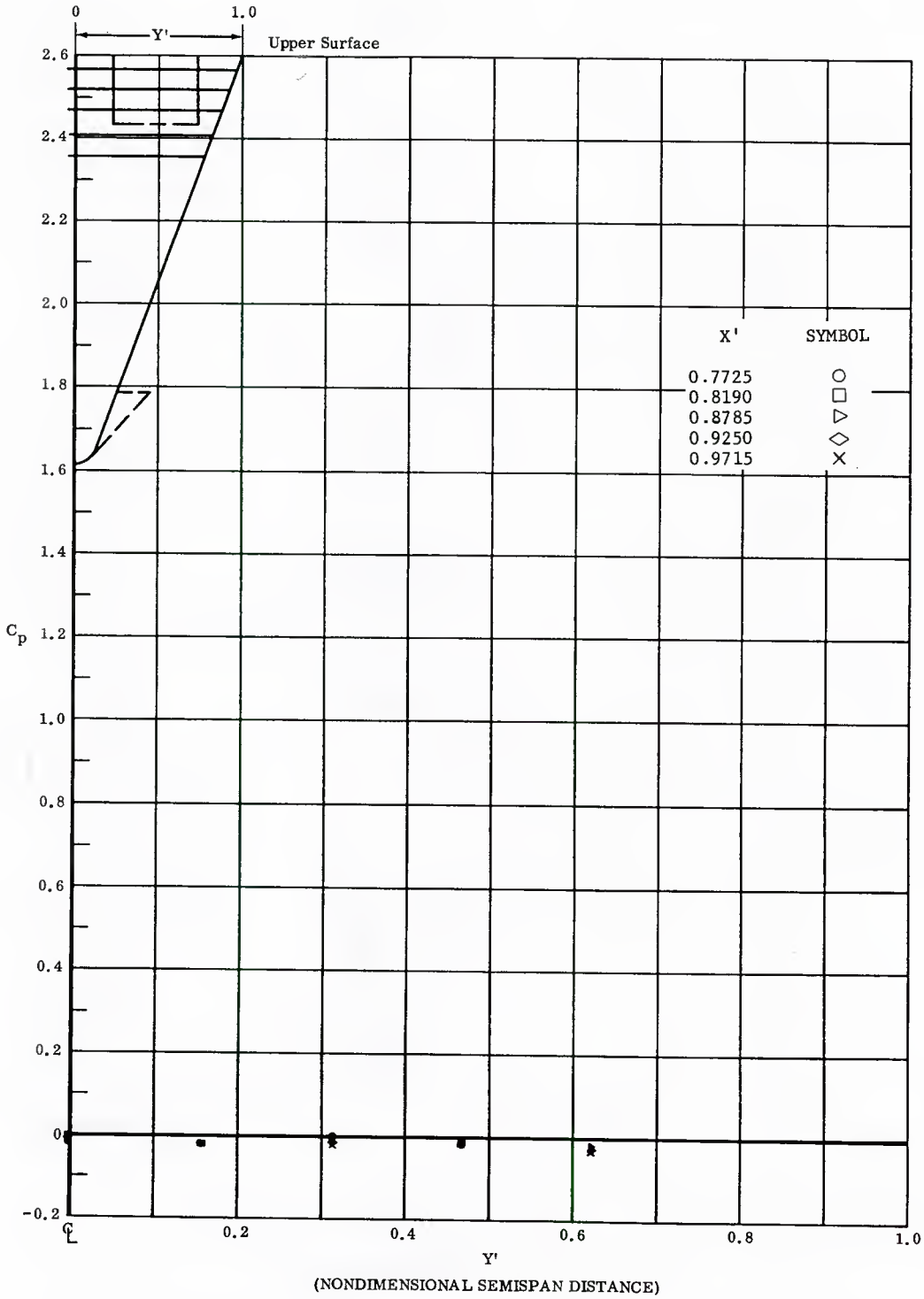

Fig. 58 Spanwise Distributions of Pressure Coefficients on Upper Surface
Basic Configuration, No Flap Deflections, α = +14.3°, β = +14°

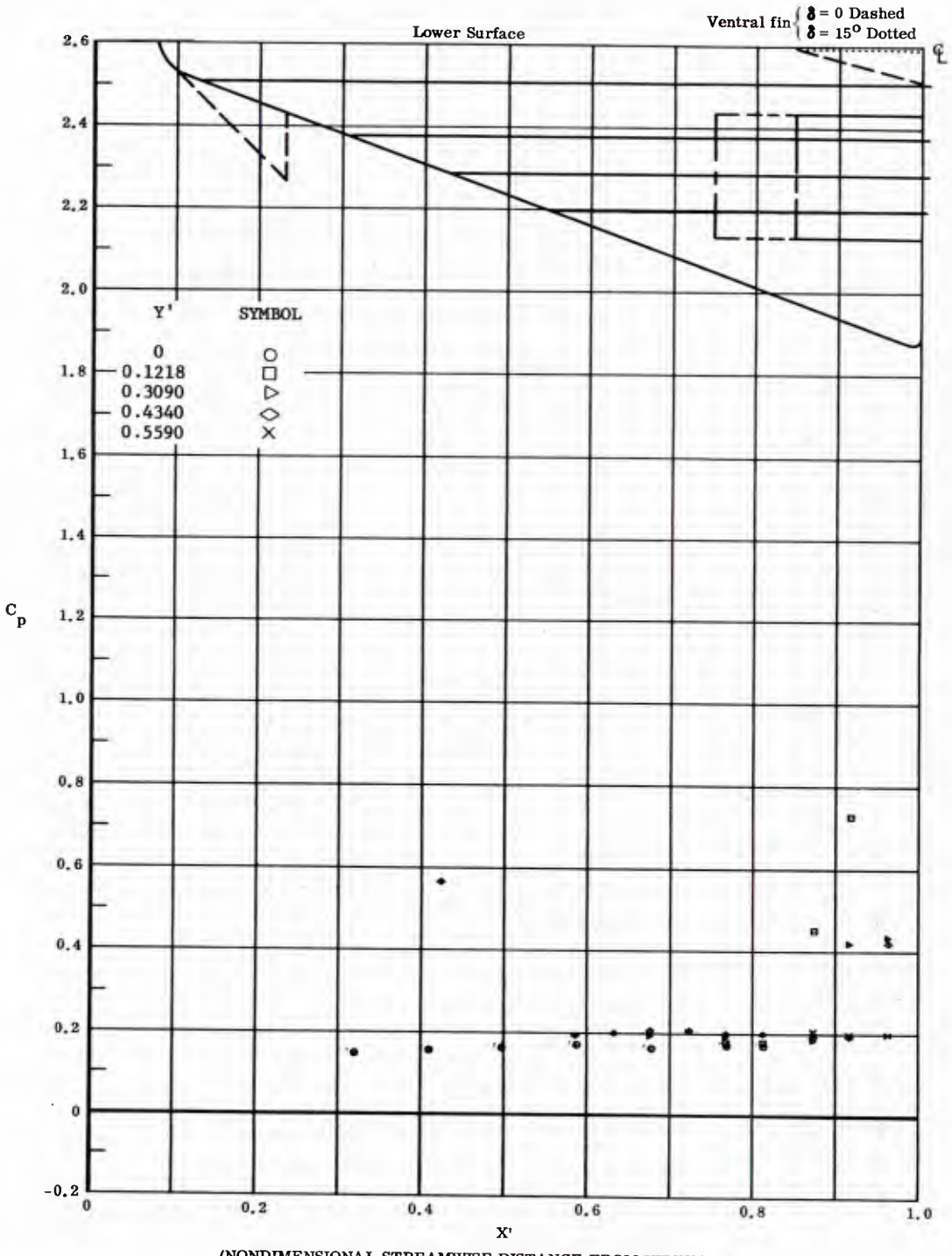

Fig. 59 Streamwise Distributions of Pressure Coefficients on Lower Surface Ventral Fin on Lower Surface Not Deflected, No Flap Deflections, α = +14.3°, β = +14°

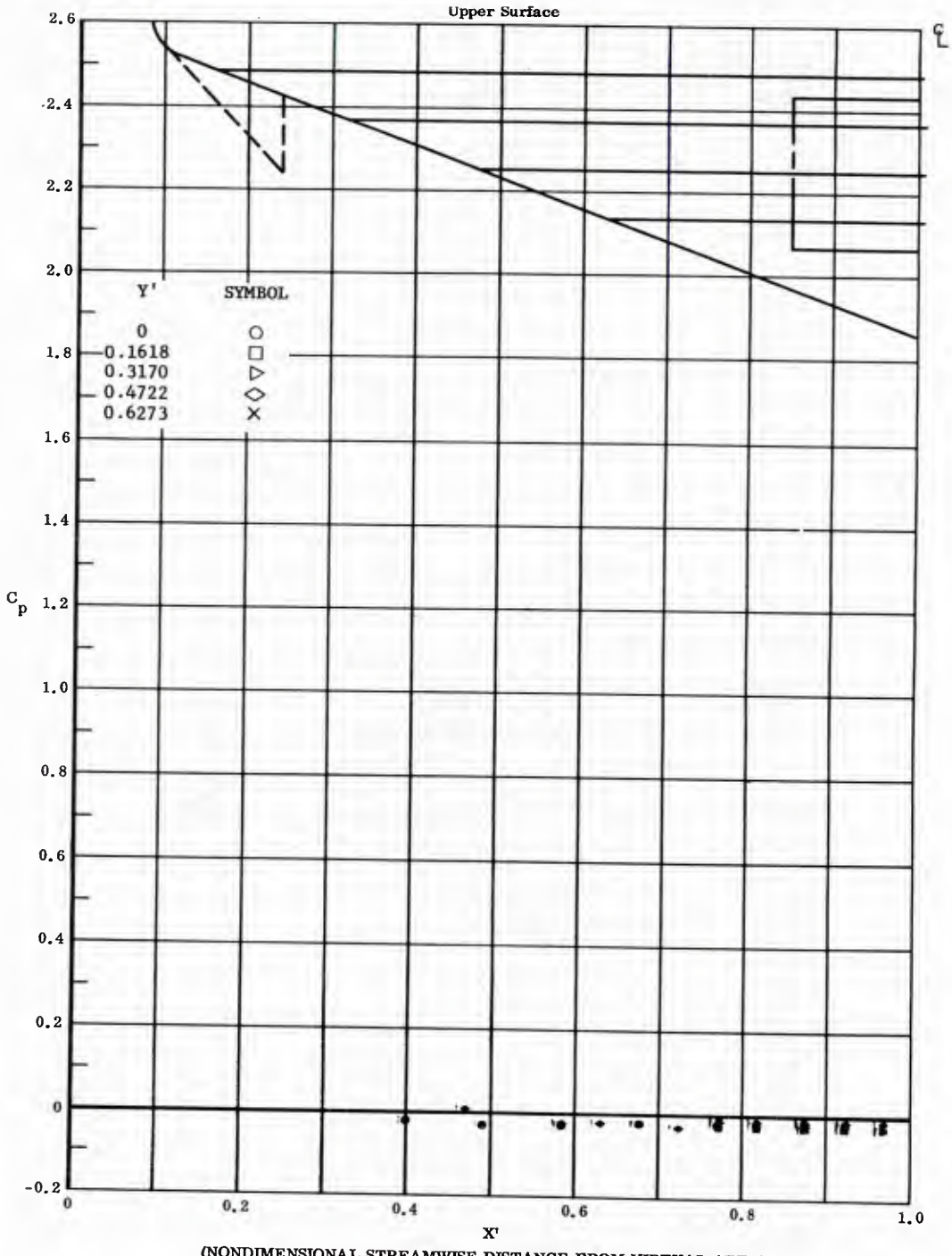

Fig. 59 Streamwise Distributions of Pressure Coefficients on Upper Surface Ventral Fin on Lower Surface Not Deflected, No Flap Deflections, $\alpha = +14.3°$, $\beta = +14°$

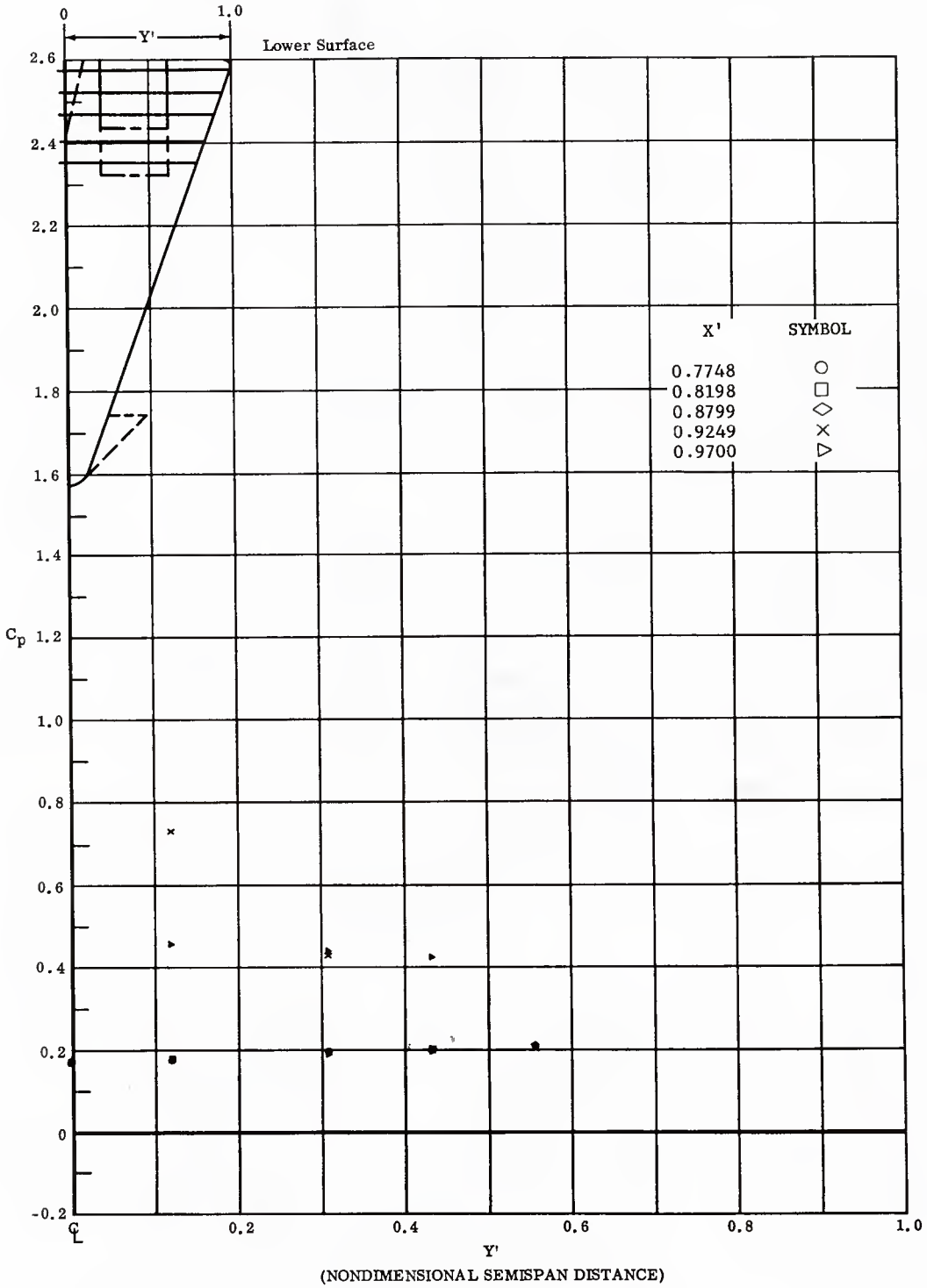

Fig. 59 Spanwise Distributions of Pressure Coefficients on Lower Surface Ventral Fin on Lower Surface Not Deflected, No Flap Deflections, $\alpha = +14.3°$, $\beta = +14°$

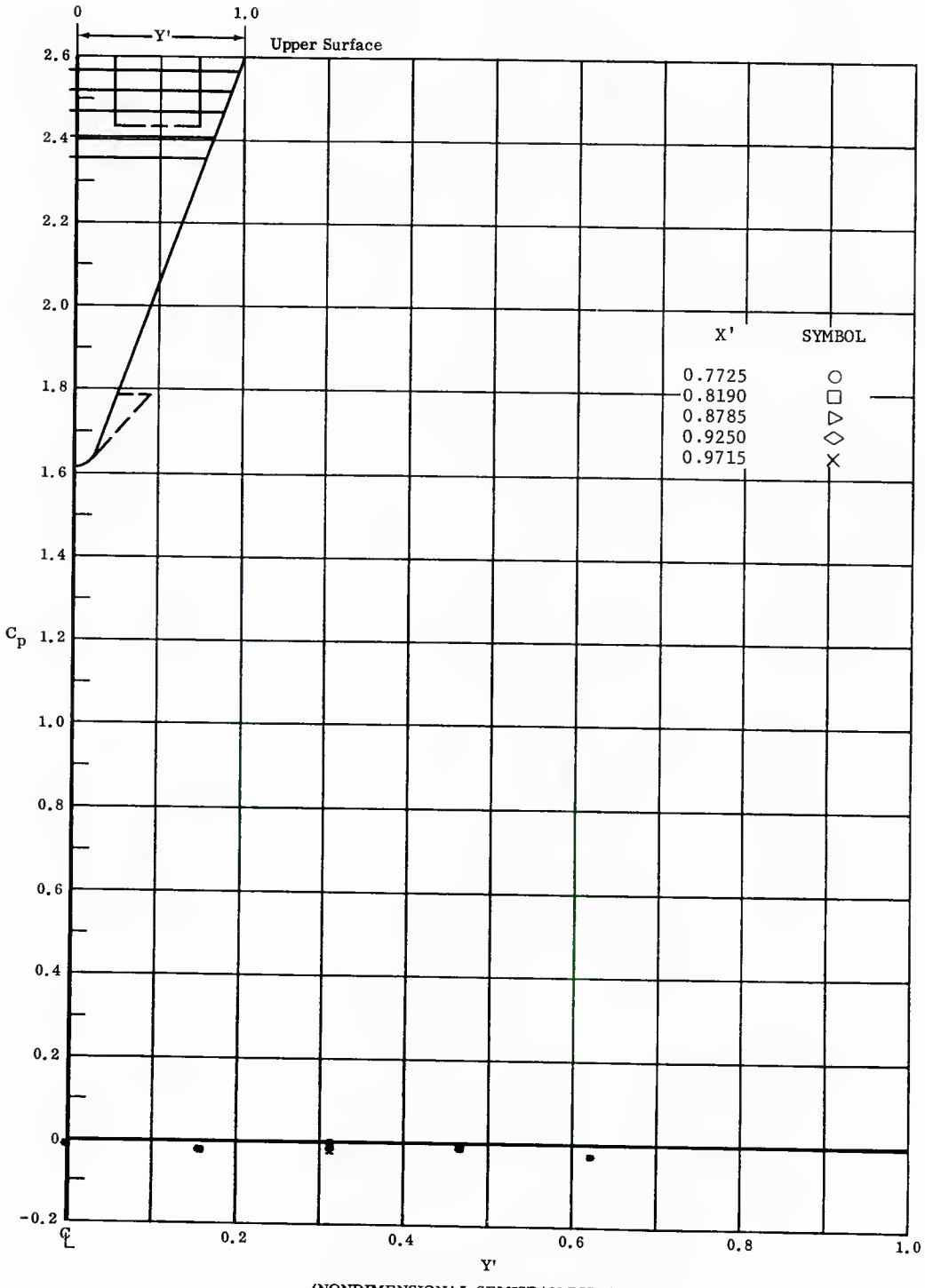

Fig. 59 Spanwise Distributions of Pressure Coefficients on Upper Surface Ventral Fin on Lower Surface Not Deflected, No Flap Deflections, α = +14.3°, β = +14°

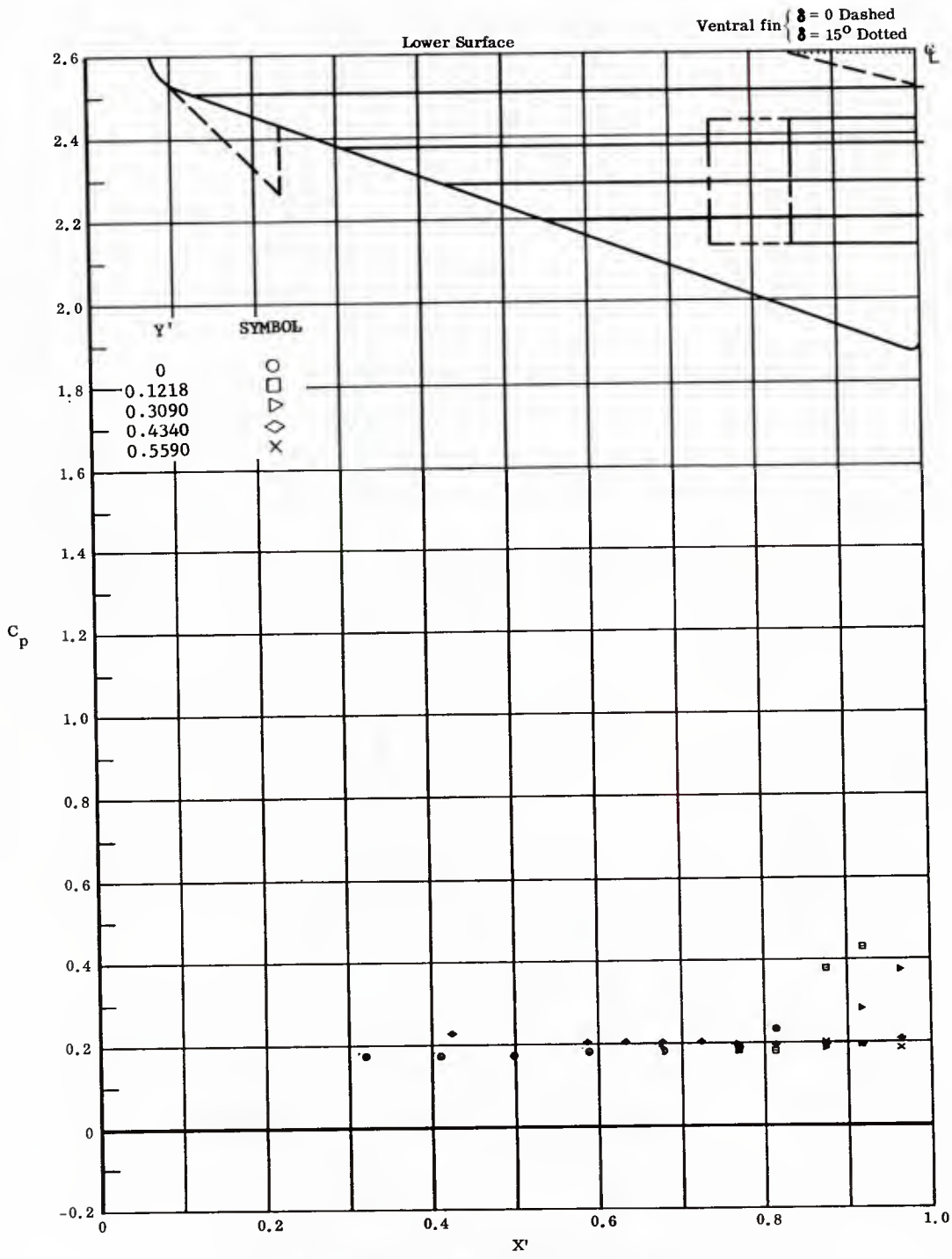

Fig. 60 Streamwise Distributions of Pressure Coefficients on Lower Surface Ventral Fin on Lower Surface Not Deflected, No Flap Deflections, $\alpha = +14.3°, \beta = 0$

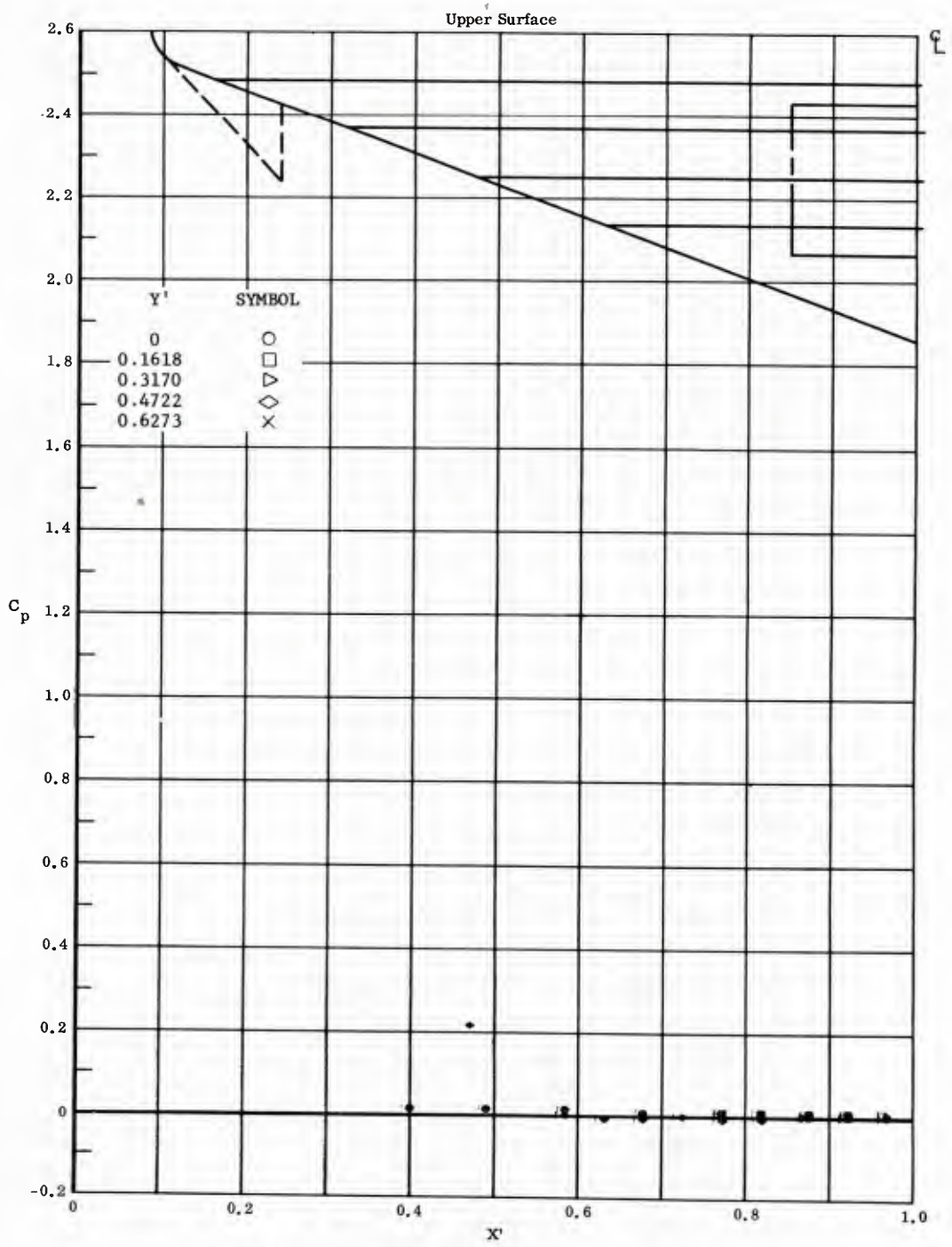

Fig. 60 Streamwise Distributions of Pressure Coefficients on Upper Surface Ventral Fin on Lower Surface Not Deflected, No Flap Deflections, $\alpha = +14.3°$, $\beta = 0$

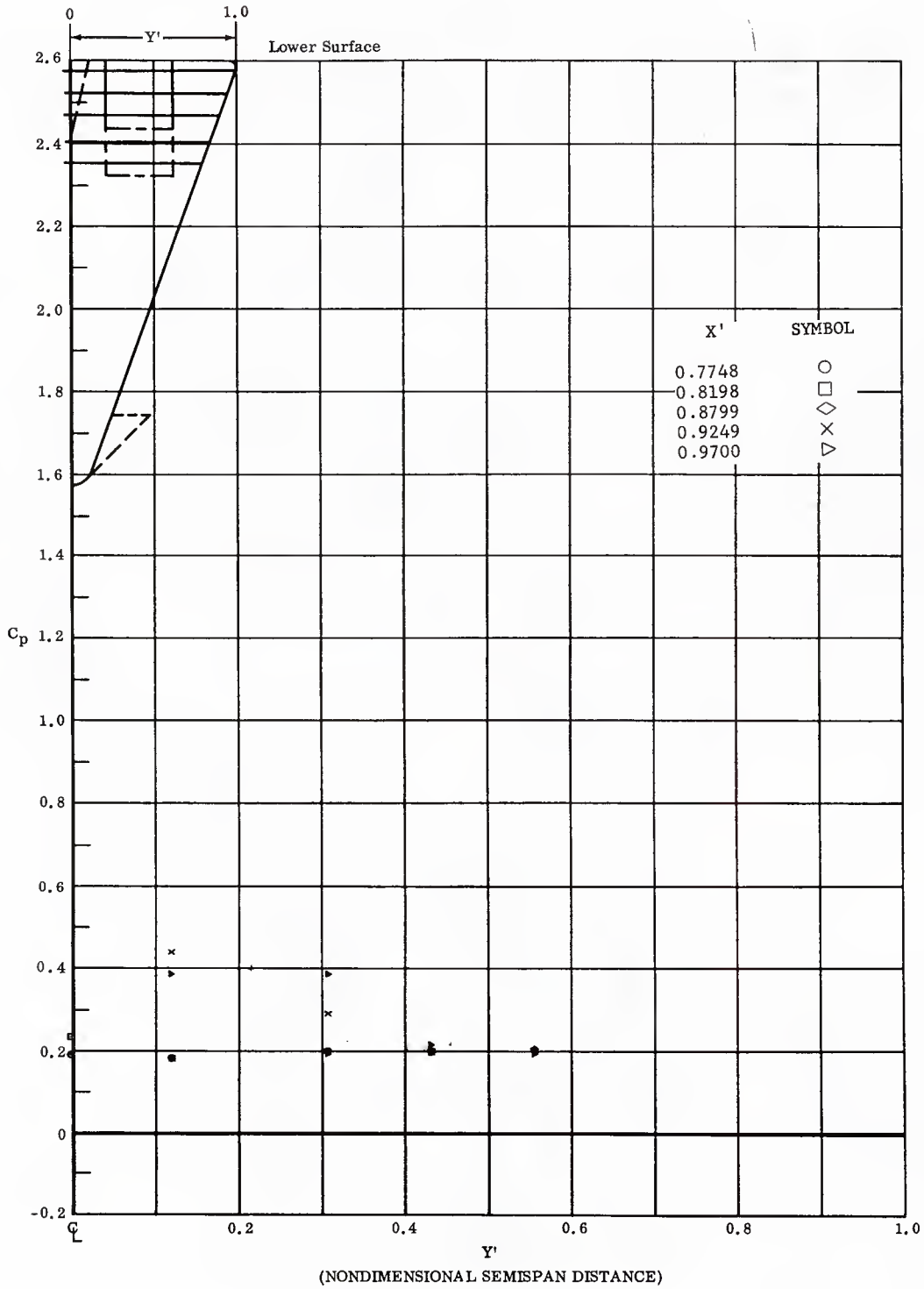

Fig. 60 Spanwise Distributions of Pressure Coefficients on Lower Surface Ventral Fin on Lower Surface Not Deflected, No Flap Deflections, $\alpha = +14.3°$, $\beta = 0$

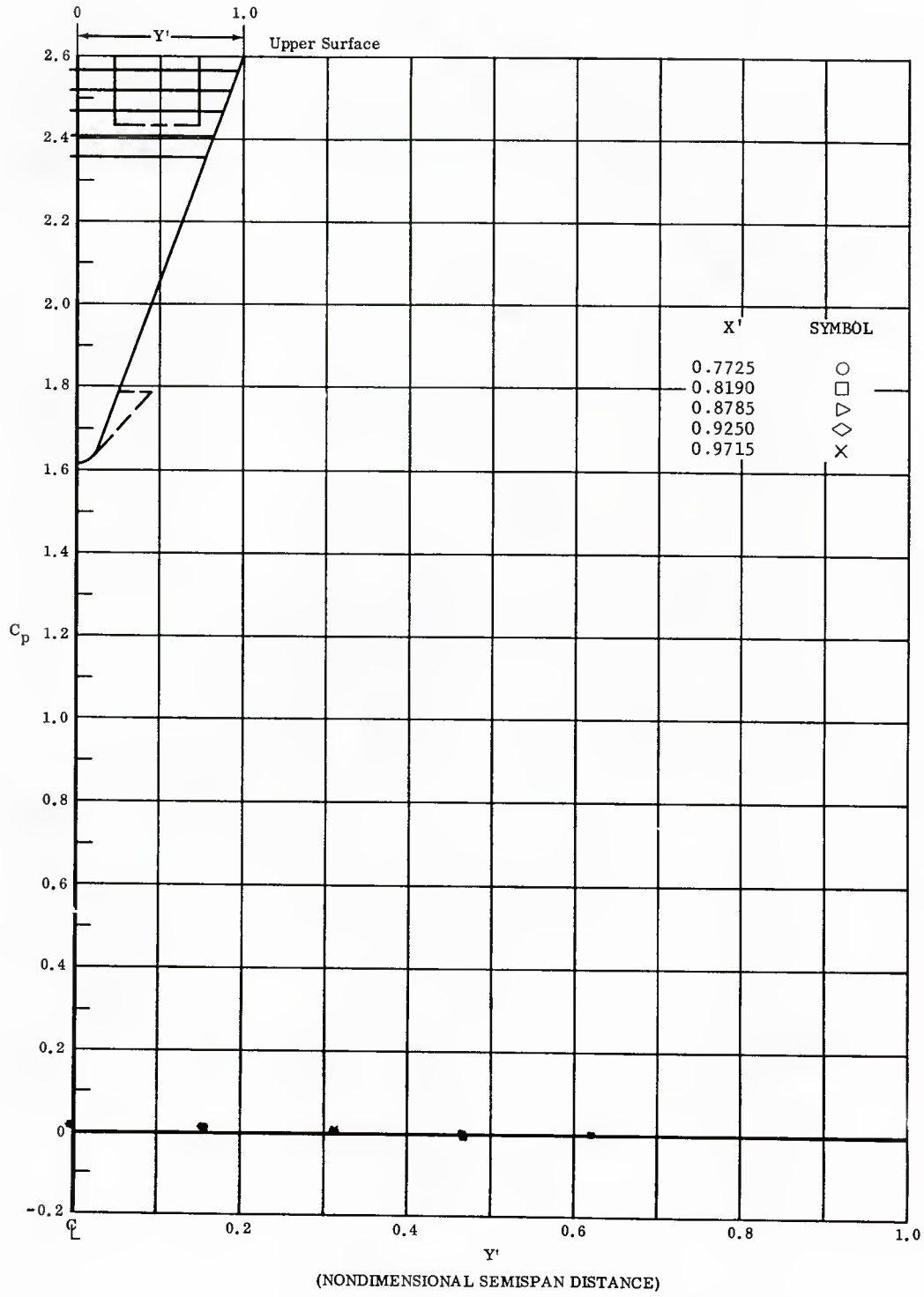

Fig. 60 Spanwise Distributions of Pressure Coefficients on Upper Surface Ventral Fin on Lower Surface Not Deflected, No Flap Deflections, $\alpha = +14.3°$, $\beta = 0$

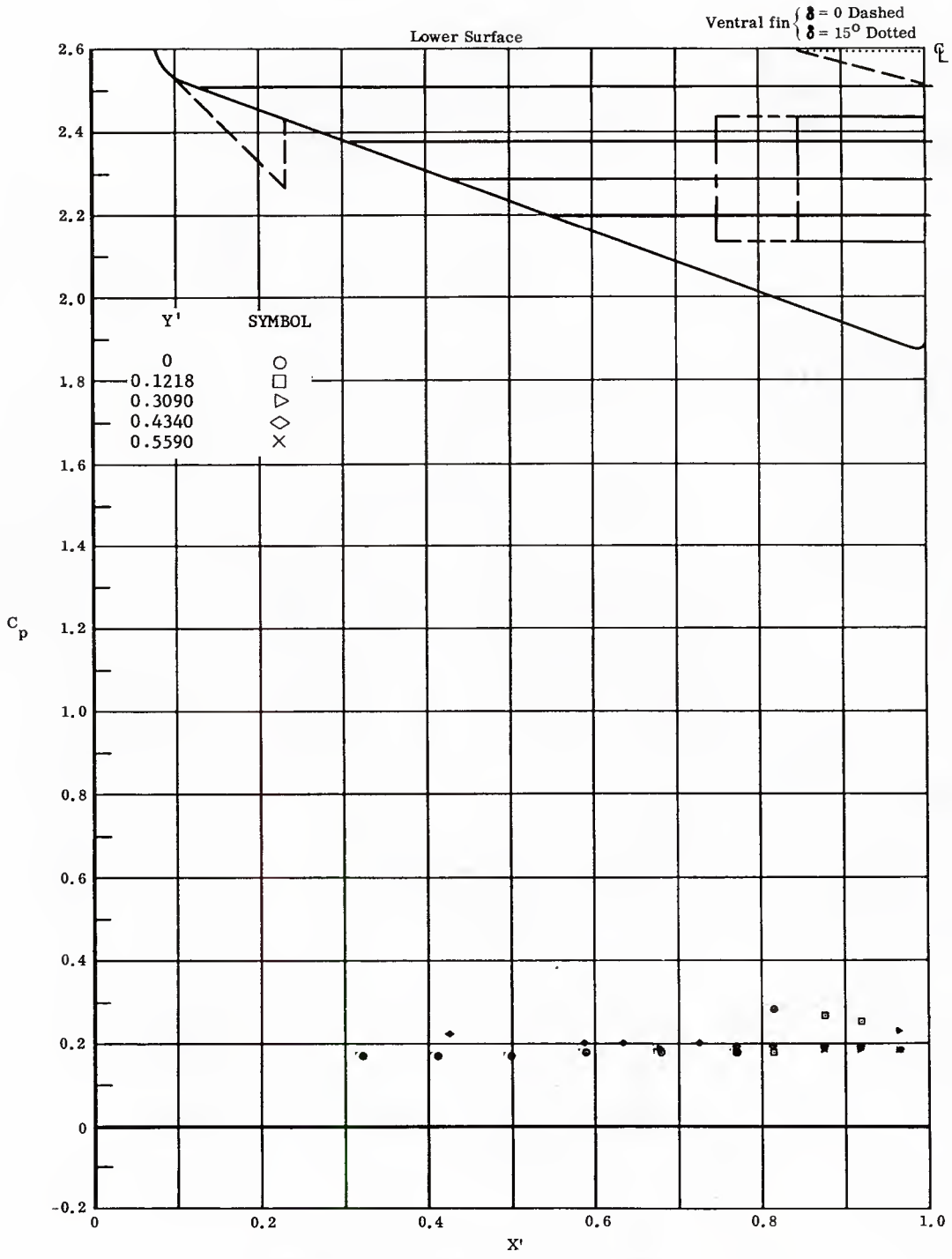

Fig. 61 Streamwise Distributions of Pressure Coefficients on Lower Surface Ventral Fin on Lower Surface Deflected 15°, No Flap Deflections, $\alpha = +14.3°, \beta = 0$

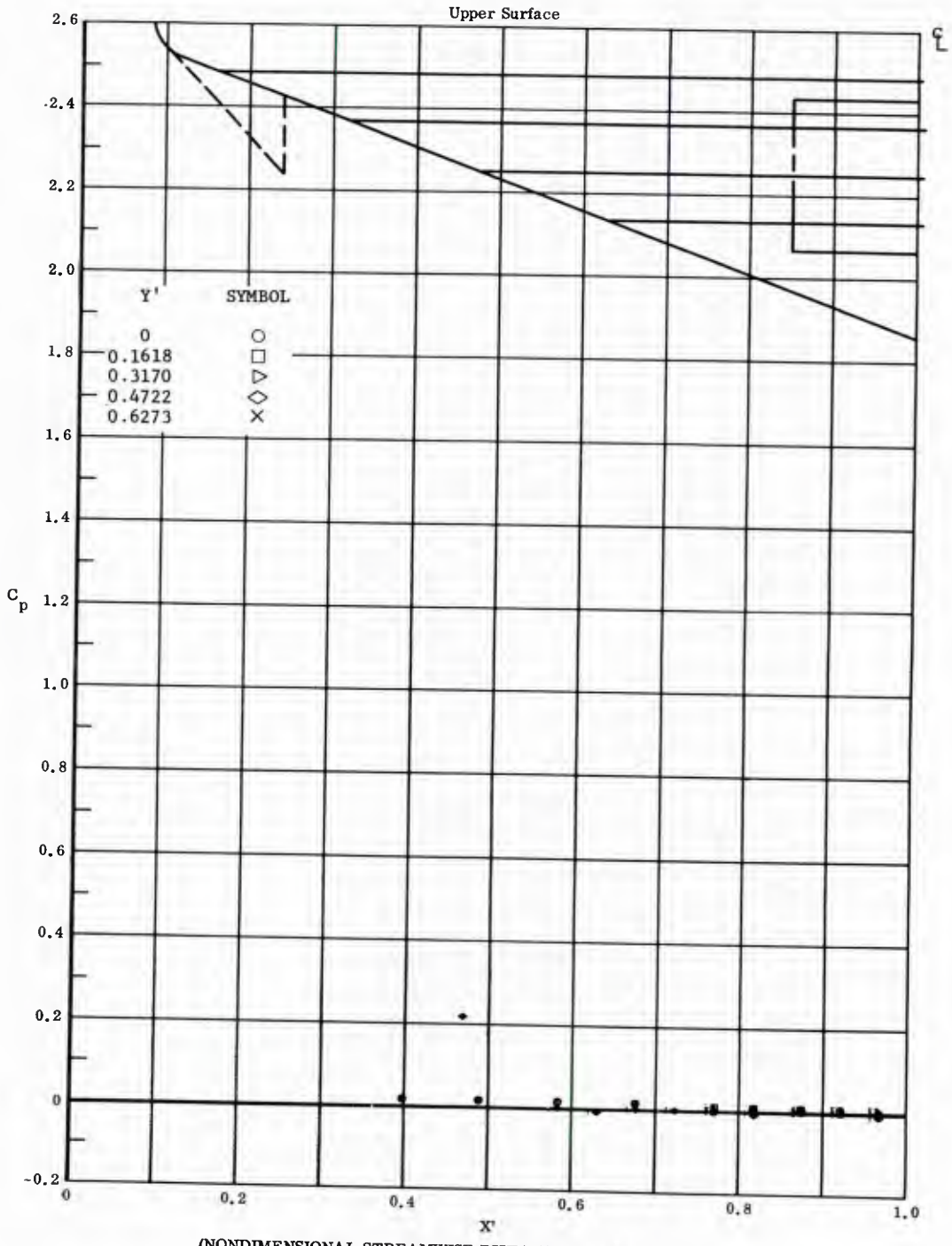

Fig. 61 Streamwise Distributions of Pressure Coefficients on Upper Surface Ventral Fin on Lower Surface Deflected 15°, No Flap Deflections, $\alpha = +14.3°$, $\beta = 0$

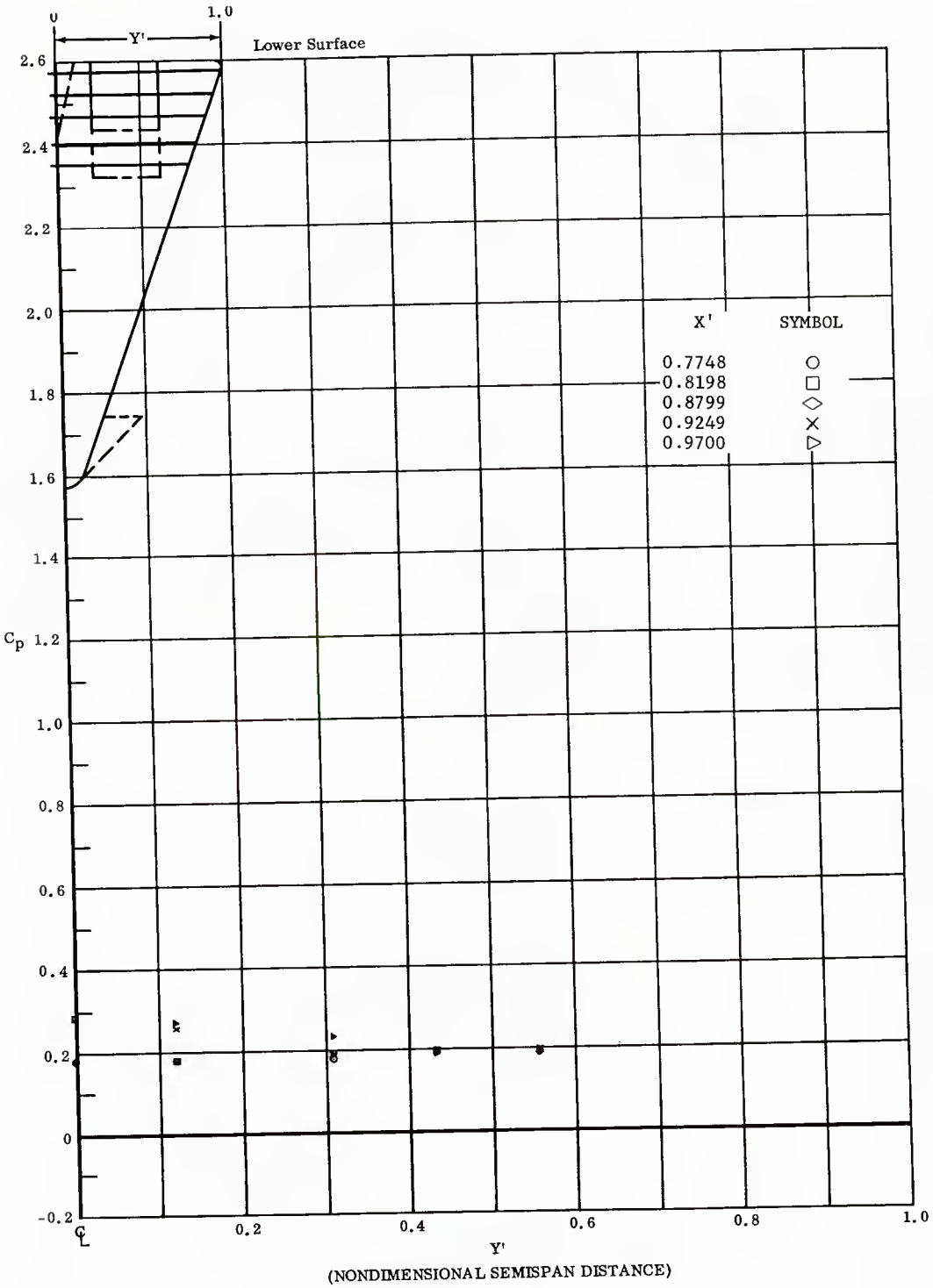

Fig. 61 Spanwise Distributions of Pressure Coefficients on Lower Surface Ventral Fin on Lower Surface Deflected 15°, No Flap Deflections, α = +14.3°, β = 0

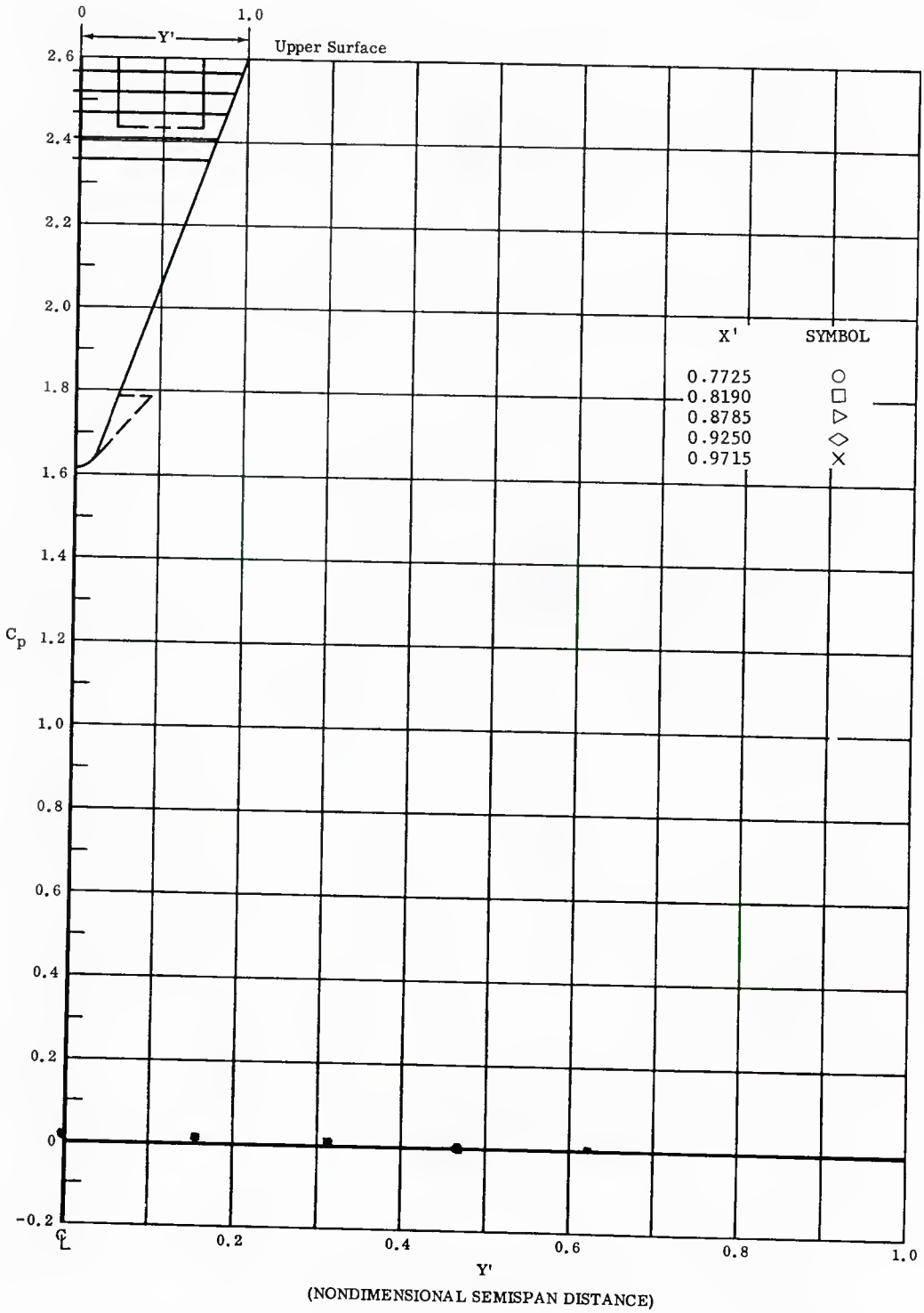

Fig. 61 Spanwise Distributions of Pressure Coefficients on Upper Surface Ventral Fin on Lower Surface Deflected 15°, No Flap Deflections, $\alpha = +14.3°$, $\beta = 0$

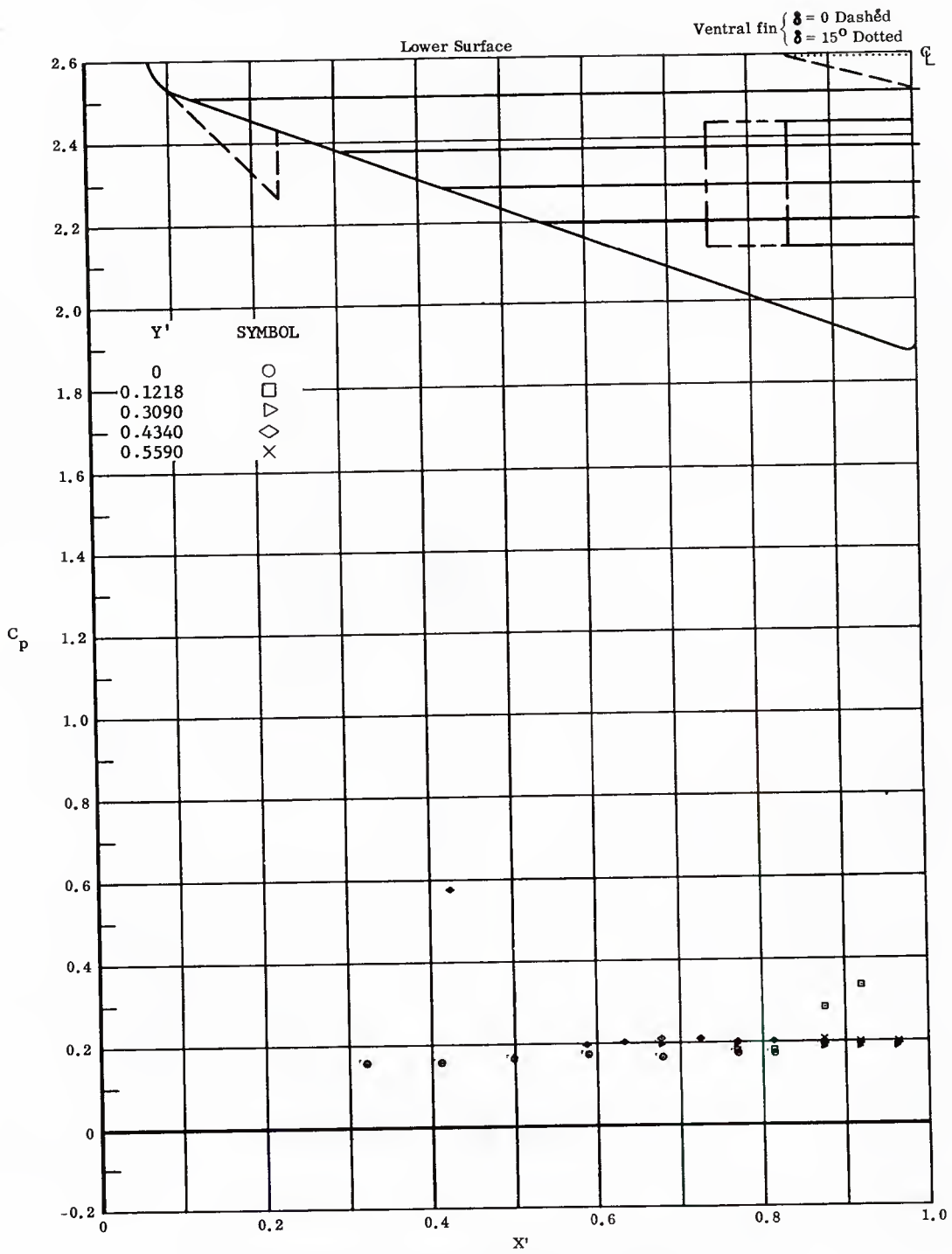

Fig. 62 Streamwise Distributions of Pressure Coefficients on Lower Surface Ventral Fin on Lower Surface Deflected 15°, No Flap Deflections, α = +14.3°, β = +14°

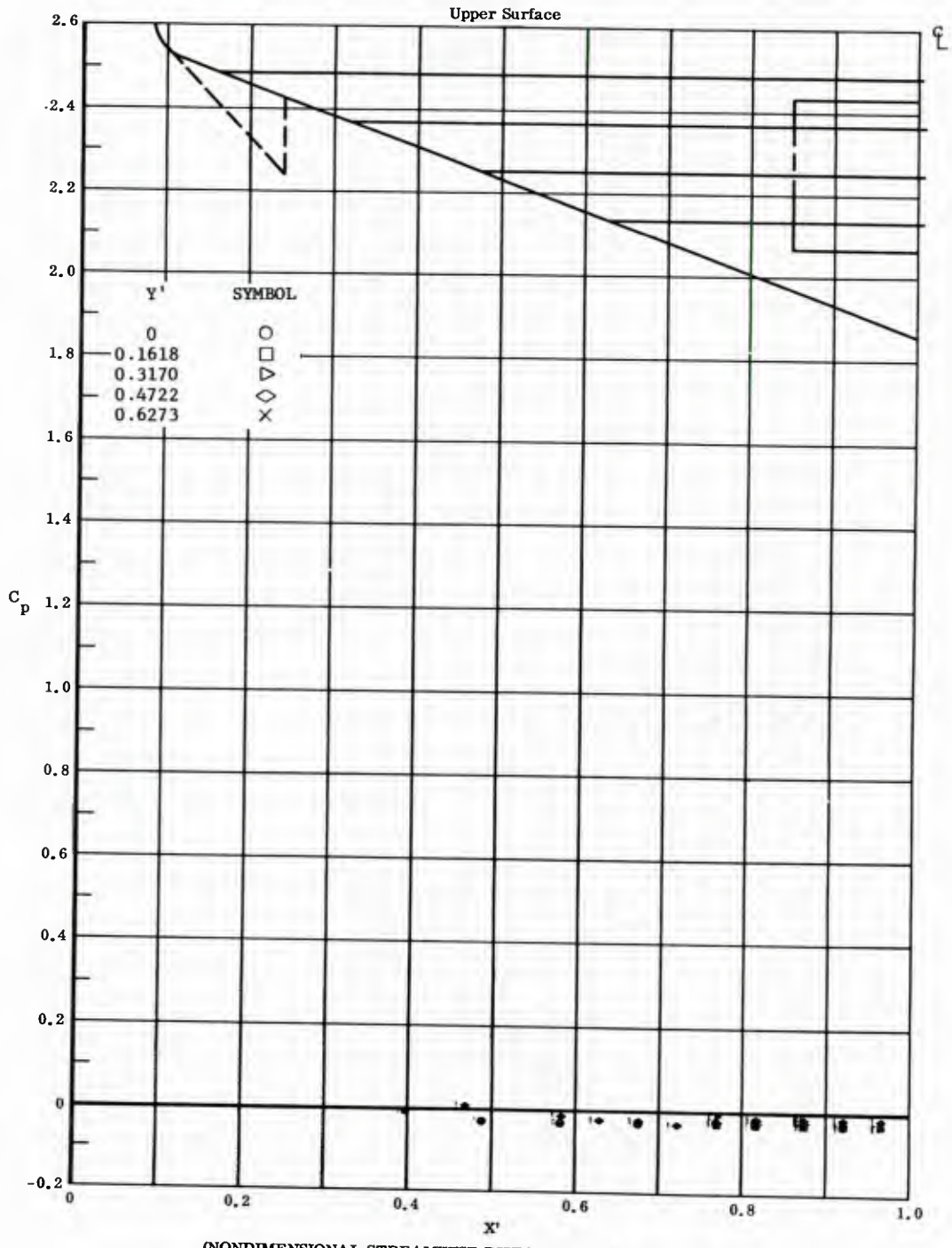

Fig. 62 Streamwise Distributions of Pressure Coefficients on Upper Surface Ventral Fin on Lower Surface Deflected 15°, No Flap Deflections, $\alpha = +14.3°$, $\beta = +14°$

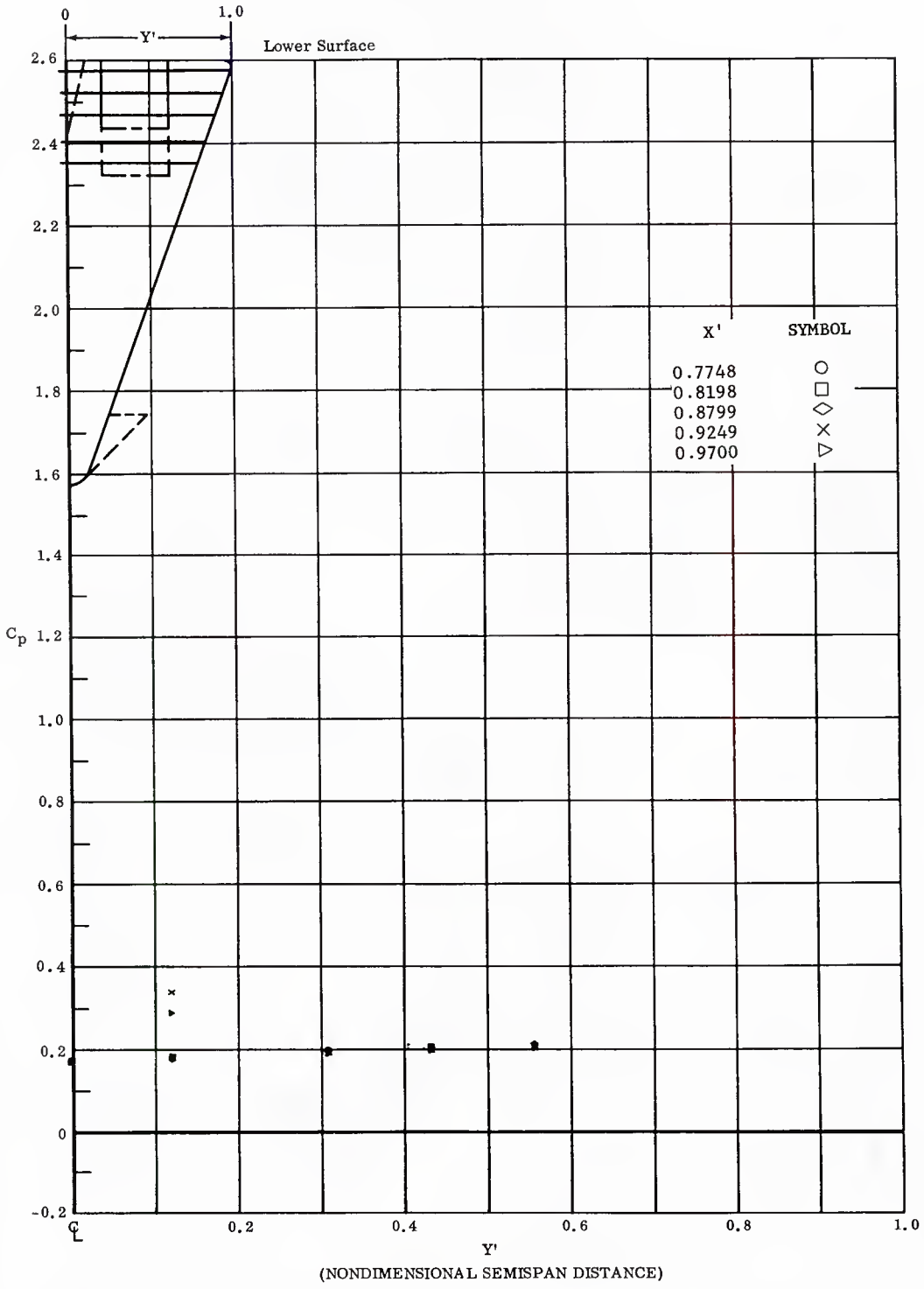

Fig. 62 Spanwise Distributions of Pressure Coefficients on Lower Surface Ventral Fin on Lower Surface Deflected 15°, No Flap Deflections, $\alpha = +14.3°$, $\beta = +14°$

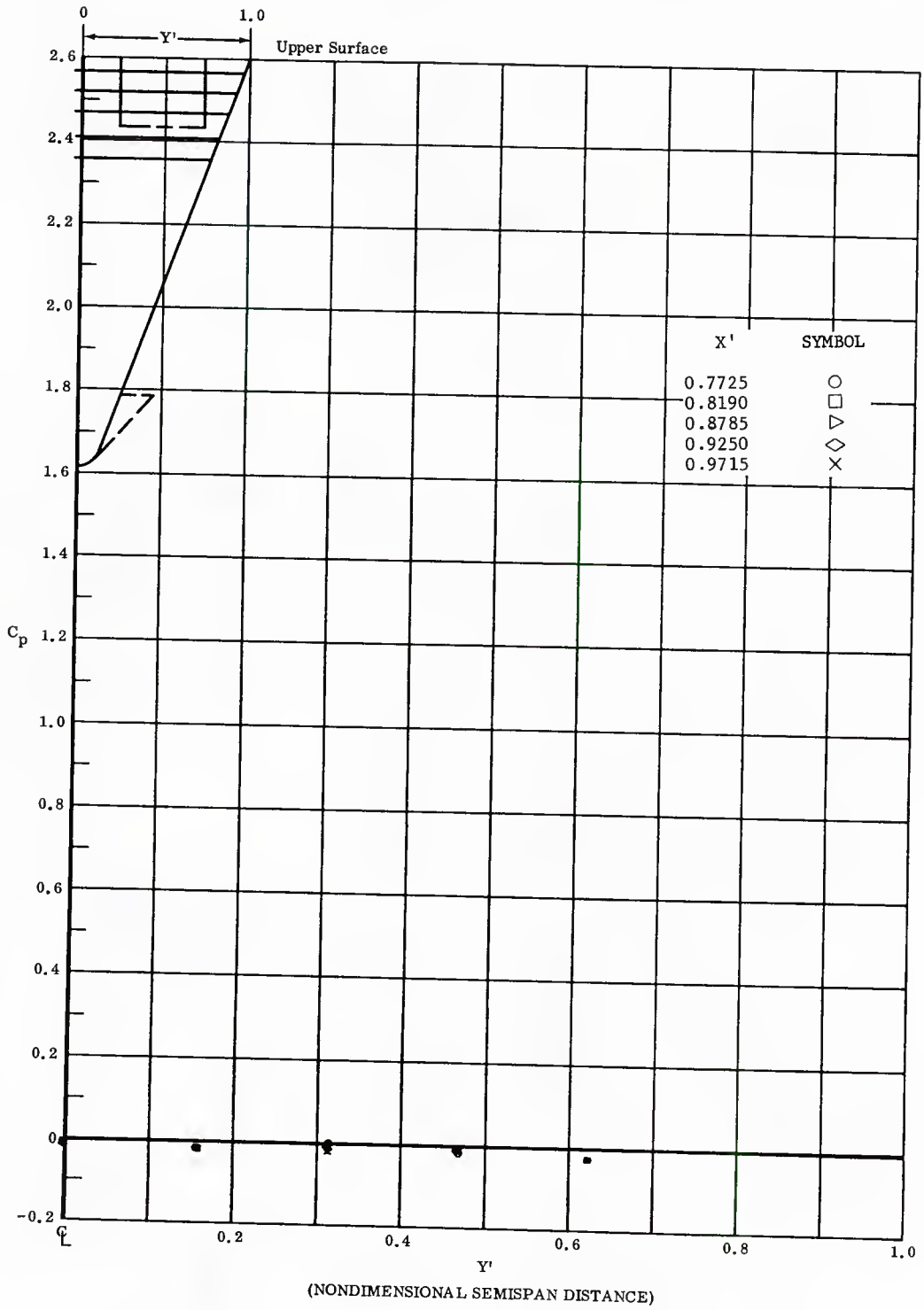

Fig. 62 Spanwise Distributions of Pressure Coefficients on Upper Surface Ventral Fin on Lower Surface Deflected 15°, No Flap Deflections, α = +14.3°, β = +14°

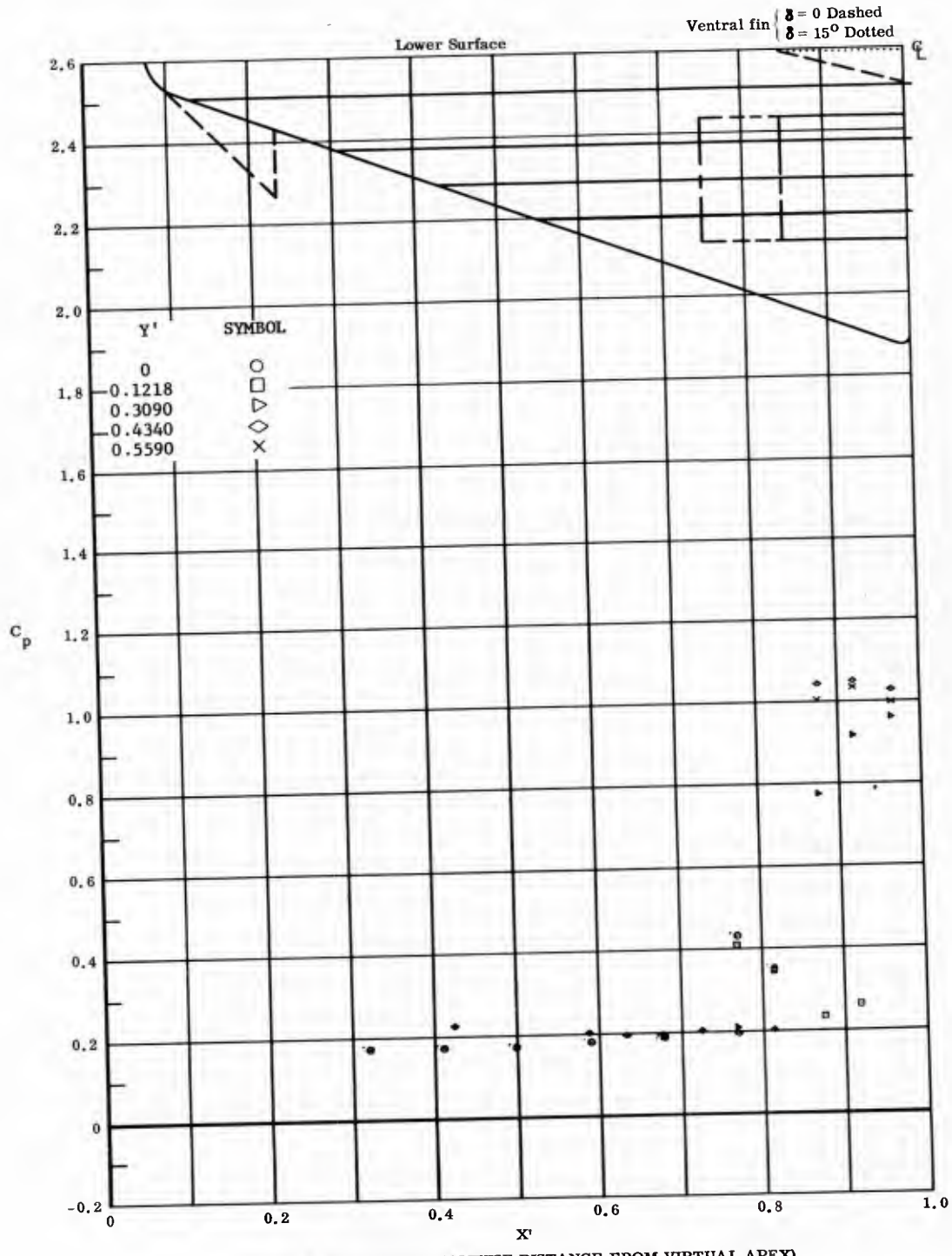

Fig. 63 Streamwise Distributions of Pressure Coefficients on Lower Surface Ventral Fin on Lower Surface Deflected 15°, Bottom Flaps Deflected 20° $\alpha = +14.3°, \beta = 0$

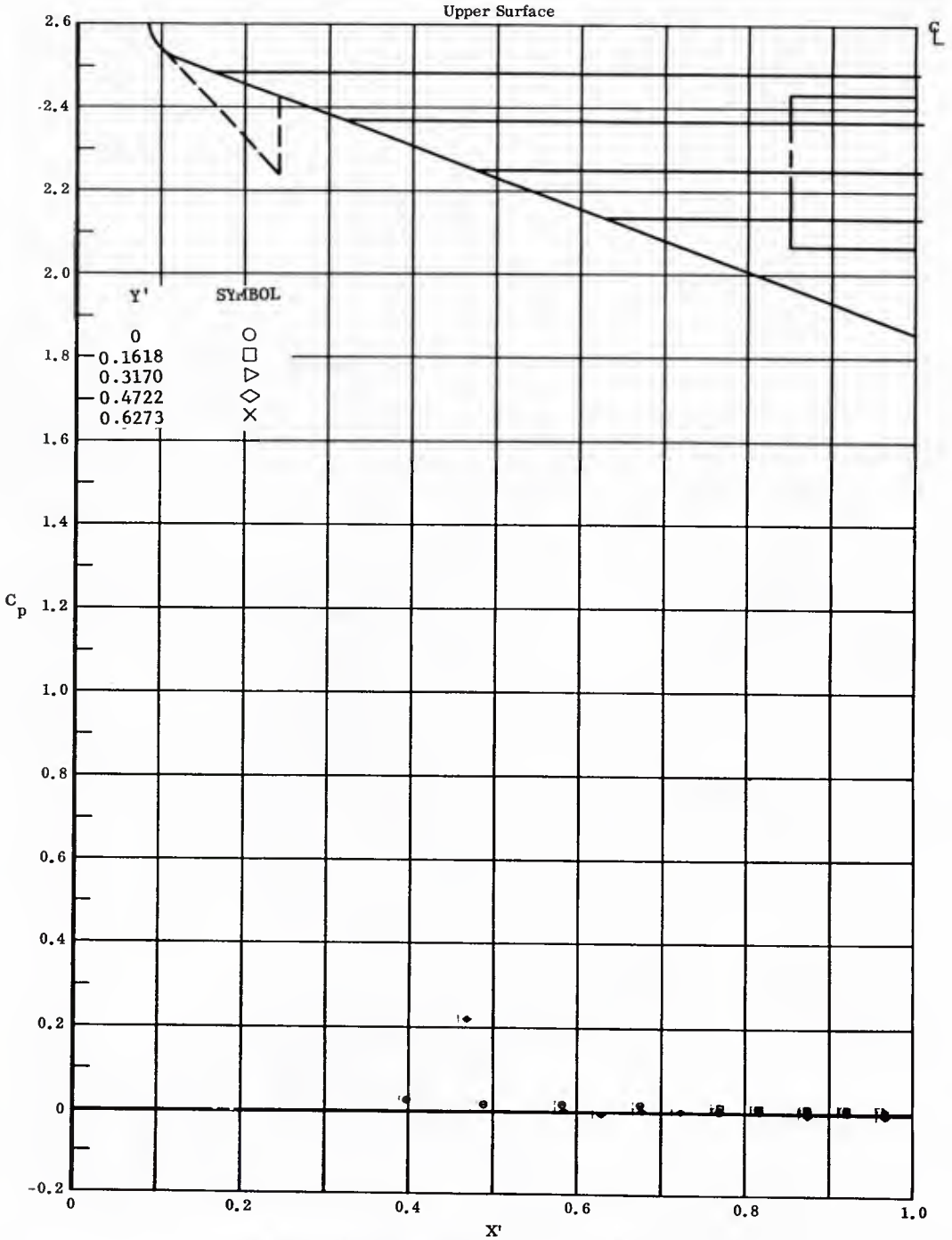

Fig. 63 Streamwise Distributions of Pressure Coefficients on Upper Surface Ventral Fin on Lower Surface Deflected 15°, Bottom Flaps Deflected 20° α = +14.3°, β = 0

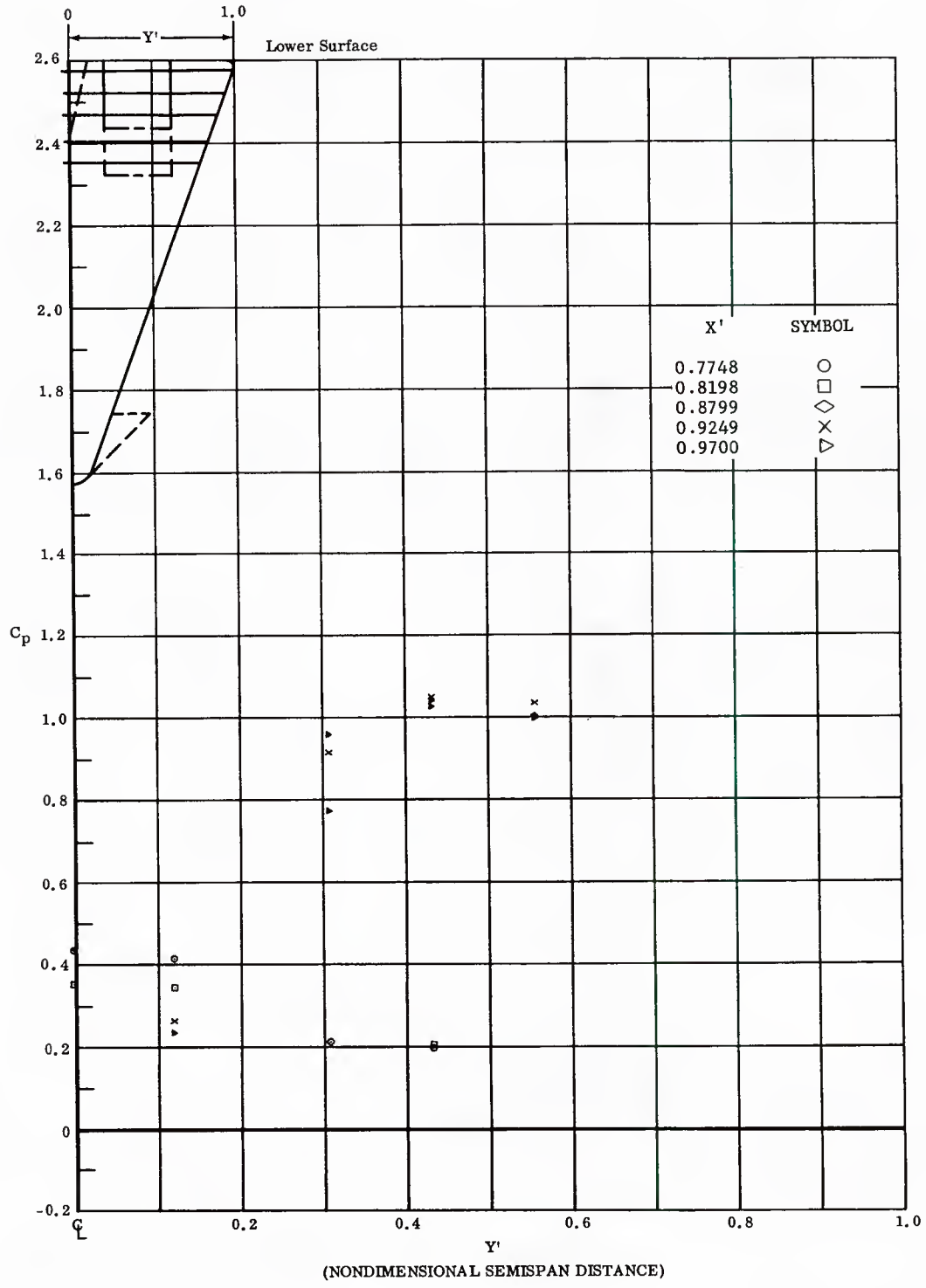

Fig. 63 Spanwise Distributions of Pressure Coefficients on Lower Surface
Ventral Fin on Lower Surface Deflected 15°, Bottom Flaps Deflected 20°
$\alpha = +14.3°$, $\beta = 0$

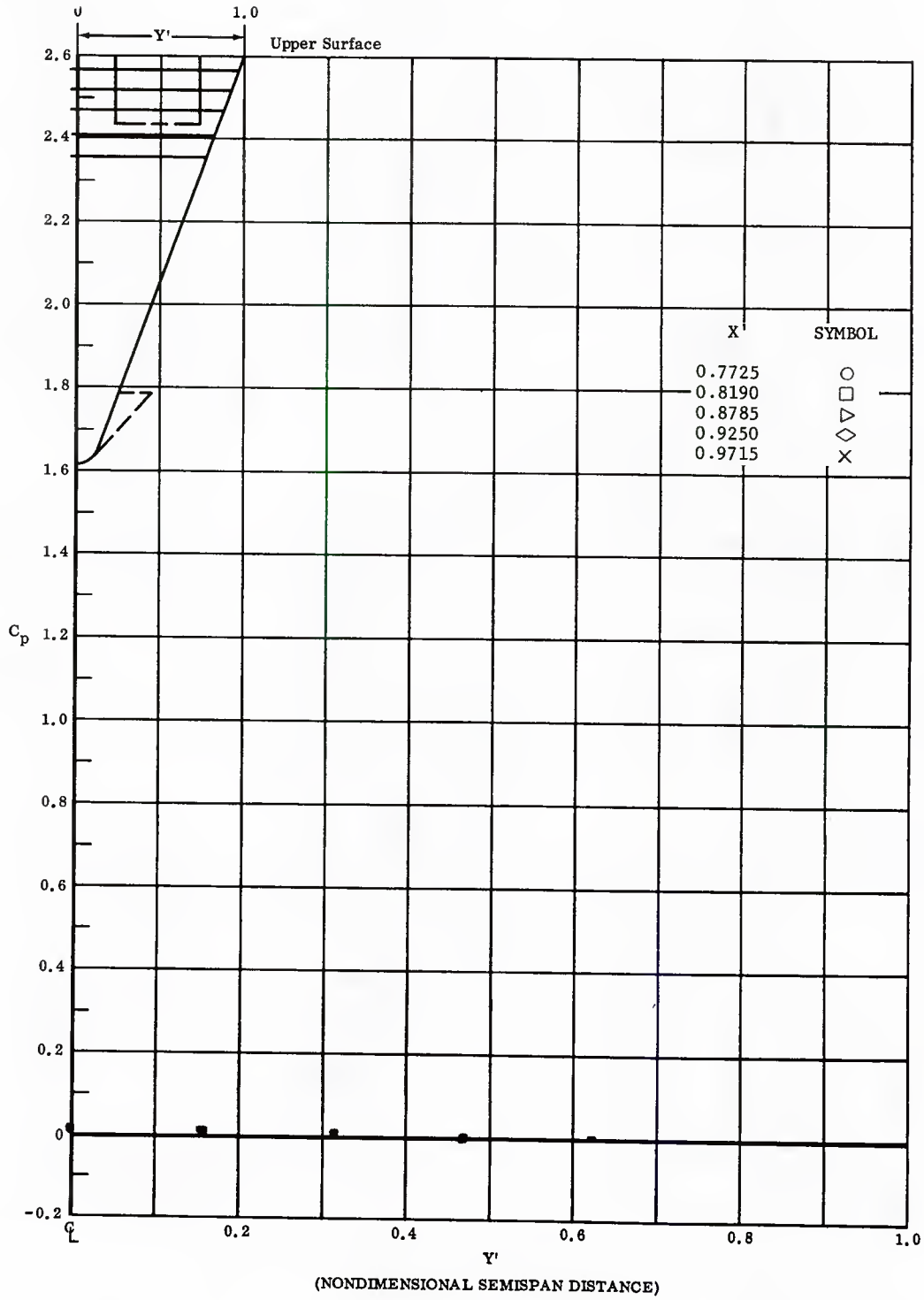

Fig. 63 Spanwise Distributions of Pressure Coefficients on Upper Surface Ventral Fin on Lower Surface Deflected 15°, Bottom Flaps Deflected 20° $\alpha = +14.3°$, $\beta = 0$

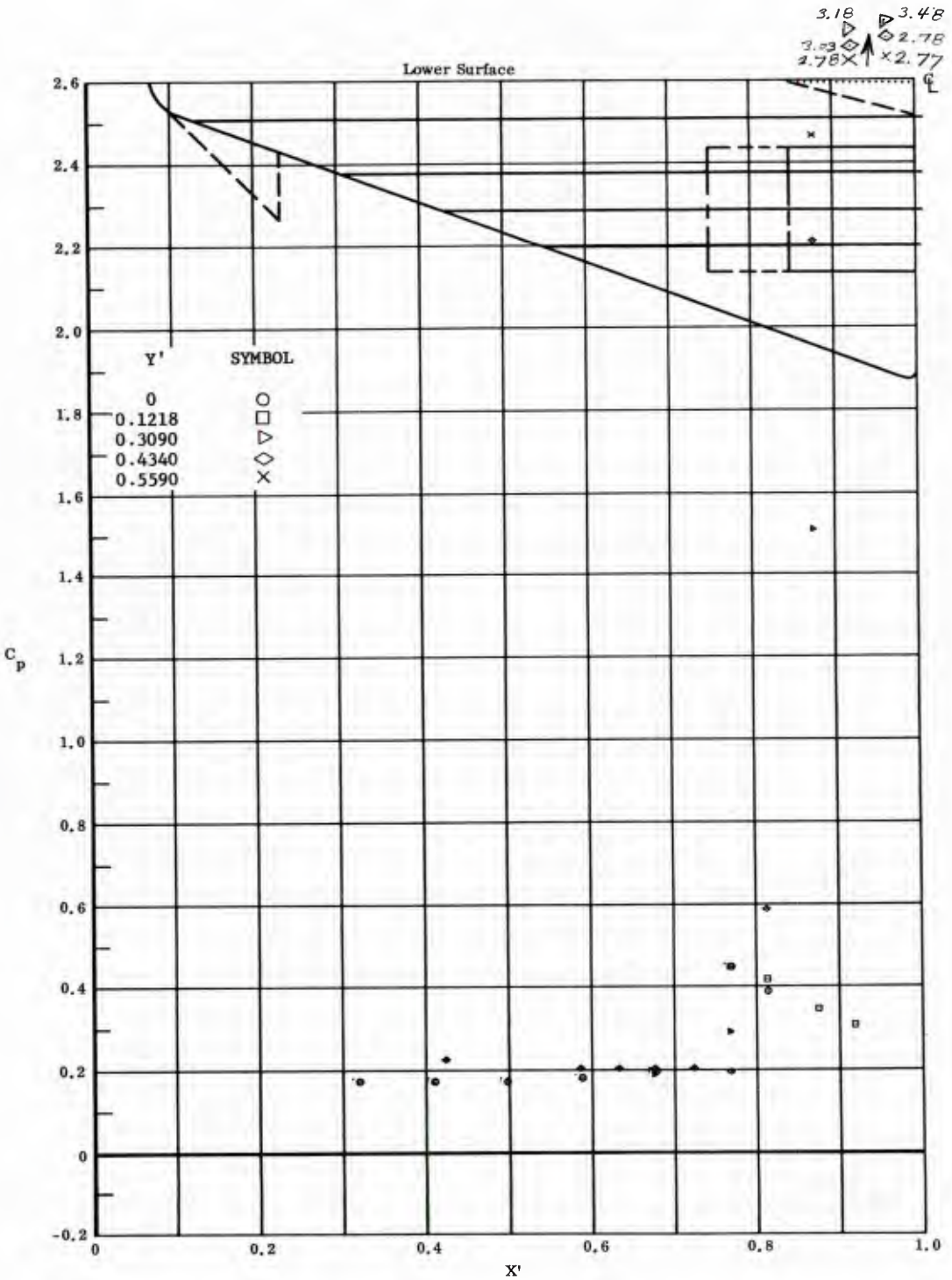

Fig. 64 Streamwise Distributions of Pressure Coefficients on Lower Surface Ventral Fin on Lower Surface Deflected 15°, Bottom Flaps Deflected 40°, α = +14.3°, β = 0

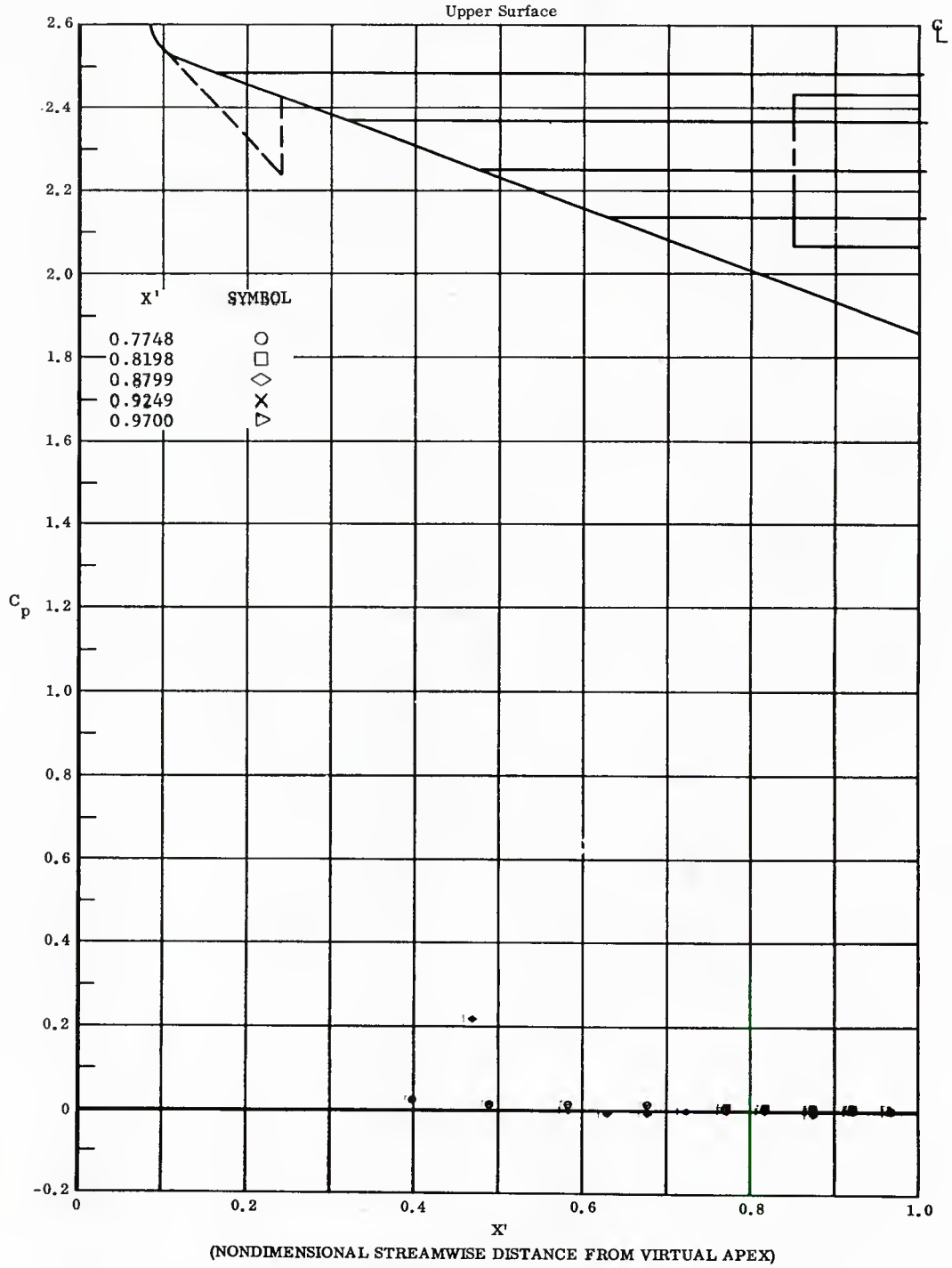

Fig. 64 Streamwise Distributions of Pressure Coefficients on Upper Surface. Ventral Fin on Lower Surface Deflected 15°, Bottom Flaps Deflected 40°, α = +14.3°, β = 0

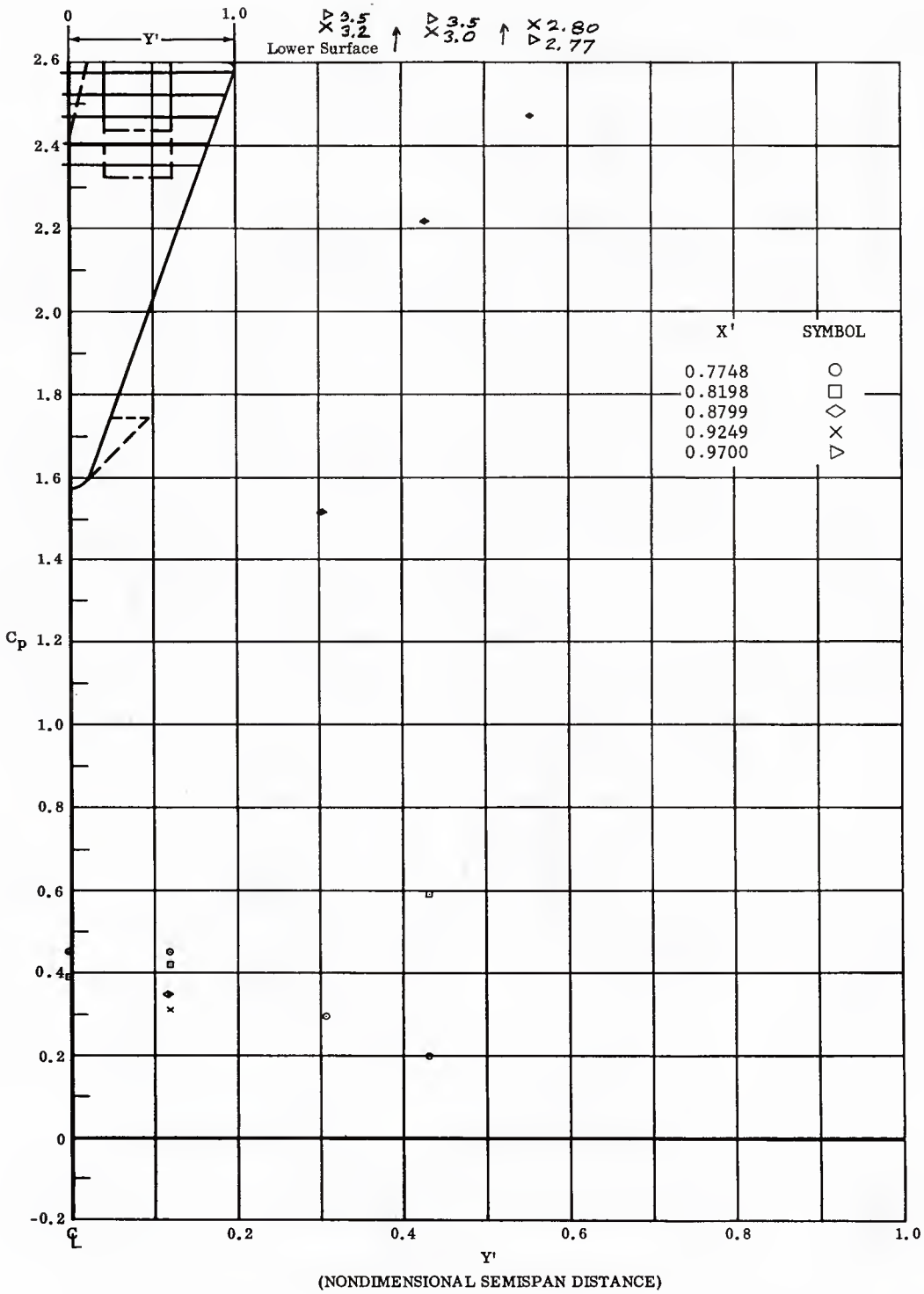

Fig. 64 Spanwise Distributions of Pressure Coefficients on Lower Surface Ventral Fin on Lower Surface Deflected 15°, Bottom Flaps Deflected 40°, $\alpha = +14.3°$, $\beta = 0$

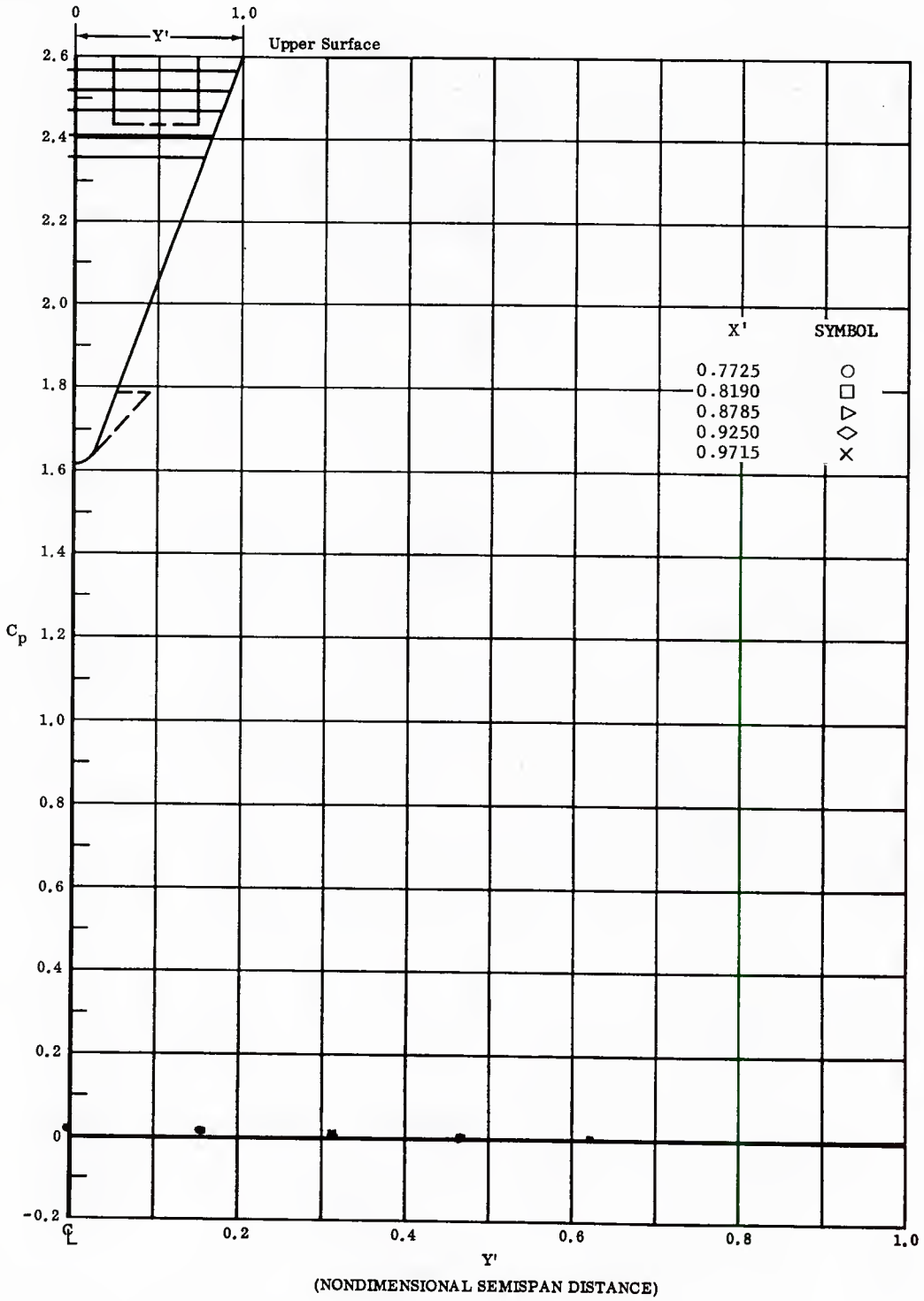

Fig. 64 Spanwise Distributions of Pressure Coefficients on Upper Surface Ventral Fin on Lower Surface Deflected 15°, Bottom Flaps Deflected 40°, α = +14.3°, β = 0

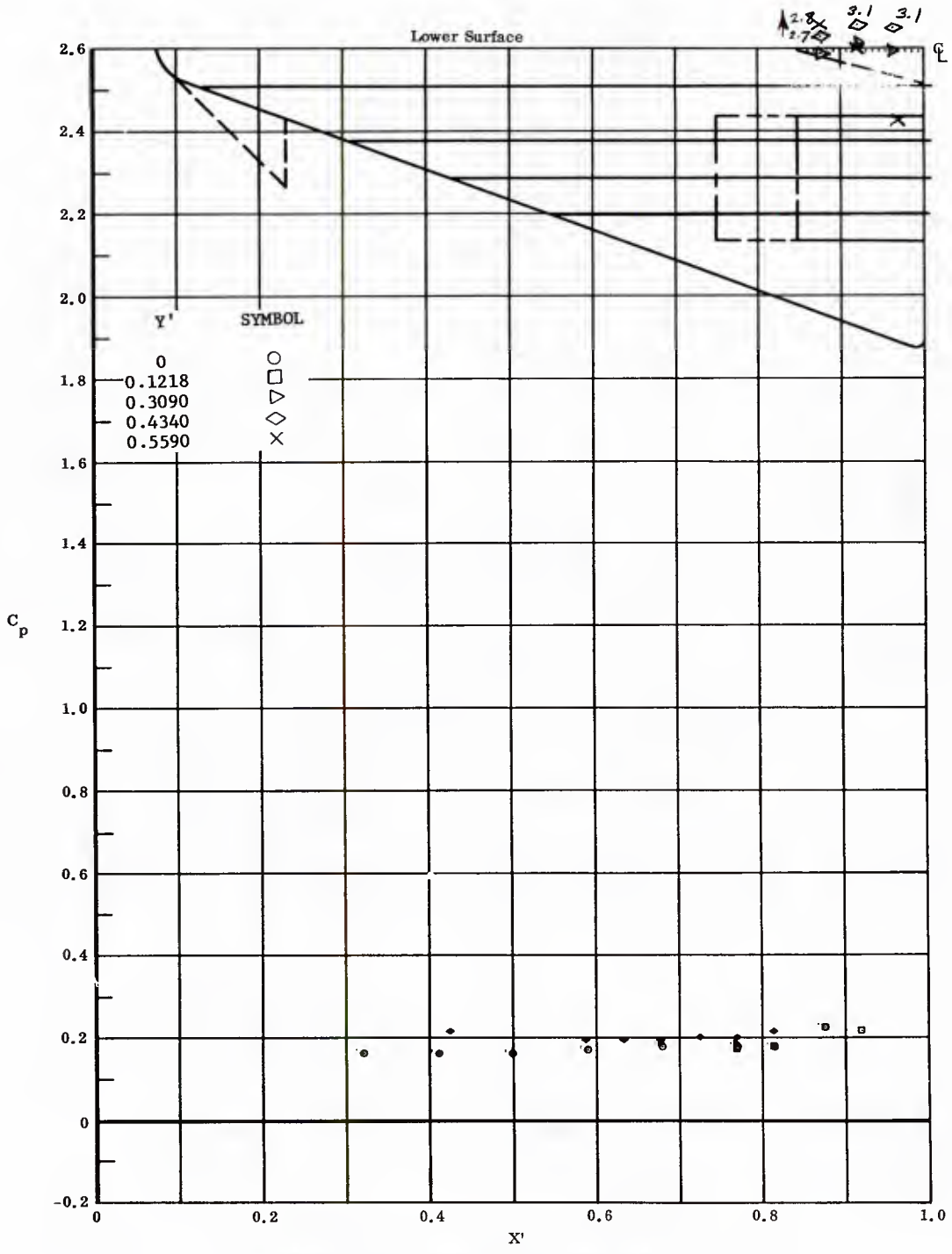

Fig. 65 Streamwise Distributions of Pressure Coefficients on Lower Surface Basic Configuration, Bottom Flaps Deflected 40°, α = +14.3°, β = 0

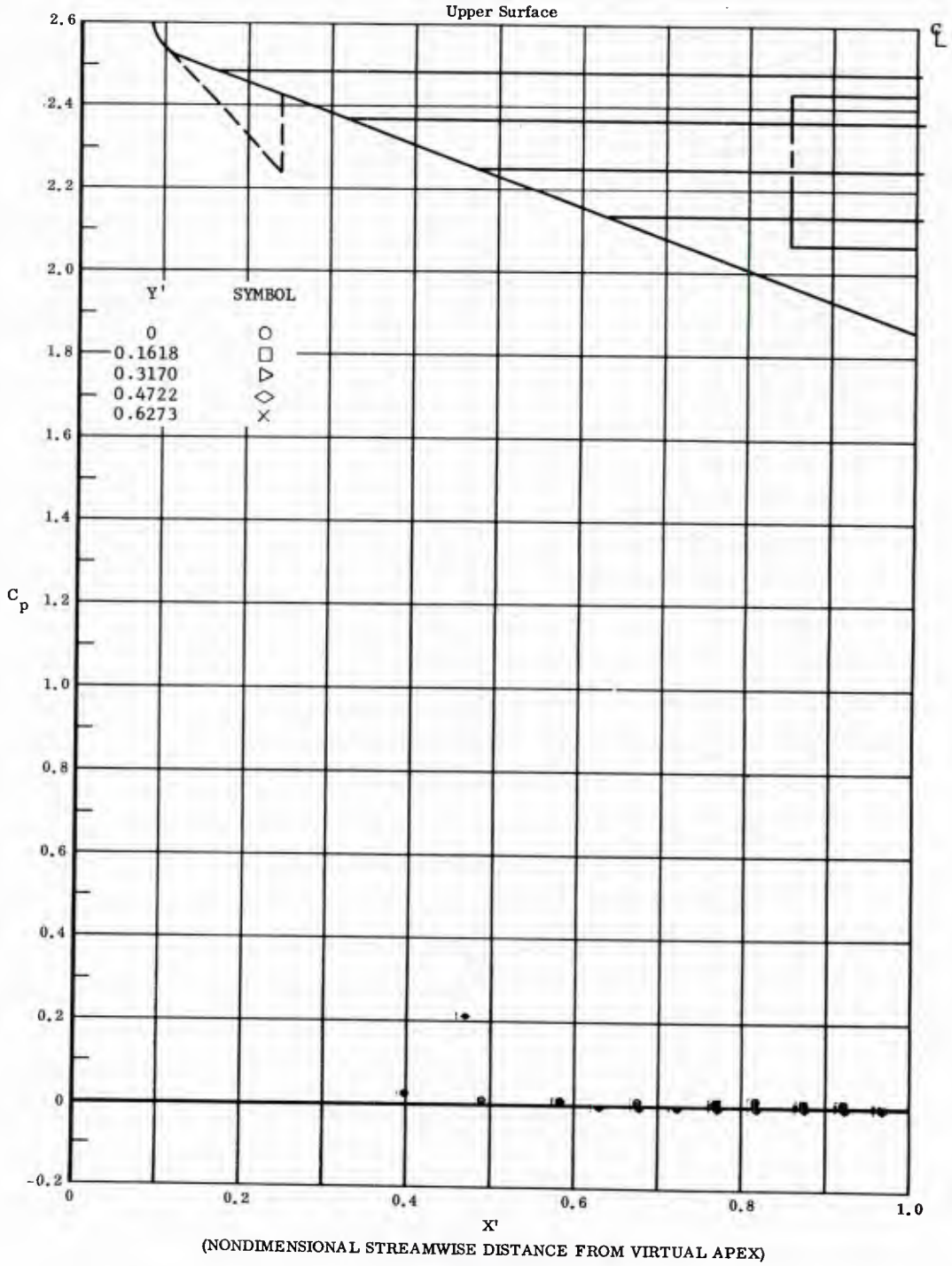

Fig. 65 Streamwise Distributions of Pressure Coefficients on Upper Surface Basic Configuration, Bottom Flaps Deflected 40°, α = +14.3°, β = 0

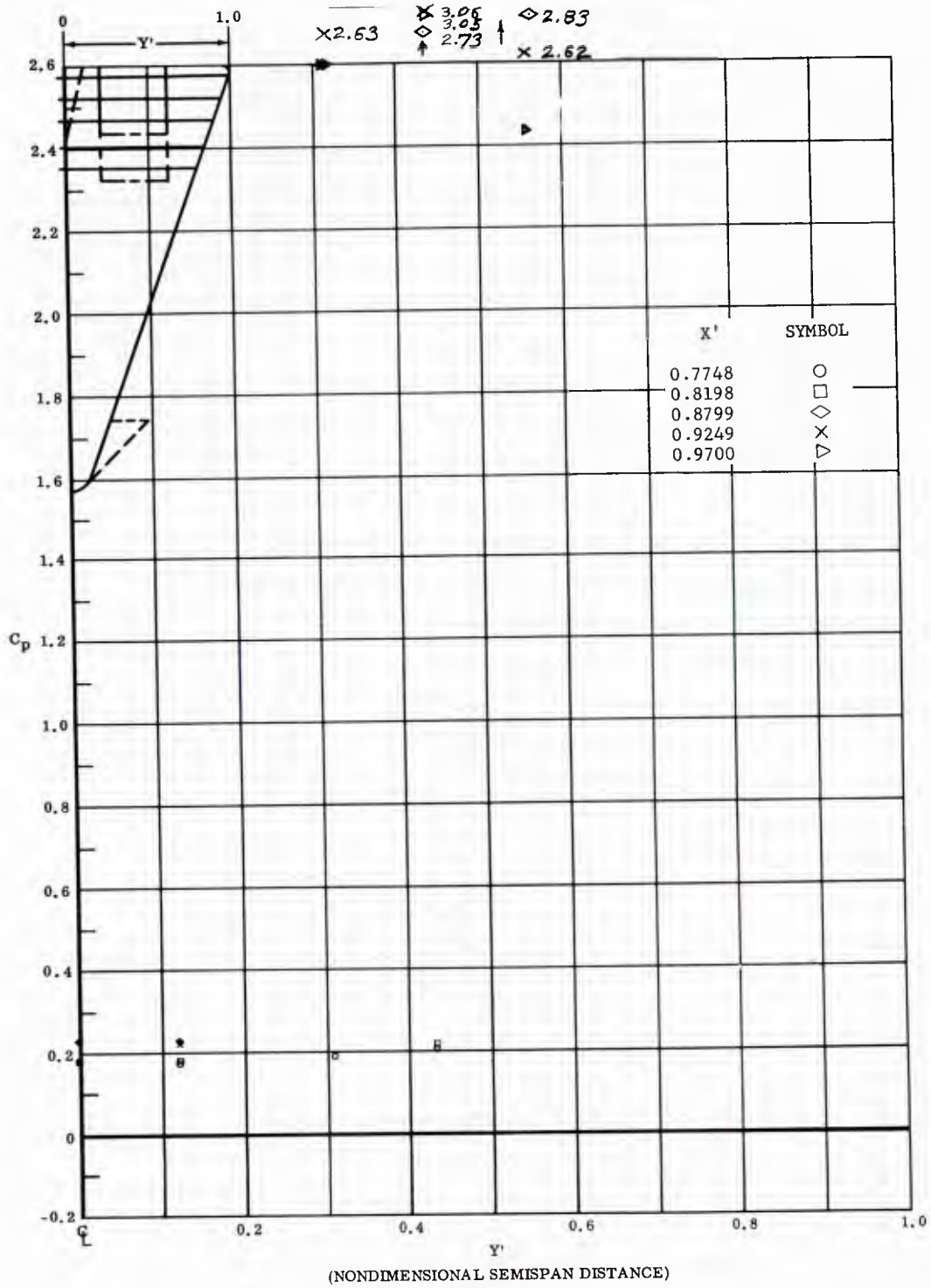

Fig. 65 Spanwise Distributions of Pressure Coefficients on Lower Surface Basic Configuration, Bottom Flaps Deflected 40°, α = +14.3°, β = 0

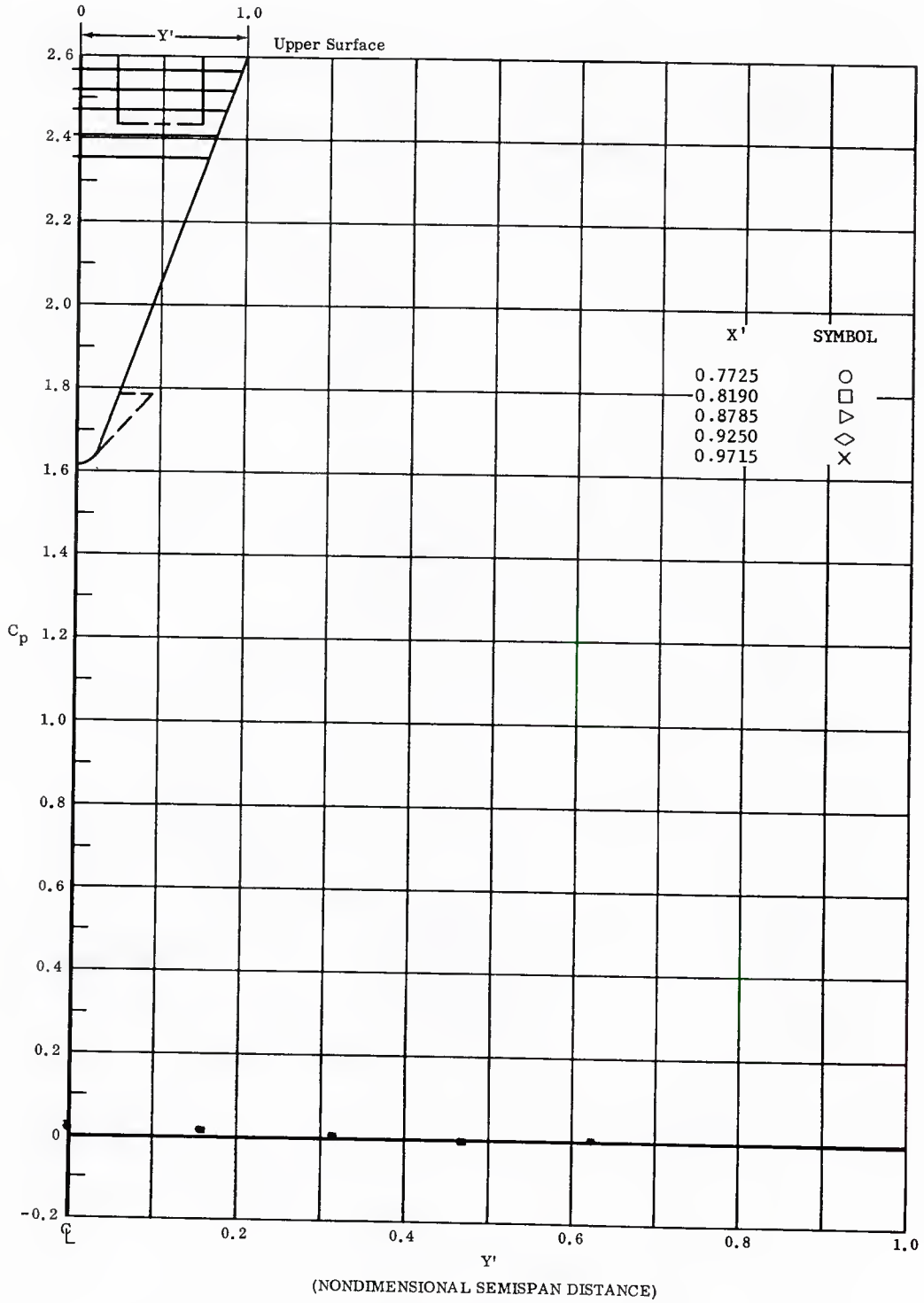

Fig. 65 Spanwise Distributions of Pressure Coefficients on Upper Surface Basic Configuration, Bottom Flaps Deflected 40°, α = +14.3°, β = 0

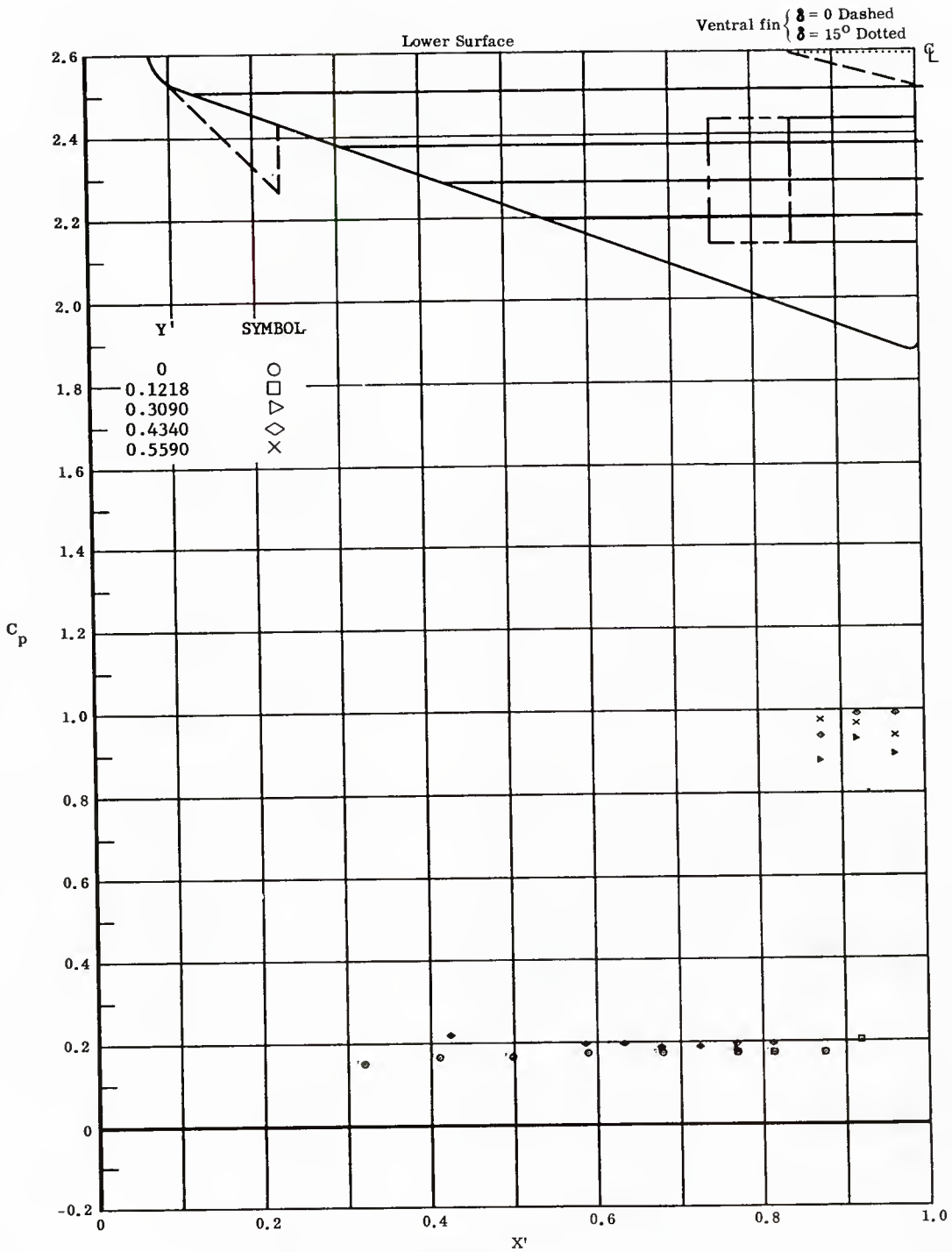

Fig. 66 Streamwise Distributions of Pressure Coefficients on Lower Surface
Basic Configuration, Bottom Flaps Deflected 20°, α = +14.3°, β = 0

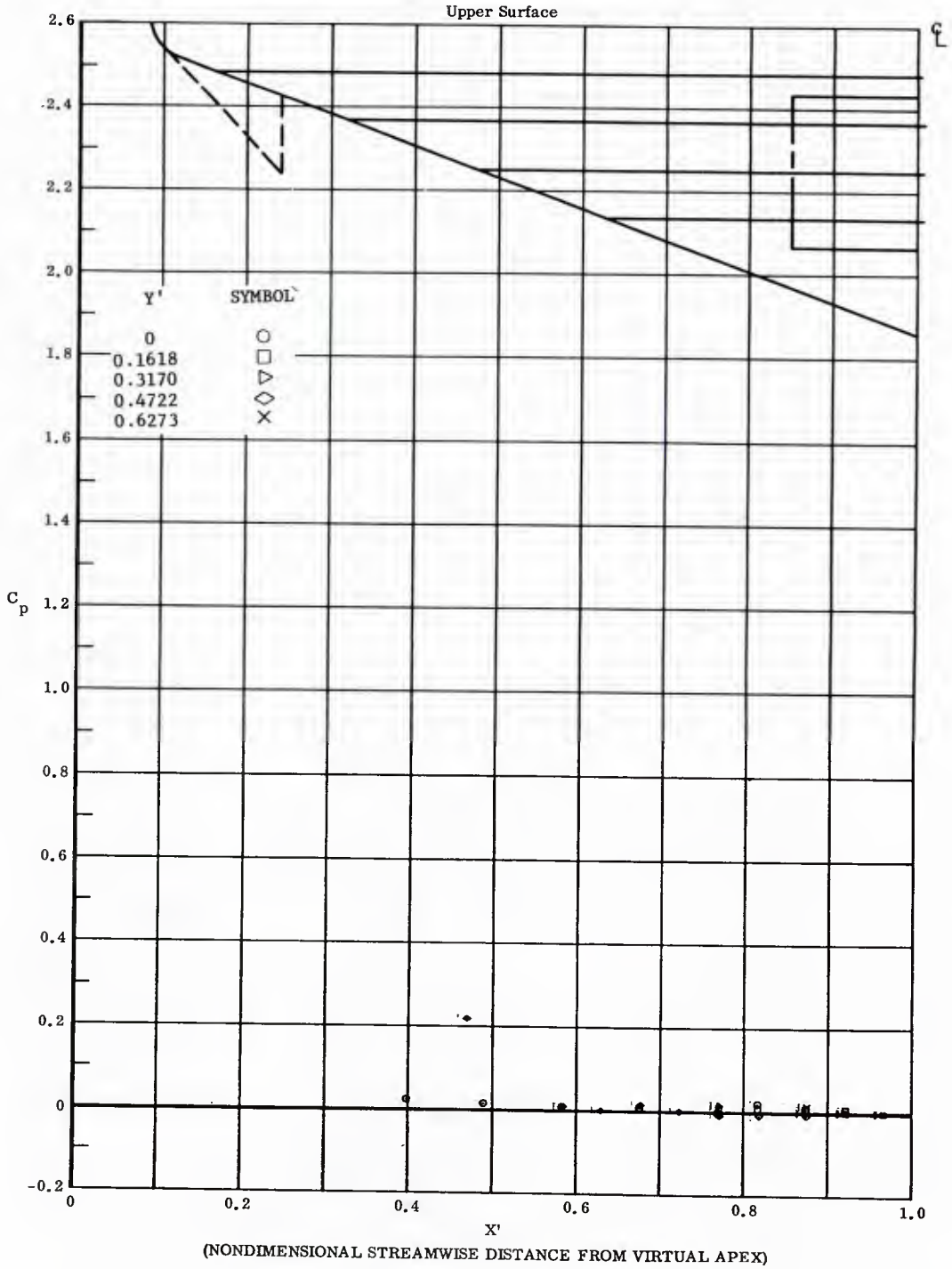

Fig. 66 Streamwise Distributions of Pressure Coefficients on Upper Surface Basic Configuration, Bottom Flaps Deflected 20°, α = +14.3°, β = 0

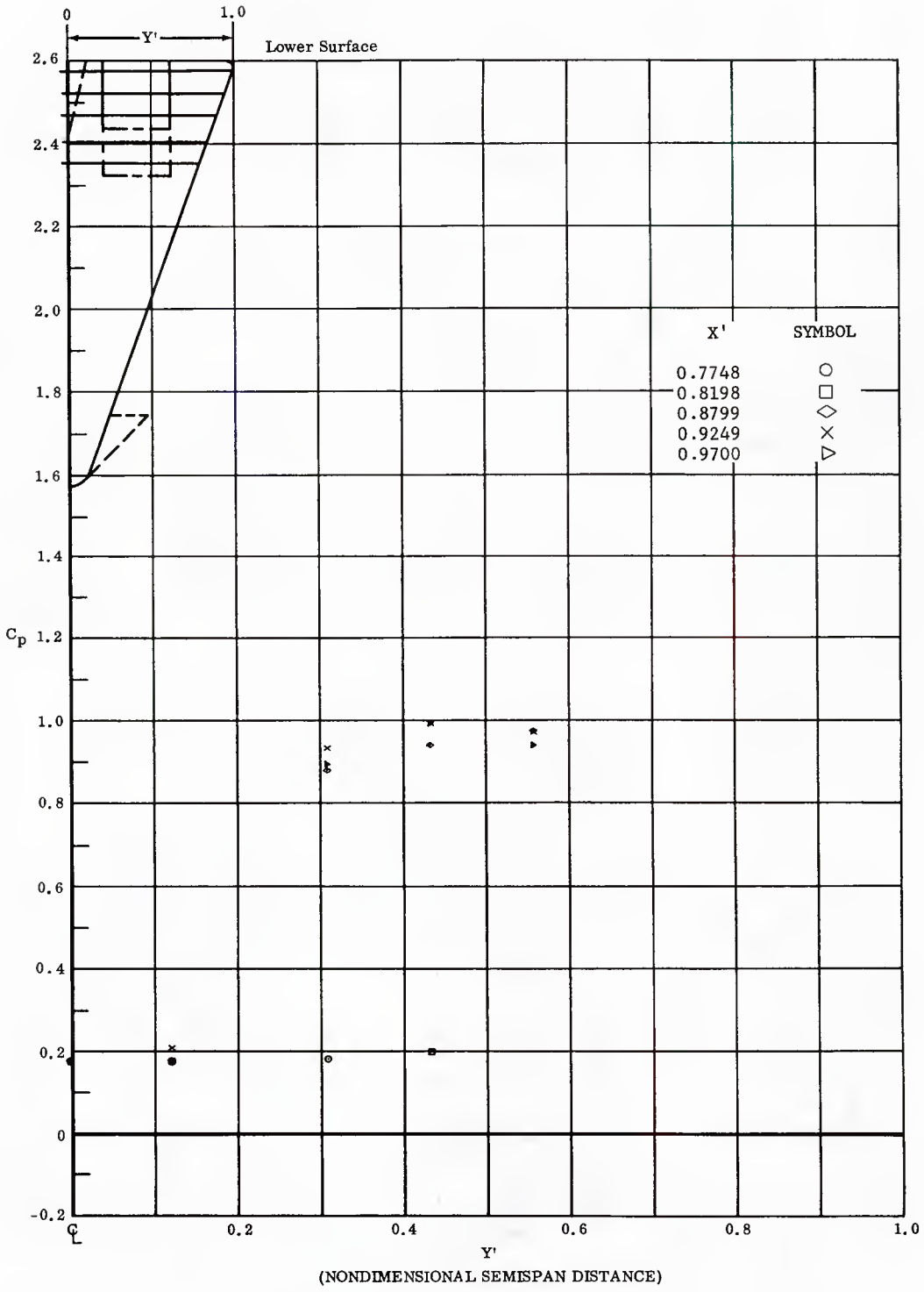

Fig. 66 Spanwise Distributions of Pressure Coefficients on Lower Surface Basic Configuration, Bottom Flaps Deflected 20°, α = +14.3°, β = 0

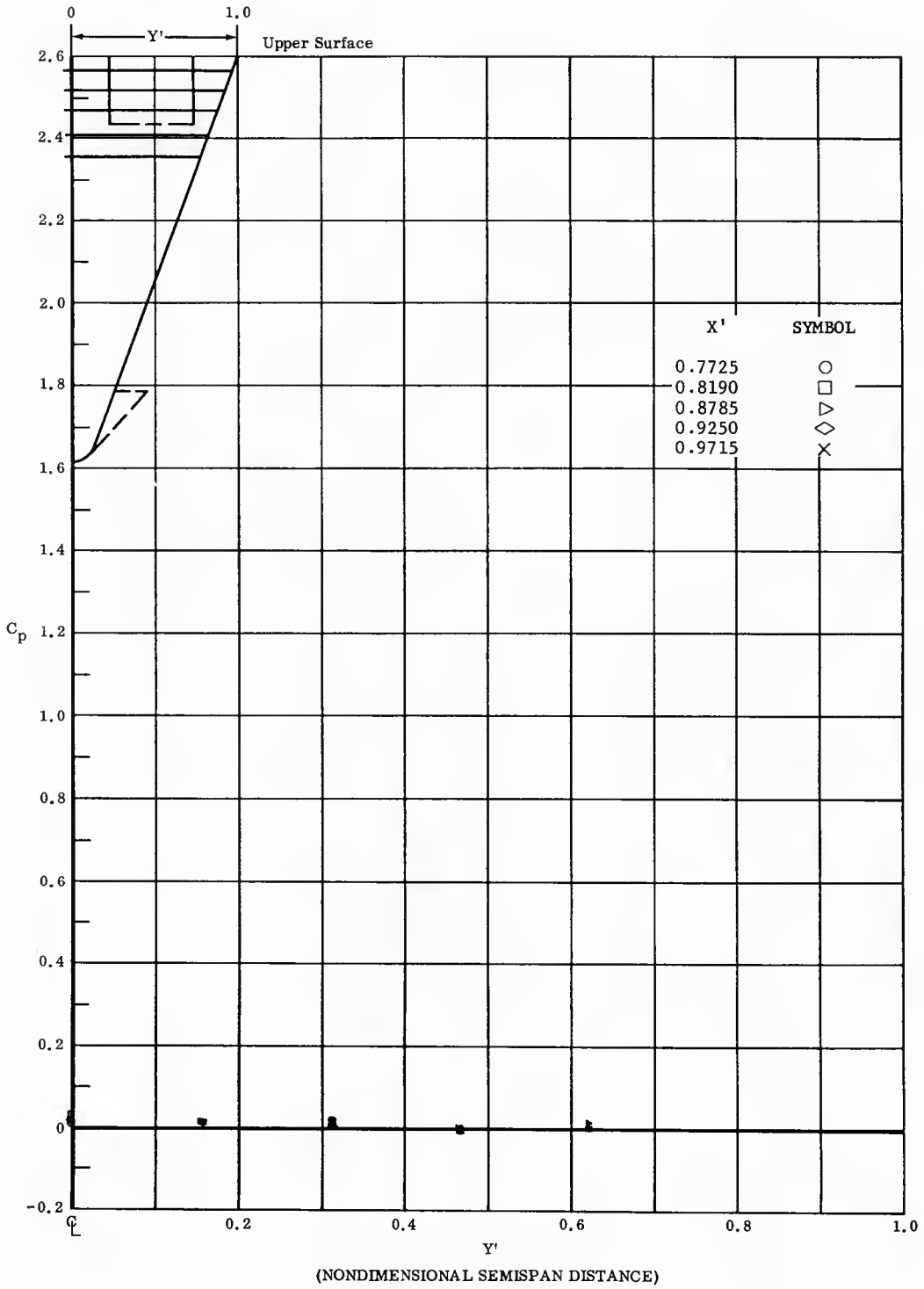

Fig. 66 Spanwise Distributions of Pressure Coefficients on Upper Surface
Basic Configuration, Bottom Flaps Deflected 20°, α = +14.3°, β = 0

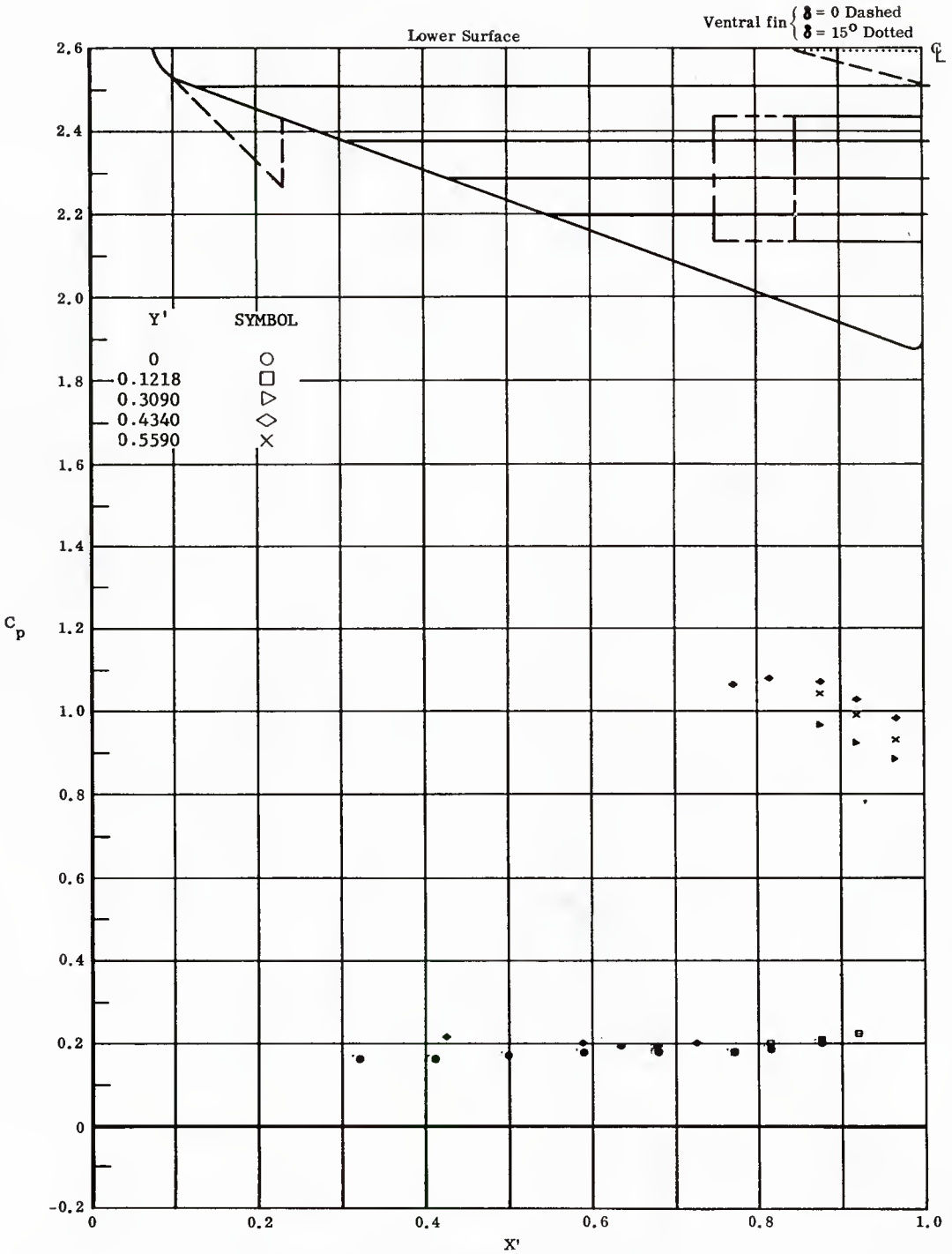

Fig. 67 Streamwise Distributions of Pressure Coefficients on Lower Surface
Extended (Long Chord) Flaps on Lower Surface,
Bottom Flaps Deflected 20°, α = +14.3°, β = 0

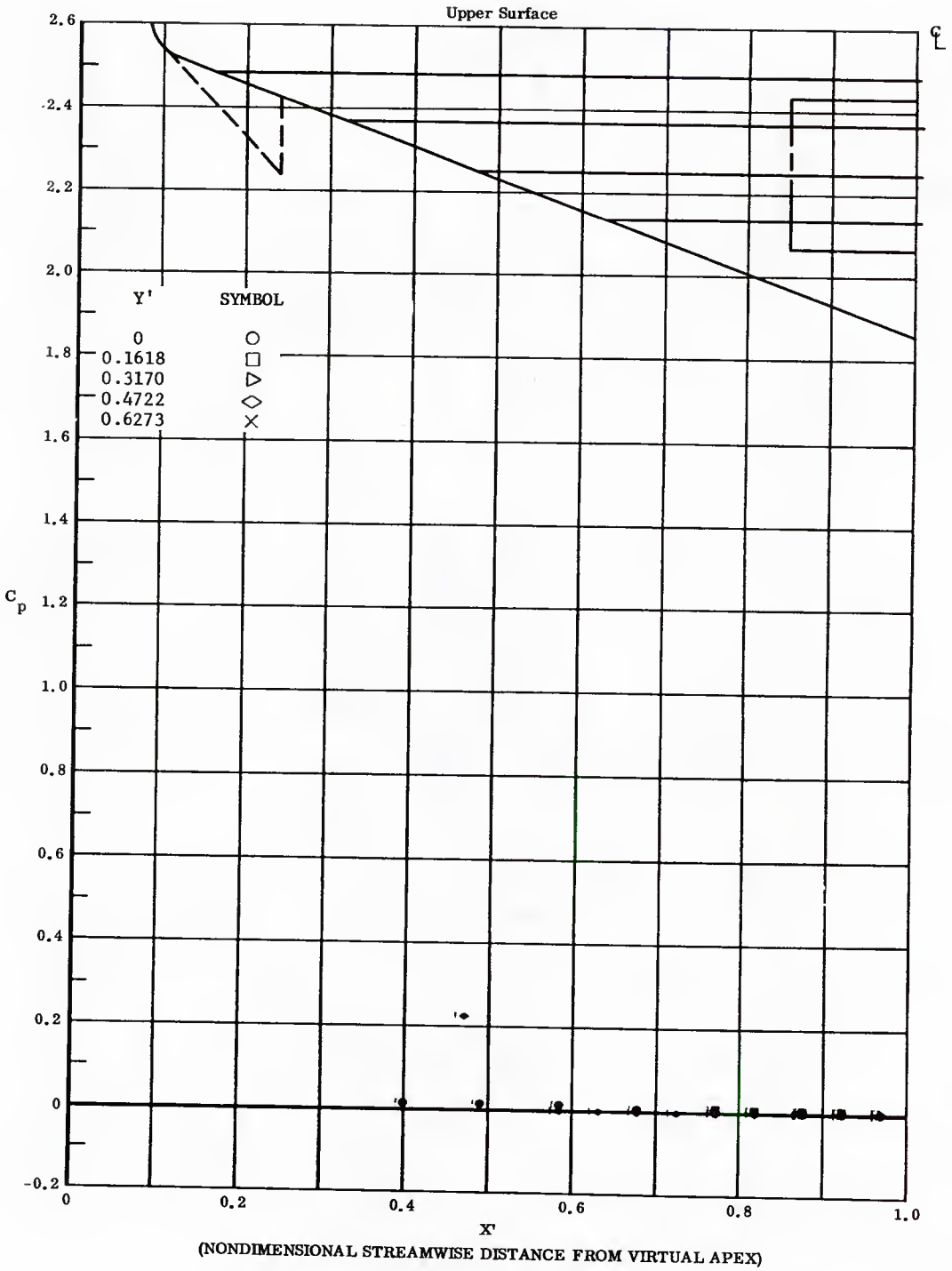

Fig. 67 Streamwise Distributions of Pressure Coefficients on Upper Surface
Extended (Long Chord) Flaps on Lower Surface,
Bottom Flaps Deflected 20°, α = +14.3°, β = 0

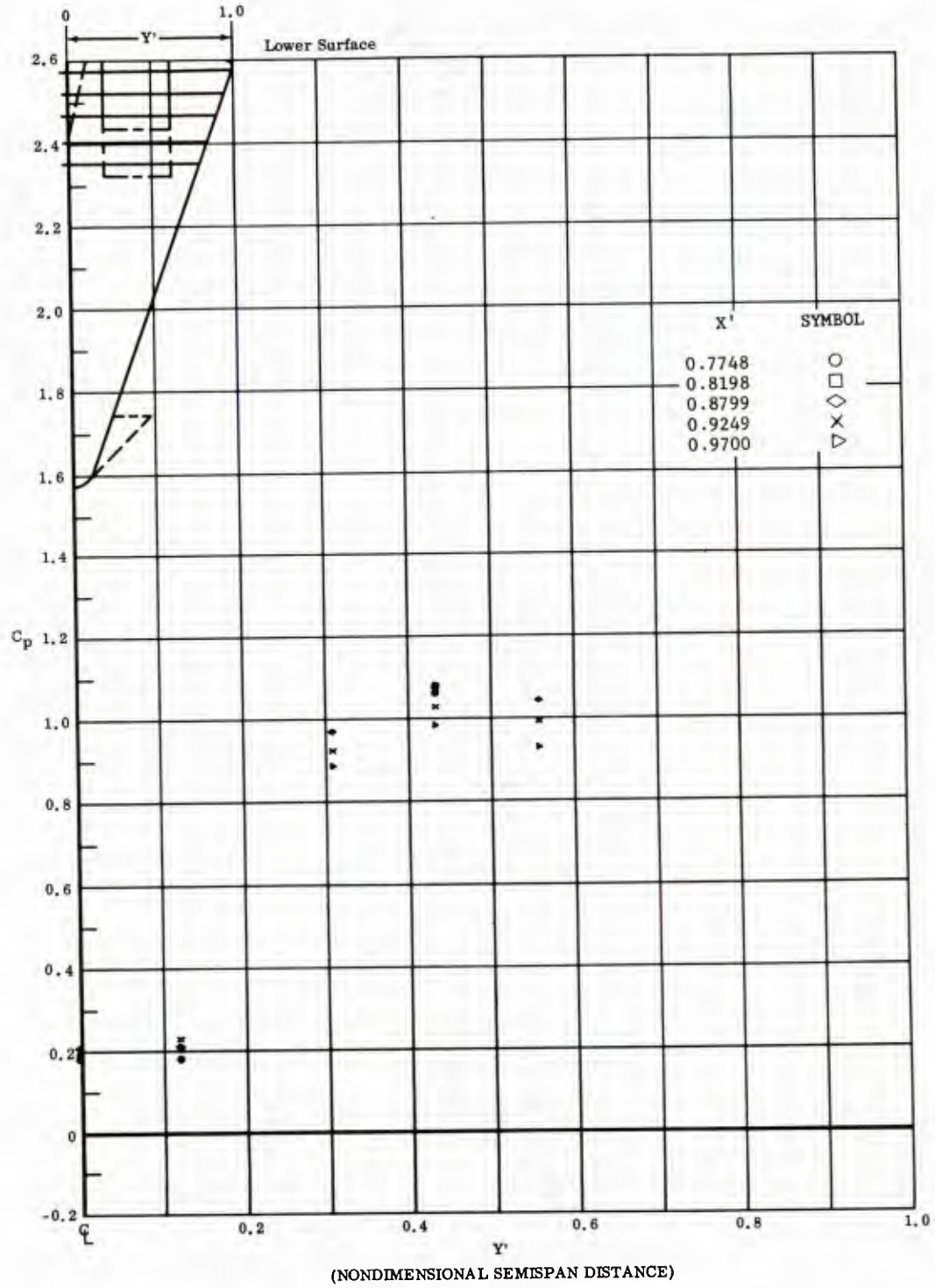

Fig. 67 Spanwise Distributions of Pressure Coefficients on Lower Surface
Extended (Long Chord) Flaps on Lower Surface,
Bottom Flaps Deflected 20°, α = +14.3°, β = 0

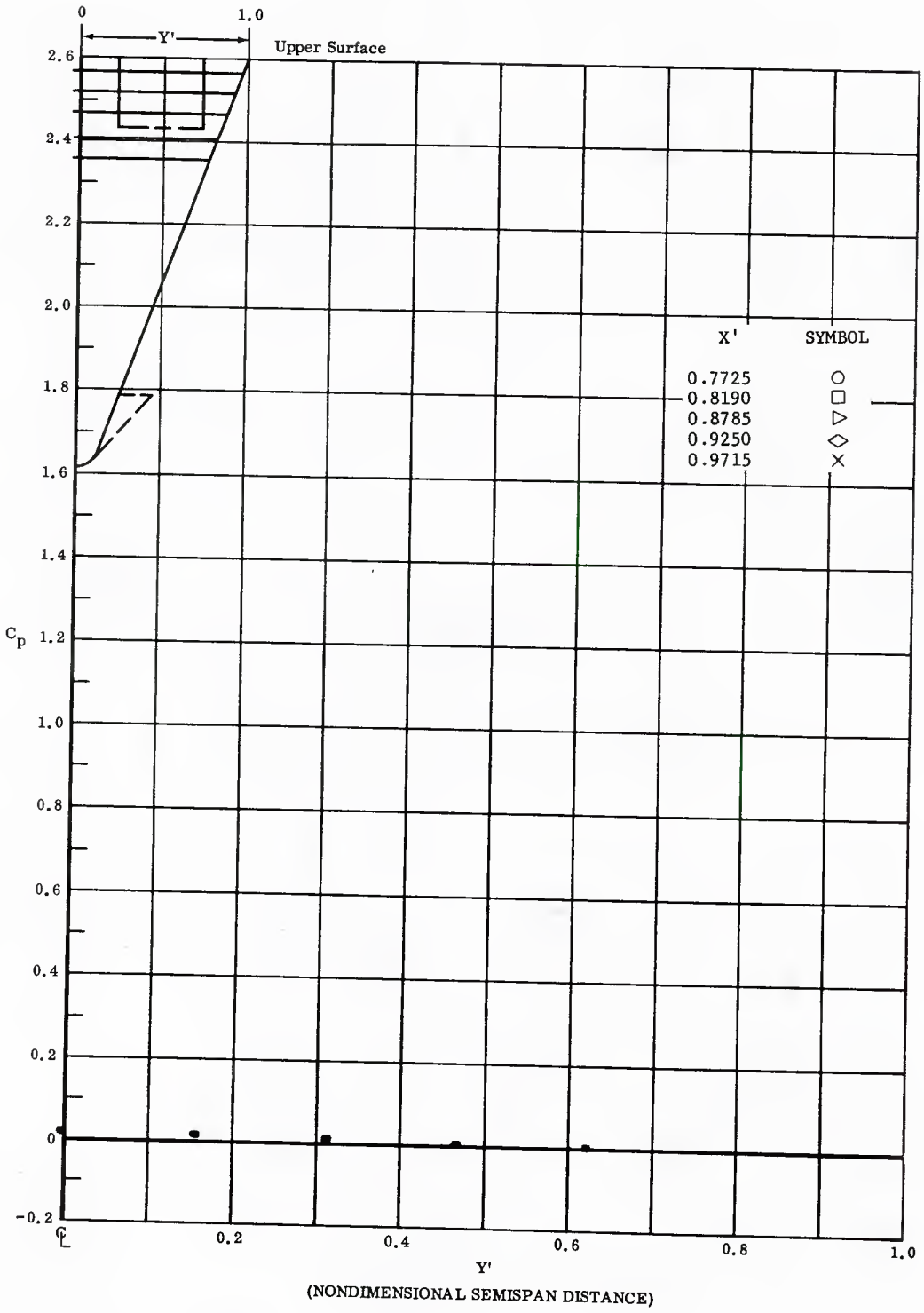

Fig. 67 Spanwise Distributions of Pressure Coefficients on Upper Surface Extended (Long Chord) Flaps on Lower Surface, Bottom Flaps Deflected 20°, α = +14.3°, β = 0

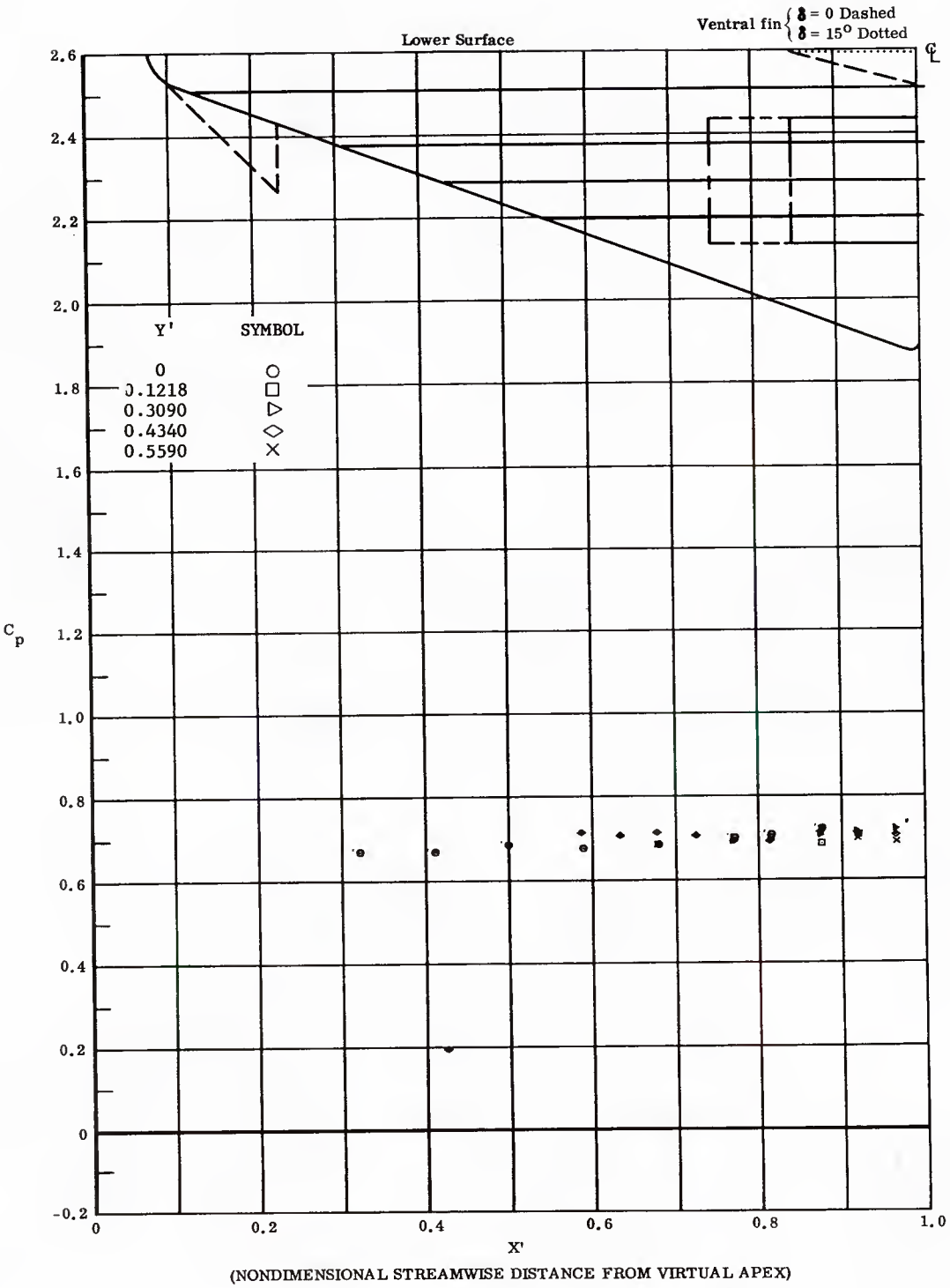

Fig. 68 Streamwise Distributions of Pressure Coefficients on Lower Surface Basic Configuration, Left and Right (Upper) Flaps Deflected -40°, α = +33°, β = 0

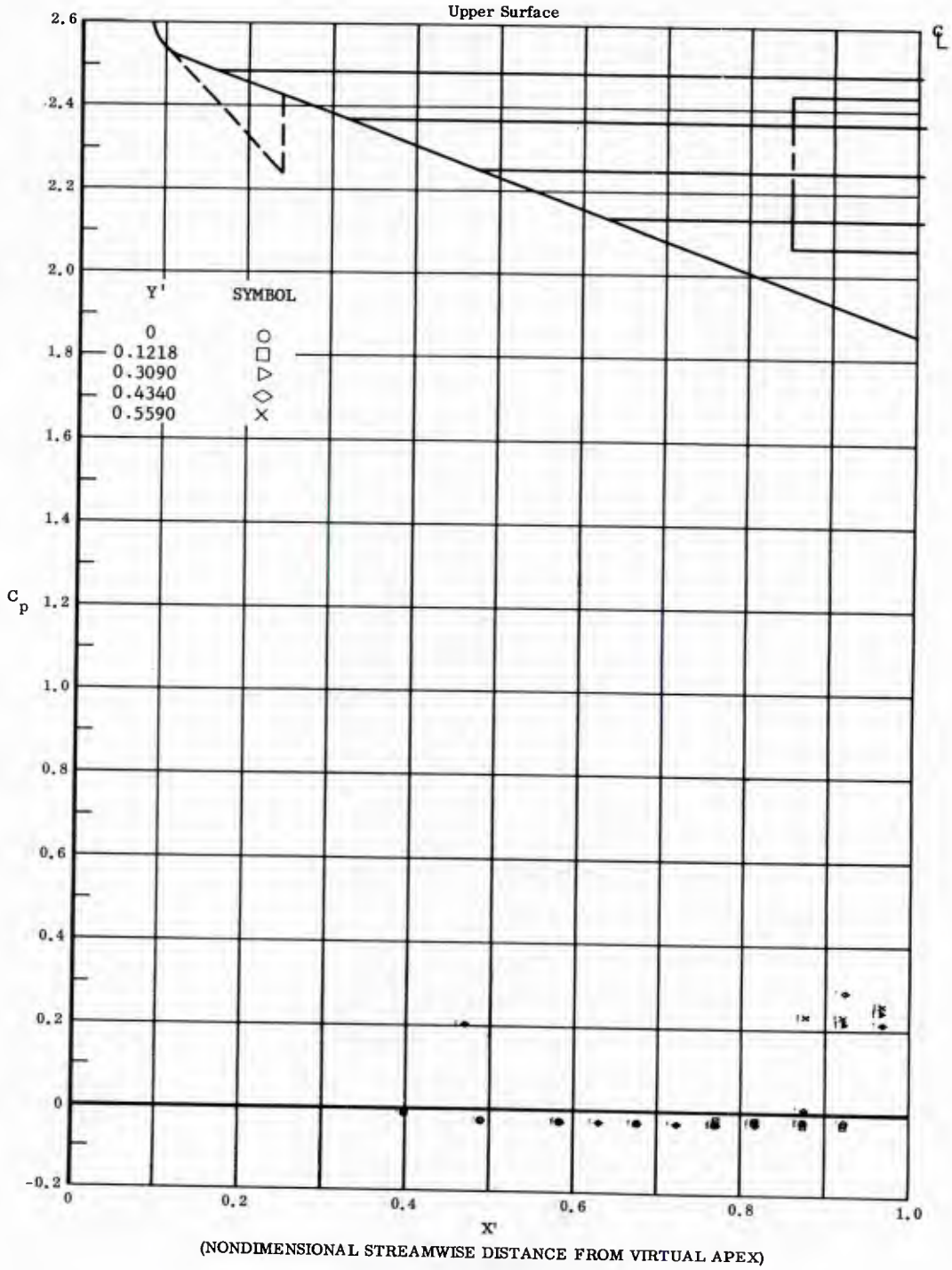

Fig. 68 Streamwise Distributions of Pressure Coefficients on Upper Surface Basic Configuration, Left and Right (Upper) Flaps Deflected -40°, α = +33°, β = 0

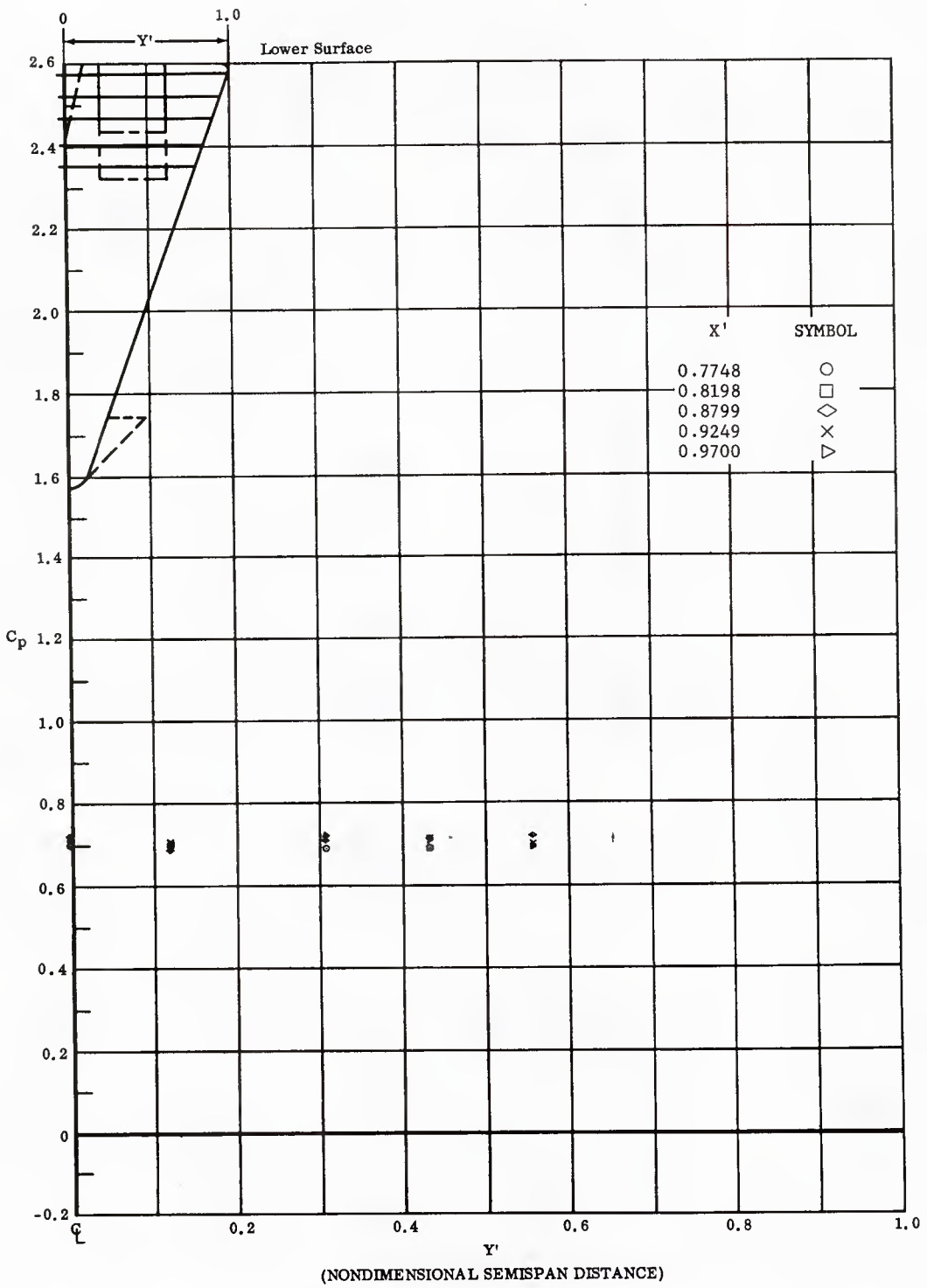

Fig. 68 Spanwise Distributions of Pressure Coefficients on Lower Surface Basic Configuration, Left and Right (Upper) Flaps Deflected -40°, α = +33°, β = 0

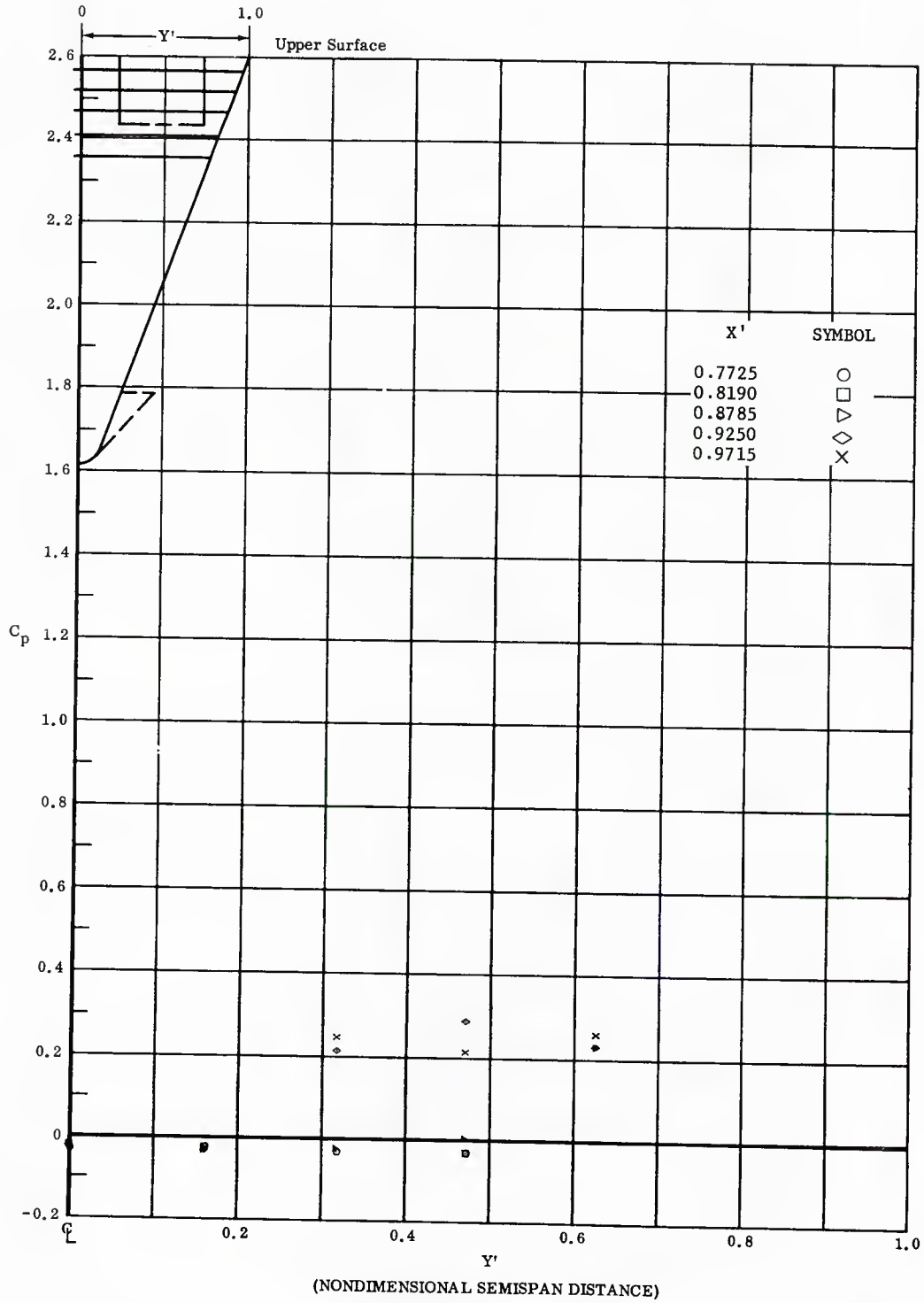

Fig. 68 Spanwise Distributions of Pressure Coefficients on Upper Surface Basic Configuration, Left and Right (Upper) Flaps Deflected -40°, α = +33°, β = 0

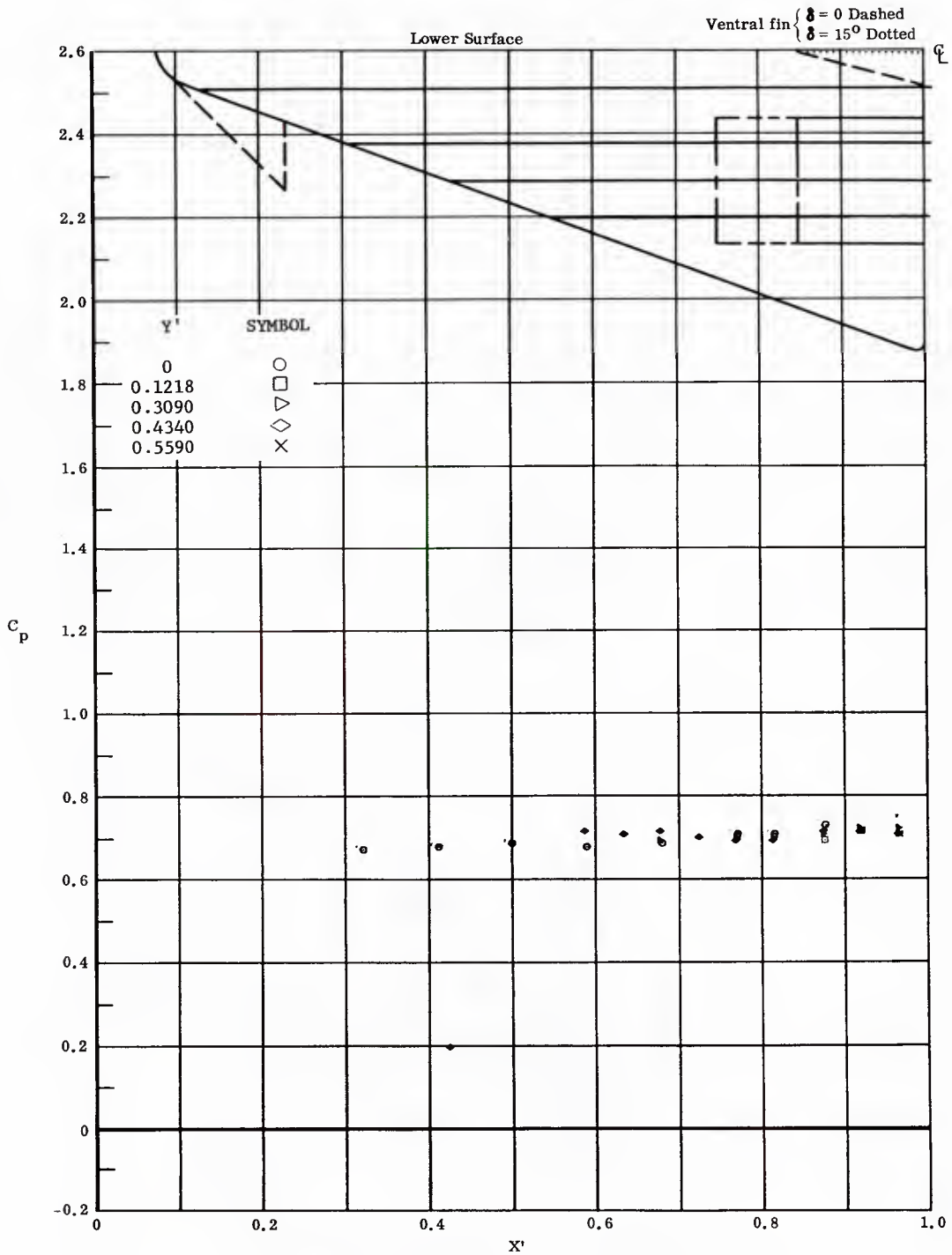

Fig. 69 Streamwise Distributions of Pressure Coefficients on Lower Surface
Basic Configuration, Left and Right (Upper) Flaps Deflected -30°,
α = +33°, β = 0

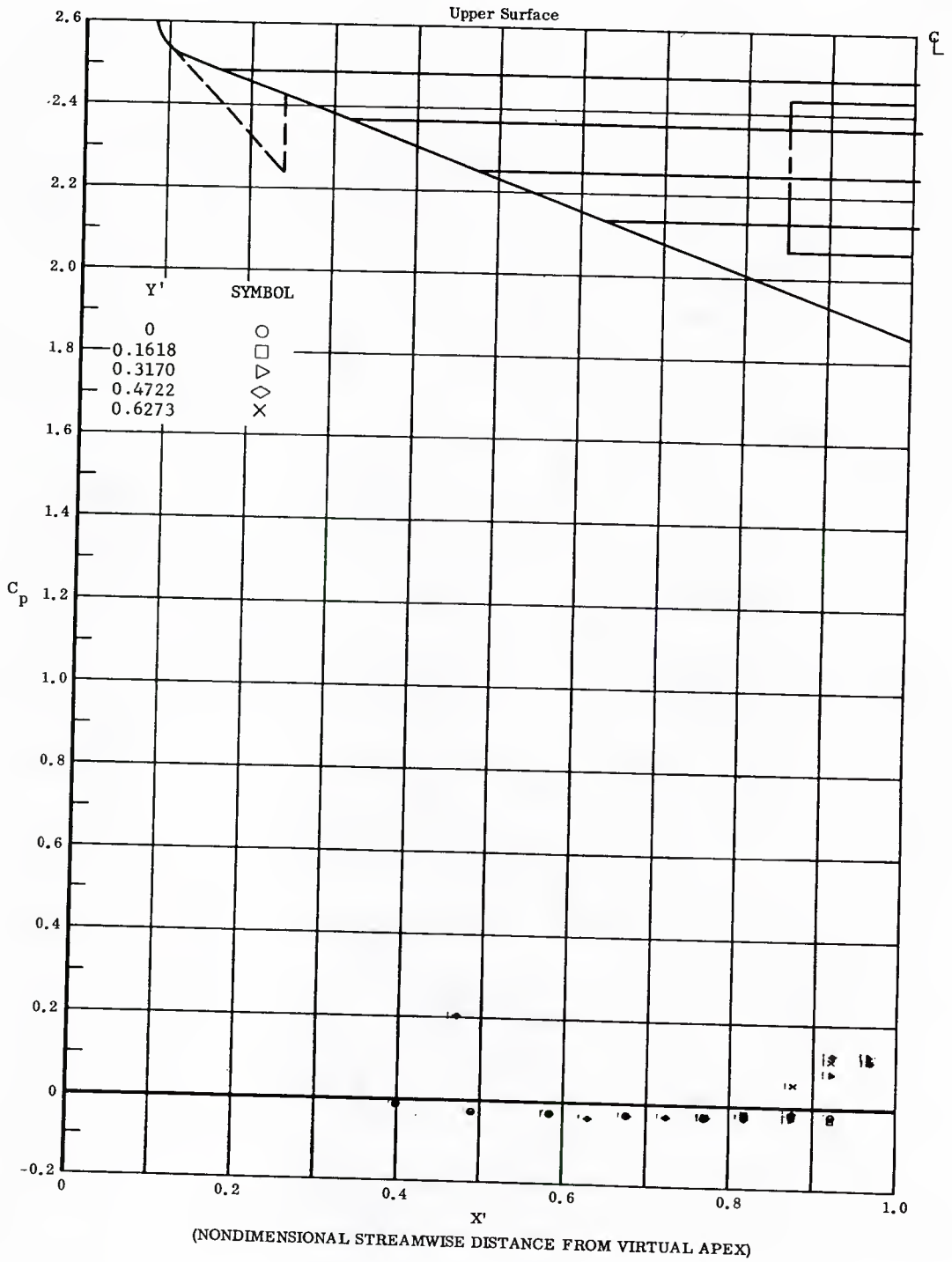

Fig. 69 Streamwise Distributions of Pressure Coefficients on Upper Surface Basic Configuration, Left and Right (Upper) Flaps Deflected -30°, α = +33°, β = 0

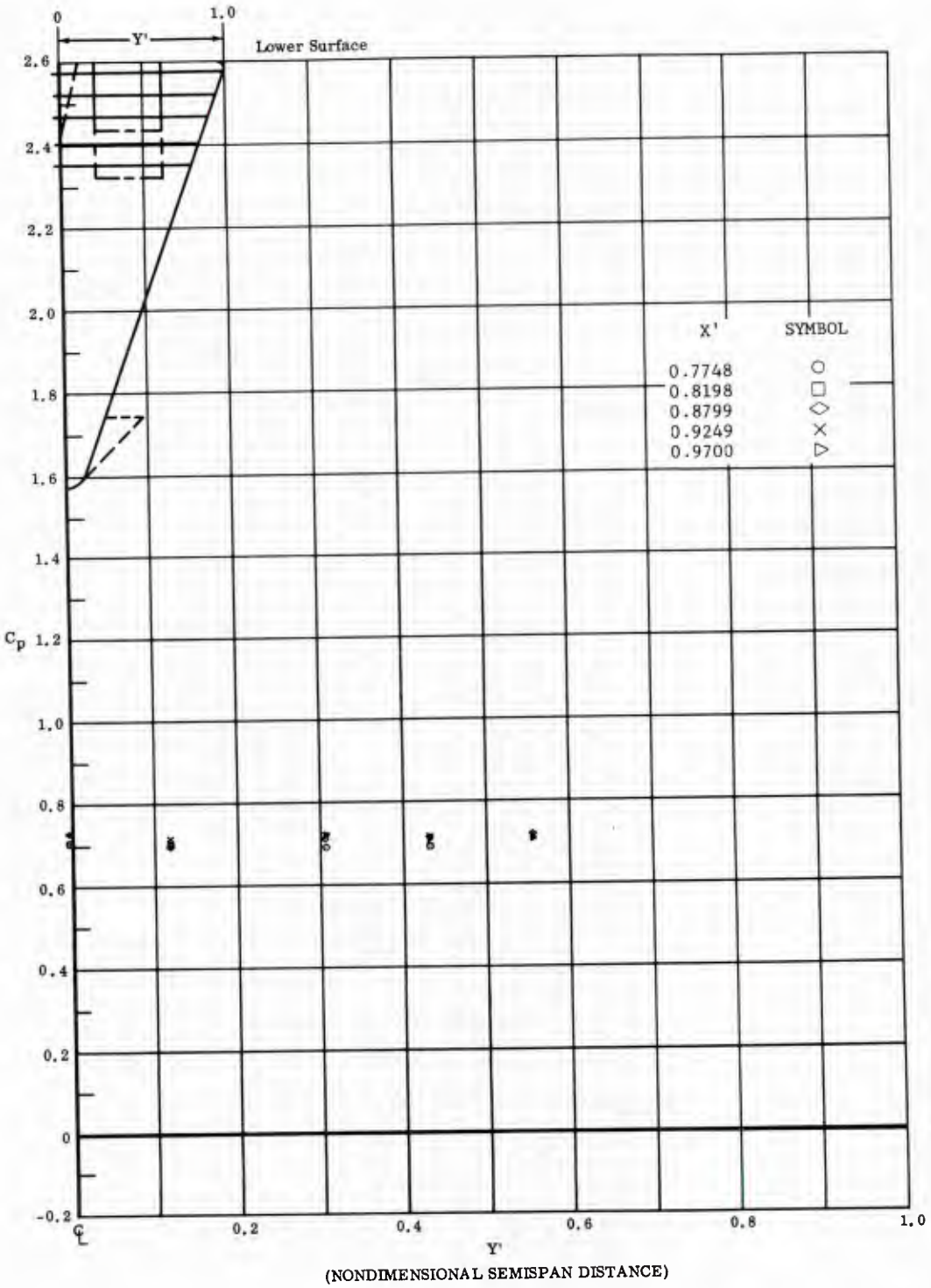

Fig. 69 Spanwise Distributions of Pressure Coefficients on Lower Surface Basic Configuration, Left and Right (Upper) Flaps Deflected -30°, α = +33°, β = 0

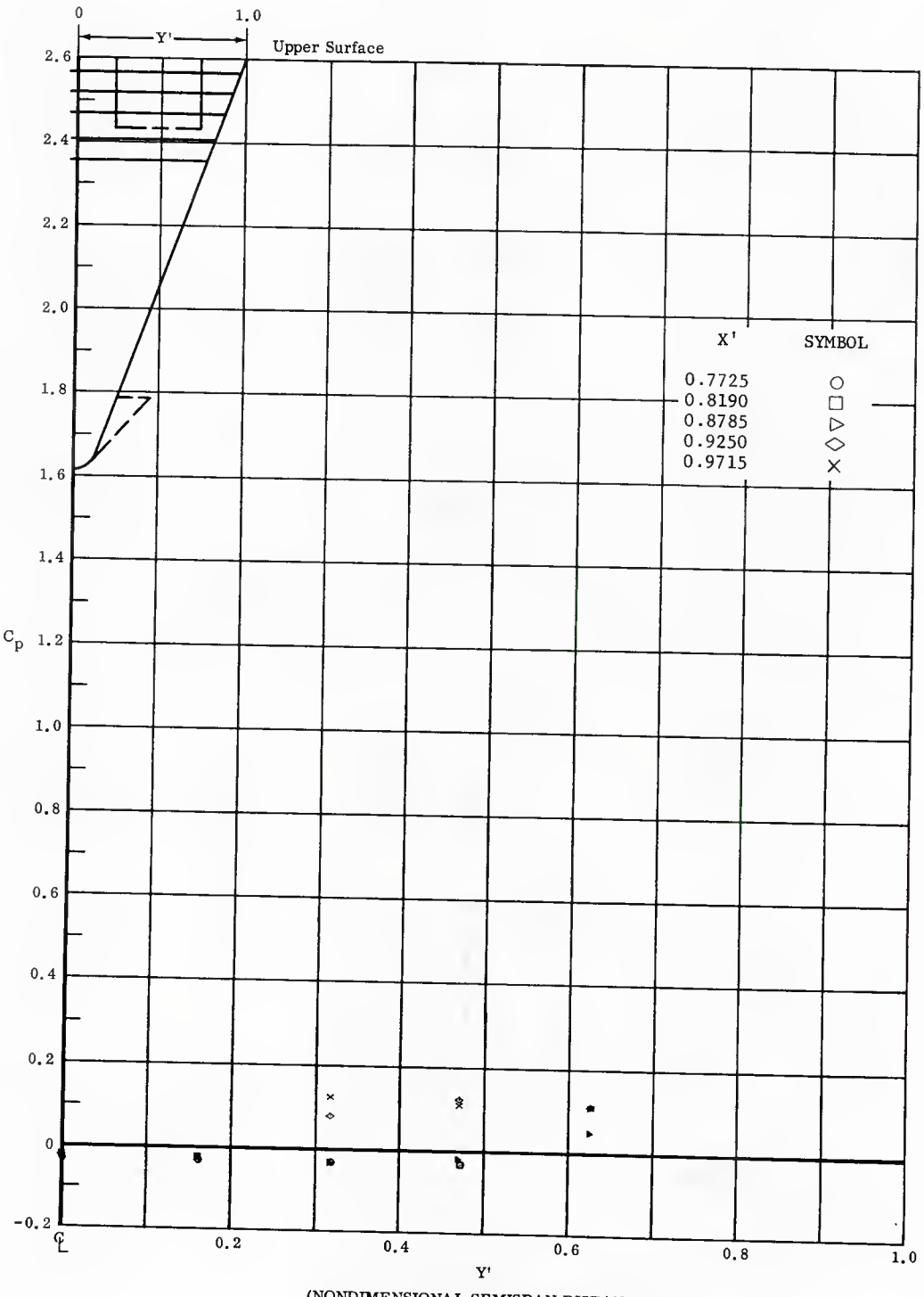

Fig. 69 Spanwise Distributions of Pressure Coefficients on Upper Surface Basic Configuration, Left and Right (Upper) Flaps Deflected -30°, $\alpha = +33°$, $\beta = 0$

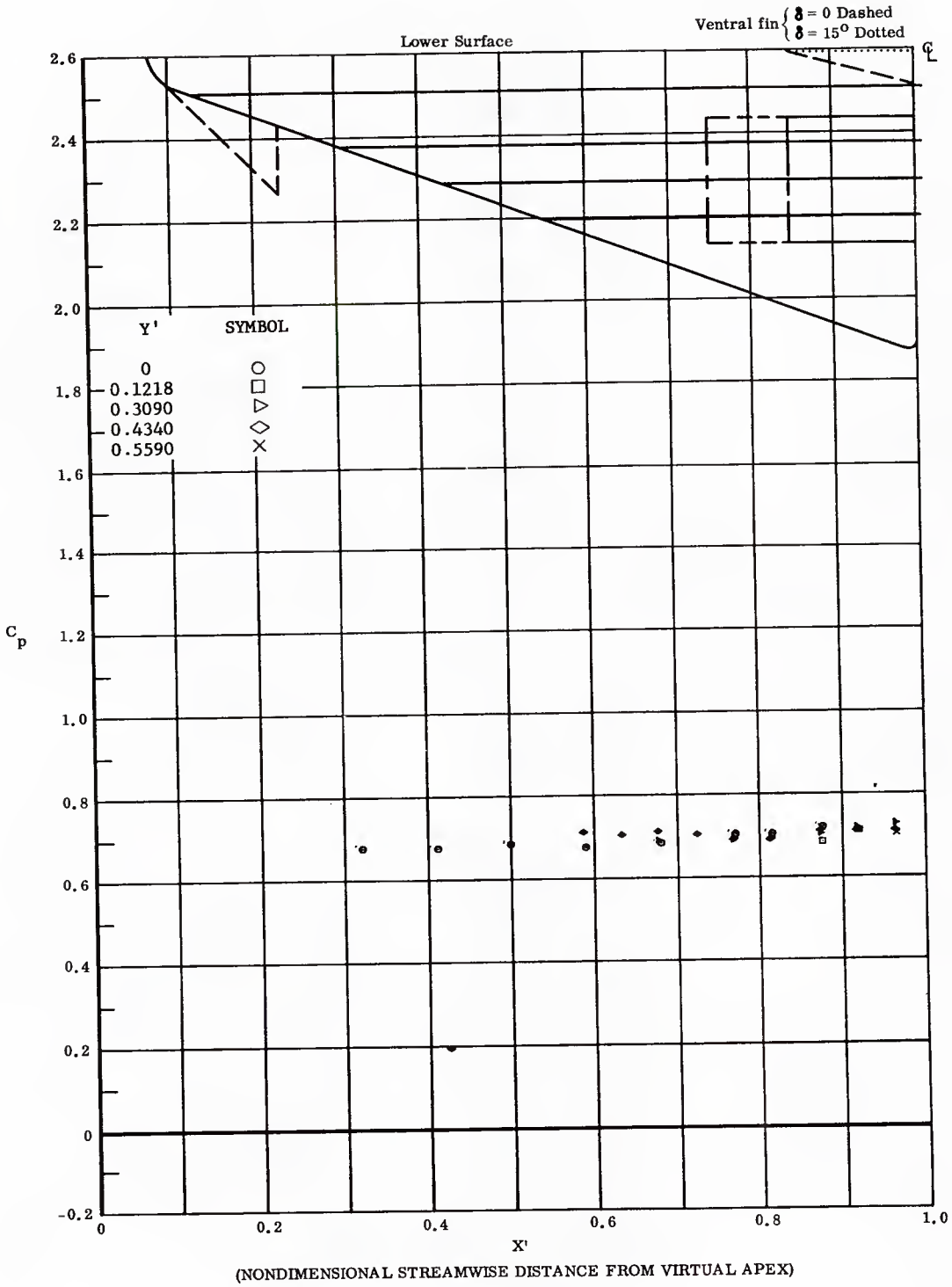

Fig. 70 Streamwise Distributions of Pressure Coefficients on Lower Surface Basic Configuration, Left and Right (Upper) Flaps Deflected -20°, $\alpha = +33°, \beta = 0$

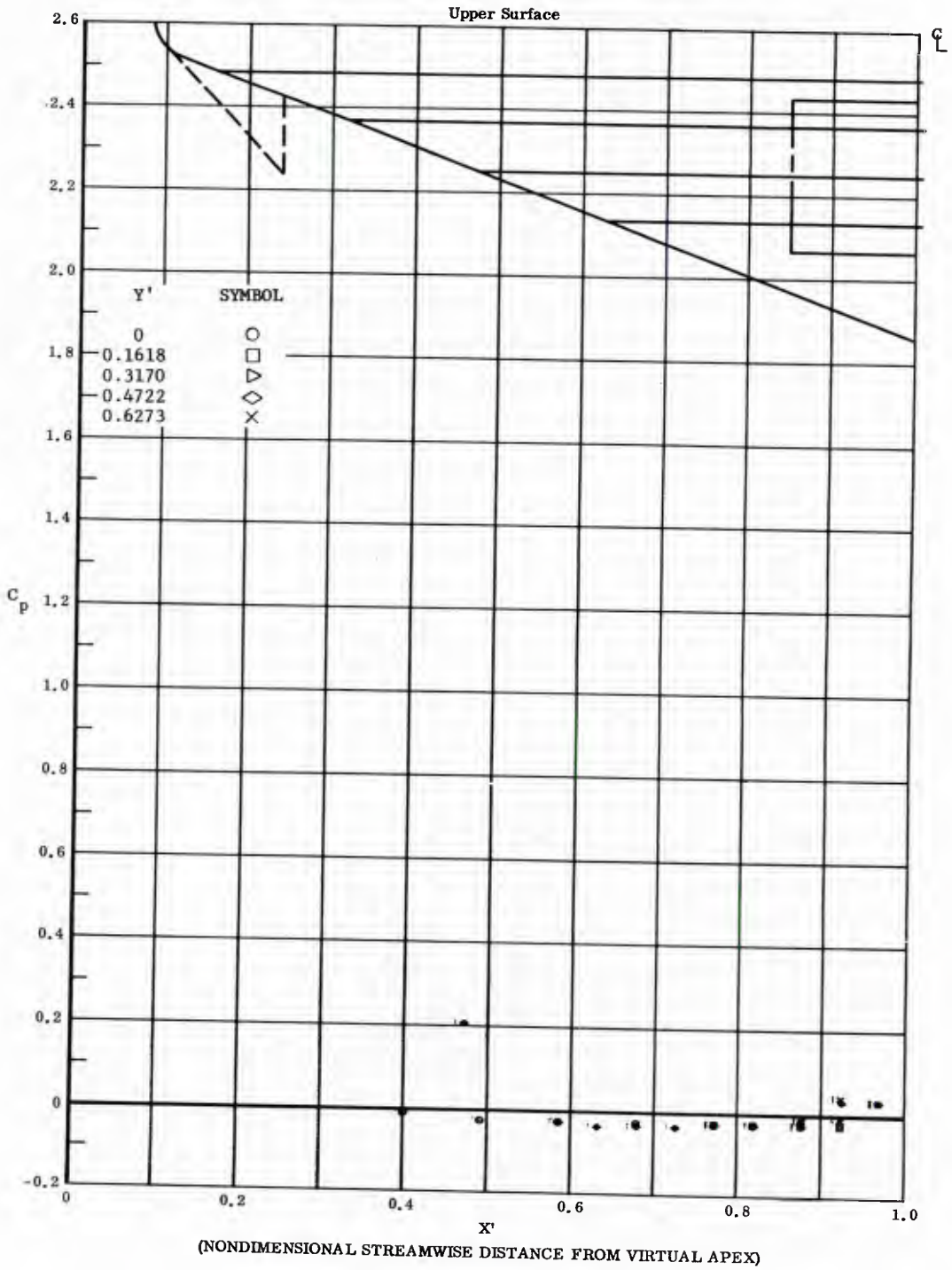

Fig. 70 Streamwise Distributions of Pressure Coefficients on Upper Surface Basic Configuration, Left and Right (Upper) Flaps Deflected -20°, α = +33°, β = 0

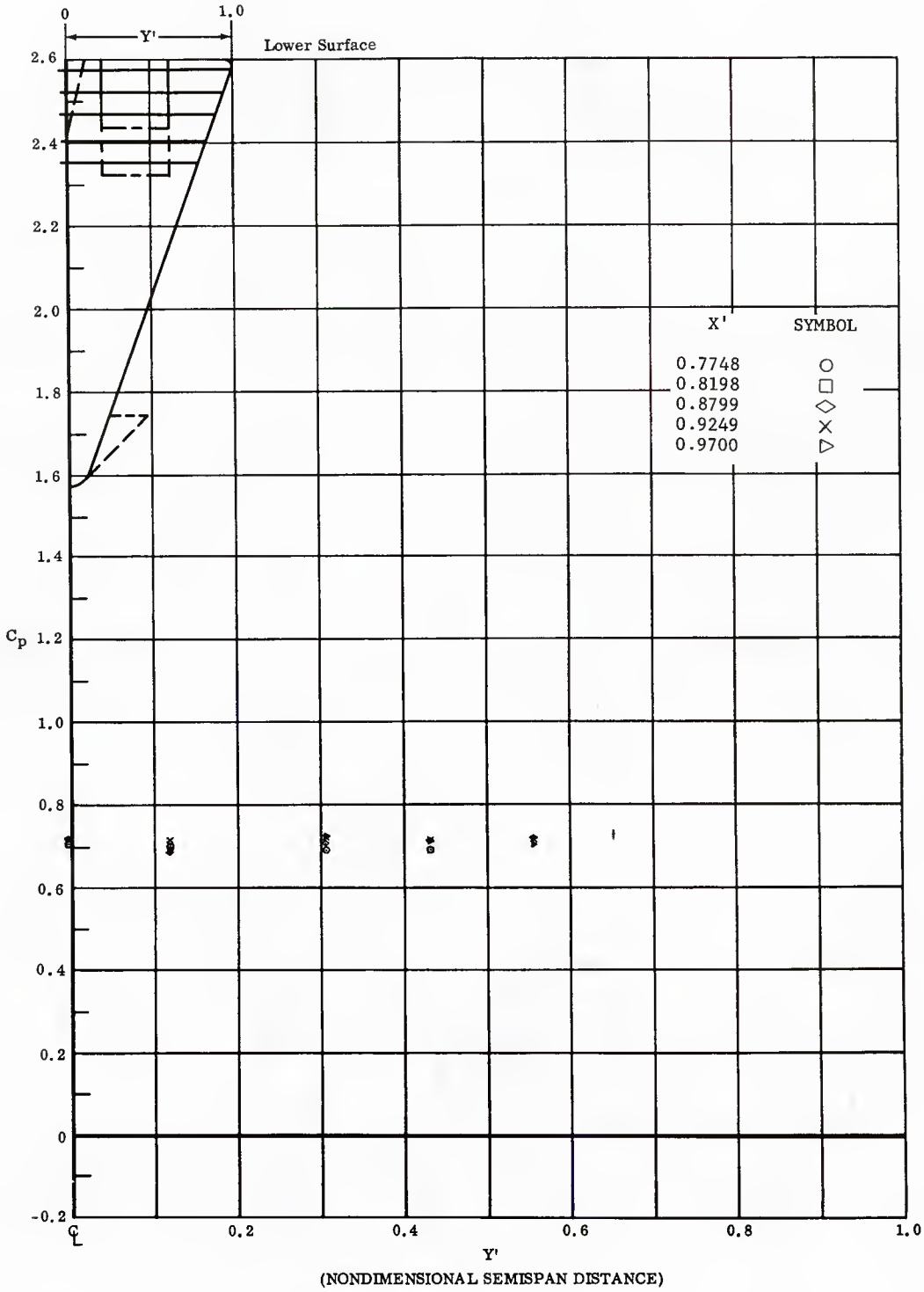

Fig. 70 Spanwise Distributions of Pressure Coefficients on Lower Surface Basic Configuration, Left and Right (Upper) Flaps Deflected -20°, $\alpha = +33°, \beta = 0$

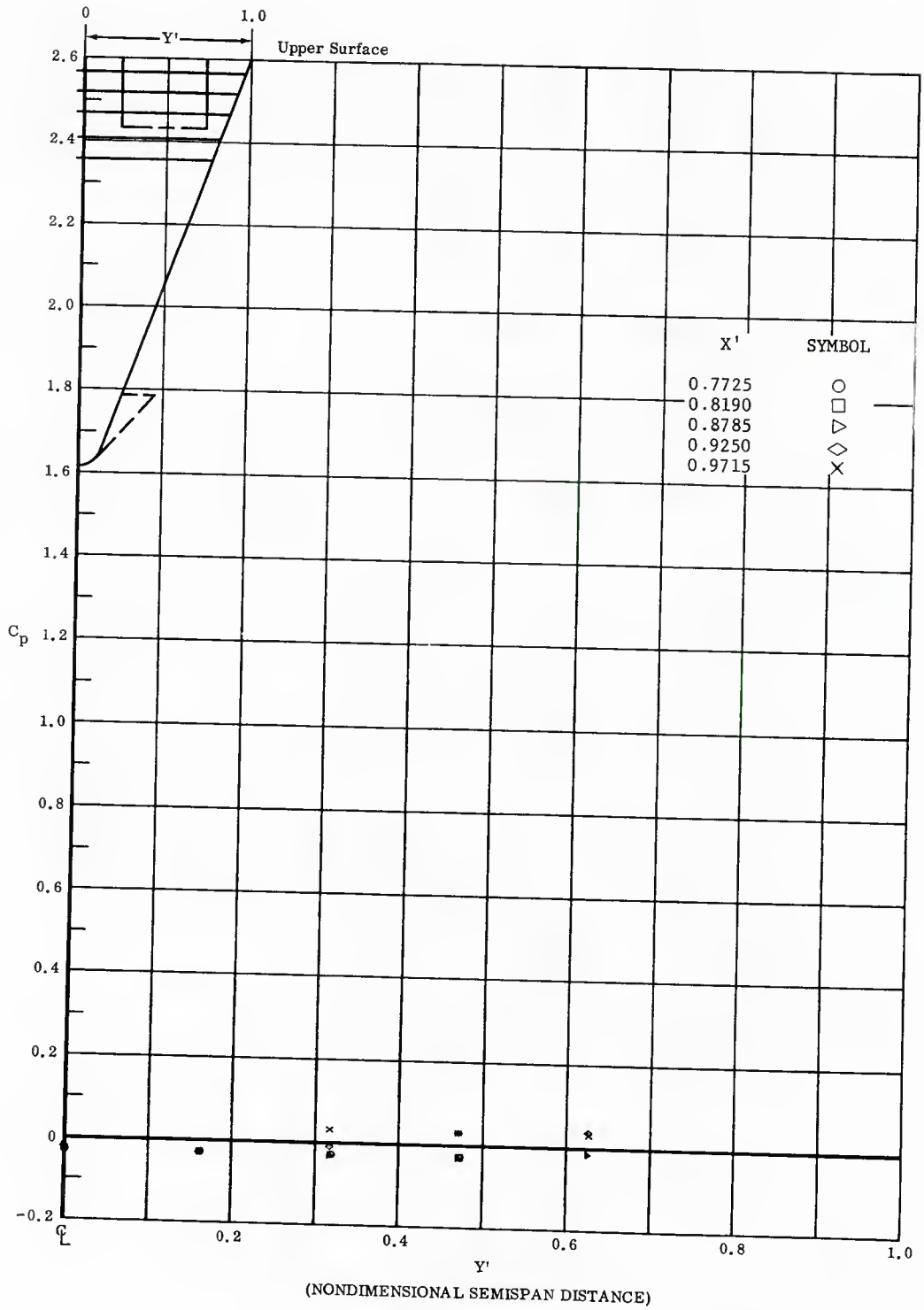

Fig. 70 Spanwise Distributions of Pressure Coefficients on Upper Surface Basic Configuration, Left and Right (Upper) Flaps Deflected -20°, $\alpha = +33°, \beta = 0$

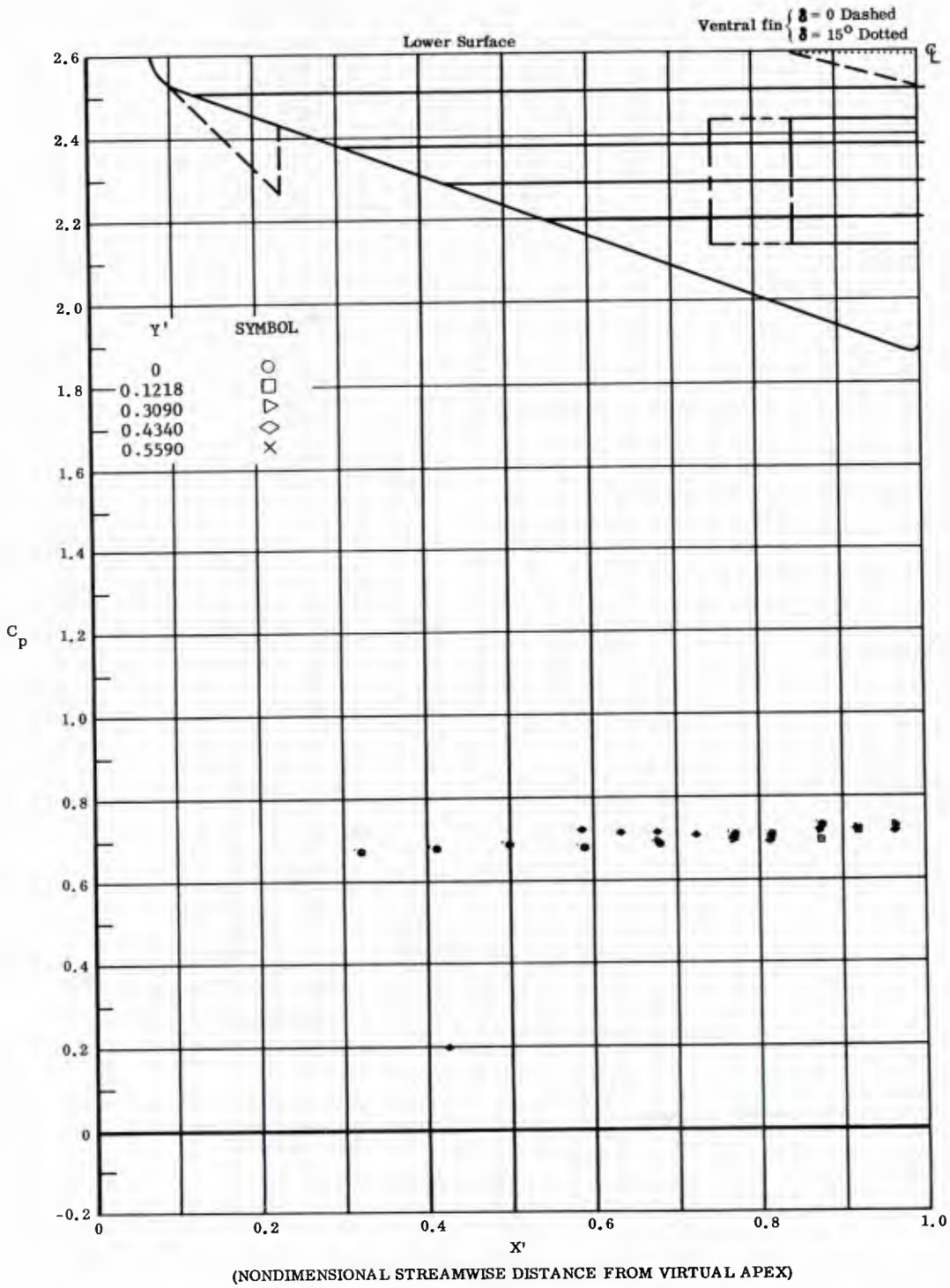

Fig. 71 Streamwise Distributions of Pressure Coefficients on Lower Surface Basic Configuration, Left and Right (Upper) Flaps Deflected -10°, $\alpha = +33°, \beta = 0$

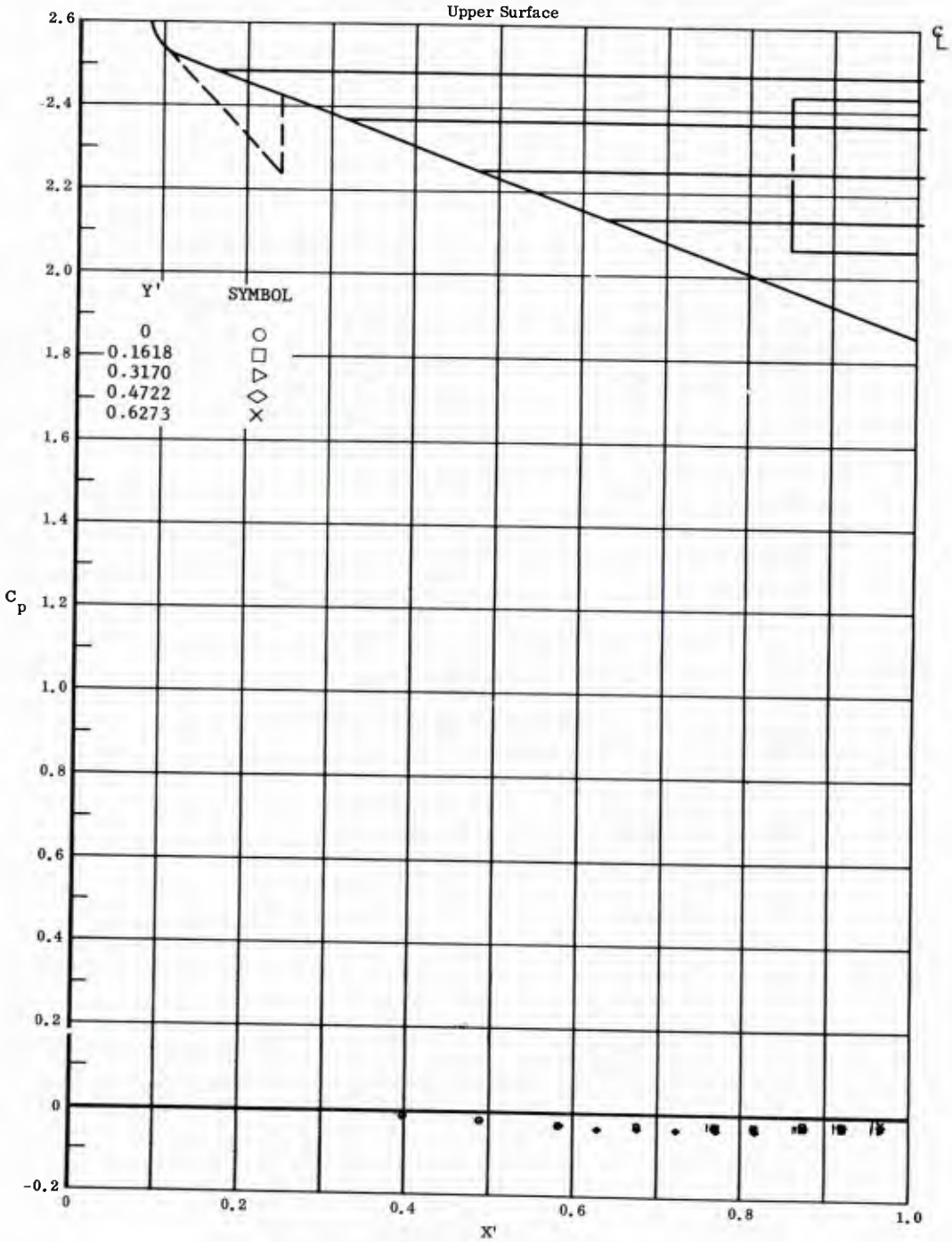

Fig. 71 Streamwise Distributions of Pressure Coefficients on Upper Surface Basic Configuration, Left and Right (Upper) Flaps Deflected -10°, α = +33°, β = 0

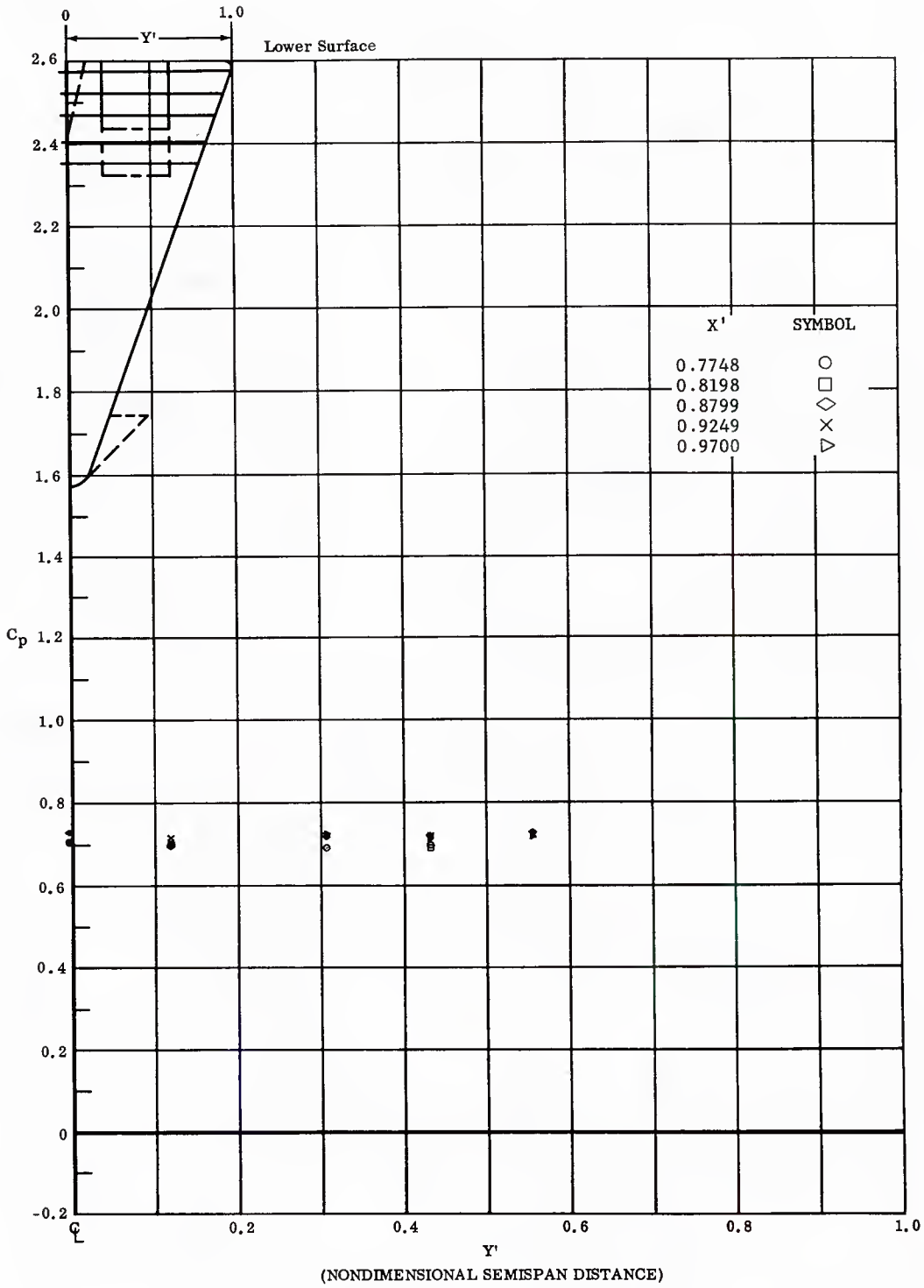

Fig. 71 Spanwise Distributions of Pressure Coefficients on Lower Surface Basic Configuration, Left and Right (Upper) Flaps Deflected -10°, α = +33°, β = 0

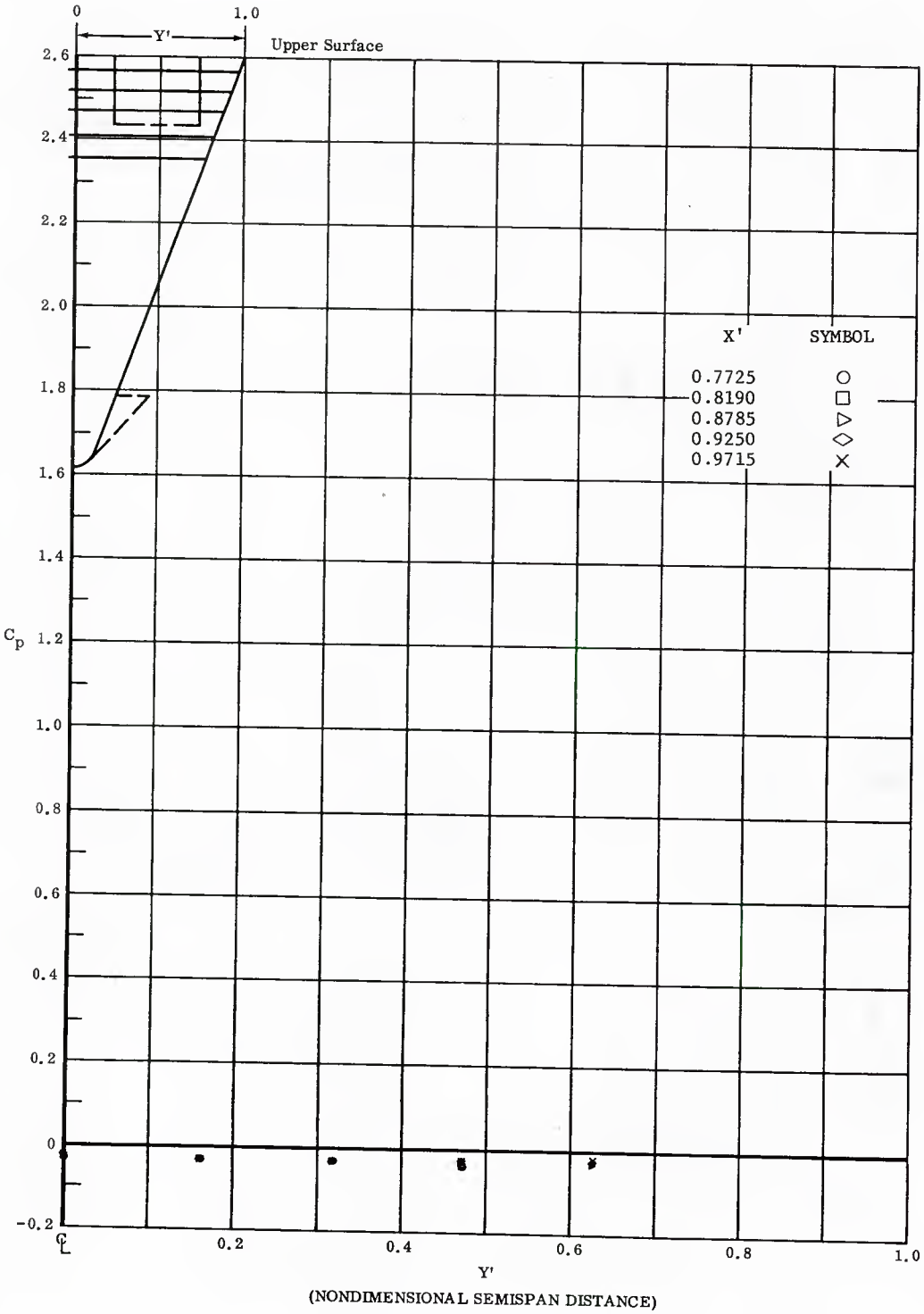

Fig. 71 Spanwise Distributions of Pressure Coefficients on Upper Surface Basic Configuration, Left and Right (Upper) Flaps Deflected -10°, $\alpha = +33°$, $\beta = 0$

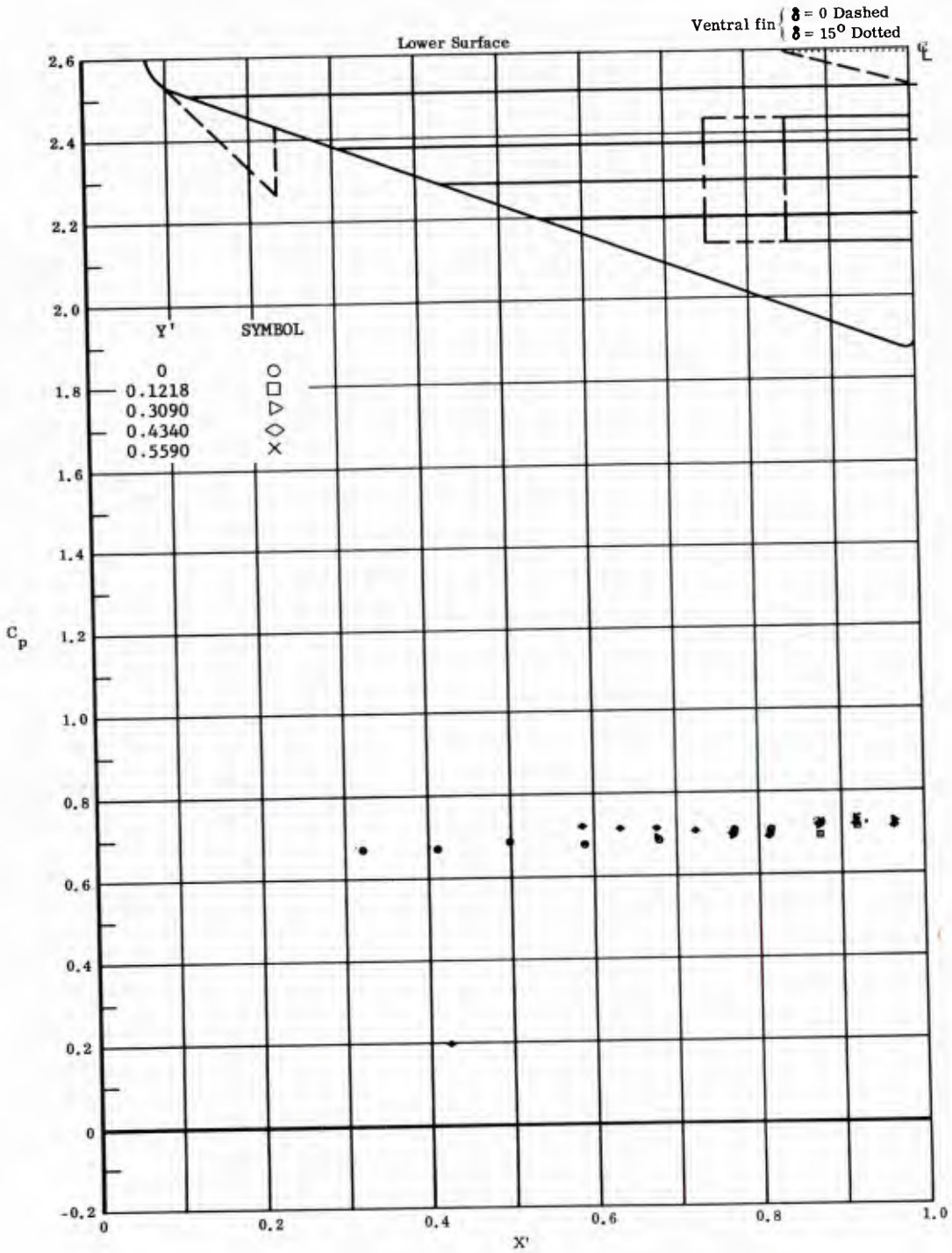

Fig. 72 Streamwise Distributions of Pressure Coefficients on Lower Surface Basic Configuration, No Flap Deflections, α = +33°, β = 0

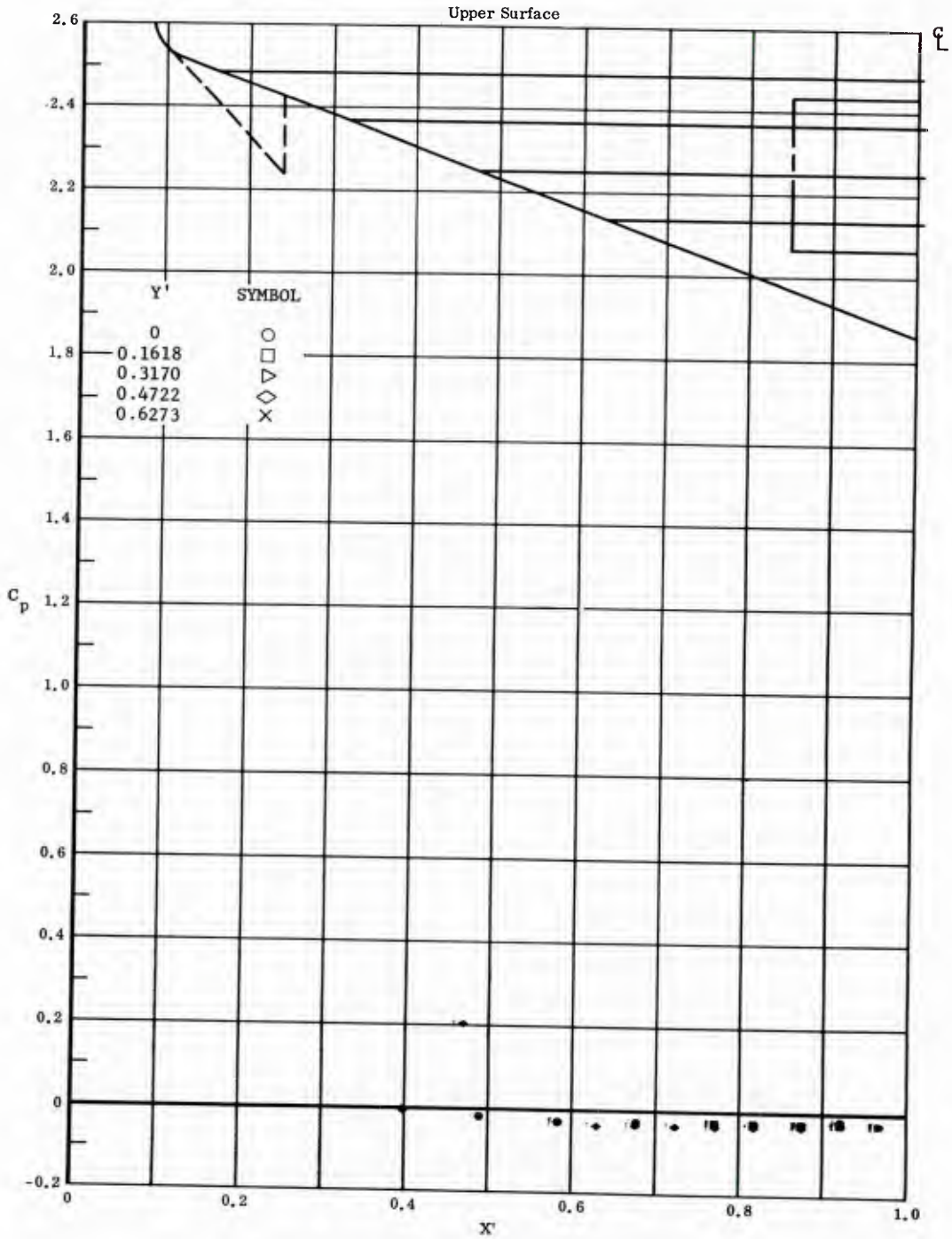

Fig. 72 Streamwise Distributions of Pressure Coefficients on Upper Surface
Basic Configuration, No Flap Deflections, α = +33°, β = 0

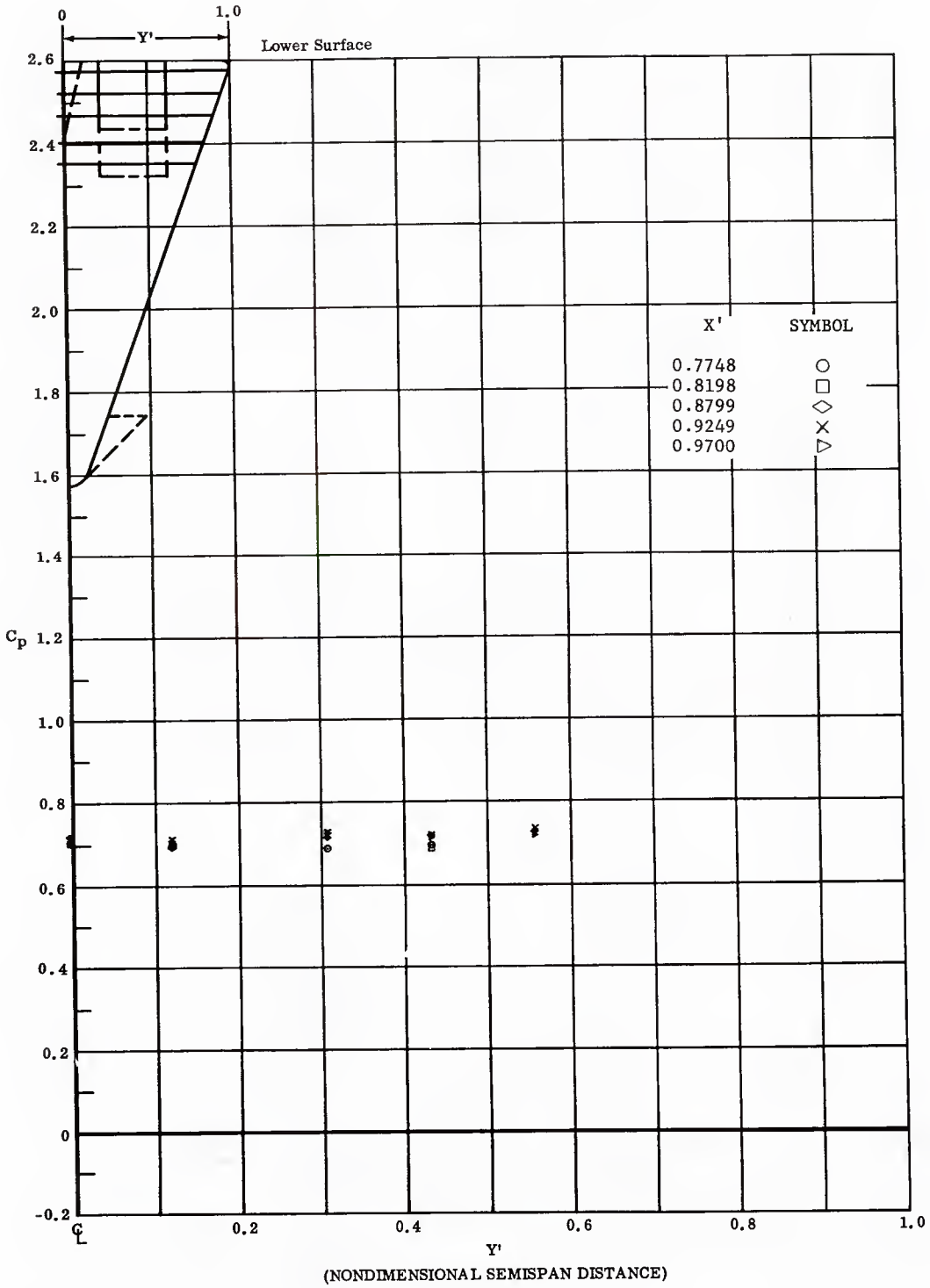

Fig. 72 Spanwise Distributions of Pressure Coefficients on Lower Surface
Basic Configuration, No Flap Deflections, α = +33°, β = 0

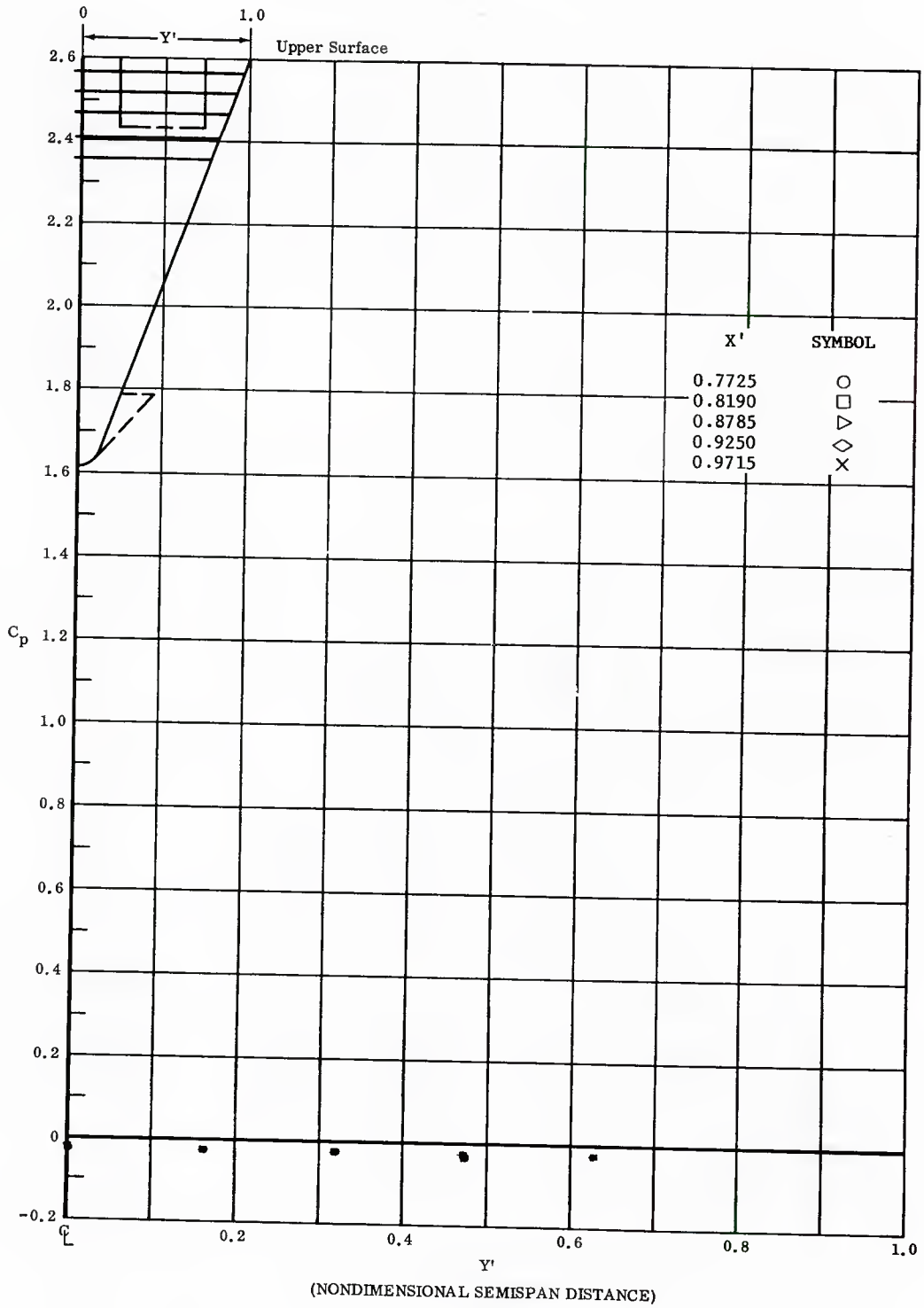

Fig. 72 Spanwise Distributions of Pressure Coefficients on Upper Surface Basic Configuration, No Flap Deflections, $\alpha = +33°$, $\beta = 0$

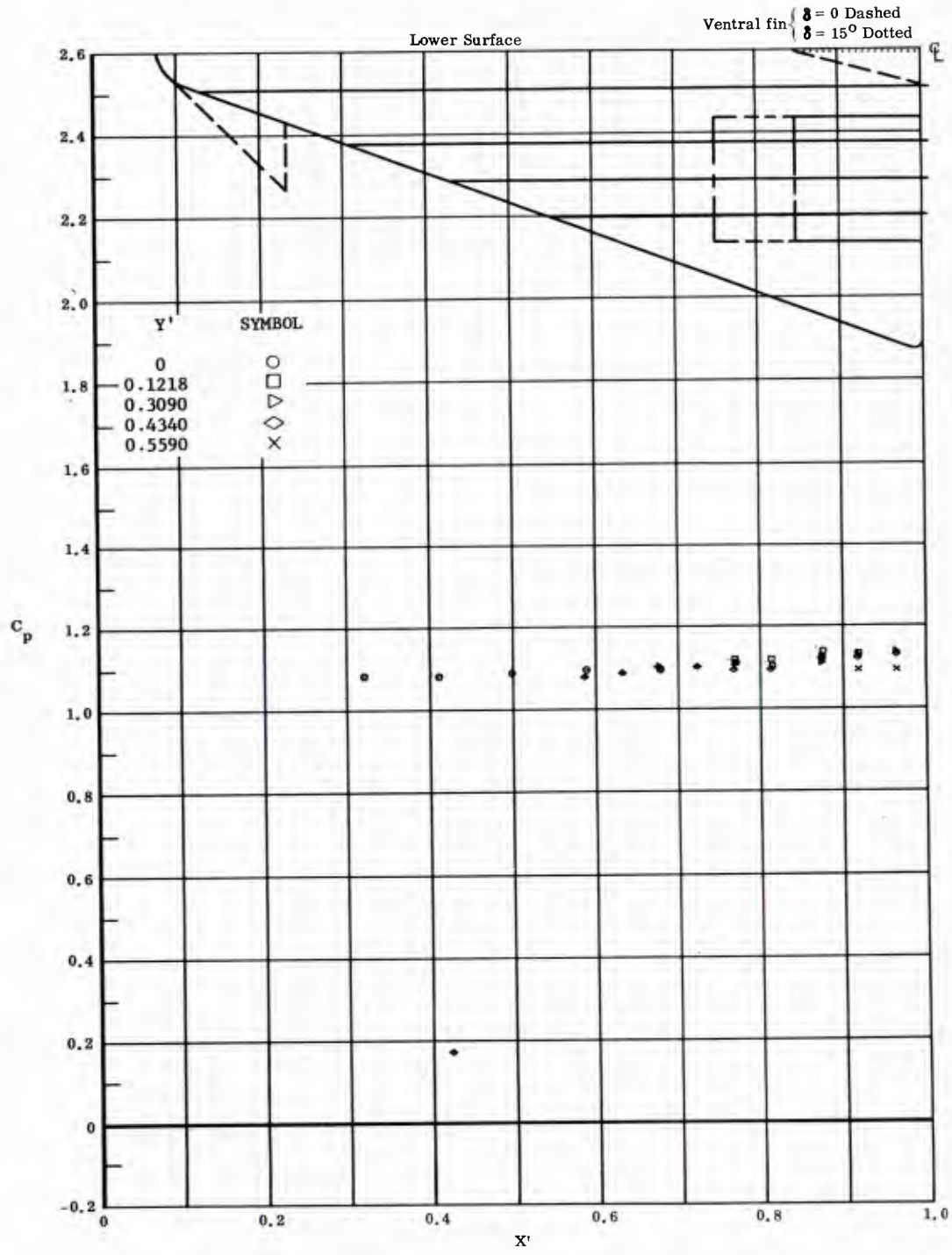

Fig. 73 Streamwise Distributions of Pressure Coefficients on Lower Surface Basic Configuration, Left and Right (Upper) Flaps Deflected -40°, $\alpha = +45°$, $\beta = 0$

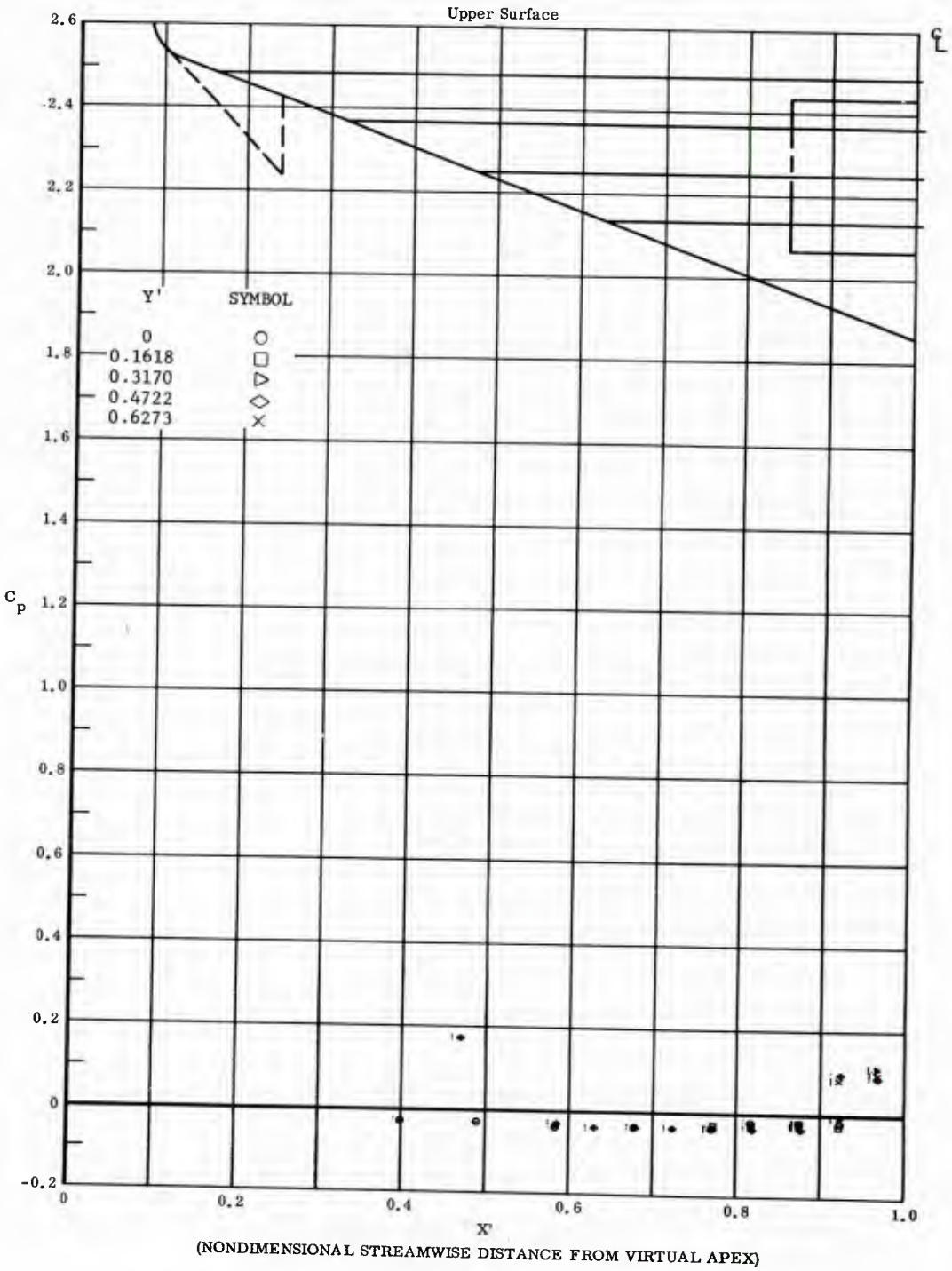

Fig. 73 Streamwise Distributions of Pressure Coefficients on Upper Surface Basic Configuration, Left and Right (Upper) Flaps Deflected -40°, $\alpha = +45°$, $\beta = 0$

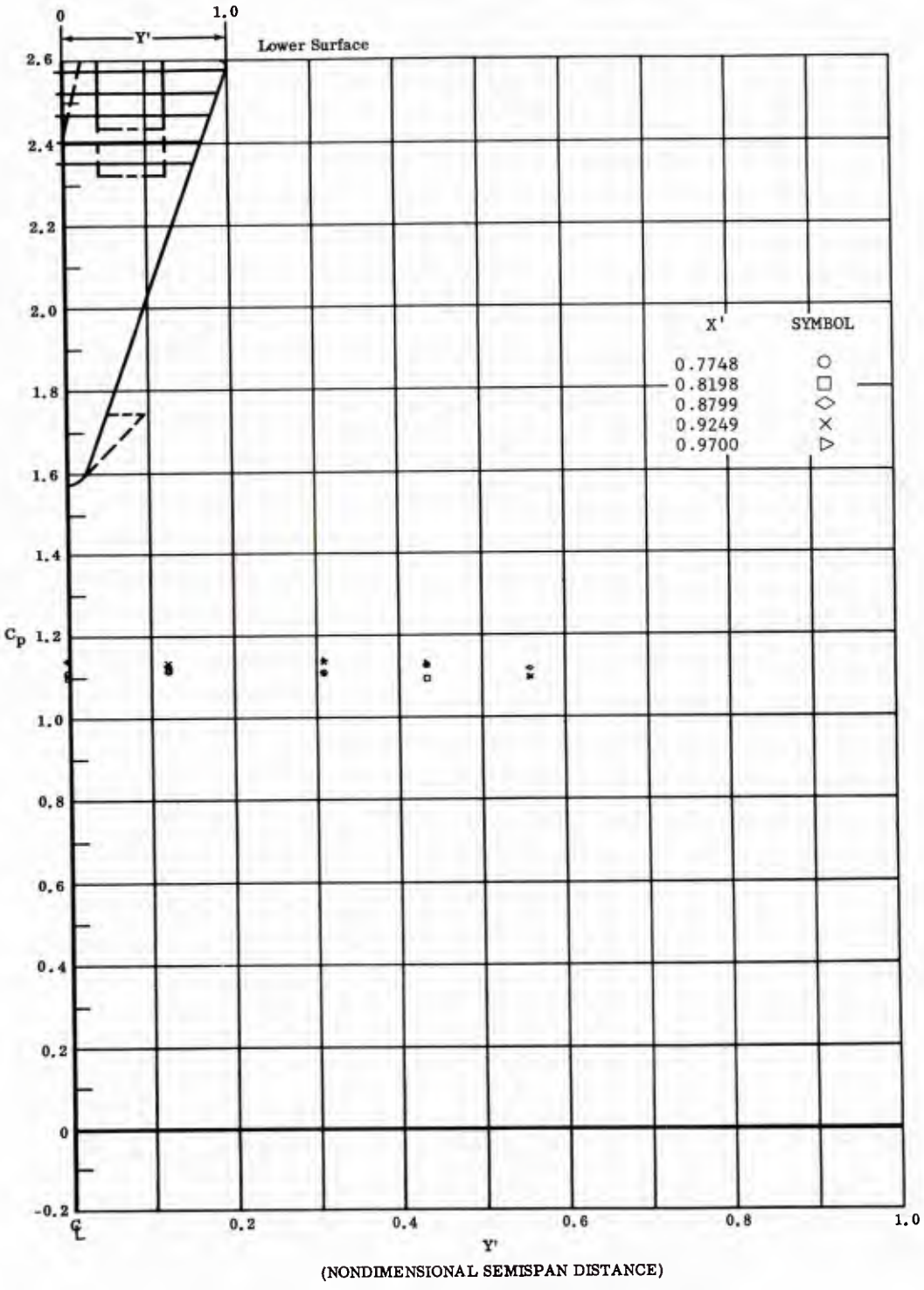

Fig. 73 Spanwise Distributions of Pressure Coefficients on Lower Surface Basic Configuration, Left and Right (Upper) Flaps Deflected -40°, $\alpha = +45°$, $\beta = 0$

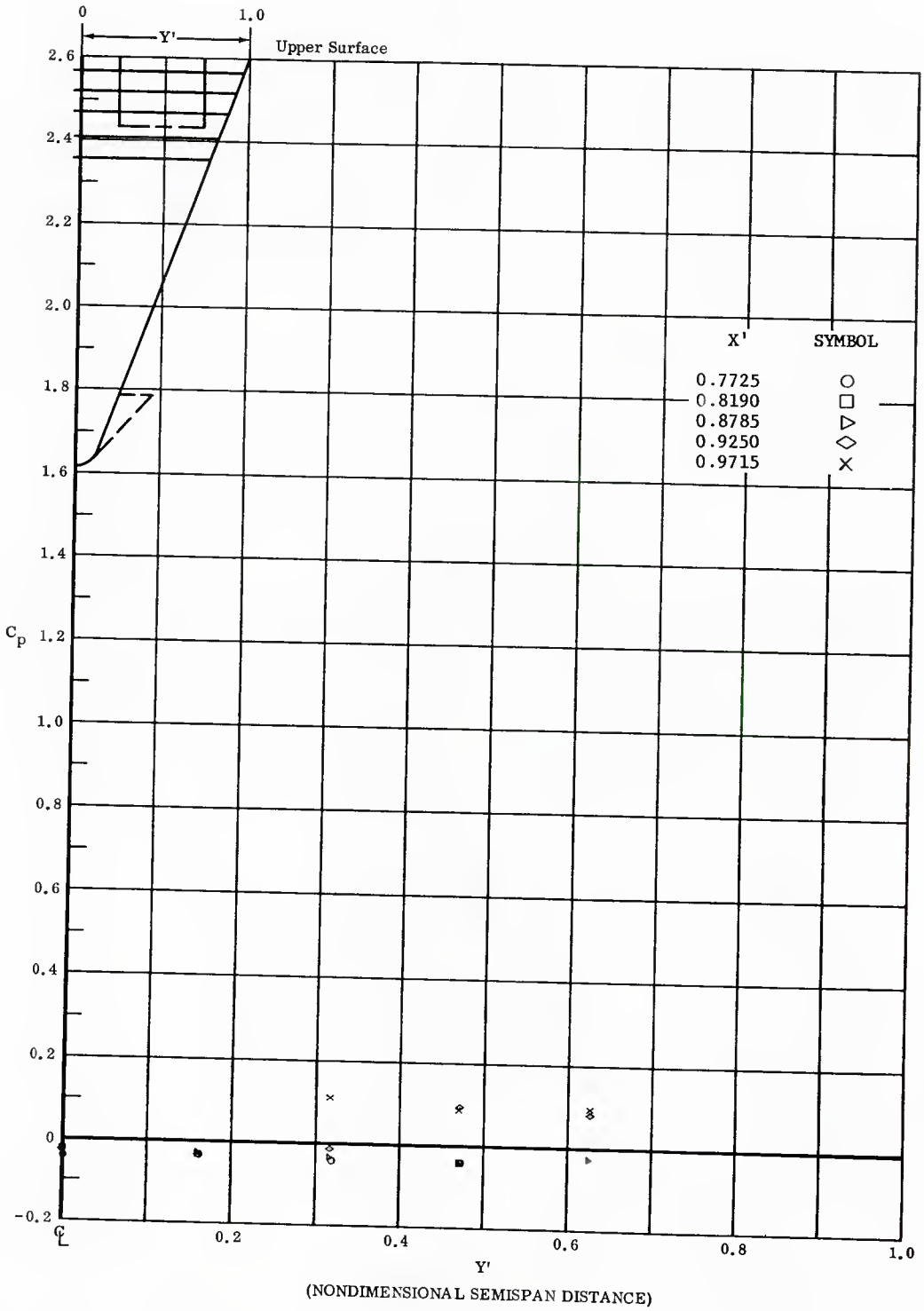

Fig. 73 Spanwise Distributions of Pressure Coefficients on Upper Surface Basic Configuration, Left and Right (Upper) Flaps Deflected -40°, $\alpha = +4^{\circ}$, $\beta = 0$

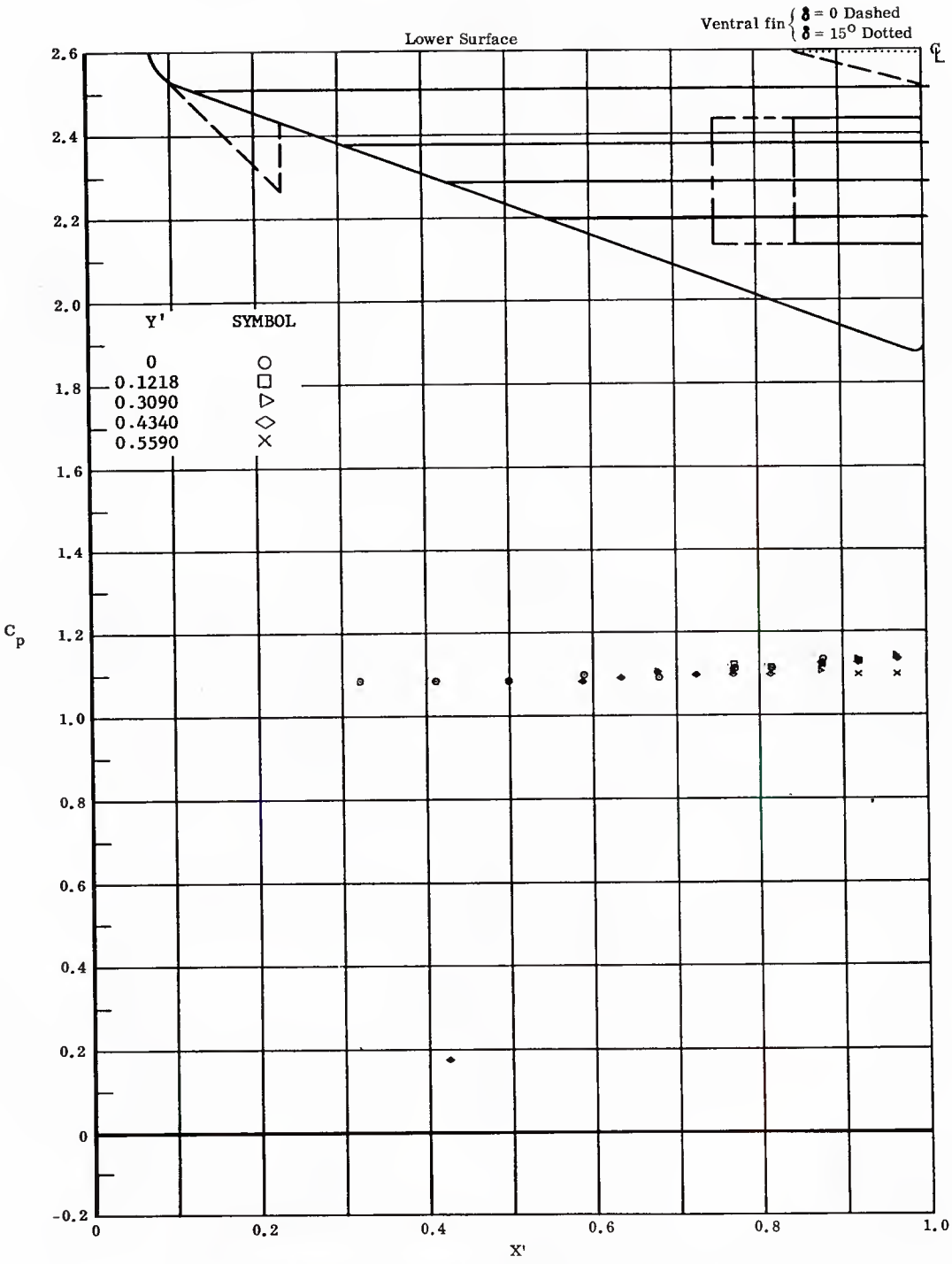

Fig. 74 Streamwise Distributions of Pressure Coefficients on Lower Surface Basic Configuration, Left and Right (Upper) Flaps Deflected -30°, $\alpha = +4.5°, \beta = 0$

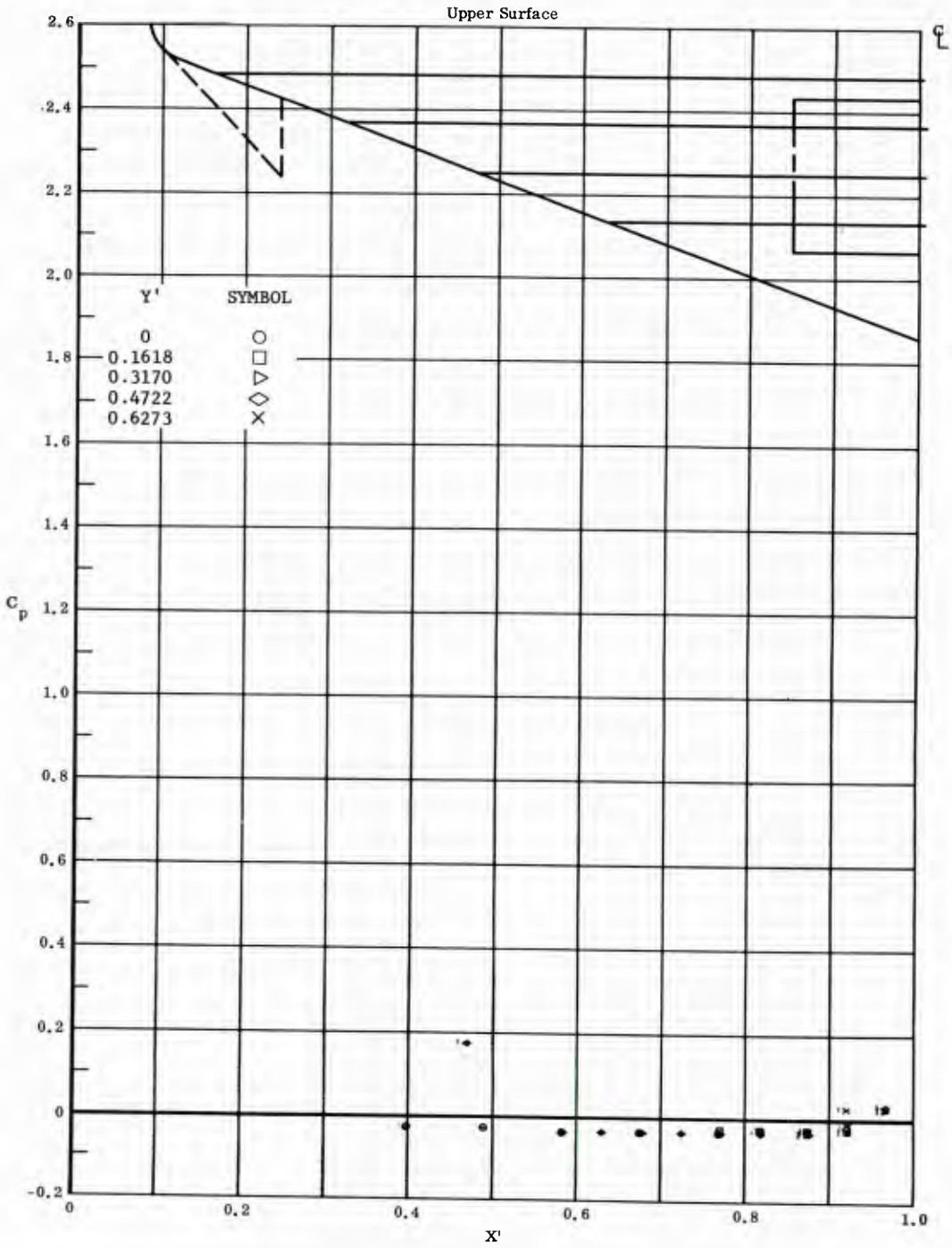

Fig. 74 Streamwise Distributions of Pressure Coefficients on Upper Surface Basic Configuration, Left and Right (Upper) Flaps Deflected -30°, $\alpha = +4.5°$, $\beta = 0$

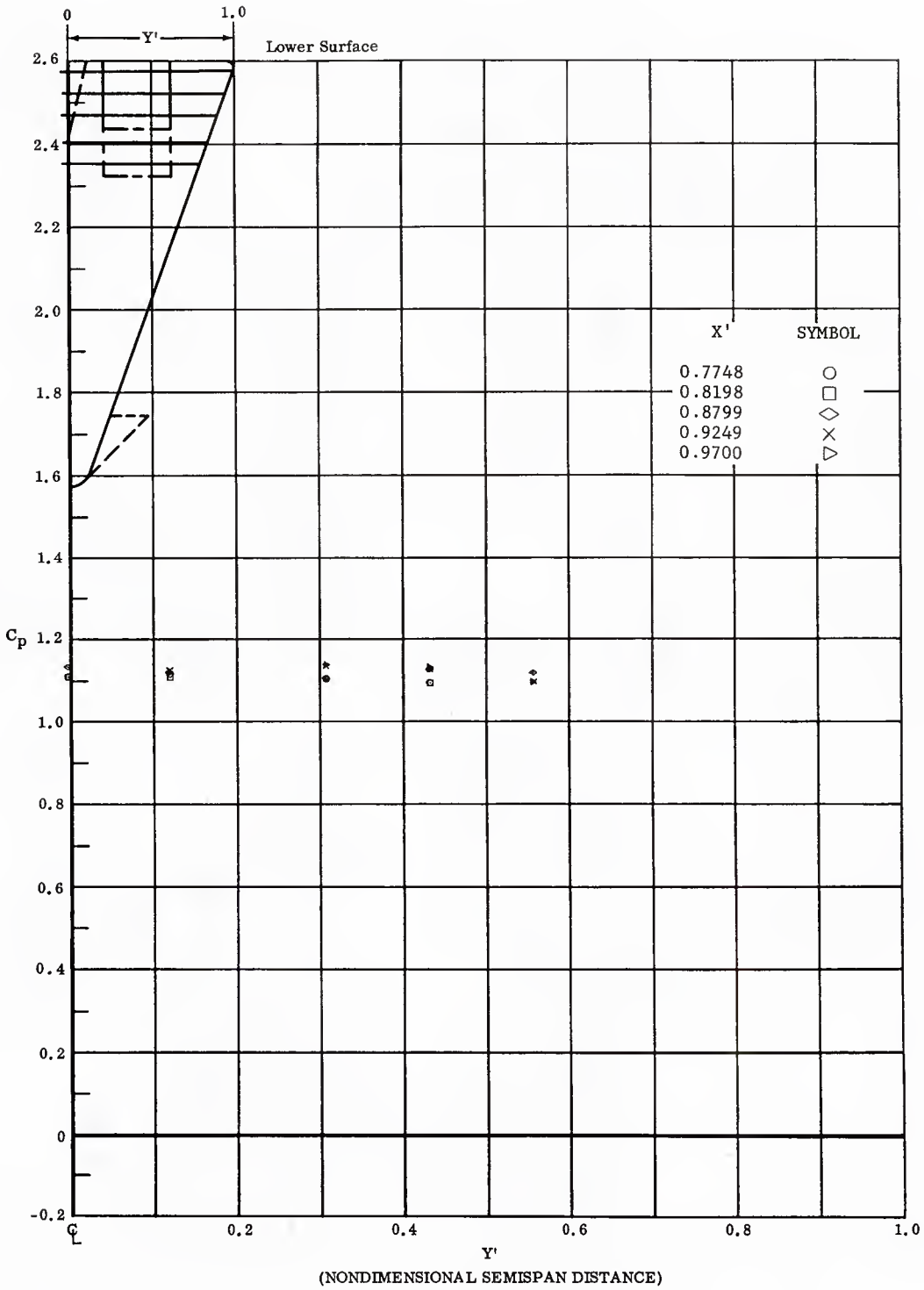

Fig. 74 Spanwise Distributions of Pressure Coefficients on Lower Surface Basic Configuration, Left and Right (Upper) Flaps Deflected -30°, $\alpha = +45°, \beta = 0$

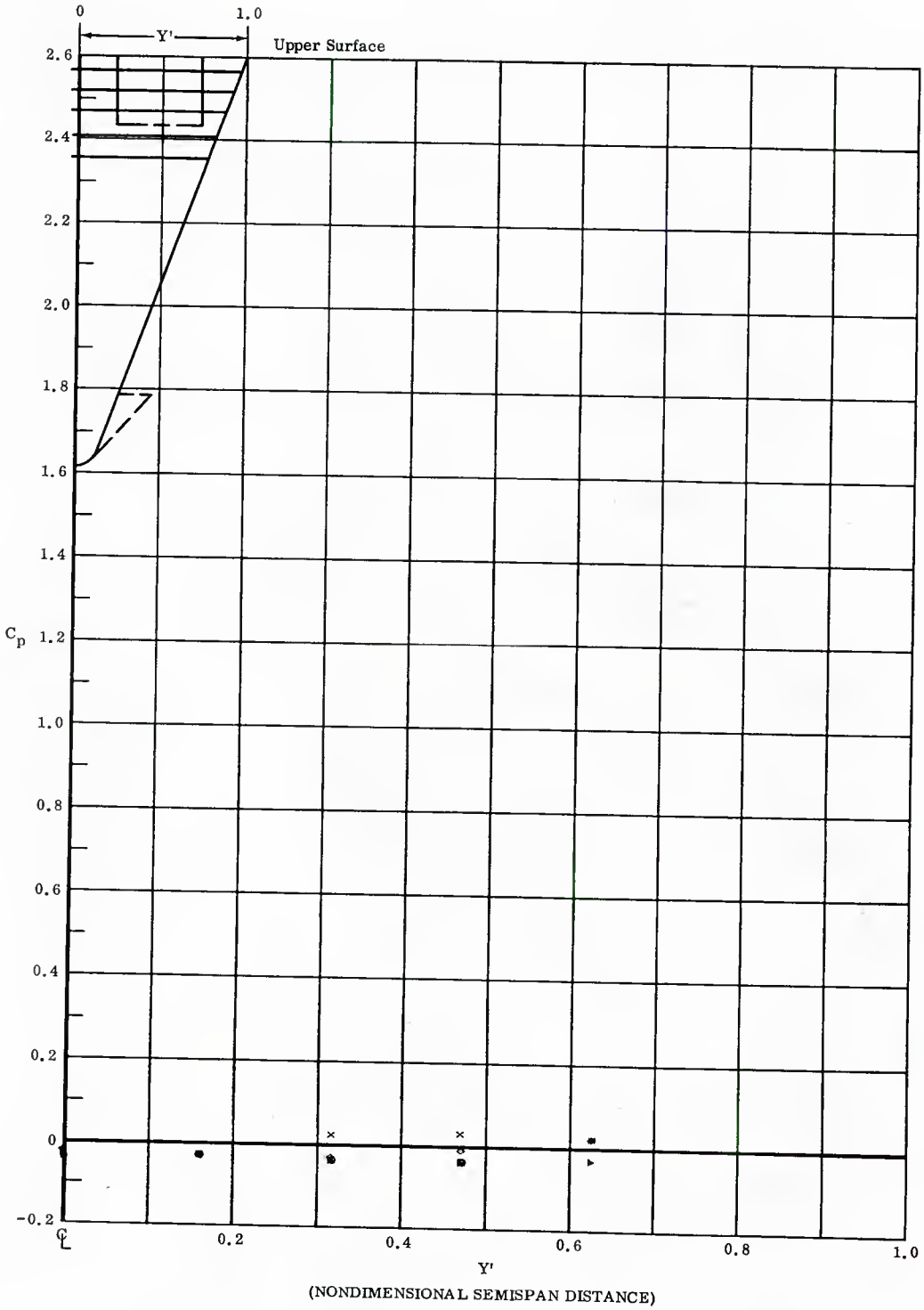

Fig. 74 Spanwise Distributions of Pressure Coefficients on Upper Surface Basic Configuration, Left and Right (Upper) Flaps Deflected -30°, α = +4.5°, β = 0

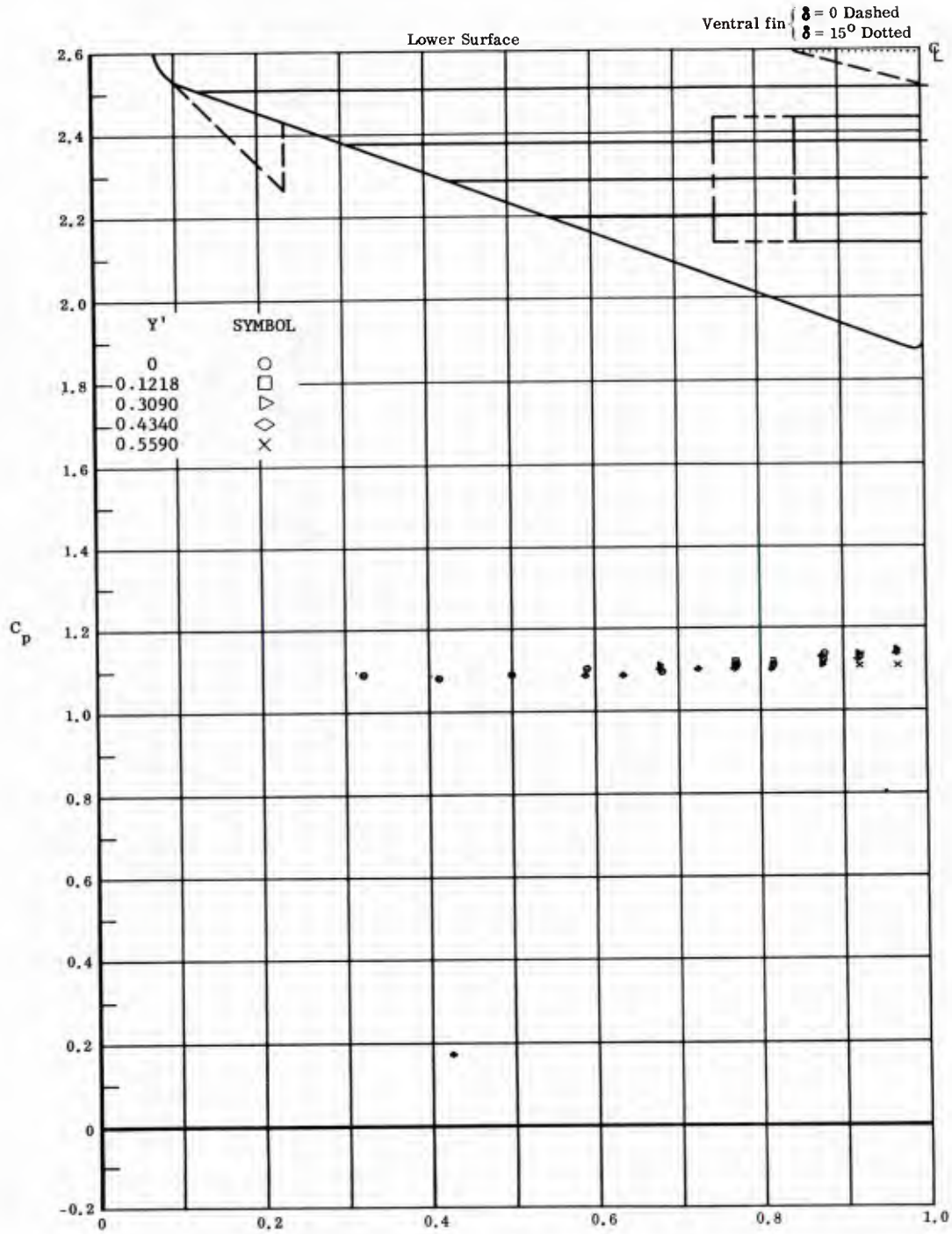

Fig. 75 Streamwise Distributions of Pressure Coefficients on Lower Surface
Basic Configuration, Left and Right (Upper) Flaps Deflected -20°
α = +45°, β = 0

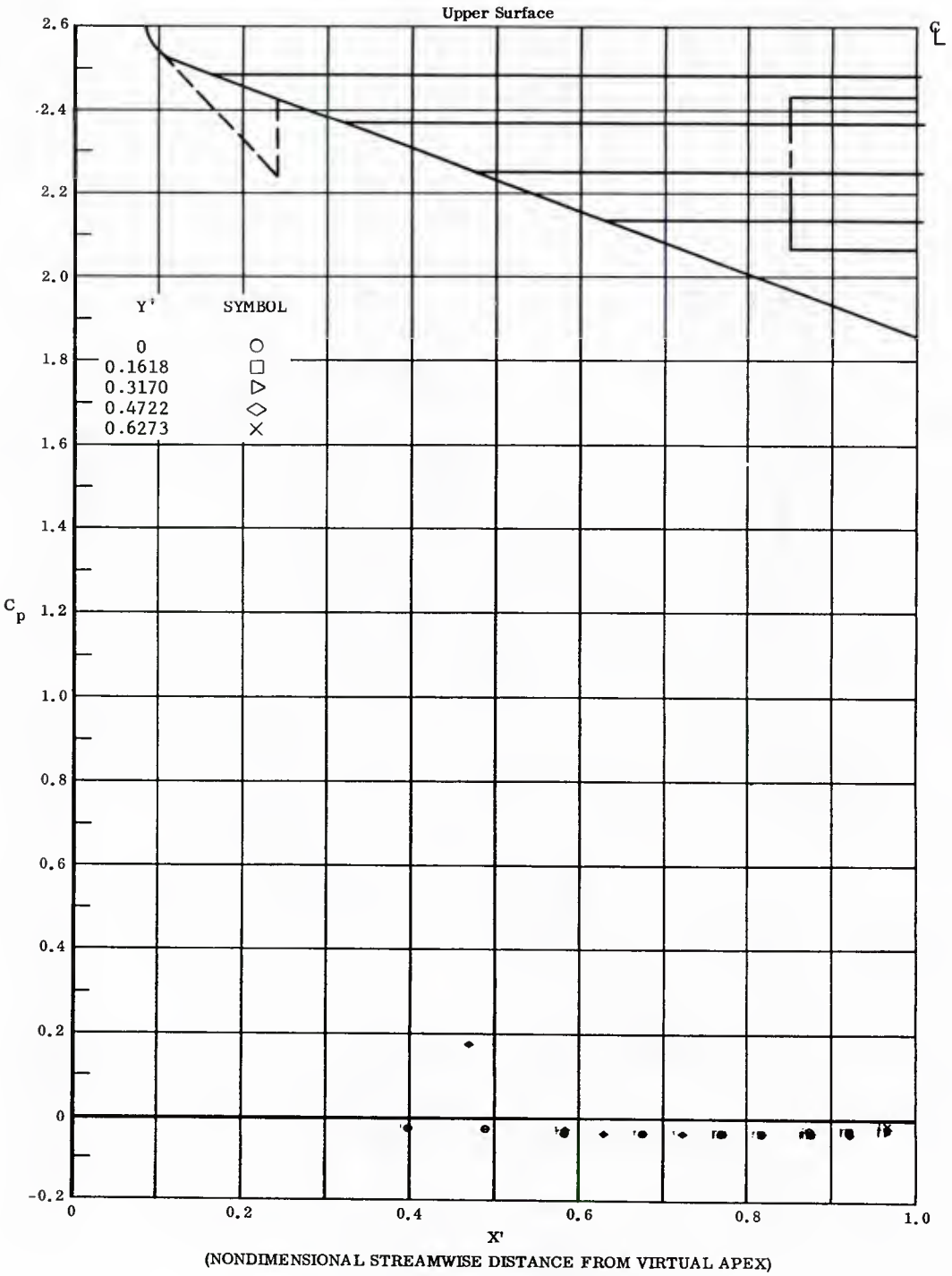

Fig. 75 Streamwise Distributions of Pressure Coefficients on Upper Surface Basic Configuration, Left and Right (Upper) Flaps Deflected -20°, $\alpha = +4.5°$, $\beta = 0$

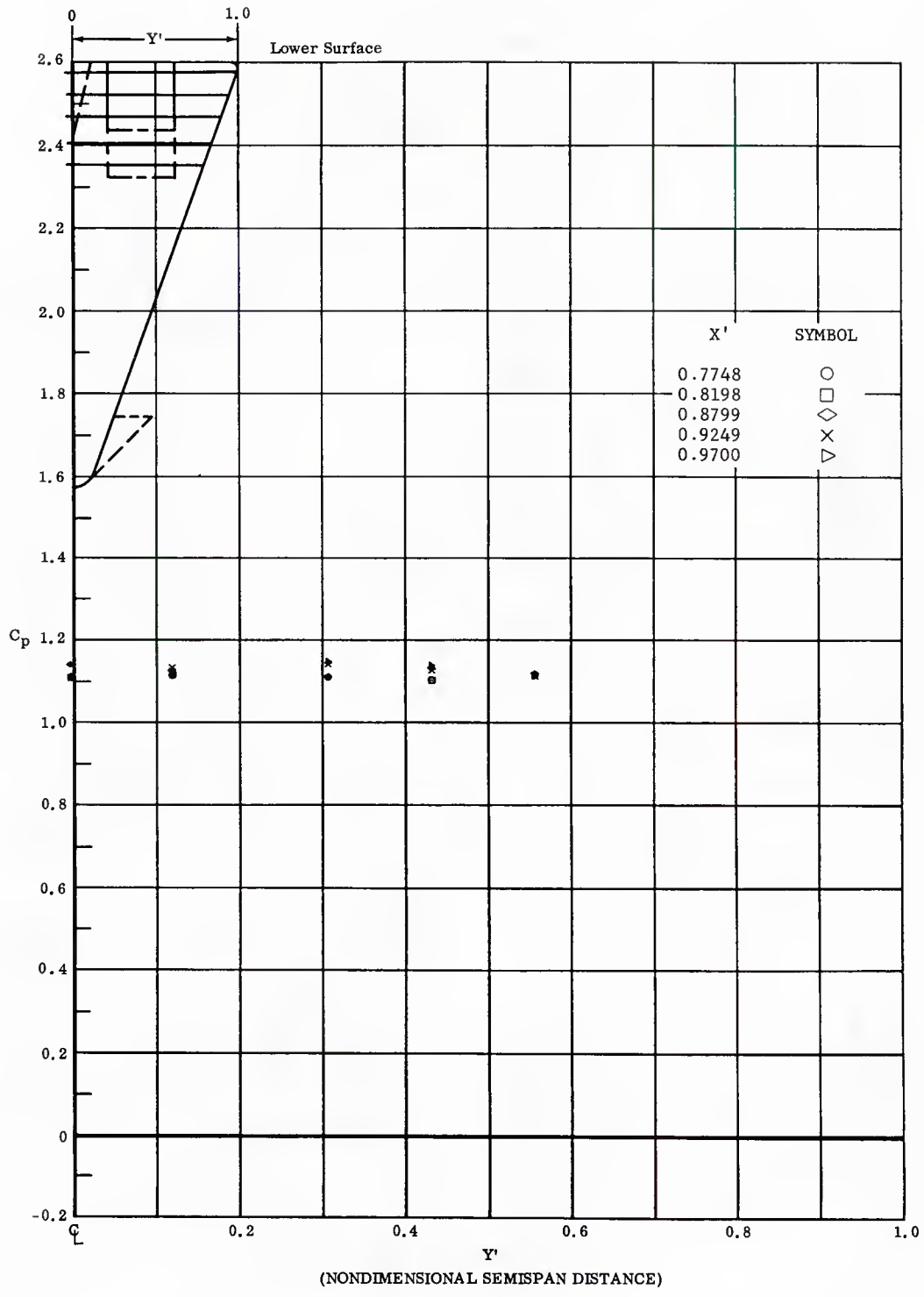

Fig. 75 Spanwise Distributions of Pressure Coefficients on Lower Surface Basic Configuration, Left and Right (Upper) Flaps Deflected -20°, $\alpha = +4.5°$, $\beta = 0$

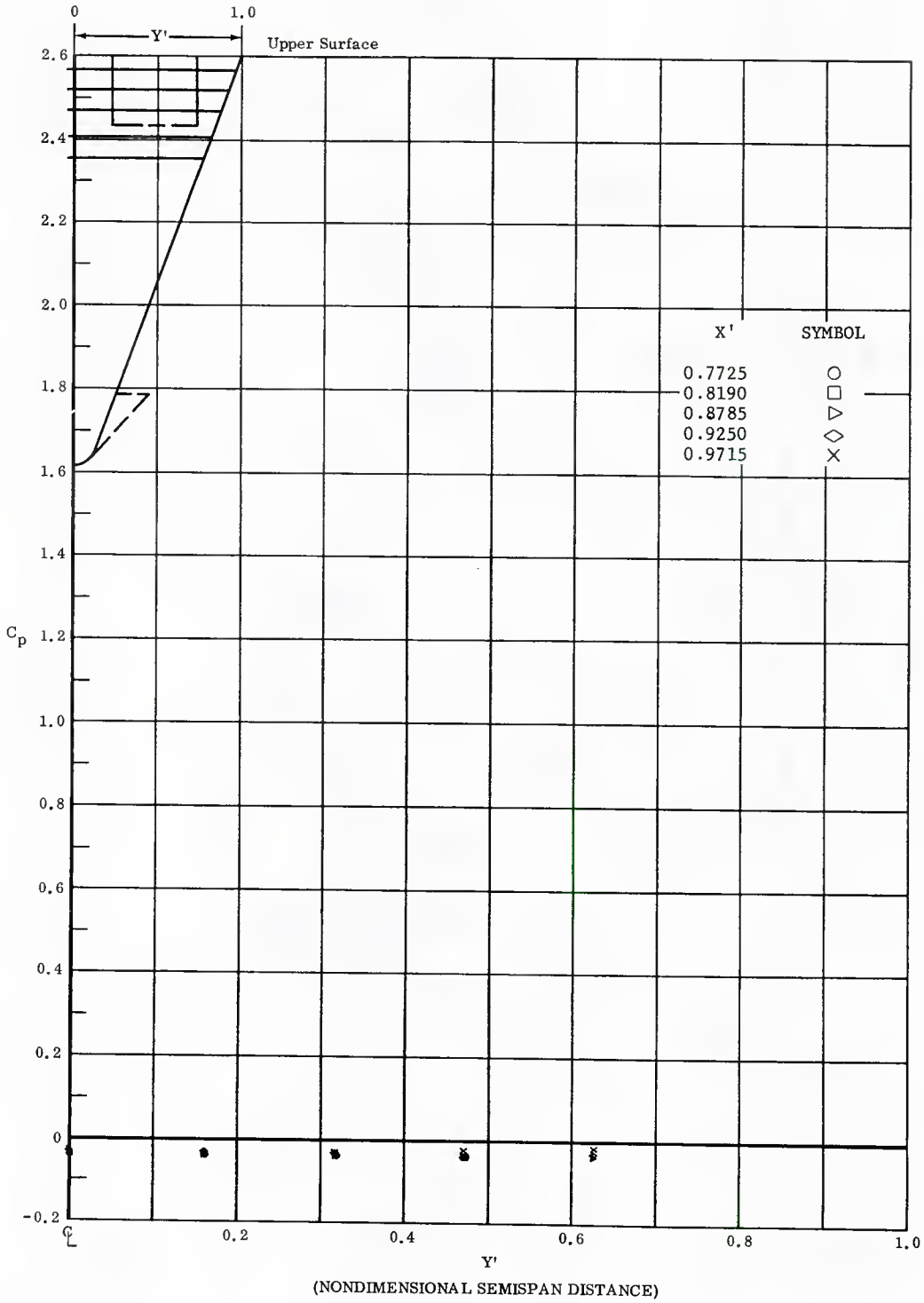

Fig. 75 Spanwise Distributions of Pressure Coefficients on Upper Surface Basic Configuration, Left and Right (Upper) Flaps Deflected -20°, α = +4.5°, β = 0

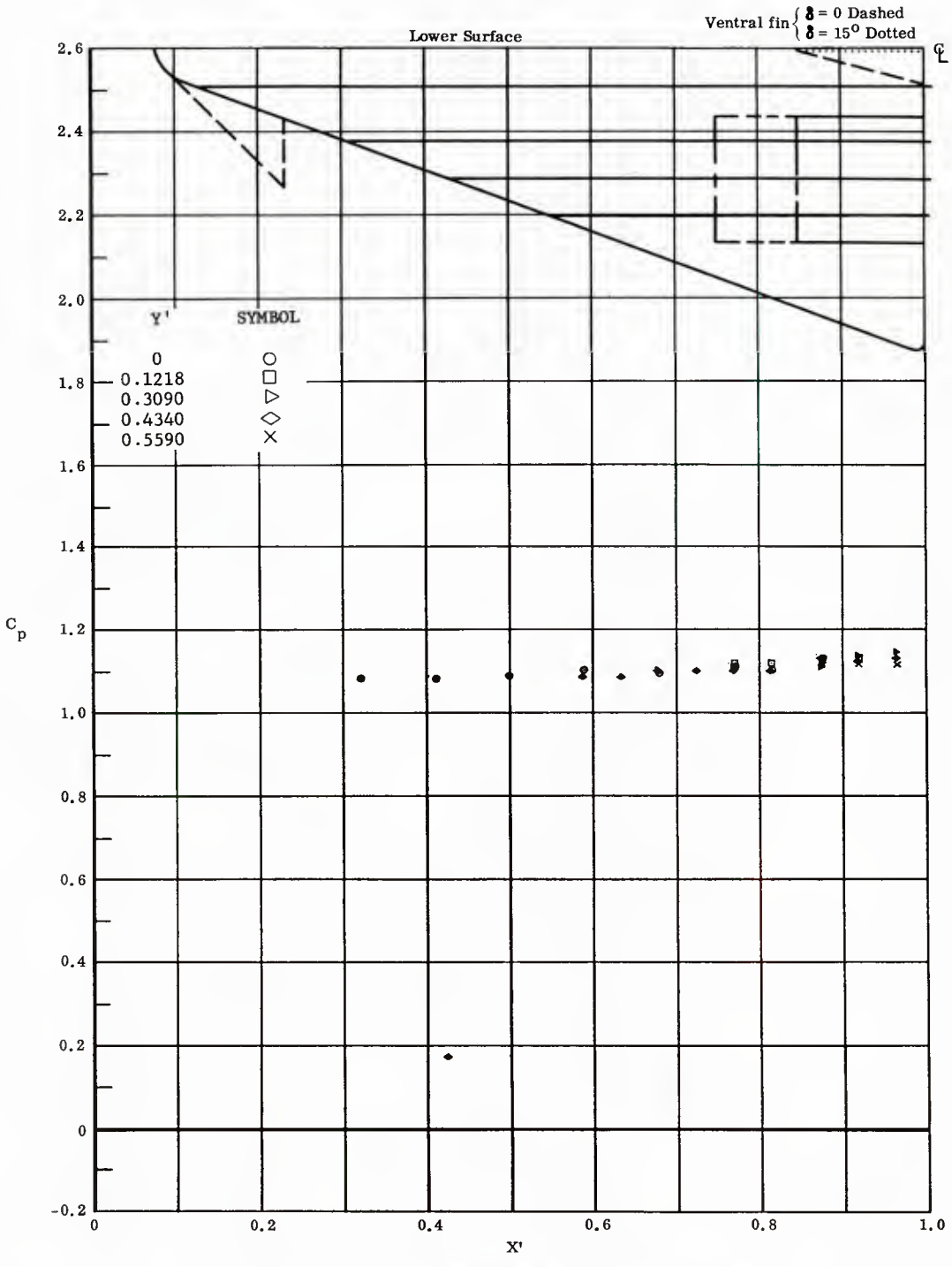

Fig. 76 Streamwise Distributions of Pressure Coefficients on Lower Surface Basic Configuration, Left and Right (Upper) Flaps Deflected -10°, $\alpha = +4.5°$, $\beta = 0$

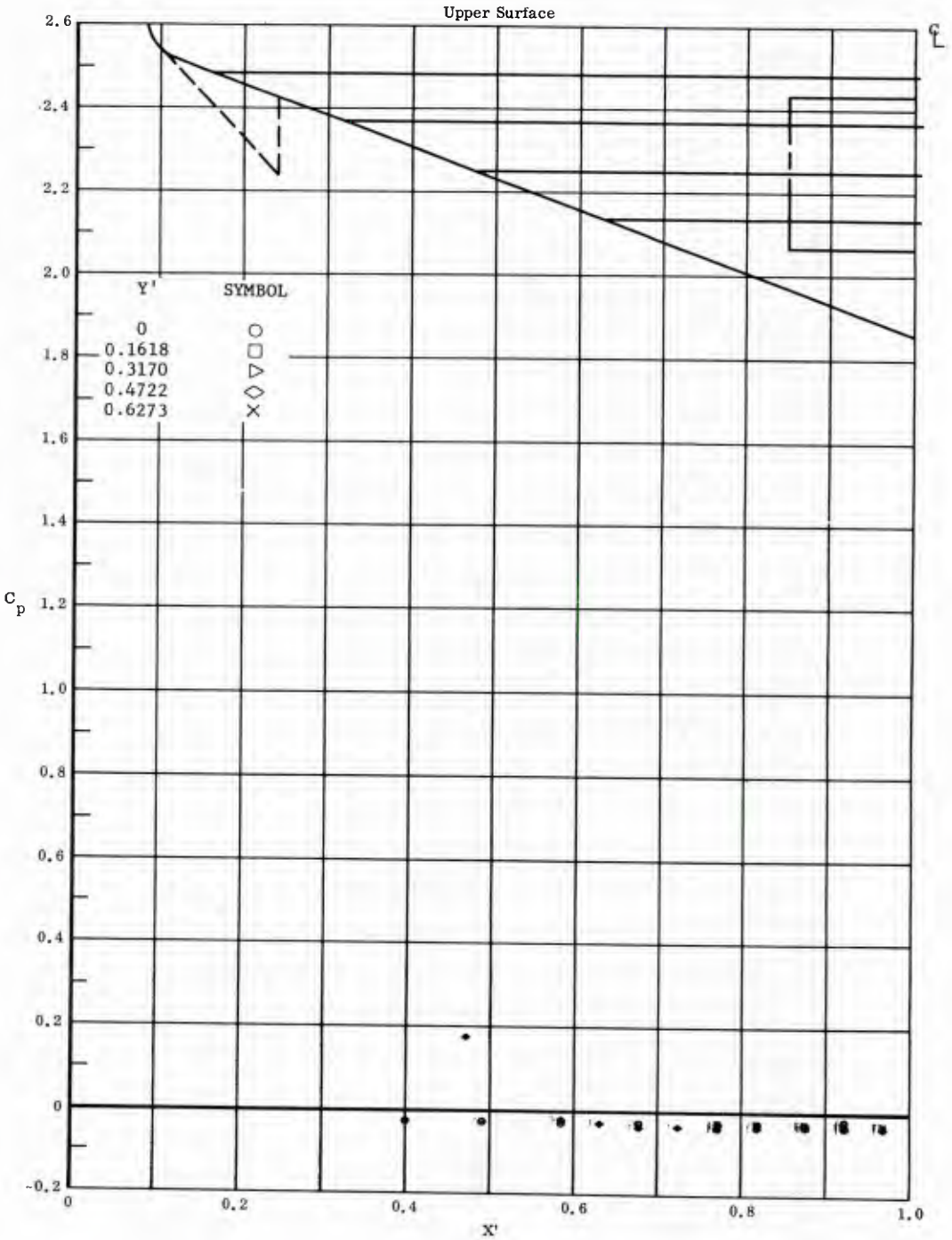

Fig. 76 Streamwise Distributions of Pressure Coefficients on Upper Surface Basic Configuration, Left and Right (Upper) Flaps Deflected -10°, $\alpha = +4.5°$, $\beta = 0$

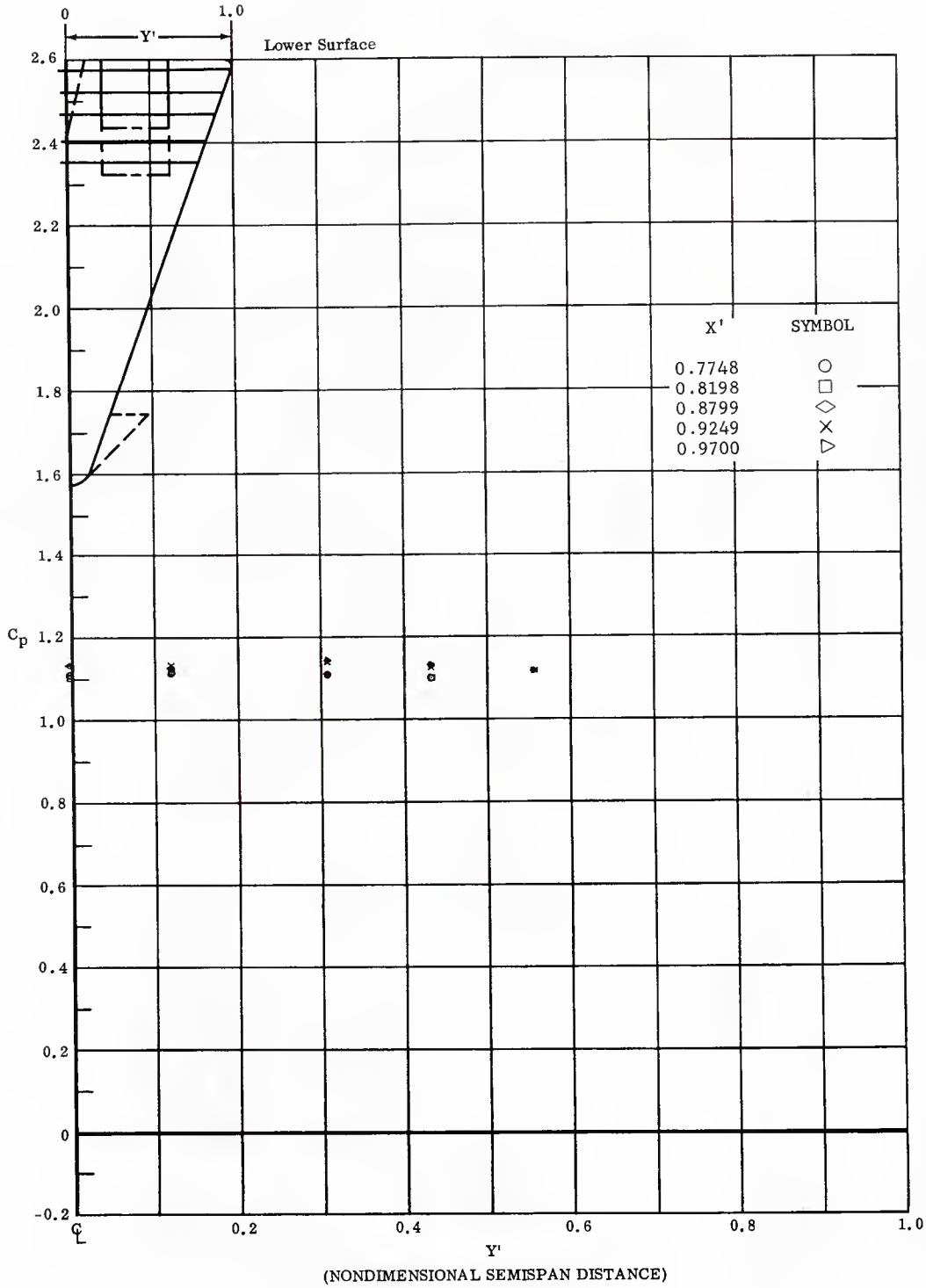

Fig. 76 Spanwise Distributions of Pressure Coefficients on Lower Surface Basic Configuration, Left and Right (Upper) Flaps Deflected -10°, $\alpha = +4.5°$, $\beta = 0$

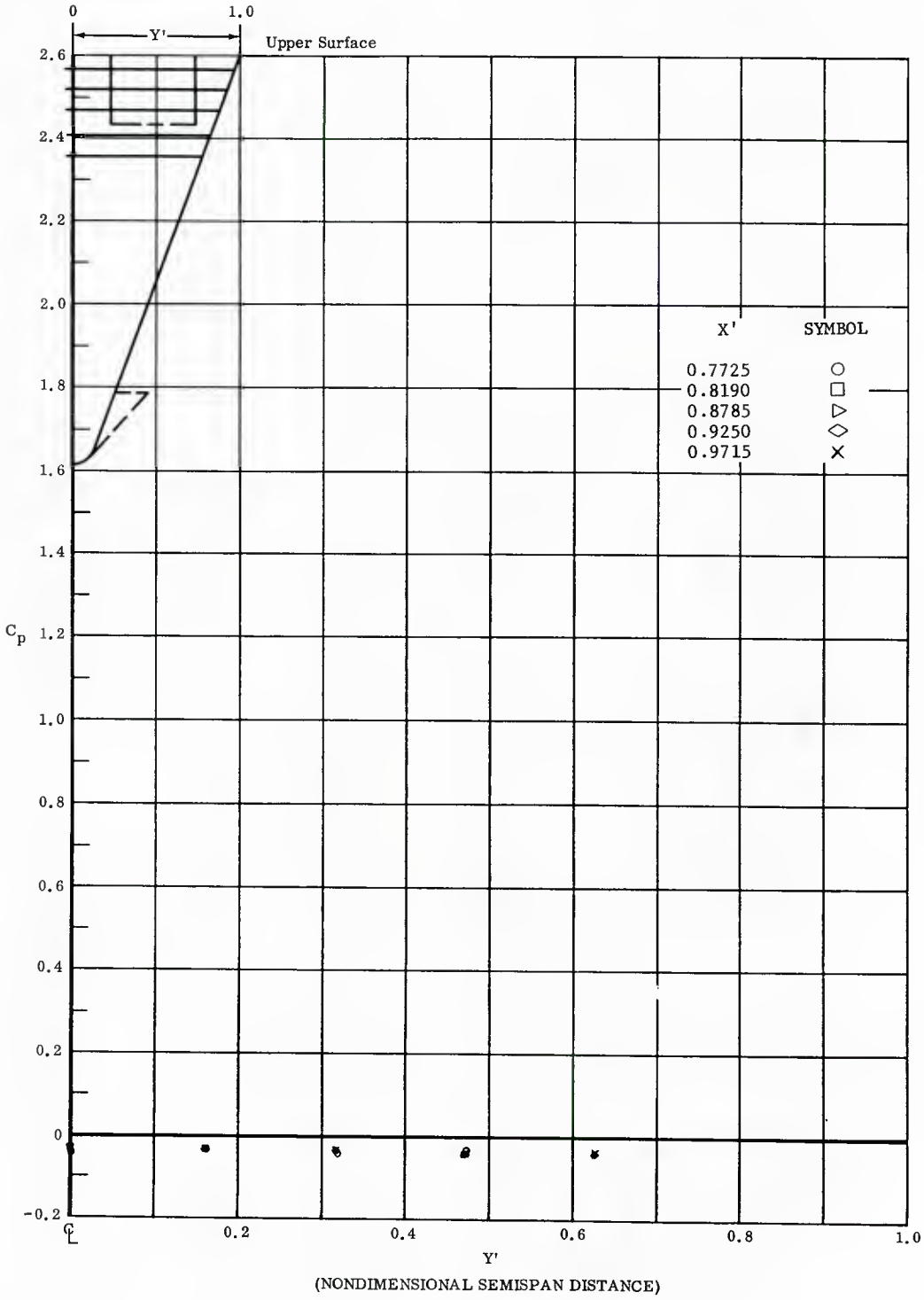

Fig. 76 Spanwise Distributions of Pressure Coefficients on Upper Surface Basic Configuration, Left and Right (Upper) Flaps Deflected -10° $\alpha = +4.5°, \beta = 0$

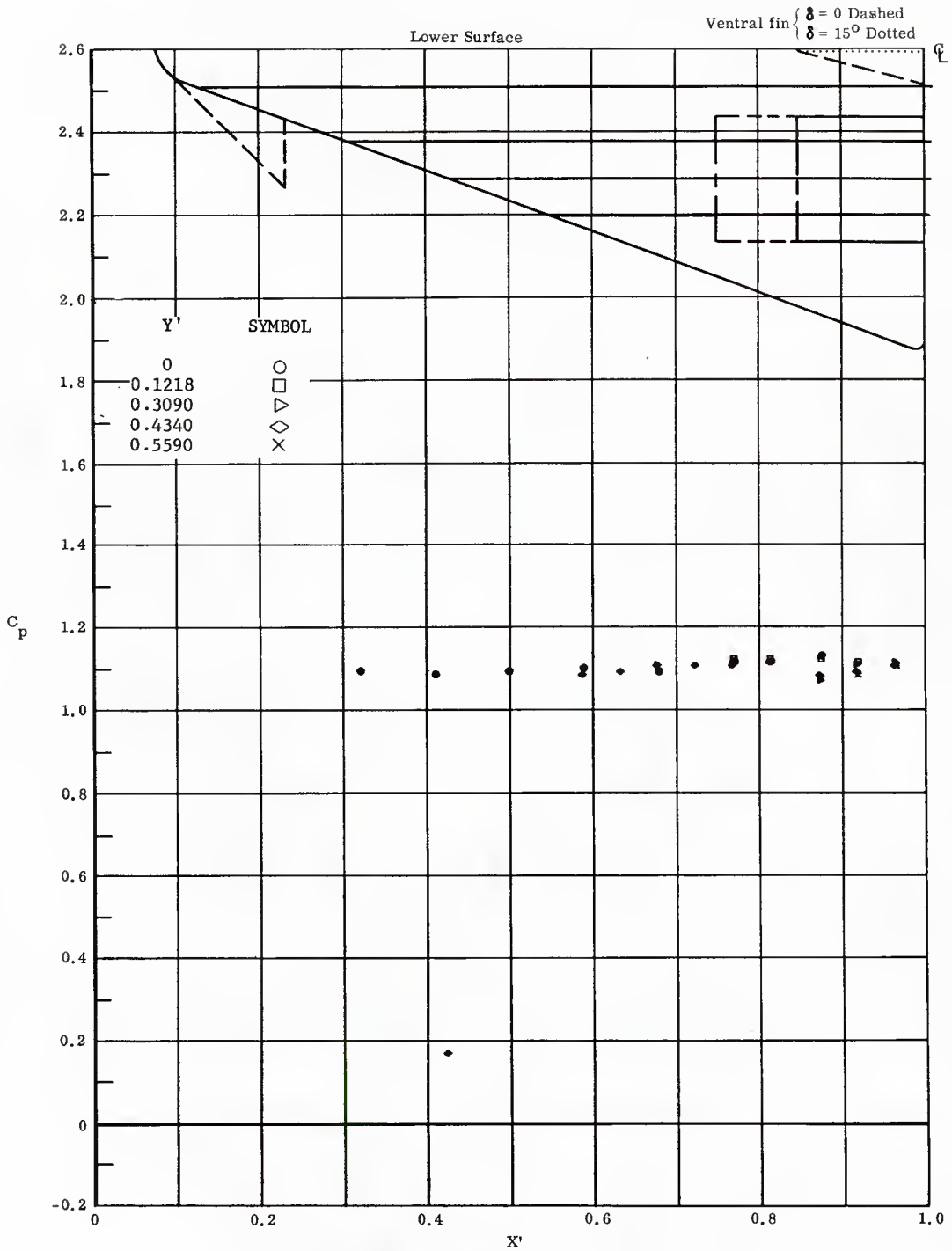

Fig. 77 Streamwise Distributions of Pressure Coefficients on Lower Surface
Basic Configuration, No Flap Deflections, $\alpha = +45°$, $\beta = 0$

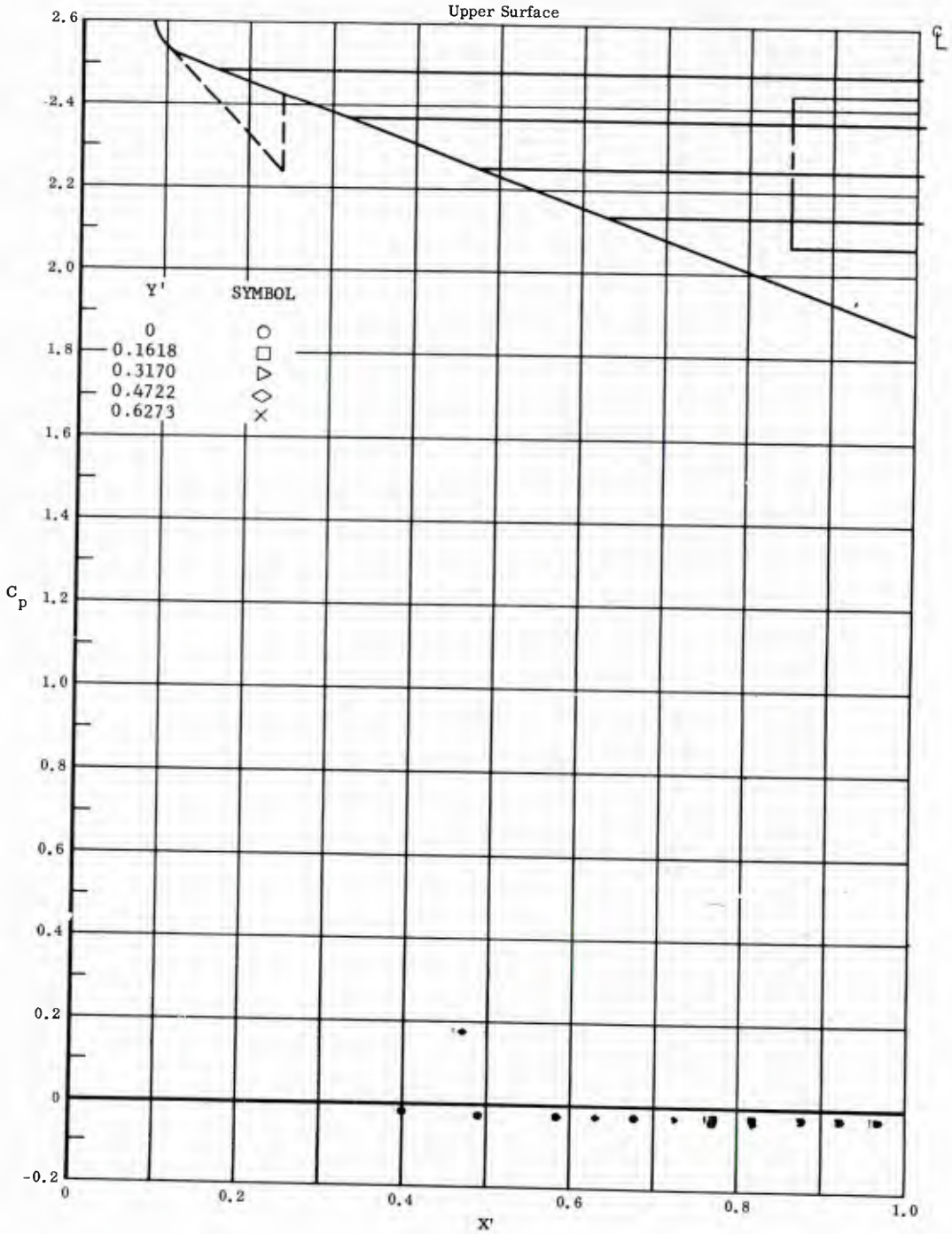

Fig. 77 Streamwise Distributions of Pressure Coefficients on Upper Surface Basic Configuration, No Flap Deflections, $\alpha = +45°$, $\beta = 0$

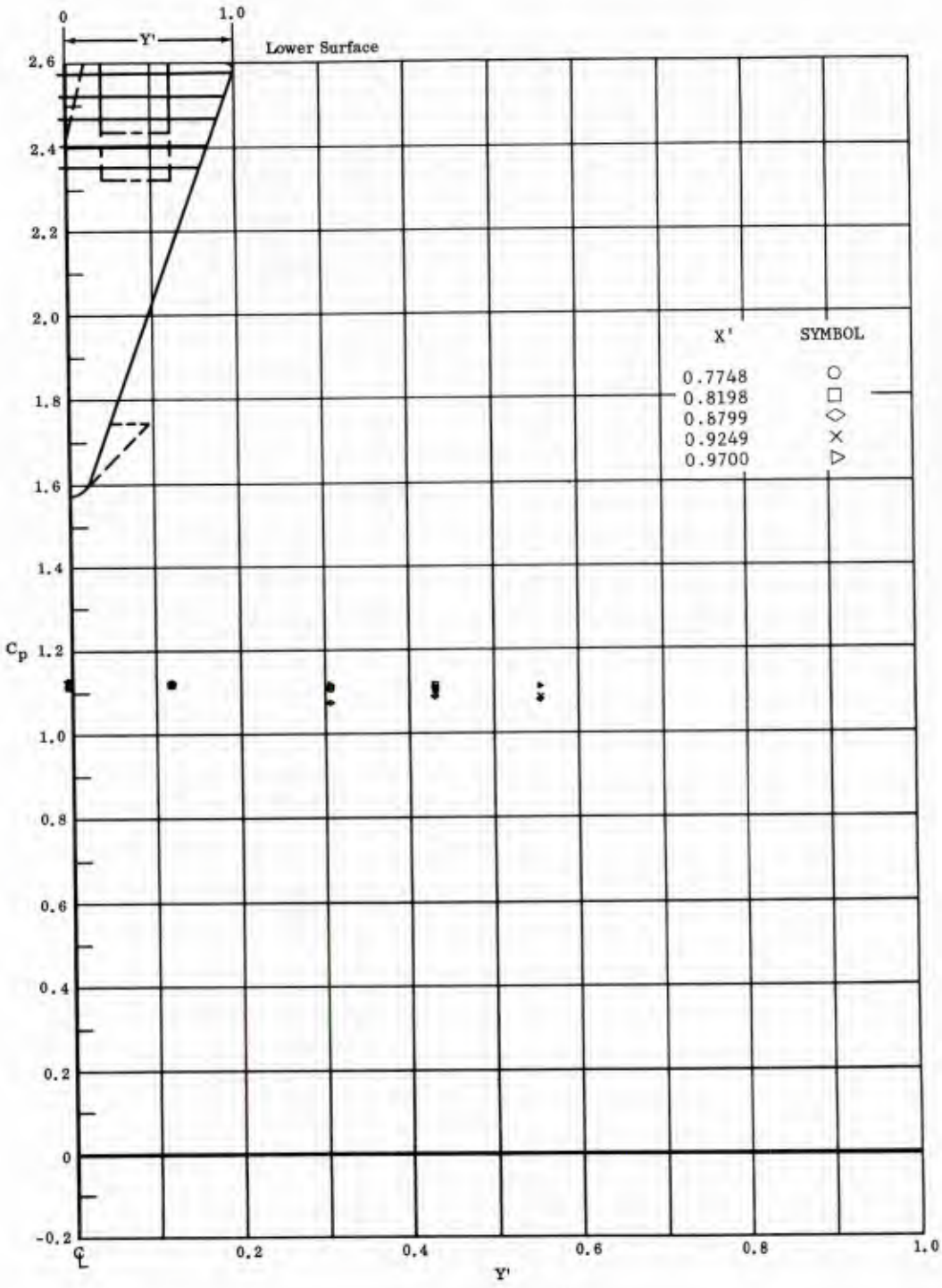

Fig. 77 Spanwise Distributions of Pressure Coefficients on Lower Surface Basic Configuration, No Flap Deflections, $\alpha = +4.5°$, $\beta = 0$

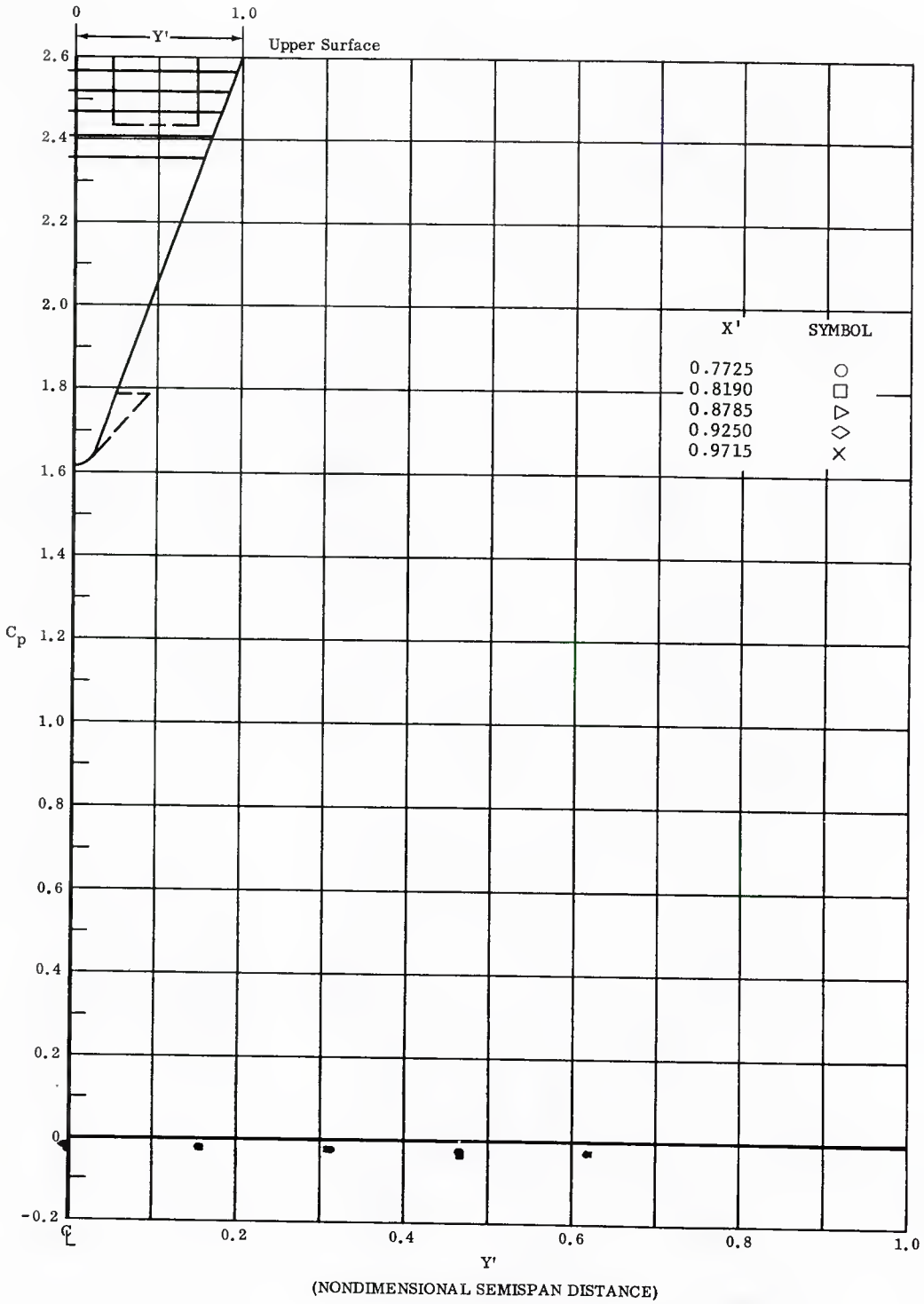

Fig. 77 Spanwise Distributions of Pressure Coefficients on Upper Surface Basic Configuration, No Flap Deflections, $\alpha = +4.5°$, $\beta = 0$

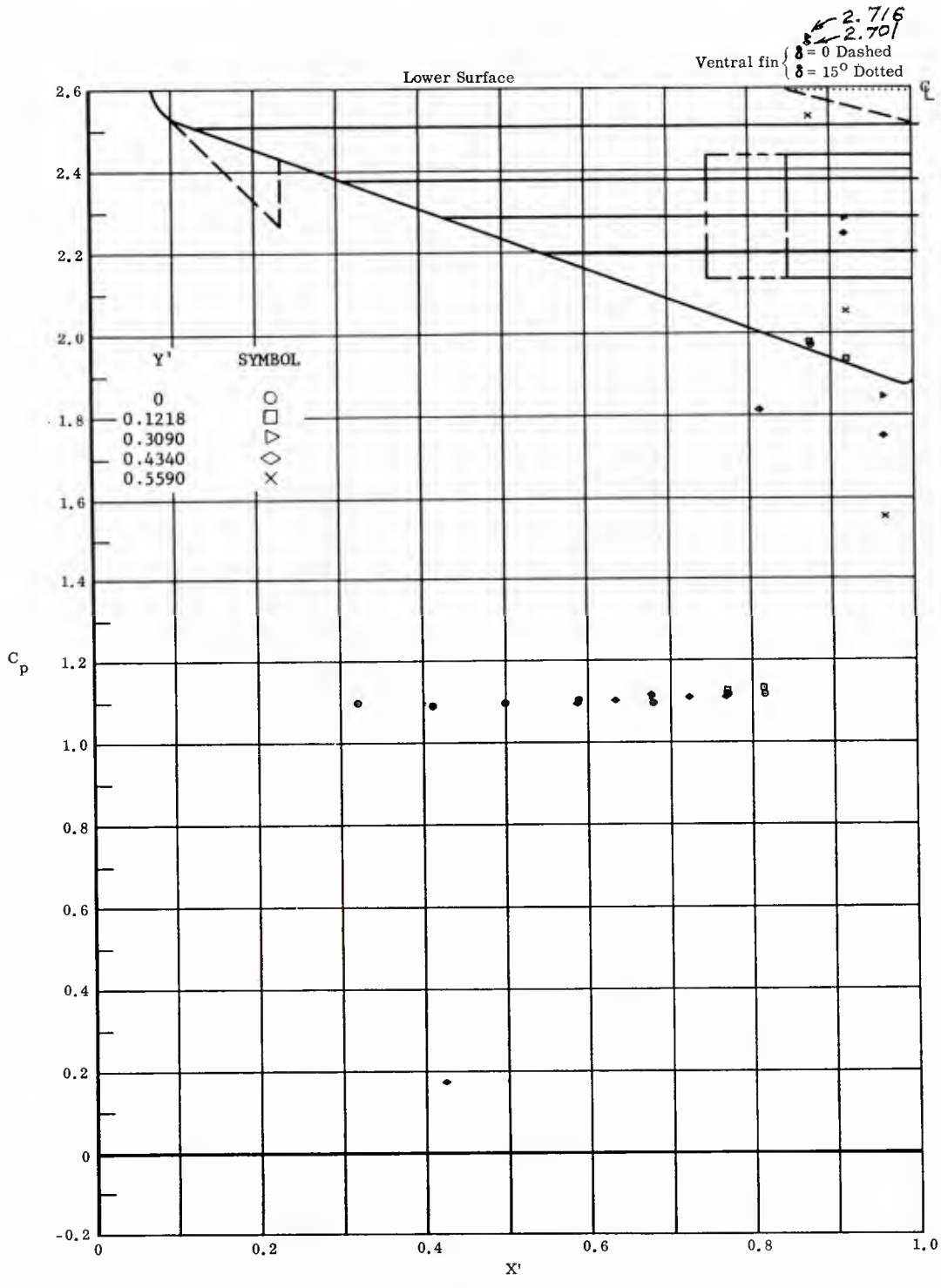

Fig. 78 Streamwise Distributions of Pressure Coefficients on Lower Surface Basic Configuration, Bottom Flaps Deflected 20°, α = +4.5°, β = 0

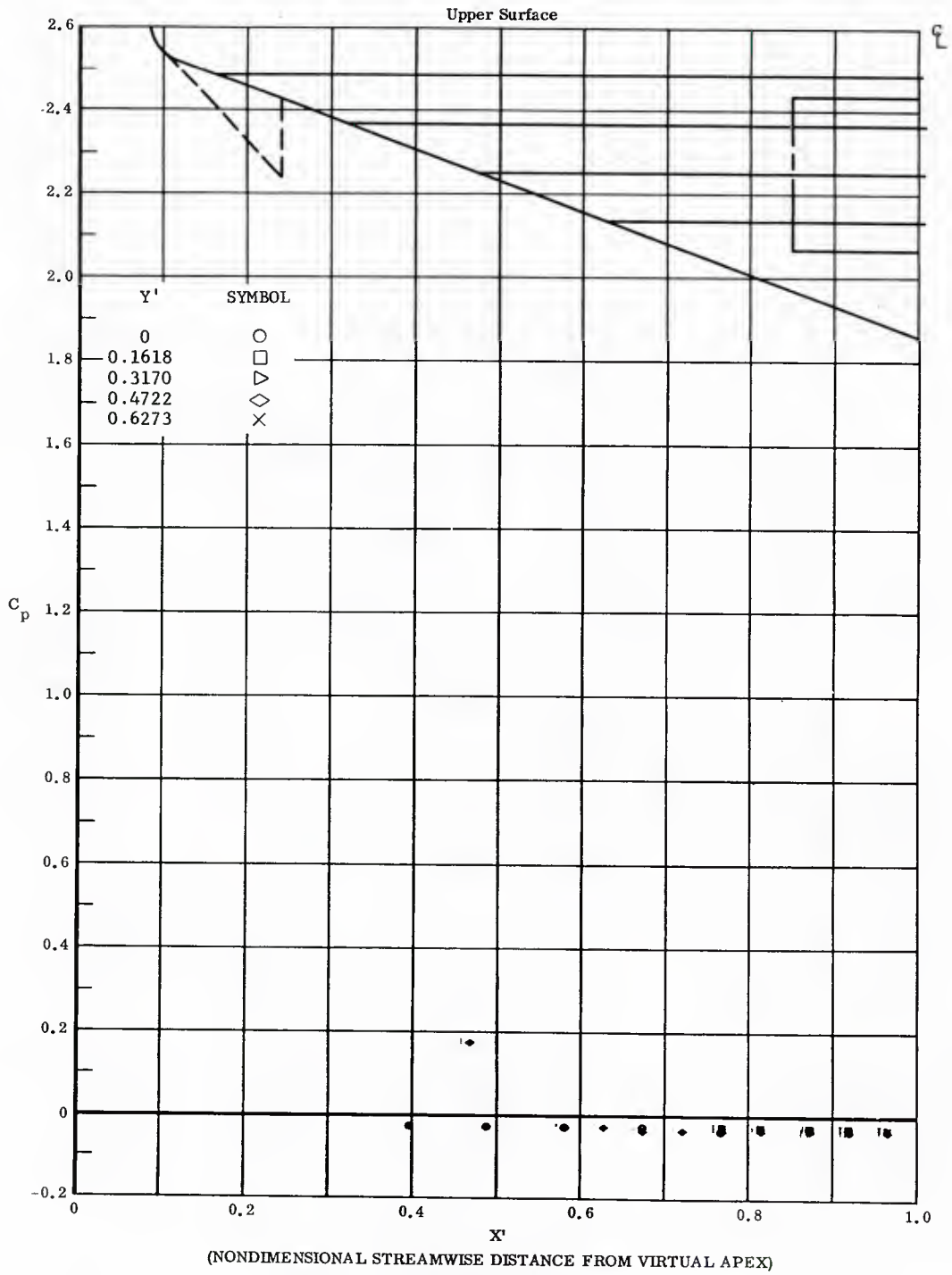

Fig. 78 Streamwise Distributions of Pressure Coefficients on Upper Surface
Basic Configuration, Bottom Flaps Deflected 20°, α = +4°, β = 0

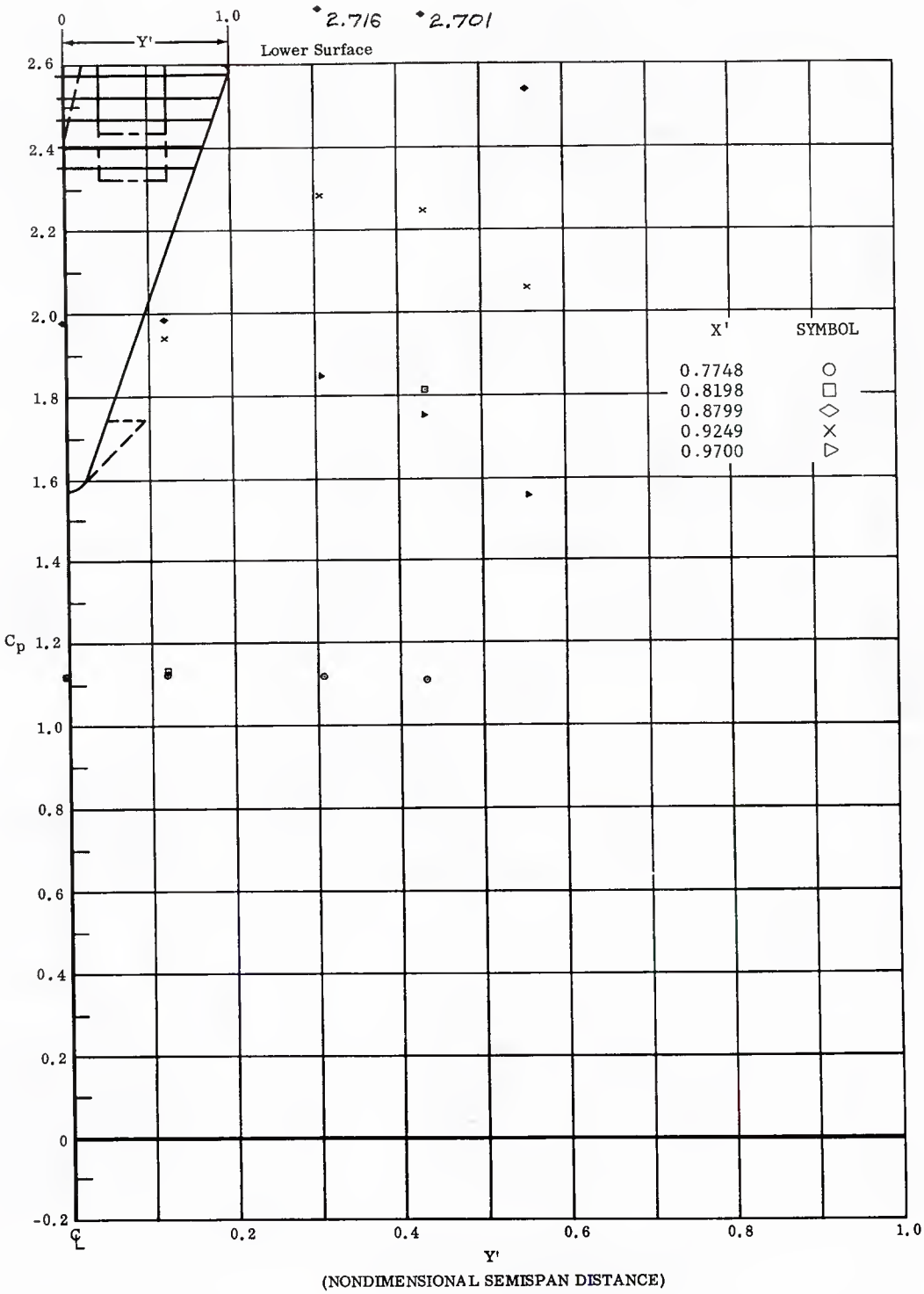

Fig. 78 Spanwise Distributions of Pressure Coefficients on Lower Surface
Basic Configuration, Bottom Flaps Deflected 20°, α = +4.5°, β = 0

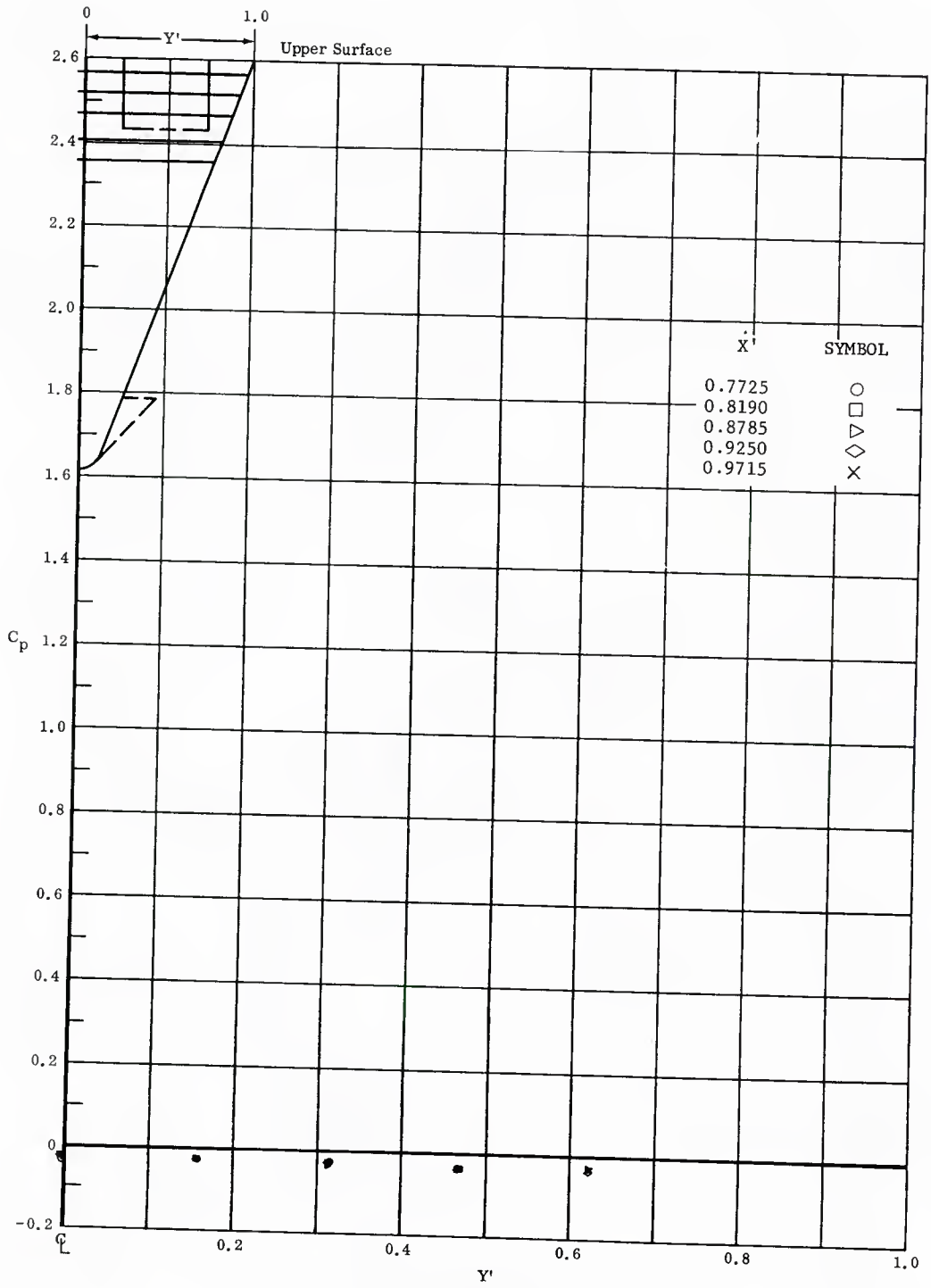

Fig. 78 Spanwise Distributions of Pressure Coefficients on Upper Surface Basic Configuration, Bottom Flaps Deflected 20°, α = +4.5°, β = 0